Svoluji k zapůjčení své dizertační práce ke studijním účelům a prosím, aby byla vedena přesná evidence vypůjčovatelů. Převzaté údaje je vypůjčovatel povinen řádně ocitovat.

Charles University

Faculty of Science

Molecular and Cell Biology, Genetics and Virology

Mgr. Vladislava Hronová

(nee / rozená Vlčková)

Molecular principles of translation reinitiation in mammals

Molekulární principy translační reiniciace v savčích buňkách

Doctoral thesis

Supervisor: Res. Prof. Leoš Shivaya Valášek, PhD

Laboratory of Regulation of Gene Expression

Institute of Microbiology of the ASCR, v. v. i.

Prague, 2017

Prohlášení:
Prohlašuji, že jsem závěrečnou práci zpracovala samostatně a že jsem uvedla všechny použité informační zdroje a literaturu. Tato práce ani její podstatná část nebyla předložena k získání jiného nebo stejného akademického titulu.

Declaration:

I hereby certify that I have written this thesis independently and that I have not used other than the cited sources. This thesis has not been submitted for any other degree or purposes.

November 2017, Prague

.....

Mgr. Vladislava Hronová

Acknowledgements

My biggest thanks belong to my supervisor Leoš Valášek, who is not only the great leader of our team but also a very inspiring personality. I would like to thank him for his support, help and guidance throughout my PhD study.

Next, I would like to thank to all members of our Laboratory of Regulation of Gene Expression for all their help and support throughout my stay in this laboratory, for their kindness and friendly approach, and for making the working environment in our lab very pleasant.

I would also like to thank my colleagues from the Academy of Science campus in Prague-Krč, particularly to all attendees of our regular Thursday/Friday seminars for all their advice, helpful suggestions and kind approach.

Finally, I thank very much to my family, namely to my mum and my husband, whose patience and great support enabled me to proceed with my scientific career and conduct this thesis.

List of abbreviations

3' UTR	3' untranslated region
40S subunit	eukaryotic small ribosomal subunit
43S PIC	preinitiation complex comprising 40S subunit, TC, eIF1, eIF1A, eIF3 and eIF5
48S PIC	preinitiation complex comprising the 43 PIC bound to mRNA
4E-BP	eIF4E-binding protein
5' UTR	5' untranslated region
60S subunit	eukaryotic large ribosomal subunit
80S ribosome	eukaryotic ribosome comprising both small and large ribosomal subunit
a/Tif32	yeast ortholog of eIF3a
a/tif32-Δ8	truncation eliminating the first 200 amino acids of the a/Tif32 subunit
A-site	aminoacyl-site of ribosome
ATF4	activating transcription factor 4
ATF5	activating transcription factor 5
ATP	adenosine triphosphate
AUG	adenine-uracil-guanine; start codon
b/Prt1	yeast ortholog of eIF3b
bp	base pair
c/Nip1	yeast ortholog of eIF3c
CDS	coding sequence
CTD	C-terminal domain
DENR-MCT-1	density regulated protein-multiple copies in T-cell lymphoma-1
eIF	eukaryotic initiation factor
eIF2α-P	phosphorylated eIF2
ER	endoplasmatic reticulum
g/Tif35	yeast ortholog of eIF3g
GADD34	growth arrest and DNA damage-inducible protein
GCN2	general control nonderepressible 2; a eIF2alpha kinase
GCN4	general control nonderepressible 4; an amino acid biosynthesis regulatory protein
GDP	guanosine diphosphate
GEF	guanine-nucleotide exchange factor
GTI	general translation initiation
GTP	guanosine triphosphate
GTPase	enzyme that can bind and hydrolyze guanosine triphosphate (GTP)
HEK	human embryonic kidney cells
HeLa	Henrietta Lacks cells
HLD	HCR1-like domain
HRI	haem regulated inhibitor; a eIF2alpha kinase
i/Tif34	yeast ortholog of eIF3i
IRES	internal ribosome entry site
ISR	integrated stress response
j/Hcr1	yeast ortholog of eIF3j
m7G-cap	7-methylguanosine cap
Met-tRNAi	methionyl initiator methionine tRNA; initiator tRNA
mTOR	mammalian target of rapamycin
NMD	nonsense-mediated mRNA decay
nt(s)	nucleotide(s)
NTD	N-terminal domain
PABP	poly(A)-binding protein
PCI	proteasome, COP9 signalosome and eIF3; a type of domain
PERK	protein kinase-like endoplasmic reticulum kinase
Pi	inorganic phosphate
PKR	double-stranded RNA (dsRNA)-activated protein kinase

PP1	protein phosphatase 1
P-site	peptidyl-site of ribosome
REI	reinitiation
RPE	reinitiation-promoting element
RPS	small ribosomal protein
RRM	RNA recognition motif
S. cerevisiae	*Saccharomyces cerevisiae*
Ser-51	serine at amino acid position 51
STE	stabilizer element
TC	ternary complex
uORF	upstream open reading frame
YAP1	yeast AP-1-like transcription factor

Abstract

Translation initiation is a multistep process resulting in the formation of the elongation-competent 80S ribosome at the AUG start codon of the mRNA to be translated into a polypeptide chain. This process is orchestrated by numerous proteins called eukaryotic initiation factors (eIFs), out of which the most multitasking one is the eukaryotic initiation factor 3 (eIF3). The main focus of our laboratory aims at the complex characterization of the multisubunit protein eIF3 and the mechanisms of its contribution to various steps of translation initiation. Besides this, we also study one of the gene-specific translational control mechanisms called reinitiation which was, at least in yeast, also shown to be promoted by eIF3.

Here I show that the N-terminal domain (NTD) of the largest subunit of yeast eIF3, a/Tif32, plays an important role not only in anchoring the eIF3 complex to the 40S small ribosomal subunit but it also critically contributes to mRNA recruitment to the 43S preinitiation complexes *in vivo*. The mRNA stabilization role of the a/Tif32-NTD at the mRNA exit channel of the 40S subunit was further confirmed in our following study by biophysical experiments. There, using *in vivo* approaches, we also demonstrated that mRNAs with longer 5´UTRs are more dependent on the stabilization role of the a/Tif32-NTD than those containing short 5´UTRs.

In other studies, where I turned my attention to the mechanism of reinitiation, we revealed novel *cis*-determinants contributing to the efficiency of reinitiation on the yeast model *GCN4* mRNA and, importantly, brought the first insights into this gene-specific regulatory mechanism in human cells on the model human *ATF4* mRNA. In detail, we discovered that similarly to the yeast *GCN4* mRNA, the reinitiation-permissive upstream ORF1 (uORF1) of *ATF4* is also surrounded by sequences that contribute to high reinitiation efficiency that this uORF allows. Moreover, we computationally predicted that the sequence immediately preceding uORF1 of *ATF4* probably folds into a specific secondary structure that seems to be conserved among mammals. Computationally designed mutations disrupting this structure obliterated the reinitiation potential of uORF1 suggesting that formation of this secondary structure critically contributes to the yet-to-be-described molecular mechanism underlying reinitiation in humans. Finally, we also demonstrated that in analogy with the reinitiation mechanism in yeasts, reinitiation in humans is also promoted by eIF3; only the contributing subunit is not eIF3a/Tif32, but eIF3h.

Thus, this PhD thesis contributed not only to our understanding of basic principles of general translation initiation in eukaryotes but also shed new light onto the molecular mechanism of reinitiation in human cells, revealing that many mechanistic aspects of this process are conserved both in higher and lower eukaryotes.

Abstrakt

Iniciace translace představuje mnohastupňový proces, který zajišťuje sestavení 80S ribosomu na AUG start kodonu molekuly mRNA, jež má být přeložena do polypeptidového řetězce. Správný průběh tohoto procesu je řízen mnoha eukaryotickými iniciačními faktory (eIFs), z nichž nejdůležitějším je eukaryotický iniciační faktor 3 (eIF3). Hlavním cílem naší laboratoře je co nejpodrobněji popsat proteinový komplex eIF3 a také způsoby, jakými tento faktor přispívá k jednotlivým krokům procesu iniciace translace. Kromě toho též zkoumáme jeden z genově specifických kontrolních mechanismů translace zvaný reiniciace, který je, alespoň u kvasinek, umožňován právě faktorem eIF3.

V této práci popisuji, že N-terminální doména (NTD) jedné z největších podjednotek kvasinkového eIF3, označované jako a/Tif32, hraje důležitou úlohu nejen ve vazbě eIF3 k 40S ribozomální podjednotce, ale taktéž významně přispívá k nasedání mRNA na 43S preiniciační komplexy *in vivo*. Stabilizační role N-terminální domény podjednotky a/Tif32 byla ověřena též v naší následující studii, a to biofyzikálními experimenty. Pomocí dalších *in vivo* přístupů jsme v této práci též dokázali, že pro mRNA s delšími 5´nepřekládanými oblastmi je stabilizační role a/Tif32-NTD důležitější než pro mRNA s krátkými 5´nepřekládanými oblastmi.

V následujících studiích, kde se zaměřuji na popis mechanismu reiniciace, jsme odhalili dosud neznámé *cis*-elementy důležité pro správné fungování reiniciace na kvasinkové modelové mRNA *GCN4*. Náš výzkum též přinesl první důležité detaily o tomto kontrolním mechanismu v lidských buňkách, a to za použití lidské modelové mRNA *ATF4.* Zjistili jsme například, že uORF1 z *ATF4*, jenž je elementem umožňujícím reiniciaci, je obklopen sekvencemi, které jsou důležité pro vysokou efektivitu reiniciace na tomto uORF. Podobně je tomu i v případě uORF1 z *GCN4,* který též umožňuje reiniciaci na této mRNA. Z našich *in silico* analýz vyplynulo, že nukleotidová sekvence předcházející uORF1 z *ATF4* pravděpodobně tvoří konkrétní sekundární strukturu, jež se zdá být konzervována mezi savci. Na základě počítačových analýz jsme vytvořili mutace, které narušily tuto strukturu, a po jejich testování jsme zjistili, že skutečně snižují schopnost uORF1 z *ATF4* podporovat reiniciaci. To nasvědčuje tomu, že přítomnost této struktury je pro efektivitu reiniciace v savčích buňkách důležitá. Na závěr jsme prokázali, že stejně jako je tomu v případě kvasinek, i reiniciace v savcích je umožňována faktorem eIF3, avšak konkrétní zúčastněnou podjednotkou není v tomto případě eIF3a/Tif32, ale eIF3h.

Tato Ph.D. práce tedy přispívá nejen k obecnému porozumění základním procesům iniciace translace, ale osvětluje též molekulární mechanismus reiniciace v lidských buňkách a odhaluje tak, že mnoho aspektů tohoto procesu zůstalo konzervováno mezi nižšími a vyššími eukaryoty.

Contents

1. Introduction 8

2. Literature review 9
- **2.1 Canonical translation initiation** 9
- **2.2 Regulation of translation initiation** 13
  - **2.2.1 Upstream ORFs (uORFs)** 13
  - **2.2.2 uORFs mediating translation reinitiation (REI)** 15
- **2.3 *GCN4* mRNA as a model of translational control *via* REI** 16
- **2.4 ATF4 (activating transcription factor 4)** 19
  - **2.4.1 ATF4 as an important player of the integrated stress response (ISR)** 19
  - **2.4.2 Upregulation of ATF4 in stress** 20
  - **2.4.3 Translational upregulation *via* REI on *ATF4* mRNA** 21

3. Aims of the study 23

4. Material and methods 24

5. List of publications 25

6. Summary of presented publications 28

7. Discussion 31
- **7.1 Role of the eIF3a/Tif32-NTD in canonical translation initiation and reinitiation** 31
- **7.2 Differences between yeast and human reinitiation** 34
- **7.3 Novel insights into human *ATF4* translational control** 35

Conclusions 39

References 40

1. Introduction

Translation is a fundamental biological process ensuring the production of proteins indispensable for every single cell's life. It contributes to important cellular processes, such as development or memory formation. Importantly, translational control of already existing mRNAs allows more rapid changes in gene expression in comparison to e.g. transcription, and thus it governs not only more permanent changes in cell physiology, but also cell homeostasis, environmental response etc. Hence, it is not surprising that it has to be perfectly regulated and that any improper translational control may lead to various human diseases, such as diabetes, cancer or neurodegenerative diseases (Sonenberg and Hinnebusch 2009). Therefore, complex understanding of the processes of translation and its regulation helps us to understand not only the general mechanisms underlying these processes but also the mechanisms underlying various human disorders.

Translation of the mRNA-encoded information into a protein is a multistep process consisting of initiation, elongation, termination and ribosomal recycling (see **Figure 1**). However, the most of its regulation occurs within its first phase – translation initiation. This step ensures a coordinated assembly of 80S ribosome, mRNA and initiator tRNA at an AUG start codon of a given mRNA molecule, which can be subsequently translated into a polypeptide chain. This delicate process is orchestrated by many effector proteins called eukaryotic initiation factors (eIFs) helping to ensure its errorless course.

The aim of my post-graduate study was to gain more insights into the process of translational initiation and its regulation. The major focus of my PhD thesis aimed at a special gene-specific translational control mechanism called reinitiation. This mechanism is known to exploit so-called short upstream open reading frames (uORFs) present in some mRNAs; however, its molecular mechanism has never been investigated in mammalian cells so far. My thesis also dealt with a general mechanism of the mRNA recruitment to the 43S PICs in eukaryotic cells, representing one of the least understood initiation steps of all. Interestingly, both the processes were shown to be promoted by the eukaryotic initiation factor 3 (eIF3).

2. Literature review

2.1 Canonical translation initiation

Initiation of translation in eukaryotes is a very sophisticated process ensuring timely and spatially coordinated assembly of the elongation-competent 80S ribosome at the AUG start codon of the mRNA to be translated into a polypeptide chain (see **Figure 1**). The formation of the 80S ribosome from 40S small ribosomal subunit, 60S large ribosomal subunit, methionyl-initiator tRNA (Met-$tRNA_i^{Met}$) and mRNA is precisely orchestrated by numerous proteins called eukaryotic initiation factors (eIFs). Notably, almost all steps of translation initiation are mediated or aided by eukaryotic initiation factor 3 (eIF3). Initiation of translation of the vast majority of eukaryotic mRNAs is mediated *via* a canonical mechanism called General Translation Initiation (GTI) that can be divided into several subsequent steps described below.

The very first step, which is also subject to a very tight regulation and represents one of the two major targets of the general translational control (Sonenberg and Hinnebusch 2009), is the formation of the so-called ternary complex (TC). The TC consists of the initiation factor eIF2, GTP and methionyl-initiator Met-$tRNA_i^{Met}$. The key step of the TC formation is the replacement of the eIF2-bound GDP, generated in the previous translation cycle, with a fresh GTP as only GTP-bound eIF2 can stably bind Met-$tRNA_i^{Met}$ to form a functional TC. This process is executed by the guanine-nucleotide exchange factor (GEF) eIF2B. Importantly, as TC enables the translational machinery to initiate the protein synthesis at an AUG start codon, the availability of TC greatly influences the general rate of protein synthesis (see also further).

The ready-to-go TC is subsequently loaded onto the 40S small ribosomal subunit with the help of eIF3, eIF1, eIF1A and eIF5, producing the so-called 43S pre-initiation complex (PIC) (reviewed in Hinnebusch and Lorsch 2012). eIF1 and eIF1A help to stabilize a specific ("open") conformation of the 40S head relative to its body, which enables the loading of the incoming mRNA. The opening of the mRNA binding channel in the 40S subunit requires certain structural changes, for example dissolving the latch formed by the helices 18 and 34 of 18S rRNA and establishment of a new interaction between RPS3 and helix 16 of 18S rRNA (Passmore et al. 2007; Llácer et al. 2015)

The 43S PIC is then recruited to the capped 5' terminus of mRNA, yielding the so-called 48S PIC. This is facilitated by the poly(A)-binding protein (PABP), eIF3 and eIF4F complex, which consists of the 7mG-cap-binding protein eIF4E, the DEAD box ATP-dependent RNA-helicase eIF4A, and eIF4G. The latter factor represents a scaffold protein which contains binding domains for (i) eIF4E and (ii) poly(A)-binding protein (PABP) in its N-terminus, and for (iii) eIF4A and (iv) eIF3 (only in mammals; see below) in its central and C-terminal regions (Imataka, Gradi, and Sonenberg 1998; Imataka and Sonenberg 1997; Morino et al. 2000; Villa et al. 2013).

These interactions enable eIF4G to bridge the 7mG-cap (bound by eIF4E) and the poly(A) tail of mRNA (bound by PABP) to form the so-called "closed-loop" mRNA structure (Wells et al. 1998). This probably serves as the means to easily recycle the components of translational machinery for a new round of initiation on the same mRNA molecule.

Notably, although this step serves as one of another crucial target for general translational control (Sonenberg and Hinnebusch 2009), it is one of the least understood steps from the translation initiation pathway. For example, the molecular mechanism of how the mRNA enters the mRNA-binding channel of the 40S subunit (i.e. whether by threading through the entire channel starting from its entrance, or by direct placement of the 7mG-cap-proximal mRNA segment into the mRNA-binding cleft) is still unknown. Moreover, it seems that this step slightly differs in lower and higher eukaryotes in terms of the participation of several eukaryotic factors: Whereas in mammals it seems that it is the eIF3 which mediates the connection between the eIF4F-mRNA and the 43S PIC, in *S. cerevisiae*, a direct eIF3-eIF4G interaction has never been detected and the yeast eIF4G does not even seem to contain the eIF3-binding domain (LeFebvre et al. 2006). Therefore, it was proposed that the contact between eIF4G and eIF3 within the yeast 48S PIC might be mediated by eIF5 (Asano et al. 2001).

Importantly, previous reports indicated that eIF3 dramatically increases the rate of mRNA recruitment both *in vitro* (Mitchell et al. 2010) and *in vivo* (Jivotovskaya et al. 2006). Moreover, yeast eIF3 was suggested to be more critical factor for mRNA recruitment than eIF4F and eIF4B (Mitchell et al. 2010). However, unambiguous *in vivo* evidence supporting a direct role of eIF3 in mRNA recruitment to the 43S PICs was lacking. Therefore, one of the aims of my thesis was to investigate the contribution of yeast eIF3 and its particular subunits to this critical initiation step.

In the next step - selection of the start codon - eukaryotic 48S PICs have to search the 5' untranslated region (5'UTR) of a given mRNA for an AUG start codon by a progressive movement called scanning. During this process, the small ribosomal subunit inspects the successive triplets on mRNA as they enter the P-site until the perfect complementarity to the anticodon of Met-tRNAi^{Met} is found (Kozak 1978). The scanning process is accompanied by the unwinding of mRNA secondary structures by helicases eIF4A and eIF4H, and a stimulatory protein eIF4B (Pestova and Kolupaeva 2002). Recently it was proposed that in higher eukaryotes, an additional helicase, DHX29, closely cooperates with eIF3 to promote scanning on highly structured mRNAs to ensure the stringency of AUG recognition (Pisareva and Pisarev 2016). During the mRNA scanning by the 48S PIC, eIF2-bound GTP is partially hydrolyzed by eIF5; however, eIF1 prevents the inorganic phosphate ion (P_i) to be totally released until the authentic AUG codon is found (Algire, Maag, and Lorsch 2005). Selection of an AUG triplet as the start codon is determined by the "strength" of adjacent nucleotide sequence called Kozak consensus sequence (Kozak 1986). Optimal Kozak sequence in mammals is gcc(A/G)ccAUGG (the A of the AUG codon is designated +1) and any deviations, especially at -3 and +4 positions, lead to decrease of translation initiation at this start

codon. In budding yeast the optimal context is typically aAaAaAAUGTCt (the most important positions are in capitals) (Hamilton, Watanabe, and de Boer 1987). The recognition of the authentic start codon triggers the dissociation of eIF1 (Cheung et al. 2007) and the irreversible release of P_i, which results in a conformational switch of the 48S PIC to the scanning-arrested ("closed") form, stabilized by a newly established interaction between eIF1A and eIF5 (Cheung et al. 2007; Maag, Algire, and Lorsch 2006; Hussain et al. 2014). These events help to fully accommodate the initiator Met-$tRNA_i^{Met}$ in the P-site of the 40S ribosomal subunit and serve as the decisive step stalling the entire machinery at this AUG start codon.

To finalize the initiation phase of translation, the scanning-arrested 48S PIC is then joined to the large ribosomal 60S subunit with the help of GTP-bound eIF5B (Pestova et al. 2000). Subunit joining triggers the ejection of all remaining eIFs occupying the intersubunit interface with the exception of eIF1A and eIF3 and most likely also eIF4F, which are localized at the opposite, solvent-exposed side of the 40S subunit (Poyry and Kaminski 2004; Mohammad et al. 2017). Finally, eIF5B-driven GTP hydrolysis stimulated by the GTPase activation center (GAC) of the 60S ribosomal subunit results in the release of eIF1A and eIF5B, leaving behind the elongation-competent 80S ribosome ready to accept an appropriate aminoacyl-tRNA into the ribosomal A-site and synthesize the first peptide bond (Shin et al. 2002). Importantly, for yeast eIF3 it was now shown *in vivo* that it stays bound to the elongating 80S ribosome for several elongation cycles, which has a great importance for its reinitiation-promoting abilities (see the Chapter 2.3).

As indicated above, the eukaryotic initiation factor eIF3 has been shown to stimulate nearly every step of translation initiation (see **Figure 1**). Moreover, eIF3 participates also in translation termination and post-termination ribosomal recycling (Pisarev, Hellen, and Pestova 2007; Beznosková et al. 2013), stop codon readthrough (Beznosková et al. 2015), nonsense-mediated decay (NMD) pathway (Isken et al. 2008), and it was shown to play the critical role also in a gene-specific translational control mechanism called reinitiation in yeasts, plants and mammals (Szamecz et al. 2008; Munzarová et al. 2011; Mohammad et al. 2017; Park et al. 2001; Pöyry et al. 2007; this PhD thesis). Such an intriguing multifunctionality of eIF3 most probably results from its huge complexity - in budding yeast, eIF3 comprises of five core essential subunits (a/Tif32, b/Prt1, c/Nip1, i/Tif34 and g/Tif35) and one eIF3-associated factor, j/Hcr1. All these subunits have corresponding orthologs in even more complex mammalian eIF3, which contains seven additional non-conserved subunits (eIF3d, e, f, h, k, l and m) plus one eIF3-associated factor, eIF3j (reviewed in Valášek et al. 2017). Based on recent structural data as well as numerous biochemical reports it has been well established that the major eIF3 part both in yeast and humans resides on the solvent-exposed side of the 40S ribosomal subunit, with several of its subunits projecting into the ribosomal interphase. Thus, eIF3 "embraces" the small ribosomal subunit from both sides which gives it the ability to control most, if not all translation initiation steps (Hashem et al. 2013; Erzberger et al. 2014; des Georges et al. 2015; Aylett et al. 2015; Llácer et al. 2015).

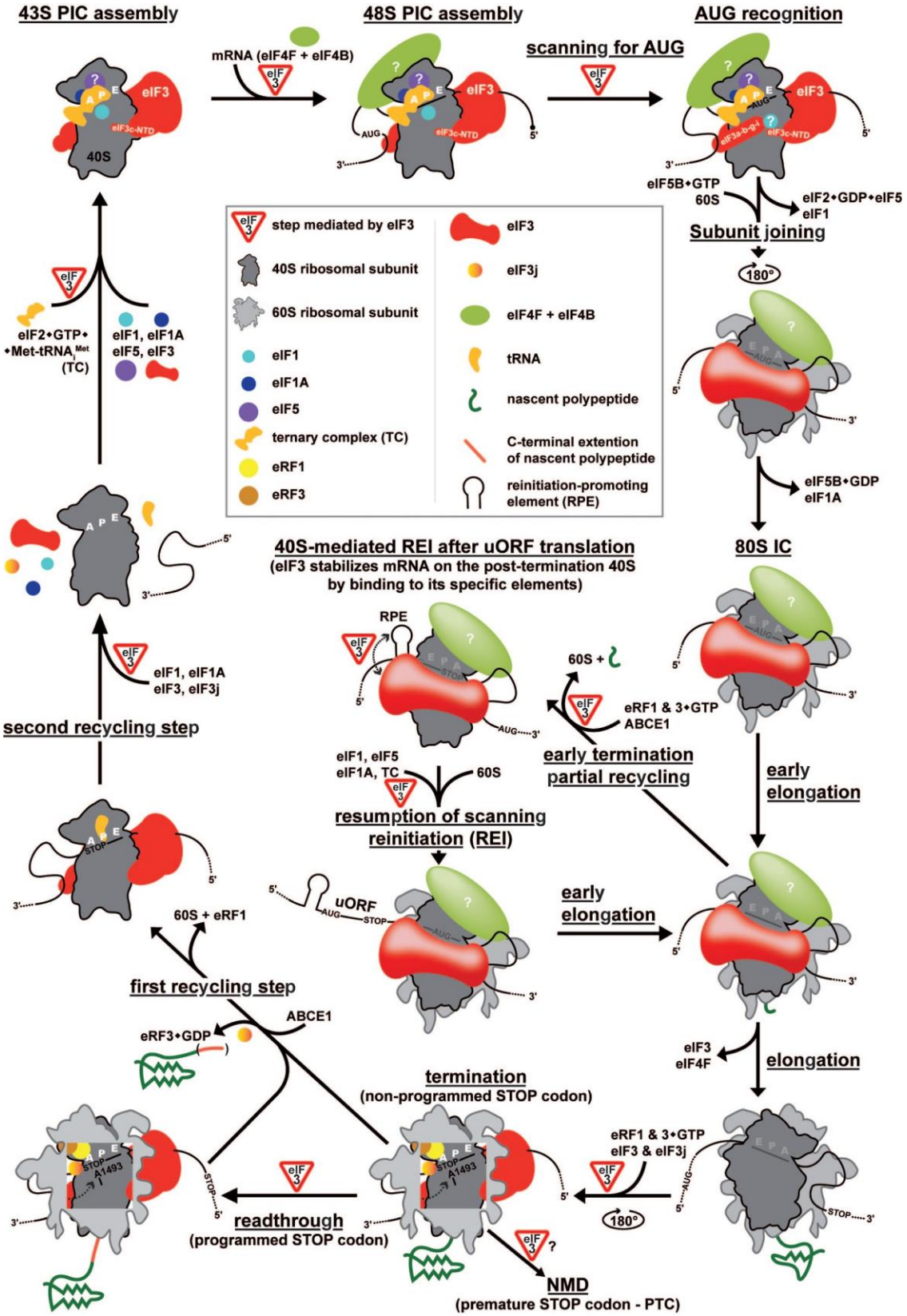

Figure 1. Schematics of the entire translational initiation cycle with 'detours' for reinitiation, programmed stop codon readthrough and the nonsense-mediated decay pathway, highlighting the role of eIF3 at the individual steps. For details, please see the main text. Adapted from Valášek et al. 2017.

2.2 Regulation of translation initiation

As indicated above, translation is an extremely energy-dependent process. Therefore it has to be tightly regulated to avoid wasting material and energy when the synthesis of new proteins is not desirable due to e.g. limited sources of nutrients. In eukaryotic cells, there are two major mechanisms of regulation of canonical translation initiation. The first one, affecting all scanning-dependent initiation events, is called general regulation and it is mediated *via* specific modifications of selected eIFs (such as eIF2-TC or eIF4F, as mentioned above). The other one is the mRNA-specific regulation that causes upregulation, silencing or degradation of only certain mRNAs in response to various stimuli. This type is mediated, for example, *via* sequence-specific RNA-binding proteins or microRNAs. This also includes the regulation by the structure and/or "composition" of the mRNA itself, for example, by presence of so-called upstream ORFs (uORFs) (reviewed in Sonenberg and Hinnebusch 2009; see also the next chapter).

One of the best-characterized mechanisms of the first type, general translational regulation, is the phosphorylation of Ser51 on the alpha (α) subunit of eIF2 employed during various stress conditions. In mammals, four eIF2α kinases have been characterized: HRI (a haem-regulated kinase that occurs presumably exclusively in erythroid cells), PKR (a kinase activated by double-stranded RNAs, typically during antiviral response), PERK (a kinase responding endoplasmic reticulum (ER) stress) and GCN2 (a kinase activated by amino acid starvation; reviewed in Pakos-Zebrucka et al. 2016). Notably, budding yeasts possess only one eIF2α kinase - GCN2. Irrespective of the type of stress, all of these kinases have one common target after they have been activated - they phosphorylate the α subunit of eIF2 on Ser51. Phosphorylation of eIF2 impedes recycling of GDP-bound eIF2 to its active GTP-bound form because this modification converts the eIF2 from a substrate to a competitive inhibitor of eIF2B, the GEF of eIF2 (Rowlands, Panniers, and Henshaw 1988). Importantly, eIF2B is present only in a limited amount in cells. As a consequence, phosphorylation of even a small percentage of eIF2 results in a complete sequestration of eIF2B leading to a rapid decrease of available TC and inhibition of general protein synthesis. In fact, TC levels affect also certain types of mRNA-specific regulation such as reinitiation, which will be described in the next chapters.

2.2.1 Upstream ORFs (uORFs)

As pointed out above, one of the potent gene-specific regulators of protein synthesis are the upstream open reading frames (uORFs). Generally, eukaryotic mRNAs are considered to be monocistronic as the majority of them contains only one main ORF usually flanked by the sequences referred to as the 5' and 3' untranslated regions (5' and 3' UTR). However, it has been shown that eukaryotic mRNAs´ 5' UTRs might contain additional short upstream ORFs, i.e. upstream elements starting with the AUG start codon followed by at least one additional coding triplet and an in-frame termination codon (UAA, UAG, UGA). These uORFs may serve as an

alternative translation initiation sites and thus influence the expression of the main coding sequence. In fact, the latest reports indicate that uORFs are surprisingly widespread among various organisms and they indeed contribute to gene expression – in yeasts, 13% of mRNAs contain short uORFs, and in humans and mice this number reaches nearly 50% (Nagalakshmi et al. 2008; Calvo, Pagliarini, and Mootha 2009; Lee et al. 2012; Johnstone, Bazzini, and Giraldez 2016). Notably, the presence of multiple uORFs seems to be enriched in certain subgroups of mRNAs, including genes coding for growth factors, transcription factors and other proto-oncogenes (Kozak 1987; Davuluri 2000), and uORF dysregulation has already been implicated in a variety of human diseases such as emergence of atherosclerosis in diabetics (Griffin et al. 2001; Barbosa, Peixeiro, and Romão 2013). The uORF-containing genes are also prominent in key cellular processes and functional classes, such as stress response (Lawless et al. 2009), meiosis (Brar et al. 2012), circadian rhythms (Janich et al. 2015) or tyrosine kinase activity (Wethmar et al. 2016). In fact, it is anticipated that with the rising number of available nucleotide sequence databases and the improvement of 5´UTR mapping, the overall number of annotated uORFs will rise.

Notably, uORFs can influence the expression of the downstream coding sequence by at least five different ways - i) general inhibition of the main ORF translation, ii) leaky scanning, iii) ribosome stalling, iv) nonsense-mediated mRNA decay (NMD) and v) reinitiation. Owing to the fact that the start codon in eukaryotes is selected by the scanning mechanism from the 5´end of mRNA and that these elements are situated upstream of the main coding sequence, uORFs are generally considered to serve as a barrier severely reducing the expression of the main gene (Kozak 1999). Indeed, a global concurrent analysis of mammalian transcriptomes and proteomes revealed that the occurrence of uORFs in mRNAs closely correlates with significantly reduced protein expression of downstream ORFs carried by these mRNAs (Calvo, Pagliarini, and Mootha 2009).

However, not all uORFs impose such a negative effect on the expression of the main ORF as the degree of reduction of the main ORF expression by this uORF is determined by its Kozak context as mentioned earlier. Intuitively, uORFs with poor initiation context are usually skipped by the 48S PICs *via* so-called leaky scanning, which mitigates their negative impact on general translation initiation (Vivier, Sollitti, and Pretorius 1999). Recognition of such uORF can be also dependent on actual cell conditions, which may alter the degree of programmed leaky scanning (Palam, Baird, and Wek 2011). So far, many examples of uORFs regulated by leaky scanning have been described (Palam, Baird, and Wek 2011; Lee, Cevallos, and Jan 2009). It is worth mentioning that degree of leaky scanning is also affected by factors eIF1 and eIF5 in an antagonistic manner, whose mRNAs are also translated by a very sophisticated mechanism employing this uORF-mediated regulatory mechanism (Ivanov et al. 2010; Loughran et al. 2012; Fijalkowska et al. 2017)

Another group of uORFs are those who affect downstream translation through their ability to mediate ribosome stalling (i.e. the translational arrest) at coding or termination codons (Wang,

Gaba and Sachs 1999). This is usually the result of the action of the nascent peptide encoded by this uORF. Such a stall at uORF termination codon prevents the ribosomes scanning from the 5´cap from reaching another downstream start site; moreover, prolonged ribosome stalling can also induce so-called nonsense-mediated mRNA decay (NMD). Even though a limited number of eukaryotic uORFs encoding arrest peptides have been reported, their number is still rising (Wei, Wu, and Sachs 2012; Sidrauski et al. 2015; Hayashi et al. 2017)

2.2.2 uORFs mediating translation reinitiation (REI)

The last group of uORFs are those that permit the small ribosomal subunit to stay mRNA-bound post-termination and resume scanning for efficient reinitiation (REI) downstream. This is enabled by an incomplete ribosome recycling where only the large ribosomal subunit is ejected after the termination, whereas the small ribosomal subunit is stabilized on the mRNA. It has been shown that the degree of permissiveness of a given uORF for efficient REI is determined by several factors: i) *cis*–acting mRNA features, which will be thoroughly described in the next chapter focused on the mechanism of REI on yeast *GCN4* mRNA, ii) the time required for the uORF translation, which is determined by the relative length of a short uORF and the translation elongation rates, and iii) various initiation factors. The last two requirements are united in the idea that eIFs important for promoting REI remain transiently associated with the elongating 80S ribosome, and the longer time the uORF is translated, the higher is the likelihood that these factors will be lost (Kozak 2001). Accordingly, REI is most efficient after short uORFs translation and its efficiency declines as the uORF is lengthened (Kozak 2001); studies indicate that uORFs longer than 10 and 30 codons in yeast and mammals, respectively, are not REI-permissive anymore (Rajkowitsch et al. 2004; Calvo, Pagliarini, and Mootha 2009). Concerning the factors necessary for efficient REI, it was shown that in yeast, eIF3 is indispensable for efficient REI (Szamecz et al. 2008; Munzarová et al. 2011; Mohammad et al. 2017; see also further). The other eIFs implicated in promoting efficient REI in mammalian cells are eIF4A and eIF4G (Poyry and Kaminski 2004; Skabkin, 2014), but the mechanism of their operation is not known yet. Finally, REI efficiency is influenced also by iv) the intercistronic distance between the uORF and the main ORF, and the presence of stable secondary structures within it (Dever 2002). This reflects the fact that the post-termination 40S traversing downstream of the uORF stop codon requires certain time for recruitment of a new TC to be able to decode the next AUG start codon. Based on Kozak (1987), the optimal distance ensuring efficient REI in mammals is 80 nts and more. Thanks to this, REI can be delicately regulated by manipulating the TC availability in cell *via* the eIF2α phosphorylation by specific protein kinases mentioned above. Thus, though the reduction in the TC availability decreases the rate of general proteosynthesis, it can paradoxically stimulate the translation of mRNAs translated *via* REI mechanism, such as mRNAs of yeast *GCN4* and its mammalian ortholog *ATF4*. The just to be described molecular mechanism of reinitiation and its

regulation *via* the levels of TC was studied mostly on the model *GCN4* mRNA from *S. cerevisiae* (Hinnebusch 2005).

It is worth mentioning, that besides *GCN4* and *ATF4* mRNAs, several more mRNAs has been experimentally proven to contain REI-permissive uORFs so far. These include mRNAs of transcription factors *YAP1* in yeast (Vilela et al. 1998), and *ATF5* and *C/EBP* in mammals (Zhou et al. 2008; Calkhoven, Müller, and Leutz 2000), together with *CD36* mRNA encoding a scavenger receptor in macrophages (Griffin et al. 2001). However, the knowledge on their regulation *via* their REI-promoting uORFs is still rudimentary.

2.3 *GCN4* mRNA as a model of translational control *via* REI

GCN4 gene encodes a master basic leucine zipper (bZIP) transcription factor that activates nearly 600 stress-related genes in response to amino acid limitation (Hinnebusch 2005). The *GCN4* mRNA contains four upstream ORFs (uORF1-4) whose interplay ensures an intricate fail-safe mechanism of the *GCN4* expression (Gunišová and Valášek 2014; see also **Figure 2**). All of these uORFs are two or three codons long and very efficiently translated; however, only the first two of them (uORF1 and uORF2) support efficient REI (Gunišová and Valášek 2014). Independent of amino acid availability, most ribosomes translate uORF1 (or immediately following uORF2, if uORF1 is skipped by leaky scanning). Both of these uORFs allow the retention of the 40S subunit on the mRNA after termination of their translation, and therefore, about a half of the post-termination 40S subunits resumes traversing downstream (Abastado et al. 1991). As soon as they reacquire a new TC, they start scanning and are able to reinitiate on the next AUG. In non-starvation conditions, eIF2-GDP is fast recycled to eIF2-GTP by its GEF eIF2B, resulting in high levels of TC formation. Thus, the post-termination 40S ribosomal subunits traversing downstream from uORF1 or uORF2 reacquire the TC quickly and reinitiate at uORF3 or uORF4, none of which supports efficient REI. The main GCN4 ORF thus remains unexpressed. In starvation conditions, however, uncharged tRNAs accumulate and activate the kinase GCN2 that phosphorylates Ser51 of the α subunit of eIF2 (Dong et al. 2000). Phosphorylation of eIF2 inhibits the function of the GEF factor eIF2B, as outlined above, which diminishes the production of TCs. As a result, the 40S subunits traversing downstream from uORF1 or uORF2 must travel much longer to reacquire a new TC. This significantly increases the likelihood that the last two REI-non-permissive uORFs are bypassed and that the 40S subunits reinitiate at the AUG of GCN4. Thus, whereas the global protein synthesis is significantly downregulated in these conditions, *GCN4* expression is induced (for the complete model, see **Figure 2**).

The long-lasting effort to characterize the molecular mechanism of reinitiation on yeast *GCN4* mRNA revealed that the high REI competence of uORF1 and uORF2 depends on several *cis*-acting features. One of the two most important ones is the AU-rich motif occurring within the first 12 nts immediately following the uORF1 stop codon (Gunišová et al. 2016), and the other one is represented by the so-called REI-promoting elements (RPEs) with a specific structural

arrangement located in the upstream regions of uORF1 and uORF2 (Munzarová et al. 2011; Gunišová and Valášek 2014). In detail, uORF1 utilizes four RPEs (i.–iv.), whereas uORF2 separately utilizes only a single RPE v. (similar in sequence with the uORF1-specific RPE i.) and, in addition, shares RPE ii. with uORF1. Besides that, it was also shown that the high REI competence of these two *GCN4* uORFs is promoted by the extreme N-terminal domain (NTD) of the a/Tif32 subunit of the eukaryotic initiation factor eIF3 (Szamecz et al. 2008). In particular, there are two separate regions within the a/Tif32-NTD, called Box 6 (amino acid residues 51–60) and 17 (residues 161–170), the mutations of which severely reduce REI permissiveness of both uORFs (Munzarová et al. 2011). Genetic epistatic experiments additionally revealed that RPE i. and iv. of uORF1 and RPE v. of uORF2 cooperate with both a/Tif32-NTD Boxes to promote efficient REI (Munzarová et al. 2011; Gunišová and Valášek 2014). Importantly, the a/Tif32-NTD is located on the 40S subunit next to the mRNA exit channel (Aylett et al. 2015), where it could theoretically come in a direct contact with these RPEs that, upon termination on uORF1 or uORF2 stop codons, have already emerged from the exit pore and became solvent-exposed. However, more experiments are necessary to reveal whether the cooperation between the a/Tif32-NTD Boxes and RPEs is based on their direct or just a functional interaction. (RPEs ii. and iii. operate in the eIF3-independent manner and the molecular mechanism of their action is unknown).

Collectively, these findings led to a hypothesis that while the eIF3-bound 40S ribosomal subunits scans through the region upstream of uORF1 (or uORF2) and subsequently translates it, the RPEs, emerging from the mRNA exit channel of the ribosome, progressively fold into a specific secondary structure. Upon termination, eIF3 interacts with the corresponding RPEs to specifically stabilize only the small ribosomal subunit on the uORF1 (or uORF2) stop codon. Thanks to the incomplete ribosomal recycling, the post-termination 40S subunit can resume traversing, and upon the acquisition of other essential eIFs reinitiate downstream as was described earlier. This process is a lot less efficient on uORFs 3 and 4 because they lack the RPEs and hence there is no eIF3-mediated 40S-stabilization effect. This theory was recently supported by recent *in vivo* evidence showing that yeast eIF3 indeed remains bound to elongating ribosomes and it interacts with the *cis*–acting elements of REI-permissive uORFs described above to render them highly REI competent (Mohammad et al. 2017).

As mentioned earlier, yeast GCN4 has its functional homolog in mammalian cells, which is called ATF4 (activating transcription factor 4). Importantly, the mRNA of *ATF4* also contains uORFs and was demonstrated to be translationally upregulated *via* reinitiation, similarly to yeast *GCN4* mRNA (Vattem and Wek 2004; Lu, Harding, and Ron 2004). One of the aims of my PhD thesis was to discover if the molecular mechanism of reinitiation is conserved in these two mRNAs. Therefore, in the next chapter I summarize the up-to-date knowledge about ATF4 regulation.

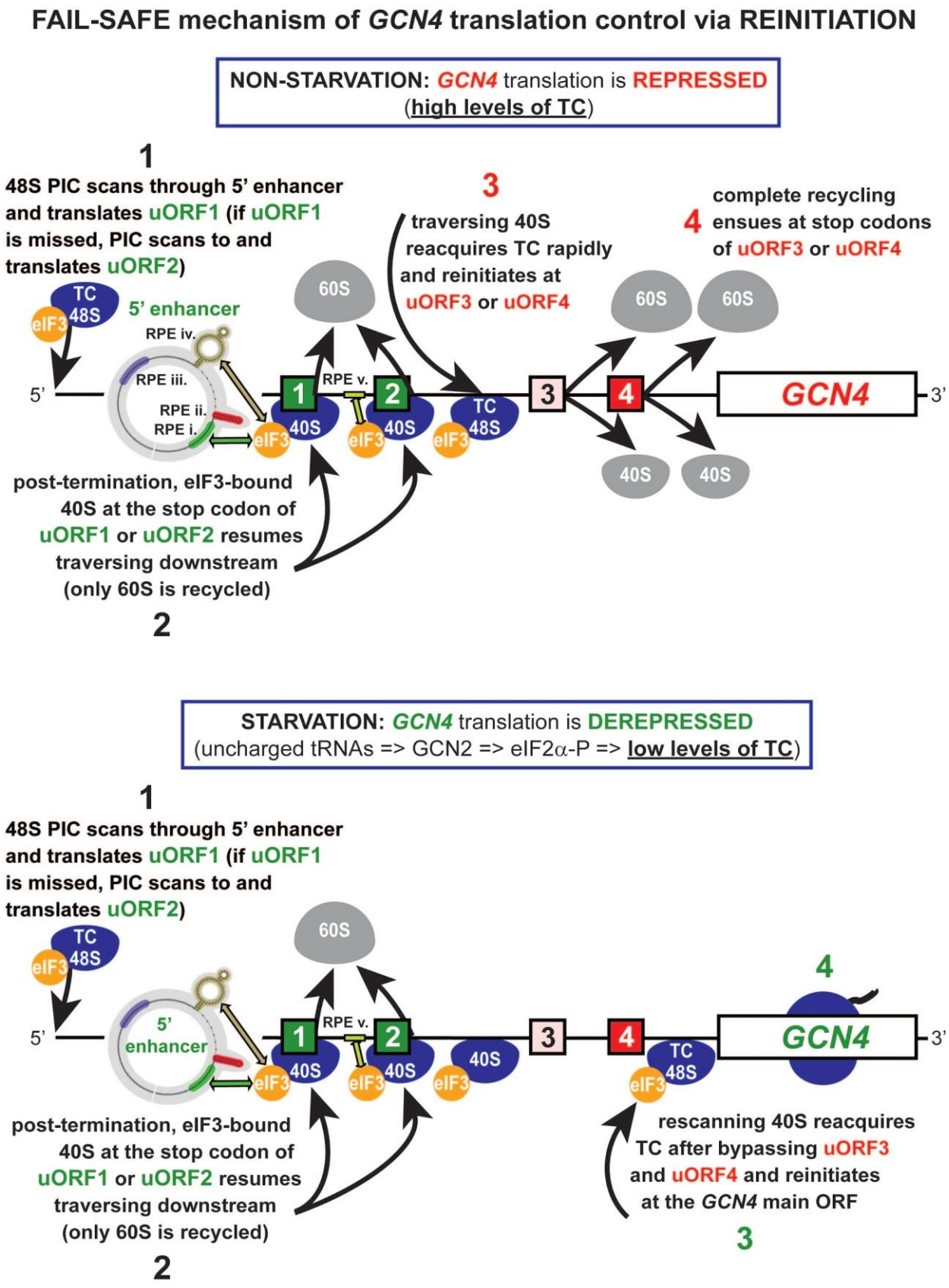

Figure 2. Model for *GCN4* translational control under non-starvation versus starvation conditions mediated *via* reinitiation in response to changing levels of the eIF2-TC. For details please see the main text. Adapted from Gunišová et al. (submitted).

2.4 ATF4 (activating transcription factor 4)

ATF4 is a basic leucine-zipper protein and, similarly to GCN4, it is a very potent transcription factor. It is upregulated in response to various stress conditions such as oxygen deprivation, amino acid deprivation, endoplasmic reticulum stress (ER stress) or oxidative stress (Harding et al. 2003; Rutkowski and Kaufman 2003; Ameri et al. 2004), the conditions collectively leading to so-called integrated stress response (ISR; see also below). Moreover, ATF4 was shown to carry out a variety of other functions - it is crucial for the long-term memory formation and neuronal plasticity (Abel et al. 1998; Pasini et al. 2015), the proliferation of fetal hematopoietic progenitors (Masuoka and Townes 2002), the differentiation of osteoblasts (Yang et al. 2004) or the formation of eye lens fibres (Tanaka et al. 1998). Not surprisingly, it was also observed to be upregulated in various types of cancer, which predetermines it to be a potential therapeutic target in cancer (reviewed in Ameri and Harris 2008).

2.4.1 ATF4 as an important player of the integrated stress response (ISR)

Undoubtedly, one of the key cellular roles of ATF4 is the activation of mammalian stress-response pathway called integrated stress response (ISR). This pathway integrates the signals from four distinct mammalian stress-responsive kinases (see the Chapter 2.2) which all phosphorylate eIF2α subunit. This event leads to the activation of specific mRNAs that enable stress response, with ATF4 as the key transcription factor (reviewed in Pakos-Zebrucka et al. 2016; see also further). The gene expression program activated by the ISR *via* ATF4 optimizes the cellular response to stress and is dependent on the cellular context, as well as on the nature and intensity of the stress stimuli. Therefore, it is not surprising that the effects of ATF4 are very broad and distinct. A comprehensive list of genes affected by ATF4 can be found in (Harding et al. 2003). Importantly, as a sustained eIF2α phosphorylation is lethal to cells in culture (Srivastava, Kumar, and Kaufman 1998), a later form of the stress response includes also a negative feedback loop that attenuates stress-induced signaling and promotes the recovery from translational inhibition. This is achieved by ATF4-mediated induction of GADD34 (growth arrest and DNA damage protein 34), which forms a complex with the catalytic subunit of PP1 (protein phosphatase 1) that specifically promotes dephosphorylation of the eIF2α-P (Ma and Hendershot 2003; Novoa et al. 2001). Interestingly, whereas PP1 is expressed ubiquitously, GADD34 expression is regulated by a similar, although not the same, eIF2α-P-regulated mechanism *via* uORFs as ATF4 (Lee, Cevallos, and Jan 2009). This allows translation to resume, and hence ensures the transient nature of protein synthesis inhibition.

Noteworthy, although the ISR is primarily a pro-survival program, exposure to severe or long-term stress can drive signaling towards the cell death. This was demonstrated by a recent

finding that forced expression of ATF4 and its downstream target CHOP might increase protein synthesis, oxidative stress and cause ATP depletion (Han et al. 2013). Thus, the activity of ATF4 is negatively modulated by several factors. First one is a pseudokinase TRB3, which is also upregulated in stress conditions and it inhibits the transcriptional activation activity of ATF4 (Ord, Meerits, and Ord 2007; Jousse et al. 2007). Furthermore, ATF4 activity was shown to be negatively regulated also by a direct interaction with mitosin/CENP-F, a human nuclear matrix protein ubiquitously expressed in interphase (Zhou et al. 2005).

2.4.2 Upregulation of ATF4 in stress

Importantly, upregulation of ATF4 in stress is not mediated only at translational level *via* the eIF2α phosphorylation and uORF-mediated reinitiation as has been widely assumed, but also the transcriptional and posttranslational regulatory mechanisms were shown to contribute to overall ATF4 upregulation.

First, it was reported that the *ATF4* mRNA levels are elevated in response to amino acid starvation and anoxia (Estes, Stoler, and Anderson 1995; Siu et al. 2002; Zhao et al. 2016); in ER stress, *ATF4* mRNA is upregulated as well, namely by the transcription factors TFEB and TFE3 (Martina et al. 2016). In contrast, however, UV radiation was shown to repress *ATF4* transcription, presumably because forced expression of ATF4 and mainly its target gene CHOP leads to increased sensitivity to UV irradiation (Dey et al. 2010). Next, *ATF4* mRNA was shown to be a direct target of a surveillance pathway called nonsense-mediated mRNA decay (NMD), which primary function is to reduce errors in gene expression by eliminating mRNA transcripts that contain premature stop codons, but it was also shown to modulate the stability of many apparently "normal" mRNAs encoding a functional, full-length protein. Here it was shown that the depletion of UPF1, the main NMD factor, results in *ATF4* mRNA stabilization, higher levels of ATF4 protein and stronger upregulation of ATF4 during chemically induced ER stress and hypoxia (Mendell et al. 2004; Gardner 2008)**.**

Importantly, ATF4 is subject also to posttranslational control. In general, endogenous ATF4 is a very unstable protein with a half-life about 30 min (Lassot et al. 2001). Additionally, two distinct mechanisms have been described that can influence ATF4 protein stability. First one is mediated by the $SCF^{\beta TrCP}$ class of mammalian E3 ubiquitin ligases which, upon phosphorylation of a specific serine residue (Ser219) in ATF4, cause degradation of ATF4 by the proteasome (Lassot et al. 2001). However, ATF4 can be also stabilized by the histone acetyltransferase p300 (HAT p300), which inhibits the ATF4 interaction with previously mentioned $SCF^{\beta TrCP}$ ubiquitin ligase (Lassot et al. 2005). Furthermore, stabilization of ATF4 was also reported in normoxia and hypoxia by prolyl hydroxylase 3-dependent hydroxylation (Koditz et al. 2007). In summary, all these observations suggest that ATF4 upregulation in stress can be induced already at transcriptional level or by posttranslational control mechanisms, and by various means.

2.4.3 Translational upregulation *via* REI on *ATF4* mRNA

The main way of the ATF4 upregulation in stress has been attributed to the translational mechanisms. The basic principle of ATF4 upregulation in stress upon eIF2α phosphorylation is, similarly to GCN4, believed to be mediated by reinitiation after translation of its short uORF1 (Vattem and Wek 2004; Lu, Harding, and Ron 2004). However, mammalian *ATF4* mRNA contains only two uORFs in its 5´leader in contrast to yeast *GCN4* mRNA containing four uORFs (see **Figure 3**). The first one of the two, uORF1, resembles the REI-permissive uORF1 of *GCN4* because it is also composed of only 9 coding nts. Moreover, the distance between its stop codon and AUG of the following uORF2 is in most species 87 nts or close to it, and according to Kozak (1987), the optimal distance ensuring efficient REI in mammals is 80 nts and more. uORF2, on the other hand, is markedly different from *GCN4*'s REI-non-permissive uORFs 3 and 4. Its length (177 nts) prevents it to be even considered as an uORF with some REI-permissive potential and, most importantly, its sequence partially overlaps the main *ATF4* ORF in a different reading frame. Thus, according to the current model, in non-stress conditions, the post-termination 40S subunits that resumed traversing after the translation of uORF1 will rebind TC quickly and reinitiate at uORF2 start codon, and ATF4 will not be translated. However, in stress conditions characterized by a drop in the TC levels in cells, the post-termination 40S subunits that resumed scanning after translation of uORF1 will skip the uORF2 start codon and reinitiate at ATF4 start codon instead (Vattem and Wek 2004; Lu, Harding, and Ron 2004).

Interestingly, reinitiation was shown to mediate the stress-dependent translational upregulation of yet another mammalian transcription factor, ATF5, whose mRNA also contains two uORFs in a constitution very similar to ATF4 (Watatani et al. 2008; Zhou et al. 2008). This transcription factor plays important roles in diverse biological processes such as cell proliferation, stress response and survival (Lenge et al. 2012) or neural progenitor cell differentiation (Angelastro et al. 2005). However, whether the molecular mechanism of its translational upregulation *via* reinitiation is similar to the mechanism of ATF4 yet-to-be described in this thesis, awaits its elucidation.

Given the fact that ATF4 and GCN4 are functional homologues and that their uORFs 1 are both permissive for reinitiation and have even the same length, it was tempting to speculate that *ATF4*'s uORF1 utilizes a REI molecular strategy analogous to that of *GCN4*'s uORF1. To answer to this long-standing question was one of the aims of my thesis, the first results of which have just recently been published (Hronová et al. 2017). Particularly, we strived to reveal whether the *ATF4* uORF1 is, similarly to the *GCN4* uORF1, also flanked by *cis*-acting sequences promoting efficient REI (called RPEs), and whether reinitiation in mammals also requires the factor eIF3 (see **Figure 3**).

Figure 3. Model of *ATF4* mRNA. Prospective REI-promoting elements (RPEs) surrounding uORF1 and their prospective interaction with eIF3 are indicated by question marks. For details please see the main text. Adapted from Gunišová et al. (submitted).

3. Aims of the study

The main aim of this thesis was to investigate the molecular mechanism of reinitiation in human cells using the model mRNA of human *ATF4*. My other aim was to further characterize the physiological importance of the N-terminal domain of the yeast eIF3a/Tif32 subunit, which was earlier implicated in promoting reinitiation on yeast *GCN4* mRNA.

Here I list all particular tasks:

- to establish and utilize an *in vivo* mRNA recruitment assay in order to characterize the N-terminal domain of a/Tif32 subunit of yeast eIF3 with respect to its potential role in this critical initiation step leading to formation of the 48S PICs
- to further employ this assay in order to experimentally confirm the role of the N-terminal domain of a/Tif32 in stabilizing the mRNA binding specifically at the 40S mRNA exit channel using various model mRNAs
- to study translation reinitiation mechanism on yeast model *GCN4* mRNA, mainly with respect to a prospective role of its 3´UTR in the translational regulation of its expression
- to set up an *in vivo* human *ATF4*-based *Firefly* luciferase reporter system in various cell lines to be able to investigate basic principles of human reinitiation
- to mutagenize the *ATF4* mRNA in order to identify specific *cis*-acting elements flanking *ATF4* uORF1 that could be responsible for high efficiency of reinitiation (REI) that this uORF allows
- to knock-down specific subunits of human eIF3 to investigate the potential role of human eIF3 in translation reinitiation on *ATF4* mRNA

4. Material and methods

The experiments studying the mRNA recruitment to the 43S PICs were carried out on the model organism *Saccharomyces cerevisiae* (budding yeast); experiments focused on translation reinitiation in mammals were done on human cell lines HEK and HeLa.

List of methods:

Yeast and bacteria cells cultivation, transformation

HEK, HeLa and MEF (mouse embryonic fibroblasts) cell lines cultivation, transfection and siRNA treatment

Nucleic acids procedures, cloning

Western blot analysis

β-galactosidase reporter assay in yeasts

Luciferase reporter assay in cell lines

Affinity tag pull downs

Preparation of yeast whole-cell extracts (WCEs)

Fractionation of yeast WCEs by sucrose gradient for analysis of the native 48S PICs

RNA isolation, reverse transcription and qPCR

FACS analysis

5. List of publications

Individual publications are enclosed at the end of this thesis.

Publication I

Structural integrity of the PCI domain of eIF3a/Tif32 is required for mRNA recruitment to the 43S pre-initiation complexes

Sohail Khoshnevis*, Stanislava Gunišová*, Vladislava Vlčková*, Tomáš Kouba, Piotr Neumann, Petra Beznosková, Ralf Ficner, and Leoš Shivaya Valášek

*These authors contributed equally to the paper as first authors.

Nucleic Acids Research. 2014 Apr 42(6): 4123–4139

PMID: 24423867

IF_{2014} 9.112

IF_{2016} 10.162

Contribution of the author: 35%; I established and performed the *in vivo* mRNA recruitment assay (based on the analysis of the amounts of model mRNAs in sucrose gradient fractions of the yeast cells using RT-qPCR) which I utilized for the characterization of the mRNA recruitment role of the N-terminal domain of a/Tif32 subunit of yeast eIF3.

Publication II

Eukaryotic translation initiation factor 3 plays distinct roles at the mRNA entry and exit channels of the ribosomal preinitiation complex

Colin Echeverría Aitken, Petra Beznosková, Vladislava Vlčková, Wen-Ling Chiu, Fujun Zhou, Leoš Shivaya Valášek, Alan G. Hinnebusch, and Jon R. Lorsch

eLife. 2016 Oct 26;5. pii: e20934

PMID: 27782884

IF_{2016} 7.725

Contribution of the author: 15%; I designed and performed the experiment shown in Figure 6E where I demonstrated *in vivo* that mRNAs with longer 5´UTRs are more dependent on the stabilization role of the a/Tif32-NTD at the 40S exit channel than those containing short 5´UTRs.

Publication III

In-depth analysis of cis-determinants that either promote or inhibit reinitiation on GCN4 after translation of its four short uORFs

Stanislava Gunišová, Petra Beznosková, Mahabub Pasha Mohammad, Vladislava Vlčková, and Leoš Shivaya Valášek

RNA. 2016 Apr 22(4):542-58

PMID: 26822200

IF_{2016} 4.605

Contribution of the author: 5%; I was involved in cloning and also carried out some experiments aimed at characterizing a suspected role of the 3´UTR in the *GCN4* translational control; it turned out that the 3´UTR does not play any role after all.

Publication IV

Does eIF3 promote reinitiation after translation of short upstream ORFs also in mammalian cells?

Vladislava Hronová, Mahabub Pasha Mohammad, Susan Wagner, Josef Pánek, Stanislava Gunišová, Jakub Zeman, Kristýna Poncová, and Leoš Shivaya Valášek

RNA Biology. 2017 Jul 26:1-8

PMID: 28745933

IF_{2016} 3.900

Contribution of the author: 70%; I was critically involved in conceiving and designing the experiments that I carried out mostly by myself. I also significantly contributed to data analysis and manuscript preparations.

Publication V

An emergency brake for protein synthesis

Vladislava Hronová and Leoš Shivaya Valášek

eLife. 2017 Apr 25;6. pii: e27085

PMID: 28440747

IF_{2016} 7.725

Contribution of the author: 40%; I significantly contributed to data analysis and manuscript preparations.

Publication VI

Embraced by eIF3: structural and functional insights into the roles of eIF3 across the translation cycle

Leoš Shivaya Valášek, Jakub Zeman, Susan Wagner, Petra Beznosková, Zuzana Pavlíková, Mahabub Pasha Mohammad, Vladislava Hronová, Anna Herrmannová, Yaser Hashem, and Stanislava Gunišová

Nucleic Acids Research. 2017 Nov 2;45(19):10948-10968.

PMID: 28981723

IF_{2016} 10.162

Contribution of the author: 10%; I contributed to manuscript preparations.

Publication VII

Please do not recycle! Translation reinitiation in microbes and higher eukaryotes

Stanislava Gunišová, Vladislava Hronová, Mahabub Pasha Mohammad, Alan G. Hinnebusch, and Leoš Shivaya Valášek

FEMS Microbiology Reviews - submitted

IF_{2016} 12.198

Contribution of the author: 20%; I wrote the sections on *ATF4* translational control and helped with manuscript preparations.

I hereby confirm that author of the thesis, Vladislava Hronová, have substantially contributed to the publications listed above. In the case of her first-author publications (unshared), she performed the major part of experimental work and contributed to the manuscript preparation.

Res. Prof. Leoš Shivaya Valášek, PhD

6. Summary of presented publications

Publication I is the result of the long-lasting effort of our laboratory to elucidate the roles of the a/Tif32 subunit of eIF3 in various steps of translation initiation. Previous studies indicated that eIF3 of *Saccharomyces cerevisiae* might play a very important role in the step of mRNA recruitment to the 43S pre-initiation complex (PIC). We identified a 10-Ala substitution (*Box37*) in the a/Tif32 subunit of *S. cerevisiae* eIF3, which reduced translation initiation rates; however, it did not seem to affect any of the steps leading to the 43S PIC assembly. Therefore, it was tempting to speculate that this *a/tif32-Box37* mutation might affect specifically the 48S PIC assembly, i.e. the mRNA recruitment step. To test this hypothesis, we measured the amounts of three model mRNAs (*RPL41a*, *DAD4* and *SME1*) associated with native 48S PICs in whole-cell extracts of formaldehyde cross-linked yeast cells that were resolved on sucrose gradients. This analysis showed that the *a/tif32-Box37* mutation indeed significantly reduces the amounts of these model mRNAs in the gradient fractions containing 48S PICs *in vivo*. Moreover, in this publication we provided also a crystal structure of the PCI domain of a/Tif32 including the Box37 region. Based on this structure we designed mutations of two specific Box37 residues, Arg363 and Lys364, which mapped onto the positively charged surface-exposed area with a potential to bind RNA, and tested their effects on mRNA recruitment by the aforementioned approach. Their substitutions with alanines also severely impaired the association of the model mRNAs with the 43S PICs *in vivo* confirming that the PCI domain of a/Tif32 ensures stable and efficient delivery of mRNAs to the 43S PICs. It should be noted that a part of this study, namely the optimization of the mRNA recruitment assay and its preliminary results, were already published in my diploma thesis.

Publication II is closely connected to the previous one as it investigates the roles of all yeast eIF3 subunits in the mRNA recruitment step. In this study, we employed a library of already characterized *S. cerevisiae* eIF3 functional variants spanning all five subunits and probed their effects on mRNA recruitment effect using an *in vitro* reconstituted system. Using this approach we revealed that mutations throughout eIF3 disrupt its interaction with the PIC and diminish its ability to accelerate recruitment to a native yeast mRNA. Importantly, using model mRNAs lacking the contacts with the 40S entry or exit channels, we revealed that the eIF3a/Tif32-NTD has a critical role in stabilizing mRNA interactions at the 40S exit channel, whereas the eIF3a/Tif32-CTD plays an ancillary role at the 40S entry channel. Moreover, the role of the a/Tif32-NTD at the 40S exit channel was further confirmed by previously used *in vivo* mRNA recruitment assay using model mRNAs varying in their 5´UTR lengths.

Publication III is a comprehensive study that helped to shed more light onto translation reinitiation (REI) mechanism on the yeast model *GCN4* mRNA. Here we subjected all four *GCN4* uORFs to a thorough analysis in order to identify all potential REI-promoting or inhibiting *cis*-determinants which might contribute to the overall efficiency of REI on *GCN4* mRNA. It turned out that uORFs 1-3 contain conserved AU-rich motif that promotes REI in position-specific, autonomous fashion similarly to the REI-promoting elements occurring in the 5′ sequences of uORF1 and uORF2. uORFs 2 and 3 were additionally shown to be flanked by transferable REI-inhibiting elements immediately following their AU-rich motifs. Moreover, it also turned out that the stop codon context of *GCN4* uORFs is crucial for their ability to either terminate translation or promote resumption of scanning. Together, this publication provided a complex overview of all *cis*-determinants of REI with their effects set in the context of the overall *GCN4* translational control and thus it helped to outline the future possible directions of exploration of this process in humans.

Publication IV brought the first insights into the molecular mechanism of reinitiation in human cells using the human *ATF4* mRNA, encoding a functional homolog of yeast GCN4. In this study, we mutagenized the sequences flanking the human *ATF4* uORF1, closely resembling the REI-permissive uORF1 of yeast GCN4, and analyzed their putative roles in human translation reinitiation on the model *ATF4* mRNA. We discovered that in striking analogy to yeasts, *ATF4* uORF1 is also surrounded by REI-promoting sequences, and that these sequences act independently to boost the REI potential of this uORF. Moreover, we predicted that the 5´sequence of *ATF4* uORF1 folds into a specific, evolutionary conserved structure that is necessary for its REI-permissive potential. Furthermore, we discovered that similarly to yeast *GCN4* mRNA, reinitiation on human *ATF4* mRNA is also promoted by eIF3, just the contributing subunit is not eIF3a/Tif32 but eIF3h. Altogether, this publication revealed that the molecular mechanism of the reinitiation is generally conserved both in yeast and humans.

Publication V is an insight article commenting a recent publication “Fail-safe control of translation initiation by dissociation of eIF2α phosphorylated ternary complexes” by Jennings et al. (2017). This publication describes a novel regulatory mechanism that enables the integrated stress response to rapidly shut down the synthesis of proteins in eukaryotic cells. As described in the Chapter 2.2, phosphorylation of eIF2α controls translation initiation by restricting the levels of active ternary complexes (TC) composed of eIF2, GTP and Met-tRNAi. The key factors controlling the activity of eIF2 are translation factors eIF2B and eIF5. Normally, eIF2B has to out-compete the eIF2-GDP-bound eIF5 in order to execute its guanine-nucleotide exchange (GEF) reaction and provide the eIF2 with a fresh GTP. After this GEF reaction is finished, eIF5 out-competes the eIF2B back, and the TC is prepared to enter a new initiation cycle. However, when TC is formed with phosphorylated eIF2 (eIF2-P), eIF2B is able to out-compete eIF2-P-bound eIF5 and thus

destabilize the already formed TC so it cannot enter a new initiation cycle anymore. Therefore we dubbed this finding “an emergency break for protein synthesis”. In our insight article, we present the functioning of the eIF2, eIF5 and eIF2B proteins as a clutch, an accelerator and a brake that create the gears of the car, and we use this resemblance to explain this novel regulatory phenomenon to a broad scientific community.

Publication VI is a comprehensive review article focused on eukaryotic initiation factor 3 (eIF3). It discusses all known eIF3 roles and provides a broad picture of the eIF3’s impact on translational control in eukaryotic cells.

Publication VII is a review article providing the current and complete knowledge on gene-specific translational control mechanism called translation reinitiation. It covers both short uORF-mediated and long ORF-mediated mechanisms of translational reinitiation in all its forms.

7. Discussion

My PhD thesis focused on the step of mRNA recruitment to the 43S PICs in yeast and the gene-specific regulatory mechanism called reinitiation in yeast and humans. Notably, both of these processes turned out to be critically promoted by eIF3, the most complex and multitasking initiation factor of all. In fact, in yeasts, both mRNA recruitment and reinitiation were shown to be promoted by the biggest eIF3 subunit, eIF3a/Tif32. Both of these functions of the eIF3a/Tif32 were mapped to its N-terminal domain (NTD), referred to as a/Tif32-NTD and containing also a PCI domain (occurring in Proteasome, COP9 signalosome and eIF3).

7.1 Role of the eIF3a/Tif32-NTD in canonical translation initiation and reinitiation

The importance of eIF3 in mRNA recruitment was indicated by several previous reports. The first one showed that depletion of the entire eIF3 complex from cells impairs model *RPL41A* mRNA recruitment *in vivo* (Jivotovskaya et al. 2006). The other one demonstrated that yeast eIF3 plays a direct role in 43S PIC binding to capped, native mRNA *in vitro*, being even more critical than eIF4F and eIF4B (Mitchell et al. 2010). In our first publication (Khoshnevis et al. 2014) we tested a specific 10-Ala substitution (*Box37*) in the N-terminally-located PCI domain of the yeast a/Tif32 and showed that it robustly reduces the recruitment of three model mRNAs to the 43S PICs *in vivo* as the only detectable defect. Moreover, based on the structure of the a/Tif32-PCI domain, which was solved by our collaborators along the way (Khoshnevis et al. 2014), we selected two basic residues located in the region of Box37 and we investigated the effect of their mutations on the mRNA recruitment as well. In analogy with the *a/tif32-Box37*, the mutations of Arg363 and Lys364 to alanines also decreased the amounts of reporter *RPL41A* mRNA in the 43S-containing fractions to the same level (*a/tif32-R363A*) or even more (*a/tif32-K364A*) when compared with the *a/tif32-Box37* mutation. Thus, all these findings together strongly suggest that this region of the PCI domain of the a/Tif32 significantly contributes to the formation and/or stability of 48S PICs and that both of these Box37 residues play a very important role in this process.

Interestingly, another study by (Chiu et al. 2010) revealed that substitutions in the KERR motif in the HCR1-like domain (HLD) located at the C-terminal half of the yeast a/Tif32 also impair binding of a model mRNA to the 43S PICs *in vivo*. However, in contrast to the PCI substitution characterized here (*Box37*), the HLD substitutions also produced phenotypes indicating reduced efficiency of scanning and AUG recognition. Hence, to our knowledge, this is the first report implicating a specific domain of an initiation factor solely in this key role *in vivo*.

A few years later, we confirmed the importance of the a/Tif32-NTD (containing also the Box37) in mRNA recruitment step by our following study employing a yeast *in vitro* reconstituted

system (Aitken, 2016). Here we used the yeast strain containing the *a/tif32-Δ8* truncation eliminating the first 200 amino acids of the a/Tif32 subunit. We demonstrated that the recruitment of a model mRNA with an AUG located near its 3´end, which produces the complex with an empty entry channel, was dramatically abolished by this mutant. In fact, the *a/tif32-Δ8* mutation mimicked the complete absence of eIF3 – there was no recruitment of this mRNA in the presence of this mutation, despite the fact that this mutant eIF3 as well as ternary complex were fully bound to the PIC (Aitken et al. 2016). On the other hand, this mutation did not affect the recruitment of a model mRNA containing the 5´proximal AUG that produces the complex with an empty exit channel, which strongly implicated this region of a/Tif32 in stabilizing mRNA binding at the 40S exit channel of the 48S PIC. Interestingly, gradual increase in the length of mRNA in the entry channel progressively rescued the *a/tif32-Δ8* defect indicating that filling the entry channel with mRNA is sufficient to restore the interactions there. This suggests that the eIF3 functions at both exit and entry channels are redundant. The ultimate proof for the mRNA stabilization role of the a/Tif32-NTD at the exit channel was provided by my *in vivo* experiments where I measured the amounts of 43S PICs-bound reporter mRNAs with an increasing 5´UTR length using the *a/tif32-Δ8 versus* WT cells (Aitken et al. 2016). Here we hypothesized that the recruitment of mRNAs with longer 5´UTRs would produce a greater defect for the mutant, as the majority of the scanning process occurs with the exit channel occupied, giving the WT PICs an advantage because they are able to make contacts with mRNA in this channel whereas *a/tif32-Δ8* mutant cells are not. Consistent with our prediction, the *a/tif32-Δ8* mutation reduced the amount of mRNA associated with native 43S PICs for all the mRNAs we tested, but had a greater defect relative to WT cells on mRNAs with longer 5'UTRs.

These results are consistent with the fact that the aforementioned *a/tif32-Δ8* truncation also impairs reinitiation on *GCN4* mRNA following translation of uORF1 and uORF2, an effect attributable to the loss of interaction between the a/Tif32-NTD and nucleotides preceding each uORF stop codon that otherwise stabilize post-termination 40S subunits and allow them to resume scanning in the presence of WT eIF3 (Szamecz et al. 2008; Munzarova et al. 2011). Moreover, it was also predicted that both of the specific Boxes (Box6 and 17) shown to promote efficient reinitiation in *GCN4* mRNA (Munzarova et al. 2011) are located close to two basic patches on the surface of the modeled N-terminal domain of a/Tif32 (Khoshnevis et al. 2014). Together, this indicates that in addition to this specific role, both of these Boxes from the a/Tif32-NTD may also nonspecifically contact all cellular mRNAs and thus contribute to their recruitment to the 43S PICs as it was shown for Box37. Notably, the aforementioned finding that the a/Tif32-NTD is able to stabilize only the mRNAs long enough to emerge from the mRNA exit channel (Aitken et al. 2016) also indicates that only the uORFs preceded by sufficiently long sequence can be stabilized by the a/Tif32-NTD to promote reinitiation downstream. This fact might thus help to distinguish the uORFs that could mediate canonical reinitiation *via* the a/Tif32-NTD.

The results obtained in the second publication of this thesis (Aitken et al. 2016) together suggest that the N-terminal part of eIF3 residing near the mRNA exit channel of 40S is crucial for stabilizing the mRNA interaction with the PIC, whereas the C-terminal arm of eIF3 located at the mRNA entry channel appears to have rather a supplementary role, based on holding the ribosome and other components of the translation machinery together and thus accelerating mRNA recruitment (Aitken et al. 2016). This model is fully supported by various other genetic and structural data that suggest that the a/Tif32 subunit wraps around the neck of the 40S subunit on its solvent-exposed side with the two arms protruding to the exit and entry mRNA channels (Szamecz et al. 2008; Chiu et al. 2010; Kouba et al. 2012; Khoshnevis et al. 2014; Aylett et al. 2015; Llácer et al. 2015). A similar position was also proposed for its mammalian ortholog eIF3a in various biochemical as well as structural studies (Pisarev et al. 2008; Hashem et al. 2013; des Georges et al. 2015). Thus, it might be proposed that that the location of eIF3a subunit on the 40S subunit is conserved, and so might be perhaps also its function. Whereas the molecular details of mRNA recruitment in mammals are not known, we are now able to compare the molecular mechanisms of translation reinitiation in yeasts and humans.

Whereas reinitiation on the yeast *GCN4* mRNA strictly requires the N-terminal part of the a/Tif32 subunit, our next study revealed that this mechanism on the mRNA encoding a human GCN4 homolog, ATF4, is promoted by a nonconserved eIF3h subunit (Hronová et al. 2017). Interestingly, the same subunit was shown to promote reinitiation also in plants (Roy et al. 2010). This difference might be explained by the fact that mammalian as well as plant eIF3 contain nearly twice as much subunits then yeasts (Valášek et al. 2017) and therefore it is very likely that in higher eukaryotes some of the subunits evolved to have specialized role(s) such as promoting REI. Accordingly, in contrast to the yeast a/Tif32, eIF3h subunit is essential neither for humans nor plants (in plants, however, it seems to be important for proper fertility; Kim et al. 2004). In any case, it is interesting to note that based on the recent structural data, human eIF3h seems to adopt a similar position on the ribosome as the REI-promoting N-terminal domain of yeast eIF3a/Tif32; i.e. right next to the mRNA exit channel (des Georges et al. 2015). This provides it with an ideal location where it could interact with the *ATF4* mRNA right emerging from the ribosome exit channel post uORF1 translation to promote resumption of scanning and REI downstream. In contrast to yeasts, however, it is still not clear whether eIF3h indeed act in a cooperation with the sequences surrounding uORF1 of *ATF4* or not.

In fact, eIF3a might also contribute to the effectivity of reinitiation in mammals, however, it is very complicated to determine its specific effect on reinitiation because the downregulation of the whole eIF3a leads to a disintegration of the whole eIF3 complex and thus severely affects general translation initiation rates (Wagner et al. 2016; Hronová et al. 2017). Therefore, even though we attempted to test the role of human eIF3a in reinitiation on *ATF4* mRNA, we were not able to detect any reinitiation-specific effect of this subunit. Nevertheless, possible future

experiments employing e.g. CRISPR/Cas system enabling us to create a mutant lacking only a part of eIF3a (e.g. its N-terminal domain), which would not affect the translation initiation rates and cell viability so dramatically, might help to answer the question whether and what part of the mammalian eIF3a contributes to the effectivity of reinitiation. In fact, the N-terminal domain of the eIF3a/Tif32 is the most conserved part of the whole protein (Kovarik et al. 1998), and the a/Tif32-Box17, shown to promote the reinitiation in yeast *GCN4* (Munzarová et al. 2011), shares the 80% similarity (8 out of 10 amino acids are the same) between *S. cerevisiae* and *H. sapiens* (VH, unpublished observations). The other REI-promoting segment, the a/Tif32-Box6, then shares the 40% similarity between these two species. Thus, it is still likely that the REI-promoting properties of eIF3a/Tif32 remained conserved both in yeast and humans, just a more specific approach is necessary to test this hypothesis.

7.2 Differences between yeast and human reinitiation

Our results obtained with human *ATF4* mRNA suggest that the general mechanism of yeast and human REI is in general conserved: In both organisms, it requires the REI-permissive uORF to be flanked by specifically structured *cis*-acting sequences interacting with specific *trans*-acting factors such as eIF3 to stabilize the post-termination 40S subunit on this uORF. However, it seems to differ in several aspects in these two organisms. First one is, as mentioned above, the involvement of different eIF3 subunits. Another difference concerns the roles of the sequences flanking the REI-permissive uORF1. First, in yeast *GCN4*, the stimulatory activity of the sequence located downstream of uORF1 was shown to be necessary for the subsequent activity of the sequence localized upstream of this uORF. Thus, the sequence downstream of uORF1 seems to be more important for the REI efficiency in yeasts (Munzarová et al. 2011). In contrast, in humans it was shown that both downstream and upstream sequences flanking the *ATF4* uORF1 act independently and the sequence upstream of *ATF4* uORF1 showed a bigger effect on REI efficiency than the sequence downstream of this uORF (Hronová et al. 2017). Next, whereas eliminating the flanking sequences around uORF1 or uORF2 of yeast *GCN4* mRNA fully abolished their REI potential (Gunišová et al. 2016), eliminating the corresponding *cis*-acting sequences flanking uORF1 of human *ATF4* reduced the efficiency of REI only by ~65%. This difference might be attributed to the nature of the two initiation factors, eIF3 and eIF4G, that have been implicated in promoting REI but whose binding significantly differ in these two organisms (Poyry and Kaminski 2004). Whereas yeast eIF3 does not directly contact eIF4G, and their contact is supposedly only bridged by eIF5 and eIF1 (Asano et al. 2001), in mammals these two proteins do interact (Korneeva et al. 2000). Therefore, if we assume that mammalian eIF3 and possibly also eIF4G are capable to persist throughout uORF translation on the mammalian 80S ribosome as it was now shown *in vivo* for yeast eIF3 (Mohammad et al. 2017), their direct contact could substantially empower the

stabilization of the post-termination 40S subunit on the mRNA. This might set the basal level of REI-permissiveness of mammalian uORFs higher than it is in yeasts, where these two factors do not directly interact. This theory is also supported by the fact that mammalian uORFs were found to be generally less repressive for REI than those in yeasts (Calvo, Pagliarini and Mootha 2009). Hence, it seems likely that mammalian uORFs are generally less inhibitory than in yeasts, and that only those uORFs that constitute a part of some sophisticated stress-related regulatory system were additionally equipped with specific *cis*-acting features that render them highly REI-permissive. This theory might also explain why the inhibitory uORF2 in mammalian *ATF4* as well as *ATF5* mRNAs is not a typical short uORF but instead it overlaps with the main coding sequence.

Besides eIF3 (and possibly eIF4G, as hinted above), little is known about other mammalian factors that could regulate uORF-mediated reinitiation in a sequence-specific manner. However, one of them might be metazoan heterodimer DENR-MCT-1. Recently, Schleich et al. (2014) discovered that these proteins specifically regulate reinitiation downstream of uORFs with a strong Kozak sequence in a specific cellular context in *Drosophila*. A follow-up study in human cells (Schleich et al. 2017) reported that in humans, DENR-MCT-1 are important only for transcripts with very short uORFs in strong Kozak sequence coding for only one, maximally two, amino acids. Interestingly, such mRNA leaders were found to be enriched for example in neuron-specific genes (Schleich et al. 2017). Strikingly, it was shown that this DENR-MCT-1 heterodimer is not required for initiation on uORF-less mRNAs (Schleich et al. 2014), apparently uncoupling REI from canonical initiation. Structural studies revealed that heterodimer DENR-MCT-1 "shares" the 40S binding site with the eIF3a-CTD and eIF3c-NTD in mammals (Lomakin et al. 2017). Therefore these authors suggested that the interplay between DENR-MCT-1 and eIF3 might represent an important factor for decision of the post-termination ribosome if to recycle both subunits or resume traversing along the mRNA to reinitiate downstream. An alternative scenario might be that these two factors may respond to different features of the sequences flanking the uORFs and, thus, promote reinitiation on different subsets of mRNAs in a mutually independent manner (Lomakin et al. 2017).

7.3 Novel insights into human *ATF4* translational control

Translational upregulation of *ATF4 via* uORF-mediated reinitiation has been widely believed to be a major contributor to its overall upregulation in stress conditions. However, many recent studies indicate that other outputs of phosphorylated eIF2α that are specific to higher eukaryotes, or even other regulatory pathways unrelated to the ISR, make important contributions to ATF4 induction. Besides translational upregulation, ATF4 accumulation might be mediated also by transcriptional upregulation and/or post-translational stabilization in various stress conditions, as already mentioned (Lassot et al. 2001, 2005; Koditz et al. 2007; Dey et al. 2010; Martina et al. 2015; Zhao

et al. 2016). Furthermore, *ATF4* mRNA stability might be regulated also by nonsense mediated mRNA decay dependent on stress (Mendell et al. 2004; Gardner et al. 2008). It should be also noted that whereas the mRNA of *GCN4* contains the specific stabilizer element (STE) preventing this mRNA to be degraded by NMD (Ruiz-Echevarría and Peltz 2000), this element has never been detected in its mammalian homolog *ATF4*. Therefore, it seems that it is the combined action of all these regulatory mechanisms and not solely the translational upregulation *via* reinitiation what ensures the boost of *ATF4* expression in certain conditions such as ER stress.

Moreover, a report by Starck et al. (2016) recently challenged the current model of *ATF4* translational upregulation by reinitiation as it revealed a high degree of peptide expression from both *ATF4* uORF1 and uORF2 during both normal growth and stress conditions. A similar finding could have been also predicted from a recent ribosome profiling measurements (Andreev et al. 2015; Sidrauski et al. 2015). Since based on the reinitiation model the high degree of uORF2 expression during stress was not anticipated, these authors suggested that either reinitiation commences after only a few 40S subunits bypass uORF2 or that translation of the ATF4 CDS is a combination of reinitiation and leaky scanning past both uORFs. The finding that uORFs are constitutively expressed even during stress with limited TC levels might also suggest that uORF translation in mammals might have an additional role during the ISR, which might provide an explanation for generally high level of ribosome occupancy within the 5´UTRs of various mRNAs expressed during stress (Andreev et al. 2015). Constitutive uORF expression could for example protect mRNAs from translational degradation during stress and thereby serve to control gene expression. Alternatively, translated uORFs could also generate bioactive peptides that might directly or indirectly regulate expression of the main CDS (Starck et al. 2016). Any way, certainly more work is needed to fully understand this phenomenon and resolve this discrepancy in the model of *ATF4* translational upregulation.

In fact, a potential function of uORF-encoded proteins in the *ATF4* mRNA leader has never been investigated. Taking into account the uORF1 short length (3 sense codons), the likelihood that uORF1-encoded peptide might have a specific function seems very low; however, longer uORF2, the amino acid sequence of which is very much conserved in various organisms, might potentially encode a functional peptide playing a role in the ATF4 expression. The fact that we identified a very strong putative hairpin in the uORF2-ATF4 overlap might indicate that the uORF2-encoded peptide could potentially cause ribosome stalling (VH, unpublished observations), like previously shown for example for the Arginine Attenuator Peptide (Wei, Wu, and Sachs 2012).

Another important unsolved question concerning the human *ATF4* expression is a role of "uORF0"; i. e. the minimal "start-stop" uORF preceding uORF1 found in the human *ATF4* 5´ leader. Even though this additional uORF has been annotated (Harding et al. 2000), its role has been never investigated so far as all of the *ATF4* translational control studies have been done using the mouse *ATF4* mRNA, which, as nearly the only higher eukaryote, does not contain it (Vattem

and Wek 2004; Lu, Harding, and Ron 2004). However, the fact that uORF0 is very much conserved among vertebrates and, at least based on the unpublished ribosome profiling data (Dmitry Andreev and Pavel Baranov, unpublished observations), is effectively recognized by ribosomes even though it is located in the very weak Kozak consensus sequence indicates that it might indeed play an important role in *ATF4* expression. In fact, we have already begun to analyze the role of this minimal uORF using the reporters where uORF0 extends into the CDS of the luciferase. By normalizing the luciferase activity of this reporter to the activity of the uORF-less construct we are able to measure the level of leaky scanning on uORF0. Our preliminary data suggest that this uORF0 is leaky scanned only in ~ 60% cases suggesting that it very likely does contribute to the overall translational regulation of the *ATF4* expression (VH, unpublished data). However, the precise mechanism of its contribution has not been determined yet.

Strikingly, a similarly minimal start-stop uORF was recently shown to induce boron-dependent ribosome stalling and subsequent mRNA degradation of the *NIP5;1* mRNA of *Arabidopsis thaliana* encoding a boric acid transporter required for efficient uptake of boron from soil (Tanaka et al. 2016). The molecular mechanism by which the boron induces ribosomal stalling remains, however, unclear. It was suggested that boron somehow blocks the dissociation of Met-tRNAi from the P-site which ultimately leads to the mRNA degradation (Mayuki Tanaka and Toru Fujiwara, personal communication). Anyway, the reproducibility of this regulation in both plant and animal transient expression system suggest that such type of regulation might be common also in eukaryotes (Tanaka et al. 2016). Thus, it might be interesting to find out in future whether the *ATF4* uORF0 might also cause a ribosome stalling leading to mRNA degradation, for example as a result of specific conditions in cell.

Apart from all this, ATF4 was recently shown to be upregulated also by a growth-stimulating mTOR pathway in the nutrient replete conditions in various mouse and human cells (Ben-Sahra et al. 2016), which seems contradictory when taking into account that ATF4 has always been considered a master regulator of the stress response. Strikingly, this mTOR-dependent ATF4 upregulation was independent of both cellular stress response and eIF2α-mediated regulation but it still seemed to require the 5´UTR of *ATF4*. A similar phenomenon was recently reported also by Park et al. (2017), who showed that the mTOR control of *ATF4* translation requires uORFs but not changes in eIF2α phosphorylation, and instead it employs the 4E-BP translational repressors. Finally, it should be also noted that according to (Chan et al. 2013), human cells express also an alternatively spliced ATF4 variant that contains four uORFs in its 5´leader and is supposedly translationally upregulated not by reinitiation but by an internal ribosomal entry site (IRES)-mediated mechanism. The IRES activity was mapped to a highly structured region that partially overlapped with the third and fourth uORF and was activated by the PERK-induced eIF2α phosphorylation. However, the physiological importance of this finding is somewhat undermined by the fact that this longer transcription variant of *ATF4* is expressed very purely and almost

exclusively only in leukocytes (Chan et al. 2013).

Together, all these observations indicate that the expression of *ATF4* is regulated by many distinct mechanisms and that the complex understanding of *ATF4* regulation is still far from complete. Therefore, the study of its regulation should be always performed cautiously and with a full awareness of other potential influences. Since ATF4 protein is upregulated by signals of the tumor microenvironment such as hypoxia, oxidative stress or ER stress protein, and it has been indeed shown to be present in greater levels in cancer when compared to normal tissue (Ameri and Harris 2008), it seems to be interesting also from a medical point of view. Therefore, revealing the molecular details of *ATF4* expression might not only contribute to our general understanding of the mechanisms of uORF-mediated regulation and stress response but it might also help to improve the human health in the future.

Conclusions

My PhD thesis brought novel insights into the molecular mechanism of the gene-specific regulatory process called reinitiation (REI) in yeasts and humans, and revealed that many mechanistic aspects of this process are conserved in these two organisms. Moreover, it also significantly contributed to our understanding of basic principles of general translation initiation in eukaryotes.

Using several independent approaches we showed that the eIF3a/Tif32-NTD (including its PCI domain) has a critical role in stabilizing mRNA interactions at the 40S exit channel. Moreover, we also solved a crystal structure of the PCI domain of the a/Tif32. Thanks to this, we identified two residues of the eIF3a/Tif32 subunit, Arg363 and Lys364, specifically contributing to the step of mRNA recruitment to the 43S PICs.

Next, we identified novel REI-promoting and inhibiting *cis*-determinants which govern translational control on the *GCN4* mRNA *via* reinitiation and thus expanded the already complex view of how expression of this gene is regulated in response to stress.

Finally, we successfully set up the human *ATF4*-based *Firefly* luciferase reporter system in HEK and HeLa cell lines and identified specific REI-promoting *cis*-acting sequences flanking the *ATF4* uORF1. We revealed that both of these sequences (5´and 3´sequences) contribute to efficiency of reinitiation on this mRNA independently. Furthermore, we computationally predicted that similarly to yeast *GCN4*, the 5´sequence of uORF1 seems to fold into a specific structure upon uORF1 translation, and that this structure is evolutionarily conserved. We also discovered that reinitiation on human *ATF4* mRNA is promoted by one of the eIF3 subunits, eIF3h.

References

Abastado, J. P., P. F. Miller, B. M. Jackson, and A. G. Hinnebusch. 1991. “Suppression of Ribosomal Reinitiation at Upstream Open Reading Frames in Amino Acid-Starved Cells Forms the Basis for GCN4 Translational Control.” *Molecular and Cellular Biology* 11 (1): 486–96.

Abel, T., K. C. Martin, D. Bartsch, and E. R. Kandel. 1998. “Memory Suppressor Genes: Inhibitory Constraints on the Storage of Long-Term Memory.” *Science* 279 (5349): 338–41.

Aitken, Colin Echeverría, Petra Beznosková, Vladislav Vlčková, Wen-Ling Chiu, Fujun Zhou, Leoš Shivaya Valášek, Alan G. Hinnebusch, and Jon R. Lorsch. 2016. “eIF3 Plays Distinct Roles at the mRNA Entry and Exit Channels of the Ribosomal Preinitiation Complex.” *eLife* doi:10.1101/072702.

Algire, Mikkel A., David Maag, and Jon R. Lorsch. 2005. “Pi Release from eIF2, Not GTP Hydrolysis, Is the Step Controlled by Start-Site Selection during Eukaryotic Translation Initiation.” *Molecular Cell* 20 (2): 251–62.

Ameri, Kurosh, and Adrian L. Harris. 2008. “Activating Transcription Factor 4.” *The International Journal of Biochemistry & Cell Biology* 40 (1): 14–21.

Ameri, Kurosh, Claire E. Lewis, Martin Raida, Heidi Sowter, Tsonwin Hai, and Adrian L. Harris. 2004. “Anoxic Induction of ATF-4 through HIF-1-Independent Pathways of Protein Stabilization in Human Cancer Cells.” *Blood* 103 (5): 1876–82.

Andreev, Dmitry E., Patrick B. F. O’Connor, Ciara Fahey, Elaine M. Kenny, Ilya M. Terenin, Sergey E. Dmitriev, Paul Cormican, Derek W. Morris, Ivan N. Shatsky, and Pavel V. Baranov. 2015. “Translation of 5’ Leaders Is Pervasive in Genes Resistant to eIF2 Repression.” *eLife* 4 (January): e03971.

Angelastro, J. M., P. D. Canoll, J. Kuo, M. Weicker, A. Costa, J. N. Bruce, and L. A. Greene. 2005. “Selective Destruction of Glioblastoma Cells by Interference with the Activity or Expression of ATF5.” *Oncogene* 25 (6): 907–16.

Asano, K., A. Shalev, L. Phan, K. Nielsen, J. Clayton, L. Valásek, T. F. Donahue, and A. G. Hinnebusch. 2001. “Multiple Roles for the C-Terminal Domain of eIF5 in Translation Initiation Complex Assembly and GTPase Activation.” *The EMBO Journal* 20 (9): 2326–37.

Aylett, Christopher H. S., Daniel Boehringer, Jan P. Erzberger, Tanja Schaefer, and Nenad Ban. 2015. “Structure of a Yeast 40S-eIF1-eIF1A-eIF3-eIF3j Initiation Complex.” *Nature Structural & Molecular Biology* 22 (3): 269–71.

Barbosa, Cristina, Isabel Peixeiro, and Luísa Romão. 2013. “Gene Expression Regulation by Upstream Open Reading Frames and Human Disease.” *PLoS Genetics* 9 (8): e1003529.

Ben-Sahra, Issam, Gerta Hoxhaj, Stéphane J. H. Ricoult, John M. Asara, and Brendan D. Manning. 2016. “mTORC1 Induces Purine Synthesis through Control of the Mitochondrial Tetrahydrofolate Cycle.” *Science* 351 (6274): 728–33.

Beznosková, Petra, Lucie Cuchalová, Susan Wagner, Christopher J. Shoemaker, Stanislava Gunišová, Tobias von der Haar, and Leoš Shivaya Valášek. 2013. “Translation Initiation Factors eIF3 and HCR1 Control Translation Termination and Stop Codon Read-through in Yeast Cells.” *PLoS Genetics* 9 (11): e1003962.

Beznosková, Petra, Susan Wagner, Myrte Esmeralda Jansen, Tobias von der Haar, and Leoš Shivaya Valášek. 2015. “Translation Initiation Factor eIF3 Promotes Programmed Stop Codon Readthrough.” *Nucleic Acids Research* 43 (10): 5099–5111.

Brar, Gloria A., Moran Yassour, Nir Friedman, Aviv Regev, Nicholas T. Ingolia, and Jonathan S. Weissman. 2012. “High-Resolution View of the Yeast Meiotic Program Revealed by Ribosome Profiling.” *Science* 335 (6068): 552–57.

Calkhoven, C. F., C. Müller, and A. Leutz. 2000. “Translational Control of C/EBPalpha and C/EBPbeta Isoform Expression.” *Genes & Development* 14 (15): 1920–32.

Calvo, Sarah E., David J. Pagliarini, and Vamsi K. Mootha. 2009. “Upstream Open Reading Frames Cause Widespread Reduction of Protein Expression and Are Polymorphic among Humans.” *Proceedings of the National Academy of Sciences of the United States of America* 106 (18): 7507–12.

Chan, Ching-Ping, Kin-Hang Kok, Hei-Man Vincent Tang, Chi-Ming Wong, and Dong-Yan Jin. 2013. “Internal Ribosome Entry Site-Mediated Translational Regulation of ATF4 Splice Variant in Mammalian Unfolded Protein Response.” *Biochimica et Biophysica Acta* 1833 (10): 2165–75.

Cheung, Yuen-Nei, David Maag, Sarah F. Mitchell, Christie A. Fekete, Mikkel A. Algire, Julie E. Takacs, Nikolay Shirokikh, Tatyana Pestova, Jon R. Lorsch, and Alan G. Hinnebusch. 2007. “Dissociation of eIF1 from the 40S Ribosomal Subunit Is a Key Step in Start Codon Selection in Vivo.” *Genes & Development* 21 (10): 1217–30.

Chiu, Wen-Ling, Susan Wagner, Anna Herrmannová, Laxminarayana Burela, Fan Zhang, Adesh K. Saini, Leos Valásek, and Alan G. Hinnebusch. 2010. “The C-Terminal Region of Eukaryotic Translation Initiation Factor 3a (eIF3a) Promotes mRNA Recruitment, Scanning, And, Together with eIF3j and the eIF3b RNA Recognition Motif, Selection of AUG Start Codons.” *Molecular and Cellular Biology* 30 (18): 4415–34.

Davuluri, R. V. 2000. “CART Classification of Human 5’ UTR Sequences.” *Genome Research* 10 (11): 1807–16.

Dever, Thomas E. 2002. “Gene-Specific Regulation by General Translation Factors.” *Cell* 108 (4): 545–56.

Dey, Souvik, Thomas D. Baird, Donghui Zhou, Lakshmi Reddy Palam, Dan F. Spandau, and Ronald C. Wek. 2010. “Both Transcriptional Regulation and Translational Control of ATF4 Are Central to the Integrated Stress Response.” *The Journal of Biological Chemistry* 285 (43): 33165–74.

Dong, J., H. Qiu, M. Garcia-Barrio, J. Anderson, and A. G. Hinnebusch. 2000. “Uncharged tRNA Activates GCN2 by Displacing the Protein Kinase Moiety from a Bipartite tRNA-Binding Domain.” *Molecular Cell* 6 (2): 269–79.

Erzberger, Jan P., Florian Stengel, Riccardo Pellarin, Suyang Zhang, Tanja Schaefer, Christopher H. S. Aylett, Peter Cimermančič, et al. 2014. “Molecular Architecture of the 40S· eIF1· eIF3 Translation Initiation Complex.” *Cell* 158 (5): 1123–35.

Estes, S. D., D. L. Stoler, and G. R. Anderson. 1995. “Normal Fibroblasts Induce the C/EBP Beta and ATF-4 bZIP Transcription Factors in Response to Anoxia.” *Experimental Cell Research* 220 (1): 47–54.

Fijalkowska, Daria, Steven Verbruggen, Elvis Ndah, Veronique Jonckheere, Gerben Menschaert, and Petra Van Damme. 2017. “eIF1 Modulates the Recognition of Suboptimal Translation Initiation Sites and Steers Gene Expression via uORFs.” *Nucleic Acids Research* 45 (13): 7997–8013.

Gardner, Lawrence B. 2008. “Hypoxic Inhibition of Nonsense-Mediated RNA Decay Regulates Gene Expression and the Integrated Stress Response.” *Molecular and Cellular Biology* 28 (11): 3729–41.

Georges, Amedee des, Vidya Dhote, Lauriane Kuhn, Christopher U. T. Hellen, Tatyana V. Pestova, Joachim Frank, and Yaser Hashem. 2015. “Structure of Mammalian eIF3 in the Context of the 43S Preinitiation Complex.” *Nature* 525 (7570): 491–95.

Griffin, E., A. Re, N. Hamel, C. Fu, H. Bush, T. McCaffrey, and A. S. Asch. 2001. “A Link between Diabetes and Atherosclerosis: Glucose Regulates Expression of CD36 at the Level of Translation.” *Nature Medicine* 7 (7): 840–46.

Gunišová, Stanislava, Petra Beznosková, Mahabub Pasha Mohammad, Vladislava Vlčková, and Leoš Shivaya Valášek. 2016. “In-Depth Analysis of Cis-Determinants That Either Promote or Inhibit Reinitiation on GCN4 mRNA after Translation of Its Four Short uORFs.” *RNA* 22 (4): 542–58.

Gunišová, Stanislava, and Leoš Shivaya Valášek. 2014. “Fail-Safe Mechanism of GCN4 Translational Control--uORF2 Promotes Reinitiation by Analogous Mechanism to uORF1 and Thus Secures Its Key Role in GCN4 Expression.” *Nucleic Acids*

Research 42 (9): 5880–93.
Hamilton, R., C. K. Watanabe, and H. A. de Boer. 1987. “Compilation and Comparison of the Sequence Context around the AUG Startcodons in Saccharomyces Cerevisiae mRNAs.” *Nucleic Acids Research* 15 (8): 3581–93.
Han, Jaeseok, Sung Hoon Back, Junguk Hur, Yu-Hsuan Lin, Robert Gildersleeve, Jixiu Shan, Celvie L. Yuan, et al. 2013. “ER-Stress-Induced Transcriptional Regulation Increases Protein Synthesis Leading to Cell Death.” *Nature Cell Biology* 15 (5): 481–90.
Harding, Heather P., Yuhong Zhang, Huiquing Zeng, Isabel Novoa, Phoebe D. Lu, Marcella Calfon, Navid Sadri, et al. 2003. “An Integrated Stress Response Regulates Amino Acid Metabolism and Resistance to Oxidative Stress.” *Molecular Cell* 11 (3): 619–33.
Harding, H. P., I. Novoa, Y. Zhang, H. Zeng, R. Wek, M. Schapira, and D. Ron. 2000. “Regulated Translation Initiation Controls Stress-Induced Gene Expression in Mammalian Cells.” *Molecular Cell* 6 (5): 1099–1108.
Hashem, Yaser, Amedee des Georges, Vidya Dhote, Robert Langlois, Hstau Y. Liao, Robert A. Grassucci, Christopher U. T. Hellen, Tatyana V. Pestova, and Joachim Frank. 2013. “Structure of the Mammalian Ribosomal 43S Preinitiation Complex Bound to the Scanning Factor DHX29.” *Cell* 153 (5): 1108–19.
Hayashi, Noriya, Shun Sasaki, Hiro Takahashi, Yui Yamashita, Satoshi Naito, and Hitoshi Onouchi. 2017. “Identification of Arabidopsis Thaliana Upstream Open Reading Frames Encoding Peptide Sequences That Cause Ribosomal Arrest.” *Nucleic Acids Research* 45 (15): 8844–58.
Hinnebusch, Alan G. 2005. “Translational Regulation of GCN4 and the General Amino Acid Control of Yeast.” *Annual Review of Microbiology* 59: 407–50.
Hinnebusch, Alan G., and Jon R. Lorsch. 2012. “The Mechanism of Eukaryotic Translation Initiation: New Insights and Challenges.” *Cold Spring Harbor Perspectives in Biology* 4 (10). doi:10.1101/cshperspect.a011544.
Hronová, Vladislava, Mahabub Pasha Mohammad, Susan Wagner, Josef Pánek, Stanislava Gunišová, Jakub Zeman, Kristýna Poncová, and Leoš Shivaya Valášek. 2017. “Does eIF3 Promote Reinitiation after Translation of Short Upstream ORFs Also in Mammalian Cells?” *RNA Biology*, July, 1–8.
Hussain, Tanweer, Jose L. Llácer, Israel S. Fernández, Antonio Munoz, Pilar Martin-Marcos, Christos G. Savva, Jon R. Lorsch, Alan G. Hinnebusch, and V. Ramakrishnan. 2014. “Structural Changes Enable Start Codon Recognition by the Eukaryotic Translation Initiation Complex.” *Cell* 159 (3): 597–607.
Imataka, H., A. Gradi, and N. Sonenberg. 1998. “A Newly Identified N-Terminal Amino Acid Sequence of Human eIF4G Binds poly(A)-Binding Protein and Functions in poly(A)-Dependent Translation.” *The EMBO Journal* 17 (24): 7480–89.
Imataka, H., and N. Sonenberg. 1997. “Human Eukaryotic Translation Initiation Factor 4G (eIF4G) Possesses Two Separate and Independent Binding Sites for eIF4A.” *Molecular and Cellular Biology* 17 (12): 6940–47.
Isken, Olaf, Yoon Ki Kim, Nao Hosoda, Greg L. Mayeur, John W. B. Hershey, and Lynne E. Maquat. 2008. “Upf1 Phosphorylation Triggers Translational Repression during Nonsense-Mediated mRNA Decay.” *Cell* 133 (2): 314–27.
Ivanov, Ivaylo P., Gary Loughran, Matthew S. Sachs, and John F. Atkins. 2010. “Initiation Context Modulates Autoregulation of Eukaryotic Translation Initiation Factor 1 (eIF1).” *Proceedings of the National Academy of Sciences of the United States of America* 107 (42): 18056–60.
Janich, Peggy, Alaaddin Bulak Arpat, Violeta Castelo-Szekely, Maykel Lopes, and David Gatfield. 2015. “Ribosome Profiling Reveals the Rhythmic Liver Translatome and Circadian Clock Regulation by Upstream Open Reading Frames.” *Genome Research* 25 (12): 1848–59.
Jennings, Martin D., Christopher J. Kershaw, Tomas Adomavicius, and Graham D. Pavitt. 2017. “Fail-Safe Control of Translation Initiation by Dissociation of eIF2α

Phosphorylated Ternary Complexes." *eLife* 6 (March). doi:10.7554/eLife.24542.
Jivotovskaya, Antonina V., Leoš Valášek, Alan G. Hinnebusch, and Klaus H. Nielsen. 2006. "Eukaryotic Translation Initiation Factor 3 (eIF3) and eIF2 Can Promote mRNA Binding to 40S Subunits Independently of eIF4G in Yeast." *Molecular and Cellular Biology* 26 (4): 1355–72.
Johnstone, Timothy G., Ariel A. Bazzini, and Antonio J. Giraldez. 2016. "Upstream ORFs Are Prevalent Translational Repressors in Vertebrates." *The EMBO Journal* 35 (7): 706–23.
Jousse, Céline, Christiane Deval, Anne-Catherine Maurin, Laurent Parry, Yoan Chérasse, Cédric Chaveroux, Renaud Lefloch, Philippe Lenormand, Alain Bruhat, and Pierre Fafournoux. 2007. "TRB3 Inhibits the Transcriptional Activation of Stress-Regulated Genes by a Negative Feedback on the ATF4 Pathway." *The Journal of Biological Chemistry* 282 (21): 15851–61.
Khoshnevis, Sohail, Stanislava Gunišová, Vladislava Vlčková, Tomáš Kouba, Piotr Neumann, Petra Beznosková, Ralf Ficner, and Leoš Shivaya Valášek. 2014. "Structural Integrity of the PCI Domain of eIF3a/TIF32 Is Required for mRNA Recruitment to the 43S Pre-Initiation Complexes." *Nucleic Acids Research* 42 (6): 4123–39.
Kim, Tae-Houn, Byung-Hoon Kim, Avital Yahalom, Daniel A. Chamovitz, and Albrecht G. von Arnim. 2004. "Translational Regulation via 5' mRNA Leader Sequences Revealed by Mutational Analysis of the Arabidopsis Translation Initiation Factor Subunit eIF3h." *The Plant Cell* 16 (12): 3341–56.
Koditz, J., J. Nesper, M. Wottawa, D. P. Stiehl, G. Camenisch, C. Franke, J. Myllyharju, R. H. Wenger, and D. M. Katschinski. 2007. "Oxygen-Dependent ATF-4 Stability Is Mediated by the PHD3 Oxygen Sensor." *Blood* 110 (10): 3610–17.
Korneeva, N. L., B. J. Lamphear, F. L. Hennigan, and R. E. Rhoads. 2000. "Mutually Cooperative Binding of Eukaryotic Translation Initiation Factor (eIF) 3 and eIF4A to Human eIF4G-1." *The Journal of Biological Chemistry* 275 (52): 41369–76.
Kouba, Tomáš, István Dányi, Stanislava Gunišová, Vanda Munzarová, Vladislava Vlčková, Lucie Cuchalová, Andreas Neueder, Philipp Milkereit, and Leoš Shivaya Valášek. 2012. "Small Ribosomal Protein RPS0 Stimulates Translation Initiation by Mediating 40S-Binding of eIF3 via Its Direct Contact with the eIF3a/TIF32 Subunit." *PloS One* 7 (7): e40464.
Kovarik, P., J. Hasek, L. Valásek, and H. Ruis. 1998. "RPG1: An Essential Gene of Saccharomyces Cerevisiae Encoding a 110-kDa Protein Required for Passage through the G1 Phase." *Current Genetics* 33 (2): 100–109.
Kozak, M. 1978. "How Do Eucaryotic Ribosomes Select Initiation Regions in Messenger RNA?" *Cell* 15 (4): 1109–23.
Kozak, M. 1986. "Point Mutations Define a Sequence Flanking the AUG Initiator Codon That Modulates Translation by Eukaryotic Ribosomes." *Cell* 44 (2): 283–92.
Kozak, M. 2001. "Constraints on Reinitiation of Translation in Mammals." *Nucleic Acids Research* 29 (24): 5226–32.
Kozak, M. 1987. "An Analysis of 5'-Noncoding Sequences from 699 Vertebrate Messenger RNAs." *Nucleic Acids Research* 15 (20): 8125–48.
Kozak, M. 1999. "Initiation of Translation in Prokaryotes and Eukaryotes." *Gene* 234 (2): 187–208.
Lassot, Irina, Emilie Estrabaud, Stephane Emiliani, Monsef Benkirane, Richard Benarous, and Florence Margottin-Goguet. 2005. "p300 Modulates ATF4 Stability and Transcriptional Activity Independently of Its Acetyltransferase Domain." *The Journal of Biological Chemistry* 280 (50): 41537–45.
Lassot, I., E. Ségéral, C. Berlioz-Torrent, H. Durand, L. Groussin, T. Hai, R. Benarous, and F. Margottin-Goguet. 2001. "ATF4 Degradation Relies on a Phosphorylation-Dependent Interaction with the SCF(betaTrCP) Ubiquitin Ligase." *Molecular and Cellular Biology* 21 (6): 2192–2202.
Lawless, Craig, Richard D. Pearson, Julian N. Selley, Julia B. Smirnova, Christopher M.

Grant, Mark P. Ashe, Graham D. Pavitt, and Simon J. Hubbard. 2009. “Upstream Sequence Elements Direct Post-Transcriptional Regulation of Gene Expression under Stress Conditions in Yeast.” *BMC Genomics* 10 (January): 7.

Lee, Sooncheol, Botao Liu, Soohyun Lee, Sheng-Xiong Huang, Ben Shen, and Shu-Bing Qian. 2012. “Global Mapping of Translation Initiation Sites in Mammalian Cells at Single-Nucleotide Resolution.” *Proceedings of the National Academy of Sciences of the United States of America* 109 (37): E2424–32.

Lee, Yun-Young, Randal C. Cevallos, and Eric Jan. 2009. “An Upstream Open Reading Frame Regulates Translation of GADD34 during Cellular Stresses That Induce eIF2α Phosphorylation.” *The Journal of Biological Chemistry* 284 (11): 6661–73.

LeFebvre, Aaron K., Nadejda L. Korneeva, Marjan Trutschl, Urska Cvek, Roy D. Duzan, Christopher A. Bradley, John W. B. Hershey, and Robert E. Rhoads. 2006. “Translation Initiation Factor eIF4G-1 Binds to eIF3 through the eIF3e Subunit.” *The Journal of Biological Chemistry* 281 (32): 22917–32.

Llácer, Jose L., Tanweer Hussain, Laura Marler, Colin Echeverría Aitken, Anil Thakur, Jon R. Lorsch, Alan G. Hinnebusch, and V. Ramakrishnan. 2015. “Conformational Differences between Open and Closed States of the Eukaryotic Translation Initiation Complex.” *Molecular Cell* 59 (3): 399–412.

Lenge, Kathleen, and Kathleen L. Lenge. 2012. “Cell Type-Dependent Function of Atf5: Where We Go from Here.” *Cell & Developmental Biology* 01 (05). doi:10.4172/2168-9296.1000e114.

Lomakin, Ivan B., Elena A. Stolboushkina, Anand T. Vaidya, Chenguang Zhao, Maria B. Garber, Sergey E. Dmitriev, and Thomas A. Steitz. 2017. “Crystal Structure of the Human Ribosome in Complex with DENR-MCT-1.” *Cell Reports* 20 (3): 521–28.

Loughran, Gary, Matthew S. Sachs, John F. Atkins, and Ivaylo P. Ivanov. 2012. “Stringency of Start Codon Selection Modulates Autoregulation of Translation Initiation Factor eIF5.” *Nucleic Acids Research* 40 (7): 2898–2906.

Lu, Phoebe D., Heather P. Harding, and David Ron. 2004. “Translation Reinitiation at Alternative Open Reading Frames Regulates Gene Expression in an Integrated Stress Response.” *The Journal of Cell Biology* 167 (1): 27–33.

Maag, David, Mikkel A. Algire, and Jon R. Lorsch. 2006. “Communication between Eukaryotic Translation Initiation Factors 5 and 1A within the Ribosomal Pre-Initiation Complex Plays a Role in Start Site Selection.” *Journal of Molecular Biology* 356 (3): 724–37.

Martina, J. A., H. I. Diab, O. A. Brady, and R. Puertollano. 2016. “TFEB and TFE3 Are Novel Components of the Integrated Stress Response.” *The EMBO Journal* 35 (5): 479–95.

Masuoka, Howard C., and Tim M. Townes. 2002. “Targeted Disruption of the Activating Transcription Factor 4 Gene Results in Severe Fetal Anemia in Mice.” *Blood* 99 (3): 736–45.

Ma, Yanjun, and Linda M. Hendershot. 2003. “Delineation of a Negative Feedback Regulatory Loop That Controls Protein Translation during Endoplasmic Reticulum Stress.” *The Journal of Biological Chemistry* 278 (37): 34864–73.

Mendell, Joshua T., Neda A. Sharifi, Jennifer L. Meyers, Francisco Martinez-Murillo, and Harry C. Dietz. 2004. “Nonsense Surveillance Regulates Expression of Diverse Classes of Mammalian Transcripts and Mutes Genomic Noise.” *Nature Genetics* 36 (10): 1073–78.

Mitchell, Sarah F., Sarah E. Walker, Mikkel A. Algire, Eun-Hee Park, Alan G. Hinnebusch, and Jon R. Lorsch. 2010. “The 5’-7-Methylguanosine Cap on Eukaryotic mRNAs Serves Both to Stimulate Canonical Translation Initiation and to Block an Alternative Pathway.” *Molecular Cell* 39 (6): 950–62.

Mohammad, Mahabub Pasha, Vanda Munzarová Pondelícková, Jakub Zeman, Stanislava Gunišová, and Leoš Shivaya Valášek. 2017. “In Vivo Evidence That eIF3 Stays Bound to Ribosomes Elongating and Terminating on Short Upstream ORFs to Promote Reinitiation.” *Nucleic Acids Research* 45 (5): 2658–74.

Morino, S., H. Imataka, Y. V. Svitkin, T. V. Pestova, and N. Sonenberg. 2000. “Eukaryotic Translation Initiation Factor 4E (eIF4E) Binding Site and the Middle One-Third of eIF4GI Constitute the Core Domain for Cap-Dependent Translation, and the C-Terminal One-Third Functions as a Modulatory Region.” *Molecular and Cellular Biology* 20 (2): 468–77.

Munzarová, Vanda, Josef Pánek, Stanislava Gunišová, István Dányi, Béla Szamecz, and Leoš Shivaya Valášek. 2011. “Translation Reinitiation Relies on the Interaction between eIF3a/TIF32 and Progressively Folded Cis-Acting mRNA Elements Preceding Short uORFs.” *PLoS Genetics* 7 (7): e1002137.

Nagalakshmi, Ugrappa, Zhong Wang, Karl Waern, Chong Shou, Debasish Raha, Mark Gerstein, and Michael Snyder. 2008. “The Transcriptional Landscape of the Yeast Genome Defined by RNA Sequencing.” *Science* 320 (5881): 1344–49.

Novoa, I., H. Zeng, H. P. Harding, and D. Ron. 2001. “Feedback Inhibition of the Unfolded Protein Response by GADD34-Mediated Dephosphorylation of eIF2alpha.” *The Journal of Cell Biology* 153 (5): 1011–22.

Ord, Daima, Kati Meerits, and Tõnis Ord. 2007. “TRB3 Protects Cells against the Growth Inhibitory and Cytotoxic Effect of ATF4.” *Experimental Cell Research* 313 (16): 3556–67.

Pakos-Zebrucka, Karolina, Izabela Koryga, Katarzyna Mnich, Mila Ljujic, Afshin Samali, and Adrienne M. Gorman. 2016. “The Integrated Stress Response.” *EMBO Reports* 17 (10): 1374–95.

Palam, Lakshmi Reddy, Thomas D. Baird, and Ronald C. Wek. 2011. “Phosphorylation of eIF2 Facilitates Ribosomal Bypass of an Inhibitory Upstream ORF to Enhance CHOP Translation.” *The Journal of Biological Chemistry* 286 (13): 10939–49.

Park, H. S., A. Himmelbach, K. S. Browning, T. Hohn, and L. A. Ryabova. 2001. “A Plant Viral ‘Reinitiation’ Factor Interacts with the Host Translational Machinery.” *Cell* 106 (6): 723–33.

Park, Yeonwoo, Andrea Reyna-Neyra, Lucas Philippe, and Carson C. Thoreen. 2017. “mTORC1 Balances Cellular Amino Acid Supply with Demand for Protein Synthesis through Post-Transcriptional Control of ATF4.” *Cell Reports* 19 (6): 1083–90.

Pasini, Silvia, Carlo Corona, Jin Liu, Lloyd A. Greene, and Michael L. Shelanski. 2015. “Specific Downregulation of Hippocampal ATF4 Reveals a Necessary Role in Synaptic Plasticity and Memory.” *Cell Reports* 11 (2): 183–91.

Passmore, Lori A., T. Martin Schmeing, David Maag, Drew J. Applefield, Michael G. Acker, Mikkel A. Algire, Jon R. Lorsch, and V. Ramakrishnan. 2007. “The Eukaryotic Translation Initiation Factors eIF1 and eIF1A Induce an Open Conformation of the 40S Ribosome.” *Molecular Cell* 26 (1): 41–50.

Pestova, Tatyana V., and Victoria G. Kolupaeva. 2002. “The Roles of Individual Eukaryotic Translation Initiation Factors in Ribosomal Scanning and Initiation Codon Selection.” *Genes & Development* 16 (22): 2906–22.

Pestova, T. V., I. B. Lomakin, J. H. Lee, S. K. Choi, T. E. Dever, and C. U. Hellen. 2000. “The Joining of Ribosomal Subunits in Eukaryotes Requires eIF5B.” *Nature* 403 (6767): 332–35.

Pisarev, Andrey V., Christopher U. T. Hellen, and Tatyana V. Pestova. 2007. “Recycling of Eukaryotic Posttermination Ribosomal Complexes.” *Cell* 131 (2): 286–99.

Pisarev, Andrey V., Victoria G. Kolupaeva, Marat M. Yusupov, Christopher U. T. Hellen, and Tatyana V. Pestova. 2008. “Ribosomal Position and Contacts of mRNA in Eukaryotic Translation Initiation Complexes.” *The EMBO Journal* 27 (11): 1609–21.

Pisareva, Vera P., and Andrey V. Pisarev. 2016. “DHX29 and eIF3 Cooperate in Ribosomal Scanning on Structured mRNAs during Translation Initiation.” *RNA* . doi:10.1261/rna.057851.116.

Poyry T Kaminski A. 2004. “What Determines Whether Mammalian Ribosomes Resume Scanning after Translation of a Short Upstream Open Reading Frame?” *Genes & Development* 18 (1): 62–75.

Poyry, Tuija A. A., Ann Kaminski, Emma J. Connell, Christopher S. Fraser, and Richard J.

Jackson. 2007. “The Mechanism of an Exceptional Case of Reinitiation after Translation of a Long ORF Reveals Why Such Events Do Not Generally Occur in Mammalian mRNA Translation.” *Genes & Development* 21 (23): 3149–62.

Rajkowitsch, Lukas, Cristina Vilela, Karine Berthelot, Carmen Velasco Ramirez, and John E. G. McCarthy. 2004. “Reinitiation and Recycling Are Distinct Processes Occurring Downstream of Translation Termination in Yeast.” *Journal of Molecular Biology* 335 (1): 71–85.

Rowlands, A. G., R. Panniers, and E. C. Henshaw. 1988. “The Catalytic Mechanism of Guanine Nucleotide Exchange Factor Action and Competitive Inhibition by Phosphorylated Eukaryotic Initiation Factor 2.” *The Journal of Biological Chemistry* 263 (12): 5526–33.

Roy, Bijoyita, Justin N. Vaughn, Byung-Hoon Kim, Fujun Zhou, Michael A. Gilchrist, and Albrecht G. Von Arnim. 2010. “The H Subunit of eIF3 Promotes Reinitiation Competence during Translation of mRNAs Harboring Upstream Open Reading Frames.” *RNA* 16 (4): 748–61.

Ruiz-Echevarría, M. J., and S. W. Peltz. 2000. “The RNA Binding Protein Pub1 Modulates the Stability of Transcripts Containing Upstream Open Reading Frames.” *Cell* 101 (7): 741–51.

Rutkowski, D. Thomas, and Randal J. Kaufman. 2003. “All Roads Lead to ATF4.” *Developmental Cell* 4 (4): 442–44.

Schleich, Sibylle, Julieta M. Acevedo, Katharina Clemm von Hohenberg, and Aurelio A. Teleman. 2017. “Identification of Transcripts with Short stuORFs as Targets for DENR•MCTS1-Dependent Translation in Human Cells.” *Scientific Reports* 7 (1): 3722.

Schleich, Sibylle, Katrin Strassburger, Philipp Christoph Janiesch, Tatyana Koledachkina, Katharine K. Miller, Katharina Haneke, Yong-Sheng Cheng, et al. 2014. “DENR-MCT-1 Promotes Translation Re-Initiation Downstream of uORFs to Control Tissue Growth.” *Nature* 512 (7513): 208–12.

Shin, Dong Hae, Hisao Yokota, Rosalind Kim, and Sung-Hou Kim. 2002. “Crystal Structure of a Conserved Hypothetical Protein from Escherichia Coli.” *Journal of Structural and Functional Genomics* 2 (1): 53–66.

Sidrauski, Carmela, Anna M. McGeachy, Nicholas T. Ingolia, and Peter Walter. 2015. “The Small Molecule ISRIB Reverses the Effects of eIF2α Phosphorylation on Translation and Stress Granule Assembly.” *eLife* 4 (February). doi:10.7554/eLife.05033.

Siu, Fai, Perry J. Bain, Rene LeBlanc-Chaffin, Hong Chen, and Michael S. Kilberg. 2002. “ATF4 Is a Mediator of the Nutrient-Sensing Response Pathway That Activates the Human Asparagine Synthetase Gene.” *The Journal of Biological Chemistry* 277 (27): 24120–27.

Sonenberg, Nahum, and Alan G. Hinnebusch. 2009. “Regulation of Translation Initiation in Eukaryotes: Mechanisms and Biological Targets.” *Cell* 136 (4): 731–45.

Srivastava, Sri P., Kotlo U. Kumar, and Randal J. Kaufman. 1998. “Phosphorylation of Eukaryotic Translation Initiation Factor 2 Mediates Apoptosis in Response to Activation of the Double-Stranded RNA-Dependent Protein Kinase.” *The Journal of Biological Chemistry* 273 (4): 2416–23.

Starck, Shelley R., Jordan C. Tsai, Keling Chen, Michael Shodiya, Lei Wang, Kinnosuke Yahiro, Manuela Martins-Green, Nilabh Shastri, and Peter Walter. 2016. “Translation from the 5’ Untranslated Region Shapes the Integrated Stress Response.” *Science* 351 (6272): aad3867.

Szamecz, Béla, Edit Rutkai, Lucie Cuchalová, Vanda Munzarová, Anna Herrmannová, Klaus H. Nielsen, Laxminarayana Burela, Alan G. Hinnebusch, and Leoš Valášek. 2008. “eIF3a Cooperates with Sequences 5’ of uORF1 to Promote Resumption of Scanning by Post-Termination Ribosomes for Reinitiation on GCN4 mRNA.” *Genes & Development* 22 (17): 2414–25.

Tanaka, Mayuki, Naoyuki Sotta, Yusuke Yamazumi, Yui Yamashita, Kyoko Miwa,

Katsunori Murota, Yukako Chiba, et al. 2016. “The Minimum Open Reading Frame, AUG-Stop, Induces Boron-Dependent Ribosome Stalling and mRNA Degradation.” *The Plant Cell* 28 (11): 2830–49.

Tanaka, T., T. Tsujimura, K. Takeda, A. Sugihara, A. Maekawa, N. Terada, N. Yoshida, and S. Akira. 1998. “Targeted Disruption of ATF4 Discloses Its Essential Role in the Formation of Eye Lens Fibres.” *Genes to Cells: Devoted to Molecular & Cellular Mechanisms* 3 (12): 801–10.

Valášek, Leoš Shivaya, Jakub Zeman, Susan Wagner, Petra Beznosková, Zuzana Pavlíková, Mahabub Pasha Mohammad, Vladislava Hronová, Anna Herrmannová, Yaser Hashem, and Stanislava Gunišová. 2017. “Embraced by eIF3: Structural and Functional Insights into the Roles of eIF3 across the Translation Cycle.” *Nucleic Acids Research* 45 (19): 10948–68.

Vattem, Krishna M., and Ronald C. Wek. 2004. “Reinitiation Involving Upstream ORFs Regulates ATF4 mRNA Translation in Mammalian Cells.” *Proceedings of the National Academy of Sciences of the United States of America* 101 (31): 11269–74.

Vilela, C., B. Linz, C. Rodrigues-Pousada, and J. E. McCarthy. 1998. “The Yeast Transcription Factor Genes YAP1 and YAP2 Are Subject to Differential Control at the Levels of Both Translation and mRNA Stability.” *Nucleic Acids Research* 26 (5): 1150–59.

Villa, Nancy, Angelie Do, John W. B. Hershey, and Christopher S. Fraser. 2013. “Human Eukaryotic Initiation Factor 4G (eIF4G) Protein Binds to eIF3c, -D, and -E to Promote mRNA Recruitment to the Ribosome.” *The Journal of Biological Chemistry* 288 (46): 32932–40.

Vivier, M. A., P. Sollitti, and I. S. Pretorius. 1999. “Functional Analysis of Multiple AUG Codons in the Transcripts of the STA2 Glucoamylase Gene from Saccharomyces Cerevisiae.” *Molecular & General Genetics: MGG* 261 (1): 11–20.

Wagner, Susan, Anna Herrmannová, Darina Šikrová, and Leoš Shivaya Valášek. 2016. “Human eIF3b and eIF3a Serve as the Nucleation Core for the Assembly of eIF3 into Two Interconnected Modules: The Yeast-like Core and the Octamer.” *Nucleic Acids Research* 44 (22): 10772–88.

Wang, Z., A. Gaba, and M. S. Sachs. 1999. “A Highly Conserved Mechanism of Regulated Ribosome Stalling Mediated by Fungal Arginine Attenuator Peptides That Appears Independent of the Charging Status of Arginyl-tRNAs.” *The Journal of Biological Chemistry* 274 (53): 37565–74.

Watatani, Yujiro, Kenji Ichikawa, Noriko Nakanishi, Maki Fujimoto, Hitoshi Takeda, Natsumi Kimura, Hidenori Hirose, Shigeru Takahashi, and Yuji Takahashi. 2008. “Stress-Induced Translation of ATF5 mRNA Is Regulated by the 5’-Untranslated Region.” *The Journal of Biological Chemistry* 283 (5): 2543–53.

Wei, Jiajie, Cheng Wu, and Matthew S. Sachs. 2012. “The Arginine Attenuator Peptide Interferes with the Ribosome Peptidyl Transferase Center.” *Molecular and Cellular Biology* 32 (13): 2396–2406.

Wells, S. E., P. E. Hillner, R. D. Vale, and A. B. Sachs. 1998. “Circularization of mRNA by Eukaryotic Translation Initiation Factors.” *Molecular Cell* 2 (1): 135–40.

Wethmar, K., J. Schulz, E. M. Muro, S. Talyan, M. A. Andrade-Navarro, and A. Leutz. 2016. “Comprehensive Translational Control of Tyrosine Kinase Expression by Upstream Open Reading Frames.” *Oncogene* 35 (13): 1736–42.

Yang, Xiangli, Koichi Matsuda, Peter Bialek, Sylvie Jacquot, Howard C. Masuoka, Thorsten Schinke, Lingzhen Li, et al. 2004. “ATF4 Is a Substrate of RSK2 and an Essential Regulator of Osteoblast Biology; Implication for Coffin-Lowry Syndrome.” *Cell* 117 (3): 387–98.

Zhao, Erhu, Jane Ding, Yingfeng Xia, Mengling Liu, Bingwei Ye, Jeong-Hyeon Choi, Chunhong Yan, et al. 2016. “KDM4C and ATF4 Cooperate in Transcriptional Control of Amino Acid Metabolism.” *Cell Reports* 14 (3): 506–19.

Zhou, Donghui, L. Reddy Palam, Li Jiang, Jana Narasimhan, Kirk A. Staschke, and Ronald C. Wek. 2008. “Phosphorylation of eIF2 Directs ATF5 Translational Control in

Response to Diverse Stress Conditions." *The Journal of Biological Chemistry* 283 (11): 7064–73.
Zhou, Xubin, Rong Wang, Libin Fan, Yan Li, Li Ma, Zhenye Yang, Wei Yu, Naihe Jing, and Xueliang Zhu. 2005. "Mitosin/CENP-F as a Negative Regulator of Activating Transcription Factor-4." *The Journal of Biological Chemistry* 280 (14): 13973–77.

Published online 13 January 2014 *Nucleic Acids Research, 2014, Vol. 42, No. 6* **4123–4139**
doi:10.1093/nar/gkt1369

Structural integrity of the PCI domain of eIF3a/TIF32 is required for mRNA recruitment to the 43S pre-initiation complexes

Sohail Khoshnevis[1,†], Stanislava Gunišová[2,†], Vladislava Vlčková[2,†], Tomáš Kouba[2], Piotr Neumann[1], Petra Beznosková[2], Ralf Ficner[1,*] and Leoš Shivaya Valášek[2,*]

[1]Department of Molecular Structural Biology, Institute for Microbiology and Genetics, George-August University, Goettingen, Germany, 37077 and [2]Laboratory of Regulation of Gene Expression, Institute of Microbiology ASCR, Videnska 1083, 142 20 Prague, the Czech Republic

Received April 19, 2013; Revised December 3, 2013; Accepted December 12, 2013

ABSTRACT

Transfer of genetic information from genes into proteins is mediated by messenger RNA (mRNA) that must be first recruited to ribosomal pre-initiation complexes (PICs) by a mechanism that is still poorly understood. Recent studies showed that besides eIF4F and poly(A)-binding protein, eIF3 also plays a critical role in this process, yet the molecular mechanism of its action is unknown. We showed previously that the PCI domain of the eIF3c/NIP1 subunit of yeast eIF3 is involved in RNA binding. To assess the role of the second PCI domain of eIF3 present in eIF3a/TIF32, we performed its mutational analysis and identified a 10-Ala-substitution (Box37) that severely reduces amounts of model mRNA in the 43–48S PICs *in vivo* as the major, if not the only, detectable defect. Crystal structure analysis of the a/TIF32-PCI domain at 2.65-Å resolution showed that it is required for integrity of the eIF3 core and, similarly to the c/NIP1-PCI, is capable of RNA binding. The putative RNA-binding surface defined by positively charged areas contains two Box37 residues, R363 and K364. Their substitutions with alanines severely impair the mRNA recruitment step *in vivo* suggesting that a/TIF32-PCI represents one of the key domains ensuring stable and efficient mRNA delivery to the PICs.

INTRODUCTION

Protein biosynthesis begins with formation of the 43S pre-initiation complex (PIC) consisting of the small ribosomal subunit, Met-tRNA$_i^{Met}$ [in the form of the ternary complex (TC) together with the eukaryotic initiation factor eIF2 in its GTP form], eIF1A, eIF1, eIF3 and eIF5 [reviewed in (1)]. In the following step, messenger RNA (mRNA) is loaded onto the 43S PIC with help of eIF3, poly(A)-binding protein (PABP) and the eIF4F factors bound to its 5′ 7-methylguanosine cap structure, producing the 48S PIC. Subsequently, usually the first AUG codon in the mRNA's 5′ UTR is recognized as the start site during the successive movement—called scanning—of the 48S PICs downstream from the cap. On AUG recognition, eIF2 in its GDP form is released from the ribosome along with several other eIFs, the 60S subunit joins the 40S•Met-tRNA$_i^{Met}$•mRNA complex in a reaction promoted by eIF5B and the resulting 80S initiation complex is on ejection of the remaining eIFs—with the exception of eIF3 and perhaps also eIF4F (2,3)—prepared for elongation.

In prokaryotes, the mRNA recruitment step is well defined and involves a direct RNA–RNA interaction between the 3′-end of 16S rRNA of the small ribosomal subunit and a specific Shine–Dalgarno sequence located in the 5′-end of mRNAs to allow direct positioning of the AUG start codon into the ribosomal P-site. In contrast, eukaryotic mRNAs do not contain anything like Shine–Dalgarno, initiating AUG is usually tens or even hundreds of nucleotides downstream from the cap and their recruitment to the 43 PICs requires the concerted action of several eIFs. This step, along with the subsequent scanning (base-to-base inspection of the mRNA's 5′ UTR), represents one of the least understood reactions in the entire eukaryotic initiation pathway. In the current textbook view, eIF3, PABP and the eIF4F complex (comprising the molecular scaffold eIF4G, to which the

*To whom correspondence should be addressed. Tel: +420 241 062 288; Fax: +420 241 062 665; Email: valasekl@biomed.cas.cz
Correspondence may also be addressed to Ralf Ficner. Tel: +49 5513 914 072; Fax: +49 5513 914 082; Email: ralf.ficner@biologie.uni-goettingen.de
Present address:
Sohail Khoshnevis, Department of Cancer Biology, The Scripps Research Institute, Jupiter, FL 33458, USA.

†These authors contributed equally to the paper as first authors.

© The Author(s) 2014. Published by Oxford University Press.
This is an Open Access article distributed under the terms of the Creative Commons Attribution License (http://creativecommons.org/licenses/by/3.0/), which permits unrestricted reuse, distribution, and reproduction in any medium, provided the original work is properly cited.

cap-binding protein eIF4E and the DEAD-box RNA helicase eIF4A bind) are proposed to be responsible for mRNA loading to the 43S PICs [reviewed in (1)]. Besides eIF4E and eIF4A, the scaffold eIF4G also interacts with PABP and, in mammals, with eIF3 (4–8). The eIF4G–eIF3 interaction has been long believed to serve as the umbilical cord connecting the eIF4F•mRNA and 43S complexes, thus mediating formation of the 48S PIC, at least in mammals [in budding yeast, where the eIF3-binding domain in eIF4G is not evident, the direct eIF3–eIF4G interaction has never been detected (9)]. However, recent *in vivo* findings suggested that not only in yeast but probably also in mammals the mRNA recruitment step might be a lot less dependent on the direct eIF4G–eIF3 contact than it has been believed so far (10–13). Consistently, recent *in vivo* and *in vitro* studies in yeast indicated that eIF3 plays a more critical role in mRNA recruitment than eIF4G (14,15). Certainly, a more systematic approach is needed to fully understand this critical initiation step that is also known to serve as one of the two major targets for the general translational control [reviewed in (16)]. The first attempt in this direction has been recently made by identifying several mutations occurring in the j/HCR1-like domain (HLD) of the eIF3a/TIF32 subunit that, besides other effects on general initiation steps, also partially affected efficiency of the model mRNA recruitment to 40S ribosomes (17).

Despite the critical importance of the multisubunit eIF3 complex in translation—in addition to the mRNA recruitment, it also promotes the TC recruitment, scanning, AUG recognition and strikingly also translation termination (17–27)—a high-resolution structural picture of both yeast and mammalian eIF3 as whole remains elusive. Only partial either crystal or nuclear magnetic resonance structures were solved for a handful of domains of some of the eIF3 subunits, alongside the low-resolution Cryo-EM structure of the 13-subunit human eIF3 (28,29). In particular, the structures of RNA recognition motif (RRM) of yeast eIF3b/PRT1 subunit (30) as well as its human ortholog alone (31) or bound to the N-terminal peptide of eIF3j/HCR1 (24), the seven-bladed β-propeller of the WD40 eIF3i/TIF34 subunit bound to the extreme C-terminal α-helix of b/PRT1 (25), the RRM of human eIF3g/TIF35 (19) and finally the atypical PCI domain-containing human eIF3k subunit (32) have been determined at atomic resolution so far. The PCI domain is a conserved bipartite domain comprising the helical bundle (HB) and winged-helix (WH) subdomains initially identified as the principal scaffold for the multisubunit 26S proteasome lid, signalosome (CSN) and eIF3 complexes (33). Yeast eIF3 contains two PCI domains, one at the N-terminus of its eIF3a/TIF32 subunit and the other at the C-terminus of eIF3c/NIP1. In fact, the 3D architecture of the eIF3c/NIP1-PCI was recently predicted *in silico* and proposed to fold into a typical bipartite arrangement (34). Most of these partial structures and the latter prediction were incorporated into a structural model of yeast eIF3 shown in Figure 1A. Importantly, the latter report also revealed for the first time that the c/NIP1-PCI domain, this typical protein–protein interacting mediator, is capable of strong binding to RNA. Later, yeast SAC3 and THP1 components of the TREX-2 transcription–export complex, both containing the PCI domain, were shown to have their WH subdomains juxtaposed in a way forming a platform that is also capable of nucleic acid binding (35).

To analyze the function of the N-terminus of a/TIF32 harboring the second PCI domain of yeast eIF3, we undertook a systematic mutagenesis of a large N-terminal segment of a/TIF32 including an N-terminal part of the PCI domain. We show that a 10-alanine substitution of residues 361–370 (designated Box37) markedly affects growth and translation initiation rates at the elevated temperature. Structural investigation of the a/TIF32-PCI domain showed that it consists of two intimately connected subdomains: an N-terminal right-handed helical domain capped by a C-terminal winged helix domain. Furthermore, we provide evidence that specifically the PCI domain of a/TIF32 (i) mediates its binding to the eIF3c/NIP1 subunit of eIF3 and (ii) that the entire N-terminal half of a/TIF32 interacts with RNA, as proposed before (2,37). Interestingly, neither the N-terminal domain nor the PCI domain alone is sufficient for this binding; however, they are both required. In addition to that, we show that α-helix 4 of the HB subdomain, and in particular its two consecutive basic residues R363 and K364, strongly contributes to mRNA recruitment of the model mRNAs to the 43S PICs *in vivo*. Although R363 is also required for stabilization of the HB fold, K364 is fully exposed to the solvent with no structural role. Further analysis of the crystal structure and the *in silico*-generated structure of the helical region preceding this domain revealed the dominance of continuous positively charged areas over the surface of the a/TIF32 N-terminal half, proposing a molecular basis for its role in RNA recruitment. In support, 10-Ala substitutions of these basic patches resulted in lethality. Taken together, because our mutants in Box37 impair the mRNA loading process as the only detectable defect *in vivo*, we propose that one of the key roles of this well-defined domain is, besides building the eIF3 core, to contact mRNAs in a non-specific manner and promote their delivery to and/or stable binding on the small ribosomal subunit. Hence, the a/TIF32-PCI domain is yet another PCI domain demonstrated to be involved in RNA binding.

MATERIALS AND METHODS

Yeast strains, plasmids and biochemical methods

Lists of strains, plasmids and oligonucleotides used in this study (Supplementary Tables S1–S3), details of their construction, as well as description of all well-established biochemical assays used throughout the study can be found in the Supplementary Data that are available at NAR online.

Cloning, expression, purification and crystallization of the a/TIF32$^{276-494}$ domain and crystal structure determination

a/TIF32$^{276-494}$ was cloned into a pGEX6P1 vector, expressed in *Escherichia coli* Rosetta2 (DE3) cells and purified via affinity and size-exclusion chromatography (SEC) (detailed purification schemes of proteins used in

A

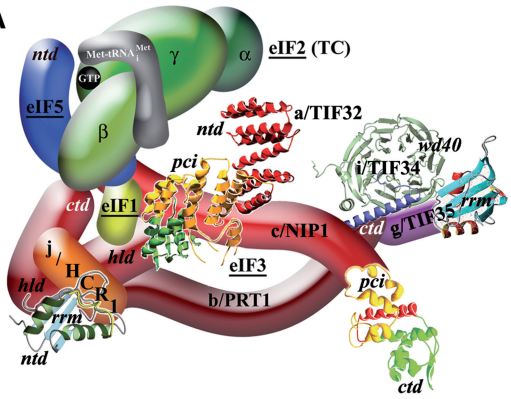

B

mutation	30°C	34°C	37°C	basic residues	description
a/TIF32 - wt	-	-	-		
a/TIF32-BOX20	let	let	let	R194,R195,K196	back RNA track
a/TIF32-BOX24	let	let	let	R235	front RNA track
a/TIF32-BOX27	let	let	let	K268	along the front RNA track below region 2
a/TIF32-BOX29	let	let	let	K288	along the front RNA track below region 2
a/TIF32-BOX31	let	let	let	K304,K305,K308	basic region 2
a/TIF32-BOX34	-	+	+++		long loop
a/TIF32-BOX35	let	let	let	R350	basic region 1
a/TIF32-BOX37	-	+	+++++	R363,K364	basic region 3
a/TIF32-BOX38	let	let	let		not involved in RNA binding surface

C

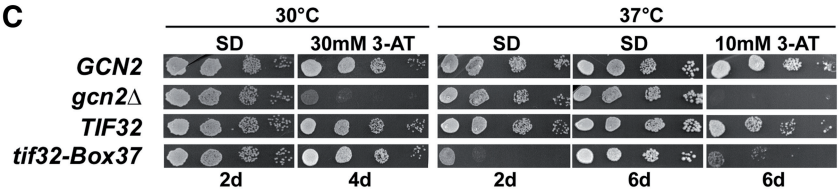

D

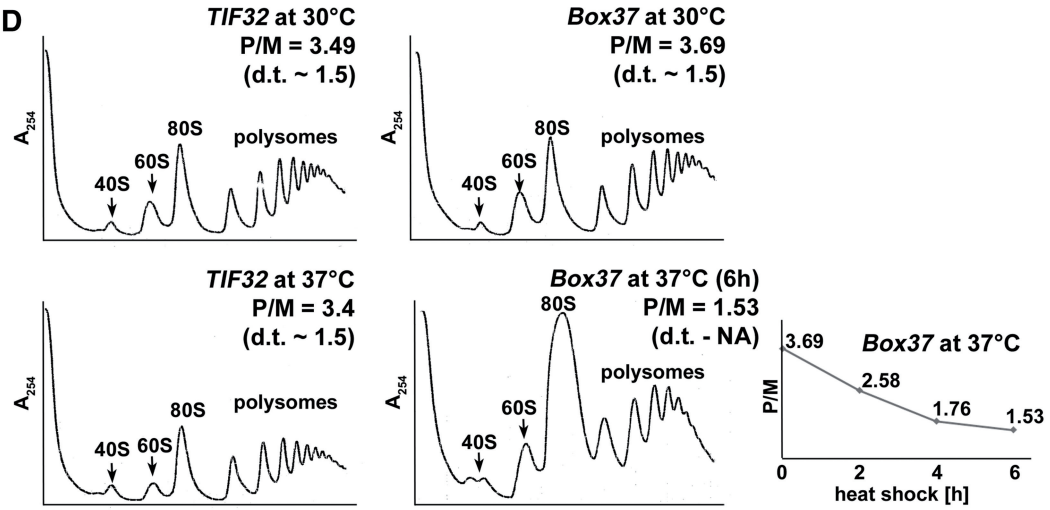

Figure 1. The 10-Ala *Box37* substitution of α-helix 4 of the HB subdomain in the a/TIF32-PCI domain reduces the translation initiation rates at the restrictive temperature. (**A**) A 3D model of eIF3 and its associated eIFs in the MFC [adapted from (25)]. *ntd*, N-terminal domain; *ctd*, C-terminal domain; *hld*, HCR1-like domain; *rrm*, RNA recognition motif; *pci*, PCI domain; TC, ternary complex. The nuclear magnetic resonance structure of the interaction between the RRM of human eIF3b (green and light blue) and the N-terminal peptide of human eIF3j (yellow) (24), the nuclear magnetic resonance structure of the C-terminal RRM of human eIF3g (19), the X-ray structure of the yeast i/TIF34–b/PRT1-CTD complex (green versus blue) (25), the X-ray structure of the a/TIF32-PCI (yellow and green) and structural prediction of the N-terminal domain of a/TIF32 (red) (both this study) and the 3D homology model of the c/NIP1-CTD (34) were used to replace the original schematic representations of the

(continued)

this study are provided in Supplementary Methods). Crystals were grown at 4°C in sitting drop vapor diffusion plates by mixing 0.8 µl of crystallization solution [100 mM HEPES, pH 7, 12% (w/v) PEG 2000, 80 mM $MnCl_2$] and 1.2 µl of protein solution (at a concentration of 6 mg/ml in the gel filtration buffer). Crystals were cryoprotected by soaking in reservoir solution supplemented with increasing concentration of PEG400 to 40% (w/v) and flash frozen in liquid nitrogen before data collection.

X-ray diffraction images were collected at 100 K at beamline 14.1 [BESSY, Berlin, Germany; (37)] equipped with a MAR Mosaic 225 mm CCD detector (Norderstedt, Germany). The oscillation images were indexed, integrated and merged using the XDS package (38,39) to the final resolution of 2.65 Å for the native and to 2.79, 2.81 and 2.97 Å for Se-Met derivative crystal (peak, inflection and remote data sets, respectively). The crystal structure of a/TIF32 was solved by means of single wavelength anomalous dispersion SAD using the Se-Met data set at the peak wavelength in SHARP/autoSHARP (40). Within autoSHARP, the heavy atom search was performed by SHELXD (41) and resulted in localizing four heavy atom positions that were further refined using SHARP followed by density modification in Solomon (42) and automatic model building in Arp/wARP (43). Structure determination and refinement procedure are discussed in detail in Supplementary Methods.

RNA-binding assay

RNA-binding studies were performed in 1× recon buffer (44). Two micromolars of *DAD4* RNA (see Supplementary Methods for transcription procedure) was mixed with 10 µM a/TIF32^{FL}, a/TIF32$^{1-494}$, a/TIF32$^{276-494}$, GST-a/TIF32$^{1-276}$ and GST in a total volume of 10 µl. After a 30-min incubation on ice, samples were mixed with native loading dye and applied to a 0.8% agarose gel supplemented with GelRed (Biotium). Electrophoresis was performed at 90 V for 30 min on ice using pre-cooled 1 × Tris acetate + ethylenediaminetetraacetic acid running buffer. The gel was subsequently exposed to ultraviolet-light to visualize nucleic acids.

Binding of the a/TIF32$^{276-494}$ domain to c/NIP1 by analytical SEC

Interaction studies were performed on an analytical Superdex 200 (10/300) column (GE Healthcare) in a buffer containing 150 mM KCl, 10 mM Hepes, pH 7.5, and 5% glycerol. Fifty micrograms of c/NIP1 (0.5 nmol), b/PRT1 (0.5 nmol) or a/TIF32$^{276-494}$ (2 nmol) in the total volume of 500 µl was loaded on the column separately or after being incubated together for 30 min.

Isothermal titration calorimetry

c/NIP1 and a/TIF32$^{276-494}$ were extensively dialyzed against ITC buffer (150 mM KCl, 10 mM Hepes, pH 7.5, 5% glycerol) and concentrated to 10 and 100 µM, respectively. The experiment was performed on a VP-ITC calorimeter (Microcal, USA). Twenty microliter aliquots of a/TIF32$^{276-494}$ were injected into the cell containing c/NIP1 every 40 s, during which the titration peak returned to the base line. Separately, seven injections of the same concentration of a/TIF32$^{276-494}$ into the buffers were performed under the same conditions to determine the heat of dilution. The titration data were analyzed using the ORIGIN software to calculate the thermodynamics parameters.

RESULTS

A specific 10-alanine substitution (*Box37*) in the a/TIF32-PCI domain results in temperature sensitivity and reduces translation initiation rates

Domain prediction programs detect two PCI domains in the yeast eIF3 complex. The first one, located at the C-terminus of c/NIP1, was previously implicated in RNA binding as the first PCI domain known to do so (34). Here we sought to investigate the role of the second PCI domain of eIF3 occurring in the N-terminal half of a/TIF32. We have recently demonstrated that the proteolytic digestion of a/TIF32 generates a fragment harboring its first 494 residues (45) suggesting that the entire a/TIF32 N-terminal half, including the PCI domain, is folded into a higher order structure. Earlier we also showed that the a/TIF32 region corresponding to amino acid (aa) residues 201 through 400, encompassing a part of the a/TIF32-PCI domain, interacts with the small ribosomal protein RPS0A (46) situated on the solvent-exposed side near the 40S mRNA exit channel (47).

To show whether the a/TIF32-PCI domain is involved in RPS0A binding and to identify specific residues that mediate this contact, we introduced Ala substitutions in consecutive blocks of 10 residues between amino acids 191 and 400 (dubbed Boxes 20–40) and tested them for growth phenotypes, first in a yeast strain containing a/

Figure 1. Continued
corresponding molecules. (**B**) Summary of the phenotypic analysis of Ala substitutions in consecutive blocks of 10 residues between amino acids 191 and 400 (dubbed Boxes 20–40). The indicated mutant alleles were introduced into the H477 strain containing a/TIF32 under control of *MET3* promoter and tested for growth in the presence of methionine. Alleles showing the Ts$^-$ or Slg$^-$ or lethal (Let) phenotypes are listed; the ± scoring system defines the wt as '–' and no growth as 5+. (**C**) The *tif32-Box37* mutation imparts the Ts$^-$ and Gcn$^-$ phenotypes. YBS52 (*GCN2 a/tif32Δ*) was transformed with YCplac111-based plasmids carrying either *a/TIF32* wt or *a/tif32-Box37* mutant alleles, and the resident YCpTIF32-His-U plasmid was evicted on 5-FOA. The resulting strains, together with isogenic strains H2880 (*GCN2 a/TIF32*; row 1) and H2881 (*gcn2Δ a/TIF32*; row 2) transformed with empty YCplac111 vector, were then spotted in four serial dilutions on SD or SD containing 10- or 30-mM 3-AT and incubated at 30°C or 37°C for up to 6 days. (**D**) The *tif32-Box37* mutation reduces the translation initiation rates at the restrictive temperature. Polysome profiles of *TIF32* wt and *tif32-Box37* mutant strains described in section B were recorded from cells cultured in YPD medium at 30°C or heat shocked at 37°C for indicated time points and subsequently treated with cycloheximide before harvesting. Whole-cell extracts were separated by velocity sedimentation through a 5–45% sucrose gradient centrifugation at 39 000 rpm for 2.5 h. The gradients were collected and scanned at 254 nm to visualize the ribosomal species. Positions of 40S, 60S and 80S species are indicated by arrows, and polysome to monosome (P/M) ratios and doubling times (d.t.) are given above the profiles. The plot indicates P/M ratios collected at various time points of heat shock.

TIF32 under control of *MET3* promoter. Several of these Ala substitutions led to lethal phenotypes (Figure 1B; see also below) in accord with our earlier observation that deletion of the first 350 residues of a/TIF32 is deleterious (18). One of these substitutions, Box37 (residues 361–370), produced strong temperature-sensitive (Ts^-) and Gcn^- phenotypes (Figure 1C), which we could analyze further for its primary defect—the Gcn^- (general control non-derepressible) phenotype indicates an impairment of the *GCN4* induction (see below). (Box34 [residues 331–340] also showed the Ts^- phenotype; however, as it was rather mild, we did not pursue this mutant any further). Careful inspection of polysome profiles carried out at the non-permissive temperature at three time points following the temperature up-shift clearly suggests that the *Box37* mutation specifically affects translation initiation rates as the run-off 80S couples accumulate at the expense of heavy polysomes, which is displayed by ~2.2-fold decrease in the polysome to monosome (P/M) ratio (Figure 1D).

Next we examined the potential effect of *Box37* on the direct interaction of the 201–400 subdomain of a/TIF32 with RPS0A in an *in vitro* binding assay as well as on the integrity of native eIF3 with eIFs 1, 2 and 5 into the ribosome-free multifactor complex (MFC) *in vivo*. Neither was found dramatically affected by this mutation (data not shown) suggesting that *Box37* did not markedly affect the mutant protein fold, if at all (see also 'Discussion' section), and also that it is not the critical anchor point between the a/TIF32-NTD and RPS0A. Despite that we still asked whether this mutation may interfere—perhaps in some indirect way—with the initial assembly of eIFs on the 40S ribosomes. Toward this end, we analyzed the distribution of selected initiation factors in *Box37* cells grown at 30°C and subsequently subjected to heat shock at 37°C for 6 h using formaldehyde cross-linking of living cells followed by high velocity sedimentation of whole-cell extracts (WCE) in sucrose density gradients (48). No reduction in the 40S-associated amounts of selected eIF3 subunits as well as eIF2 and eIF5 was observed in heat-shocked cells (Figure 2B). On the contrary, when normalizing to the levels of 40S species, we detected ~1.5-fold accumulation of the latter eIFs in heat-shocked cells compared with cells grown at the permissive temperature. Wild-type (wt) cells showed rather decreased, but definitely not increased, amounts of eIFs in 40S fractions on heat shock (Figure 2A). This suggests that the rate-limiting step that is impaired in *Box37* follows the 43S PIC assembly.

The *tif32-Box37* mutation imparts severe Gcn^- phenotype that is not caused by post-assembly defects in the initiation pathway

To examine what step is affected by *Box37*, we used the translational control mechanism of *GCN4*, which depends on four short upstream open reading frame (uORFs) found in its mRNA leader and has been adapted to serve as an experimental tool for monitoring various translational steps [reviewed in (49)]. The expression of *GCN4*, a transcriptional activator of many biosynthetic genes, is delicately regulated in a nutrient-dependent manner by the GCN2 kinase. Under nutrient-replete conditions, the kinase is inactive and the *GCN4* expression is repressed. On amino acid starvation, GCN2 becomes activated and derepresses *GCN4* synthesis by reducing the steady-state levels of the TC. Mutants defective in the TC formation and/or its recruitment to the 40S subunit mimic starvation conditions and constitutively derepress *GCN4* even under nutrient-replete conditions, producing the Gcd^- phenotype. Conversely, mutants that fail to derepress *GCN4* under starvation conditions provoke the Gcn^- phenotype, which typically signals defects in the steps following assembly of 43–48S PICs, such as processivity of scanning, AUG recognition or subunit joining.

The fact that *Box37* displayed the severe Gcn^- phenotype at the restrictive temperature (Figure 1C), which is characterized by a failure to grow in the presence of an inhibitor of histidine biosynthetic genes—3-aminotriazole (3-AT), prompted us to use a battery of *GCN4-lacZ* reporter constructs with specific modifications in the *GCN4* mRNA leader. These have been successfully used in the past to reveal malfunctioning in scanning processivity, scanning rates, stringency of AUG selection or in subunit joining (2,17,19,20,24,25,50). First, we tested the wt *GCN4-lacZ* reporter plasmid to verify the true nature of the Gcn^- phenotype in *Box37* cells and found that the degree of *GCN4-lacZ* induction was ~4-fold reduced in mutant (showing rather low ~2-fold induction) versus wt (showing standard ~8-fold induction) cells. This clearly indicates that the inability to compete with 3-AT on plates is a direct consequence of an insufficient *GCN4* derepression in response to 3-AT. Surprisingly, detailed analysis of all potential post-assembly defects described above did not reveal any clearly distinguishable defects; we only noticed that most of the constructs showed generally reduced β-galactosidase activities in mutant *versus* wt strains. Taking this into consideration, plus the fact that yeast eIF3 has been recently implicated in serving as one of the major factors ensuring stable mRNA binding to 40S ribosomes (14,15,17), low levels of wt *GCN4-lacZ* induction could be explained by a failure to recruit or stably accommodate mRNAs on the 43S PICs to form the 48S PICs poised for scanning. Interestingly, a similar phenotype was only recently reported for the eIF4G mutant *tif4632-7R* (51). In fact, this particular defect could also explain increased amounts of eIFs on 40S ribosomes that we observed in heat-shocked mutant cells (Figure 2B), as an increased number of 40S species bound only by the initial set of factors promoting the Met-$tRNA_i^{Met}$ recruitment would be expected to accumulate in such defective cells. In further support, the '40S' peak in polysome profiles recorded with heat-shocked *Box37* cells is divided into two equally large sub-peaks, whereas only one dominant peak (the heavier one) occurs in wt cells (Figure 1D). In our previous work (9), we proposed that the lighter sub-peak corresponds to 'naked' 40S ribosomes combined with the 43S PICs and the heavier one to the 48S PICs. Hence, occurrence of two 40S sub-peaks in the heat-shocked mutant cells could be explained by slower conversion of 43S PICs into 48S PICs due to impaired mRNA recruitment (see below). To shed light on the molecular mechanism by which a/TIF32-PCI domain

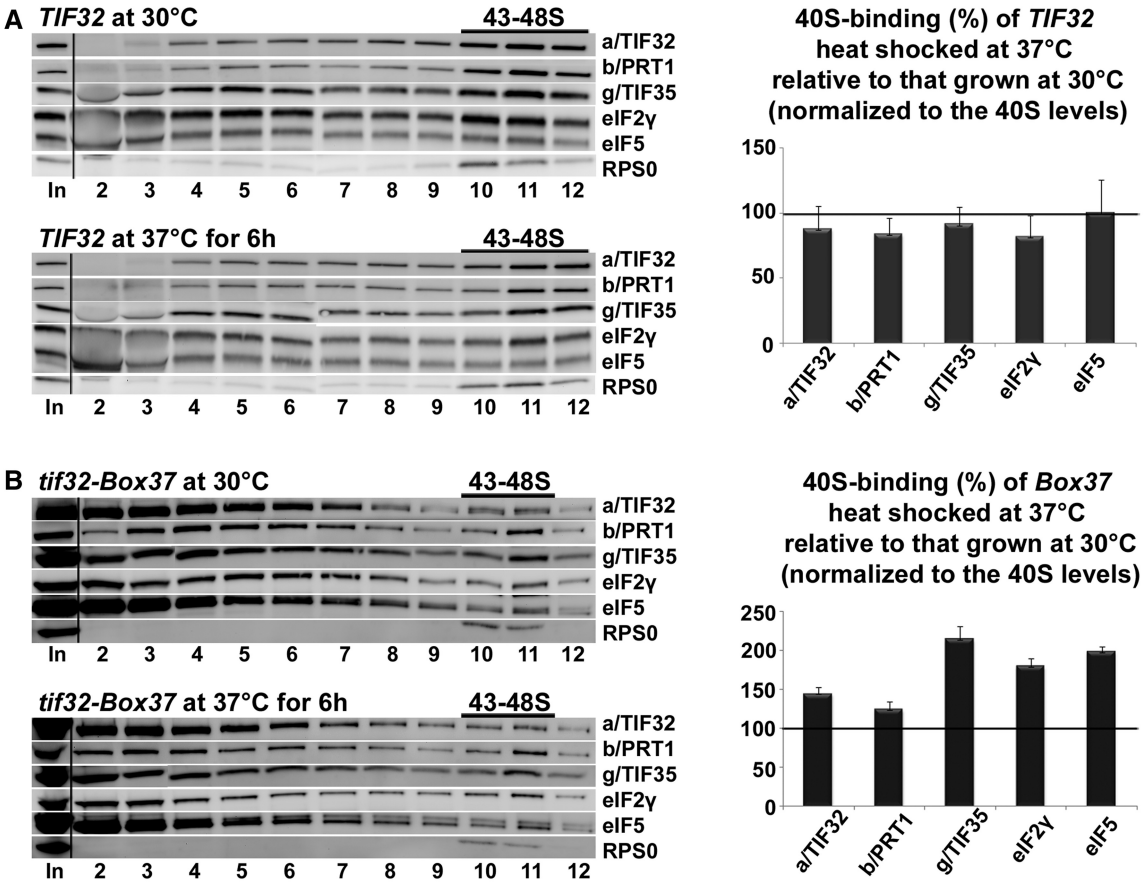

Figure 2. The *tif32-Box37* substitution results in accumulation of the 43S PICs. The *tif32-Box37* mutant strain (**B**) and its corresponding wt (**A**) described in Figure 1C were grown in YPD medium at 30°C or heat shocked at 37°C for 6 h and cross-linked with 2% HCHO before harvesting. Whole-cell extracts were prepared, separated on a 7.5–30% sucrose gradient by centrifugation at 41 000 rpm for 5 h and 5% of each fraction was loaded on the gel and subjected to western blot analysis. 'In' shows 5% input. Proportions of the 40S-bound proteins relative to the amount of 40S subunits were calculated using Quantity One software (BioRad) from at least three independent experiments. The resulting values obtained with cells grown at 30°C were set to 100% and those obtained with heat-shocked cells were expressed as percentages of the 30°C-grown cells in the histogram on the right (SDs are given).

would facilitate the recruitment of mRNA to the ribosome, we set forth to determine its 3D structure at atomic resolution.

Purification, crystallization and structure determination of the a/TIF32 PCI domain

The N-terminal region of a/TIF32 was previously identified as a stable protein domain (45). As mentioned previously, this region is predicted to harbor a PCI domain preceded by several α-helices. PCI domains are made up of two subdomains: N-terminal helical repeats followed by a C-terminal-winged helix motif. While the C-terminal winged helix motif can be fairly accurately predicted, the prediction of the exact length of the N-terminal subdomain of a/TIF32 turned out to be difficult. Because we did not obtain crystals of the entire N-terminal domain of a/TIF32, we systematically removed helices from the N-terminus, keeping the C-terminus at residue 494. However, most of the constructs led to insoluble proteins. The most soluble fragment was obtained by removing the first 275 residues (Supplementary Figure S1). This fragment was crystallized in a solution containing 100 mM HEPES, pH 7, 12% PEG 2000 (w/v), 80 mM $MnCl_2$. Crystals grew at 4°C to the maximum size in 1 week. Cryoprotection was achieved by soaking crystals in several drops containing the crystallization solution and increasing concentration of PEG400. Sudden increase of the PEG400 concentration caused cracks in the crystal and had a severe effect on the diffraction quality. The crystal structure of a/TIF32$^{276\text{-}494}$ was solved by single wavelength anomalous dispersion using a selenomethionine (SeMet) derivative and refined to the final resolution of 2.65 Å. The asymmetric unit (AU) is composed of two molecules of a/TIF32$^{276-494}$, which corresponds to a solvent content of 45%. Although the first molecule in the AU (chain A in the pdb file) is almost complete, the second molecule is only partially defined in the electron density map. The crystallographic statistics for data processing and refinement are presented in Table 1.

Crystal structure analysis

The crystal structure of a/TIF32$^{276–494}$ consists of two intimately connected subdomains; an N-terminal right-handed helical bundle capped by a C-terminal winged

Table 1. Data collection, phasing and refinement statistics

	Native	Peak	Inflection	High remote	Low remote
Data collection					
Wavelength (Å)	0.933400	0.979540	0.979690	0.977260	0.982450
Resolution (Å)	50.00–2.65 (2.75–2.65)	50.00–2.79 (2.89–2.79)	50.00–2.81 (2.91–2.81)	50.00–2.97 (3.07–2.97)	50.00–2.97 (3.07–2.97)
Space group	I 2_1 3	I 2_1 3	I 2_1 3	I 2_1 3	I 2_1 3
Cell parameters:					
a = b = c (Å)	137.137	137.63	137.99	138.06	137.75
$\alpha = \beta = \gamma = 90$ (°)					
R_{merge} (%)	5.9 (78.0)	10.4 (83.4)	10.8 (88.7)	8.8 (60.2)	10.2 (71.7)
$I/\delta I$	17.76 (1.83)	21.44 (2.16)	21.7 (2.0)	23.21 (2.77)	21.36 (2.53)
$CC_{(1/2)}$ (%)	99.9 (66.2)				
Completeness (%)	99.5 (99.8)	99.6 (96.5)	99.7 (97.3)	99.9 (100)	99.8 (99.9)
Redundancy	3.67 (3.71)	4.41 (3.48)	4.44 (3.58)	4.93 (4.92)	3.89 (3.88)
Anomalous correlation		56 (11)	35 (7)	35 (4)	16 (11)
Mean anomalous difference (SigAno)		1.724 (0.849)	1.285 (0.794)	1.269 (0.806)	0.997 (0.845)
Refinement					
Resolution (Å)	48.48–2.65 (2.75–2.65)				
Number of reflections	12 582				
R_{work}/R_{free} (%)	24.89/28.61				
Number of atoms					
Protein	3037				
B-factors (Å^2					
Protein	118.70				
Entity nr. 1/2	81.5/168.8				
R.m.s deviations					
Bond lengths (Å)	0.006				
Bond angles (°)	1.26				
PDB code	4K51				

The $CC_{1/2}$ is the correlation coefficient between two randomly selected half data sets as described in (52).

helix (WH) domain (Figure 3A). The helical bundle (HB) is composed of three pairs of antiparallel helices with structural resemblance to tetratricopeptide repeats (TPR). Helices 3 and 4 are connected via a long loop and a short helix. Residues 342–344 of this loop are poorly visible in the electron density and therefore likely to be flexible. Interestingly, residues 337–362, which form the loop and the helix connecting helices 3 and 4, are not present in the structure of any of the known PCI domains. The winged helix sub-domain shows the canonical α-β-α-α-β-β topology with an N-terminal elongated helix, which is kinked at the beginning. The structure of the WH subdomain is well conserved among known PCI structures. The orientation of the WH relative to the HB is held by several hydrogen bonds and van der Waals interactions between helix 7 (the first helix of WH) and different helices from HB. Most notably, R431 of helix 7, E392 of helix 5 and R363 of helix 4 are tightly linked by hydrogen bonds locking these three helices in place (Figure 3B). R363 and the adjacent K364 together with R431 contribute to a positively charged surface on the concave face of the protein, proposing a function for this region in mRNA recruitment (see below). Y420 and L424 of helix 7 make van der Waals interactions with the side chain of L330 of helix 3. Y420 makes a hydrogen bond with H299 of helix 2, which also interacts with S331 of helix 3. Interestingly, all these residues are highly conserved among eukaryotes, suggesting that maintaining the relative orientation of WH and HB might have a functional relevance (Supplementary Figure S2).

In fact, a/TIF32 is one of the most conserved core eIF3 subunits among eukaryotes. Interestingly, the highest degree of conservation is observed in its N-terminal region, including the PCI domain (Supplementary Figure S2). The majority of the conserved residues were found to be in the hydrophobic core of a/TIF32$^{276–494}$, pointing to their importance in the folding of this domain. We mapped the highly conserved residues on the surface of a/TIF32$^{276-494}$ using ConSurf server (53). Although no region with particularly high degree of conservation was found throughout the surface, scattered regions of high conservation were found to be surrounded by less conserved residues mainly at the concave surface of the protein (Figure 4A).

Comparison of the a/TIF32 PCI domain with other known PCI structures

Comparison of the structure of a/TIF32$^{276–494}$ with PCI domains from RPN6 [proteasomal protein, PDB code 3TXN, (54)], CSN7 [COP9-signalosome subunit, PDB code 3CHM, (55)], eIF3k (eIF3 subunit, PDB code 1RZ4, (56)], SAC3 and THP1 [TREX-2 components, PDB code 3T5V, (35)] reveals high degree of structural similarity despite little sequence conservation (Figure 4B). The highest structural conservation is observed for the C-terminal WH subdomain, whereas the N-terminal HB is more divergent. In all these structures, HB sub-domains show an overall right-handed superhelical arrangement of α-helices with characteristics

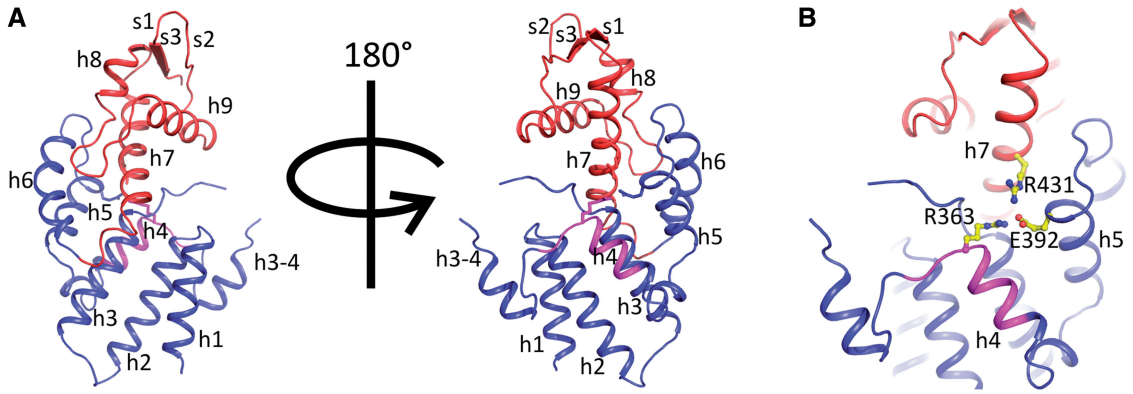

Figure 3. The overall structure of the PCI domain of a/TIF32. (**A**) Cartoon representation of a/TIF32$^{276–494}$ crystal structure. The helical bundle and the winged helix motif are colored blue and red, respectively. Box37 (residues 361–370) within helix 4 is shown in magenta. α-helices and β-strands are denoted as h and s, respectively. (**B**) Interactions between HB and WH sub-domains. HB and WH are held together via hydrogen bonding between helices 4, 5 and 7 (h4, h5 and h7). Residues involved in these interactions are R363 (h4), E392 (h5) and R431 (h7) and are presented as sticks.

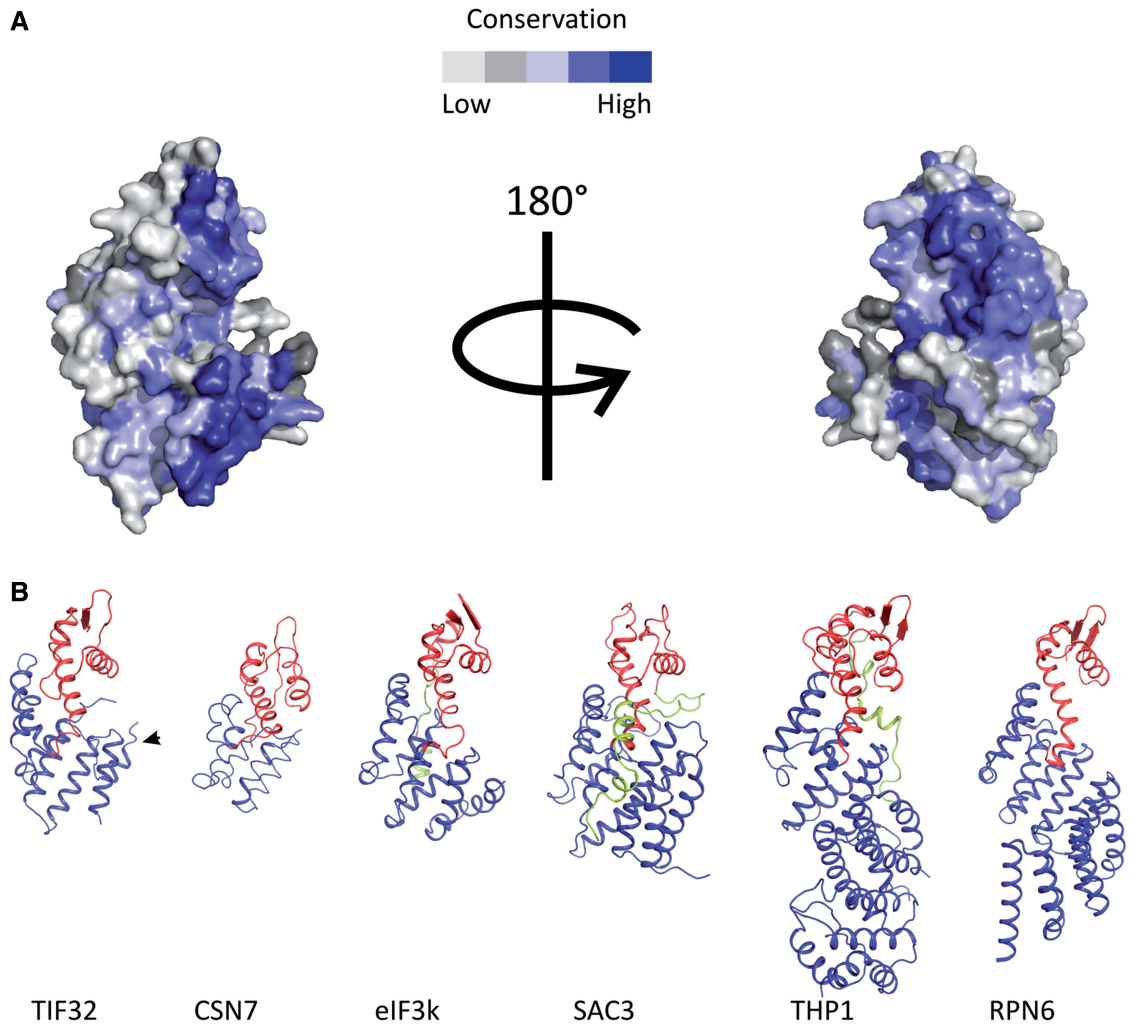

Figure 4. Conserved residues of a/TIF32 and comparison of the 3D structures of different PCI domains. (**A**) Conserved residues of a/TIF32. Surface representation of the conservation of residues among a/TIF32 from different organisms was performed using ConSurf server. (**B**) Comparison of the 3D structures of different PCI domains. In all structures, the HB and WH sub-domains are depicted in blue and red, respectively. C-terminal extensions of the WH, if present, are colored green. In the a/TIF32 PCI domain, the extra helix 3–4 is marked by an arrow.

of both HEAT [**H**untingtin, elongation factor 3 (**E**F3), protein phosphatase 2A (PP2**A**) and the yeast kinase **T**OR1] and TPR helical repeats. While eIF3k has 11 helices, which form 3 HEAT repeats, and CNS7 consists of 6 helices forming a pair of HEAT repeats, one of which resembles an ARM motif, RPN6 and THP1 structures have longer N-terminal extensions of TPR-like repeats. RPN6 contains five pairs of TPR-like repeats forming a twisted solenoid arrangement, whereas Thp1 forms a straighter arrangement that is capped by a helical bundle at the N-terminus formed by four α-helices [for a review see (57)]. Our a/TIF32 structure consists of six helices with a superhelical arrangement. An extra helix connecting helices 3 and 4 is a novel feature of a/TIF32 compared with the other PCI domains. This region is relatively conserved among eIF3a from different eukaryotes.

The PCI domain of a/TIF32 directly mediates its binding to c/NIP1

PCI domains are known to be protein interaction sites (33). a/TIF32, the largest subunit of yeast eIF3, has been implicated in building the core of eIF3 by interacting with c/NIP1 and b/PRT1, two other large eIF3 subunits (18,58). We had previously purified a stable complex between a/TIF32$^{1–494}$ and c/NIP1$^{244–812}$ (45). To find out whether the PCI domain of a/TIF32 (276–494) *per se* mediates this binding, we performed analytical SEC with purified c/NIP1 and a/TIF32$^{276–494}$. While each of the proteins elutes as a single peak from the column, the mixture of two proteins results in two peaks, with one having the same retention volume as a/TIF32$^{276–494}$ alone (as it was used in excess over c/NIP1 to promote complex formation) and the other one shifting toward the smaller volumes compared with c/NIP1 indicating the formation of a complex (Figure 5A). To dissect the thermodynamics of this binding, we performed isothermal titration calorimetry (ITC) using a/TIF32$^{276–494}$ and c/NIP1. The results indicated the formation of a complex with the stoichiometric ratio of nearly 1 (0.944), the dissociation constant (K_d) of 158 nM and a relatively large enthalpy change of −10.23 kcal/mol (Figure 5B). As expected (59), no binding was detected between b/PRT1 and a/TIF32$^{276–494}$ as judged by no change in the retention volumes of the mixture of the two proteins on analytical SEC compared with those of each protein alone (Figure 5C). Hence, the binding of a/TIF32 to b/PRT1 is most likely mediated via the C-terminal part of a/TIF32, as we recently also showed by *in vitro* reconstitution experiments (45).

RNA-binding properties of the a/TIF32-PCI domain

Winged helix motives are well-known nucleic acid binding modules (60). It is therefore likely, but not necessarily self-evident, for a given PCI domain to modulate an interaction with nucleic acids. As mentioned previously, there are two PCI domains in yeast eIF3; one in the N-terminal region of a/TIF32 under study here and the other one in the C-terminal region of c/NIP1, which was recently implicated in RNA binding as the first PCI domain ever found to do so (34). To test whether the a/TIF32-PCI domain is also capable of binding to RNA, we performed electrophoretic mobility shift assay with different fragments of a/TIF32 and *DAD4* mRNA, which is one of the smallest naturally occurring mRNAs in yeast. A stretch of 30 adenosine nucleotides was added to the 3′-end of the mRNA during transcription to mimic the polyA tail of the mRNA. While full-length and the entire N-terminal domain (1–494) of a/TIF32 bound to the mRNA, a/TIF32$^{276–494}$ failed to interact with the mRNA (Figure 5D). This may suggest an RNA-binding activity for the N-terminal region of a/TIF32 before residue 276. To check this, a/TIF32$^{1–276}$ was purified as a GST-fusion protein and tested for binding to *DAD4* mRNA. However, this fragment also failed to bind to the mRNA. This can be explained in several ways; GST-a/TIF32$^{1–276}$ is not properly folded, or the mRNA-binding site is masked by the GST or the RNA-binding site at the N-terminal region of a/TIF32 is distributed over a wide range of residues, both before and after residue 276. It has to be acknowledged here that the concentrations of RNA and protein used in this assay are relatively high and as such might produce non-specific RNA–protein interactions. However, this is of a minor concern as (i) only the entire N-terminal fragment of a/TIF32$^{1–494}$ and not its N- and C-terminal halves interacted with RNA in our assay and (ii) a protein implicated in mRNA recruitment to ribosomes like a/TIF32 is expected to have general non-specific RNA-binding properties.

The *tif32-Box37* mutation specifically diminishes mRNA recruitment to the 43S PICs *in vivo*

With several lines of experimental evidence and predictions from the 3D structure all pointing at the importance of the PCI domain for mRNA recruitment, we next decided to examine the effects of *Box37* on the 48S PIC assembly. To do that, we measured the amounts of three model mRNAs associated with native 48S PICs in whole-cell extracts of formaldehyde (HCHO) cross-linked cells that were resolved on sucrose gradients as described above according to (17). One of the model mRNAs—*RPL41A*—was successfully used in the latter and other studies, and the use of the other two—*DAD4* and *SME1*—was established here to provide broad specificity of our analysis. We specifically chose these mRNAs because they are rather short and thus minimize the 'contamination' effects of large mRNAs assembled into mRNPs that often run in heavy sucrose fractions like ribosomal species (17) and could lead to serious misinterpretations of the mRNA recruitment data. In addition, these experiments were conducted using isogenic strains lacking one of the genes encoding the 60S protein RPL11 (*RPL11B*), as the reduced level of 60S subunits resulting in a reduced rate of subunit joining increases the concentration of 48S PICs in *rpl11BΔ* cells (14). This is a necessary arrangement that increases the peak of mRNAs associated with the 48S PICs relative to the free mRNPs and significantly

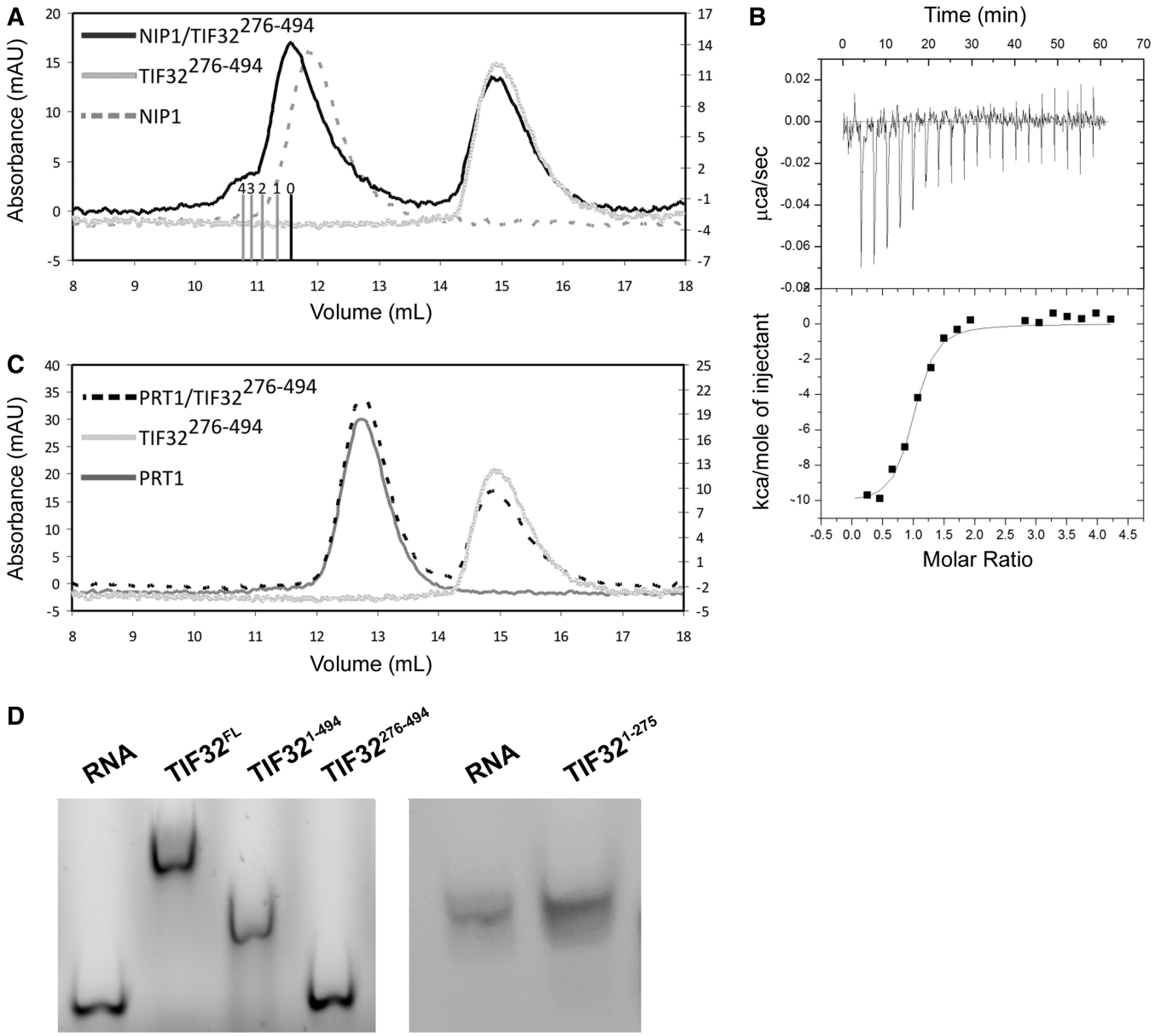

Figure 5. Protein and RNA-binding properties of a/TIF32$^{276\text{-}494}$. (**A**) Interaction of a/TIF32$^{276–494}$ with other major components of eIF3. SEC chromatogram of a/TIF32$^{276–494}$ interaction with c/NIP1. The shift to the smaller volume in the case of the mixture of two proteins indicates a complex formation. Bars indicate different ratios of a/TIF32$^{276–494}$ to c/NIP1, with 0 being only c/NIP1 and 4 being four molecules of a/TIF32$^{276–494}$ bound to c/NIP1. The small peak at 10.8 ml after mixing a/TIF32$^{276–494}$ and c/NIP1 is most probably an artifact of SEC due to incubation of the complex at room temperature for 30 min. (**B**) Isothermal calorimetric titration of c/NIP1 with a/TIF32$^{276–494}$. The upper panel shows raw data of heat effect (in mcal s^{-1}). The lower panel shows the fitted binding isotherms. The data points were obtained by integration of heat signals plotted against the molar ratio of a/TIF32$^{276–494}$ to c/NIP1 in the reaction cell. The solid line represents a calculated curve using the best fit parameters obtained by a non-linear least squares fit. (**C**) The mixture of a/TIF32$^{276–494}$ and b/PRT1 behaves the same as the sum of both proteins individually. (**D**) RNA binding activity of different regions of a/TIF32. Both full-length and the entire N-terminal domain of a/TIF32 bind to RNA. In contrast, a/TIF32$^{276–494}$ or a/TIF32$^{1–276}$ does not disturb the electrophoretic mobility of the mRNA.

facilitates quantification of the 48S-bound species (17). Using real-time quantitative reverse transcription-polymerase chain reaction to assay the three reporter mRNAs and 18S rRNA in 12–13 collected fractions, we found that heat-shocked *Box37* significantly shifts distribution of all three mRNAs from 40S-containing fractions toward the top, indicating a substantial underutilized pool of free mRNPs (Figure 6A, B, and D, and Supplementary Figure S3). Relative amounts of all three mRNAs in PICs of mutant versus wt cells are shown in the corresponding Tables in Figure 6E and Supplementary Figure S3. This experiment was repeated several times with similar results. Taken together, we propose that the *tif32-Box37* 10-Ala substitution primarily impairs the assembly or stability of the 48S PICs. In other words, the α-helix 4 of the HB subdomain encompassing residues 361 through 370 markedly contributes to the stable mRNA recruitment to 43S PICs *in vivo*.

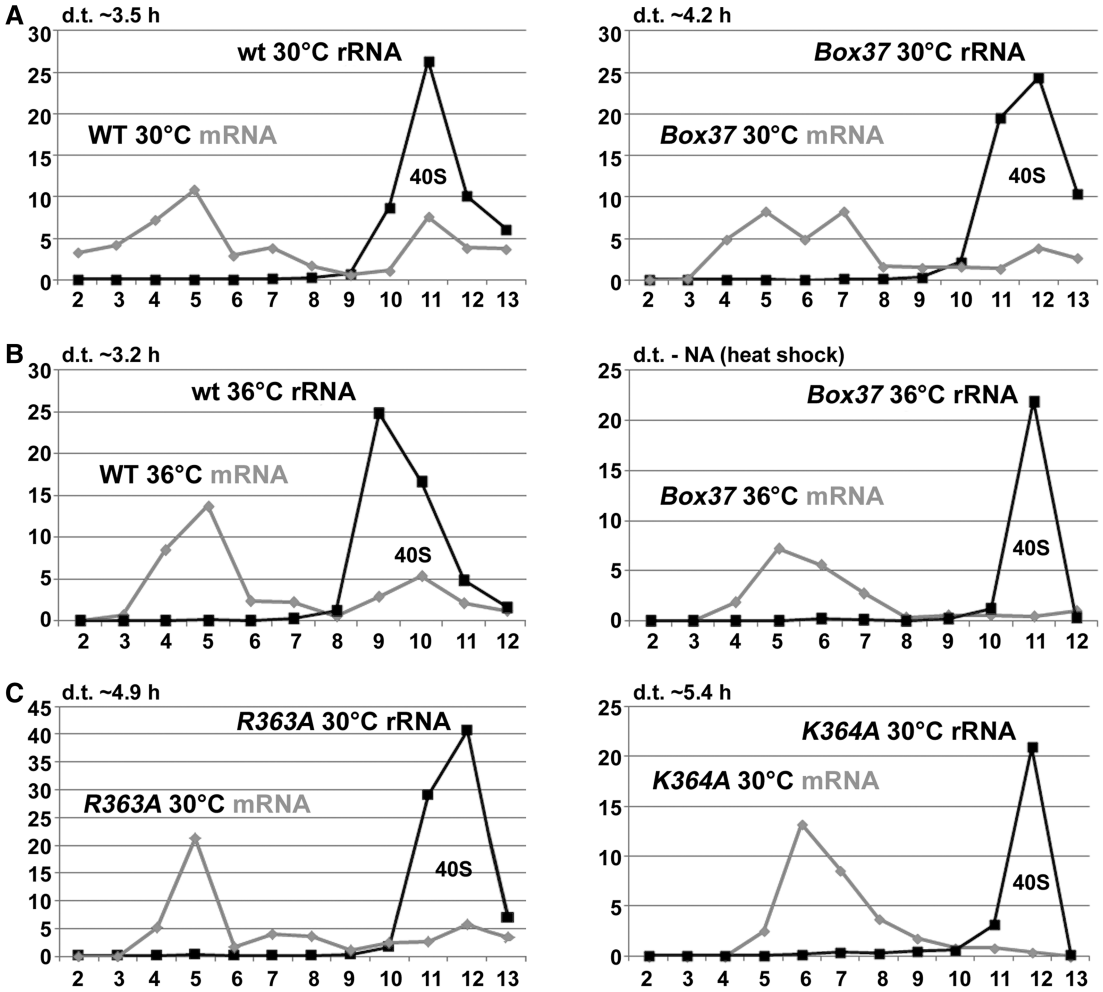

D

	DISTRIBUTION ACROSS the GRADIENTS			
	30°C		36°C	
	the amount (%) corresponding to *RPL41A* mRNA in:			
	free RNPs	PICs	free RNPs	PICs
WT	**68.3** ± 5.5	**31.7** ± 5.5	**74.9** ± 4.6	**25.1** ± 4.6
Box37	**84.2** ± 4.1	**15.8** ± 4.1	**91.2** ± 0.6	**8.8** ± 0.6
R363A	**82.3** ± 6.4	**17.7** ± 6.4	**ND**	**ND**
K364A	**89.8** ± 1.9	**10.1** ± 1.9	**ND**	**ND**

E

RELATIVE AMOUNT of *RPL41A* mRNA in PICs in MUTANT vs. WT CELLS			p-value	
	30°C	36°C	30°C	36°C
WT	**1**	**1**		
Box37	**0.5**	**0.35**	0.008	0.004
R363A	**0.56**	**ND**	0.014	
K364A	**0.32**	**ND**	0.002	

Figure 6. The *tif32-Box37*, *-R363A* and *-K364A* substitutions eliminate mRNA association with 43S PICs *in vivo*. (**A–C**) The isogenic *rpl11bΔ* strains carrying indicated *TIF32* mutations were cultured, cross-linked and separated as described in Figure 2. Total RNA was extracted from each of 12–13 fractions, and the amounts of 18S rRNA and *RPL41A* mRNA were measured by real-time quantitative polymerase chain reaction. The amounts of mRNA and 18S rRNA were calculated as $2^{-Ct} \times 10^{-7}$ and $2^{-Ct} \times 10^{-4}$, respectively. (**D** and **E**) The distribution of *RPL41A* mRNA across all fractions and its relative amounts in mutants versus wt in 18S rRNA containing fractions were calculated. Student's *t* test (*P*-value) indicated that the value for each mutant differed significantly from that for the wt.

Solvent-exposed K364 of the a/TIF32-PIC domain promotes mRNA recruitment

As mentioned previously, two N-terminal residues of the α-helix 4 of the HB subdomain (mutated in *Box37*) are R363 and K364. Whereas R363 is certainly required for stabilization of the HB fold (Figure 3B), K364 is fully exposed to the solvent with no structural role. However, both residues are part of the apparent continuous surface rich in basic residues with a fair probability to interact with RNA (region 3 in Figure 7B). Because the Ala-substitution of Box37 dramatically reduced the *RPL41A* mRNA amounts in the 40S-containing fractions *in vivo* (Figure 6A and B), it was tempting to speculate that these two residues actually mediate the mRNA transfer onto the 43 PICs. To address this question, we substituted both residues with alanine and examined the effects of these individual substitutions on *RPL41A* mRNA association with PICs *in vivo* as described above. As shown in Figure 6C–E and Supplementary Figure S4, both single substitutions decreased growth rates (by ~2-fold) already at 30°C and, most importantly, markedly reduced the *RPL41A* mRNA amounts associated with the PICs. These observations thus strongly suggest that both residues play an important role in the ability of the PCI domain of a/TIF32 to stimulate formation of the 48S PICs. Interestingly, of the two, *K364A* had a stronger effect on mRNA recruitment (the relative amounts of *RPL41A* mRNA in PICs are reduced by ~70%) as well as on the growth rates than *R363A* (showing ~45% reduction in the relative amounts of *RPL41A*, the effect of which was comparable with the effect of *Box37*; see 'Discussion' section for further details). Taken together, we propose that one of the key roles of the a/TIF32-PCI domain is, besides building the eIF3 core, to contact mRNAs in a non-specific manner and promote their delivery to and/or stable binding on the small ribosomal subunit.

Structural basis for the RNA binding of the a/TIF32-PCI domain

Secondary structure prediction suggests the dominance of helical repeats in the N-terminal region of a/TIF32, preceding the crystallized fragment. The sequence-based structure prediction using Phyre2 (62) suggests that the N-terminal HB probably extends further than six helices similar to the extended twisted character of THP1 and RPN6 (see above). Therefore, we built a chimeric molecule *in silico* from the predicted domain (residues 1–275) and the crystallized fragment (residues 276–494, Figure 7A). The relative orientation of the two domains was confirmed by performing protein–protein docking using HEX software (Supplementary Figure S5) (63). Analysis of the surface charge distribution of the predicted piece of the structure shows the dominance of positively charged patches, which form two continuous surfaces on the front and back of this N-terminal region of a/TIF32 implying a possible role in RNA binding (Figure 7B, left and right, respectively). Even though the crystallized fragment does not show an accumulation of charge density that would be comparable with a/TIF32$^{1–276}$, the

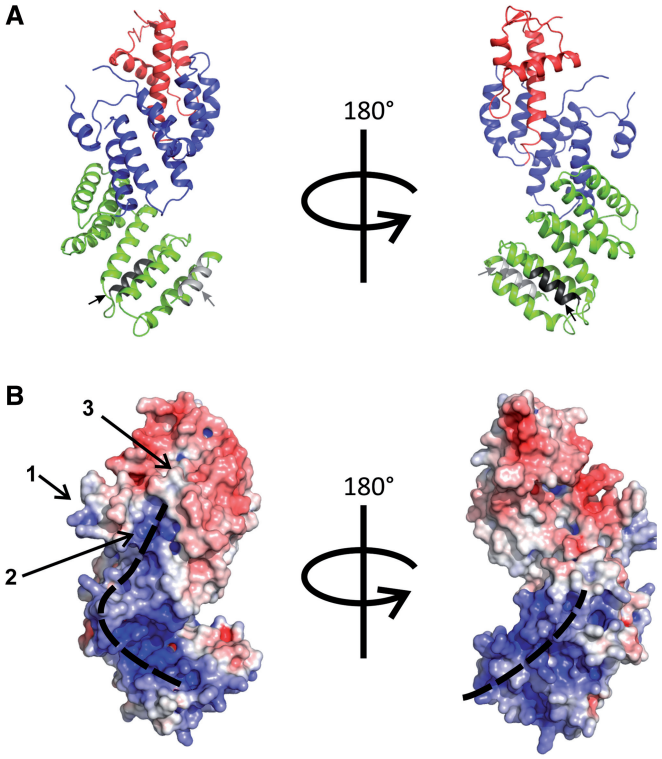

Figure 7. A proposed model of the entire a/TIF32-NTD. The crystal structure (residues 276–494) was extended by a homology-based prediction of residues 1–275. (**A**) The ribbon representation of the chimeric molecule. The WH and HB sub-domains of the crystal structure and the predicted helical extension are depicted in red, blue and green, respectively. Within the predicted region, Box6 (residues 51–60) and Box17 (residues 161–170) (see the text for details) are shown in light and dark gray, respectively, and are further marked by arrows of the same color. (**B**) Surface charge distribution of the chimeric molecule as calculated by APBS (61) plugin in PyMol (The PyMOL Molecular Graphics System, Version 1.0r1 Schrödinger, LLC.) shows the dominance of the basic side chains over the surface of the N-terminal helical extension (the predicted model). Two major patches of positive charges on opposite sides of the molecule are marked. Three major positive patches on the surface of the crystal structure are shown (left; 1, 2 and 3; the latter is created by the juxtaposition of residues R363, K364 and R431—see the text for details), which collectively form a basic area that aligns with the continuous basic patch on the front side of the N-terminal extension.

short α-helix connecting helices 3 and 4 of the PCI domain harbors several positively charged side chains, rendering it relatively basic (region 1, Figure 7B). Adjacent to this region is another patch of positive charge density on the concaved side of the structure made by K304, K305 and K308 of helix 2 (region 2, Figure 7B), followed by the last, only modestly basic region created by the juxtaposition of residues R363, K364 and R431 at the site where the HB joins the WH (region 3, Figure 7B). Together, these three regions constitute an overall basic area, which is, to some extent, aligned with the continuous positive charges on the surface of the modeled N-terminal fragment. Note that the first two of the latter residues from region 3 were experimentally implicated in promoting the mRNA loading to the 43S PICs *in vivo* (Figure 6). Moreover, 10-Ala substitutions of Box20 (the back RNA track of the NTD containing R194, R195 and K196), Box24 (the front RNA

track containing R235), Box27 and Box29 (along the front RNA track below region 2 containing K268 and K288, respectively), Box31 (region 2 containing K304, K305 and K308) and Box35 (region 1 containing R350) produced lethal phenotypes (summarized in Figure 1B), indicating that they might be critical for mRNA recruitment. Although we cannot rule out a lot simpler explanation for the observed lethality—a defect in protein folding—the fact that no other Box mutants (with the only exception of Box38), including those in the PCI domain, were deleterious may speak in favor of a defect in RNA binding. Taken altogether, it is tempting to speculate that both the N-terminal and PCI domains of a/TIF32 promote mRNA recruitment in a co-operative manner, with the a/TIF32$^{1–276}$ part probably making a bigger contribution to the overall binding. This is, in fact, consistent with our observations that neither the crystallized PCI fragment alone nor the N-terminal domain of a/TIF32 displayed any RNA-binding activity in solution, whereas the entire N-terminal half of a/TIF32 encompassing both of these domains did bind to the transcribed mRNA *in vitro* (Figure 5D).

DISCUSSION

We reported previously that depletion of the entire eIF3 complex from cells impaired model *RPL41A* mRNA recruitment *in vivo* (14) and, furthermore, yeast eIF3 was later demonstrated to play a direct role in 43S PIC binding to capped, native mRNA *in vitro*, being even more critical than eIF4F and eIF4B (15). In this study, we showed that Ala substitutions in the α-helix 4 of the HB subdomain of the N-terminal PIC domain of a/TIF32, the crystal structure of which was solved at 2.65-Å resolution, robustly reduce the recruitment of three model mRNAs to the 43S PICs *in vivo* as the only detectable defect. Thus, these findings strongly suggest that this region of the a/TIF32-PCI significantly contributes to the formation of 48S PICs. In addition, our observation that several 10-Ala substitutions specifically mapping onto the mutually interconnected basic patches that we predicted to constitute the a/TIF32-NTD surface (Figure 7B; one of the patches includes the HB α helix 4) result in lethality further supports the idea that the entire N-terminal half of a/TIF32 is significantly involved in mRNA loading onto the 43S PICs, although we cannot rule out the protein folding effects. Importantly, in our recent study (17), substitutions in the KERR motif in the HLD located at the C-terminal half of the a/TIF32 were also shown to impair 40S-binding of model mRNA to the 43S PICs. However, in contrast to the PCI substitutions characterized here, the HLD substitutions also produced phenotypes indicating reduced efficiency of scanning and AUG recognition. Hence, to our knowledge, this is the first report implicating a specific domain of an initiation factor solely in this key role *in vivo*.

Actually, the additional post-assembly phenotypes associated with the HLD versus PCI substitutions can be most likely attributed to the fact that the CTD of a/TIF32 interacts *in vitro* with an 18S rRNA segment containing h16–h18 (64) and with RPS2 and RPS3 (17), all occurring nearby the mRNA entry pore on the solvent side of the 40S subunit (47) (Figure 8). It is believed that RPS3 plays a key role in opening and closing of the mRNA entry channel latch, stabilizing the closed position by interacting with h34 but interacting with h16 on the solvent side of the 40S subunit to promote the open-latch conformation (65). These latch movements are believed to play a critical role for the initial mRNA loading onto the 43S PICs and/or during the subsequent start codon selection process (65,66). Based on that, we naturally proposed that the a/TIF32-CTD can, by interacting with RPS3, h16 or h18, modulate the mRNA entry channel latch as a way of influencing the transition from open to closed PIC conformations during mRNA loading and scanning for AUG recognition (17). In support, hydroxyl radical cleavage mapping of mammalian eIF3 in the 48S PICs also suggested that proportions of its eIF3a and eIF3d subunits interact with h16 (67). Ribosomal location of the a/TIF32-PCI domain can be, on the other hand, predicted from the well-established interaction between RPS0A and the a/TIF32 segment spanning residues 201–400 (2,46,64). Incidentally, a significant contributor to this binding is the C-terminal tail of RPS0A, which is highly acidic (46), indicating an ionic character of its interaction with the basic a/TIF32-NTD. Consistently, a subunit of rabbit eIF3 was only recently predicted to contact RPS1 and 26 that are both situated next to RPS0 (29). Importantly, RPS0A occurs near the mRNA exit not the entry pore (Figure 8); i.e. relatively far from the 'latch feature' that thus should not be affected by the PCI mutations. In agreement, no phenotypes indicating dramatic post-assembly defects were observed using the *GCN4* translational mechanism as a genetic tool.

In detail, we found two basic residues (R363 and K364) located at the beginning of helix 4, which together with R431 of helix 7 constitute a positively charged patch on the surface of a/TIF32-PCI domain (Figure 7B, region 3). To test whether the mRNA recruitment defect observed for the Ala substitution of the entire helix 4 (in Box37) originates from the perturbation of this basic surface, each of these Box37 residues was mutated to Ala. Both *R363A* and *K364A* mutations did impair the recruitment of *RPL41A* mRNA to the 43S PICs *in vivo*, with the latter displaying a more pronounced defect than *Box37* and *R363A* (Figure 6). Attempts to purify the N-terminal half of a/TIF32 harboring *Box37*, *R363A* or *R363A K364A* mutations to examine the effects of helix 4 mutations on the *in vitro* RNA-binding property of the a/TIF32-NTD yielded poorly expressed and/or largely insoluble proteins in the bacterial expression strains that we used. Poor expression and insolubility could be attributed to problems in the folding of the a/TIF32-PCI domain, as R363 plays an important role in bringing helices 4, 5 and 7 together and maintaining the proper relative orientation of the WH and HB subdomains (Figure 3B). However, the folding problem in the context of the entire a/TIF32 would be most likely only minor provided that *Box37* dramatically affects neither the integrity of eIF3 nor the assembly of the MFC *in vivo*. Nevertheless, it is still possible that some minor misfolding stands behind the

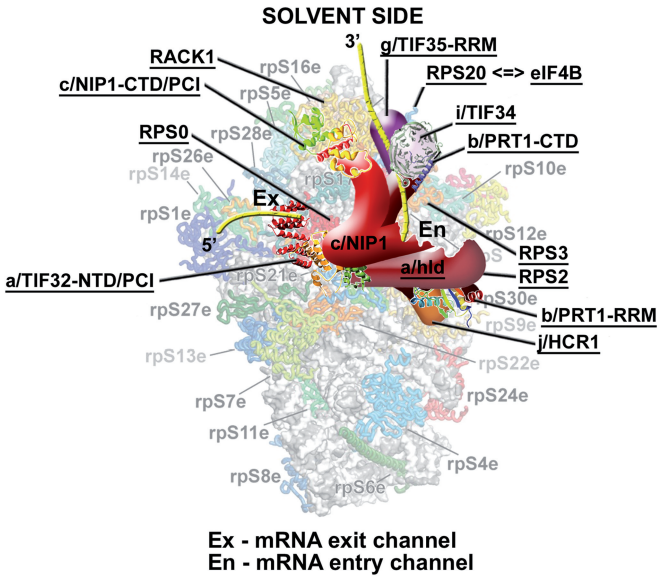

Figure 8. A model of eIF3 on the 40S ribosome spanning the mRNA exit and entry channels. The crystal structure of the 40S subunit is shown from the solvent side with ribosomal proteins shown as cartoons in individual colors; rRNA is shown as gray surface [adapted from (47)]. A hypothetical location of *Saccharomyces cerevisiae* eIF3 on the back side of the 40S subunit is based on the published interactions between RACK1 and the c/NIP1-CTD/PCI (34); RPS0 and the a/TIF32-NTD/PCI (2,46,64); RPS2 and j/HCR1 (24); RPS2 and 3 and the a/TIF32-CTD (17); helices 16-18 of 18S rRNA and the a/TIF32-CTD (64); and RPS3 and 20 and g/TIF35 (19). The extreme N- and C-terminal domains of c/NIP1 and a/TIF32, respectively, are predicted to interact with the interface side of the 40S subunit (64), as hinted. The recently published interaction between RPS20 and eIF4B is indicated by a double-headed arrow (69). Positions of all eIF3 subunits as well as RACK1, RPS0, 2, 3 and 20 are highlighted in bold. Schematic representations of i/TIF34 bound to the b/PRT1-CTD, the b/PRT1-RRM, the a/TIF32-NTD/PCI and the c/NIP1-CTD/PCI were replaced with the X-ray structures (25,30) or the 3D structural model (34), respectively. The yellow lines represent mRNA.

observed differences in the degree of impairment of mRNA recruitment in *Box37* and *R363A* versus *K364A* mutants. It could perhaps indirectly affect some step preceding mRNA binding that would thus become rate-limiting and specifically reduce the net effect on the mRNA recruitment impairment in *Box37* and *R363A* mutants. In contrast to R363, K364 is fully exposed to the solvent and therefore less critical for the folding of the a/TIF32-PCI domain, if at all. Consistently, its Ala substitution produced a soluble protein that, however, did not show any significant effect in our *in vitro* RNA-binding assay (data not shown). The ostensible paradox that *K364A* resulted in severe impairment of mRNA recruitment *in vivo* but did not affect the a/TIF32-NTD RNA binding *in vitro* could be explained by proposing that either our RNA-binding assay is not sensitive enough to detect the impact of *K364A* on the a/TIF32 ability to directly interact with mRNAs, or that the undisputable contribution of K364 to mRNA recruitment is indirect. In the latter case, it could be exerted in co-operation with other mRNA binding and recruitment-promoting eIFs, such as those associated with eIF4G, which most probably also bind to the solvent-exposed side of the 48S PICs as eIF3 does, at least based on their predicted locations [reviewed in (1)]. For example, this region of a/TIF32 could contact 18S rRNA (rather than mRNA) in such a way that it is not required to anchor eIF3 to the ribosome but to make 40S-bound eIF3 to adopt an 'RNA-recruitment-competent' conformation to enable stable binding of incoming mRNA-bound eIF4F complex to start scanning.

Along these lines, the ribosomal position of yeast eIF4B—a factor previously implicated in promoting ribosomal scanning by stimulating the helicase activity of eIF4A and by holding on to the single-stranded regions created by eIF4A (68)—has been only recently mapped. It was shown to interact *in vitro* with RPS20 (69) that is situated on the 40S head right above the mRNA entry pore (47) (Figure 8); its head-location around RPS20 was also corroborated by hydroxyl radical probing. The tight 40S-binding of eIF4B was then demonstrated to play a critical role in its novel unexpected role in promoting mRNA recruitment to 43S PICs. Interestingly, eIF4B interacts with g/TIF35 (70), earlier implicated in promoting processivity of scanning through stable secondary structures (19), and g/TIF35 in turn interacts with RPS20 and also RPS3 (19). Recently, we proposed that the scaffold b/PRT1 subunit serves to connect two eIF3 modules at each of its termini: (i) a/TIF32-HLD-CTD–j/HCR1 at the N-terminal RRM and (ii) i/TIF34–g/TIF35 at the extreme C-terminal α-helix, both of which surround the mRNA entry pore working together to fine-tune scanning and the AUG selection process (25) (Figure 8). Hence, it is tempting to speculate that although these two modules co-operate with eIF4B (via its contacts with g/TIF35 and RPS20) and possibly also with eIF4A in stimulating mRNA recruitment and promoting scanning for AUG, the a/TIF32-PCI co-operates with eIF4G—since time immemorial implicated in bridging the 40S–mRNA contact—to ensure mRNA loading onto the 43S PIC as their primary role. In fact, recent mutational analysis of yeast eIF4G showed that two of its functionally important RNA-binding elements, RNA2 and RNA3, do not critically contribute to formation of the eIF4G–PABP mRNPs suggesting that they could contribute to the function of eIF4G in recruitment of the 43S PIC to mRNAs (71), perhaps hand in hand with the a/TIF32-PCI and other factors. Even though the interaction between eIF3 and eIF4G has never been shown in yeast, in contrast to mammals (6,72), it does not mean that it cannot be established directly in the PIC or that eIF4G and a/TIF32-PCI could not work together without actually being bound to each other. In fact, earlier findings showing that several eIF3 subunits can directly interact with mRNA (2,19,34,67,73,74) may suggest that incoming mRNA is 'grabbed by many hands'—some more, some less contributory—that could be physically and spatially independent of each other; however, collectively they would ensure proper and timely mRNA delivery to the mRNA-binding channel of the 40S ribosomes. Alternatively, as proposed before, the eIF3–eIF4G contact could be bridged by eIF5, which simultaneously interacts with eIF4G and with the extreme NTD of the c/NIP1 subunit of eIF3 (9,26). However, given the fact

that eIF5 is most likely situated on the interface side of the 40S (75), whereas eIF4G is expected to occur on its solvent-exposed side [see (1) for the current view of factor's occupancy on the 40S subunit], this possibility seems unlikely. Furthermore, the stimulatory function of eIF5 on mRNA recruitment to the PIC was not observed in a reconstituted yeast system (15) and a mutation in the eIF5-CTD that disrupts its interaction with eIF4G impaired 43S binding to mRNA only *in vitro* (9). Hence, the eIF5 contribution to this important initiation step, if any, awaits further examination. Without a doubt, detailed structural information about interactions of eIF3 subunits with the 40S ribosome, mRNA and other eIFs including eIF4B and eIF4G will be essential in deciphering molecular details of their critical roles in 43S attachment to mRNA.

Finally, we previously identified two N-terminal mutations in *tif32-Box6* and *17*, which produce the severe Gcn^- phenotype in an additive manner by disturbing the ability of 40S ribosomes to resume scanning after translating uORF1 to reinitiate on *GCN4* (36). Here we predict that they are both located close to two basic patches on the surface of the modeled N-terminal domain of a/TIF32 (Figure 7A). This supports our earlier proposal that both Boxes specifically contact reinitiation-promoting elements (RPEs) occurring in the 5′ UTR of uORF1 in the *GCN4* mRNA leader to stabilize the 40S subunit on uORF1 post-termination to resume scanning for efficient reinitiation downstream. Furthermore, it also indicates that in addition to this specific role, both segments may also non-specifically contact all cellular mRNAs and thus contribute to their recruitment to the 43S PICs.

ACCESSION NUMBERS

The atomic coordinates have been deposited in the Protein Data Bank, www.rcsb.org (PDB ID code 4K51).

SUPPLEMENTARY DATA

Supplementary Data are available at NAR Online.

ACKNOWLEDGEMENTS

The authors are thankful to Béla Szamecz and István Danyi for help with cloning, to the laboratory of Petr Svoboda from IMG ASCR in Prague for their help with qPCR experiments and to all members of our laboratories for insightful discussions. The authors also thank Helmholtz-Zentrum Berlin (HZB, Germany) for the allocation of synchrotron radiation beamtime and for financial support.

FUNDING

The Wellcome Trust [090812/Z/09/Z to L.S.V.]; Czech Science Foundation [305/10/0335 to L.S.V.]. Funding for open access charge: Wellcome Trust.

Conflict of interest statement. None declared.

REFERENCES

1. Valášek,L.S. (2012) 'Ribozoomin' – Translation initiation from the perspective of the ribosome-bound Eukaryotic Initiation Factors (eIFs). *Curr. Protein Pept. Sci.*, **13**, 305–330.
2. Szamecz,B., Rutkai,E., Cuchalova,L., Munzarova,V., Herrmannova,A., Nielsen,K.H., Burela,L., Hinnebusch,A.G. and Valášek,L. (2008) eIF3a cooperates with sequences 5′ of uORF1 to promote resumption of scanning by post-termination ribosomes for reinitiation on GCN4 mRNA. *Genes Dev.*, **22**, 2414–2425.
3. Pöyry,T.A., Kaminski,A. and Jackson,R.J. (2004) What determines whether mammalian ribosomes resume scanning after translation of a short upstream open reading frame? *Genes Dev.*, **18**, 62–75.
4. Imataka,H., Gradi,A. and Sonenberg,N. (1998) A newly identified N-terminal amino acid sequence of human eIF4G binds poly (A)-binding protein and functions in poly(A)-dependent translation. *EMBO J.*, **17**, 7480–7489.
5. Imataka,H. and Sonenberg,N. (1997) Human eukaryotic translation initiation factor 4G (eIF4G) possesses two separate and independent binding sites for eIF4A. *Mol. Cell. Biol.*, **17**, 6940–6947.
6. Korneeva,N.L., Lamphear,B.J., Hennigan,F.L. and Rhoads,R.E. (2000) Mutually cooperative binding of eukaryotic translation initiation factor (eIF) 3 and eIF4A to human eIF4G-1. *J. Biol. Chem.*, **275**, 41369–41376.
7. Lamphear,B.J., Kirchweger,R., Skern,T. and Rhoads,R.E. (1995) Mapping of functional domains in eukaryotic protein synthesis initiation factor 4G (eIF4G) with picornaviral proteases. *J. Biol. Chem.*, **270**, 21975–21983.
8. Morino,S., Imataka,H., Svitkin,Y.V., Pestova,T.V. and Sonenberg,N. (2000) Eukaryotic translation initiation factor 4E (eIF4E) binding site and the middle one-third of eIF4GI constitute the core domain for cap-dependent translation, and the C-terminal one-third functions as a modulatory region. *Mol. Cell. Biol.*, **20**, 468–477.
9. Asano,K., Shalev,A., Phan,L., Nielsen,K., Clayton,J., Valášek,L., Donahue,T.F. and Hinnebusch,A.G. (2001) Multiple roles for the carboxyl terminal domain of eIF5 in translation initiation complex assembly and GTPase activation. *EMBO J.*, **20**, 2326–2337.
10. Hinton,T.M., Coldwell,M.J., Carpenter,G.A., Morley,S.J. and Pain,V.M. (2007) Functional analysis of individual binding activities of the scaffold protein eIF4G. *J. Biol. Chem.*, **282**, 1695–1708.
11. Ramirez-Valle,F., Braunstein,S., Zavadil,J., Formenti,S.C. and Schneider,R.J. (2008) eIF4GI links nutrient sensing by mTOR to cell proliferation and inhibition of autophagy. *J. Cell Biol.*, **181**, 293–307.
12. Park,E.H., Zhang,F., Warringer,J., Sunnerhagen,P. and Hinnebusch,A.G. (2011) Depletion of eIF4G from yeast cells narrows the range of translational efficiencies genome-wide. *BMC Genomics*, **12**, 68.
13. Clarkson,B.K., Gilbert,W.V. and Doudna,J.A. (2010) Functional overlap between eIF4G isoforms in *Saccharomyces cerevisiae*. *PLoS One*, **5**, e9114.
14. Jivotovskaya,A., Valášek,L., Hinnebusch,A.G. and Nielsen,K.H. (2006) Eukaryotic translation initiation factor 3 (eIF3) and eIF2 can promote mRNA binding to 40S subunits independently of eIF4G in yeast. *Mol. Cell. Biol.*, **26**, 1355–1372.
15. Mitchell,S.F., Walker,S.E., Algire,M.A., Park,E.-H., Hinnebusch,A.G. and Lorsch,J.R. (2010) The 5′-7-methylguanosine cap on eukaryotic mRNAs serves both to stimulate canonical translation initiation and to block an alternative pathway. *Mol. Cell*, **39**, 950–962.
16. Sonenberg,N. and Hinnebusch,A.G. (2009) Regulation of translation initiation in eukaryotes: mechanisms and biological targets. *Cell*, **136**, 731–745.
17. Chiu,W.-L., Wagner,S., Herrmannová,A., Burela,L., Zhang,F., Saini,A.K., Valášek,L. and Hinnebusch,A.G. (2010) The C-terminal region of eukaryotic translation initiation factor 3a (eIF3a) promotes mRNA recruitment, scanning, and, together with eIF3j and the eIF3b RNA recognition motif, selection of AUG start codons. *Mol. Cell. Biol.*, **30**, 4415–4434.

18. Valášek,L., Nielsen,K.H. and Hinnebusch,A.G. (2002) Direct eIF2-eIF3 contact in the multifactor complex is important for translation initiation *in vivo*. *EMBO J.*, **21**, 5886–5898.
19. Cuchalová,L., Kouba,T., Herrmannová,A., Danyi,I., Chiu,W.-l. and Valášek,L. (2010) The RNA recognition motif of eukaryotic translation initiation factor 3g (eIF3g) is required for resumption of scanning of posttermination ribosomes for reinitiation on GCN4 and together with eIF3i stimulates linear scanning. *Mol. Cell. Biol.*, **30**, 4671–4686.
20. Nielsen,K.H., Szamecz,B., Valasek,L.J., Jivotovskaya,A., Shin,B.S. and Hinnebusch,A.G. (2004) Functions of eIF3 downstream of 48S assembly impact AUG recognition and GCN4 translational control. *EMBO J.*, **23**, 1166–1177.
21. Valášek,L., Nielsen,K.H., Zhang,F., Fekete,C.A. and Hinnebusch,A.G. (2004) Interactions of eukaryotic translation initiation factor 3 (eIF3) subunit NIP1/c with eIF1 and eIF5 promote preinitiation complex assembly and regulate start codon selection. *Mol. Cell. Biol.*, **24**, 9437–9455.
22. Kovarik,P., Hašek,J., Valášek,L. and Ruis,H. (1998) RPG1: an essential gene of *saccharomyces cerevisiae* encoding a 110-kDa protein required for passage through the G1 phase. *Curr. Genet.*, **33**, 100–109.
23. Nielsen,K.H., Valášek,L., Sykes,C., Jivotovskaya,A. and Hinnebusch,A.G. (2006) Interaction of the RNP1 motif in PRT1 with HCR1 promotes 40S binding of eukaryotic initiation factor 3 in yeast. *Mol. Cell. Biol.*, **26**, 2984–2998.
24. ElAntak,L., Wagner,S., Herrmannová,A., Karásková,M., Rutkai,E., Lukavsky,P.J. and Valášek,L. (2010) The indispensable N-terminal half of eIF3j co-operates with its structurally conserved binding partner eIF3b-RRM and eIF1A in stringent AUG selection. *J. Mol. Biol.*, **396**, 1097–1116.
25. Herrmannová,A., Daujotyte,D., Yang,J.C., Cuchalová,L., Gorrec,F., Wagner,S., Danyi,I., Lukavsky,P.J. and Valášek,L.S. (2012) Structural analysis of an eIF3 subcomplex reveals conserved interactions required for a stable and proper translation pre-Initiation complex assembly. *Nucleic Acids Res.*, **40**, 2294–2311.
26. Karaskova,M., Gunisova,S., Herrmannova,A., Wagner,S., Munzarova,V. and Valasek,L.S. (2012) Functional characterization of the role of the N-terminal domain of the c/Nip1 subunit of eukaryotic initiation factor 3 (eIF3) in AUG recognition. *J. Biol. Chem.*, **287**, 28420–28434.
27. Beznosková,P., Cuchalová,L., Wagner,S., Shoemaker,C.J., Gunišová,S., Von der Haar,T. and Valášek,L.S. (2013) Translation initiation factors eIF3 and HCR1 control translation termination and stop codon read-through in yeast cells. *PLoS Genet.*, **9**, e1003962.
28. Querol-Audi,J., Sun,C., Vogan,J.M., Smith,M.D., Gu,Y., Cate,J.H. and Nogales,E. (2013) Architecture of human translation initiation factor 3. *Structure*, **21**, 920–928.
29. Hashem,Y., des Georges,A., Dhote,V., Langlois,R., Liao,H.Y., Grassucci,R.A., Hellen,C.U., Pestova,T.V. and Frank,J. (2013) Structure of the mammalian ribosomal 43S preinitiation complex bound to the scanning factor DHX29. *Cell*, **153**, 1108–1119.
30. Khoshnevis,S., Neumann,P. and Ficner,R. (2010) Crystal structure of the RNA recognition motif of yeast translation initiation factor eIF3b reveals differences to human eIF3b. *PLoS One*, **5**, e12784.
31. ElAntak,L., Tzakos,A.G., Locker,N. and Lukavsky,P.J. (2007) Structure of eIF3b RNA recognition motif and its interaction with eIF3j: structural insights into the recruitment of eIF3b to the 40 S ribosomal subunit. *J. Biol. Chem.*, **282**, 8165–8174.
32. Wei,Z., Xue,Y., Xu,H. and Gong,W. (2006) Crystal structure of the C-terminal domain of *S.cerevisiae* eIF5. *J. Mol. Biol.*, **359**, 1–9.
33. Pick,E., Hofmann,K. and Glickman,M.H. (2009) PCI complexes: beyond the proteasome, CSN, and eIF3 troika. *Mol. Cell*, **35**, 260–264.
34. Kouba,T., Rutkai,E., Karasková,M. and Valášek,L.S. (2012) The eIF3c/NIP1 PCI domain interacts with RNA and RACK1/ASC1 and promotes assembly of the pre-initiation complexes. *Nucleic Acids Res.*, **40**, 2683–2699.
35. Ellisdon,A.M., Dimitrova,L., Hurt,E. and Stewart,M. (2012) Structural basis for the assembly and nucleic acid binding of the TREX-2 transcription-export complex. *Nat. Struct. Mol. Biol.*, **19**, 328–336.
36. Munzarová,V., Pánek,J., Gunišová,S., Dányi,I., Szamecz,B. and Valášek,L.S. (2011) Translation reinitiation relies on the interaction between eIF3a/TIF32 and progressively folded cis-acting mRNA elements preceding short uORFs. *PLoS Genet.*, **7**, e1002137.
37. Mueller,U., Darowski,N., Fuchs,M.R., Forster,R., Hellmig,M., Paithankar,K.S., Puhringer,S., Steffien,M., Zocher,G. and Weiss,M.S. (2012) Facilities for macromolecular crystallography at the Helmholtz-Zentrum Berlin. *J. Synchrotron Radiat.*, **19**, 442–449.
38. Kabsch,W. (2010) Integration, scaling, space-group assignment and post-refinement. *Acta Crystallogr. D Biol. Crystallogr.*, **66**, 133–144.
39. Kabsch,W. (2010) Xds. *Acta Crystallogr. D Biol. Crystallogr.*, **66**, 125–132.
40. Vonrhein,C., Blanc,E., Roversi,P. and Bricogne,G. (2007) Automated structure solution with autoSHARP. *Methods Mol. Biol.*, **364**, 215–230.
41. Sheldrick,G.M. (2010) Experimental phasing with SHELXC/D/E: combining chain tracing with density modification. *Acta Crystallogr. D Biol. Crystallogr.*, **66**, 479–485.
42. Abrahams,J.P. and Leslie,A.G. (1996) Methods used in the structure determination of bovine mitochondrial F1 ATPase. *Acta Crystallogr. D Biol. Crystallogr.*, **52**, 30–42.
43. Langer,G., Cohen,S.X., Lamzin,V.S. and Perrakis,A. (2008) Automated macromolecular model building for X-ray crystallography using ARP/wARP version 7. *Nat. Protoc.*, **3**, 1171–1179.
44. Acker,M.G., Kolitz,S.E., Mitchell,S.F., Nanda,J.S. and Lorsch,J.R. (2007) *Methods in Enzymology*, Vol. 430. Academic Press, pp. 111–145.
45. Khoshnevis,S., Hauer,F., Milon,P., Stark,H. and Ficner,R. (2012) Novel insights into the architecture and protein interaction network of yeast eIF3. *RNA*, **18**, 2306–2319.
46. Kouba,T., Danyi,I., Gunišová,S., Munzarová,V., Vlčková,V., Cuchalová,L., Neueder,A., Milkereit,P. and Valášek,L.S. (2012) Small ribosomal protein RPS0 stimulates translation initiation by mediating 40S-binding of eIF3 via its direct contact with the eIF3a/TIF32 subunit. *PLoS One*, **7**, e40464.
47. Rabl,J., Leibundgut,M., Ataide,S.F., Haag,A. and Ban,N. (2011) Crystal structure of the eukaryotic 40S ribosomal subunit in complex with initiation factor 1. *Science*, **331**, 730–736.
48. Valášek,L., Szamecz,B., Hinnebusch,A.G. and Nielsen,K.H. (2007) *In vivo* stabilization of preinitiation complexes by formaldehyde cross-linking. *Methods Enzymol.*, **429**, 163–183.
49. Hinnebusch,A.G. (2005) Translational regulation of GCN4 and the general amino acid control of yeast. *Annu. Rev. Microbiol.*, **59**, 407–450.
50. Fekete,C.A., Mitchell,S.F., Cherkasova,V.A., Applefield,D., Algire,M.A., Maag,D., Saini,A.K., Lorsch,J.R. and Hinnebusch,A.G. (2007) N- and C-terminal residues of eIF1A have opposing effects on the fidelity of start codon selection. *EMBO J.*, **26**, 1602–1614.
51. Singh,C.R., Watanabe,R., Chowdhury,W., Hiraishi,H., Murai,M.J., Yamamoto,Y., Miles,D., Ikeda,Y., Asano,M. and Asano,K. (2012) Sequential eukaryotic translation initiation factor 5 (eIF5) binding to the charged disordered segments of eIF4G and eIF2beta stabilizes the 48S preinitiation complex and promotes its shift to the initiation mode. *Mol. Cell. Biol.*, **32**, 3978–3989.
52. Karplus,P.A. and Diederichs,K. (2012) Linking crystallographic model and data quality. *Science*, **336**, 1030–1033.
53. Ashkenazy,H., Penn,O., Doron-Faigenboim,A., Cohen,O., Cannarozzi,G., Zomer,O. and Pupko,T. (2012) FastML: a web server for probabilistic reconstruction of ancestral sequences. *Nucleic Acids Res.*, **40**, W580–W584.
54. Pathare,G.R., Nagy,I., Bohn,S., Unverdorben,P., Hubert,A., Korner,R., Nickell,S., Lasker,K., Sali,A., Tamura,T. *et al.* (2012) The proteasomal subunit Rpn6 is a molecular clamp holding the core and regulatory subcomplexes together. *Proc. Natl Acad. Sci. USA*, **109**, 149–154.

55. Dessau,M., Halimi,Y., Erez,T., Chomsky-Hecht,O., Chamovitz,D.A. and Hirsch,J.A. (2008) The *Arabidopsis* COP9 signalosome subunit 7 is a model PCI domain protein with subdomains involved in COP9 signalosome assembly. *Plant Cell*, **20**, 2815–2834.
56. Wei,Z., Zhang,P., Zhou,Z., Cheng,Z., Wan,M. and Gong,W. (2004) Crystal structure of human eIF3k, the first structure of eIF3 subunits. *J. Biol. Chem.*, **279**, 34983–34990.
57. Ellisdon,A.M. and Stewart,M. (2012) Structural biology of the PCI-protein fold. *Bioarchitecture*, **2**.
58. Asano,K., Phan,L., Anderson,J. and Hinnebusch,A.G. (1998) Complex formation by all five homologues of mammalian translation initiation factor 3 subunits from yeast *Saccharomyces cerevisiae*. *J. Biol. Chem.*, **273**, 18573–18585.
59. Valášek,L., Phan,L., Schoenfeld,L.W., Valášková,V. and Hinnebusch,A.G. (2001) Related eIF3 subunits TIF32 and HCR1 interact with an RNA recoginition motif in PRT1 required for eIF3 integrity and ribosome binding. *EMBO J.*, **20**, 891–904.
60. Gajiwala,K.S. and Burley,S.K. (2000) Winged helix proteins. *Curr. Opin. Struct. Biol.*, **10**, 110–116.
61. Baker,N.A., Sept,D., Joseph,S., Holst,M.J. and McCammon,J.A. (2001) Electrostatics of nanosystems: application to microtubules and the ribosome. *Proc. Natl Acad. Sci. USA*, **98**, 10037–10041.
62. Kelley,L.A. and Sternberg,M.J.E. (2009) Protein structure prediction on the Web: a case study using the Phyre server. *Nat. Protoc.*, **4**, 363–371.
63. Ritchie,D.W., Kozakov,D. and Vajda,S. (2008) Accelerating and focusing protein-protein docking correlations using multi-dimensional rotational FFT generating functions. *Bioinformatics*, **24**, 1865–1873.
64. Valášek,L., Mathew,A., Shin,B.S., Nielsen,K.H., Szamecz,B. and Hinnebusch,A.G. (2003) The yeast eIF3 subunits TIF32/a and NIP1/c and eIF5 make critical connections with the 40S ribosome *in vivo*. *Genes Dev.*, **17**, 786–799.
65. Passmore,L.A., Schmeing,T.M., Maag,D., Applefield,D.J., Acker,M.G., Algire,M.A., Lorsch,J.R. and Ramakrishnan,V. (2007) The eukaryotic translation initiation factors eIF1 and eIF1A induce an open conformation of the 40S ribosome. *Mol. Cell*, **26**, 41–50.
66. Lomakin,I.B. and Steitz,T.A. (2013) The initiation of mammalian protein synthesis and mRNA scanning mechanism. *Nature*, **500**, 307–311.
67. Pisarev,A.V., Kolupaeva,V.G., Yusupov,M.M., Hellen,C.U.T. and Pestova,T.V. (2008) Ribosomal position and contacts of mRNA in eukaryotic translation initiation complexes. *EMBO J.*, **27**, 1609–1621.
68. Rogers,G.W. Jr, Richter,N.J., Lima,W.F. and Merrick,W.C. (2001) Modulation of the helicase activity of eIF4A by eIF4B, eIF4H, and eIF4F. *J. Biol. Chem.*, **276**, 30914–30922.
69. Walker,S.E., Zhou,F., Mitchell,S.F., Larson,V.S., Valasek,L., Hinnebusch,A.G. and Lorsch,J.R. (2013) Yeast eIF4B binds to the head of the 40S ribosomal subunit and promotes mRNA recruitment through its N-terminal and internal repeat domains. *RNA*, **19**, 191–207.
70. Vornlocher,H.P., Hanachi,P., Ribeiro,S. and Hershey,J.W.B. (1999) a 110-kilodalton subunit of translation initiation factor eIF3 and an associated 135-kilodalton protein are encoded by the *Saccharomyces cerevisiae* TIF32 and TIF31 genes. *J. Biol. Chem.*, **274**, 16802–16812.
71. Park,E.-H., Walker,S.E., Lee,J.M., Rothenburg,S., Lorsch,J.R. and Hinnebusch,A.G. (2010) Multiple elements in the eIF4G1 N-terminus promote assembly of eIF4G1[bull]PABP mRNPs *in vivo*. *EMBO J.*, **30**, 302–316.
72. LeFebvre,A.K., Korneeva,N.L., Trutschl,M., Cvek,U., Duzan,R.D., Bradley,C.A., Hershey,J.W. and Rhoads,R. (2006) Translation initiation factor eIF4G-1 binds to eIF3 through the eIF3e subunit. *J. Biol. Chem.*, **281**, 22917–22932.
73. Asano,K., Kinzy,T.G., Merrick,W.C. and Hershey,J.W.B. (1997) Conservation and diversity of eukaryotic translation initiation factor eIF3. *J. Biol. Chem.*, **272**, 1101–1109.
74. Block,K.L., Vornlocher,H.P. and Hershey,J.W.B. (1998) Characterization of cDNAs encoding the p44 and p35 subunits of human translation initiation factor eIF3. *J. Biol. Chem.*, **273**, 31901–31908.
75. Luna,R.E., Arthanari,H., Hiraishi,H., Nanda,J., Martin-Marcos,P., Markus,M.A., Akabayov,B., Milbradt,A.G., Luna,L.E., Seo,H.C. *et al.* (2012) The C-terminal domain of eukaryotic initiation factor 5 promotes start codon recognition by its dynamic interplay with eIF1 and eIF2beta. *Cell Rep.*, **1**, 689–702.

eLIFE elifesciences.org

RESEARCH ARTICLE

Eukaryotic translation initiation factor 3 plays distinct roles at the mRNA entry and exit channels of the ribosomal preinitiation complex

Colin Echeverría Aitken[1], Petra Beznosková[2], Vladislava Vlčkova[2], Wen-Ling Chiu[3†], Fujun Zhou[1], Leoš Shivaya Valášek[2*], Alan G Hinnebusch[3*], Jon R Lorsch[1*]

[1]Laboratory on the Mechanism and Regulation of Protein Synthesis, Eunice Kennedy Shriver National Institute of Child Health and Human Development, National Institutes of Health, Bethesda, United States; [2]Laboratory of Regulation of Gene Expression, Institute of Microbiology ASCR, Prague, Czech Republic; [3]Laboratory of Gene Regulation and Development, Eunice Kennedy Shriver National Institute of Child Health and Human Development, National Institutes of Health, Bethesda, United States

Abstract Eukaryotic translation initiation factor 3 (eIF3) is a central player in recruitment of the pre-initiation complex (PIC) to mRNA. We probed the effects on mRNA recruitment of a library of *S. cerevisiae* eIF3 functional variants spanning its 5 essential subunits using an in vitro-reconstituted system. Mutations throughout eIF3 disrupt its interaction with the PIC and diminish its ability to accelerate recruitment to a native yeast mRNA. Alterations to the eIF3a CTD and eIF3b/i/g significantly slow mRNA recruitment, and mutations within eIF3b/i/g destabilize eIF2•GTP•Met-tRNA$_i$ binding to the PIC. Using model mRNAs lacking contacts with the 40S entry or exit channels, we uncovered a critical role for eIF3 requiring the eIF3a NTD, in stabilizing mRNA interactions at the exit channel, and an ancillary role at the entry channel requiring residues of the eIF3a CTD. These functions are redundant: defects at each channel can be rescued by filling the other channel with mRNA.
DOI: 10.7554/eLife.20934.001

***For correspondence:** valasekl@biomed.cas.cz (LSV); ahinnebusch@nih.gov (AGH); jon.lorsch@nih.gov (JRL)

Present address: †PharmaEssentia Corp., Taipei, Taiwan

Competing interest: See page 25

Funding: See page 25

Received: 25 August 2016
Accepted: 25 October 2016
Published: 26 October 2016

Reviewing editor: Nahum Sonenberg, McGill University, Canada

This is an open-access article, free of all copyright, and may be freely reproduced, distributed, transmitted, modified, built upon, or otherwise used by anyone for any lawful purpose. The work is made available under the Creative Commons CC0 public domain dedication.

Introduction

The goal of translation initiation is to assemble the ribosome at the start (AUG) codon of an mRNA in a state ready to begin reading the message and synthesizing the corresponding protein. This represents one of the most important readings of the genetic code because initiation at the wrong site results in extended, truncated or out of frame translation products. To ensure faithful identification of the start codon, translation initiation in eukaryotes follows a complex, multi-step pathway which requires the participation of 12 initiation factors (eIFs) (reviewed in: (***Aitken and Lorsch, 2012***; ***Hinnebusch, 2014***; ***Jackson et al., 2010***; ***Sonenberg and Hinnebusch, 2009***; ***Valášek, 2012***). The process begins with the formation of a 43S pre-initiation complex (PIC), in which the initiator methionyl tRNA (Met-tRNA$_i$) is initially positioned as a tRNA$_i$•eIF2•GTP ternary complex (TC) on the small (40S) ribosomal subunit. The 43S PIC further contains eIF1 and eIF1A bound, respectively, near the 40S P and A sites, as well as eIF5 and eIF3. GTP hydrolysis by eIF2 can proceed within the PIC, but the release of inorganic phosphate (P$_i$) is blocked by the presence of eIF1. With the collaboration of eIF4B and the eIF4F complex composed of eIF4A, eIF4G, and eIF4E, the PIC is then loaded onto the

eLife digest Cells use the genetic information stored within genes to build proteins, which are largely responsible for performing the molecular tasks essential for life. The ribosome is the molecular machine that translates the information within genes to assemble proteins in all cells, from bacteria to humans. To make a protein, the corresponding gene is first copied to make molecules of messenger ribonucleic acid (or mRNA for short). Then the ribosome binds to the mRNA in a process called translation initiation.

Cells tightly regulate translation initiation so that they can decide which proteins to make, according to their needs and in response to changes in the environment. In fact, regulation of translation initiation is often disrupted during viral infections, cancer and other human diseases. A set of proteins called translation initiation factors drive translation initiation; the largest and least understood of these is called eIF3.

Cells are unable to load the mRNA onto the ribosome without eIF3, which has two "arms" that sit near where the mRNA enters and exits the ribosome. Aitken et al. used mutant forms of eIF3 from genetically modified yeast to investigate how the arms of the protein work, and if they help the ribosome hold onto the mRNA.

These experiments show that the two arms of eIF3 have unique roles. One arm sits near where mRNA exits the ribosome and is important for holding onto the mRNA. The other arm – which is near where mRNA enters the ribosome – helps hold the ribosome and other components of the translation machinery together. This arm may also help to open and close the channel through which messenger RNA enters the ribosome. The next challenges are to find out the precise role this arm plays in translation – in particular, how it helps to open and close the channel in the ribosome, and whether this helps the ribosome load the messenger RNA or even move along it.

DOI: 10.7554/eLife.20934.002

5' end of the mRNA, from which it scans in the 3' direction to locate the AUG codon, thus generating the 48S PIC. Both loading onto the mRNA and subsequent scanning are facilitated by an open conformation of the PIC enforced by the binding of eIF1. Recognition of the AUG codon triggers eviction of eIF1, gating P_i release by eIF2 and provoking a transition from the open PIC conformation to a closed conformation that arrests scanning. Joining of a 60S ribosomal subunit completes assembly of the 80S initiation complex, which can then proceed to the elongation cycle.

The largest of the initiation factors is eIF3, a multisubunit complex that binds the 40S subunit and has been implicated in events throughout the initiation pathway (***Hinnebusch, 2006***, ***2011***; ***Valásek, 2012***). In humans, eIF3 is composed of 13 individual subunits. In the yeast *S. cerevisiae*, eIF3 comprises 5 essential subunits thought to represent a core complex capable of performing the essential tasks of eIF3: eIF3a, eIF3b, eIF3c, eIF3i, and eIF3g. A sixth nonessential and nonstoichiometric subunit, eIF3j, associates loosely with the complex (***Elantak et al., 2010***; ***Fraser et al., 2004***; ***Nielsen et al., 2006***; ***Valasek et al., 2001a***), though its role during initiation remains unclear (***Beznosková et al., 2013***; ***Fraser et al., 2007***; ***Mitchell et al., 2010***). Genetic and biochemical evidence indicate that eIF3 stabilizes both the 43S (***Asano et al., 2000***; ***Kolupaeva et al., 2005***; ***Maag et al., 2005***; ***Valášek et al., 2003***) and 48S PIC (***Chiu et al., 2010***; ***Khoshnevis et al., 2014***; ***Phan et al., 2001***) and interacts with TC (***Valášek et al., 2002***), eIF1 (***Fletcher et al., 1999***; ***Valasek et al., 2004***), eIF1A (***Olsen et al., 2003***), and eIF5 (***Asano et al., 2001***; ***Phan et al., 1998***), as well as with the 40S subunit near both the mRNA entry and exit channels (***Kouba et al., 2012a***, ***2012b***; ***Pisarev et al., 2008***; ***Valášek et al., 2003***). eIF3 also plays roles in loading the mRNA onto the PIC (***Jivotovskaya et al., 2006***; ***Mitchell et al., 2010***; ***Pestova and Kolupaeva, 2002***) and in scanning of the mRNA to locate the start codon (***Chiu et al., 2010***; ***Cuchalova et al., 2010***; ***Karásková et al., 2012***; ***Nielsen et al., 2006***; ***Valasek et al., 2004***). How eIF3 contributes to these diverse events is not yet clear.

Recent results have highlighted the role of eIF3 in mRNA recruitment to the PIC. The depletion of eIF3 from yeast cells sharply decreases the amount of mRNA associated with PICs in vivo (***Jivotovskaya et al., 2006***). In vitro, yeast eIF3 is required for detectable recruitment of native mRNAs in the yeast reconstituted translation initiation system (***Mitchell et al., 2010***). Mutations in

the C-terminal domain (CTD) of eIF3a, which interacts with the 40S subunit near the mRNA entry channel, impair mRNA recruitment in yeast cells without affecting the integrity of the PIC (**Chiu et al., 2010**). The eIF3a N-terminal domain (NTD) interacts functionally with mRNA near the exit channel, enhancing reinitiation upon translation of the upstream open reading frame 1 (uORF1) and uORF2 of *GCN4* mRNA in a manner dependent on the sequence upstream of these two uORFs (**Gunišová et al., 2016**; **Gunišová and Valášek, 2014**; **Munzarová et al., 2011**; **Szamecz et al., 2008**). Consistent with this, mammalian eIF3 can be cross-linked to mRNA at positions 8–17 nucleotides upstream of the AUG codon (**Pisarev et al., 2008**), near the exit channel, and a mutation within the eIF3a NTD, which has been located near the exit channel in structures of the PIC, interferes with mRNA recruitment in yeast cells (**Khoshnevis et al., 2014**).

How eIF3 might intervene at both the mRNA entry and exit channels of the PIC was illuminated recently by a series of structural studies. Initial structural information — based on separate lower resolution Cryo-EM reconstructions — placed mammalian eIF3 on the solvent-exposed face of the 40S subunit, near the platform, but did not reveal interactions in either the entry or exit channel (**Siridechadilok et al., 2005**). Subsequent studies in the presence of the helicase DHX29 refined this placement, identifying two main points of contact near the 40S platform, as well as potential peripheral domains of eIF3 near the 40S head above the platform and below DHX29 nearer the mRNA entry channel (**Hashem et al., 2013**).

More recently, high-resolution Cryo-EM reconstructions of mammalian eIF3 bound to a PIC containing DHX29 (**Georges, des et al., 2015**) and of yeast eIF3 bound either to a 40S•eIF1•eIF1A complex (**Aylett et al., 2015**) or to a partial 48S PIC containing mRNA (**Llácer et al., 2015**) (**Figure 1A–C**, py48S-closed structure) have revealed this interaction in molecular detail. In these structures, eIF3 (shown in blues and reds from py48S-closed structure) is found bound primarily to the 40S (light grey) solvent face, via two main points of contact. First, the eIF3a (dark blue) NTD and eIF3c (light blue) CTD PCI (**P**roteasome/**C**op9/e**I**F3) domains form a heterodimer that binds below the platform, near the mRNA exit channel pore (**Figure 1B**). A second contact is formed closer to the mRNA entry-channel side of the PIC (**Figure 1A**), in the vicinity of helix 16 (h16) and helix 18 (h18) of the 40S rRNA. This contact is made by the eIF3b (light blue) β-propeller domain, consistent with its described interaction with uS4 (**Liu et al., 2014**), and is likely connected to the first contact via a previously identified interaction between the eIF3b RRM and the eIF3a CTD (**Valasek et al., 2001b**; **Valášek et al., 2002**), which likely spans the solvent face (**Figure 1C**). In both the mammalian structure and the yeast eIF3•40S•eIF1•eIF1A structure, the eIF3i and eIF3g subunits are found above the eIF3b subunit, near the solvent-face opening of the mRNA entry channel; with the exception of the non-essential eIF3j subunit, no density for eIF3 was observed on the intersubunit face of the 40S in these structures. In the partial 48S structure (**Figure 1B**), the eIF3c (light blue) NTD extends from the eIF3a/eIF3c PCI heterodimer near the exit channel towards the intersubunit face, projecting near the P-site, where it appears to interact with eIF1 (pink). Near the entry channel, the eIF3a CTD extends away from eIF3b (**Figure 1A**), wrapping around the 40S, spanning the intersubunit face, and nearly meeting the eIF3c NTD near the P-site, effectively encircling the 43S PIC (**Figure 1C**). In this structure, the eIF3i (maroon) and eIF3g (red) subunits are located together with the eIF3b C-terminal region on the intersubunit face near the A site and below the intersubunit-face opening of the mRNA entry channel, where eIF3i interacts with the eIF2γ portion of the TC (green and charcoal). In a recent structure of mammalian eIF3 bound to an apparently late-stage initiation complex, eIF3i was found at a distinct location on the intersubunit face of the PIC, leading to the suggestion that the density observed near TC in the yeast py48S-closed structure is in fact the β-propeller of eIF3b and not eIF3i (**Simonetti et al., 2016**).

While these recent structures illuminate several important contacts between eIF3 and the PIC, the identification of less well-resolved domains of eIF3, as well as the proposed placement of unresolved regions of the complex rest heavily on a host of interactions previously identified in genetic and biochemical studies. These studies established interactions between the eIF3a CTD and the eIF3b RRM **Valasek et al., 2001b**), the 40S latch components uS3/uS5 and h16/18 (**Chiu et al., 2010**; **Valášek et al., 2003**), and with TC at its extreme C-terminus (**Valášek et al., 2002**). The C-terminal region of eIF3b was previously shown to be required for binding of eIF3i and eIF3g (**Asano et al., 1998**; **Herrmannová et al., 2012**), the latter of which was observed to interact with uS3 and uS10 (**Cuchalova et al., 2010**). These observations delineate a network of interactions between the eIF3a CTD, eIF3b, eIF3i, and eIF3g, and place them either in the vicinity of the entry channel or projecting

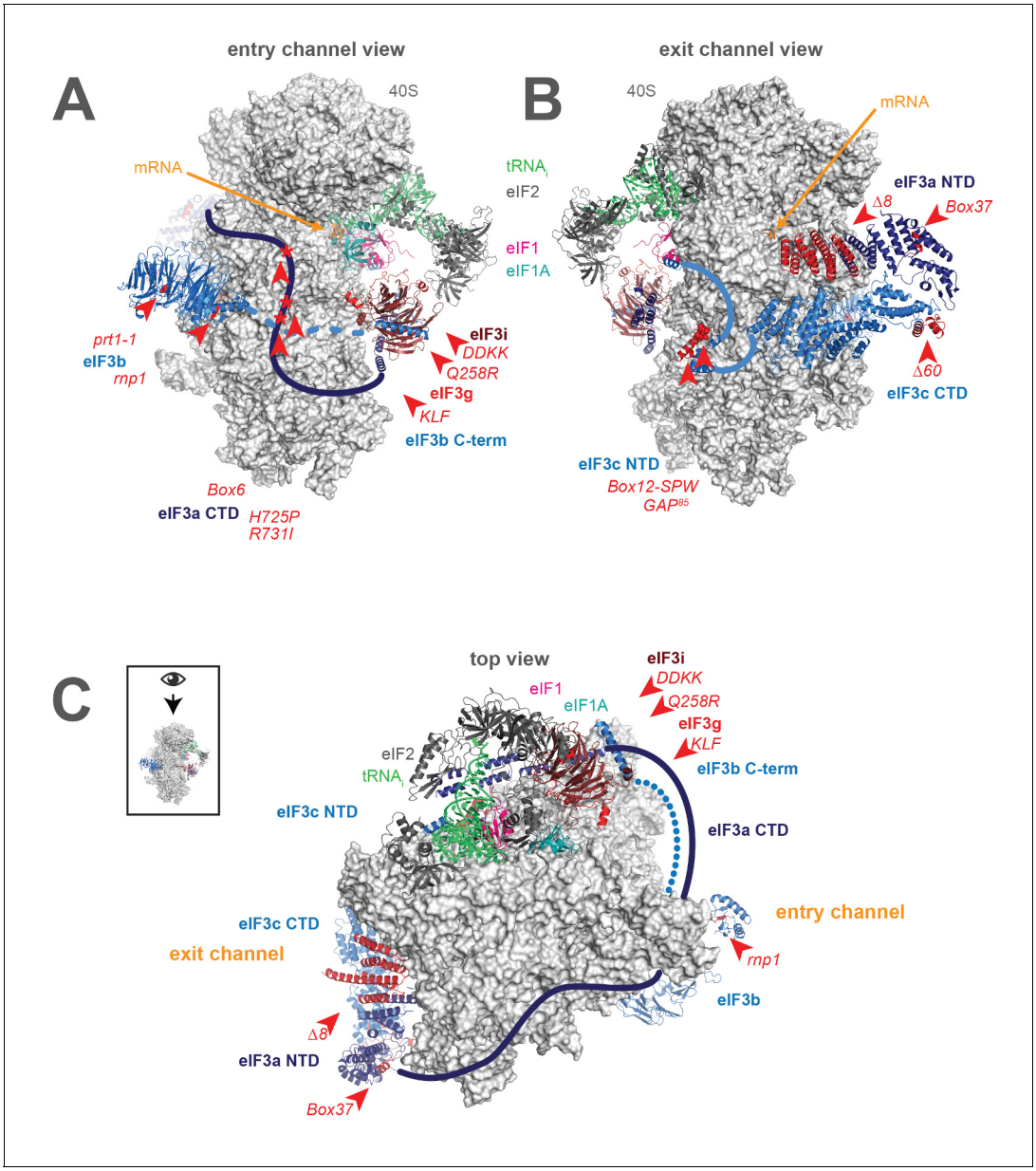

Figure 1. A library of *S. cerevisiae* eIF3 functional variants affected by mutations spanning all five essential subunits. Three views of the cryo-EM structure of eIF3 bound to the partial yeast 48S PIC in the closed conformation (py48S-closed), as reported by Llacer, *et al.* The 40S subunit is shown in light grey, with resolved domains of eIF3 shown as ribbons and unresolved regions cartooned as solid or dotted lines: eIF3a is shown in dark blue, eIF3c and eIF3b in light blue, eIF3i in maroon, and eIF3g in red. The location of mutations throughout eIF3 are shown colored in red and indicated by red arrowheads; the eIF3i and eIF3g subunits are also depicted in red hues owing to their absence in the a/b/c subcomplex resulting from the *DDKK* mutation in eIF3i. The mRNA (orange), Met-tRNA$_i$ (green), eIF2 (charcoal), eIF1 (pink), and eIF1A (teal) are also visible in this structure. (**A**) View looking towards the mRNA entry channel, with the 40S intersubunit face on the right, and the solvent face on the left. (**B**) Opposite view looking towards the mRNA exit channel, with the 40S intersubunit face on the left, and the solvent face on the right. (**C**) View of the PIC looking down at the 40S head, showing the relative orientation of the entry- and exit-channel arms of eIF3 and its contacts on the 40S solvent face. The PIC is oriented such that the intersubunit face appears at the top, while the solvent face appears at the bottom.

DOI: 10.7554/eLife.20934.003

towards the 40S intersubunit face. Other studies identified interactions between the eIF3a NTD and uS2 (***Valášek et al., 2003***; ***Kouba et al., 2012b***), the eIF3c CTD and RACK1 (***Kouba et al., 2012a***), and between the eIF3c NTD and both eIF5 and eIF1 (***Asano et al., 2000***; ***Valasek et al., 2004***). This final observation, together with the discovery of mutations in the eIF3c NTD that affect the fidelity

of start-codon recognition (**Valasek et al., 2004**; **Karásková et al., 2012**), supports the putative identification of regions of density near the P site in the py48S-closed structure (**Llácer et al., 2015**).

Together with this previous work, structural studies reveal the presence of eIF3 not just on the 40S solvent face, but near the functional centers of the PIC. In particular, eIF3 appears to project arms into or near both the mRNA entry and exit channels (**Figure 1C**). Based on their apparent locations near either the solvent-face or intersubunit-face openings of the mRNA entry channel, eIF3i, eIF3g, the C-terminal region of eIF3b, and the eIF3a CTD together compose the entry-channel arm. The exit-channel arm comprises the eIF3a NTD and eIF3c CTD PCI heterodimer located below the platform at the solvent-face opening of the mRNA exit channel. The presence of eIF3 subunits at both mRNA channels, near the P site, and encircling the PIC does not, however, clarify the mechanistic nature of their involvement during steps of the initiation pathway. These regions of eIF3 might participate actively in these events, interacting and collaborating with the 40S, mRNA, and initiation factors to stimulate mRNA recruitment, scanning, and start-codon recognition. eIF3 might also alter the conformation of the PIC to indirectly enhance the efficiency of these steps or serve as a scaffold upon which other factors can bind.

To interrogate the mechanistic roles of the domains of eIF3, we purified a library of *S. cerevisiae* eIF3 variants – all of which were previously characterized in vivo (**Chiu et al., 2010**; **Cuchalova et al., 2010**; **Herrmannová et al., 2012**; **Karásková et al., 2012**; **Khoshnevis et al., 2014**; **Kouba et al., 2012a**; **Nielsen et al., 2004**, **2006**; **Szamecz et al., 2008**) – to probe their effects on steps and interactions in the translation initiation pathway in an in vitro-reconstituted yeast translation system (**Acker et al., 2007**; **Algire et al., 2002**; **Mitchell et al., 2010**). This library contains variants with mutations spanning the five essential subunits of eIF3 (**Table 1**). The phenotypes associated with these mutants suggest defects in 40S binding, 43S PIC formation, mRNA recruitment, scanning, and start-codon recognition. Our results demonstrate that regions throughout the eIF3 complex contribute to its interaction with the PIC and its role in mRNA recruitment. In particular, the mRNA entry-channel arm of eIF3 and eIF3b appear to play a role in stabilizing TC binding to the PIC and accelerating mRNA recruitment. In contrast, the mRNA exit channel arm of eIF3 is required to stabilize the binding of mRNA within the PIC, and this function can be attributed to the extreme N-terminal region of the eIF3a subunit.

Results

The eIF3 variants in this study can be divided into four categories (**Table 1**). The first contains mutations in the components of the eIF3 entry channel arm (**Figure 1A**). This includes mutations to the eIF3i (*Q258R, DDKK*) and eIF3g (*KLF*) subunits (**Asano et al., 1998**; **Cuchalova et al., 2010**; **Herrmannová et al., 2012**). The eIF3i *DDKK* mutation disrupts the interaction between the eIF3i/g module and eIF3b, resulting in the dissociation of eIF3i/g from the sub-complex containing the a, b, and c subunits (**Herrmannová et al., 2012**); eIF3 purified from *DDKK* cells yields the WT eIF3a/b/c sub-complex. These mutations produce phenotypes consistent with scanning defects, and in the case of the *DDKK* mutation also reduce binding of eIF3 to the 43S PIC in vivo. Also included in this group are mutations to the eIF3a CTD (*H725P, R731I, Box6*) (**Valasek et al., 1998**; **Chiu et al., 2010**), which has not been resolved in recent structural models but was shown to interact with the RRM of eIF3b (**Valasek et al., 2001b**), as well as with 40S components near the mRNA entry channel: uS5, uS3, h16, and h18 (**Chiu et al., 2010**; **Valášek et al., 2003**). These mutations affect mRNA recruitment, scanning, and codon recognition in vivo, perhaps by affecting the equilibrium between the open and closed states of the 43S PIC.

The second group of mutations affects residues of eIF3b located at the solvent face of the 40S subunit (**Figure 1A**). The *prt1-1* mutation was the first functional variant of eIF3 to be identified (**Evans et al., 1995**; **Hartwell and McLaughlin, 1969**) and is a point-substitution (S555F) within the eIF3b β-propeller domain that contacts the 40S subunit and is connected to the eIF3i/g module of the entry-channel arm via the C-terminal segment of eIF3b (**Herrmannová et al., 2012**). The *rnp1* mutation is within the eIF3b N-terminal RRM domain (**Nielsen et al., 2006**), which interacts with the eIF3a CTD portion of the entry-channel arm (**Valasek et al., 2001b**). Both eIF3b mutations give rise to a complex portfolio of phenotypes consistent with defects in 40S binding, 43S PIC formation, scanning, and codon recognition (**Nielsen et al., 2004**, **2006**).

Table 1. Putative mechanistic defects attributed to eIF3 variants. Table describing the putative mechanistic defects attributed to each eIF3 variant within our library. Variants are organized according to their general location within the PIC (left column) and by the subunit or subunit domain (second column from left) in which the associated mutation occurs (allelic designation in third column from left). The specific identity of the mutation affecting each variant (second column from right) and the putative mechanistic defects previously attributed to each variant (final column, see text for references) are described.

Location	Subunit	Variant	Mutation	Putative defects
Entry channel	eIF3a/Tif32 CTD	*H725P*	H725P	mRNA recruitment scanning codon recognition
		R731I	R731I	
		Box6	Alanine substitution of ^{692}LDLDTIKQVI^{701}	
	eIF3i/Tif34	*Q258R*	Q258R	scanning
		DDKK	D207K/D224K	40S binding 43S PIC formation scanning start codon recognition
	eIF3g/Tif35	*KLF*	K194A/L235A/F237A	scanning
Solvent face	eIF3b/Prt1	*prt1-1*	S555F	40S binding 43S PIC formation scanning start codon recognition
		rnp1	Alanine substitution of ^{124}KGFLVE^{130}	
Exit channel	eIF3c/Nip1 CTD	*Δ60*	C-terminal truncation of aa 753–813	40S binding 43S PIC formation
	eIF3a/Tif32 NTD	*Δ8*	N-terminal truncation of aa 1–200	40S binding 43S PIC formation re-initiation
		Box37	Alanine substitution of ^{361}PTRKEMLQSI^{370}	mRNA recruitment
P site	eIF3c/Nip1 NTD	*GAP^{85}*	Deletion of aa 60–144	eIF1 binding start codon recognition
		Box12-SPW	K111S/K114P/K116W	

DOI: 10.7554/eLife.20934.004

The next group includes mutations to regions of eIF3 located near the mRNA exit channel of the 40S ribosomal subunit (***Figure 1B***). Among these are a 200 amino acid N-terminal truncation of the eIF3a PCI domain (*Δ8*), as well as a multiple alanine substitution deeper within the eIF3a PCI domain (*Box37*). The *Δ8* mutation disrupts a previously identified interaction between eIF3a and uS2 (***Valášek et al., 2003***), apparently weakening the eIF3:40S interaction (***Szamecz et al., 2008***), whereas the *Box37* substitution predominantly reduces mRNA association with native PICs in vivo (***Khoshnevis et al., 2014***). The final mutant in this group is a 60 amino acid C-terminal truncation of the eIF3c PCI domain (*Δ60*) that reduces the amount of both eIF3 and eIF5 in 43S PICS, apparently by disrupting interactions with the ribosome-associated protein RACK1 and the 18S rRNA (***Kouba et al., 2012a***).

Lastly, we investigated mutations within the N-terminal region of eIF3c (*GAP^{85}*, *Box12-SPW*) that is thought to project near the P site and mediate interactions with eIF1 near the decoding center of the 40S subunit (***Figure 1B***). These mutations affect the amount of eIF1 bound to 43S PICs and appear to interfere with stringent selection of the AUG start-codon (***Karásková et al., 2012***).

Both the mRNA entry and exit channel arms of eIF3 and the eIF3b subunit contribute to stabilizing eIF3 interaction with the 43S complex

Genetic approaches have identified mutations in eIF3 that reduce its abundance in native 43S or 48S PICs in vivo, suggesting the altered residues are involved in interactions with the 40S ribosomal

subunit or other components of the PIC. This interpretation is corroborated by structural studies that identify points of contact between the 43S PIC and eIF3, as described above. To directly interrogate the contributions of the eIF3 subunits to the 43S:eIF3 interaction, we first examined the ability of each eIF3 variant to bind 43S complexes in vitro. To this end, we assembled 43S complexes using purified 40S subunits, saturating levels of eIF1 and eIF1A, and a limiting concentration of TC containing initiator $tRNA_i^{Met}$ charged with [^{35}S]-methionine, and incubated them with increasing concentrations of each variant (***Figure 2A,B***). Native gel electrophoresis of the reactions enables separation of free $tRNA_i$ from TC bound to both 43S and 43S•eIF3 complexes. In the absence of AUG-containing mRNA, and at the low concentrations of 40S subunits required to measure the affinity of eIF3 for the 43S complex, there is a significant population of free 40S subunits that can compete for eIF3 and complicate the measurement of 43S•eIF3 complex formation. However, because all TC-containing species are resolved by this method, the amount of free eIF3 (as opposed to total eIF3) can be calculated from measured dissociation constants, enabling us to determine the affinity of eIF3 for the 43S complex under these conditions (***Figure 2—figure supplement 1***).

Both wild-type (WT) and variant forms of eIF3 exhibit apparently cooperative binding to the 43S PIC, as evidenced by sigmoidal binding isotherms (***Figure 2—figure supplement 2A***). This behavior may reflect the requirement for stable interaction between the five subunits of the complex prior to binding the PIC. We modeled binding data using both a standard Langmuir binding isotherm and the cooperative Hill curve, and obtained similar results with both methods (***Figure 2—figure supplement 2B***). Because fitting with the Hill equation more accurately models the data (***Figure 2—figure supplement 2A***), those results are discussed below. The Hill constants resulting from the fits are measures of apparent cooperativity, but we cannot yet ascribe a molecular interpretation to them.

WT eIF3 binds tightly to the 43S complex, with a dissociation constant (K_D) near or below ($\leq$38 nM; ***Figure 2C***, left panel) the concentration of 40S subunits used in the experiment (30 nM). Mutations in the entry channel arm of eIF3 appear to weaken its binding by up to ~3 fold (***Figure 2C***, left panel). Two of the eIF3a CTD mutations in this region, *H725P* and *R731I*, which alter the KERR motif of the eIF3a CTD Hcr1-like Domain (HLD), decrease the apparent affinity of eIF3 for the 43S PIC by ~2 and ~3 fold, respectively. The *Box6* mutant, which is also located within the eIF3a HLD but is outside the KERR motif, does not affect the apparent affinity of eIF3 for the 43S complex. The a/b/c sub-complex lacking the i and g subunits exhibits ~2 fold weaker apparent affinity for the 43S PIC than the WT factor, whereas the eIF3i *Q258R* and the eIF3g *KLF* mutations do not manifest any effect on the 43S:eIF3 interaction. In contrast, the *prt1-1* and *rnp1* mutations in eIF3b, which connects the entry channel arm to the 40S solvent face, also weaken the 43S:eIF3 affinity ~2 and ~3 fold, respectively.

We observe similarly modest effects in the case of the exit-channel mutants of the eIF3a NTD, the *Δ8* truncation and *Box37* substitution. Both weaken the apparent 43S:eIF3 affinity by ~2 fold or less. The *Δ60* mutation within the eIF3c PCI domain, which is also located near the exit channel, does not affect the 43S:eIF3 affinity. Nearer to the P site, the *Box12-SPW* mutation in the N-terminal region of eIF3c weakens the 43S:eIF3 interaction ~2 fold, whereas the GAP^{85} mutation also located within the eIF3c NTD does not appear to affect the binding of eIF3 to 43S PICs.

To examine the effects of these mutations on the affinity of eIF3 for 48S PICs, we repeated these experiments in the presence of saturating amounts of an unstructured, AUG-containing model mRNA (***Figure 2C***, right panel). As with our 43S PIC binding experiments, these experiments produced apparently cooperative binding behavior. WT eIF3 binds 48S PICs tightly ($K_D \leq$ 38 nM), similar to what we observed for 43S PICs lacking mRNA. The absence of the i and g subunits in the a/b/c sub-complex weakens the apparent eIF3:48S interaction by nearly three-fold, as do the *prt1-1* and *rnp1* mutations in eIF3b, by nearly three-fold and more than four-fold, respectively. We also observe ~2 fold reductions in apparent eIF3 affinity for 48S complexes with mutations in the exit channel arm of eIF3 (*Δ8* and *Box37*) and the *Box12-SPW* mutation in the N-terminal region of eIF3c. In fact, the apparent affinity of most of the eIF3 variants for 48S PICs is similar to that observed for 43S PICs lacking mRNA, perhaps because their apparent 43S PIC affinity, even in the absence of mRNA, is tighter than the resolution of our assay. An alternative explanation is that stabilizing contacts with the mRNA are offset by changes in the complex that weaken other interactions with eIF3. In contrast, both the *H725P* and *R731I* substitutions within the eIF3a CTD display higher apparent affinities in the presence of mRNA than in its absence, perhaps because mRNA contributes interactions with eIF3 that can supplement those disrupted by these mutations. It is also possible that both

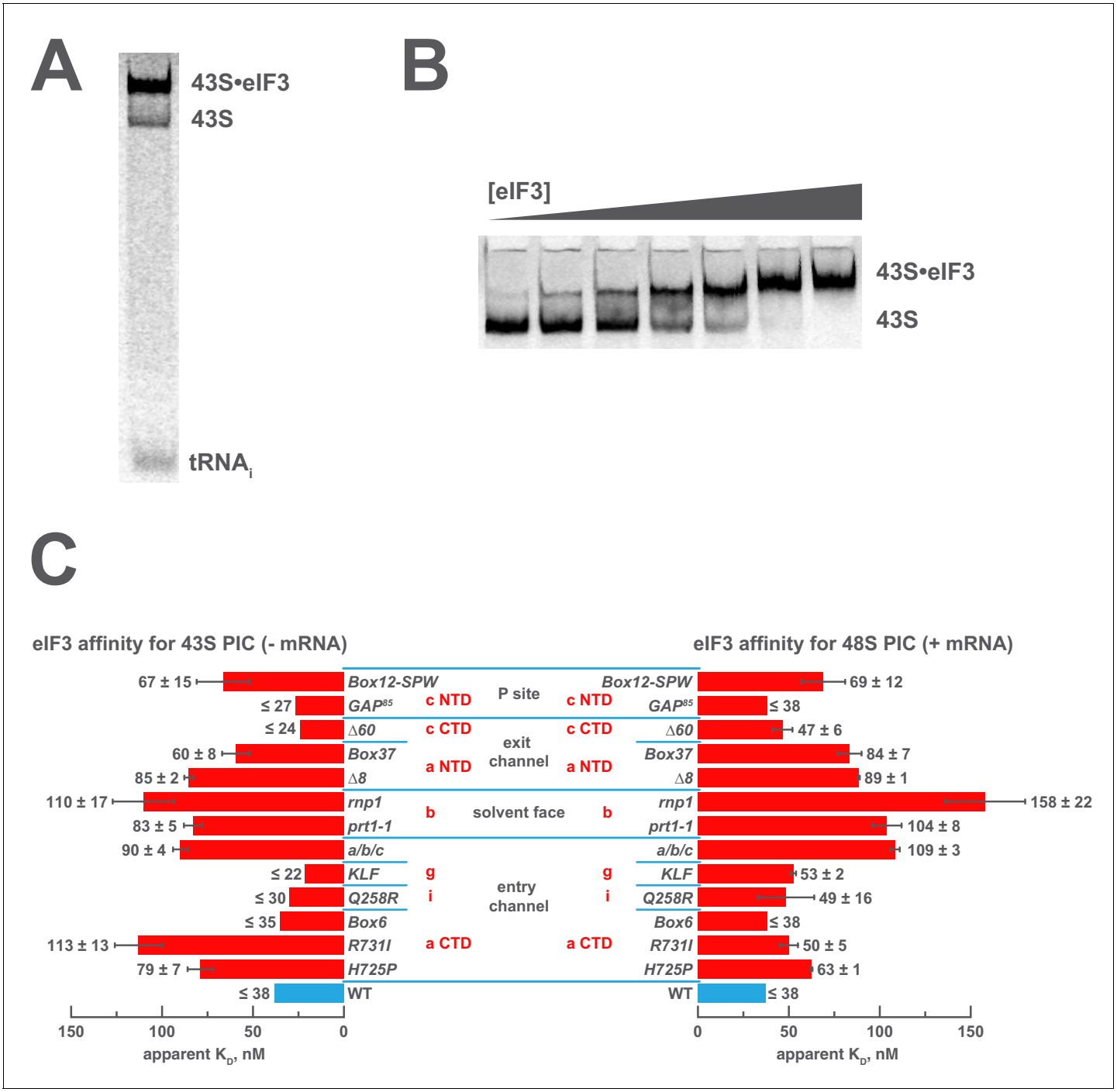

Figure 2. Mutations in the mRNA entry- or exit-channel arms of eIF3 or in eIF3b destabilize eIF3 binding to the PIC. (**A**) Binding of ternary complex containing [^{35}S]-Met-tRNA$_i^{Met}$ to 40S ribosomal subunits in the presence of eIF1, eIF1A, and WT or mutant eIF3 was measured using a native gel-shift assay, which separates free [^{35}S]-Met-tRNA$_i^{Met}$ from that bound to 43S PICs alone or 43S PICs containing eIF3 (43S·eIF3). (**B**) The titration of eIF3 into reactions containing 43S PICs produces a well-resolved gel-shift that monitors the binding of eIF3 to the PIC. The amounts of [^{35}S]-Met-tRNA$_i^{Met}$ free, bound to 43S PICs, and bound to 43S•eIF3 complexes were quantified and analyzed as described in ***Figure 2—figure supplement 1***. (**C**) The apparent equilibrium dissociation constant (K_D) of WT (blue bars) and eIF3 variants (red bars) for the PIC, both in the absence (left) and presence (right) of mRNA, obtained by fitting the data with the Hill equation (see ***Figure 2—figure supplement 2B***). Bars and errors represent mean and SEM, respectively (as determined by individual fitting of each experiment), of ≥2 experiments. Owing to the conditions of these assays, apparent affinities ≤ 30 nM likely represent upper limits.

DOI: 10.7554/eLife.20934.005

The following source data and figure supplements are available for figure 2:

Figure 2 continued on next page

Figure 2 continued

Source data 1. Individual eIF3:43S and eIF3:48S dissociation constant measurements.
DOI: 10.7554/eLife.20934.006
Figure supplement 1. Calculating the affinity of eIF3 for PICs under conditions where free 40S subunits compete for binding.
DOI: 10.7554/eLife.20934.007
Figure supplement 2. Comparison of hyperbolic and Hill equations for modeling eIF3 binding to the PIC.
DOI: 10.7554/eLife.20934.008

variants, which appear to affect the transition between open and closed conformations of the PIC in vivo (***Chiu et al., 2010***), bind more readily to the closed conformation of the PIC stabilized by AUG-containing mRNA. Presumably, the contribution of these effects to the affinity of WT eIF3 for 48S complexes is masked by its already tight interaction with the 43S PIC lacking mRNA.

Nonetheless, these results suggest that both the eIF3 entry- and exit-channel arms, together with eIF3b, contribute to stabilizing eIF3 binding to the PIC. This is consistent with structural and genetic evidence identifying multiple points of contact between eIF3 and the 40S subunit (***Aylett et al., 2015***; ***Chiu et al., 2010***; ***Llácer et al., 2015***; ***Valášek et al., 2003***). Accordingly, impairing any single interaction with these mutations does not dramatically destabilize eIF3 binding to the 43S PIC.

The eIF3 entry channel arm and eIF3b stabilize TC association with the 43S PIC

We next interrogated the contributions of the eIF3 subunits to stabilizing TC binding to the PIC by measuring the dissociation constant of TC in 43S complexes assembled with each eIF3 variant. These experiments employed the assay described above, only each eIF3 variant was included at saturating levels relative to its measured affinity for the 43S PIC and the concentration of 40S subunits was varied. We have previously reported the thermodynamic coupling between TC binding to the 43S complex and the presence of mRNA with an AUG codon in the 40S P site. In the presence of AUG-containing model mRNA, the affinity of TC for the 43S PIC is ~10 pM (***Kolitz et al., 2009***); in the absence of mRNA this affinity is reduced by 4 orders of magnitude to 104 ± 15 nM (***Figure 3***, left panel). WT eIF3 stabilizes TC binding to the 43S PIC by ~7 fold, resulting in an affinity of 15 ± 1 nM in the absence of mRNA (***Figure 3***, left panel). For most eIF3 variants, this affinity is not significantly altered. However, the a/b/c sub-complex lacking the i and g subunits weakens the 43S:TC interaction ~ 3 fold, as does the *prt1-1* mutation in the eIF3b β-propeller domain. The eIF3b RRM mutation *rnp1* has a slightly smaller effect on 43S:TC affinity, weakening it ~ 2 fold (***Figure 3***, left panel).

Intriguingly, three mutations – *R731I* and *Box6* in the eIF3a CTD and GAP^{85} in the eIF3c NTD – appear to modestly increase the affinity of TC relative to the effect of WT eIF3. Several mutations also reduce the endpoints of TC recruitment observed at saturating concentrations of 40S subunits: *Box12-SPW*, *rnp1* and *R731I* (***Figure 3***, right panel). Previous work has suggested that such reductions may be due to a shift in the balance of complexes between two conformational states: one in which TC is stably bound and one in which it dissociates during gel electrophoresis (***Kapp et al., 2006***; ***Kolitz et al., 2009***). It is possible that these states are related to the open and closed conformations of the PIC and that eIF3 modulates their relative stabilities.

Our results suggest that segments of eIF3b, the eIF3a CTD, and eIF3 i/g module – which constitute the eIF3 entry-channel arm and its attachment point on the 40S solvent face – contribute, together with the eIF3c NTD, to stabilizing TC binding to the 43S PIC, perhaps by modulating the PIC conformation or by interacting indirectly or directly with TC. The latter explanation would be consistent with the structure of the py48S-closed complex, in which the i and g subunits are found on the intersubunit face, resting against eIF2γ (***Llácer et al., 2015***) The effects of the eIF3c NTD mutants GAP^{85} and *Box12-SPW* might occur as a result of indirect interactions with TC, consistent with their effects on eIF1 binding (***Karásková et al., 2012***).

Regions throughout eIF3 collaborate to drive mRNA recruitment

To dissect the contributions of regions throughout eIF3 to mRNA recruitment, we followed the kinetics and extent of recruitment in the presence of each eIF3 variant in vitro. For those variants that

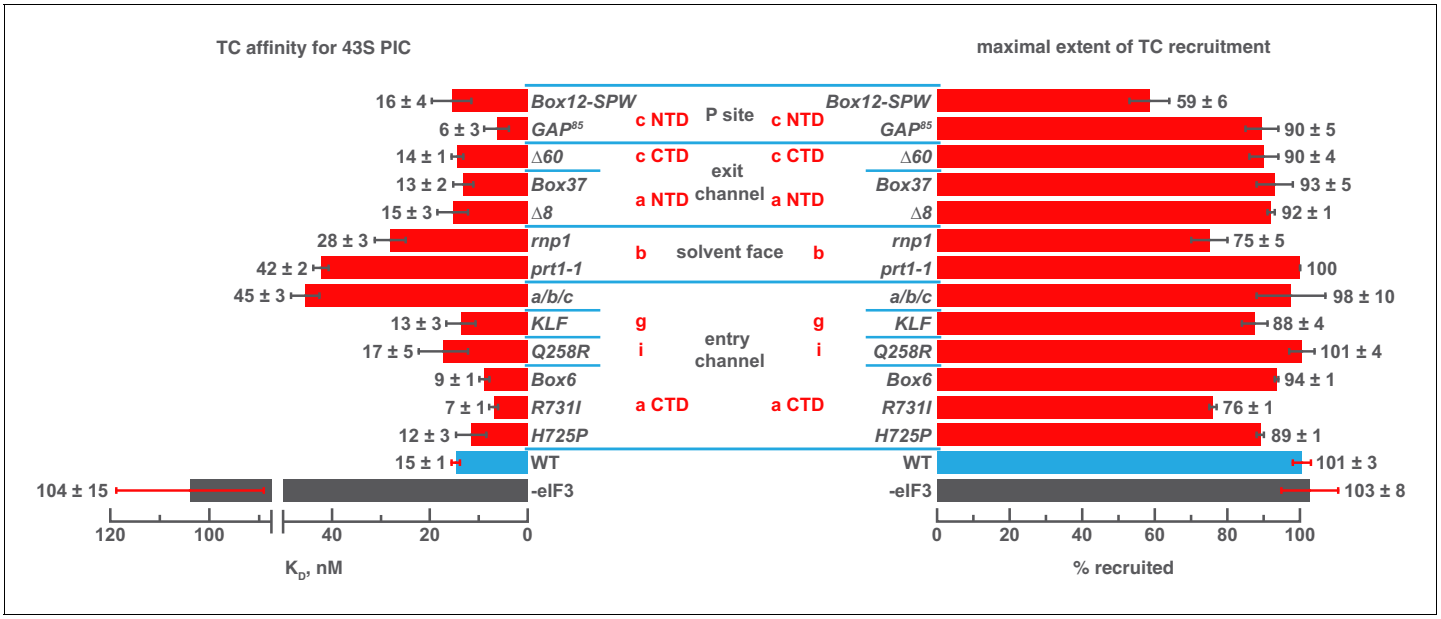

Figure 3. Mutations in the mRNA entry-channel arm of eIF3 or in eIF3b destabilize binding of TC to the PIC. The K_D of TC (left) or maximal extent of TC recruitment (right) observed for PICs assembled either in the absence of eIF3 (grey bar), or the presence of either WT (blue bar) or variant eIF3 (red bars). Bars and errors represent mean and SEM, respectively (as determined by individual fitting of each experiment), of ≥2 experiments.

DOI: 10.7554/eLife.20934.009

The following source data is available for figure 3:

Source data 1. Individual measurements of ternary complex binding (dissociation constants and reaction extents) to 43S PICs.

DOI: 10.7554/eLife.20934.010

produced temperature-sensitive phenotypes in vivo, we additionally assayed recruitment at 37˚C. In these experiments, 43S complexes were formed in the presence of saturating concentrations of TC, eIF1, eIF1A, eIF5, eIF4A, eIF4B, eIF4E•eIF4G, and eIF3; the concentrations of eIF3 and TC were chosen such that they would saturate binding for all variants. Once formed, 43S complexes were incubated with a natural mRNA (*RPL41A*) radio-labeled via a [^{32}P]-5′-7-methylguanosine cap. Individual time points were loaded onto a running native polyacrylamide gel, which stops further mRNA binding and resolves free mRNA from mRNA recruited to form 48S complexes (***Figure 4A–B***). The observed 48S complex band is dependent on the presence of an AUG codon in the mRNA (***Mitchell et al., 2010***) (***Figure 4—figure supplement 1A***), and recruitment of capped *RPL41A* mRNA is highly dependent on the presence of both eIF4A and ATP in this in vitro system (***Mitchell et al., 2010***; Yourik, Aitken, Zhou, and Lorsch, unpublished), indicating that it is an active, energy-dependent process. Together, these data suggest that this assay reports on the combined rates of all steps — from initial attachment of mRNA to start-codon recognition — required to form a stable, detectable 48S complex. Hereafter, we will refer to these combined processes simply as 'mRNA recruitment.'

We have previously reported that eIF3 is required for observable recruitment of native mRNA in the reconstituted yeast translation initiation system (***Mitchell et al., 2010***), consistent with its requirement in vivo (***Jivotovskaya et al., 2006***). In the presence of WT eIF3, mRNA recruitment occurs with an apparent rate constant of 0.27 ± 0.023 min^{-1} (***Figure 4B***, light blue circles; ***Figure 4C***). Mutations throughout eIF3 slow this process. The most dramatic effect occurs in the presence of the a/b/c sub-complex, which slows recruitment more than 10-fold and reduces its endpoint nearly five-fold (***Figure 4B***, orange circles; ***Figure 4C***). In contrast, the *Q258R* mutation in eIF3i and the *KLF* mutation in eIF3g have little effect on the kinetics of *RPL41A* mRNA recruitment, indicating that they do not alter regions of these subunits that are critical for rapid loading of mRNA onto the PIC. These mutations confer in vivo phenotypes consistent with defects in either the rate of scanning, as in the case of *Q258R*, or in the processivity of scanning through stable secondary structures, in the case of *KLF*. It is possible that these defects are not rate-limiting for recruitment of the

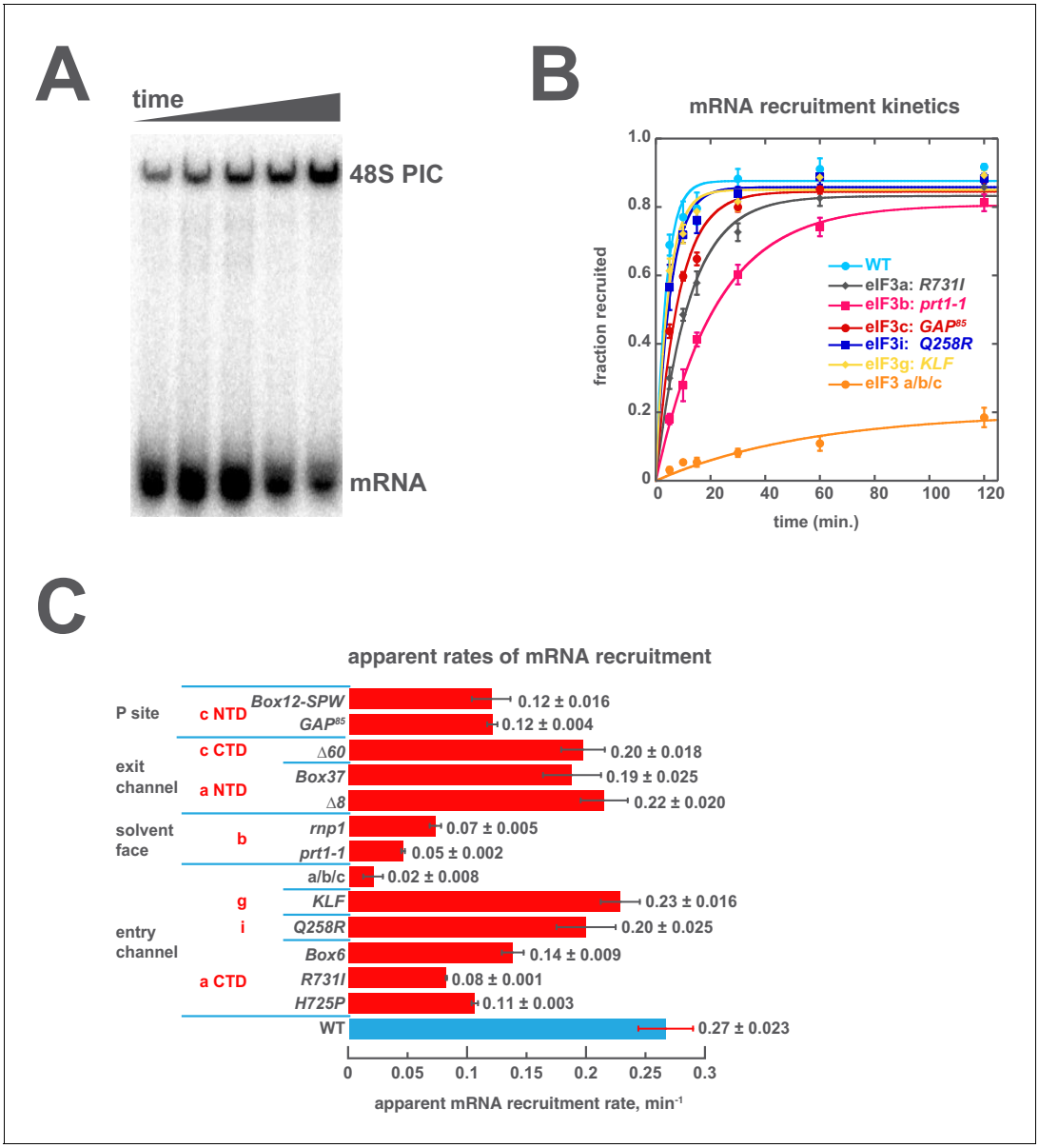

Figure 4. Mutations throughout the eIF3 complex compromise its ability to accelerate recruitment of capped native *RPL41A* mRNA to the PIC. (**A**) mRNA recruitment reactions were quenched at appropriate time points on a running native gel to separate free [^{32}P]-capped *RPL41A* mRNA from mRNA recruited to form 48S PICs. The bands were quantified to determine the fraction of total mRNA bound at each time point. (**B**) Individual time courses were fit with single-exponential rate equations to determine the observed rate constant for each experiment. (**C**) The observed rates of mRNA recruitment of capped *RPL41A* mRNA measured in the presence of WT (blue bar) and variants of eIF3 (red bars). Bars and errors represent mean values and SEM, respectively (as determined by individual fitting of each experiment), of ≥2 experiments.

DOI: 10.7554/eLife.20934.011

The following source data and figure supplements are available for figure 4:

Source data 1. Individual observed apparent rates for *RPL41A* mRNA recruitment.

DOI: 10.7554/eLife.20934.012

Figure supplement 1. The recruitment of unstructured model mRNAs to the PIC depends on the presence of an AUG codon and 40S subunits.

DOI: 10.7554/eLife.20934.013

Figure supplement 2. Comparison of the kinetics of mRNA recruitment for WT and variant eIF3 at 26°C and 37°C.

DOI: 10.7554/eLife.20934.014

RPL41A mRNA, which possesses a relatively short (22 nt) 5′ UTR lacking highly-structured elements. These defects may become rate-limiting in the recruitment of mRNAs with longer, more-structured 5′ UTRs. Nonetheless, the fact that both the extent and rate of recruitment of *RPL41A* mRNA are severely compromised when eIF3 is replaced with the a/b/c sub-complex, together with the previous observation that the loss of eIF3i and eIF3g from the eIF3 complex in vivo critically compromises scanning arrest (**Herrmannová et al., 2012**), is consistent with our interpretation that this assay is sensitive to scanning defects.

The *R731I, H725P,* and *Box6* mutations within the eIF3a CTD slow mRNA recruitment by approximately 2- to 3-fold, further implicating the eIF3 entry channel arm in the mechanism of mRNA recruitment. The eIF3b mutations *prt1-1* and *rnp1* also slow recruitment, by approximately 4- to 5-fold. Aside from the loss of the i and g subunits, these are the strongest effects we observe on the kinetics of recruitment, suggesting that eIF3b also contributes significantly to rapid mRNA recruitment, perhaps by anchoring the entry-channel arm of eIF3 to the solvent face. The eIF3c NTD mutations *GAP*^{85}and *Box12-SPW*, thought to be located on the opposite side of the PIC near the P site, also slow mRNA recruitment by ~2 fold. Mutations within the eIF3 exit channel arm, either in the eIF3a NTD (*Δ8* and *Box37*) or the eIF3c CTD (*Δ60*) PCI domains, only slightly reduce the rate of mRNA recruitment; nonetheless, *Box37* significantly slows recruitment at 37˚C (**Figure 4—figure supplement 2**), consistent with its temperature-sensitive phenotype in vivo (**Khoshnevis et al., 2014**). Overall, the kinetic defects conferred by mutations throughout eIF3 suggest a requirement for proper collaboration between its different subunits in coordinating rapid mRNA recruitment to the PIC.

One possible explanation for the mRNA recruitment defects we observe in the presence of the eIF3 variants is that mutations in eIF3 affect its ability to collaborate with other factors involved in the mechanism of mRNA recruitment. The eIF4 factors – eIF4A, eIF4B, eIF4E, and eIF4G – have previously been shown to play critical roles during mRNA recruitment both in vivo and in vitro (reviewed in: **Hinnebusch, 2011**; **Jackson et al., 2010**; **Sonenberg and Hinnebusch, 2009**). Our system recapitulates the requirement for these factors in the recruitment of capped natural mRNAs (**Mitchell et al., 2010**) and was previously employed to demonstrate that the absence of eIF4B increases the concentration of eIF4A required for efficient mRNA recruitment (**Walker et al., 2013**), consistent with the genetic interaction between these two factors (**Coppolecchia et al., 1993**; **de la Cruz et al., 1997**). However, varying the concentration of either eIF4A, eIF4B, or eIF4E•eIF4G in mRNA recruitment reactions confirmed that these factors were still saturating for each eIF3 variant under the conditions of our experiments (data not shown). These results suggest that the mRNA recruitment defects we observe do not arise from diminished interaction of the eIF4 factors with the PIC caused by the mutations in eIF3. Moreover, because TC was included at a concentration that saturates its binding in the presence of all variants, we can rule out the possibility that the observed defects are downstream effects of TC binding defects. These in turn imply that eIF3 acts directly to coordinate events during mRNA recruitment, rather than simply helping to recruit TC or the eIF4 factors.

eIF3 stabilizes the binding of mRNA at the exit channel

The fact that eIF3 is required for mRNA recruitment both in vivo and in vitro and that mutations to both the entry and exit channel arms of eIF3 appear to disrupt mRNA recruitment in vivo (**Chiu et al., 2010**; **Khoshnevis et al., 2014**) suggests that its presence at the mRNA entry and exit channels of the 43S PIC might be central to this role. To investigate the role played by eIF3 at the mRNA entry and exit channels, we next asked how the formation of 48S PICs is affected by the presence or absence of mRNA in each of these channels, and whether eIF3 contributes to the formation of these complexes.

To this end, we replaced the *RPL41A* mRNA in the mRNA recruitment assay with a series of [^{32}P]-5′-7-methylguanosine-capped, unstructured model mRNAs, 50 nucleotides in length, in which the location of the AUG codon – located in the 40S P site of the final 48S PIC – dictates the amount of mRNA present in the mRNA entry and exit channels upon start codon recognition (**Figure 5A–C**, left panels; **Figure 5—figure supplement 1**). Based on structural models, the mRNA entry channel can accommodate at least 9 nucleotides 3′ of the AUG start codon, and the exit channel is filled with 10 nucleotides 5′ of the AUG. As before, we monitored the recruitment of these [^{32}P]-5′-7-

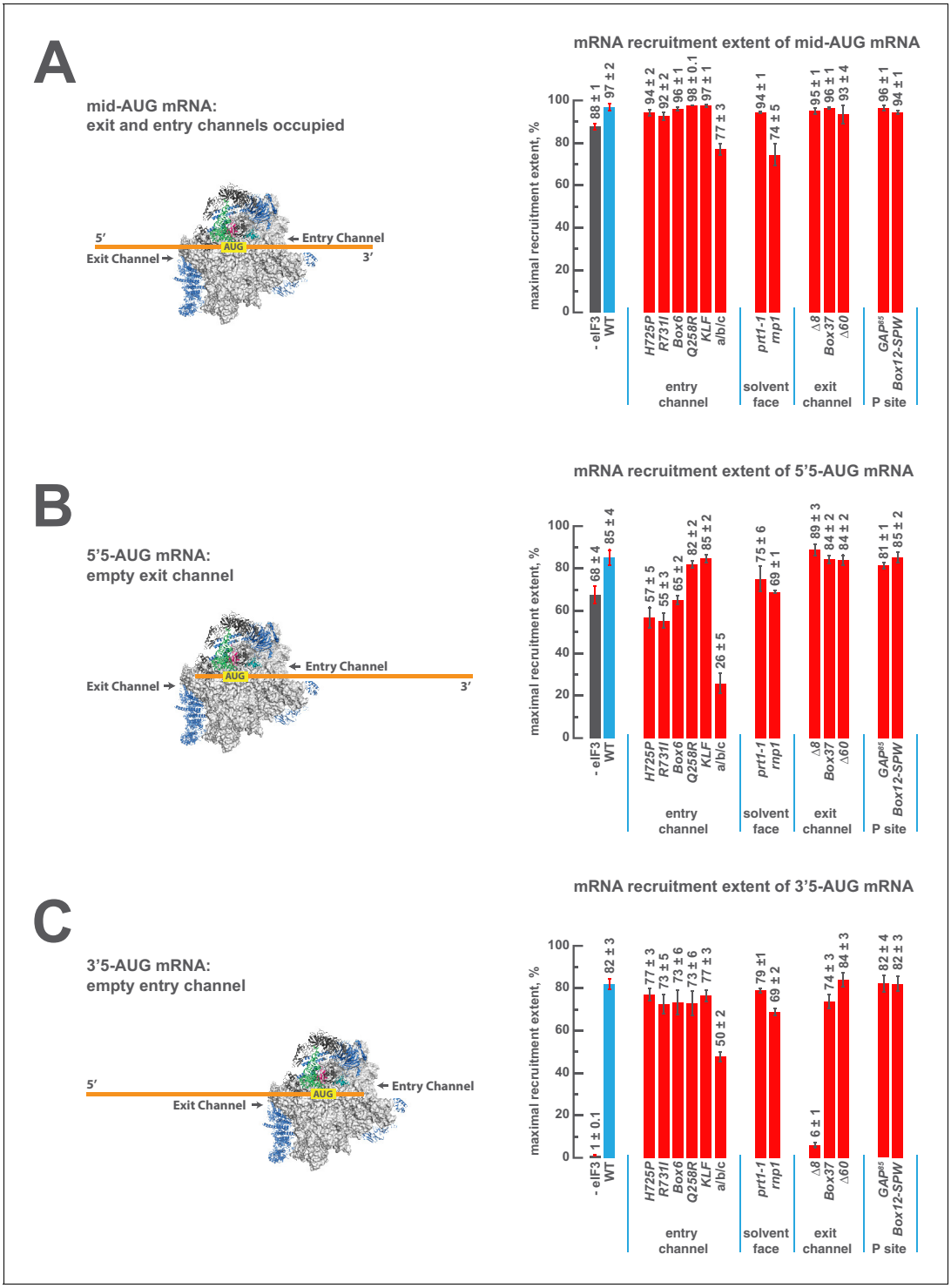

Figure 5. eIF3 strongly stabilizes binding of mRNA at the exit channel of the PIC in a manner dependent on the eIF3a NTD. (**A**) The maximal extent of mid-AUG mRNA recruited in the absence of eIF3 (grey bar), or in the presence of either WT (blue bar) or variant eIF3 (red bars). The locations of sequences 5′ or 3′ of the AUG in the PIC, with AUG in the P site, are shown schematically on the left, indicating that both the mRNA entry and exit channels of the PIC are fully occupied. Bars and errors represent mean and SEM, respectively, of ≥2 experiments. (**B**) The maximal extent of 5′5-AUG mRNA recruited in the absence of eIF3, or in the presence of either WT or variant eIF3. As shown on the left, 5′5 AUG mRNA programs a recruited complex in which only the mRNA entry channel is fully occupied, and thus is sensitized to changes in that channel. (**C**) The maximal extent of 3′5-AUG mRNA recruited in the absence of eIF3, or in the presence of either WT or variant eIF3. The 3′5-AUG programs a recruited complex in which only the mRNA exit channel is occupied (left), and thus is sensitized to changes in that channel.

DOI: 10.7554/eLife.20934.015

Figure 5 continued on next page

Figure 5 continued

The following source data and figure supplements are available for figure 5:

Source data 1. Individual measurements of recruitment extent.

DOI: 10.7554/eLife.20934.016

Figure supplement 1. Short, unstructured model mRNAs with distinct start codon positions.

DOI: 10.7554/eLife.20934.017

Figure supplement 2. eIF3 accelerates the recruitment of unstructured model mRNAs.

DOI: 10.7554/eLife.20934.018

Figure supplement 3. The mRNA recruitment extent defects observe for entry- and exit-channel variants of eIF3 are not exacerbated in the absence of the eIF4 factors.

DOI: 10.7554/eLife.20934.019

methylguanosine-capped mRNAs in the presence of saturating concentrations of TC, eIF1, eIF1A, eIF5, eIF4A, eIF4B, eIF4E•eIF4G, and eIF3.

In the presence of eIF3, recruitment of a 50 nucleotide mRNA with a centrally positioned AUG codon at nucleotides 24–26 ('mid-AUG') occurs within 15 s, faster than the time resolution of our assay. In the absence of eIF3, however, recruitment proceeds at least two orders of magnitude more slowly, at an apparent rate of 0.02 ± 0.004 min^{-1} (***Figure 5—figure supplement 2A***). We observe a similar acceleration of 48S assembly by eIF3 with mRNAs in which the AUG codon occurs 5 nt from the 5' end (5'5-AUG) or 5 nt from the 3' end (3'5-AUG) (***Figure 5—figure supplement 2B–C***).

In contrast, the maximal extent of recruitment of the mid-AUG mRNA is similar in both the presence and absence of eIF3 (***Figure 5A***, grey and blue bars). The extent of mRNA recruitment observed – determined by the endpoint of the reaction defined by multiple time-course experiments – is a function of how much mRNA is recruited in solution and how stably the mRNA is bound within the 48S PIC during gel electrophoresis. Thus, while eIF3 dramatically accelerates the recruitment of the mid-AUG mRNA, it is largely dispensable for stabilizing the binding of the mid-AUG mRNA to this 48S complex, in which both the mRNA entry and exit channels are occupied. Again, mRNA recruitment is strongly dependent on the presence of an AUG codon (***Figure 4—figure supplement 1A–B***), consistent with the interpretation that our assay detects the 48S PIC formed upon start-codon recognition; we similarly observe no recruitment in the absence of 40S subunits (***Figure 4—figure supplement 1C***). Presumably owing to the unstructured nature of the model mRNAs, none requires any of the eIF4 factors for maximum recruitment (***Figure 5—figure supplement 3A–D***, black bars; and data not shown).

We next asked if eIF3 contributes to the stable binding of the 5'5-AUG mRNA, whose recruitment results in a 48S PIC in which the mRNA exit channel is mostly unoccupied, but the entry channel is full (***Figure 5B***, left). The ability to bind this mRNA, as compared to the mid-AUG mRNA, reports on the consequences of disrupting interactions between the 43S PIC and mRNA in the exit channel. In the presence of eIF3, we observe a modest decrease in the extent of recruitment of 5'5-AUG mRNA as compared to mid-AUG mRNA, suggesting that the absence of mRNA in the exit channel slightly destabilizes its binding to the 48S PIC (***Figure 5***, compare blue bars in A and B).

This destabilization resulting from an empty exit channel should make the binding of mRNA to the 48S PIC more dependent on interactions elsewhere within the complex, and thus further sensitize it to disruptions within the entry channel. If eIF3 provides important contacts with mRNA at the entry channel, then its absence should further destabilize mRNA binding in complexes formed on the 5'5-AUG mRNA, in which contacts in the exit channel have already been lost. We observe a moderate decrease in the extent of recruitment in the absence of eIF3 (***Figure 5B***, grey and blue bars), somewhat greater than that observed on the mid-AUG mRNA (***Figure 5A***, grey and blue bars), suggesting that eIF3 makes a moderate contribution to stable binding of mRNA in the entry channel ($p<0.01$, unpaired, two-tailed t test for -eIF3/+eIF3 ratio on 5'5-AUG mRNA vs. on midAUG mRNA, ***Figure 5A and B***, grey and blue bars).

Turning to the 3'5-AUG mRNA, which produces a 48S PIC with the exit channel filled but the entry channel mostly empty, we again observe a modest decrease in recruitment compared to that of mid-AUG mRNA, in the presence of eIF3 (***Figure 5A and C***, blue bars), consistent with the loss of interactions in the entry channel destabilizing mRNA binding to the PIC. Strikingly, however, we observe almost no recruitment of 3'5-AUG mRNA in the absence of eIF3 (***Figure 5C***, grey and blue

bars). Because complexes formed on 3'5-AUG mRNA contain almost no mRNA in the entry channel, they would be expected to be hypersensitive to loss of mRNA interactions in or around the exit channel. Thus, whereas stabilization of mRNA binding in the entry channel does not strongly depend on eIF3 (***Figure 5B***, grey and blue bars), stable binding of mRNA in the exit channel is fully dependent on eIF3. This dependence implicates eIF3 in stabilizing the binding of mRNA either inside or just outside of the exit channel.

The eIF3a NTD is required for stabilizing the binding of mRNA at the exit channel

We next determined whether mutations in the entry- and exit-channel arms of eIF3 mimic the effects we observe in the absence of eIF3 when either mRNA channel is left empty. As before, all experiments were performed under conditions where binding of TC and each eIF3 variant to the 43S PIC is saturated.

We see no effects on the extent of 48S PIC formation on mid-AUG mRNA – where both channels are occupied – when WT eIF3 is replaced by several eIF3 variants affecting the entry or exit channel arms of the factor, consistent with the observation that WT eIF3 is largely dispensable for the stable binding of mRNA within this complex (***Figure 5A***, blue and red bars). However, the a/b/c sub-complex lacking the i and g subunits confers a modest reduction in endpoint of recruitment slightly greater than that observed even in the absence of the entire eIF3 complex, again highlighting the importance of these subunits to the overall mRNA recruitment process. The *rnp1* variant, which harbors a mutation in the eIF3b RRM located on the 40S solvent face, also confers a similar reduction, perhaps because disruption of this region interferes with the organization of the entry-channel arm to which it connects.

Recruitment of the 5'5-AUG mRNA, which forms a 48S PIC with the exit channel largely empty, produces a different pattern of effects (***Figure 5B***, blue and red bars). Although WT eIF3 only moderately contributes to stable binding of mRNA within this complex, the eIF3a CTD mutations *H725P, R731I*, and *Box6* located within the entry channel arm diminish recruitment to essentially the same reduced level observed in the absence of eIF3. This suggests that these mutations impair the moderate contribution of the entry channel arm of eIF3 to stabilizing mRNA binding. Though the eIF3g *KLF* and eIF3i *Q258R* mutations do not destabilize the binding of the 5'5-AUG mRNA, its binding is dramatically reduced in the presence of the a/b/c sub-complex lacking the i and g subunits, even as compared to the absence of eIF3. This is consistent with its modest dominant negative effect on mid-AUG mRNA binding, and suggests that the conformation of the PIC might be altered when these subunits are missing such that the binding of mRNA is destabilized. None of the defects conferred by *H725P, R731I*, or the a/b/c subcomplex is exacerbated by the absence of eIF4A, eIF4B, or eIF4E•4G (***Figure 5—figure supplement 3A***), indicating that the eIF3 entry channel arm contributes directly to recruitment of this mRNA, and does not do so simply by binding to these factors. Consistent with the fact that mRNA is already absent from the exit channel in the 5'5-AUG complex, we observe no effects of the eIF3 exit-channel mutations *Δ8*, *Box37*, and *Δ60*.

In contrast, recruitment of the 3'5-AUG mRNA, which produces a complex with an empty entry channel, is dramatically impaired by the *Δ8* truncation. This mutation, which eliminates the first 200 amino acids of the eIF3a NTD PCI domain in the factor's exit-channel arm, mimics the complete absence of eIF3; we observe no recruitment of the 3'5-AUG mRNA in the presence of *Δ8* eIF3 (***Figure 5C***), despite the fact that this mutant factor and TC are both fully bound to the PIC under these conditions (***Figure 2C***, ***Figure 3***). Together with the absence of any effect of the *Δ8* mutant on recruitment of the 5'5-AUG mRNA (***Figure 5***, compare Δ8 in B and C), this implicates this region of eIF3a in stabilizing mRNA binding at the exit channel of the 48S PIC. We do not observe any defect in the case of the *Box37* mutation, which maps further into the eIF3a NTD PCI domain, outside the region removed by the *Δ8* truncation. We similarly observe no effect in the presence of the *Δ60* truncation of the eIF3c PCI domain.

Whereas the absence of mRNA in the entry channel sensitizes complexes formed on the 3'5-AUG mRNA to the *Δ8* deletion at the exit channel, it should conversely confer insensitivity to changes at the already vacant entry channel. Accordingly, mutations throughout the eIF3a CTD (*H725P, R731I, Box6*), eIF3i (*Q258R*), and eIF3g (*KLF*) components of the entry-channel arm do not result in reduced formation of the 3'5-AUG complex (***Figure 5C***). This stands in contrast to the effects of *H725P, R731I*, and *Box6* on the 5'5-AUG mRNA (***Figure 5B***), underscoring the deduced defects in entry

channel interactions for these variants. Although we still observe a defect in the presence of the a/b/c sub-complex, this effect is weaker than that observed with the 5′5-AUG complex (***Figure 5***, compare a/b/c in panel B and C). We suggest that the lack of the i and g subunits prevents the factor from promoting the conformation of the PIC needed for optimal mRNA binding.

The destabilization of mRNA binding caused by eIF3 mutations in either channel can be rescued by sufficient mRNA in the opposite channel

We next set out to determine the minimal length of mRNA in the exit and entry channels required to rescue the defects observed above when those channels are empty. To probe the positions of interactions in the exit channel we measured the extent of recruitment of a model mRNA in which the AUG codon is 11 nucleotides from the 5′-end (5′11-AUG), resulting in a complex with the exit channel mostly occupied, and compared it to the recruitment observed on the 5′5-AUG mRNA, which leaves the exit channel mostly empty and is sensitive to certain entry-channel arm mutations in eIF3. The addition of the six extra nucleotides in the 5′11-AUG mRNA relative to 5′5-AUG mRNA fully or partially rescues the recruitment defects for all of the three eIF3 variants affected by mutations in the eIF3a CTD, leading to recruitment extents nearly as high as those observed with the mid-AUG mRNA that fills the exit channel and extends beyond it (***Figure 6A***). The 5′11-AUG mRNA also partially rescues the defects we observed in the absence of eIF3 and with the a/b/c sub-complex (***Figure 6A***). The ability of 11 nucleotides upstream of the AUG to rescue the destabilizing effects of entry channel mutants is not diminished by the absence of any of the eIF4 factors (eIF4A, eIF4B, eIF4E•eIF4G), suggesting that the interactions restored upon filling the exit channel are with either the 40S subunit itself or with eIF3 at the exit channel pore (***Figure 5—figure supplement 3C***). Consistent with this, the cryo-EM structure of a 48S PIC containing eIF3 shows the −10 nucleotide of the mRNA emerging from the constriction between the 40S head and platform, approximately 15 Å from the position of the eIF3a NTD (***Figure 6B***) (***Llácer et al., 2015***).

We similarly measured the amount of mRNA in the entry channel required to rescue the strong defect in recruitment we observed with the eIF3a Δ*8* mutant for 3′5-AUG mRNA that leaves the entry channel largely vacant (***Figure 6C***). The 3′11-AUG mRNA, which programs a recruited complex with 11 nucleotides in the entry channel, partially rescues recruitment in the presence of the Δ*8* variant, to an endpoint of 28 ± 1% of total mRNA recruited, but is not sufficient to restore recruitment to the levels observed on the mid-AUG mRNA (***Figure 5A***). Increasing the length of mRNA in the entry channel to 14 and 17 nucleotides progressively rescues the defect, resulting in endpoints of approximately 85 ± 1% and 90 ± 0.3%, respectively (***Figure 6C***). These extents of recruitment approach those observed in the presence of the Δ*8* variant for both the 5′5-AUG and mid-AUG mRNAs (***Figure 5A–B***), which both result in a fully-occupied entry channel, suggesting that between 14 and 17 nucleotides of mRNA is sufficient to restore interactions there. The rescue of recruitment we observe with Δ*8* and the 5′14-AUG mRNA is not markedly affected by the absence of any eIF4 factor, or eIF5 (***Figure 5—figure supplement 3D***), suggesting that the interactions restored upon filling the entry channel with 14 nucleotides are with either the PIC itself or eIF3. While mRNA is not visible in the entry channel of recent structures of the 48S PIC containing eIF3, a previous structure of a partial 48S complex lacking eIF3 shows the mRNA up to position +12, where it threads past the 40S latch and projects towards a constriction between uS5, uS3, and eS30, and near h16 (***Figure 6D***) (***Hussain et al., 2014***). These 40S components might stabilize mRNA binding by interacting with nucleotides located 14–17 bases downstream of the AUG.

Given the dramatic effect on mRNA recruitment we observe with the eIF3 Δ*8* mutant whenever interactions in the entry channel are disrupted, we wondered how these effects might manifest themselves in vivo. Because the cell likely contains no mRNAs resembling the 3′5-AUG mRNA, in which the AUG codon is followed by only 5 nucleotides, we instead reasoned that the Δ*8* eIF3 mutant, which is insensitive to the absence of mRNA in the exit channel, might confer a relatively weaker recruitment defect relative to WT cells on mRNAs with extremely short 5′-UTRs, because the majority of mRNA recruitment and scanning on these mRNAs will occur while the exit channel remains empty. In this case, both WT and mutant cells will have the same lack of contacts between mRNA and the PIC in the exit channel. In contrast, the recruitment of mRNAs with longer 5′-UTRs would produce a greater defect for the mutant, as the majority of the scanning process occurs with the exit channel occupied, giving WT PICs an advantage because they are able to make contacts with mRNA in this channel whereas Δ*8* mutant cells are not. To investigate this, we quantified the

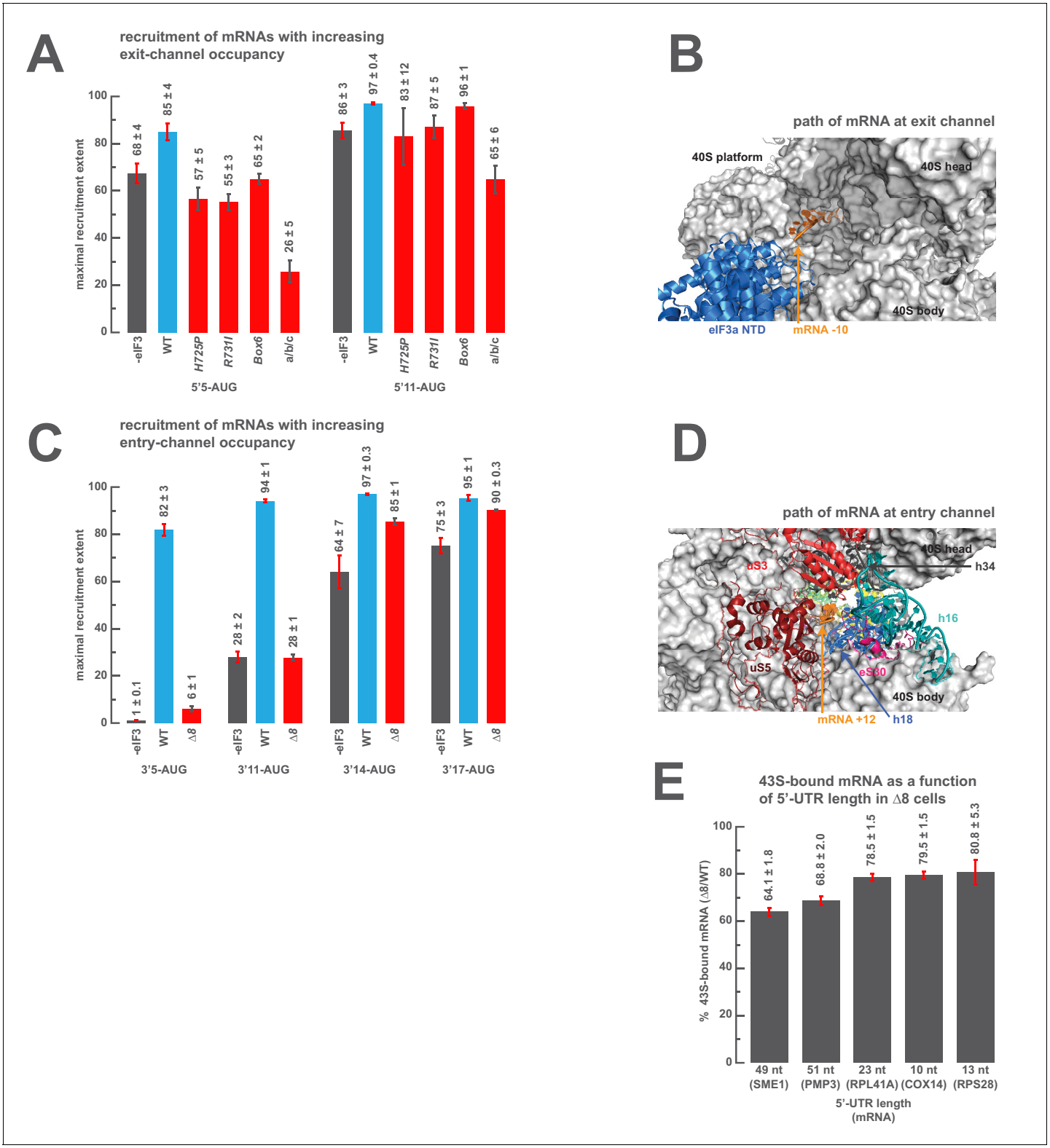

Figure 6. The presence of sufficient mRNA in the opposite channel rescues the destabilization of mRNA binding caused by mutations in the entry- or exit-channel arms of eIF3. (**A**) Bars represent the maximal extent of recruitment of mRNAs that program complexes with either 5 (5'5-AUG) or 11 (5'11-AUG) nucleotides in the mRNA exit channel, in the absence of eIF3 (grey bars) or in the presence of either WT eIF3 (blue bars) or variants with mutations near the mRNA entry channel (red bars). Bars and errors represent mean and SEM, respectively, of ≥2 experiments. (**B**) The path of mRNA (orange) at the exit channel of the 40S subunit (grey) in the py48S-closed structure (***Llácer et al., 2015***). mRNA is visualized up to the −10 nucleotide,

Figure 6 continued on next page

Figure 6 continued

where it emerges from the exit channel pore and is located approximately 15 Å from the eIF3a NTD (blue). (**C**) Bars represent the maximal extent of recruitment of mRNAs with 5 (3'5-AUG), 11 (3'11-AUG), 14 (3'14-AUG), or 17 (3'17-AUG) nucleotides in the entry channel in the absence of eIF3 (grey bars) or in the presence of either WT eIF3 (blue bars) or the Δ*8* variant (red bars). Bars and errors represent mean and SEM, respectively, of ≥2 experiments. (**D**) The path of mRNA (orange) at the entry channel of the 40S subunit (grey) in the py48S PIC lacking eIF3 (***Hussain et al., 2014***). mRNA is visualized up to the +12 nucleotide, where it emerges from the 40S latch composed of h34 (charcoal), h18 (blue), and uS3 (red), and projects towards a constriction formed by uS5 (burgundy), uS3 (red), and eS30 (pink), near h16 (teal). (**E**) The amount of mRNA cross-linked to PICs in Δ*8* cells, as a percentage of mRNA cross-linked to PICs in WT cells, determined for five mRNAs with decreasing 5'-UTR lengths. Bars and errors represent means and SD from two independent biological replicates.

DOI: 10.7554/eLife.20934.020

The following source data is available for figure 6:

Source data 1. Individual measurements of recruitment extent and of the amount of mRNA associated with 43S PICs in vivo.

DOI: 10.7554/eLife.20934.021

amount of mRNA associated with native 43S complexes in vivo, stabilized by formaldehyde cross-linking of living yeast cells, for several mRNAs with different 5' UTR lengths, in strains expressing either WT or the Δ*8* variant of eIF3a. Consistent with our prediction, the Δ*8* mutation reduces the amount of mRNA associated with native 43S PICs for all the mRNAs we tested, but has a greater defect relative to WT cells on mRNAs with longer 5'UTRs (***Figure 6E***).

Discussion

Despite, and perhaps because of its involvement throughout the translation initiation pathway, the precise molecular roles of eIF3 during the component events of initiation remain unclear. Nonetheless, eIF3 has emerged as a pivotal player in the events that bring the PIC to the mRNA, and ultimately to the start codon. Structural models revealing eIF3 at the 40S solvent face but projecting arms near both the mRNA entry and exit channels, as well as genetic and biochemical evidence consistent with eIF3 operating in these regions, suggest the compelling possibility that eIF3 mediates events such as mRNA recruitment and scanning via these appendages. Our data indicate that while regions throughout eIF3 collaborate to stabilize its binding to the 43S PIC and directly promote mRNA recruitment, the mRNA entry- and exit-channel arms of eIF3 play distinct roles within the PIC. The eIF3 exit-channel arm — and in particular the eIF3a NTD — is required to stabilize the binding of mRNA at the exit channel within the 48S PIC (***Figure 7***). In contrast, the entry-channel arm helps to stabilize mRNA binding in the entry channel but also participates in stabilizing TC binding to the PIC and in accelerating mRNA recruitment (***Figure 7***).

eIF3 binds the PIC via multiple interactions and contributes directly to mRNA recruitment

Our results support the idea that the binding of eIF3 to the PIC is mediated by multiple interactions. Mutations in both the eIF3a CTD and NTD, eIF3b, eIF3c, as well as the simultaneous absence of eIF3i and eIF3g weaken the affinity of eIF3 for the PIC. This is consistent with the multiple contacts observed between eIF3 and the PIC in recent structures (***Aylett et al., 2015***; ***Georges, des et al., 2015***; ***Llácer et al., 2015***), and with the diverse set of interactions between eIF3 subunits and components of the PIC identified in genetic and biochemical studies (***Asano et al., 2000***; ***Chiu et al., 2010***; ***Pisarev et al., 2008***; ***Szamecz et al., 2008***; ***Valásek, 2012***; ***Valášek et al., 2003***). Notably, we observe that none of the eIF3 variants displays a severe defect in PIC binding, despite the fact that several directly affect regions that appear to interact with the 40S subunit in the py48S-closed structure or target previously identified interactions. This suggests that because the factor makes multiple contacts with the PIC, no single interaction is itself essential for binding.

Our results further support a direct role for eIF3 in promoting mRNA recruitment. None of the eIF3 variants we tested that significantly slow recruitment of *RPL41A* mRNA do so as a result of the concentrations of TC, eIF4A, eIF4B, or eIF4E•eIF4G becoming limiting under the conditions of our assay. While this does not preclude an interaction between eIF3 and these other factors, it does suggest that eIF3 contributes directly to mRNA recruitment. This is consistent with our previous finding that eIF3 is essential, whereas eIF4G and eIF4B are only rate-enhancing, for recruitment of *RPL41A*

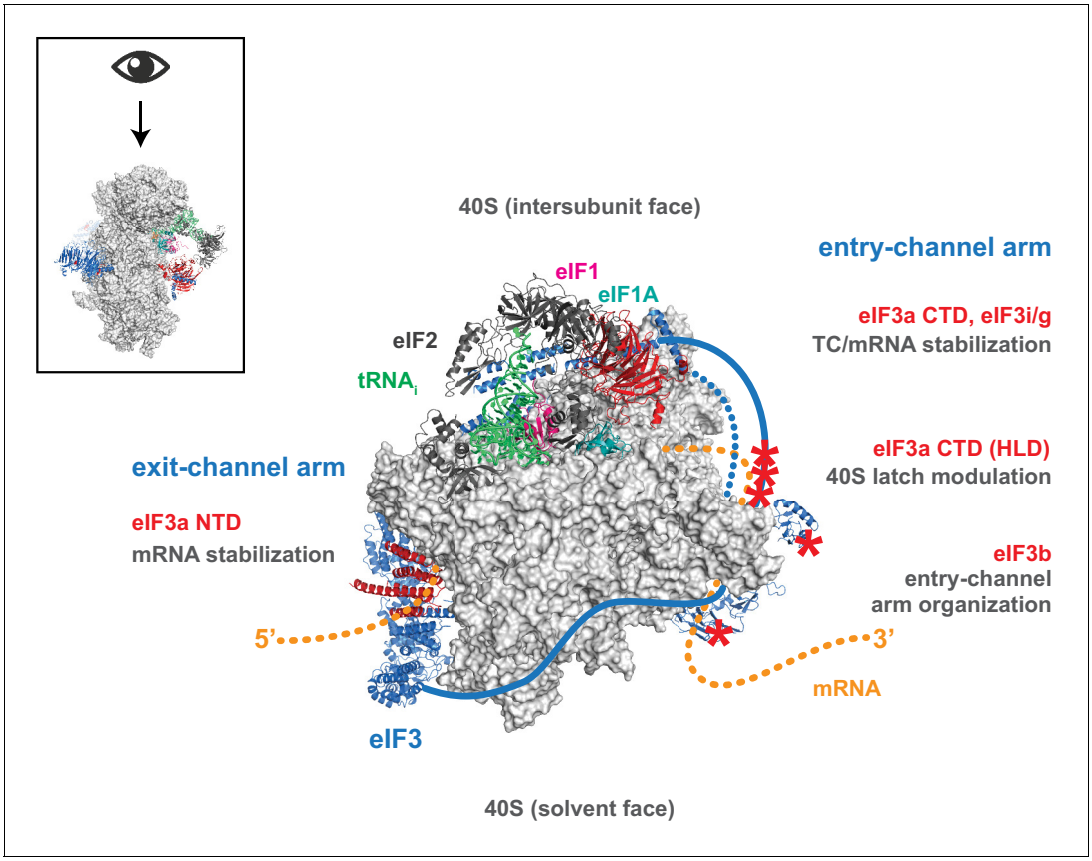

Figure 7. Distinct roles for the mRNA entry- and exit-channel arms of eIF3. A proposed model for the roles of the eIF3 entry- and exit-channel arms during translation initiation. The py48S-closed complex is shown from above (boxed schematic), looking down at the head of the 40S (light grey), with the solvent face at the bottom, and the intersubunit face at the top with Met-tRNA$_i$ (green), eIF2 (dark grey), eIF1 (pink), and eIF1A (teal) bound to the decoding center. eIF3 is shown in blue, with areas of interest highlighted in red or denoted with red asterisks; resolved regions of eIF3 are depicted as ribbons, with unresolved regions cartooned as solid or dashed lines. The mRNA is cartooned in orange, entering the PIC though the entry channel at right, and exiting at the pore near the platform at left. Our results suggest that the eIF3 exit-channel arm, and specifically the eIF3a NTD, is critical for stabilizing mRNA binding to the PIC at the exit channel, whereas the eIF3a CTD (unresolved regions appear as solid blue line) and eIF3i/g enhance the stability of mRNA interactions at the entry-channel. The entry-channel arm and its attachment to the solvent face via eIF3b (unresolved regions appear as dashed blue line) is also important for stabilizing TC binding to the PIC and promoting steps that control the kinetics of mRNA recruitment, perhaps as a function of modulating the 40S latch.

DOI: 10.7554/eLife.20934.022

mRNA in vitro (***Mitchell et al., 2010***), and with the observation that depletion of eIF3 from yeast essentially abolishes recruitment of the *RPL41A* mRNA in vivo (***Jivotovskaya et al., 2006***).

The eIF3 entry-channel arm stabilizes TC binding to the PIC and is important for recruitment of native mRNA

Our results point to a role for the eIF3 entry channel arm — comprising the eIF3a CTD, eIF3i, eIF3g, and eIF3b — in stabilizing both eIF3 and TC binding to the PIC, and making important contributions to the mechanism of mRNA recruitment. In our experiments, WT eIF3 binds tightly to both 43S and 48S PICs and strongly stabilizes TC binding to the PIC in the absence of mRNA. The strong stabilization of TC binding we observe is consistent with genetic evidence that eIF3 promotes TC recruitment in vivo (***Asano et al., 2000***; ***Phan et al., 2001***; ***Valasek et al., 2004***; ***Valášek et al., 2002***).

In contrast, the a/b/c sub-complex lacking eIF3i and eIF3g displays weakened affinity for both 43S and 48S PICs (***Figure 2C***) and diminishes the affinity of the PIC for TC relative to that observed with WT eIF3 (***Figure 3***). In a structure of yeast eIF3 bound to the 40S•eIF1•eIF1A complex (***Aylett et al., 2015***), eIF3i and eIF3g are found distant from TC on the solvent-face side of the PIC above the eIF3b β-propeller domain, and appear to interact with eIF3b but not with the 40S subunit.

This position agrees with the placement of eIF3i in the structure of mammalian eIF3 bound to a complex containing DHX29 (**Georges, des et al., 2015**), though eIF3g was not resolved. In the yeast py48S-closed PIC (**Llácer et al., 2015**), however, these subunits are found at the intersubunit face below the A site, together with the C-terminus of eIF3b; both eIF3i and eIF3g appear to interact with the 40S and eIF3i appears to contact the eIF2γ subunit of TC, consistent with our observation that the absence of eIF3i and eIF3g weakens the binding of both TC and eIF3 to the PIC. Further evidence of a role for eIF3i and eIF3g in contributing to PIC binding by eIF3 is provided by the in vivo effects of the eIF3i *DDKK* mutation, which results in the dissociation of both of these subunits from the eIF3 complex and reduces the amount of a/b/c sub-complex bound to PICs in vivo (**Herrmannová et al., 2012**).

Most strikingly, we observe that the a/b/c sub-complex lacking eIF3i and eIF3g is essentially unable to promote the recruitment of capped *RPL41A* mRNA to the PIC (**Figure 4B–C**). This stands in contrast to a previous study where the affinity-purified a/b/c sub-complex rescued mRNA recruitment in heat-treated extracts from *prt1-1* cells (**Phan et al., 2001**). However, these extracts were not deprived of WT eIF3, perhaps enabling reconstitution of the complex with WT eIF3i and g subunits. In fact, the simultaneous loss of eIF3i and eIF3g from the eIF3 complex in *DDKK* cells produces phenotypes consistent with significant defects in scanning and start-codon recognition (**Herrmannová et al., 2012**). Because mRNA recruitment in our assay depends on the presence of an AUG codon, the kinetics we observe may report not only on initial mRNA attachment, but also on the subsequent events of scanning and start-codon recognition, suggesting an inability to efficiently scan and recognize the AUG codon in the absence of eIF3i and g prevents efficient *RPL41A* recruitment. In light of the severe mRNA recruitment defects we observe in the simultaneous absence of eIF3i and eIF3g, it is notable that neither the *Q258R* eIF3i mutation nor the *KLF* eIF3g mutation confer significant defects in mRNA recruitment. One possible explanation for these apparently opposed observations is that these mutations, which appear to affect either the rate or processivity of scanning, confer defects that are not rate limiting on the *RPL41A* mRNA employed in our assays, whose 5′ UTR is relatively short. It will be interesting to see the effects of these and other mutations that affect the efficiency of scanning by the PIC on the in vitro recruitment of natural mRNAs with longer, more structured 5′ UTRs.

Both proposed locations for eIF3i and eIF3g place them adjacent to the mRNA entry channel, either on the solvent or intersubunit face of the PIC (**Cuchalova et al., 2010**; **Aylett et al., 2015**; **Llácer et al., 2015**). Together with our observation that these subunits are critical for *RPL41A* mRNA recruitment in vitro and scanning and start-codon recognition in vivo (**Cuchalova et al., 2010**; **Herrmannová et al., 2012**), the observation that these subunits appear at the intersubunit face in structures containing mRNA, but at the solvent face in structures lacking mRNA further suggests that the mRNA entry channel arm of eIF3 might undergo a large-scale conformational change upon initial binding of the mRNA which could facilitate processive scanning and its arrest.

The *H725P and R731I* mutations within the eIF3a CTD also interfere with eIF3 binding to the PIC (**Figure 2C**) and, together with the *Box6* mutation, significantly slow the kinetics of *RPL41A* mRNA recruitment (**Figure 4C**). In contrast to the absence of the eIF3i and eIF3g subunits, these mutations do not appear to reduce the affinity of the PIC for TC (**Figure 3**), consistent with the observation that the interaction between eIF3a and eIF2 occurs in a region downstream of these mutations (**Valášek et al., 2002**). Though structures of eIF3 bound to various states of the PIC have yet to completely resolve the eIF3a CTD, previous work has established interactions between it and the eIF3b RRM (**Valasek et al., 2001b**), components of the 40S latch (**Chiu et al., 2010**; **Valášek et al., 2003**), and TC (**Valášek et al., 2002**), locating it near the entry channel and even projecting towards the intersubunit face. These observations enabled its proposed placement in the yeast py48S-closed structure, where it spans the intersubunit face, nearly encircling the PIC (**Llácer et al., 2015**). The binding defects we observe may result from disruptions to interactions between the eIF3a CTD and 40S latch; these disruptions might also affect the opening and closing of the latch, explaining the recruitment defects conferred by eIF3a CTD mutations. Consistent with this, all three eIF3a CTD mutations reduce the amount of *RPL41A* mRNA associated with PICs in vivo (**Chiu et al., 2010**). In particular, both the *H725P and R731I* mutations impair mRNA recruitment without affecting upstream events in vivo, and appear to affect the equilibrium between the open and closed conformations of the PIC.

We further observe a similar profile of effects in the presence of mutations to eIF3b. The *prt1-1* and *rnp1* mutations in the eIF3b β-propeller and RRM domains, respectively, disrupt both eIF3 and TC binding to the PIC (***Figure 2C*** and ***Figure 3***), and slow *RPL41A* mRNA recruitment (***Figure 4C***). In fact, these mutations confer the strongest kinetic effects we observe on native mRNA recruitment. Consistent with these results, both mutations produce in vivo phenotypes suggesting significant defects in scanning and start-codon recognition (***Nielsen et al., 2004***, ***2006***) and both have also been shown to reduce the amount of eIF3 associated with PICs either in cells or, in the case of *prt1-1*, in extracts. In several structures of eIF3 bound to the PIC, the eIF3b β-propeller domain is seen interacting with the 40S solvent face, below h16 (***Figure 7***) (***Aylett et al., 2015***; ***Georges, des et al., 2015***; ***Llácer et al., 2015***), consistent with its known interaction with uS4 (***Liu et al., 2014***). The eIF3b C-terminus, which appears together with eIF3i and eIF3g at the intersubunit face in the yeast py48S-closed structure, has been shown to mediate interactions with eIF3i (***Asano et al., 1998***; ***Herrmannová et al., 2012***). Together with the our results and the previous observation that the eIF3b RRM interacts with the eIF3a CTD (***Valasek et al., 2001b***), these raise the possibility that eIF3b contributes to the working of the eIF3 entry-channel arm by anchoring it to the 40S solvent face and, via its RRM and C-terminal regions, organizing its constituent components. The *prt1-1* and *rnp1* mutations might disrupt this mechanistic nexus, explaining the diverse set of defects they confer.

Another possibility is that eIF3b contributes more directly to mRNA recruitment, either from its position below the entrance to the mRNA entry channel on the solvent face as observed in the majority of structures, or by relocating to the intersubunit face. A recent report located mammalian eIF3i to a distinct location on the intersubunit face and suggested that the eIF3b β-propeller instead interacts with TC in the yeast 48S PIC (***Simonetti et al., 2016***). While this model would not explain the TC binding defects we observe in the absence of eIF3i and eIF3g, it would nonetheless still be consistent with the defects in TC affinity that we observe in the presence of eIF3b mutants and with a role for the eIF3 entry channel arm in stabilizing TC binding to the PIC.

The eIF3 exit-channel arm and the eIF3c NTD contribute to PIC binding and mRNA recruitment

Both the *Δ8* truncation and the *Box37* substitution in the eIF3a NTD diminish the affinity of eIF3 for 43S and 48S PICs. Consistent with this, structures of both yeast and mammalian eIF3 bound to various states of the PIC reveal the PCI domain in the eIF3a NTD, and specifically residues within the region truncated in the *Δ8 mutant*, as well as the eIF3c C-terminal PCI domain, contacting the 40S on its solvent face, below the platform (***Aylett et al., 2015***; ***Georges, des et al., 2015***; ***Llácer et al., 2015***). Moreover, the eIF3a NTD has been shown to interact with uS2 (***Valášek et al., 2003***; ***Kouba et al., 2012b***) which is located in this vicinity, and the *Δ8* truncation reduces the amount of eIF3 associated with PICs in vivo (***Szamecz et al., 2008***). In contrast, the *Box37* mutation, which confers a Ts$^-$ phenotype in vivo, appears to primarily affect mRNA recruitment in cells (***Khoshnevis et al., 2014***). In fact, we observe a significant defect in *RPL41A* mRNA recruitment at 37°C in the presence of *Box37* eIF3 (***Figure 4—figure supplement 2***). Based on structures, the *Box37* mutation does not appear to occur on the surface of the eIF3a PCI domain that faces the mRNA exit channel pore (***Llácer et al., 2015***), and thus may exert its effects indirectly by disrupting this domain, as suggested previously (***Khoshnevis et al., 2014***).

Elsewhere, the *Box12-SPW* and *GAP^{85}* mutations to the eIF3c NTD also slow native mRNA recruitment. Both mutations are in a region that appears to interact with eIF1 and both affect the amount of eIF1 associated with PICs and the accuracy of start-codon recognition in vivo (***Karásková et al., 2012***). The defects we observe are consistent with the observation that mRNA recruitment in our assay depends on codon-recognition (***Figure 4—figure supplement 1A–B***). The *Box12-SPW* mutation additionally weakens the affinity of eIF3 for the PIC. While this region has not been well-resolved in structural studies, regions of the eIF3c NTD were modeled on the 40S intersubunit face below the platform in the yeast py48S-closed structure, suggesting that this putative interaction might contribute to stabilizing eIF3 binding to the PIC (***Llácer et al., 2015***). Another possibility is that both mutations exert their effects on PIC binding via their effects on the eIF3:eIF1 interaction.

The eIF3a NTD is critical for stabilizing mRNA binding at the exit channel

To investigate the molecular role of eIF3 in stabilizing mRNA binding to the PIC at both the entry and exit channels, we followed the recruitment of a series of capped model mRNAs in which the placement of the AUG codon enables us to control the amount of mRNA in either channel. These experiments reveal that, while eIF3 is dispensable for stabilizing the binding of mRNA when both the entry and exit channels are occupied, it is essential for doing so when the entry channel is empty and the complex thus depends on interactions with mRNA in the exit channel. Previous work demonstrated that mammalian eIF3 can be cross-linked to mRNA at positions −8 thru −17 (relative to the AUG at +1 to +3), indicating its proximity to mRNA nucleotides just inside the entry channel (−8 to −10) and protruding from the entry channel pore (−11 to −17) (**Pisarev et al., 2008**). Consistent with this, our results indicate that eIF3 stabilizes the binding of mRNA to the PIC at this location.

In fact, our results localize this role to the eIF3a NTD; the *Δ8* truncation mimics the absence of eIF3 in its inability to stabilize the binding of mRNA to 48S PICs in which the entry channel is mostly empty (**Figure 5C**). This is consistent with the observation that the *Δ8* truncation impairs reinitiation on *GCN4* mRNA following translation of uORF1 and uORF2, an effect attributable to the loss of interaction between the eIF3a NTD and nucleotides 5′ of each uORF stop codon that otherwise stabilize post-termination 40S subunits and allow them to resume scanning in the presence of WT eIF3 (**Gunišová et al., 2016**; **Munzarová et al., 2011**; **Szamecz et al., 2008**). This role of the eIF3a NTD is also consistent with its placement immediately adjacent to the exit-channel pore in several structures of eIF3 bound to the 40S, in both yeast and mammals (**Aylett et al., 2015**; **Georges, des et al., 2015**; **Llácer et al., 2015**). In the cryo-EM structure of a yeast 48S PIC containing eIF3, the −10 nucleotide of the mRNA is visible as it begins to emerge from the exit channel at the solvent face (**Figure 6B**); we showed that the presence of 11 nucleotides within the exit channel is sufficient to rescue the destabilization caused by mutations affecting the entry channel arm of eIF3 (**Figure 6A**). This effect suggests that the eIF3a NTD might serve to extend the mRNA exit channel behind the 40S platform, interacting directly with mRNA as it emanates from the exit-channel pore. Another possibility is that the eIF3a NTD influences the conformation of the exit channel, promoting stable interaction between the mRNA and components of the 40S within the channel. Thus, the established stimulatory effects on translation initiation conferred by a minimum 5′UTR length and favorable sequence context just upstream of the start codon might also depend on proper interactions of 5′UTR nucleotides with the 40S exit channel, and hence, could be influenced by the eIF3a-NTD.

In contrast to its essential role in the binding of mRNA at the exit channel, eIF3 more modestly stabilizes mRNA binding at the entry channel. And yet, the absence of eIF3, or the presence of eIF3 variants with eIF3a-CTD mutations *H725P*, *R731I*, or *Box6*, all reduce binding of a model mRNA in which the exit channel is empty but the entry channel is filled (**Figure 5B**); these binding defects are largely rescued by increasing the amount of mRNA upstream of the AUG codon to fill the exit channel completely (**Figure 6A**). These results implicate the eIF3a CTD in stabilizing mRNA interactions at the entry channel of the PIC in a manner that is redundant with mRNA interactions at the entry channel involving the eIF3a NTD. Consistent with this, the presence of increasing amounts of mRNA in the entry channel progressively rescues the destabilization of mRNA binding to the PIC conferred by the *Δ8* variant, which is defective for interactions at the exit channel (**Figure 6C**). These observations might reflect the importance of a constriction of the mRNA entry channel formed by a movement of the 40S head that appears to be triggered by start codon recognition (**Llácer et al., 2015**; **Zhang et al., 2015**). This head movement also closes the latch on the entry channel, a feature composed of interactions between 18S rRNA helices 18 and 34 and ribosomal proteins uS3/uS5, which might contribute to scanning arrest upon start-codon recognition (**Llácer et al., 2015**). One explanation for our finding that full rescue of the *Δ8* exit channel defect requires filling the entry channel with ~14–17 nucleotides is that this represents the minimum length of mRNA required to fully engage the 40S components of the entry channel in its restricted conformation within the closed PIC and to also pass through the constriction created by the closed latch and interact with elements beyond it, which could include the eIF3a CTD. In fact, the structure of a partial yeast 48S complex lacking eIF3 (py48S) shows that 9 nt 3′ of the AUG codon (nucleotide + 12) is long enough to pass beyond h18/h34, but not past uS3/uS5 (**Figure 6D**) (**Hussain et al., 2014**). It is notable that, with the

exception of h34, every 40S component of the latch has been implicated in interactions with eIF3 (**Chiu et al., 2010**; **Valášek et al., 2003**).

Interestingly, the a/b/c sub-complex lacking the i and g subunits produces a stronger defect in recruitment of the model mRNA lacking contacts in the exit channel compared to the absence of eIF3 itself, perhaps because the absence of the i and g subunits alters the conformation of this entry channel arm, inducing a conformation of the PIC or of eIF3 itself that inhibits mRNA binding to the PIC. This might occur as a result of disruptions to the proposed rearrangement of the entry-channel arm upon mRNA binding to the PIC. In the end, the role of the eIF3 entry channel arm appears distinct from its counterpart at the exit channel (**Figure 7**). Whereas it contributes more subtly to stabilizing mRNA binding to the PIC, it contributes indirectly to mRNA recruitment by stabilizing TC binding and, as evidenced by its importance in the recruitment of natural mRNA, participates in events that control the rate of mRNA recruitment or scanning, perhaps by responding to the presence of mRNA within the PIC and by modulating the conformation of the 40S latch.

The work presented here provides greater understanding of how the individual subunits of eIF3 contribute to its interaction with the PIC, and to the component events of the initiation pathway. In particular, our results dissect the distinct roles played by eIF3 at the mRNA entry and exit channels, and how these contribute to the events of mRNA recruitment. Future work is required to better understand the molecular details of these contributions, particularly in the entry channel, where eIF3 appears to play a more subtle mechanistic role, perhaps collaborating with the 40S itself to mediate interaction with the mRNA. It will also be interesting to determine how, if at all, yeast eIF3 collaborates with the other mRNA recruitment factors to drive this event.

Materials and methods

Purification and preparation of reagents

40S ribosomal subunits and individual initiation factors were purified as previously described (**Acker et al., 2007**; **Mitchell et al., 2010**). eIF3 variants were purified from corresponding strains using the same method as for the wild-type factor, with the modification that cells were grown in the appropriate selective media throughout. Initiator $tRNA_i^{Met}$ was transcribed in vitro using His_6-tagged T7 RNA polymerase and subsequently methionylated with purified N-terminal His_6-tagged *E. coli* methionyl-tRNA synthetase as previously described (**Walker and Fredrick, 2008**), using either unlabeled methionine or [^{35}S]-methionine (PerkinElmer, Waltham, MA). All mRNAs were transcribed in vitro and purified as previously described (**Mitchell et al., 2010**). mRNAs were capped using the vaccinia virus D1/D12 capping enzyme as previously described (**Mitchell et al., 2010**). *RPL41A* mRNA was capped at a concentration of 5 µM, in the presence 50 mM Tris-HCl (pH 7.8), 1.25 mM $MgCl_2$, 6 mM KCl, 2.5 mM DTT, 50 µM GTP, 100 µM S-adenosylmethionine, 2 µCi/µL α-[^{32}P]-GTP [Perkin Elmer], 125 nM capping enzyme, 1 U/µL RiboLock RNase Inhibitor [Invitrogen]). Model mRNAs were capped at a concentration of 50 µM under similar conditions, except the concentration of cold GTP was increased to 100 µM to ensure it remained in excess of the mRNA. Capping reactions were incubated at 37°C for 90 min, and mRNAs were subsequently purified using the RNeasy mini kit (Qiagen). Model mRNAs were purified via a modified RNeasy mini kit protocol: 10 µL capping reactions were brought to 30 µL total volume using RNase-free water, followed by addition of 320 µL RLT buffer (Qiagen) and mixing by vortexing. Upon mixing, 525 µL of 100% ethanol was added, and the resultant solution was mixed by careful pipetting. Half of this mixture was loaded on to an RNeasy spin column and centrifuged at ≥8000 ×g for 15 s, after which the flowthrough was discarded, and the remaining mixture was loaded onto the column and centrifuged, and the flowthrough again discarded. The column was then sequentially washed once with 700 µL of RWT buffer (Qiagen) and twice with 500 µL buffer RPE (Qiagen), with each wash followed by centrifugation for 15 s at ≥8000 ×g and disposal of the flowthrough. Upon the final wash, centrifugation at ≥8000 ×g was extended to 60 s and performed twice, with the flowthrough discarded each time, to ensure complete drying of the column. Purified RNA was then eluted by addition of 30 µL RNase-free water to the column and centrifugation for 60 s at ≥8000 ×g.

Biochemical assays

The affinity of WT and variant eIF3 for 43S and 48S PICs was determined using a gel-shift assay monitoring [^{35}S]-Met-tRNA$_i^{Met}$ (**Acker et al., 2007**; **Mitchell et al., 2010**). 43S complexes (in the absence of mRNA) were formed in the presence of 1 μM eIF1, 1 μM eIF1A, 200 nM eIF2, 1 mM GDPNP•Mg^{2+}, 2 nM [^{35}S]-Met-tRNA$_i^{Met}$, and 30 nM 40S subunits in 1X Recon buffer (30 mM HEPES-KOH pH 7.4, 100 mM KOAc pH 7.6, 3 mM $Mg(OAc)_2$, 2 mM DTT). The concentration of WT or variant eIF3 was titrated between 30 nM and 500 nM. 48S complexes (including mRNA) were formed in the presence of 1 μM uncapped AUG-containing model mRNA, 1 μM eIF1, 1 μM eIF1A, 200 nM eIF2, 1 mM GDPNP•Mg^{2+}, 2 nM [^{35}S]-Met-tRNA$_i^{Met}$, and 20 nM 40S subunits. The concentration of either WT or variant eIF3 was titrated between 30 nM and 500 nM for both. 10 μL reactions were incubated at 26˚C for 2 hr, after which they were mixed with 2 μL loading buffer (0.05% xylene cyanol, 0.05% bromophenol blue, 50% sucrose in 1X Recon buffer) and resolved on a 4% polyacrylamide (37.5:1 acrylamide:bisacrylamide) gel prepared in 1X THEM (34 mM Tris Base, 57 mM HEPES, 0.1 mM EDTA, 2.5 mM $MgCl_2$) gel run at 25 W for 45 min using 1X THEM as the running buffer. Upon completion, gels were placed on Whatman paper, covered with plastic wrap, and exposed for at least 15 h to a phosphor screen inside a cassette wrapped in plastic wrap at −20˚C. Cooled cassettes were removed from refrigeration at −20˚C and allowed to warm at room temperature for approximately 10 min prior to removal of the plastic wrap and scanning of the phosphor screen using a Typhoon FLA 9500 imager (GE Life Sciences). The fraction of eIF3-bound PICs was determined from the signal of free and eIF3-bound PIC bands. Data were modeled with both Langmuir and Hill-binding isotherms to determine the apparent K_D.

The affinity of 43S PICs for TC was determined using a previously-described gel-shift assay monitoring [^{35}S]-Met-tRNA$_i^{Met}$ (**Acker et al., 2007**; **Kolitz et al., 2009**). Complexes were formed in the presence of 1 μM eIF1, 1 μM eIF1A, 200 nM eIF2, 1 mM GDPNP, 1 nM [^{35}S]-Met-tRNA$_i^{Met}$, and 500 nM eIF3 in 1X Recon buffer (30 mM HEPES-KOH pH 7.4, 100 mM KOAc pH 7.6, 3 mM $Mg(OAc)_2$, 2 mM DTT). The concentration of 40S subunits was titrated between 10 nM and 320 nM. Reactions were incubated at 26˚C for 2 hr and subsequently resolved on a 4% native THEM gel run at 25 W for 45 min. Gels were exposed and quantified as above, with the fraction of TC binding quantified as the ratio of signal from bands representing eIF3-bound PICs and free TC. Data were modeled with a Langmuir isotherm to determine the apparent K_D.

The kinetics and extent of mRNA recruitment to reconstituted 43S PICs were determined using a previously-described gel-shift assay monitoring [^{32}P]-capped mRNA (**Mitchell et al., 2010**). PICs were assembled in the presence of 1 μM eIF1, 1 μM eIF1A, 300 nM eIF2, 200 nM Met-tRNA$_i^{Met}$, 400 nM eIF3, 2 μM eIF4A, 300 nM eIF4B, 50 nM eIF4E•eIFG, 300 nM eIF5, and 30 nM 40S subunits in 1X Recon buffer (30 mM HEPES-KOH pH 7.4, 100 mM KOAc pH 7.6, 3 mM $Mg(OAc)_2$, 2 mM DTT) and incubated 10 min at 26˚C. Reactions were initiated by the simultaneous addition of ATP•Mg^{2+} and the appropriate [^{32}P]-capped mRNA to final concentrations of 2 mM and 15 nM, respectively. For kinetic measurements, 4 μL aliquots were removed at appropriate time points, added to 1 μl of loading buffer and quenched by loading on a 4% native THEM gel running at 200 V. Gels were exposed and quantified as above, with the fraction of mRNA recruitment quantified as the fraction of signal in the band representing 48S PICs per lane. Data were fit with single-exponential rate equations to obtain the observed rate constant of mRNA recruitment. To measure the maximal extent of recruitment at completion, reactions were similarly resolved on a 4% native THEM gel upon incubation for 2 hr at 26˚C, at which point all reactions had proceeded to completion as judged by prior kinetic experiments. For experiments containing *RPL41A* mRNA, gels were run for 1 hr at 200 V. For experiments containing 50 nt model mRNAs, gels were run 45 min at 200 V.

In vivo assays

The analysis of native 48S PICs was performed as previously described (**Chiu et al., 2010**; **Khoshnevis et al., 2014**). Cells were cultured at 30˚C to $OD600_{600}$ = 1 and cross-linked with 1% formaldehyde prior to being harvested. Whole Cell Extracts were prepared in breaking buffer (20 mM Tris-HCl, pH 7.5, 50 mM KCl, 10 mM $MgCl_2$, 1 mM dithiothreitol [DTT], 5 mM NaF, 1 mM phenylmethylsulfonyl fluoride [PMSF], 1× Complete Protease Inhibitor Mix tablets without EDTA [Roche]), and 25 A260 units were separated on a 7.5% to 30% sucrose gradient by centrifugation at 41,000 rpm for 5 hr in a SW41Ti rotor. Total RNA was isolated from 500 μL of each of 13 gradient

fractions by hot-phenol extraction, and resuspended in 26 µL of diethyl pyrocarbonate-treated H_2O. Prior to RNA isolation, 3 µL of TATAA Universal RNA Spike I (Tataa Biocenter) was added to each fraction as a normalization control. 3 µL of total RNA were subjected to reverse transcription using the High Capacity cDNA Reverse Transcription Kit (Applied Biosystems). Aliquots of cDNA were diluted six-fold, and qPCR amplifications were performed on 2 µL of diluted cDNA in 10 µL reaction mixtures prepared with the 5x HOT FIREPol EvaGreen qPCR Supermix (Solis Biodyne) and primers for RPL41A (0.3 µM), 18S rRNA, PMP3, SME1, COX14, RPS28A and spike (0.4 µM) using the CFX384 Real-Time System (Biorad).

Acknowledgements

The authors would like to acknowledge Tom Dever for his thoughtful and critical suggestions. This work was supported by the Intramural Research Program (JRL and AGH) of the National Institutes of Health (NIH), NIH grant GM62128 (previously to JRL), and by Wellcome Trust grant 090812/B/09/Z and the Centrum of Excellence of the Czech Science Foundation P305/12/G034 (both to LSV). CEA was further supported by an NIH minority supplement to NIH grant GM62128 and by a Leukemia and Lymphoma Society CDP Fellowship.

Additional information

Competing interests

AGH: Reviewing editor, *eLife*. The other authors declare that no competing interests exist.

Funding

Funder	Grant reference number	Author
National Institutes of Health	Intramural Research Program	Colin Echeverría Aitken Wen-Ling Chiu Fujun Zhou Alan G Hinnebusch Jon R Lorsch
Leukemia and Lymphoma Society	5199-12	Colin Echeverría Aitken
Wellcome Trust	090812/B/09/Z	Leoš Shivaya Valášek
Centrum of Excellence of the Czech Science Foundation	P305/12/G034	Leoš Shivaya Valášek
National Institutes of Health	GM62128	Jon R Lorsch

The funders had no role in study design, data collection and interpretation, or the decision to submit the work for publication.

Author contributions

CEA, Purified all the eIF3 variants with assistance from Petra and Wen-Ling. Together with Jon, Alan, and Leos, he conceived of all the in-vitro experiments, which he performed himself. Wrote the first draft of the manuscript, which he further revised and edited with Jon, Alan, and Leos. Conception and design, Acquisition of data, Analysis and interpretation of data, Drafting or revising the article; PB, Created the strains for expressing and purifying all eIF3 variants, with the exception of those created by Wen-Ling. Petra additionally helped with the purification of several eIF3 variants. Drafting or revising the article, Contributed unpublished essential data or reagents; VV, Performed the in vivo mRNA crosslinking experiments. Acquisition of data; W-LC, Created the strains for expressing and purifying H725P, R731I, and box6 eIF3, and helped with these purifications. Contributed unpublished essential data or reagents; FZ, Created the constructs for in-vitro transcription of the unstructured model mRNAs. Contributed unpublished essential data or reagents; LSV, AGH, JRL, Conception and design, Analysis and interpretation of data, Drafting or revising the article

Author ORCIDs
Alan G Hinnebusch, http://orcid.org/0000-0002-1627-8395
Jon R Lorsch, http://orcid.org/0000-0002-4521-4999

References

Acker MG, Kolitz SE, Mitchell SF, Nanda JS, Lorsch JR. 2007. Reconstitution of yeast translation initiation. *Methods in Enzymology* **430**:111–145. doi: 10.1016/S0076-6879(07)30006-2, PMID: 17913637

Aitken CE, Lorsch JR. 2012. A mechanistic overview of translation initiation in eukaryotes. *Nature Structural & Molecular Biology* **19**:568–576. doi: 10.1038/nsmb.2303, PMID: 22664984

Algire MA, Maag D, Savio P, Acker MG, Tarun SZ, Sachs AB, Asano K, Nielsen KH, Olsen DS, Phan L, Hinnebusch AG, Lorsch JR. 2002. Development and characterization of a reconstituted yeast translation initiation system. *RNA* **8**:382–397. doi: 10.1017/S1355838202029527, PMID: 12008673

Asano K, Clayton J, Shalev A, Hinnebusch AG. 2000. A multifactor complex of eukaryotic initiation factors, eIF1, eIF2, eIF3, eIF5, and initiator tRNA(Met) is an important translation initiation intermediate in vivo. *Genes & Development* **14**:2534–2546. doi: 10.1101/gad.831800, PMID: 11018020

Asano K, Phan L, Anderson J, Hinnebusch AG. 1998. Complex formation by all five homologues of mammalian translation initiation factor 3 subunits from yeast Saccharomyces cerevisiae. *Journal of Biological Chemistry* **273**:18573–18585. doi: 10.1074/jbc.273.29.18573, PMID: 9660829

Asano K, Shalev A, Phan L, Nielsen K, Clayton J, Valásek L, Donahue TF, Hinnebusch AG. 2001. Multiple roles for the C-terminal domain of eIF5 in translation initiation complex assembly and GTPase activation. *The EMBO Journal* **20**:2326–2337. doi: 10.1093/emboj/20.9.2326, PMID: 11331597

Aylett CH, Boehringer D, Erzberger JP, Schaefer T, Ban N. 2015. Structure of a yeast 40S-eIF1-eIF1A-eIF3-eIF3j initiation complex. *Nature Structural & Molecular Biology* **22**:269–271. doi: 10.1038/nsmb.2963, PMID: 25664723

Beznosková P, Cuchalová L, Wagner S, Shoemaker CJ, Gunišová S, von der Haar T, Valášek LS. 2013. Translation initiation factors eIF3 and HCR1 control translation termination and stop codon read-through in yeast cells. *PLoS Genetics* **9**:e1003962. doi: 10.1371/journal.pgen.1003962, PMID: 24278036

Brachmann CB, Davies A, Cost GJ, Caputo E, Li J, Hieter P, Boeke JD. 1998. Designer deletion strains derived from Saccharomyces cerevisiae S288C: a useful set of strains and plasmids for PCR-mediated gene disruption and other applications. *Yeast* **14**:115–132. doi: 10.1002/(SICI)1097-0061(19980130)14:2<115::AID-YEA204>3.0.CO;2-2, PMID: 9483801

Chiu WL, Wagner S, Herrmannová A, Burela L, Zhang F, Saini AK, Valásek L, Hinnebusch AG. 2010. The C-terminal region of eukaryotic translation initiation factor 3a (eIF3a) promotes mRNA recruitment, scanning, and, together with eIF3j and the eIF3b RNA recognition motif, selection of AUG start codons. *Molecular and Cellular Biology* **30**:4415–4434. doi: 10.1128/MCB.00280-10, PMID: 20584985

Coppolecchia R, Buser P, Stotz A, Linder P. 1993. A new yeast translation initiation factor suppresses a mutation in the eIF-4A RNA helicase. *The EMBO Journal* **12**:4005–4011. PMID: 8404866

Cross FR. 1997. 'Marker swap' plasmids: convenient tools for budding yeast molecular genetics. *Yeast* **13**:647–653. doi: 10.1002/(SICI)1097-0061(19970615)13:7<647::AID-YEA115>3.0.CO;2-#, PMID: 9200814

Cuchalová L, Kouba T, Herrmannová A, Dányi I, Chiu WL, Valásek L. 2010. The RNA recognition motif of eukaryotic translation initiation factor 3g (eIF3g) is required for resumption of scanning of posttermination ribosomes for reinitiation on GCN4 and together with eIF3i stimulates linear scanning. *Molecular and Cellular Biology* **30**:4671–4686. doi: 10.1128/MCB.00430-10, PMID: 20679478

de la Cruz J, Iost I, Kressler D, Linder P. 1997. The p20 and Ded1 proteins have antagonistic roles in eIF4E-dependent translation in saccharomyces cerevisiae. *PNAS* **94**:5201–5206. doi: 10.1073/pnas.94.10.5201, PMID: 9144215

des Georges A, Dhote V, Kuhn L, Hellen CU, Pestova TV, Frank J, Hashem Y. 2015. Structure of mammalian eIF3 in the context of the 43S preinitiation complex. *Nature* **525**:491–495. doi: 10.1038/nature14891, PMID: 26344199

Elantak L, Wagner S, Herrmannová A, Karásková M, Rutkai E, Lukavsky PJ, Valásek L. 2010. The indispensable N-terminal half of eIF3j/HCR1 cooperates with its structurally conserved binding partner eIF3b/PRT1-RRM and with eIF1A in stringent AUG selection. *Journal of Molecular Biology* **396**:1097–1116. doi: 10.1016/j.jmb.2009.12.047, PMID: 20060839

Evans DR, Rasmussen C, Hanic-Joyce PJ, Johnston GC, Singer RA, Barnes CA. 1995. Mutational analysis of the Prt1 protein subunit of yeast translation initiation factor 3. *Molecular and Cellular Biology* **15**:4525–4535. doi: 10.1128/MCB.15.8.4525, PMID: 7623843

Fletcher CM, Pestova TV, Hellen CU, Wagner G. 1999. Structure and interactions of the translation initiation factor eIF1. *The EMBO Journal* **18**:2631–2637. doi: 10.1093/emboj/18.9.2631, PMID: 10228174

Fraser CS, Berry KE, Hershey JW, Doudna JA. 2007. eIF3j is located in the decoding center of the human 40S ribosomal subunit. *Molecular Cell* **26**:811–819. doi: 10.1016/j.molcel.2007.05.019, PMID: 17588516

Fraser CS, Lee JY, Mayeur GL, Bushell M, Doudna JA, Hershey JW. 2004. The j-subunit of human translation initiation factor eIF3 is required for the stable binding of eIF3 and its subcomplexes to 40 S ribosomal subunits in vitro. *Journal of Biological Chemistry* **279**:8946–8956. doi: 10.1074/jbc.M312745200, PMID: 14688252

Giaever G, Chu AM, Ni L, Connelly C, Riles L, Véronneau S, Dow S, Lucau-Danila A, Anderson K, André B, Arkin AP, Astromoff A, El-Bakkoury M, Bangham R, Benito R, Brachat S, Campanaro S, Curtiss M, Davis K,

Deutschbauer A, et al. 2002. Functional profiling of the Saccharomyces cerevisiae genome. *Nature* **418**:387–391. doi: 10.1038/nature00935, PMID: 12140549

Gietz RD, Sugino A. 1988. New yeast-Escherichia coli shuttle vectors constructed with in vitro mutagenized yeast genes lacking six-base pair restriction sites. *Gene* **74**:527–534. doi: 10.1016/0378-1119(88)90185-0, PMID: 3073106

Gietz RD, Woods RA. 2002. Transformation of yeast by lithium acetate/single-stranded carrier DNA/polyethylene glycol method. *Methods in Enzymology* **350**:87–96. doi: 10.1016/S0076-6879(02)50957-5, PMID: 12073338

Gunišová S, Beznosková P, Mohammad MP, Vlčková V, Valášek LS. 2016. In-depth analysis of cis-determinants that either promote or inhibit reinitiation on GCN4 mRNA after translation of its four short uORFs. *RNA* **22**:542–558. doi: 10.1261/rna.055046.115, PMID: 26822200

Gunišová S, Valášek LS. 2014. Fail-safe mechanism of GCN4 translational control–uORF2 promotes reinitiation by analogous mechanism to uORF1 and thus secures its key role in GCN4 expression. *Nucleic Acids Research* **42**:5880–5893. doi: 10.1093/nar/gku204, PMID: 24623812

Hartwell LH, McLaughlin CS. 1969. A mutant of yeast apparently defective in the initiation of protein synthesis. *PNAS* **62**:468–474. doi: 10.1073/pnas.62.2.468, PMID: 5256225

Hashem Y, des Georges A, Dhote V, Langlois R, Liao HY, Grassucci RA, Hellen CU, Pestova TV, Frank J. 2013. Structure of the mammalian ribosomal 43S preinitiation complex bound to the scanning factor DHX29. *Cell* **153**:1108–1119. doi: 10.1016/j.cell.2013.04.036, PMID: 23706745

Herrmannová A, Daujotyte D, Yang JC, Cuchalová L, Gorrec F, Wagner S, Dányi I, Lukavsky PJ, Valásek LS. 2012. Structural analysis of an eIF3 subcomplex reveals conserved interactions required for a stable and proper translation pre-initiation complex assembly. *Nucleic Acids Research* **40**:2294–2311. doi: 10.1093/nar/gkr765, PMID: 22090426

Hinnebusch AG. 2006. eIF3: a versatile scaffold for translation initiation complexes. *Trends in Biochemical Sciences* **31**:553–562. doi: 10.1016/j.tibs.2006.08.005, PMID: 16920360

Hinnebusch AG. 2011. Molecular mechanism of scanning and start codon selection in eukaryotes. *Microbiology and Molecular Biology Reviews* **75**:434–467. doi: 10.1128/MMBR.00008-11, PMID: 21885680

Hinnebusch AG. 2014. The scanning mechanism of eukaryotic translation initiation. *Annual Review of Biochemistry* **83**:779–812. doi: 10.1146/annurev-biochem-060713-035802, PMID: 24499181

Hussain T, Llácer JL, Fernández IS, Munoz A, Martin-Marcos P, Savva CG, Lorsch JR, Hinnebusch AG, Ramakrishnan V. 2014. Structural changes enable start codon recognition by the eukaryotic translation initiation complex. *Cell* **159**:597–607. doi: 10.1016/j.cell.2014.10.001, PMID: 25417110

Jackson RJ, Hellen CU, Pestova TV. 2010. The mechanism of eukaryotic translation initiation and principles of its regulation. *Nature Reviews Molecular Cell Biology* **11**:113–127. doi: 10.1038/nrm2838, PMID: 20094052

Jivotovskaya AV, Valásek L, Hinnebusch AG, Nielsen KH. 2006. Eukaryotic translation initiation factor 3 (eIF3) and eIF2 can promote mRNA binding to 40S subunits independently of eIF4G in yeast. *Molecular and Cellular Biology* **26**:1355–1372. doi: 10.1128/MCB.26.4.1355-1372.2006, PMID: 16449648

Kapp LD, Kolitz SE, Lorsch JR. 2006. Yeast initiator tRNA identity elements cooperate to influence multiple steps of translation initiation. *RNA* **12**:751–764. doi: 10.1261/rna.2263906, PMID: 16565414

Karásková M, Gunišová S, Herrmannová A, Wagner S, Munzarová V, Valášek L. 2012. Functional characterization of the role of the N-terminal domain of the c/Nip1 subunit of eukaryotic initiation factor 3 (eIF3) in AUG recognition. *Journal of Biological Chemistry* **287**:28420–28434. doi: 10.1074/jbc.M112.386656, PMID: 22718758

Khoshnevis S, Gunišová S, Vlčková V, Kouba T, Neumann P, Beznosková P, Ficner R, Valášek LS. 2014. Structural integrity of the PCI domain of eIF3a/TIF32 is required for mRNA recruitment to the 43S pre-initiation complexes. *Nucleic Acids Research* **42**:4123–4139. doi: 10.1093/nar/gkt1369, PMID: 24423867

Kolitz SE, Takacs JE, Lorsch JR. 2009. Kinetic and thermodynamic analysis of the role of start codon/anticodon base pairing during eukaryotic translation initiation. *RNA* **15**:138–152. doi: 10.1261/rna.1318509, PMID: 19029312

Kolupaeva VG, Unbehaun A, Lomakin IB, Hellen CU, Pestova TV. 2005. Binding of eukaryotic initiation factor 3 to ribosomal 40S subunits and its role in ribosomal dissociation and anti-association. *RNA* **11**:470–486. doi: 10.1261/rna.7215305, PMID: 15703437

Kouba T, Dányi I, Gunišová S, Munzarová V, Vlčková V, Cuchalová L, Neueder A, Milkereit P, Valášek LS. 2012b. Small ribosomal protein RPS0 stimulates translation initiation by mediating 40S-binding of eIF3 via Its direct contact with the eIF3a/TIF32 subunit. *PLoS One* **7**:e40464. doi: 10.1371/journal.pone.0040464

Kouba T, Rutkai E, Karaskova M, Valasek LS. 2012a. The eIF3c/NIP1 PCI domain interacts with RNA and RACK1/ASC1 and promotes assembly of translation preinitiation complexes. *Nucleic Acids Research* **40**:2683–2699. doi: 10.1093/nar/gkr1083

Kovarik P, Hasek J, Valásek L, Ruis H. 1998. RPG1: an essential gene of saccharomyces cerevisiae encoding a 110-kDa protein required for passage through the G1 phase. *Current Genetics* **33**:100–109. doi: 10.1007/s002940050314, PMID: 9506897

Liu Y, Neumann P, Kuhle B, Monecke T, Schell S, Chari A, Ficner R. 2014. Translation initiation factor eIF3b contains a nine-bladed β-propeller and interacts with the 40S ribosomal subunit. *Structure* **22**:923–930. doi: 10.1016/j.str.2014.03.010, PMID: 24768115

Llácer JL, Hussain T, Marler L, Aitken CE, Thakur A, Lorsch JR, Hinnebusch AG, Ramakrishnan V. 2015. Conformational differences between open and closed states of the eukaryotic translation initiation complex. *Molecular Cell* **59**:399–412. doi: 10.1016/j.molcel.2015.06.033, PMID: 26212456

Maag D, Fekete CA, Gryczynski Z, Lorsch JR. 2005. A conformational change in the eukaryotic translation preinitiation complex and release of eIF1 signal recognition of the start codon. *Molecular Cell* **17**:265–275. doi: 10.1016/j.molcel.2004.11.051, PMID: 15664195

Mitchell SF, Walker SE, Algire MA, Park EH, Hinnebusch AG, Lorsch JR. 2010. The 5′-7-methylguanosine cap on eukaryotic mRNAs serves both to stimulate canonical translation initiation and to block an alternative pathway. *Molecular Cell* **39**:950–962. doi: 10.1016/j.molcel.2010.08.021, PMID: 20864040

Munzarová V, Pánek J, Gunišová S, Dányi I, Szamecz B, Valášek LS. 2011. Translation reinitiation relies on the interaction between eIF3a/TIF32 and progressively folded cis-acting mRNA elements preceding short uORFs. *PLoS Genetics* **7**:e1002137. doi: 10.1371/journal.pgen.1002137, PMID: 21750682

Nielsen KH, Szamecz B, Valásek L, Jivotovskaya A, Shin BS, Hinnebusch AG. 2004. Functions of eIF3 downstream of 48S assembly impact AUG recognition and GCN4 translational control. *The EMBO Journal* **23**:1166–1177. doi: 10.1038/sj.emboj.7600116, PMID: 14976554

Nielsen KH, Valásek L, Sykes C, Jivotovskaya A, Hinnebusch AG. 2006. Interaction of the RNP1 motif in PRT1 with HCR1 promotes 40S binding of eukaryotic initiation factor 3 in yeast. *Molecular and Cellular Biology* **26**: 2984–2998. doi: 10.1128/MCB.26.8.2984-2998.2006, PMID: 16581774

Olsen DS, Savner EM, Mathew A, Zhang F, Krishnamoorthy T, Phan L, Hinnebusch AG. 2003. Domains of eIF1A that mediate binding to eIF2, eIF3 and eIF5B and promote ternary complex recruitment in vivo. *The EMBO Journal* **22**:193–204. doi: 10.1093/emboj/cdg030, PMID: 12514125

Pestova TV, Kolupaeva VG. 2002. The roles of individual eukaryotic translation initiation factors in ribosomal scanning and initiation codon selection. *Genes & Development* **16**:2906–2922. doi: 10.1101/gad.1020902, PMID: 12435632

Phan L, Schoenfeld LW, Valásek L, Nielsen KH, Hinnebusch AG. 2001. A subcomplex of three eIF3 subunits binds eIF1 and eIF5 and stimulates ribosome binding of mRNA and tRNA(i)Met. *The EMBO Journal* **20**:2954–2965. doi: 10.1093/emboj/20.11.2954, PMID: 11387228

Phan L, Zhang X, Asano K, Anderson J, Vornlocher HP, Greenberg JR, Qin J, Hinnebusch AG. 1998. Identification of a translation initiation factor 3 (eIF3) core complex, conserved in yeast and mammals, that interacts with eIF5. *Molecular and Cellular Biology* **18**:4935–4946. doi: 10.1128/MCB.18.8.4935, PMID: 9671501

Pisarev AV, Kolupaeva VG, Yusupov MM, Hellen CU, Pestova TV. 2008. Ribosomal position and contacts of mRNA in eukaryotic translation initiation complexes. *The EMBO Journal* **27**:1609–1621. doi: 10.1038/emboj.2008.90, PMID: 18464793

Simonetti A, Brito Querido J, Myasnikov AG, Mancera-Martinez E, Renaud A, Kuhn L, Hashem Y. 2016. eIF3 peripheral subunits rearrangement after mRNA binding and start-codon recognition. *Molecular Cell* **63**:206–217. doi: 10.1016/j.molcel.2016.05.033, PMID: 27373335

Siridechadilok B, Fraser CS, Hall RJ, Doudna JA, Nogales E. 2005. Structural roles for human translation factor eIF3 in initiation of protein synthesis. *Science* **310**:1513–1515. doi: 10.1126/science.1118977, PMID: 16322461

Sonenberg N, Hinnebusch AG. 2009. Regulation of translation initiation in eukaryotes: mechanisms and biological targets. *Cell* **136**:731–745. doi: 10.1016/j.cell.2009.01.042, PMID: 19239892

Szamecz B, Rutkai E, Cuchalová L, Munzarová V, Herrmannová A, Nielsen KH, Burela L, Hinnebusch AG, Valásek L. 2008. eIF3a cooperates with sequences 5′ of uORF1 to promote resumption of scanning by post-termination ribosomes for reinitiation on GCN4 mRNA. *Genes & Development* **22**:2414–2425. doi: 10.1101/gad.480508, PMID: 18765792

Valásek L, Hasek J, Nielsen KH, Hinnebusch AG. 2001a. Dual function of eIF3j/Hcr1p in processing 20 S pre-rRNA and translation initiation. *Journal of Biological Chemistry* **276**:43351–43360. doi: 10.1074/jbc.M106887200, PMID: 11560931

Valásek L, Mathew AA, Shin BS, Nielsen KH, Szamecz B, Hinnebusch AG. 2003. The yeast eIF3 subunits TIF32/a, NIP1/c, and eIF5 make critical connections with the 40S ribosome in vivo. *Genes & Development* **17**:786–799. doi: 10.1101/gad.1065403, PMID: 12651896

Valásek L, Nielsen KH, Hinnebusch AG. 2002. Direct eIF2-eIF3 contact in the multifactor complex is important for translation initiation in vivo. *The EMBO Journal* **21**:5886–5898. doi: 10.1093/emboj/cdf563, PMID: 12411506

Valásek L, Nielsen KH, Zhang F, Fekete CA, Hinnebusch AG. 2004. Interactions of eukaryotic translation initiation factor 3 (eIF3) subunit NIP1/c with eIF1 and eIF5 promote preinitiation complex assembly and regulate start codon selection. *Molecular and Cellular Biology* **24**:9437–9455. doi: 10.1128/MCB.24.21.9437-9455.2004, PMID: 15485912

Valásek L, Phan L, Schoenfeld LW, Valásková V, Hinnebusch AG. 2001b. Related eIF3 subunits TIF32 and HCR1 interact with an RNA recognition motif in PRT1 required for eIF3 integrity and ribosome binding. *The EMBO Journal* **20**:891–904. doi: 10.1093/emboj/20.4.891, PMID: 11179233

Valásek L, Trachsel H, Hasek J, Ruis H. 1998. Rpg1, the Saccharomyces cerevisiae homologue of the largest subunit of mammalian translation initiation factor 3, is required for translational activity. *Journal of Biological Chemistry* **273**:21253–21260. doi: 10.1074/jbc.273.33.21253, PMID: 9694884

Valásek LS. 2012. 'Ribozoomin'–translation initiation from the perspective of the ribosome-bound eukaryotic initiation factors (eIFs). *Current Protein & Peptide Science* **13**:305–330. doi: 10.2174/138920312801619385, PMID: 22708493

Walker SE, Fredrick K. 2008. Preparation and evaluation of acylated tRNAs. *Methods* **44**:81–86. doi: 10.1016/j.ymeth.2007.09.003, PMID: 18241790

Walker SE, Zhou F, Mitchell SF, Larson VS, Valasek L, Hinnebusch AG, Lorsch JR. 2013. Yeast eIF4B binds to the head of the 40S ribosomal subunit and promotes mRNA recruitment through its N-terminal and internal repeat domains. *RNA* **19**:191–207. doi: 10.1261/rna.035881.112, PMID: 23236192

Zhang F, Saini AK, Shin BS, Nanda J, Hinnebusch AG. 2015. Conformational changes in the P site and mRNA entry channel evoked by AUG recognition in yeast translation preinitiation complexes. *Nucleic Acids Research* **43**:2293–2312. doi: 10.1093/nar/gkv028, PMID: 25670678

Appendix 1

Supplementary materials and methods

Yeast strain constructions

A list of all strains used throughout this study can be found in ***Appendix 1—table 1***.

To create PBH57 (*prb1Δ pep4Δ tif34Δ* YEp-TIF34) and PBH42 (*prb1Δ pep4Δ tif35Δ* YEp-TIF35), *LEU2*–based covering plasmids YEp111-MET-TIF34-L and YEp111-MET-TIF35-L, expressing *TIF34* or *TIF35* under the control of the methionine promoter, respectively, were first introduced into strain BJ5465 (*prb1Δ pep4Δ*) strain using the lithium acetate yeast transformation protocol (***Gietz and Woods, 2002***). The resulting transformants were first selected on SC media lacking leucine and methionine. Positively scoring clones were subsequently transformed with the *tif34Δ::hisG::URA3::hisG* (pTZ-tif34Δ) and *tif35Δ::hisG::URA3::hisG* (B444) disruption cassettes, respectively, to delete a gene encoding a given eIF3 subunit. The Ura^+ colonies were selected on SC-URA plates and the uracil auxothrophy was subsequently regained by growing the transformants on medium containing 5-fluoroorotic acid (5-FOA). Successful completion of these genetic manipulations was verified by growing the resulting strains, auxotrophic for uracil, on plates supplemented with or lacking methionine. Only those cells where a chromosomal allele encoding a given eIF3 subunit was deleted, failed to grow on media containing methionine. Thus generated and verified strains were finally transformed with YEp-TIF34 and YEp-TIF35 and the leucine auxotrophy (a loss of the original covering plasmids YEp111-MET-TIF34-L and YEp111-MET-TIF35-L, respectively) was regained by growing the cells in liquid media containing leucine for several rounds of exponential growth and selecting for clones that grew in the absence of uracil but not in the absence of leucine in the media. The resulting strains were named PBH57 (*prb1Δ pep4Δ tif34Δ* YEp-TIF34) and PBH42 (*prb1Δ pep4Δ tif35Δ* YEp-TIF35).

To create PBH44 (*prb1Δ pep4Δ prt1Δ* YEpPRT1-U) and PBH56 (*prb1Δ pep4Δ nip1Δ* YEpNIP1-His-U), *TRP1*–based covering plasmids YCpAH-MET-PRT1-W and YCpMJ-MET-NIP1-W, expressing *PRT1* and *NIP1* under the control of the methionine promoter, respectively, were first introduced into the BJ5465 (*prb1Δ pep4Δ*) strain using the LiAc yeast transformation protocol. The resulting transformants were first selected on SC media lacking tryptophan and methionine. Positively scoring clones were subsequently transformed with the *prt1Δ::hisG::URA3::hisG* (B3289) and *nip1Δ::hisG::URA3::hisG* (pLV10) disruption cassettes, respectively, to delete a gene of a given eIF3 subunit. The URA+ colonies were selected on SC-URA plates and the uracil auxothrophy was subsequently regained by growing the transformants on 5-FOA containing plates. Successful completion of these genetic manipulations was verified by growing the resulting strains, auxotrophic for uracil, on plates supplemented with or lacking methionine. Only those cells where a chromosomal allele of a given eIF3 subunit was completely deleted failed to grow on media containing methionine. Thus generated and verified strains were finally transformed with YEpPRT1-U and YEpNIP1-His-U and the tryptophan auxotrophy (a loss of the original covering plasmids YCpAH-MET-PRT1-W and YCpMJ-MET-NIP1-W, respectively) was regained by growing the cells in liquid media containing tryptophan for several rounds of exponential growth and selecting for those clones that did grow in the absence of uracil but not in the absence of tryptophan in the media. The resulting strains were named PBH44 (*prb1Δ pep4Δ prt1Δ* YEpPRT1-U) and PBH56 (*prb1Δ pep4Δ nip1Δ* YEpNIP1-His-U).

To produce PBH65, PBH66 and PBH67 overexpressing all eIF3 subunits, PBH56 (*prb1Δ pep4Δ nip1Δ* YEpNIP1-His-U) was first subjected to double transformation with YEpPRT1-His-TIF34-TIF35-W/YEpTIF32-nip1-Δ60-L, YEpPRT1-His-TIF34-TIF35-W/Yep3TIF32-nip_GAP85-L or YEpPRT1-His-TIF34-TIF35-W/Yep3TIF32-nip_Box12-SPW-L, respectively. The resulting double transformants were selected on SC-LEU-TRP but +URA to minimize the number of revertants generated during this procedure for unknown reasons. The resident

URA3-based YEpNIP1-His-U plasmid carrying was contra-selected against on SC plates containing 5-FOA.

To produce PBH54 and PBH55 overexpressing all eIF3 subunits, PBH44 (*prb1Δ pep4Δ prt1Δ* YEpPRT1-U) was first subjected to double transformation with YEpprt1-rnp1-His-TIF34-TIF35-W/YEpTIF32-NIP1-L or with YEpprt1-1-His-TIF34-TIF35-W / YEpTIF32-NIP1-L, respectively. The resulting double transformants were selected on SC-LEU-TRP but +URA to minimize the number of revertants. The resident *URA3*-based YEpPRT1-U plasmid carrying was contra-selected against on SC plates containing 5-FOA.

To produce PBH51 and PBH143 overexpressing all eIF3 subunits, WLCY12 (*prb1Δ pep4Δ tif32Δ* YCp*TIF32*-His-U) was first subjected to double transformation with YEpPRT1-His-TIF34-TIF35-W/YEptif32-Δ8-NIP1-L or YEpPRT1-His-TIF34-TIF35-W/Yep3tif32_BOX37-NIP-L, respectively. The resulting double transformants were selected on SC-LEU-TRP but +URA to minimize the number of revertants. The resident *URA3*-based YCp*TIF32*-His-U plasmid carrying was contra-selected against on SC plates containing 5-FOA.

To produce PBH71 and PBH73 overexpressing all eIF3 subunits, PBH57 (*prb1Δ pep4Δ tif34Δ* YEp-TIF34) was first subjected to double transformation with YEpPRT1-His-tif34_DDKK-TIF35-W/YEpTIF32-NIP1-L or with YEpPRT1-His-tif34_Q258R-TIF35-W/YEpTIF32-NIP1-L, respectively. The resulting double transformants were selected on SC-LEU-TRP but +URA to minimize the number of revertants. The resident *URA3*-based YEp-TIF34 plasmid carrying was contra-selected against on SC plates containing 5-FOA.

To produce PBH76 overexpressing all eIF3 subunits, PBH42 (*prb1Δ pep4Δ tif35Δ* YEp-TIF35) was first subjected to double transformation with YEpPRT1-His-TIF34-tif35_KLF-W/YEpTIF32-NIP1-L. The resulting double transformants were selected on SC-LEU-TRP but +URA to minimize the number of revertants. The resident *URA3*-based YEp-TIF35 plasmid carrying was contra-selected against on SC plates containing 5-FOA.

To create strains WLCY11 and WLCY12, protease-deficient yeast strains BJ5464 (MATα *ura3-52 trp1 leu2-Δ1 his3-Δ200 pep4::HIS3 prb1-Δ1.6R can1 GAL*$^+$) and BJ5465 (*MATa ura3-52 trp1 leu2- Δ1 his3-Δ200 pep4::HIS3 prb1-Δ1.6 can1 GAL*$^+$) were each transformed with single-copy (sc) plasmid p3908/YCpTIF32-His-U (*TIF32 URA3*), respectively, and then with a PCR fragment containing the *tif32Δ::KanMX4* allele amplified from the appropriate deletion mutant from the *Saccharomyces* Genome Deletion Project (***Giaever et al., 2002***), purchased from Research Genetics, selecting for resistance to G418.

WLCY12 was transformed with high-copy (hc) plasmid p3127/yEp-PRT1His-TIF34HA-TIF35FL-Leu (*PRT1-His TIF34-HA TIF35-FLAG LEU2*) to create strain WLCY13.

To create strains WLCY14 to WLCY17, WLCY11 was transformed with pWCB23, pWCB24, pWCB25, and pWCB26, respectively, and the resident *TIF32/NIP1/URA3* plasmid was evicted on medium containing 5-fluoro-orotic acid (5-FOA).

To generate yeast strains WLCY18 to WLCY21 for over-expressing eIF3 subunits, haploid strains WLCY14 to WLCY17 were mated to WLCY13, selecting for diploids on SC-LWU plates, and the resident *TIF32/NIP1/URA3* plasmid was evicted using 5-FOA.

Plasmid constructions

A list of all the plasmids and PCR primers used throughout this study can be found in ***Appendix 1—tables 2*** and ***3***, respectively.

To insert the coding sequences for the 8xHis tag into the overexpressing vector YEpPRT1-TIF34-TIF35-U, the fusion PCR was performed using the following pairs of primers PRT1-SpeI – PRT1-8xHis-PstI-R and PRT1-8xHis-F – PRT1-SphI-R, with YEpPRT1-TIF34-TIF35-U as a template. The PCR products thus obtained were used in a 1:1 ratio as templates for a third PCR amplification with primers PRT1-SpeI and PRT1-SphI-R. The resulting PCR product was

digested with *Spe*I-*Sph*I and inserted into *Spe*I-*Sph*I-digested YEpPRT1-TIF34-TIF35-U producing YEpPRT1-His-TIF34-TIF35-U.

To produce YEpPRT1-His-TIF34-TIF35-W, *URA3* was replaced by *TRP1* by cutting YEpPRT1-His-TIF34-TIF35-U with *Ahd*I-*Sac*I and replacing the ~4 kb fragment with the ~3.7 kb long *Ahd*I-*Sac*I-digested fragment from YEp112.

YEpTIF32-NIP1-L was generated by PCR using primers MJRNIP1Sal-Xba and NIP1-noHis-BamHI-R, and YEpTIF32-NIP1-His-L as a template. The resulting PCR product was digested with *Xba*I-*Bam*HI and inserted into *Xba*I-*Bam*HI cleaved YEpTIF32-NIP1-His-L to produce YEpTIF32-NIP1-L.

YEpTIF32-nip1-Δ60-L was generated by PCR using primers MJRNIP1Sal-Xba and PBNIPD60-BamHI-R, and YEpTIF32-NIP1-L as a template. The resulting PCR product was digested with *Xba*I-*Bam*HI and inserted into *Xba*I-*Bam*HI cleaved YEpTIF32-NIP1-L.

YEpprt1-1-His-TIF34-TIF35-W was generated by PCR using primers PRT1-SpeI and PRT1-8xHis-PstI-R, and pLPY202 as a template. The resulting PCR product was digested with *Spe*I-*Pst*I and inserted into *Spe*I-*Pst*I cleaved YEpPRT1-His-TIF34-TIF35-W.

To produce YEpprt1-rnp1-His-TIF34-TIF35-W, ~ 2.3 kb fragment digested from p4473 with *Spe*I-*Ahd*I was inserted into *Spe*I-*Ahd*I cleaved YEpPRT1-His-TIF34-TIF35-W.

To produce YEptif32-Δ8-NIP1-L, ~ 3.2 kb fragment digested from YEptif32-Δ8-NIP1-His-L with *Msc*I-*Pst*I was inserted into *Msc*I-*Pst*I cleaved YEpTIF32-NIP1-L

To produce Yep3tif32_BOX37-NIP-L, fragment digested from YCp-a/tif32-Box37-H with *Msc*I-*Bsg*I was inserted into *Msc*I-*Bsg*I cleaved YEpTIF32-NIP1-L.

To produce Yep3TIF32-nip_GAP85-L, fragment digested from YCpNIP1-GAP85 with *Sca*I-*Xba*I was inserted into *Sca*I-*Xba*I cleaved YEpTIF32-NIP1-L.

To produce YEp3TIF32-nip_Box12-SPW-L, fragment digested from YCpNIP1-Box12-SPW with *Sca*I-*Xba*I was inserted into *Sca*I-*Xba*I cleaved YEpTIF32-NIP1-L.

YEpPRT1-His-tif34_Q258R-TIF35-W was generated by PCR using primers PBTIF34SacI and TIF34-SmaI-R, and YCpL-i/tif34-HA-3 as a template. The resulting PCR product was digested with *Sma*I-*Sac*I and inserted into *Sma*I-*Sac*I cleaved YEpPRT1-His-TIF34-TIF35-W.

YEpPRT1-His-tif34_DDKK-TIF35-W was generated by PCR using primers PBTIF34SacI and TIF34-SmaI-R, and YCp-i/TIF34-D207K-D224K-HA as a template. The resulting PCR product was digested with *Sma*I-*Sac*I and inserted into *Sma*I-*Sac*I cleaved YEpPRT1-His-TIF34-TIF35-W.

YEpPRT1-His-TIF34-tif35_KLF-W was generated by PCR using primers TIF35-SphI and TIF35-SmaI-R, and YCp22-g/TIF35-KLF as a template. The resulting PCR product was digested with *Sma*I-*Sph*I and inserted into *Sma*I-*Sph*I cleaved YEpPRT1-His-TIF34-TIF35-W.

YCpAH-MET-PRT1-W was generated by PCR using primers AH-PRT1-SalI and AH-PRT1-HindIII-R, and pGAD-PRT1 as a template. The resulting PCR product was digested with *Sal*I-*Bam*HI and inserted into *Sal*I-*Bam*HI cleaved YCplac22MET-W.

To produce YEp111-MET-TIF35-L, fragment containing *TIF35* digested from pGAD-TIF35 with *Bam*HI-*Pst*I and fragment containing MET3 promotor digested from YCpLV06 with *Bam*HI-*Eco*RI were inserted into *Pst*I-*Eco*RI cleaved YCplac111.

YEp111-MET-TIF34-L was generated by PCR using primers AH-PRT1-SalI and AH-PRT1-HindIII-R, and pGAD-TIF34 as a template. The resulting PCR product was digested with *Bam*HI-*Pst*I and inserted into *Bam*HI-*Pst*I cleaved YEp111-MET-TIF35-L.

YEpPRT1-U was created by inserting the *Hin*dIII-*Pst*I digested PCR product obtained with primers LVPRT1-5' and LVPRT1-3'R using genomic DNA obtained from yeast strain BY4741 as template into *Hin*dIII-*Pst*I digested YEplac195.

YEpPRT1-TIF35-U was created by inserting the *Sph*I-*Sal*I digested PCR product obtained with primers LVTIF35-5′ and LVTIF35-3′R using genomic DNA obtained from yeast strain BY4741 as template into *Sph*I-*Sal*I digested YEpPRT1-U.

YEpPRT1-TIF34-TIF35-U was created by inserting the *Sma*I-*Sac*I digested PCR product obtained with primers LVTIF34-5′ and LVTIF34-3′R using genomic DNA obtained from yeast strain BY4741 as template into *Sma*I-*Sac*I digested YEpPRT1-TIF35-U.

To produce YEpTIF32-NIP1-His-L, 4.7kbp-fragment containing *TIF32* digested from p3131 with *Sac*I-*Pst*I was inserted into *Sac*I-*Pst*I cleaved YEpNIP1-His-L.

To produce YEptif32-Δ8-NIP1-His-L, fragment digested from pRSTIF32-Δ8-His with *Msc*I-*Pst*I was inserted into *Msc*I-*Pst*I cleaved YEpTIF32-NIP1-His-L.

pWCB27, pWCB28, pWCB29 were made by inserting the *Pst*I-*Msc*I fragments from pWLCB01, p4577, and pRS-a/tif32-box6-His-L, respectively, into p3131 digested with *Pst*I and *Msc*I. Because *Pst*I cuts in the middle of *tif32-box6*, intact ORF DNA was obtained by partial digestion of pRS-a/tif32-box6-His-L.

pWCB23, pWCB24, pWCB25, and pWCB26, containing *TRP1*, were generated from p3131, pWCB27, pWCB28, pWCB29 by using the marker swap plasmid pUT11.

Appendix 1—table 1. Yeast strains used in this study.

Strain	Genotype	Source or reference
BY4741	*MATa his3Δ0 leu2Δ0 met15Δ0 ura3Δ0*	(**Brachmann et al., 1998**)
BJ5465	*MATa ura3-52 trp1 leu2- Δ1 his3-Δ200 pep4::HIS3 prb1-Δ1.6 can1 GAL*$^+$	Elizabeth Jones
WLCY12	*MATa ura3-52 trp1 leu2-Δ1 his3-Δ200 pep4::HIS3 prb1-Δ1.6 can1 GAL*$^+$ *tif32Δ::kanMX4* p3908 sc[*TIF32, NIP1, URA3*]	This study
PBH42	*MATa ura3-52 trp1 leu2-Δ1 his3-Δ200 pep4::HIS3 prb1-Δ1.6R can1 TIF35-del GAL+* (YEp-TIF35)	This study
PBH44	*MATa ura3-52 trp1 leu2-Δ1 his3-Δ200 pep4::HIS3 prb1-Δ1.6R can1 prt1-Δ GAL+* (YEpPRT1-U)	This study
PBH51	*MATa ura3-52 trp1 leu2-Δ1 his3-Δ200 pep4::HIS3 prb1-Δ1.6R can1 GAL+ tif32Δ::KanMX4* (YEpPRT1-His-TIF34-TIF35-W, YEptif32-Δ8-NIP1-L)	This study
PBH143	*MATa ura3-52 trp1 leu2-Δ1 his3-Δ200 pep4::HIS3 prb1-Δ1.6R can1 GAL+ tif32Δ::KanMX4* (YEpPRT1-His-TIF34-TIF35-W, Yep3tif32_BOX37-NIP-L)	This study
PBH54	*MATa ura3-52 trp1 leu2-Δ1 his3-Δ200 pep4::HIS3 prb1-Δ1.6R can1 prt1-Δ GAL+* (YEpprt1-rnp1-His-TIF34-TIF35-W, YEpTIF32-NIP1-L)	This study
PBH55	*MATa ura3-52 trp1 leu2-Δ1 his3-Δ200 pep4::HIS3 prb1-Δ1.6R can1 prt1-Δ GAL+* (YEpprt1-1-His-TIF34-TIF35-W, YEpTIF32-NIP1-L)	This study
PBH56	*MATa ura3-52 trp1 leu2-Δ1 his3-Δ200 pep4::HIS3 prb1-Δ1.6R can1 nip1-Δ GAL+* (YEpNIP1-His-U)	This study
PBH57	*MATa ura3-52 trp1 leu2-Δ1 his3-Δ200 pep4::HIS3 prb1-Δ1.6R can1 tif34-Δ GAL+* (YEp-TIF34)	This study
PBH65	*MATa ura3-52 trp1 leu2-Δ1 his3-Δ200 pep4::HIS3 prb1-Δ1.6R can1 nip1-Δ GAL+* (YEpPRT1-His-TIF34-TIF35-W, YEpTIF32-nip1-Δ60-L)	This study
PBH66	*MATa ura3-52 trp1 leu2-Δ1 his3-Δ200 pep4::HIS3 prb1-Δ1.6R can1 nip1-Δ GAL+* (YEpPRT1-His-TIF34-TIF35-W, Yep3TIF32-nip_GAP85-L)	This study
PBH67	*MATa ura3-52 trp1 leu2-Δ1 his3-Δ200 pep4::HIS3 prb1-Δ1.6R can1 nip1-Δ GAL+* (YEpPRT1-His-TIF34-TIF35-W, Yep3TIF32-nip_Box12-SPW-L)	This study
PBH71	*MATa ura3-52 trp1 leu2-Δ1 his3-Δ200 pep4::HIS3 prb1-Δ1.6R can1 tif34-Δ GAL+* (YEpPRT1-His-tif34_DDKK-TIF35-W, YEpTIF32-NIP1-L)	This study
PBH73	*MATa ura3-52 trp1 leu2-Δ1 his3-Δ200 pep4::HIS3 prb1-Δ1.6R can1 tif34-Δ GAL+* (YEpPRT1-His-tif34_Q258R-TIF35-W, YEpTIF32-NIP1-L)	This study

Appendix 1—table 1 continued on next page

Appendix 1—table 1 continued

Strain	Genotype	Source or reference
PBH76	MATa ura3-52 trp1 leu2-Δ1 his3-Δ200 pep4::HIS3 prb1-Δ1.6R can1 TIF35-Δ GAL+ (YEpPRT1-His-TIF34-tif35_KLF-W, YEpTIF32-NIP1-L)	This study
WLCY11	*MATα ura3-52 trp1 leu2-Δ1 his3-Δ200 pep4::HIS3 prb1-Δ1.6R can1 GAL$^+$ tif32Δ::kanMX4* p3908 sc[*TIF32, NIP1, URA3*]	This study
WLCY13	*MATa ura3-52 trp1 leu2-Δ1 his3-Δ200 pep4::HIS3 prb1-Δ1.6 can1 GAL$^+$ tif32Δ::kanMX4* p3908 sc[*TIF32, NIP1, URA3*] p3127 hc[*PRT1-His, TIF34-HA, TIF35-FLAG, LEU2*]	This study
WLCY14	*MATα ura3-52 trp1 leu2-Δ1 his3-Δ200 pep4::HIS3 prb1-Δ1.6R can1 GAL$^+$ tif32Δ::kanMX4* p5237 hc[*TIF32, NIP1, TRP1*]	This study
WLCY15	*MATα ura3-52 trp1 leu2-Δ1 his3-Δ200 pep4::HIS3 prb1-Δ1.6R can1 GAL$^+$ tif32Δ::kanMX4* p5238 hc[*tif32-H725P, NIP1, TRP1*]	This study
WLCY16	*MATα ura3-52 trp1 leu2-Δ1 his3-Δ200 pep4::HIS3 prb1-Δ1.6R can1 GAL$^+$ tif32Δ::kanMX4* p5239 hc[*tif32-R731I, NIP1, TRP1*]	This study
WLCY17	*MATα ura3-52 trp1 leu2-Δ1 his3-Δ200 pep4::HIS3 prb1-Δ1.6R can1 GAL$^+$ tif32Δ::kanMX4* p5240 hc[*tif32-box6, NIP1, TRP1*]	This study
WLCY18	*MATa/MATα ura3-52/ura3-52 trp1/trp1 leu2-Δ1/leu2-Δ1 his3-Δ200/his3-Δ200 pep4::HIS3/pep4::HIS3 prb1-Δ1.6R/prb1-Δ1.6R can1/can1 GAL$^+$/GAL$^+$ tif32Δ::kanMX4/tif32Δ::kanMX* p5237 hc[*TIF32, NIP1, TRP1*] p3127 hc[*PRT1-His, TIF34-HA, TIF35-FLAG, LEU2*]	This study
WLCY19	*MATa/MATα ura3-52/ura3-52 trp1/trp1 leu2-Δ1/leu2-Δ1 his3-Δ200/his3-Δ200 pep4::HIS3/pep4::HIS3 prb1-Δ1.6R/prb1-Δ1.6R can1/can1 GAL$^+$/GAL$^+$ tif32Δ::kanMX4/tif32Δ::kanMX* p5238 hc[*tif32-H725P, NIP1, TRP1*] p3127 hc[*PRT1-His, TIF34-HA, TIF35-FLAG, LEU2*]	This study
WLCY20	*MATa/MATα ura3-52/ura3-52 trp1/trp1 leu2-Δ1/leu2-Δ1 his3-Δ200/his3-Δ200 pep4::HIS3/pep4::HIS3 prb1-Δ1.6R/prb1-Δ1.6R can1/can1 GAL$^+$/GAL$^+$ tif32Δ::kanMX4/tif32Δ::kanMX* p5239 hc[*tif32-R731I, NIP1, TRP1*] p3127 hc[*PRT1-His, TIF34-HA, TIF35-FLAG, LEU2*]	This study
WLCY21	*MATa/MATα ura3-52/ura3-52 trp1/trp1 leu2-Δ1/leu2-Δ1 his3-Δ200/his3-Δ200 pep4::HIS3/pep4::HIS3 prb1-Δ1.6R/prb1-Δ1.6R can1/can1 GAL$^+$/GAL$^+$ tif32Δ::kanMX4/tif32Δ::kanMX* p5240 hc[*tif32-box6, NIP1, TRP1*] p3127 hc[*PRT1-His, TIF34-HA, TIF35-FLAG, LEU2*]	This study

DOI: 10.7554/eLife.20934.023

Appendix 1—table 2. Plasmids used in this study. High-copy, low-copy, and single-copy plasmids are designated hc, lc. and sc, respectively.

Plasmid	Description	Source of reference
pLV10	hc vector containing *nip1Δ::hisG::URA3::hisG* disruption cassette	(**Valasek et al., 2004**)
p4473 (pRS315-prt1-rnp1-His)	lc *LEU2* vector containing *prt1-rnp1-His*	(**Nielsen et al., 2006**)
pTZ-tif34Δ	hc vector containing *tif34Δ::hisG::URA3::hisG* disruption cassette	(**Asano et al., 1998**)
B3289	hc vector containing *prt1Δ::hisG::URA3::hisG* disruption cassette	(**Nielsen et al., 2004**)
B444	hc vector containing *tif35Δ::hisG::URA3::hisG* disruption cassette	(**Cuchalova et al., 2010**)
YCpMJ-MET-NIP1-W	sc *TRP1* vector containing *NIP1* under *MET3* promotor	(**Karásková et al., 2012**)
YCpAH-MET-PRT1-W	sc *TRP1* vector containing *PRT1* under *MET3* promotor	This study
pGAD-PRT1	*PRT1* ORF cloned into pGAD424	(**Asano et al., 1998**)
YCplac22MET-W	sc cloning vector with conditional *MET3* promoter, *TRP1* plasmid from YCplac22	K. Nasmyth

Appendix 1—table 2 continued on next page

Appendix 1—table 2 continued

Plasmid	Description	Source of reference
pLPY202	lc *URA3* vector containing *prt1-1*-His	(**Phan et al., 2001**)
YEp112	hc *TRP1* vector	(**Gietz and Sugino, 1988**)
YEp111-MET-TIF34-L	hc *LEU2* vector containing *TIF34* under *MET3* promotor	This study
pGAD-TIF34	*TIF34* ORF cloned into pGAD424	(**Asano et al., 1998**)
YCpLV06	sc *LEU2* vector containing *TIF32* under *MET3* promotor	(**Kovarik et al., 1998**)
YCplac111	sc *LEU2* vector	(**Gietz and Sugino, 1988**)
pGAD-TIF35	*TIF35* ORF cloned into pGAD424	(**Asano et al., 1998**)
YEp111-MET-TIF35-L	hc *LEU2* vector containing *TIF35* under *MET3* promotor	This study
YEpNIP1-His-U	hc *URA3* vector containing *NIP1-His*	(**Valášek et al., 2002**)
YEpprt1-1-His-TIF34-TIF35-W	hc *TRP1* vector containing *prt1-1-His*, *TIF34* and *TIF35*	This study
YEpPRT1-His-TIF34-TIF35-W	hc *TRP1* vector containing *PRT1-His*, *TIF34* and *TIF35*	This study
YEpprt1-rnp1-His-TIF34-TIF35-W	hc TRP1 vector containing *prt1-rnp1-His*, *TIF34* and *TIF35*	This study
YEpPRT1-His-TIF34-TIF35-U	hc *URA3* vector containing *PRT1-His*, *TIF34* and *TIF35*	This study
YEpPRT1-U	hc *URA3* vector containing *PRT1*	This study
YEplac195	hc *URA3* vector	(**Gietz and Sugino, 1988**)
YEpPRT1-TIF35-U	hc *URA3* vector containing *PRT1* and *TIF35*	This study
YEpPRT1-TIF34-TIF35-U	hc *URA3* vector containing *PRT1*, *TIF34* and *TIF35*	This study
YEpTIF32-NIP1-L	hc *LEU2* vector containing *TIF32* and *NIP1*	This study
YEpTIF32-NIP1-His-L	hc *LEU2* vector containing *TIF32* and *NIP1-His*	This study
YEpNIP1-His-L	hc *LEU2* vector containing *NIP1-His*	(**Valášek et al., 2002**)
YEpTIF32-nip1-Δ60-L	hc *LEU2* vector containing *TIF32* and *NIP1* truncated by 60 amino acid residues in its CTD	This study
YEptif32-Δ8-NIP1-His-L	hc *LEU2* vector containing *TIF32* with the deletion of first 200aa and *NIP1-His*	This study
pRSTIF32-Δ8-His	lc *TIF32-Δ8-His*[200–964], *LEU2* plasmid from pRS315	(**Valášek et al., 2002**)
YEptif32-Δ8-NIP1-L	hc *LEU2* vector containing *TIF32* truncated by 200 amino acid residues in its NTD and *NIP1*	This study
YEp-TIF34	hc *URA3* vector containing *TIF34*	(**Asano et al., 1998**)
YEp-TIF35	hc *URA3* vector containing *TIF35*	(**Asano et al., 1998**)
Yep3tif32_BOX37-NIP-L	hc *LEU2* vector containing *TIF32* with ten alanine substitution in its NTD and *NIP1*	This study
YCp-a/tif32-Box37-H	sc *tif32-Box37-His* in *LEU2* plasmid, from YCplac111	(**Khoshnevis et al., 2014**)
YEp3TIF32-nip_Box12-SPW-L	hc *LEU2* vector containing *TIF32* and *NIP1* containing K113S/K116P/K118W substitutions in Box12	This study
YCpNIP1-Box12-SPW	sc *NIP1-His* containing K113S/K116P/K118W substitutions in Box12; *LEU2* plasmid from YCplac111	(**Karásková et al., 2012**)
Yep3TIF32-nip_GAP85-L	hc *LEU2* vector containing *TIF32* and *NIP1* containing deletion of 85 residues (Val^{60}- Asn144)	This study

Appendix 1—table 2 continued on next page

Appendix 1—table 2 continued

Plasmid	Description	Source of reference
YCpNIP1-GAP85	sc *NIP1-His* containing deletion of 85 residues (Val^{60}-Asn^{144}); *LEU2* plasmid from YCplac111	{Karaskova:2012ce}
YEpPRT1-His-tif34_Q258R-TIF35-W	hc *TRP1* vector containing *PRT1-His*, *tif34-Q258R* and *TIF35*	This study
YCpL-i/tif34-HA-3	sc *tif34-HA-Q258R* in *LEU2* plasmid from YCplac111	(**Cuchalova et al., 2010**)
YEpPRT1-His-tif34_DDKK-TIF35-W	hc *TRP1* vector containing *PRT1-His*, *TIF34* containing D207K and D224K mutations and *TIF35*	This study
YCp-i/TIF34-D207K-D224K-HA	sc *TIF34-HA* containing D207K and D224K mutations in *LEU2* plasmid from YCplac111	(**Herrmannová et al., 2012**)
YEpPRT1-His-TIF34-tif35_KLF-W	hc TRP1 vector containing *PRT1-His*, *TIF34* and *tif35-KLF*	This study
YCp22-g/TIF35-KLF	sc *TIF35-KLF-His* in*TRP1* plasmid from YCplac22	(**Cuchalova et al., 2010**)
pWCB27	hc *NIP1*, *tif32-H725P*, *URA3* plasmid, from YEplac195	This study
pWCB28	hc *NIP1*, *tif32-R731I*, *URA3* plasmid, from YEplac195	This study
pWCB29	hc *NIP1*, *tif32-box6*, *URA3* plasmid, from YEplac195	This study
pWLCB01	*tif32-H725P-His* in lc *LEU2* plasmid, from pRS315	(**Chiu et al., 2010**)
p4577 (pRS-a/tif32-R731I-His-L)	*tif32-R731I-His* in lc *LEU2* plasmid, from pRS315	(**Chiu et al., 2010**)
pRS-a/tif32-box6-His-L	*tif32-box6-His* in lc *LEU2* plasmid, from pRS315	(**Chiu et al., 2010**)
p3131 (pLPY-NIP1-TIF32)	hc *NIP1*, *TIF32*, *URA3* plasmid, from YEplac195	(**Phan et al., 2001**)
p3908 (YCp-a/TIF32-His-U)	sc *TIF32-His URA3* plasmid	(**Valášek et al., 2003**)
pWCB23	hc *NIP1*, *TIF32*, *TRP1* plasmid, from YEplac195	This study
pWCB24	hc *NIP1*, *tif32-H725P*, *TRP1* plasmid, from YEplac195	This study
pWCB25	hc *NIP1*, *tif32-R731I*, *TRP1* plasmid, from YEplac195	This study
pWCB26	hc *NIP1*, *tif32-box6*, *TRP1* plasmid, from YEplac195	This study
pUT11	*URA3* to *TRP1* marker swap plasmid	(**Cross, 1997**)
p3127 (pLPY-PRT1His-TIF34HA-TIF35FL-Leu)	hc *PRT1-His*, *TIF34-HA*, *TIF35-FLAG*, *LEU2* plasmid from YEplac 181	(**Phan et al., 2001**)

DOI: 10.7554/eLife.20934.024

Appendix 1—table 3. Primers used in this study.

Primer name	Primer sequence (5´to 3´)
MJNIP1Sal-Xba	AGCAAAGAGTCAAGAAAGTTTCTA
NIP1-noHis-BamHI-R	TTATTGGATCCTCAACGACGATTTGATGGTGGGTTAAGACG
PBNIPD60-BamHI-R	CCCCGGATCCTCACACCTTATTTTCTGGAAGATC
PRT1-8xHis-F	ATTTCATGAACTTACGGGCTTGTATGTAAA
PRT1-8xHis-PstI-R	TTTACATACAAGCCCGTAAGTTCATGAAATCTGCAGTTAGTGGTGGT GGTGGTGGTGGTGGTGTTCGACCTTTTCCTTTGTTTCTTCCAAAAC
PRT1-SpeI	GACGTGAAGACTAGTGTGTTC
PRT1-SphI-R	TGCGTCTACTTGTGCATGCAT
PBTIF34SacI	AGTGAATTCGAGCTCCTTATTCAGCGG
TIF34-SmaI-R	TTATTCCCGGGTTAATTAGCTTCTTGCATGTGCTC
TIF35-SphI	AATAAGCATGCACAAGTAGACGCACCTAAAAG

Appendix 1—table 3 continued on next page

Appendix 1—table 3 continued

Primer name	Primer sequence (5′to 3′)
TIF35-SmaI-R	TTATTCCCGGGCTATTCCTTAACCTTAGGTTTGGA
AH-PRT1-SalI	ATATATGTCGACATGACTACCGAGACTTTCGAA
AH-PRT1-HindIII-R	GTCCAAAGCTTCTGAATAAGCCCT
OJ-TIF34	attcggatccatatgaaggctatcaaattaacaggt
OJ-TIF34-R	atctctgcagttaattagcttcttgcatgtgctctttt
LVPRT1-5′	aataaAAGCTTAGGGCGATCTGCTACAGGAAGCTA
LVPRT1-3′R	aataaCTGCAGGCATGCATACAAAGATAATAGAGCCTATT
LVTIF35-5′	aataaGCATGCACAAGTAGACGCACCTAAAAGTCC
LVTIF35-3′R	aataaGTCGACACATATTCACGACAGCCTCTGAGC
LVTIF34-5′	aataaGAGCTCAAActcgagGAGCTGATAAAACCCTACACTACGGTGTAA
LVTIF34-3′R	CGCCTATGCCCGGGAACTGCATAC

DOI: 10.7554/eLife.20934.025

In-depth analysis of *cis*-determinants that either promote or inhibit reinitiation on *GCN4* mRNA after translation of its four short uORFs

STANISLAVA GUNIŠOVÁ, PETRA BEZNOSKOVÁ, MAHABUB PASHA MOHAMMAD, VLADISLAVA VLČKOVÁ, and LEOŠ SHIVAYA VALÁŠEK

Laboratory of Regulation of Gene Expression, Institute of Microbiology AS CR, Prague 142 20, Czech Republic

ABSTRACT

Translational control in eukaryotes is exerted by many means, one of which involves a ribosome translating multiple cistrons per mRNA as in bacteria. It is called reinitiation (REI) and occurs on mRNAs where the main ORF is preceded by a short upstream uORF(s). Some uORFs support efficient REI on downstream cistrons, whereas some others do not. The mRNA of yeast transcriptional activator *GCN4* contains four uORFs of both types that together compose an intriguing regulatory mechanism of its expression responding to nutrients' availability and various stresses. Here we subjected all *GCN4* uORFs to a comprehensive analysis to identify all REI-promoting and inhibiting *cis*-determinants that contribute either autonomously or in synergy to the overall efficiency of REI on *GCN4*. We found that the 3′ sequences of uORFs 1–3 contain a conserved $AU_{1\text{-}2}A$/$UUAU_2$ motif that promotes REI in position-specific, autonomous fashion such as the REI-promoting elements occurring in 5′ sequences of uORF1 and uORF2. We also identified autonomous and transferable REI-inhibiting elements in the 3′ sequences of uORF2 and uORF3, immediately following their AU-rich motif. Furthermore, we analyzed contributions of coding triplets and terminating stop codon tetranucleotides of *GCN4* uORFs showing a negative correlation between the efficiency of reinitiation and efficiency of translation termination. Together we provide a complex overview of all *cis*-determinants of REI with their effects set in the context of the overall *GCN4* translational control.

Keywords: translational control; reinitiation; uORF; *cis*-regulation; *GCN4*

INTRODUCTION

Translational control of one of yeast's most influential stress-related transcription factors, GCN4, represents undoubtedly the best-studied model of eukaryotic translation reinitiation (REI) (Hinnebusch 2005; Gunišová and Valášek 2014). REI is a gene-specific regulatory mechanism exploiting the presence of short upstream uORFs in mRNA leaders (i.e., 5′ untranslated regions—5′ UTRs) of various genes. The molecular key to this potentially abundant regulation (Davuluri et al. 2000; Iacono et al. 2005; Calvo et al. 2009; Hood et al. 2009; Zhou et al. 2010) is the ability of some of these short uORFs (in yeast up to five codons in length [Vilela et al. 1998; Rajkowitsch et al. 2004; Szamecz et al. 2008], in plants up to 16 [von Arnim et al. 2014], and in mammals up to 30 codons [Kozak 2005]) to retain the 40S ribosomal subunit on the same mRNA molecule even after they have been translated and the large 60S subunit has been recycled by the ribosome recycling factors (for review, see Jackson et al. 2012; Valášek 2012). Such post-termination 40S subunits are then able to resume scanning downstream, and upon acquisition of the new ternary complex (TC), composed of Met-$tRNA_i^{Met}$ and eukaryotic initiation factor eIF2 in its GTP form, they are able to recognize the AUG start codon of the next ORF and reinitiate translation thereon.

Generally speaking, short uORFs in principle impose a functional barrier for sufficient expression of a downstream main ORF. This repressive effect of uORFs can be, however, alleviated under specific conditions, such as various types of stress, in order to boost expression of some regulatory uORF-containing mRNAs that help the cell to cope with sudden environmental changes. It has been shown that the efficiency of REI depends on four main factors: (i) time required for uORF translation, which is determined by the relative length of uORF and the translation elongation rate; (ii) its 5′ and 3′ flanking sequences, which contain specific *cis*-acting features

Corresponding authors: gunisova@biomed.cas.cz, valasekl@biomed.cas.cz

Article published online ahead of print. Article and publication date are at http://www.rnajournal.org/cgi/doi/10.1261/rna.055046.115.

© 2016 Gunišová et al. This article is distributed exclusively by the RNA Society for the first 12 months after the full-issue publication date (see http://rnajournal.cshlp.org/site/misc/terms.xhtml). After 12 months, it is available under a Creative Commons License (Attribution-NonCommercial 4.0 International), as described at http://creativecommons.org/licenses/by-nc/4.0/.

with poorly understood molecular roles; (iii) translation initiation factors (eIFs) involved in the primary initiation event such as the eIF3 and eIF4F complexes, which are believed to remain associated with the ribosome throughout the short elongation as well as termination and recycling phases; and (iv) its distance to the next open reading frame, which determines the likelihood of acquisition of the new TC by the post-termination 40S ribosome that has resumed scanning (Kozak 1987; Dever et al. 1992; Pöyry et al. 2004; Szamecz et al. 2008; Cuchalová et al. 2010; Roy et al. 2010; Munzarová et al. 2011).

The classical REI-dependent mRNA of *GCN4* containing a total of four short uORFs has been studied in great detail for several decades; it has been found to be very sensitive to the TC levels that are changing in response to different nutrient conditions and to rely mainly on the first REI-permissive uORF1 and the last REI-nonpermissive uORF4 (reviewed in Hinnebusch 2005 and recently revised in Gunišová and Valášek 2014). Briefly, the first of the four uORFs is efficiently translated under both nutritional replete and deplete conditions, and after its translation the post-termination 40S subunit remains attached to the mRNA and resumes scanning downstream for REI at the next AUG. In nonstressed cells, where the TC levels are high, nearly all of the rescanning ribosomes can rebind the TC before reaching one of the last two distant uORFs (uORFs 3 and 4), neither of which supports efficient REI. As a result, ribosomes terminating on one of these two uORFs undergo the full ribosomal recycling step, which prevents them from reaching and translating the main *GCN4* ORF (Supplemental Fig. S1).

Under starvation conditions, the GCN2 kinase phosphorylates eIF2, which suspends formation of new TCs in the cytoplasm. Consequently, post-termination 40S ribosomes traveling from the uORF1 stop codon downstream will require more time to rebind the TC to be able to recognize the next AUG start codon. This will allow a large proportion of them to bypass uORF3 and uORF4 and reacquire the TC downstream from uORF4 but still upstream of the *GCN4* start codon (Supplemental Fig. S1). Thus, whereas the global protein synthesis is significantly down-regulated under nutrient deplete conditions, protein expression of the GCN4 transcriptional activator is concurrently induced.

The second REI-permissive uORF, uORF2 with ~80%–90% of the uORF1 REI activity, occurs only 56-nt downstream from uORF1 and serves as a backup of uORF1 to capture all ribosomes that leaky scanned past the uORF1 AUG (Gunišová and Valášek 2014), especially during stress conditions that seem to increase the frequency of leaky scanning in general (Lee et al. 2009; Raveh-Amit et al. 2009; Palam et al. 2011; Sundaram and Grant 2014). This ensures that the maximum capacity of this intriguing regulatory system is met. Similarly, two consecutive uORFs with minimal or no REI-promoting potential occurring further downstream (uORF3 that allows approximately five times less efficient REI than the first two uORFs, but still approximately four times more efficient REI than REI-nonpermissive uORF4) also prevent "leakiness" of this system but during nutrient replete conditions (Gunišová and Valášek 2014). Hence the tightness of *GCN4* translational control is ensured by a fail-safe mechanism that effectively prevents or triggers *GCN4* expression under nutrient replete or deplete conditions, respectively.

The exceptionally high REI potential of uORF1 and uORF2 has been ascribed to (i) their 5′ sequences (Grant et al. 1995) containing several REI-promoting elements (RPEs) that together make up the so-called 5′ enhancer with a specific structural arrangement (Munzarová et al. 2011; Gunišová and Valášek 2014), (ii) the stimulatory role of N-terminal domain (NTD) of the a/TIF32 subunit of the eukaryotic initiation factor eIF3 (Szamecz et al. 2008) that sits near the 40S mRNA exit channel (Valášek et al. 2003; Kouba et al. 2012; Aylett et al. 2015), and, in the case of uORF1, also to (iii) the first 10 nt immediately following the uORF1 stop codon (Grant and Hinnebusch 1994), and (iv) the third coding triplet of uORF1 in combination with its 3′ UTR (Grant and Hinnebusch 1994).

With respect to known molecular functions of these features, some of the RPEs were shown to functionally interact with the a/TIF32-NTD, and this interaction, the exact nature of which still awaits determination, was implicated in stabilizing the post-termination 40S subunits on stop codons of both REI-permissive uORFs in order to facilitate the resumption of scanning downstream (Szamecz et al. 2008; Munzarová et al. 2011; Gunišová and Valášek 2014). The stretch of the first 10 nt past the uORF1 stop codon was owing to its relatively low GC content proposed to allow the 40S subunit to promptly resume scanning, in contrast to the corresponding GC-rich sequence of uORF4, because it would not permit strong base-pairing interactions with the 40S subunit (Grant and Hinnebusch 1994). However, we recently noted that the 3′ sequences of the other two *GCN4* uORFs (2 and 3) have a very similar AU content to uORF1, yet uORF3 permits only poor REI (Munzarová et al. 2011). Hence the idea that it is simply the high AU content of the uORF1 3′ sequence that makes it so robustly REI permissive does not seem to be so unequivocal anymore (Jackson et al. 2012).

With the recent outburst of new findings on the *GCN4* translation control that in some cases clarified and/or extended the earlier observations but in some others led to revised hypotheses, we wished to systematically analyze all potential *cis*-determinants that either promote or inhibit REI on *GCN4* after translation of its uORFs in one complex study. Based on this study we also postulate "reinitiation rules" that can be generalized for any short uORF in yeast (please see the Conclusion section).

RESULTS AND DISCUSSION

Proper functioning of the 3′ sequences immediately following stop codons of *GCN4* uORFs is not determined by their AU content

A considerable difference in the efficiency of resumption of scanning following translation of the REI-permissive

uORF1 vs. REI-nonpermissive uORF4 in the *GCN4* mRNA leader was found to be attributable to the distinct 3′ sequences following the termination codons of these two uORFs. Replacing the sequence of 25-nt downstream from the uORF1 stop codon with the corresponding nucleotides from uORF4 disabled the uORF1-promoted REI on *GCN4* by a great deal (Miller and Hinnebusch 1989). It was originally proposed that this difference is due to a varying AU content of these 3′ sequences, with uORF1 being more AU-rich (the AU content of 25 nt after uORF1 stop codon is 80%) than uORF4 (60%) (Fig. 1A; Grant and Hinnebusch 1994).

In our recent work, however, we noted that the 3′ sequences of the other two uORFs of *GCN4* are similarly AU-rich as the uORF1 3′ sequence by itself; the second REI-permissive uORF2 shows the highest AU content (88%), while the AU content of uORF3 that is only modestly REI-permissive is comparable to that of uORF1 (76%) (Fig. 1A; Munzarová et al. 2011; Gunišová and Valášek 2014). Therefore, if the degree of AU-richness is the sole factor determining the REI-promoting activity of the 3′ sequences in general, at least a part of the REI potential of uORF2 and probably the whole REI potential of uORF3 could be explained by employment of the REI-promoting 3′ sequences of these two uORFs.

To test this possibility, we substituted 25 nt immediately following stop codons of uORF2 and uORF3 with the corresponding sequence of REI-nonpermissive uORF4 in the same way as it was done previously for uORF1. In all our constructs, only the uORF under study was functional while the start codons of the other three uORFs were mutated out. Note that since the uORF4 start codon is separated from the uORF3 stop codon by only 13 nt, the 3′ sequence of the *uORF3-3333* construct contains the mutated out uORF4 start codon (Fig. 1A). This mutation, however, does not change the overall AU content of the uORF3 3′ sequence.

Also note that we divided the sequences constituting and flanking all four uORFs into four segments, A through D, for each uORF (Fig. 1B) according to Munzarová et al. (2011). In short, segment A is 166 bp in length (from position −181 to −16 relative to the uORF1-4 AUG start codons) and corresponds to the 5′ REI-promoting sequences of uORF1 (Szamecz et al. 2008; Munzarová et al. 2011); segment B designated previously as the linker is 15-bp long (−15 to −1); segment C contains coding triplets and the stop codon; and segment D encompasses 25 bp immediately following the stop codon that corresponds to the 3′ REI-promoting sequence of uORF1 (Miller and Hinnebusch 1989; Munzarová et al. 2011; Gunišová and Valášek 2014). Mutual replacements of these segments among all four uORFs that feature in the whole study are always indicated by the sequence of ABCD segments expressed as numbers 1–4, indicating which uORF each particular segment comes from: For example, a hypothetical *uORF1-1234* construct would correspond to segment A from uORF1 followed by B from uORF2, C from uORF3, and D from uORF4, all situated in the uORF1 position.

With respect to the aforementioned substitutions, replacing the 3′ sequence (segment D) of uORF1 with that of uORF4 (*uORF1-1114*) reduced its REI potential down to ∼31% (Fig. 1C), as reported before (Miller and Hinnebusch 1989). Replacing also the segment C along with D of uORF1 with those of uORF4 (*uORF1-1144*) further reduced its REI activity, almost to the basal level corresponding to the activity of REI-nonpermissive uORF4 (*uORF1-4444*), as also observed before (Fig. 1C; Miller and Hinnebusch 1989; Munzarová et al. 2011; Gunišová and Valášek 2014). This illustrates the magnitude of the 3′ sequence contribution to the REI potential of uORF1, as its loss leads to a remarkable impairment (∼69% drop in this experimental setup) of the uORF1 ability to allow resumption of scanning of post-termination ribosomes. Similar replacements of uORF2 and uORF3 in *uORF2-2224* and *uORF3-3334* did not decrease but actually increased REI activities of both uORFs (Fig. 1C). These findings indicate that (i) the REI potential of uORF2 and uORF3 does not depend on their AU-rich 3′ sequences, and thus (ii) the degree of AU content per se does not play the key role in rendering the 3′ sequences active in promoting REI. They also contradict our earlier suggestion that the GC-rich 3′ sequence of uORF4 functions as the REI inhibitor that can suppress the resumption of scanning from any REI-permissive uORF (Gunišová and Valášek 2014). The fact that the presence of the GC-rich segment D of uORF4 allows even more efficient REI on the middle two uORFs, mainly on uORF3, will be explained below.

The 3′ sequences of uORF1 and uORF2 operate autonomously in the position-specific manner

Since uORF1 seems to be the only uORF utilizing the 3′ sequence for its REI-promoting activity, we next asked whether the 3′ sequences of uORF2 and uORF3 with a similar AU content would also work for uORF1. Interestingly, only the presence of the uORF2 3′ sequence (*uORF1-1112*) was able to functionally replace the uORF1 3′ sequence (Fig. 1D). The 3′ sequence of uORF3 (*uORF1-1113*) decreased the uORF1-mediated REI activity by nearly the same margin as the 3′ sequence of uORF4 (*uORF1-1114*), which will also be explained below. The fact that uORF1 can also utilize the 3′ sequence of uORF2 suggested that its function could be position specific. To examine this, we first attempted to activate the REI enhancing potential of the uORF2 3′ sequence by placing the whole uORF2 ABCD block in the position of uORF1 (*uORF1-2222*). As a control, we replaced segment 2D with that of uORF4 in *uORF1-2224*. However, this replacement had nearly the same effect as when uORF2 occurred in its authentic position—its REI activity mildly increased but did not decrease (cf. Supplemental Figs. S1C, S2A), which further illustrates that uORF2 cannot utilize its 3′ sequence to increase its REI potential. Since comparison of ratios of reinitiation vs. initiation rates for uORF1 and uORF2 showed that uORF1 resumes scanning with

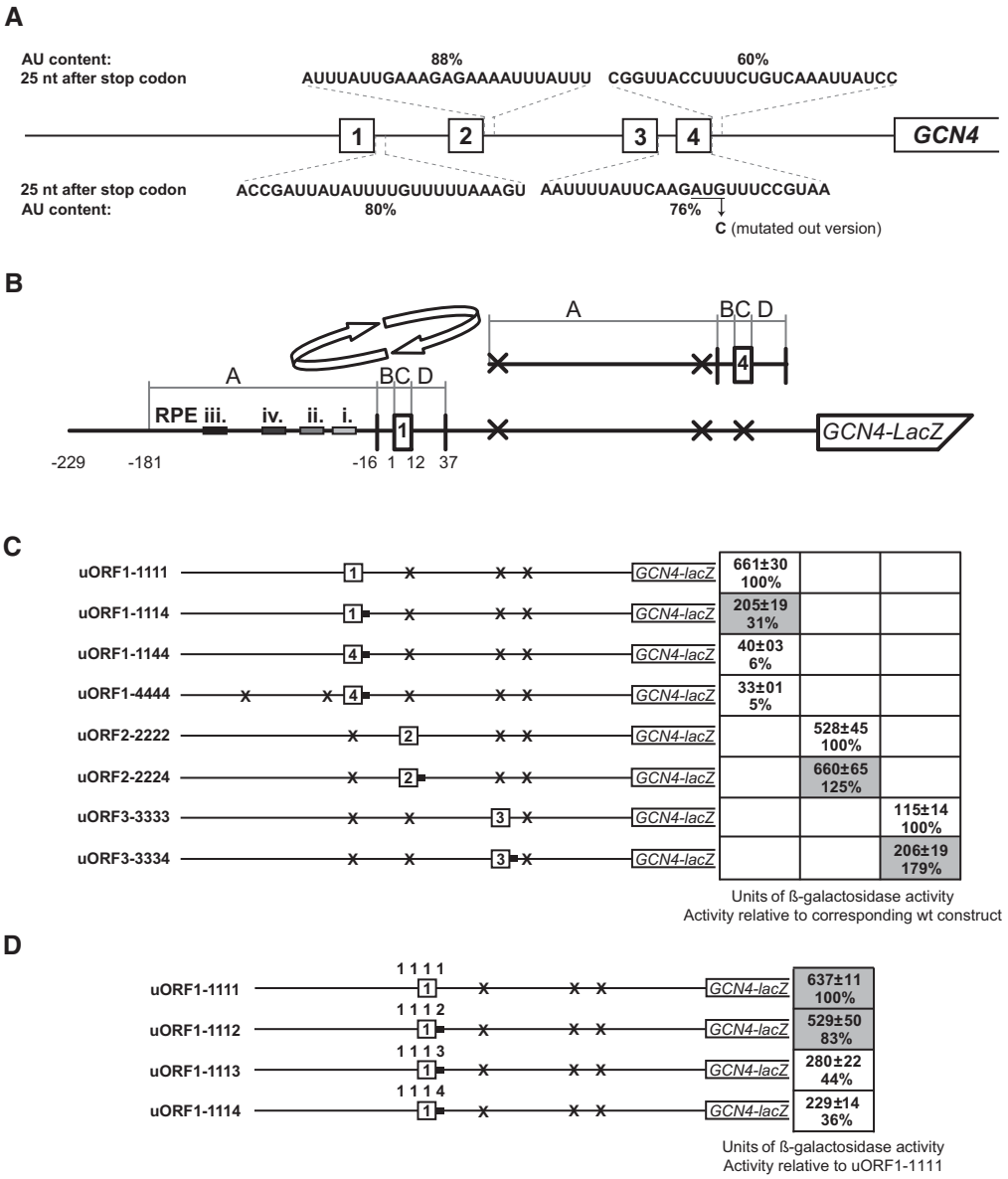

FIGURE 1. uORF1 is the only uORF utilizing its 3′ flanking sequence for its REI-promoting activity. (*A*) Schematic of the *GCN4* leader containing four short uORFs (1–4). The first 25 nt of 3′ flanking sequences (segments D) immediately following stop codon of each uORF are depicted together with the percentage of their AU content. In the uORF3 3′ sequence, the start codon of uORF4 is underlined and arrow indicates G to C substitution used to mutate it out (see text for further details). (*B*) Schematic showing the *GCN4-lacZ* construct containing solitary uORF1, the surrounding sequences of which were divided into four separate segments (A1–D1; see text for further details). Arrows indicate replacements of these segments with the corresponding segments (A4–D4) surrounding uORF4, shown to the *right* of the arrows. Crosses indicate positions of other uORFs in which start codons were mutated out. Gray bars indicate sequence positions of individual uORF1-specific RPEs. Replacements with the corresponding segments surrounding uORF2 and uORF3 that are not depicted were done in the analogous way; adapted from Munzarová et al. (2011). (*C*) Solitary uORFs from the *GCN4* mRNA leader in their authentic positions and their derivatives with their 3′ sequences replaced by the corresponding segment of uORF4 (indicated by the black bar) were introduced into the YSG2 strain. Additional replacements of indicated uORF1 segments by those of uORF4 were also prepared as a control. The resulting transformants were precultured in minimal media overnight, diluted to $OD_{600} \sim 0.35$, and grown for an additional 6 h; the β-galactosidase activities were measured in the WCEs and expressed in units of nmol of *o*-nitrophenyl-β-d-galactopyranoside hydrolyzed/min/mg of protein. The mean values and standard deviations obtained from at least three independent measurements with five independent transformants and activities of the respective constructs relative to their corresponding wt constructs are given in the table. Differences in β-galactosidase activities between *uORF2–2224* and its wt *uORF2-2222* were analyzed by Student's *t*-test and the calculated $P = 0.1335$. (*D*) The 3′ sequence of solitary uORF1 from the *GCN4* mRNA leader in its authentic position was replaced by corresponding segments of the other three uORFs and the resulting constructs were introduced into the YSG2 strain and analyzed as described in panel *C*. Differences in β-galactosidase activities between *uORF1-1112* and its wt *uORF1-1111* were analyzed by Student's *t*-test and the calculated $P = 0.0911$.

~14% higher efficiency than uORF2 (Supplemental Fig. S2B), we propose that it could be in fact the ability of uORF1 to utilize the 3′ sequence expressed in its higher efficiency of resumption of scanning that to a great deal lies behind the small but reproducible difference (from 10% to 20%) in the overall REI efficiency between both uORFs that we routinely observe (Gunišová and Valášek 2014).

Next we tested whether or not the 3′ sequence of uORF1, and as a proof of principle also that of uORF2, can operate from the position of uORF1 regardless of the nature of the preceding three segments. If yes, it would indicate (i) its autonomy and (ii) position specificity. To do that, we moved the whole uORF4 ABCD block into the position of uORF1 (*uORF1-4444*), and replaced segment D with the corresponding segments from the remaining three uORFs (*uORF1-4441*, *uORF1-4442*, and *uORF1-4443*) (Fig. 2A). As a control, we carried out the same D replacements (*uORF4-4441*, *uORF4-4442*, and *uORF4-4443*) also in the authentic position of uORF4 (*uORF4-4444*) (Fig. 2B). Remarkably, uORF1, and to a slightly smaller degree also uORF2 3′ sequences, did increase the REI potential of uORF4 (by approximately twofold), but only when situated in the position of uORF1. The 3′ sequence of uORF3, on the other hand, had the opposite effect on both setups, which is in accord with our findings shown in Figure 1C (see *uORF3-3333* vs. *uORF3-3334*), and we explain it below. Taken together, these results indicate that the REI-promoting 3′ sequence of uORF1, and analogously also that of uORF2, does function autonomously, at least to a certain degree, but its activity is position-restricted. To further support this conclusion, we carried out the D replacements of uORF3 in its authentic position (*uORF3-3333*) and showed that neither uORF1 nor uORF2 3′ sequences (*uORF3-3331* and *uORF3-3332*) had any stimulatory impact on REI allowed by this uORF. Predictably, the authentic 3′ sequence of uORF3 showed the weakest REI activity of all (Supplemental Fig. S3).

What could determine the position specificity for the REI-promoting action of the 3′ sequence of uORF1? In theory it

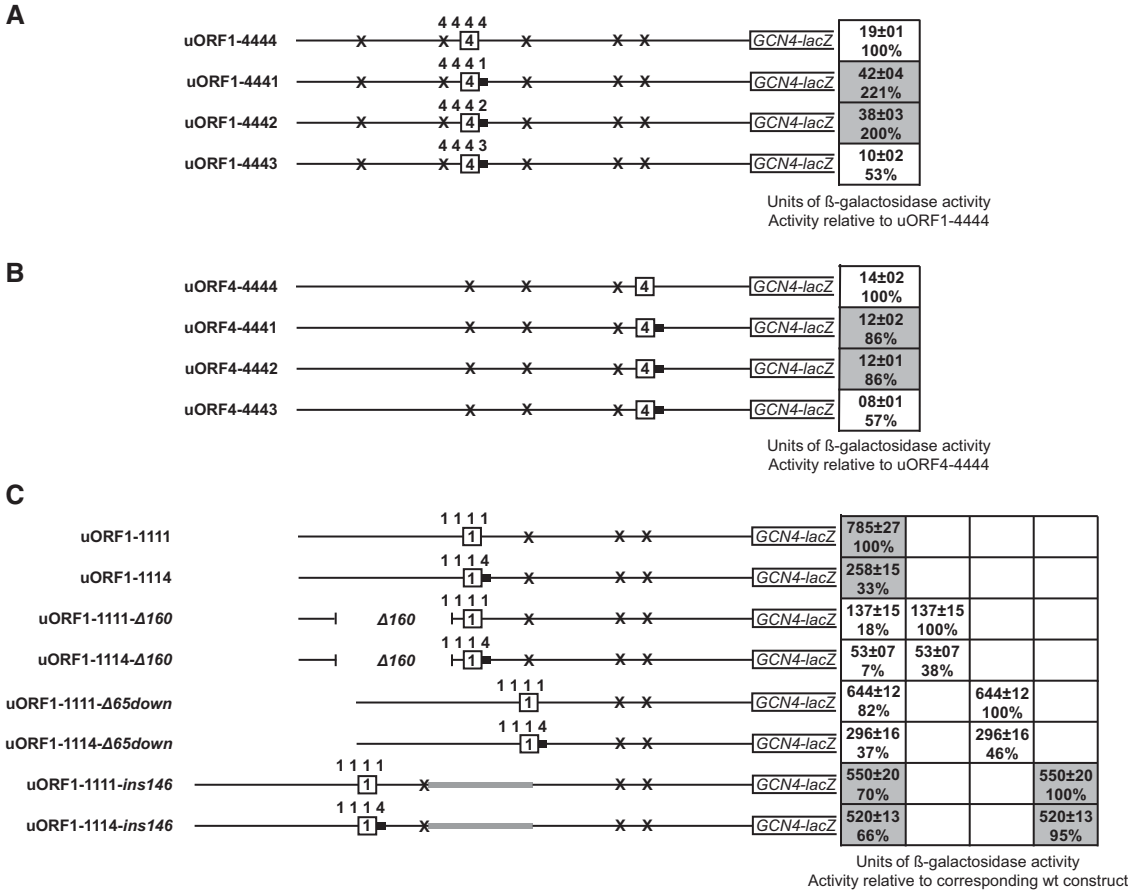

FIGURE 2. Function of the REI-promoting 3′ sequence is position specific. (*A*) The 3′ sequence of solitary uORF4 from the *GCN4* mRNA leader with its authentic flanking sequences (A4–D4) situated in the position of uORF1 was replaced by corresponding segments of the other three uORFs and analyzed as described in Figure 1C. (*B*) Same as in *A* except that the 3′ sequence substitutions were done in the authentic position of uORF4. (*C*) Solitary uORF1 or its derivative containing the 3′ sequence substitution for the corresponding segment of uORF4 situated it the authentic uORF1 position were modified as indicated and analyzed as described in Figure 1C. Differences in β-galactosidase activities between *uORF1-1111-Δ65down*, *uORF1-1111-ins146*, or *uORF1-1114-ins146* and their wt *uORF1-1111* were analyzed by Student's *t*-test and the calculated $P = 0.0014$, 0.0001, or 0.0001, respectively.

could simply be its distance either from the 5′ end of *GCN4* mRNA or from the *GCN4* main gene. To investigate this, we measured (i) the impact of shortening the distance between uORF1 start codon and the 5′ end, or (ii) shortening or (iii) prolonging the distance between the uORF1 3′ sequence and the *GCN4* start codon on the REI potential of wild-type uORF1 using the *1114* versions of all constructs designed for this purpose as a tool (Fig. 2C). We assumed that if any of our manipulations eliminate the REI-promoting activity of the 3′ sequence of uORF1, their replacement with the 3′ sequence of uORF4 would then show genetic epistasis; i.e., would not lead to any further decrease in the REI activity.

Shortening the distance from the 5′ end by the deletion of 160-nt upstream of uORF1 containing all four REI-promoting elements (RPEs) (*uORF1-1111-Δ160*) dramatically decreased the REI potential of uORF1, as expected (Szamecz et al. 2008), but had only marginal, if any, impact on the autonomous activity of the uORF1 3′ sequence (*uORF1-1114-Δ160*) (Fig. 2C, compare 100% vs. 33% and 100% vs. 38%). Hence the distance of the uORF1 3′ sequence from the 5′ end of *GCN4* mRNA does not seem to determine the position-specific phenomenon of the 3′ sequences.

Next we examined the potential importance of the distance of the uORF1 3′ sequence from the *GCN4* ORF. First we deleted 65 nt downstream from the uORF1 segment D, placing uORF1 directly into the uORF2 position (*uORF1-1111-Δ65down)*. This deletion decreased REI on *GCN4* by ∼18% compared to the wild-type *uORF1-1111* construct (Fig. 2C). It can be explained by two effects: (i) impaired function of the 3′ sequence of uORF1 due to its altered position; (ii) shortening the distance that the 40S ribosomes scanning downstream from uORF1 need to reacquire the new ternary complex (TC) in order to become REI-competent, as demonstrated before (Dever et al. 1992). Since the same deletion in the *uORF1-1114-Δ65down* construct reduced REI on *GCN4* to a smaller degree than in the wild-type *uORF1-1114* construct (Fig. 2C, compare 46% to 33%), we believe that the observed drop in the REI activity of *uORF1-1111-Δ65down* is the combination of both aforementioned effects.

In a complementary approach, we prolonged the distance of uORF1 from the *GCN4* start by insertion of 146 nt representing two copies of the previously identified segment S1 downstream from the 3′ sequence of uORF1 (Abastado et al. 1991) (*uORF1-1111-ins146*). Hypothetically, increasing the uORF1–*GCN4* distance should increase the REI on *GCN4*, as the scanning 40S ribosomes would gain even more time (thanks to a longer distance) to reacquire the TC on their way downstream from uORF1. Disruption of a prospective position-specific role of the uORF1 3′ sequence would counteract this effect, producing either no increase of the REI activity on *GCN4* or even a decrease. Replacement of the uORF1 3′ sequence with that of uORF4 should then be epistatic; and this is exactly what we observed (Fig. 2C). The double S1 insertion in the *uORF1-1111-ins146* construct reduced REI on *GCN4* by ∼30% and had virtually the same effect; i.e., the reduction by ∼34% was also seen with the *uORF1-1114-ins146* construct. These observations thus demonstrate that moving the uORF1 3′ sequence further away from the *GCN4* start codon completely abrogates its REI-promoting activity. Taken together, both shortening and lengthening approaches further support our theory that the action of the uORF1 3′ sequence is, within some limited range of tolerance, position-specific.

The question that still remains unanswered is how this feature operates at the molecular level. Taking into account our earlier suggestion that the action of the 3′ sequence of uORF1 is a prerequisite for the action of 5′-based RPEs of uORF1 (Munzarová et al. 2011), we propose the following two options. The RPEs are, in cooperation with eIF3, believed to stabilize the post-termination 40S subunit on the *GCN4* mRNA after the 60S subunit has been recycled in order to facilitate its resumption of scanning. If true, the 3′ sequence of uORF1 that during termination is buried in the mRNA binding channel could, for example, expedite the ribosomal recycling of the large subunit by stabilizing the post-termination 80S ribosomes at the stop codon. It was recently shown that post-termination 80S ribosomes are not stably anchored at the stop codon and can migrate in both directions to codons that are cognate to the P-site deacylated tRNA (Skabkin et al. 2013). Such instability may lead to an undesirable accumulation of nonrecycled aberrant ribosomal complexes in the vicinity of the stop codon, which would indeed dampen the efficiency of REI. With this role, however, it would be hard to reconcile the position specificity of the uORF1 3′ sequence; i.e., its functional requirement to be situated within a defined distance from the *GCN4* start codon.

This requirement brings us to the second option, as it could suggest that the uORF1 3′ sequence interacts with some downstream sequence and/or *trans*-acting factor bound to a downstream sequence. And since it is buried in the terminating 80S ribosome, as hinted above, this prospective interaction could not be formed before completion of the first recycling step involving the 60S subunit dissociation (Pisarev et al. 2007). The purpose of this contact could be to prevent the last recycling step; i.e., dissociation of mRNA from the 40S subunit. Only if this is ensured, the RPEs in co-operation with eIF3 could further strengthen this stabilization effect and enable resumption of scanning of post-termination 40S subunits downstream. Changing the position of the uORF1 3′ sequence with respect to the *GCN4* start site may prevent formation of this interaction, resulting in diminished REI efficiency of uORF1, which we observed.

The 3′ sequences of the first three uORFs contain the conserved, REI-promoting AU-rich motif and at the same time, in the case of uORFs 2 and 3, also inhibitory elements further downstream

The puzzling similarity of the AU-richness of the 3′ sequences of uORF1–3 combined with their differential effects on

GCN4 REI observed in Figure 1D prompted us to inspect the composition of the 3′ sequences of these three uORFs in greater detail. We revealed a potential AU-rich motif ($AU_{1\text{-}2}A/UUAU_2$) specifically occurring within the first 12 nt of segment D of only the first three uORFs (Fig. 3A). To examine whether this motif solely carries the REI-promoting activity of the 3′ sequences of uORFs 1 and 2, and perhaps even of uORF3, we replaced either the first 1–12 nt or the immediately following 13–25 nt of the uORF1 segment D with the corresponding sequences of the other three uORFs and measured the β-galactosidase activities of the resulting constructs. In the case of uORF2, we not only observed that its $AU_{1\text{-}2}A/UUAU_2$ motif-containing 1 through 12 nt sequence behaved as efficiently as the native uORF1 3′ sequence (~102% for *uORF1-1112*$^{1\text{-}12}$), but also that its 13 through 25 nt sequence (*uORF1-1112*$^{13\text{-}25}$) had a modest inhibitory effect on the REI activity of uORF1 (Fig. 3). In the case of uORF3, the first 12 nt containing the AU-rich motif showed only modestly decreased activity compared to the native uORF1 3′ sequence (~79% for *uORF1-1113*$^{1\text{-}12}$), whereas its 13 through 25 nt sequence (*uORF1-1113*$^{13\text{-}25}$) displayed a robust inhibitory effect. Strikingly, this inhibitory effect is dominant over the stimulatory effect of the AU-motif, which perfectly explains why replacing the entire segment D of uORF1 (Fig. 1D) or of uORF4 in the uORF1 position (Fig. 2A) with the same segment of uORF2 or uORF3 reduced the efficiency of REI by varying degree despite their similar AU content. These findings also suggest that the modest dominant inhibitory impact of 13–25 nt of uORF2 3′ sequence (further documented in Fig. 1C; Supplemental Fig. S2A) further contributes to the difference in the overall REI efficiency between uORF1 and uORF2.

Replacing the first 12 nt of the uORF1 segment D with the same uORF4 sequence (*uORF1-1114*$^{1\text{-}12}$) completely eliminated the stimulatory effect of the uORF1 3′ sequence, whereas the replacement of the following 13–25 nt (*uORF1-1114*$^{13\text{-}25}$) had no effect whatsoever (Fig. 3B), clearly suggesting that the 13 through 25 nt segment of uORF4 has no inhibitory effect. This observation explains why the D segment replacement of uORF2 and uORF3 with that of uORF4 increased their overall REI activity (Fig. 1C). Importantly, it was previously suggested that the first 10 (and not 12) nt of

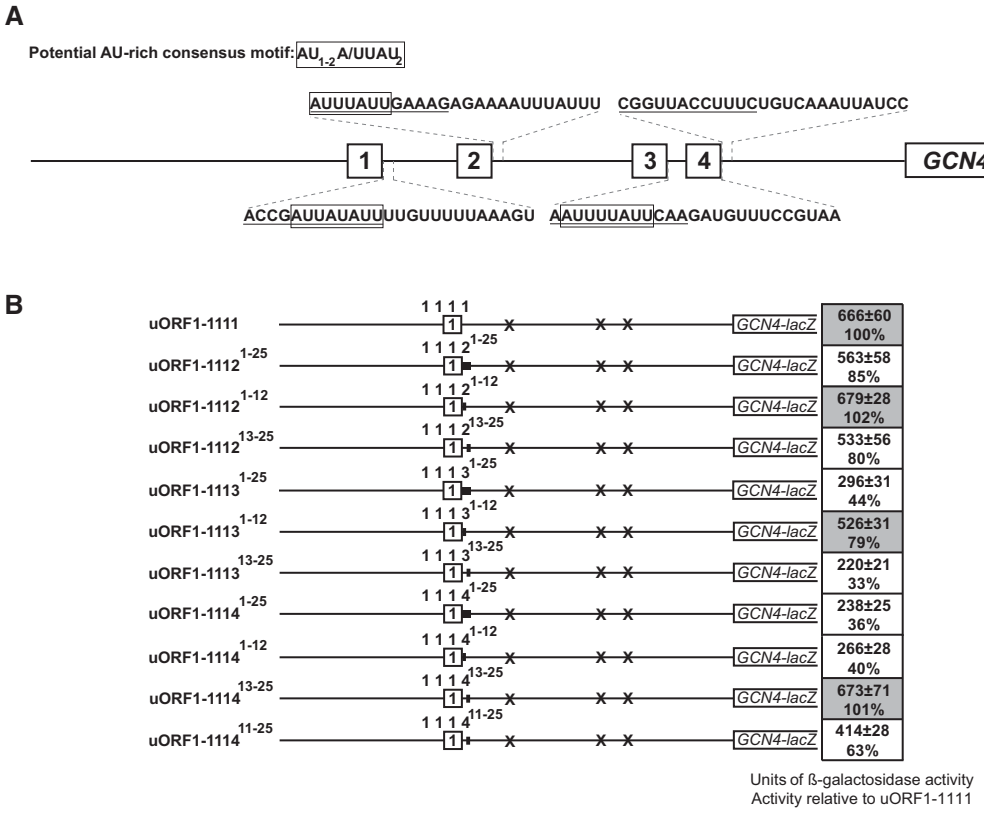

FIGURE 3. The presence of the specific AU-rich motif determines the REI-promoting activity of the 3′ sequence. (*A*) Schematic of the *GCN4* mRNA leader adapted from Figure 1A. The specific AU-rich motif (shown in frame) is present within the first 12 nt of the 3′ sequences of uORF1, 2, and 3; the first 12 nt of the 3′ sequence of each uORF are underlined. (*B*) The "full-length" 3′ sequence (1–25) of solitary uORF1 from the *GCN4* mRNA leader in its authentic position or its parts represented by the first 12 nt (1–12) or second 13 nt (13–25), or 15 nt in the case of uORF4 (11–25), were replaced by corresponding segments of the other three uORFs and analyzed as described in Figure 1C. Differences in β-galactosidase activities between *uORF1-1112*, *uORF1-1112*$^{13\text{-}25}$, *uORF1-1113*$^{1\text{-}12}$, or *uORF1-1114*$^{11\text{-}25}$ and their wt *uORF1-1111* were analyzed by Student's *t*-test and the calculated $P = 0.25$, 0.1469, 0.0722, or 0.0052, respectively.

the 3′ sequence of uORF1 suffice for its full function (Miller and Hinnebusch 1989), which leaves out the last 2 nt from the AU-rich motif. To reconcile these and our observations, we replaced the 11–25 nt of the uORF1 3′ sequence with the corresponding region of uORF4 (*uORF1-1114*$^{11\text{-}25}$) and observed that the REI activity on *GCN4* dropped down to 63%, in contrast to the 13–25 nt replacement showing 100% activity (Fig. 3B). Hence at least in our experimental setup, it is not the first 10 but the first 12 nt that encompass the entire $AU_{1\text{-}2}A/UUAU_2$ motif needed for the full REI potential of the uORF1 3′ sequence.

Taken together, our findings strongly suggest that the specific AU-rich motif occurring within the first 12 nt of segment D of uORF1, uORF2, and uORF3 is solely responsible for the REI-promoting function of the 3′ sequence, provided that it is situated at or near the authentic position of uORF1. As can be seen, however, sequences immediately following this motif also play an important role in this regulatory mechanism as they, at least in the case of uORFs 2 and 3, negatively influence their overall REI potential. Since uORF2 and uORF3 stimulate REI in the AU-rich motif-independent manner (Fig. 1C), and since these inhibitory sequences are transferable also to the ABCD blocks of uORF1 and uORF4, it is conceivable that they also act autonomously and impact a different REI step than that involving the action of the $AU_{1\text{-}2}A/UUAU_2$ motif.

The exact length of uORF1 and uORF2 coding sequences is critical for their maximal REI activity that shows a partially autonomous character

In our effort to systematically assess individual contributions of sequences flanking the REI-permissive uORFs to their REI capacity, we also wished to examine the potential contribution of the uORF1 and uORF2 coding sequences (CDS) per se. Early experiments done in the Hinnebusch laboratory suggested that the last coding triplet, which is represented by TGC coding cysteine for uORF1 and CCG coding proline for uORF4, does somehow contribute to the remarkable difference in the efficiency of REI between these two uORFs (Miller and Hinnebusch 1989; Grant and Hinnebusch 1994). Interestingly, the second REI-permissive uORF, uORF2, also contains a cysteine codon (TGT) as its last sense codon as uORF1, only it is one codon shorter (Fig. 4A). The same kind of similarity for the last sense codon also applies to uORF3 and REI-nonpermissive uORF4, as uORF3, like uORF4, contains the CCG triplet coding proline (Fig. 4A).

In analogy with our previous approach (Fig. 1D), we first replaced the CDS of uORF1 with CDSs of the other three uORFs (*uORF1-1121*, *uORF1-1131*, and *uORF1-1141*). None of them could work in place of uORF1 as efficiently as uORF1 by itself, not even the Cys codon-containing REI-permissive uORF2; the REI activity of these three replacements was reduced by ~51% to 70% (Fig. 4B). This is in agreement with an earlier study where the activity of *uORF1-1141* was measured in the strain deleted for the *GCN4* pathway-specific GCN2 kinase (Miller and Hinnebusch 1989). Hence we propose that not only the character of the last coding triplet but also the exact length of the uORF1 CDS is critical for its function. In support, extending the length of the two-codonal uORF2 by insertion of the uORF1 GCT Ala codon immediately after the uORF2 start codon (*uORF2-2212*) reduced its REI activity by 40% (Fig. 4C). Our findings thus clearly imply that the authentic length of both REI-permissive uORFs has to be maintained for their optimal activity. This could matter, for example, due to the fact that even slight alterations of their length may interfere with proper functioning of their 5′ and/or 3′ sequences.

To find out whether or not the CDSs of uORF1 and uORF2 can at least to some degree stimulate REI independently of their flanking, REI-promoting sequences, we replaced the uORF4 segment C from the uORF4 ABCD block situated either in the position of uORF1 (*uORF1-4444*) (Fig. 4D) or in its authentic position (*uORF4-4444*) (Fig. 4E) with those of uORF1 (*uORF1-4441* and *uORF4-4441*) or uORF2 (*uORF1-4442* and *uORF4-4442*). Regardless of the placement of the uORF4 ABCD block, the presence of CDSs of both REI-permissive uORFs did increase the efficiency of REI by ~26% to 44%. However, since segment C replacements in the uORF1 ABCD block showed >50% decrease in its REI activity (Fig. 4B), it is intuitive that a fully autonomous contribution of CDSs of both REI-permissive uORFs should lead to a larger, approximately twofold increase, which we did not observe. Hence we conclude that both uORFs per se have some inherent ability to promote REI independently of other sequences that is not position-specific, in contrast to the 3′ AU-rich motif. Not surprisingly, however, they also functionally interact with their flanking sequences to maximize their REI potential. Generally speaking, a REI-permissive uORF can be viewed as the complex unit with several independent and/or mutually interdependent contributors with peculiar attributes such as the CDS length.

The CCG triplet coding proline negatively impacts REI efficiency and at least in yeast has a predictable value in this respect

To investigate the causality of the aforementioned occurrence of the Cys triplet as the ultimate coding triplet in REI-permissive uORFs 1 and 2, and of the Pro triplet as the ultimate coding triplet in uORF3 and uORF4, we first inspected the *GCN4* mRNA leaders of closely or distantly related yeast species to *Saccharomyces cerevisiae* (Fig. 5A). With the exception of *Candida glabrata*, there is a clear conserved tendency for all other species to preserve Cys and Pro as the last coding triplets in at least the first and last short uORF, respectively. In the case of *C. glabrata*, the Cys triplet occurs in uORF3 and is followed by long uORF4 that is, owing to its length, by definition strictly REI-nonpermissive (Vilela et al. 1998; Szamecz et al. 2008). Therefore, this regulatory setup simply

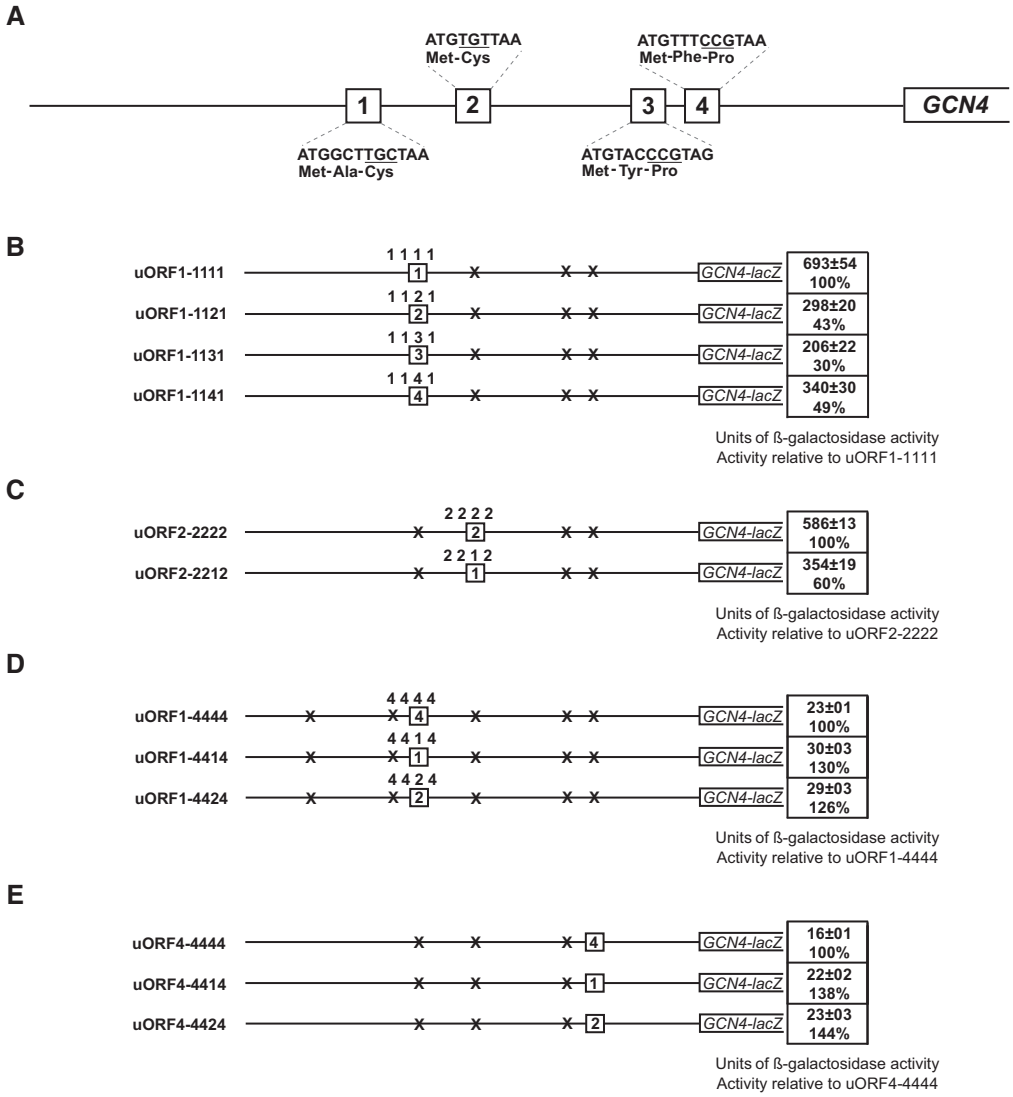

FIGURE 4. Sequence composition and length but not the position of uORF1 and uORF2 CDSs define their REI permissiveness. (*A*) Schematic of the *GCN4* leader containing four short uORFs (1–4). For each uORF, nucleotide as well as amino acid sequences are shown. The triplets of the last sense codon are underlined. (*B*) The CDS (segment C) of solitary uORF1 from the *GCN4* mRNA leader in its authentic position was replaced by corresponding segments of the other three uORFs and analyzed as described in Figure 1C. (*C*) The CDS of solitary uORF2 from the *GCN4* mRNA leader in its authentic position was replaced by corresponding segment of uORF1 and analyzed as described in Figure 1C. (*D*) The CDS of solitary uORF4 from the *GCN4* mRNA leader with its authentic flanking sequences (A4–D4) situated in the position of uORF1 was replaced by corresponding segments of uORF1 and 2 and analyzed as described in Figure 1C. Differences in β-galactosidase activities between *uORF1-4414* or *uORF1-4424* and their wt *uORF1-4444* were analyzed by Student's *t*-test and the calculated $P = 0.0572$ or 0.094, respectively. (*E*) Same as in *D* except that the CDS substitutions were tested in the authentic position of uORF4. Differences in β-galactosidase activities between *uORF4-4414* or *uORF4-4424* and their wt *uORF4-4444* were analyzed by Student's *t*-test and the calculated $P = 0.0275$ or 0.0581, respectively.

does not require featuring Pro as the ultimate coding triplet of the last uORF.

The question is, what stands behind this phenomenon? Is it the Cys/Pro triplet or the identity of these two residues per se? To examine that, we systematically substituted the ultimate coding triplet individually in all four *GCN4* uORFs and measured the resulting REI activities. Recoding the cysteine triplet of uORF1 [*uORF1-1111-Cys (TGT)*] or uORF2 [*uORF2-2222-Cys (TGC)*] showed almost no impact on REI of these uORFs (Fig. 5B,C), which contrasts with the remarkable increase in REI seen when the analogous uORF1 recoding was tested in early days, however, in the artificial setup with the genuine uORF1 3′ sequence replaced with the corresponding 3′ sequence of uORF4 (Grant and Hinnebusch 1994). In fact, our measurements are perfectly consistent with another work by the same group, where the REI activity was measured for the synonymous uORF1 cysteine substitutions under starvation conditions using a minimalistic construct lacking uORF2 and uORF3 and no significant changes were found (Miller and Hinnebusch

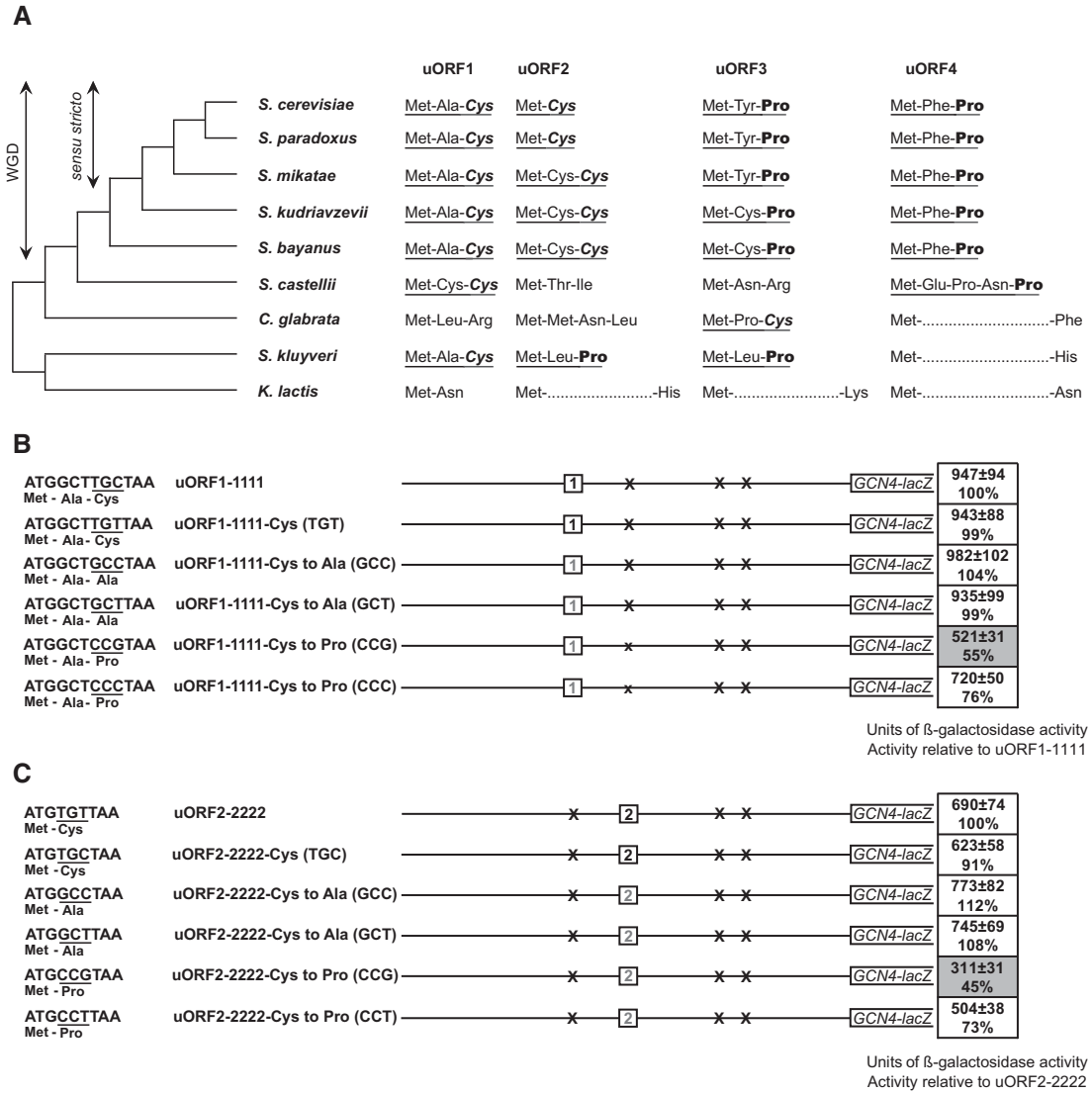

FIGURE 5. Insertion of the CCG triplet as the last sense codon of uORF1 and uORF2 inhibits their REI activity. (*A*) The conservation of Cys and Pro codons in short uORFs from the *GCN4* mRNA leaders of yeast species related to *S. cerevisiae.* The uORFs are presented as identified in Cvijović et al. (2007). uORFs containing Cys (in italics) and Pro (in bold) triplets as their last sense codons are underlined. In longer uORFs, the sequence of their CDSs is represented by a dotted line. WGD, whole-genome duplication. (*B*) The TGC cysteine codon of solitary uORF1 from the *GCN4* mRNA leader in its authentic position was replaced by indicated cysteine, alanine, and proline substitutions and analyzed as described in Figure 1C. Differences in β-galactosidase activities between *uORF1-1111-Cys* to *Pro (CCC)* and its wt *uORF1-1111* were analyzed by Student's *t*-test and the calculated $P = 0.0648$. (*C*) The TGT cysteine codon of solitary uORF2 from the *GCN4* mRNA leader in its authentic position was replaced by indicated cysteine, alanine, and proline substitutions and analyzed as described in Figure 1C. Differences in β-galactosidase activities between *uORF2-2222-Cys* to *Pro (CCT)* and its wt *uORF2-2222* were analyzed by Student's *t*-test and the calculated $P = 0.0554$.

1989). Hence we conclude that both cysteine codons of uORF1 and uORF2 utilizing the same Cys-tRNA are similarly efficient in promoting REI. In addition, our findings further support the idea that it is most probably the length of the CDSs of uORF1 and uORF2 and not the differing Cys triplet that stands behind their inability to replace each other in their authentic environment (Fig. 4B,C).

To examine whether it is the cysteine residue per se that lies behind this phenomenon, we substituted the cysteine codons of uORF1 (TGC) and uORF2 (TGT) with two different alanine codons: (i) GCC [*uORF1-1111-Cys* to *Ala (GCC)* and *uORF2-2222-Cys* to *Ala (GCC)*], and (ii) GCT [*uORF1-1111-Cys* to *Ala (GCT)* and *uORF2-2222-Cys* to *Ala (GCT)*]. Like the cysteine substitutions, neither of the Ala substitutions had any effect on either uORF (Fig. 5B,C). Hence the REI permissiveness of uORF1 and uORF2 CDSs does not exclusively depend on the presence of a cysteine codon as the last coding triplet, as suggested before (Grant and Hinnebusch 1994). It also does not seem to strictly depend on the AU vs. GC content, as proposed by Grant

and Hinnebusch (1994), because the changes that increased or decreased the AU content showed no effect (Fig. 5B,C). This implies that the third codon can most probably tolerate a wide range of codons as long as these do not interfere with the resumption of scanning.

Finally, we substituted Cys codons in both REI-permissive uORFs with the supposedly inhibitory proline CCG triplet from uORFs 3 and 4 [*uORF1-1111-Cys* to *Pro (CCG)* and *uORF2-2222-Cys* to *Pro (CCG)*] as well as with the other two proline triplets; CCC for uORF1 [*uORF1-1111-Cys* to *Pro (CCC)*] and CCT for uORF2 [*uORF2-2222-Cys* to *Pro (CCT)*] (Fig. 5B,C). Whereas the latter CCT and CCC substitutions led to ~24%–27% drop in the REI activity on both uORFs, the CCG triplet produced the most robust ~45%–55% reduction. A similar decrease was also seen when the CCG substitution in uORF2 was made in the construct where the entire uORF2 ABCD block was placed in the position of uORF1 (data not shown). These findings correspond well with our uORF1 segment C replacement data (Fig. 4B), where introduction of the corresponding uORF4 segment in *uORF1-1141* also reduced the REI efficiency by ~51%. This suggests that at least for uORF1 the entire negative effect could be solely attributable to the presence of the last coding CCG triplet.

Importantly, we cannot explain the observed difference among the three tested Pro triplets by their varying codon optimality, because it simply does not correlate with the amounts of distinct types of Pro-tRNAs specific to these triplets. Hence, we propose that both the presence of proline as the ultimate residue and also some peculiar attributes of the CCG codon beyond codon optimality act together to maximize the inhibitory impact on REI after translation of short uORFs that are not meant to promote efficient resumption of scanning. Consistently, replacing the CCG Pro triplet in uORF3 and uORF4 with the uORF1 TGC cysteine codon relieved the CCG-mediated inhibition of REI after uORF3 and uORF4 translation to some degree (Supplemental Fig. S4).

The proline residue is known for its unusual conformation that, due to its limited spatial rotation during peptide bond formation, slows down the incorporation of this residue into the nascent polypeptide chain and therefore negatively influences the speed of translation (Wohlgemuth et al. 2008; Pavlov et al. 2009). Since uORF1 and uORF2 are very short, the presence of the slowing down Pro as the last residue could theoretically interfere with the time-sensitive formation of the interaction between uORF1 and uORF2 RPEs and their interacting factor eIF3. In support, prolonging the time of uORF1 proteosynthesis by extending its coding region by up to five codons gradually decreased its REI potential (Szamecz et al. 2008). The difference observed among the three tested Pro triplets could then be caused by a specific character of the CCG sequence that might, for example, interfere with proper stop codon recognition for effective translation termination.

The sequence composition of the uORF3 and uORF4 second codon and markedly differing termination efficiency makes the difference in the REI activity between these two uORFs

As mentioned above, we previously established that the inherent REI activity of uORF3 represents ~13%–18% of the maximum REI capacity allowed by uORF1, whereas uORF4 goes down to ~3%–5% (Munzarová et al. 2011; Gunišová and Valášek 2014). Therefore, we wished to uncover what determines the approximately fourfold higher REI activity of uORF3 compared to uORF4. In our earlier work, we demonstrated that the modest REI potential of uORF3 does not depend on any of the uORF1- and/or uORF2-specific RPEs and, accordingly, it does not require intact eIF3 (Gunišová and Valášek 2014). Here we ruled out the possibility that this difference could be caused by the uORF3's ability to utilize the AU-rich motif contained within its 3′ sequence (Fig. 1C; Supplemental Fig. S3). Hence the only option left was the CDS of both uORFs, where only two differences can be found: (i) the second codon that is represented by TAC encoding Tyr in uORF3 and TTT encoding Phe in uORF4, and (ii) the stop codon that is represented by TAG in uORF3 and TAA in uORF4 (Fig. 6A). Looking at their 12-nt sequences per se, these two uORFs differ only by 3 nt.

To investigate what lies behind this difference, we prepared the uORF3- and uORF4-based constructs, where each aspect at which they differ was individually or in combinations swapped between them and examined for REI activity (Fig. 6B). The Tyr to Phe substitution of uORF3 [*uORF3-3333-Tyr* to *Phe (TTT)*] markedly decreased its activity (down to ~55%) (Fig. 6B). A milder decrease down to ~71% was obtained when the stop codon of uORF3 was replaced with that of uORF4 (*uORF3-3333-TAA*), however, a combination of both of these substitutions in *uORF3-3333-Tyr* to *Phe (TTT)-TAA* showed an additive effect by allowing only ~42% of the intrinsic REI activity of wild-type uORF3 (Fig. 6B). Interestingly, whereas the stop codon swap in uORF4 (*uORF4-4444-TAG*) showed no effect, the Phe to Tyr substitution of uORF4 [*uORF4-4444-Phe* to *Tyr (TAC)*] increased the REI activity by ~1.7-fold and their subsequent combination in *uORF4-4444-Phe* to *Tyr (TAC)-TAG* also led to an additive effect by increasing the intrinsic REI potential of uORF4 by approximately twofold (Fig. 6B). Our results thus indicate that the differences in the composition of the uORF3 and uORF4 CDSs are indeed at least partially responsible for their different REI permissiveness.

Next we analyzed the effect of the second sense codon in greater detail because it seemed to have a bigger influence on efficiency of resumption of scanning over the identity of the stop codon. To find out whether it is the encoded amino acid or a particular triplet that makes the difference, we tested both existing Tyr codons (original TAC and synonymous TAT) and both existing Phe codons (original TTT and synonymous TTC) in both uORFs of interest. Luckily, the

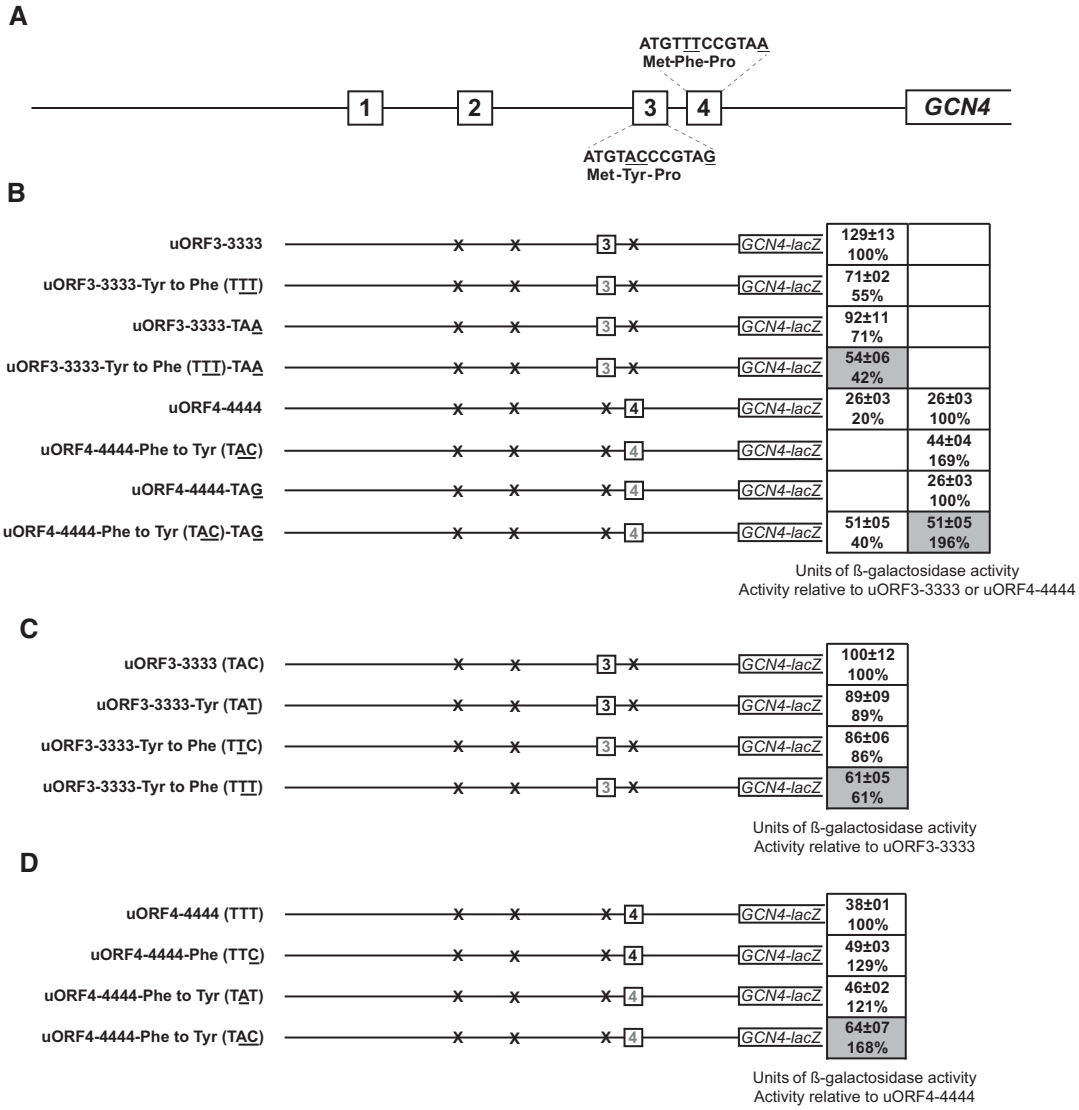

FIGURE 6. The differences in the sequence composition of the uORF3 and uORF4 CDSs are responsible for their varying REI permissiveness. (*A*) Schematic of the *GCN4* leader adapted from Figure 4A. Nucleotide as well as amino acid sequences of only uORF3 and uORF4 are depicted. The different nucleotides between these two uORFs are underlined. (*B*) The CDSs of solitary uORF3 and uORF4 from the *GCN4* mRNA leader in their authentic positions were modified by indicated substitutions and analyzed as described in Figure 1C. Differences in β-galactosidase activities between *uORF3-3333-TAA* and its wt *uORF3-3333,* or *uORF3-3333-Tyr* to *Phe (TTT)* and *uORF3-3333-Tyr* to *Phe (TTT)-TAA,* or *uORF4-4444-Phe* to *Tyr (TAC)* and *uORF4-4444-Phe* to *Tyr (TAC)-TAG* were analyzed by Student's *t*-test and the calculated $P = 0.0609$, 0.0275, or 0.3033, respectively. (*C*) Same as in *B* except that a different set of solitary uORF3 substitutions was used. Differences in β-galactosidase activities between *uORF3-3333-Tyr* to *Phe (TTT)* and its wt *uORF3-3333* were analyzed by Student's *t*-test and the calculated $P = 0.0171$. (*D*) Same as in *B* except that a different set of solitary uORF4 substitutions was used.

interpretation of these analyses is simplified by the fact that both existing Tyr and Phe codons are recognized by a single Tyr- or Phe-tRNA, respectively. Therefore, there should be no unspecific influence on the effect of our substitutions. Out of these three possible substitutions only Phe (TTT), changing two out of three original bases in *uORF3-3333-Tyr* to *Phe (TTT)*, produced by far the most dramatic reduction in the uORF3 REI activity (down to ~61%) (Fig. 6C). Similarly, the Tyr (TAC) substitution, changing two out of three original bases in *uORF4-4444-Phe* to *Tyr (TAC)*, produced by far the largest increase (by ~1.7-fold) in the uORF4 REI activity (Fig. 6D). All other substitutions that changed only one out of three bases of both uORFs [*uORF3-3333-Tyr (TAT)* and *uORF3-3333-Tyr* to *Phe (TTC)* in Fig. 6C, and *uORF4-4444-Phe (TTC)* and *uORF4-4444-Phe* to *Tyr (TAT)* in Fig. 6D] altered the efficiency of REI only modestly. Since the same amino acid encoded by two different triplets that are, however, recognized by the same tRNA produced a marked difference in REI activity, we can conclude that it is not the identity of an amino acid

residue or of a tRNA by which it is delivered, but the sequence composition of the uORF3 and uORF4 second codon that contributes to the difference in the REI potential between these two uORFs.

Because the full remake of uORF3 into uORF4 in the authentic position of uORF3 [*uORF3-3333-Tyr* to *Phe (TTT)-TAA*] reduces its REI activity only approximately twofold, and at the same time the full remake of uORF4 into uORF3 in the authentic position of uORF4 [*uORF4-4444-Phe* to *Tyr (TAC)-TAG*] increases its REI activity also only approximately twofold, there must clearly be some other factor outside of their CDSs that further contributes to the approximately fourfold difference in REI activity between uORF3 and uORF4. We hypothesized that this factor could lie in the identity of the base immediately following the stop codon (the so-called +4 nucleotide), which is known to strongly influence the efficiency of stop codon recognition (see, for example, Beznosková et al. 2015b). In particular, cytosine at the +4 position is the leakiest base with respect to efficiency of translation termination among all four bases at all three stop codons (Beznosková et al. 2015a; Dabrowski et al. 2015). Hence, we rationalized that an uORF with a poorer stop codon context allowing increased frequency of stop codon readthrough would extend its translation beyond its genuine stop codon, which would in turn decrease its efficiency of REI. Interestingly, the TAA stop codon of uORF4 is followed by C and TAG of uORF3 by A (Figs. 1A, 7A), and indeed our dual-luciferase reporter assay revealed that uORF4 has ~3.7-fold increased frequency of readthrough compared to uORF3 (Fig. 7B). As a control, we used the TGA stop codon with the C at the +4 position (TGA-C), which is known to allow relatively high levels of readthrough (Beznosková et al. 2015b). Notably, readthrough on uORF4 is even ~1.5-fold higher than readthrough on this very rare terminating tetranucleotide with the so-called programmed readthrough. Hence we propose that the fact that ~3.7-times more ribosomes fail to terminate at uORF4 compared to uORF3 does further contribute to its overall REI nonpermissiveness and thus to the difference in REI activity between these two uORFs.

If true, the combination of the full remake of uORF4 into uORF3 [*uORF4-RT-Phe* to *Tyr (TAC)-TAG*] with a substitution of the +4 nucleotide C of uORF4 for A of uORF3 (*uORF4-RT-TAAA*) into one construct [*uORF4-RT-Phe* to *Tyr (TAC)-TAGA*] should reduce the frequency of readthrough down to the levels observed for wt uORF3; and this is exactly what we observed. Whereas individual mutations reduced readthrough by similar ~2.6-fold, their combination displayed an approximately fourfold decrease [Fig. 7B; compare 24% of *uORF4-RT-Phe* to *Tyr (TAC)-TAGA* with 27% of *uORF3-RT*]. Consistently, the same trend but in a reverse order was seen when we substituted the +4 nucleotide C of uORF4 for A of uORF3 and measured the REI efficiency using the *GCN4-LacZ* construct (*uORF4-4444-TAAA*). It increased the overall REI activity of uORF4 by ~1.6-fold (164%) and the same substitution in the full remake of uORF4 into uORF3 [*uORF4-4444-Phe* to *Tyr (TAC)-TAGA*] increased the overall REI activity from approximately twofold (209%) to approximately threefold (291%), which is now close to the aforementioned approximately fourfold difference between both uORFs (Fig. 7C). We thus conclude that the combination of the sequence composition of the uORF3 and uORF4 second codon and the identity of the stop codon tetranucleotide is what makes the major contribution to the difference in the REI potential between these two uORFs.

Individual and combined effects of all *cis*-elements that determine REI permissiveness of uORF1 and uORF2

To capture our in-depth analysis, we gradually combined mutations in all identified REI-promoting *cis*-determinants of uORF1 as well as uORF2 in an effort to compare their individual contributions to the overall REI potential of both REI-permissive uORFs. First, we side-by-side evaluated individual contributions of (i) the RPEs i.–iv. that are situated in segment A of uORF1 (Munzarová et al. 2011; Gunišová and Valášek 2014), (ii) the CDS of uORF1 and in particular of its third sense codon, and (iii) the 3′ sequence of uORF1. The biggest contribution comes from the RPEs (*uORF1-1111-Δ160*; ~79% drop), some of which like RPE i. and iv. require intact eIF3 for their function. The RPEs are followed by the autonomous 3′ sequence (*uORF1-1114*; ~67% drop), and the uORF1 third sense codon [*uORF1-1111-Cys* to *Pro (CCG)*; ~49% drop] (Fig. 8A). Concurrent removal of the two biggest contributors in *uORF1-1114-Δ160* displayed a robust decrease in the REI activity (down to ~8%), strongly suggesting that their contributions are independent ($0.21 \times 0.33 = 0.07$, which pretty much equals the obtained 8%). A relatively smaller additive effect was observed when the removal of all RPEs was combined with the Cys to Pro substitution in *uORF1-1111-Δ160-Cys* to *Pro (CCG)* (16%), indicating their partial interdependence ($0.21 \times 0.51 = 0.11$, which is smaller than the obtained 16%). Testing the combination of the Cys to Pro substitution with the removal of the uORF1 3′ sequence in the hypothetical *uORF1-only-1114-Cys* to *Pro (CCG)* construct is meaningless, because we previously showed that the otherwise autonomous activity of RPEs follows and in fact requires a prior action of the uORF1 3′ sequences (Munzarová et al. 2011). Therefore, with respect to its minimal activity (~6%), the *uORF1-1144* construct shown in Figure 1C basically mimics the elimination of all three contributors in *uORF1-1114-Δ160-Cys* to *Pro (CCG)* reaching the uORF4-like basal REI activity (~5%) (Fig. 8A).

Finally, removal of the eIF3-independent RPE ii. together with the uORF2-specific, eIF3-dependent RPE v. (Gunišová and Valášek 2014), situated in the uORF2 segment A (*uORF2-2222-Δ233*), reduced the efficiency of REI by a robust ~77%, whereas the Cys to Pro substitution of the

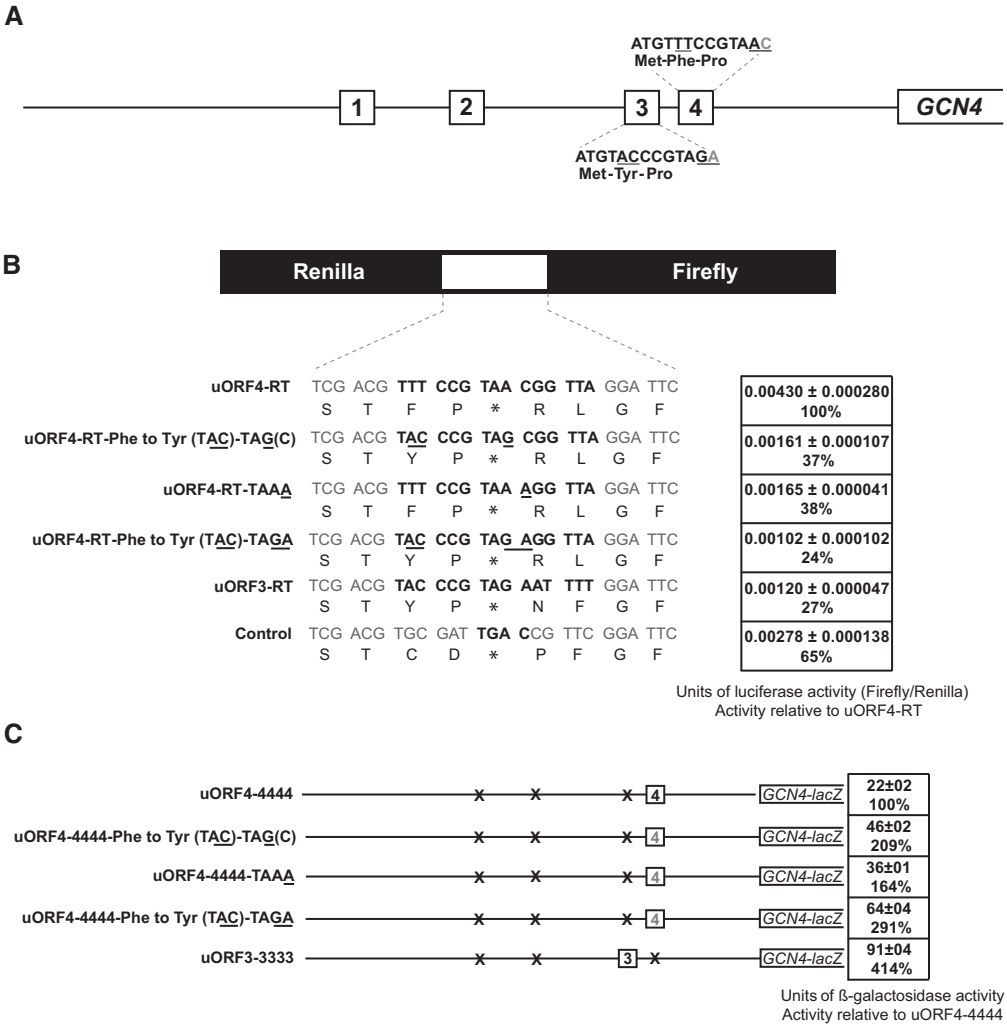

FIGURE 7. Poor termination efficiency at the uORF4 stop codon strongly contributes to the difference in the REI efficiency between uORF3 and uORF4. (*A*) Modified schematic from Figure 6A, in addition depicting the nucleotide following the stop codon of uORF3 and uORF4 (the +4 base; in gray). (*B*) Schematic of the standard dual luciferase readthrough reporter constructs adapted from Keeling et al. (2004). In the linker region, the 15-nt long termination sequences of uORF3 or uORF4 with their derivatives, as well as the control TGA-C terminating tetranucleotide, are shown in bold. The uORF4 derivatives have all their substitutions gradually turning them into wt uORF3 underlined. All indicated constructs were introduced into the PBH156 strain and the resulting transformants were grown in SD and processed for stop codon readthrough measurements as described in Materials and Methods. Values of luciferase activity are represented as mean values and standard deviations obtained from five independent transformants, and each experiment was repeated at least three times. Differences in luciferase activities between *uORF4-RT-Phe* to *Tyr (TAC)-TAG* or *uORF4-RT-TAAA* and their wt *uORF4-RT*, and between *uORF4-RT* and control *TGAC* plasmid were analyzed by Student's *t*-test and the calculated $P = 0.0039$ or 0.0004, and 0.0012, respectively. (*C*) The difference in the nucleotide following the stop codon of uORF3 and uORF4 (the +4 base) contributes to their varying REI permissiveness. Solitary uORF4 from the *GCN4* mRNA leader in its authentic position was modified by indicated substitutions from uORF3 and analyzed as described in Figure 1C. Differences in β-galactosidase activities between *uORF4-4444-TAAA* and its wt *uORF4-4444* were analyzed by Student's *t*-test and the calculated $P = 0.0002$.

uORF2 last coding triplet [*uORF2-2222-Cys* to *Pro (CCG)*] showed a similar reduction to that observed for uORF1 (~56% drop in REI) (Fig. 8B). Hence, as in the case of uORF1, the major contributor to the uORF2 REI potential is represented by its RPEs. Elimination of both of these *cis*-determinants at the same time in *uORF2-2222-Δ233-Cys* to *Pro (CCG)* expectedly reached the uORF4-like basal level of REI (~5%) (Fig. 8B), clearly illustrating the absolute independence of the uORF2 REI activity on its 3′ sequences, as shown above.

Conclusion

Our systematic analysis of all potential *cis*-determinants that either promote or inhibit reinitiation on *GCN4* mRNA revealed the following attributes of individual uORFs (summarized in Fig. 9). The 3′ sequences of uORFs 1–3, in particular the first 12 nt immediately following their stop codons, contain a conserved $AU_{1\text{-}2}A/UUAU_2$ motif that promotes REI independently of other REI-promoting elements but only when situated at the defined distance from the *GCN4* AUG

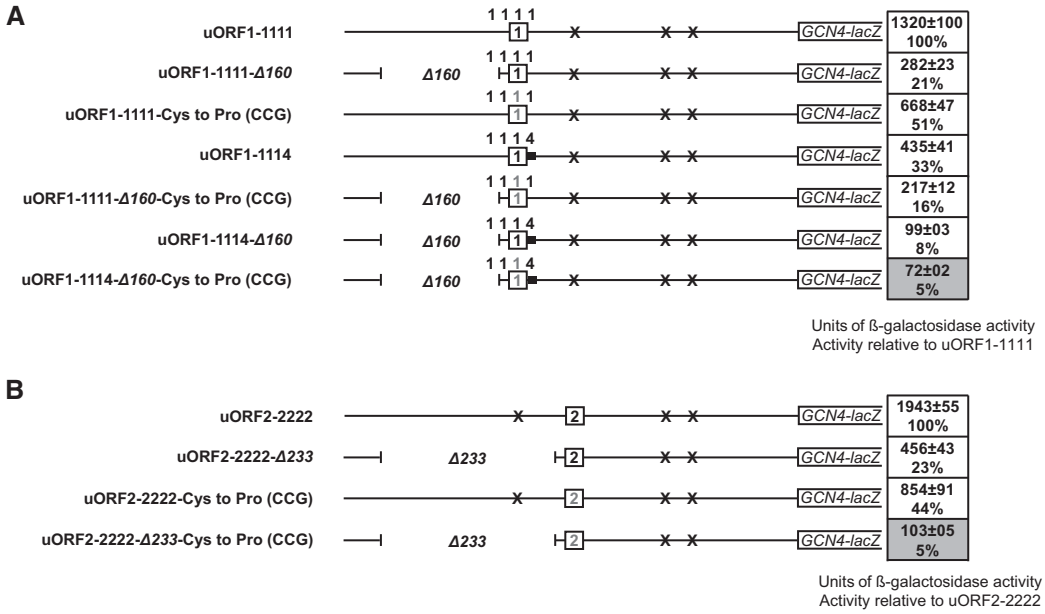

FIGURE 8. Combined effects of mutations in *cis*-determinants of uORF1 and uORF2 on their REI permissiveness. (*A*) The REI permissiveness of uORF1 is determined by three *cis*-factors: RPEs situated in the 5′ sequence, CDS, and the 3′ sequence. Solitary uORF1 from the *GCN4* mRNA leader in its authentic position and its derivatives containing the indicated mutations were analyzed as described in Figure 1C. Differences in β-galactosidase activities between *uORF1-1111-Δ160* and *uORF1-1111-Δ160-Cys* to *Pro (CCG)*, or *uORF1-1114-Δ160* and *uORF1-1114-Δ160-Cys* to *Pro (CCG)* were analyzed by Student's *t*-test and the calculated $P = 0.0369$ or 0.0001, respectively. (*B*) REI permissiveness of uORF2 is determined by two *cis*-factors: RPEs situated in the 5′ sequence and CDS. Solitary uORF2 from the *GCN4* mRNA leader in its authentic position and its derivatives containing the indicated mutations were analyzed as described in Figure 1C.

start codon, in principle corresponding to the position of uORF1. Hence, despite carrying this autonomous motif in their 3′ sequences, uORF2 and uORF3 do not utilize it. Intriguingly, the 3′ sequences of specifically these two uORFs in addition contain inhibitory elements that immediately follow the AU-rich motif and decrease the REI potential of these two uORFs. Interestingly, these inhibitory elements are transferable and function irrespectively of their distance from the *GCN4* start codon. Furthermore, we also revealed that the authentic length of both REI-permissive uORFs has to be maintained for their optimal activity and that the last coding triplet can most probably tolerate a wide range of codons with the exception of the REI-inhibiting proline CCG triplet. Indeed, specifically this Pro triplet occurs as the last triplet in uORF3 and uORF4 and, in fact, features in all ultimate uORFs in the *GCN4* mRNA leaders across yeast species. Finally, we show that the approximately four-fold difference between the REI potential of modestly REI-permissive uORF3 and REI-nonpermissive uORF4 does not lie in the supposedly inhibitory 3′ sequence of uORF4, as suggested before (Gunišová and Valášek 2014), but is manifested through the specific effects of the sequence composition of their second codon and of the identity of their stop codon tetranucleotide, which together impact the efficiency of stop

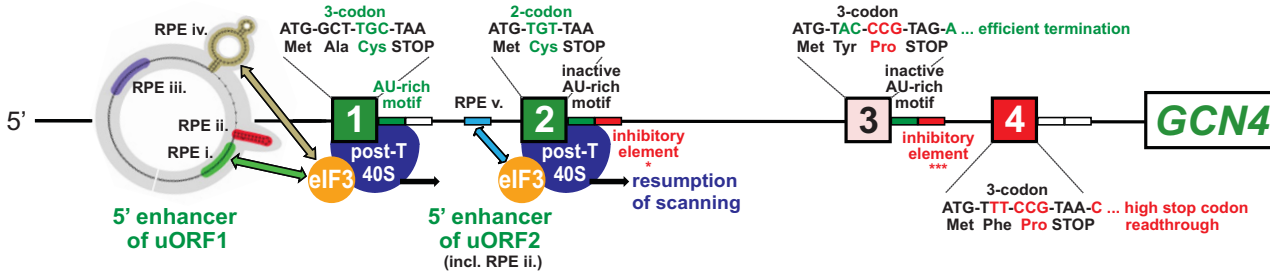

FIGURE 9. Summary of all *cis*-determinants that either promote or inhibit reinitiation on *GCN4* after translation of its four short uORFs. Schematics of the 5′ enhancers of uORF1 and 2 containing their respective RPEs, some of which functionally interact with eIF3 to promote resumption of scanning, were taken from Gunišová and Valášek (2014). Green color-coding generally indicates stimulatory effects of the corresponding *cis*-factors on efficiency of REI, whereas red color-coding indicates inhibitory effects (with the exception of RPE ii. of uORF1, which is also stimulatory); the number of asterisks *below* the inhibitory elements of the uORF2 and uORF3 3′ sequences illustrates the degree of their inhibition as determined experimentally. Please see text for further details.

codon recognition in a positive (uORF3) or negative (uORF4) way. In other words, we demonstrate for the first time that there is a direct negative correlation between the efficiency of reinitiation and efficiency of translation termination. Collectively this comprehensive approach pictures an intriguing complexity of this delicate regulatory system that depends on several REI-promoting as well as inhibiting features that mutually fine-tune their often autonomous effects on the overall efficiency of REI on *GCN4* mRNA in order to keep it as low as possible during nonstarvation conditions or as high as possible during starvation/stress conditions.

Even though there is a prevailing opinion that practically each short uORF is different and there are no generalizable rules that would apply to a majority of them (Wethmar 2014), we can conclude the following. The presence of the CCG triplet encoding proline as the last coding triplet most probably signals very poor REI potential of a given uORF, at least in yeast. Conversely, the presence of the RPE i.-like and/or RPE v.-like sequence motif not far upstream of a given short uORF, as well as the presence of the AU-rich motif immediately following the stop codon, might signal increased permissiveness for REI. An additional indicator of the REI permissiveness could be the presence of a structural element resembling the secondary structure of the uORF1 RPE iv., which can also be found in the 5′ enhancer of the solitary uORF preceding the *YAP1* gene (Munzarová et al. 2011).

MATERIALS AND METHODS

Yeast strains, plasmids, and other biochemical methods

Lists of strains (Supplemental Table S1), plasmids (Supplemental Table S2), and PCR primers (Supplemental Table S3) used in this study and details of their construction can be found in the Supplemental Material. β-Galactosidase assays were conducted as described previously (Mueller et al. 1987; Grant and Hinnebusch 1994). For all β-galactosidase values recorded with mutant constructs that differed from their respective wt constructs by <40%, the *P*-values were calculated and are given in the corresponding figure legends.

Stop codon readthrough assay

Dual luciferase assay was performed using the Dual Luciferase Reporter Assay System (Promega). Briefly, yeast strain PBH156 was transformed with the indicated dual luciferase reporter nonsense control plasmid pTH477 (Fig. 7A) as well as with the sense codon (CAA) plasmid pTH460 and pSG358, pSG362, pSG349, pSG365, or pSG350. The experiments and data analysis were carried out according to the Microtiter plate-based dual luciferase protocol developed by Merritt et al. (2010) and commercially distributed by Promega. Assays were done in quintuplicates ($n = 5$), the data are expressed as the mean ± SD, and each experiment was repeated at least three times. Resulting luciferase activity in each strain was expressed as the firefly/Renilla luciferase activity (nonsense or all indicated pSG plasmids) divided by the firefly/Renilla luciferase activity (sense). For further details, please see Keeling et al. (2004).

SUPPLEMENTAL MATERIAL

Supplemental material is available for this article.

ACKNOWLEDGMENTS

We are thankful to Josef Pánek for computational analysis, to Olga Krýdová for technical and administrative assistance, and to the members of the Valášek laboratory for helpful suggestions. This research was supported by the Czech Science Foundation Grant P305-11-0172.

Received October 26, 2015; accepted December 18, 2015.

REFERENCES

Abastado JP, Miller PF, Jackson BM, Hinnebusch AG. 1991. Suppression of ribosomal reinitiation at upstream open reading frames in amino acid-starved cells forms the basis for *GCN4* translational control. *Mol Cell Biol* **11:** 486–496.

Aylett CH, Boehringer D, Erzberger JP, Schaefer T, Ban N. 2015. Structure of a yeast 40S-eIF1-eIF1A-eIF3-eIF3j initiation complex. *Nat Struct Mol Biol* **22:** 269–271.

Beznosková P, Gunisova S, Valasek LS. 2015a. Rules of UGA-N decoding by near-cognate tRNAs and analysis of readthrough on short uORFs in yeast. *RNA* doi: 10.1261/rna.054452.115.

Beznosková P, Wagner S, Jansen ME, von der Haar T, Valášek LS. 2015b. Translation initiation factor eIF3 promotes programmed stop codon readthrough. *Nucleic Acids Res* **43:** 5099–5111.

Calvo SE, Pagliarini DJ, Mootha VK. 2009. Upstream open reading frames cause widespread reduction of protein expression and are polymorphic among humans. *Proc Natl Acad Sci* **106:** 7507–7512.

Cuchalová L, Kouba T, Herrmannová A, Dányi I, Chiu W-l, Valášek L. 2010. The RNA recognition motif of eukaryotic translation initiation factor 3g (eIF3g) is required for resumption of scanning of postermination ribosomes for reinitiation on GCN4 and together with eIF3i stimulates linear scanning. *Mol Cell Biol* **30:** 4671–4686.

Cvijović M, Dalevi D, Bilsland E, Kemp GJ, Sunnerhagen P. 2007. Identification of putative regulatory upstream ORFs in the yeast genome using heuristics and evolutionary conservation. *BMC Bioinformatics* **8:** 295.

Dabrowski M, Bukowy-Bieryllo Z, Zietkiewicz E. 2015. Translational readthrough potential of natural termination codons in eukaryotes —the impact of RNA sequence. *RNA Biol* **12:** 950–958.

Davuluri RV, Suzuki Y, Sugano S, Zhang MQ. 2000. CART classification of human 5′ UTR sequences. *Genome Res* **10:** 1807–1816.

Dever TE, Feng L, Wek RC, Cigan AM, Donahue TD, Hinnebusch AG. 1992. Phosphorylation of initiation factor 2 α by protein kinase GCN2 mediates gene-specific translational control of *GCN4* in yeast. *Cell* **68:** 585–596.

Grant CM, Hinnebusch AG. 1994. Effect of sequence context at stop codons on efficiency of reinitiation in *GCN4* translational control. *Mol Cell Biol* **14:** 606–618.

Grant CM, Miller PF, Hinnebusch AG. 1995. Sequences 5′ of the first upstream open reading frame in *GCN4* mRNA are required for efficient translational reinitiation. *Nucleic Acids Res* **23:** 3980–3988.

Gunišová S, Valášek LS. 2014. Fail-safe mechanism of GCN4 translational control–uORF2 promotes reinitiation by analogous mechanism to uORF1 and thus secures its key role in GCN4 expression. *Nucleic Acids Res* **42:** 5880–5893.

Hinnebusch AG. 2005. Translational regulation of GCN4 and the general amino acid control of yeast. *Annu Rev Microbiol* **59:** 407–450.

Hood HM, Neafsey DE, Galagan J, Sachs MS. 2009. Evolutionary roles of upstream open reading frames in mediating gene regulation in fungi. *Annu Rev Microbiol* **63:** 385–409.

Iacono M, Mignone F, Pesole G. 2005. uAUG and uORFs in human and rodent 5′ untranslated mRNAs. *Gene* **349:** 97–105.

Jackson RJ, Hellen CU, Pestova TV. 2012. Termination and post-termination events in eukaryotic translation. *Adv Protein Chem Struct Biol* **86:** 45–93.

Keeling KM, Lanier J, Du M, Salas-Marco J, Gao L, Kaenjak-Angeletti A, Bedwell DM. 2004. Leaky termination at premature stop codons antagonizes nonsense-mediated mRNA decay in *S. cerevisiae*. *RNA* **10:** 691–703.

Kouba T, Dányi I, Gunišová S, Munzarová V, Vlčková V, Cuchalová L, Neueder A, Milkereit P, Valášek LS. 2012. Small ribosomal protein RPS0 stimulates translation initiation by mediating 40S-binding of eIF3 via its direct contact with the eIF3a/TIF32 subunit. *PLoS One* **7:** e40464.

Kozak M. 1987. Effects of intercistronic length on the efficiency of reinitiation by eukaryotic ribosomes. *Mol Cell Biol* **7:** 3438–3445.

Kozak M. 2005. Regulation of translation via mRNA structure in prokaryotes and eukaryotes. *Gene* **361:** 13–37.

Lee YY, Cevallos RC, Jan E. 2009. An upstream open reading frame regulates translation of GADD34 during cellular stresses that induce eIF2α phosphorylation. *J Biol Chem* **284:** 6661–6673.

Merritt GH, Naemi WR, Mugnier P, Webb HM, Tuite MF, von der Haar T. 2010. Decoding accuracy in eRF1 mutants and its correlation with pleiotropic quantitative traits in yeast. *Nucleic Acids Res* **38:** 5479–5492.

Miller PF, Hinnebusch AG. 1989. Sequences that surround the stop codons of upstream open reading frames in *GCN4* mRNA determine their distinct functions in translational control. *Genes Dev* **3:** 1217–1225.

Mueller PP, Harashima S, Hinnebusch AG. 1987. A segment of *GCN4* mRNA containing the upstream AUG codons confers translational control upon a heterologous yeast transcript. *Proc Natl Acad Sci* **84:** 2863–2867.

Munzarová V, Pánek J, Gunišová S, Dányi I, Szamecz B, Valášek LS. 2011. Translation reinitiation relies on the interaction between eIF3a/TIF32 and progressively folded *cis*-acting mRNA elements preceding short uORFs. *PLoS Genet* **7:** e1002137.

Palam LR, Baird TD, Wek RC. 2011. Phosphorylation of eIF2 facilitates ribosomal bypass of an inhibitory upstream ORF to enhance CHOP translation. *J Biol Chem* **286:** 10939–10949.

Pavlov MY, Watts RE, Tan Z, Cornish VW, Ehrenberg M, Forster AC. 2009. Slow peptide bond formation by proline and other *N*-alkylamino acids in translation. *Proc Natl Acad Sci* **106:** 50–54.

Pisarev AV, Hellen CU, Pestova TV. 2007. Recycling of eukaryotic posttermination ribosomal complexes. *Cell* **131:** 286–299.

Pöyry TA, Kaminski A, Jackson RJ. 2004. What determines whether mammalian ribosomes resume scanning after translation of a short upstream open reading frame? *Genes Dev* **18:** 62–75.

Rajkowitsch L, Vilela C, Berthelot K, Ramirez CV, McCarthy JE. 2004. Reinitiation and recycling are distinct processes occurring downstream of translation termination in yeast. *J Mol Biol* **335:** 71–85.

Raveh-Amit H, Maissel A, Poller J, Marom L, Elroy-Stein O, Shapira M, Livneh E. 2009. Translational control of protein kinase Cη by two upstream open reading frames. *Mol Cell Biol* **29:** 6140–6148.

Roy B, Vaughn JN, Kim BH, Zhou F, Gilchrist MA, Von Arnim AG. 2010. The h subunit of eIF3 promotes reinitiation competence during translation of mRNAs harboring upstream open reading frames. *RNA* **16:** 748–761.

Skabkin MA, Skabkina OV, Hellen CU, Pestova TV. 2013. Reinitiation and other unconventional posttermination events during eukaryotic translation. *Mol Cell* **51:** 249–264.

Sundaram A, Grant CM. 2014. A single inhibitory upstream open reading frame (uORF) is sufficient to regulate *Candida albicans* GCN4 translation in response to amino acid starvation conditions. *RNA* **20:** 559–567.

Szamecz B, Rutkai E, Cuchalová L, Munzarová V, Herrmannová A, Nielsen KH, Burela L, Hinnebusch AG, Valášek L. 2008. eIF3a cooperates with sequences 5′ of uORF1 to promote resumption of scanning by post-termination ribosomes for reinitiation on GCN4 mRNA. *Genes Dev* **22:** 2414–2425.

Valášek LS. 2012. 'Ribozoomin'—translation initiation from the perspective of the ribosome-bound eukaryotic initiation factors (eIFs). *Curr Protein Pept Sci* **13:** 305–330.

Valášek L, Mathew AA, Shin BS, Nielsen KH, Szamecz B, Hinnebusch AG. 2003. The yeast eIF3 subunits TIF32/a, NIP1/c, and eIF5 make critical connections with the 40S ribosome in vivo. *Genes Dev* **17:** 786–799.

Vilela C, Linz B, Rodrigues-Pousada C, McCarthy JE. 1998. The yeast transcription factor genes YAP1 and YAP2 are subject to differential control at the levels of both translation and mRNA stability. *Nucleic Acids Res* **26:** 1150–1159.

von Arnim AG, Jia Q, Vaughn JN. 2014. Regulation of plant translation by upstream open reading frames. *Plant Sci* **214:** 1–12.

Wethmar K. 2014. The regulatory potential of upstream open reading frames in eukaryotic gene expression. *Wiley Interdiscip Rev RNA* **5:** 765–778.

Wohlgemuth WA, Safonova O, Engelhardt M, Freitag M, Wölfle K, Kirchhof K. 2008. Improvement of the quality of life concerning the health of patients with peripheral arterial disease (PAD) after successful bypass surgery. *Vasa* **37:** 338–344.

Zhou F, Roy B, von Arnim AG. 2010. Translation reinitiation and development are compromised in similar ways by mutations in translation initiation factor eIF3h and the ribosomal protein RPL24. *BMC Plant Biol* **10:** 193.

RNA Biology

ISSN: 1547-6286 (Print) 1555-8584 (Online) Journal homepage: http://www.tandfonline.com/loi/krnb20

Does eIF3 promote reinitiation after translation of short upstream ORFs also in mammalian cells?

Vladislava Hronová, Mahabub Pasha Mohammad, Susan Wagner, Josef Pánek, Stanislava Gunišová, Jakub Zeman, Kristýna Poncová & Leoš Shivaya Valášek

To cite this article: Vladislava Hronová, Mahabub Pasha Mohammad, Susan Wagner, Josef Pánek, Stanislava Gunišová, Jakub Zeman, Kristýna Poncová & Leoš Shivaya Valášek (2017): Does eIF3 promote reinitiation after translation of short upstream ORFs also in mammalian cells?, RNA Biology, DOI: 10.1080/15476286.2017.1353863

To link to this article: https://doi.org/10.1080/15476286.2017.1353863

View supplementary material

Accepted author version posted online: 26 Jul 2017.
Published online: 26 Jul 2017.

Submit your article to this journal

Article views: 181

View related articles

View Crossmark data

Full Terms & Conditions of access and use can be found at
http://www.tandfonline.com/action/journalInformation?journalCode=krnb20

Download by: [Charles University in Prague] **Date:** 25 November 2017, At: 10:11

RNA BIOLOGY
2017, VOL. 0, NO. 0, 1–8
https://doi.org/10.1080/15476286.2017.1353863

Taylor & Francis
Taylor & Francis Group

POINT OF VIEW

Check for updates

Does eIF3 promote reinitiation after translation of short upstream ORFs also in mammalian cells?

Vladislava Hronová[a,b], Mahabub Pasha Mohammad[a], Susan Wagner[a], Josef Pánek[c], Stanislava Gunišová[a], Jakub Zeman[a], Kristýna Poncová[a], and Leoš Shivaya Valášek[a]

[a]Laboratory of Regulation of Gene Expression, Institute of Microbiology ASCR, Videnska, Prague, the Czech Republic; [b]Department of Genetics and Microbiology, Faculty of Science, Charles University in Prague, Vinicna, Prague, the Czech Republic; [c]Laboratory of Bioinformatics, Institute of Microbiology ASCR, Videnska, Prague, the Czech Republic

ABSTRACT

Reinitiation after translation of short upstream ORFs (uORFs) represents one of the means of regulation of gene expression on the mRNA-specific level in response to changing environmental conditions. Over the years it has been shown-mainly in budding yeast-that its efficiency depends on *cis*-acting features occurring in sequences flanking reinitiation-permissive uORFs, the nature of their coding sequences, as well as protein factors acting *in trans*. We earlier demonstrated that the first two uORFs from the reinitiation-regulated yeast *GCN4* mRNA leader carry specific structural elements in their 5′ sequences that interact with the translation initiation factor eIF3 to prevent full ribosomal recycling post their translation. Actually, this interaction turned out to be instrumental in stabilizing the mRNA·40S post-termination complex, which is thus capable to eventually resume scanning and reinitiate on the next AUG start site downstream. Recently, we also provided important *in vivo* evidence strongly supporting the long-standing idea that to stimulate reinitiation, eIF3 has to remain bound to ribosomes elongating these uORFs until their stop codon has been reached. Here we examined the importance of eIF3 and sequences flanking uORF1 of the human functional homolog of yeast *GCN4, ATF4*, in stimulation of efficient reinitiation. We revealed that the molecular basis of the reinitiation mechanism is conserved between yeasts and humans.

ARTICLE HISTORY
Received 26 May 2017
Revised 28 June 2017
Accepted 28 June 2017

KEYWORDS
ATF4; eIF3; GCN4; mRNA; ribosome; reinitiation; translational control

Downloaded by [Charles University in Prague] at 10:11 25 November 2017

Introduction

Translation of mRNA has four stages: initiation, elongation, termination, and ribosome recycling. During recycling, the post-termination 80S ribosome is first split into the small 40S and large 60S subunits by the energy-depended action of ABCE1.[1] However, mRNA and deacylated tRNA remain bound to the small subunit and must be removed in the second step by a joint action of either canonical initiation factors eIF1, eIF1A and eIF3, or by eIF2D (also known as Ligatin) or by the heterodimer MCT1-DENR.[2-5] As such, ribosome recycling can be considered as the link between translation termination and initiation because termination, recycling and initiation use several factors in common, like for example eIF3.[6-8] Even though ribosome recycling naturally captures the translational cycle, there are specific exceptions where the completion of the full recycling step is undesirable or even detrimental, and the termination reaction is followed by reinitiation (REI) on the same mRNA molecule at a site downstream of the stop codon (reviewed in[6,9,10]). Translation reinitiation is a gene-specific regulatory mechanism where upon translation of the so-called REI-permissive short upstream ORF (uORF) only the large 60S subunit and deacylated tRNA are recycled, whereas the mRNA is retained on the post-termination 40S subunit to allow REI downstream. It has been well established that most of relatively widespread uORFs across all eukaryotic genomes in principle inhibits expression of the main ORF by preventing the fully recycled ribosome to reach its start site. Hence, existence of REI-permissive uORFs, which are often part of intricate regulatory circuits together with REI-non-permissive uORFs, is very critical as it enables-upon various stimuli-efficient expression of a main ORF. Importantly, various oncogenes, proteins involved in differentiation, development, cell cycle, stress response, learning and memory forming can be found on the list of REI-regulated mRNAs (see for example[11-13]).

Practically since the onset of this scientific direction, the textbook example of an mRNA regulated *via* REI has been the yeast *GCN4* gene encoding a very potent transcriptional activator.[14] The *GCN4* mRNA contains four short uORFs in its 5′ leader, out of which the first two (uORF1 and uORF2) are highly REI-permissive, while the remaining two (uORF3 and uORF4) allow only negligible levels of REI.[15,16] Their specific effects in combination with stress-induced changes in the level of one of the key initiating complexes composed of Met-tRNA$_i^{Met}$ and eIF2·GTP (the so-called ternary complex-TC) create a fail-safe mechanism that allows *GCN4* translation only under specific stresses.[15,17] The trick is that the distance between the REI-permissive vs. non-permissive uORFs is long enough that under non-stress conditions (characteristic of high TC levels)

CONTACT Leoš Shivaya Valášek valasekl@biomed.cas.cz Laboratory of Regulation of Gene Expression, Institute of Microbiology ASCR, Videnska 1083, Prague, Czech Republic, 14220.

Supplemental data for this article can be accessed on the publisher's website.

© 2017 Taylor & Francis Group, LLC

Downloaded by [Charles University in Prague] at 10:11 25 November 2017

most of the post-termination 40S ribosomes scanning downstream from uORF1 or uORF2 stop codons will reacquire the TC before AUG of uORF3 or uORF4 has been reached-as a result the GCN4 protein cannot be made. At the same time, it is short enough to ensure that under specific stress conditions (characteristic of low TC levels, when longer time is needed to reacquire the TC), majority of these ribosomes will rebind the TC after bypassing the REI-non-permissive uORFs-as a result these will be skipped and the *GCN4* translation eventually initiated. Over the years it has been demonstrated that the REI potential of uORF1 and uORF2 is determined by: (i) the presence of the AU-rich motif in the 3′ sequence; (ii) their defined length and coding triplets composition; (iii) specific REI-promoting elements (RPEs) situated in their 5′ sequences; and (iv.) the functional interaction of some of the RPEs (namely RPE i. and iv. of uORF1 and RPE v. of uORF2) with the N-terminal domain (NTD) of the a/TIF32 subunit of the translation initiation factor 3 (eIF3) within the context of the post-termination mRNA·40S complex.[15,16,18-24] The favorable location of the a/TIF32-NTD on the 40S subunit next to the mRNA exit channel[25-27] led to an idea that while the eIF3-bound 40S ribosome scans through the region upstream of uORF1 (or uORF2) and translates it as the fully assembled 80S ribosome still bound by eIF3, the RPEs progressively fold into a specific secondary structure. Upon termination, eIF3 interacts with these RPEs to specifically stabilize only the small ribosomal subunit on the uORF1 (or uORF2) stop codon. Thanks to this incomplete ribosomal recycling, the post-termination 40S subunit can, upon acquisition of other essential eIFs, subsequently resume scanning for REI downstream.[21] Actually, continued presence of some eIFs on early elongating ribosomes as a prerequisite for efficient REI had been a long standing hypothesis[18] that was strongly supported by our most recent yeast work.[28] With the help of a newly developed *in vivo* RNA-protein Ni^{+2} pull down (Rap-Nip) assay we have clearly demonstrated that eIF3 does travel with early elongating ribosomes and interacts with RPEs *in vivo*, and this eIF3s ability is critical for stimulation of efficient reinitiation downstream of REI-promoting uORFs. Besides eIF3, the mRNA-delivery eIF4F complex, and particularly the central one-third fragment of eIF4G interacting with eIF3 and eIF4A, was also suggested to remain bound to early elongation ribosomes and promote efficient REI, at least in an *in vitro* reconstituted mammalian system.[29] However, firm experimental evidence is lacking in this case.

Here we set out to examine whether the just described molecular mechanism of REI relying on *cis*-acting features of REI-permissive uORFs and eIF3 is conserved between yeasts and humans. We used an extensively studied mRNA encoding transcriptional activator ATF4 (the mammalian functional homolog of yeast GCN4) that contains two uORFs as a reporter that we mutagenized. We also knocked down several eIF3 subunits, in particular eIF3a (implicated in REI in yeasts[21]) and eIF3h (shown to stimulate REI in plants[30,31]), and checked their effects on REI efficiency in human cells. Our analysis revealed that the *ATF4*s uORF1 is in analogy to uORF1 of *GCN4* also surrounded by *cis*-acting features, with those occurring in its 5′ leader specifically structured, that ensure its permissiveness for REI. Furthermore, we also show that human eIF3h (like its plant counterpart) enhances efficiency of REI.

Novel insights into the molecular mechanism of reinitiation in human cells

Sequences flanking uORF1 of ATF4 substantially increase its reinitiation potential

As mentioned above, mammalian *ATF4* mRNA contains only two uORFs in its leader in contrast to four uORFs of yeast *GCN4* (Fig. 1A). However, only the first uORF1 of the two fulfills the requirements of a typical short uORF with a REI-potential because it is composed of only three sense codons and the distance between its stop codon and AUG of uORF2 is in most species 87 nucleotides or close to it. (Based on Kozak 1987,[32] the optimal distance ensuring efficient REI in mammals is 80 nt and more.) This could enable a similar mode of regulation under stress vs. non-stress conditions like in the case of *GCN4* despite the fact that *ATF4*s uORF2 is markedly different from *GCN4*s uORFs 3 and 4. It is too long to be even considered as an uORF with some REI potential (59 amino acids residues) and, most importantly, its sequence partially overlaps the *ATF4* ORF in a different reading frame. Therefore, according to the current model, all ribosomes that reinitiate on uORF2 will under normal conditions terminate past the *ATF4* AUG and thus prevent its translation.[33,34] Nonetheless, taking into account the striking similarity between the *GCN4*s and *ATF4*s uORF1 with respect to their arrangement and proposed function, we were curious to examine what else they have in common. In other words, we asked whether *ATF4*s uORF1 utilizes an identical molecular strategy to that of *GCN4*s uORF1.

To answer this question, we first isolated total RNA from human HEK293T cells and using the 5′ RLM-RACE system from Ambion, generated cDNA carrying full-length 5′ UTR of human *ATF4* and precisely mapped its transcriptional start site (Fig. 1C). We then replaced the 5′ and 3′ sequences (either individually or in combination) of human *ATF4*s uORF1, which might hypothetically correspond to the 5′ RPEs and 3′ AU-rich motif of *GCN4*s uORF1, with stretches of supposedly linear (CAA)n triplets (Fig. 1A). In detail, we replaced 69 nts upstream of uORF1 (in "CAAup") and 25 nts downstream of uORF1 (in "CAAdown"); in addition we combined these mutations in a single construct "CAAup+down." The resulting mutant variants were introduced into the uORF1-only *ATF4-Luc* construct containing solitary uORF1 kindly provided by the Wek's laboratory[33] and the luciferase activity, as an indicator of the REI efficiency, was measured in HEK293T cells and normalized to mRNA levels of individual constructs. Please note that the inhibitory effect of uORF2 was neutralized by mutating its AUG to AGG implying that these constructs could be analyzed without using a stress inducer. As shown in Fig. 1B, both sequences flanking uORF1 are-in a striking analogy to the *GCN4*s uORF1-required for efficient REI. Replacement of the 5′ sequence ("CAAup") decreased the REI efficiency to a greater extent (down to ~47%) than the replacement of the 3′ sequence ("CAAdown;" down to ~71%), suggesting that its contribution is significantly greater. Interestingly, the opposite is true in case of the *GCN4*s uORF1[21]. The combination of both mutations ("CAA up+-down") produced a fully additive effect-downregulation to ~35% (Fig. 1B). Together these findings strongly indicate that both upstream and downstream sequences of uORF1

Downloaded by [Charles University in Prague] at 10:11 25 November 2017

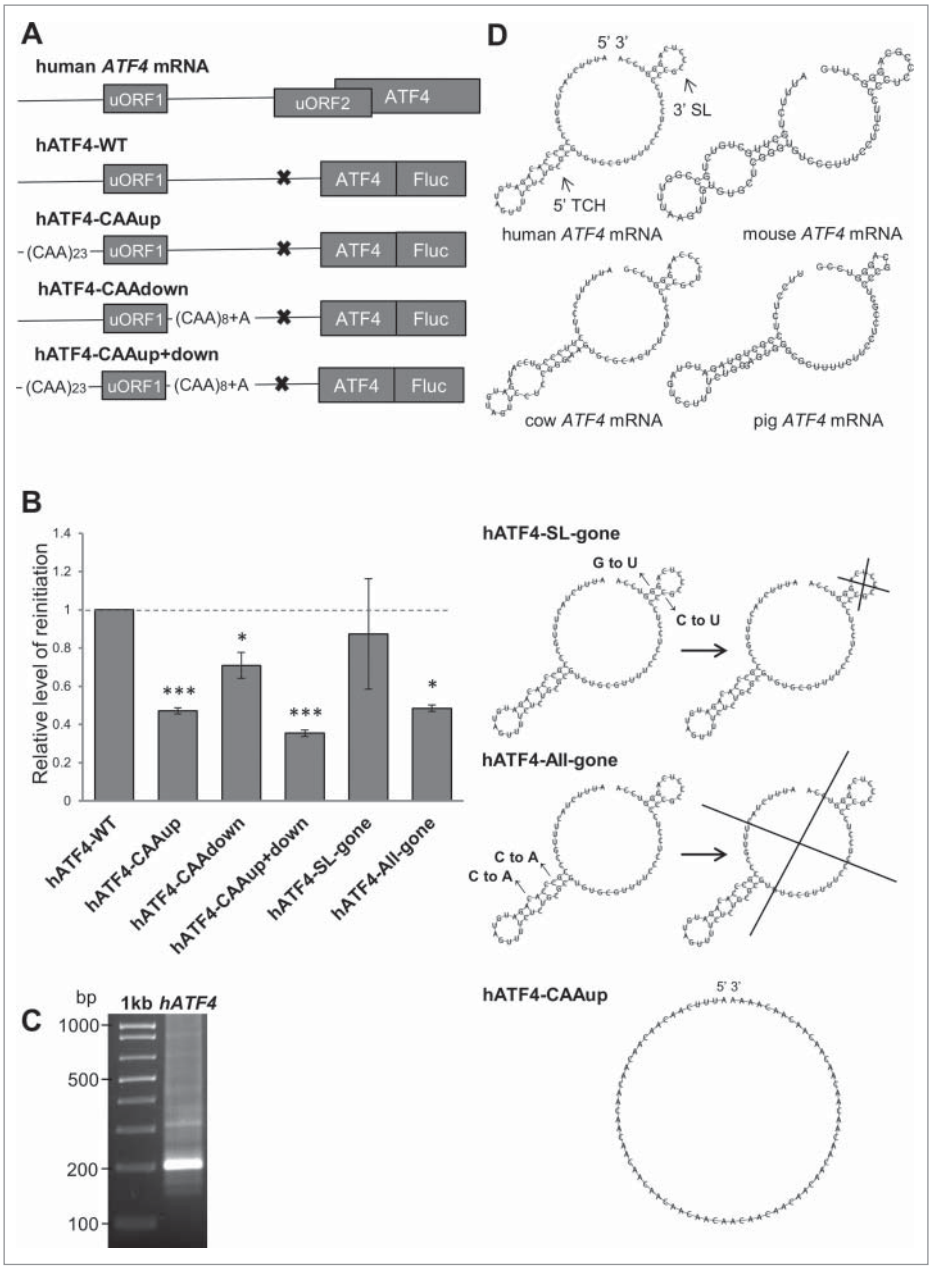

Figure 1. Flanking sequences of human *ATF4*s uORF1 individually contribute to ensure its high propensity for reinitiation. A) Schematics of the human *ATF4* mRNA and mutagenized constructs used in this study. Please note that the inhibitory effect of uORF2 was neutralized by mutating its AUG to AGG to simplify the analysis, because thus modified constructs could be analyzed without using a stress inducer. In "CAAup," a major part of the original sequence upstream of uORF1 was replaced by 23 CAA triplets (the transcriptional start site and 9 nts immediately preceding AUG of uORF1 that are buried in the mRNA binding channel of the ribosome terminating on uORF1 were left intact, as in case of *GCN4*s uORF1[21]); in "CAAdown," the original sequence encompassing 25 nts immediately following the stop codon of uORF1 was replaced by 7 CAA triplets followed by one CAAA tetranucleotide; in "CAAup+down," both of these substitutions were combined. B) All constructs shown in A) were transfected into HEK293T cells and subjected to Dual luciferase assay normalized to mRNA levels (Fluc/Rluc) as described in Materials and Methods. The statistical analysis was performed using One sample *t* test; statistical significance is indicated by stars (one star means $P \leq 0.05$, 3 stars $P \leq 0.001$). C) 5RLM-RACE of human *ATF4* cDNA prepared from total RNA derived from HEK293T cells. DNA sample was separated by gel electrophoresis in a 2% agarose gel, cut out and processed to be sequenced (the obtained sequence indeed corresponded to the 5′ UTR of human *ATF4* mRNA - NM_182810 in NCBI). Size markers in base pairs are indicated in the left. D) Secondary structure predictions of the entire 5′ sequence of *ATF4*s uORF1 in indicated mammals as determined by the RNA Vienna package software.[35] The bottom panels depict the "CAAup" mutation and 2 double-point substitutions engineered to disrupt either the individual structures or the 5′ UTR fold as whole. Please see the main text for further details.

independently contribute to its overall REI potential by more than 60%, suggesting that this important translational control mechanism is evolutionary conserved.

Given the fact that the 5′ sequence of the *GCN4*s uORF1, as well as the 5′ sequence of a single uORF of another yeast transcriptional activator YAP1, contain specific structural and sequence-specific REI-promoting *cis*-acting features, the RPEs,[21] we next investigated whether the 5′ sequence of *ATF4*s uORF1 also adopt some specific structure, and if so, whether it is also important for efficient REI. Therefore, we subjected the entire region preceding the *ATF4* uORF1 to *in silico* modeling by the RNA Vienna package software.[35] As in case of *GCN4*, our prediction was based on the fact that the 5′ sequence is not a standalone molecule with a rigid structure but its fold forms

Downloaded by [Charles University in Prague] at 10:11 25 November 2017

and changes dynamically as the sequence emerges from the ribosomal mRNA exit pore.[21] Hence, we divided the 5′ UTR of uORF1 into two consecutive segments and first folded the extreme 5′ segment, which formed a stable triple-circle hairpin ("5′ TCH") (Fig. 1D). After that we added the other segment and continued with modeling of the entire 5′ sequence as it emerged from the mRNA exit pore with the initially identified 5′ triple-circle hairpin structure "pre-folded." As a result, a stem-loop formed proximal to the 3′ end ("3′ SL"), in addition to the 5′ triple-circle hairpin. These structures and their spacing not only resemble similar structures representing *GCN4*s RPEs ii. and iv.,[21] they also seem to be very well conserved at least among other mammalian species (Fig. 1D).

To examine the prospective physiologic importance of these structures, we further used *in silico* modeling to design and test minimal mutations disrupting one or the other structure using the same reporter system as described above. The first mutation, "SL-gone" (where C64 and G73 were both mutated to Us), was designed to disrupt the 3′ stem-loop; however, its effect on luciferase activity was very mild (~13% reduction) indicating that this stem-loop contributes to REI only negligibly (Fig. 1B). We did not find any computational prediction that would disrupt selectively only the 5′ triple-circle hairpin, hence as the second mutation we chose "All-gone" (where C17 and C21 were both mutated to As), which disrupts both structures. Strikingly, the effect of this mutation showed the same dramatic drop in the luciferase activity as the "CAAup" construct (down to ~49%) strongly suggesting that the 5′ triple-circle hairpin highly likely is what lies behind the REI-promoting effect of 5′ sequences of *ATF4* uORF1 (Fig. 1B). However, at present we cannot tell whether it is the entire specific structure or only some sequential motif within this structure, like for example the apical circle that is required for its function in promoting REI.

eIF3h promotes translation reinitiation in human cells

As mentioned above, RPE i. and iv. of the *GCN4*s uORF1 specifically interact with the N-terminal domain of the a/TIF32 subunit of eIF3 and this interaction is instrumental for stabilizing the 40S·mRNA post-termination complex. Hence the next obvious question we asked was whether human eIF3 also contributes to efficient REI on the *ATF4* mRNA. To our knowledge, the prospective role of eIF3a in REI has never been tested in the past; however, there are a few reports implicating the eIF3h subunit in REI in plants.[30,31] To address this question, we individually reduced the eIF3a and eIF3h expression by knocking them down with On-target plus siRNA system (Dharmacon) as described before,[36,37] and measured the luciferase activity in thus treated HeLa cells transfected with human *ATF4-Luc* constructs bearing either uORF1 alone ("uORF1-only") or none of the uORFs ("d-all") (Fig. 2A). The latter construct was used for normalization purposes. As a control we used cells treated with non-targeting siRNA, as well as cells knocked down for eIF3k. The knock down efficiency for all 3 eIF3 subunits was as observed before[37]-expression was reduced by ~70–80% (Fig. 2B). Please note that we used HeLa instead of HEK293T cells owing to the fact that the efficiency of downregulation of all eIF3 subunits is significantly greater in HeLa cells.[36] Also note that the eIF3k knock down results in the loss of only two non-essential subunits (eIF3k by itself and its interacting partner eIF3l) from the rest of human 12-subunit eIF3, the eIF3h knock down eliminates itself plus both eIF3kandl, whereas the eIF3a knock down pretty much destroys the entire eIF3 complex leaving intact only the "Yeast-Like-Core" assembly composed of the eIF3b–eIF3i–eIF3g subunits (Fig. 2B).[36,37] As shown in Fig. 2C, the eIF3k knock down displayed practically no impact on the efficiency of REI; similarly the eIF3a knock down produced only an insignificantly modest reduction (by ~11%). However, the eIF3h knock down led to a statistically significant reduction by ~34%. Importantly, the eIF3a knock down as the only knock down downregulated general translation initiation rates as judged from our measurements of the "d-all" construct; this is expected given the detrimental consequences of the eIF3a knock down on the overall integrity of the entire eIF3 complex and its function in general initiation.[36,37] Hence, we cannot conclude anything specific regarding its involvement in REI in mammals. However, the fact that the eIF3h knock down (co-downregulating also the expression of the eIF3kandl dimer) clearly impacted the efficiency of REI, whereas the eIF3k knock down (co-downregulating only the eIF3kandl dimer) showed no impact whatsoever, suggests that eIF3h does enhance efficiency of REI also in humans.

Concluding remarks

Two questions we asked in this article were: (1) Is there any mechanistic resemblance in the *modus operandi* between REI-permissive uORFs from mRNA leaders of functional homologs from two rather diverse eukaryotic organisms like yeasts (*GCN4*) and humans (*ATF4*)?; and (2) Does eIF3a and/or eIF3h promote reinitiation in mammals? The answer is yes to both questions. Flanking sequences of *ATF4*s uORF1 independently contribute to significantly boost the basic level of REI that this uORF allows. In addition, its 5′ sequence contains two well conserved structural features-the 5′ triple-circle hairpin and the 3′ stem-loop-that resemble the structural features of *GCN4*s uORF1 and the former of which seems to be fully responsible for the observed effect. Finally, whether or not eIF3a promotes REI as in budding yeast cannot be judged from our analysis; however, eIF3h does seem to be involved like in plants. In fact, it is interesting to note that human eIF3h seems to adopt a similar position on the ribosome to the REI-promoting N-terminal domain of yeast eIF3a/TIF32; i.e., right next to the mRNA exit channel (Fig. 2D), where it could interact with the 5′ triple-circle hairpin post uORF1 translation. This further supports the idea that in the 12-subunit eIF3 complex, eIF3h has a direct role in stimulating reinitiation.

According to recent reports, uORFs occur at a much higher frequency in mammalian (~45%) mRNAs than in yeast (~13%).[11,38-40] Yeast studies on *GCN4* and *YAP1* mRNA leaders,[16,21,41] as well as an early report examining REI efficiency of randomly generated uORFs[42] strongly suggest that majority of yeast uORFs are severely REI-non-permissive. Even though uORFs are prevalent translational repressors also in mammals,[43,44] there is a prevailing notion that uORFs in mammalian mRNAs (including randomly laboratory-designed uORFs)

Downloaded by [Charles University in Prague] at 10:11 25 November 2017

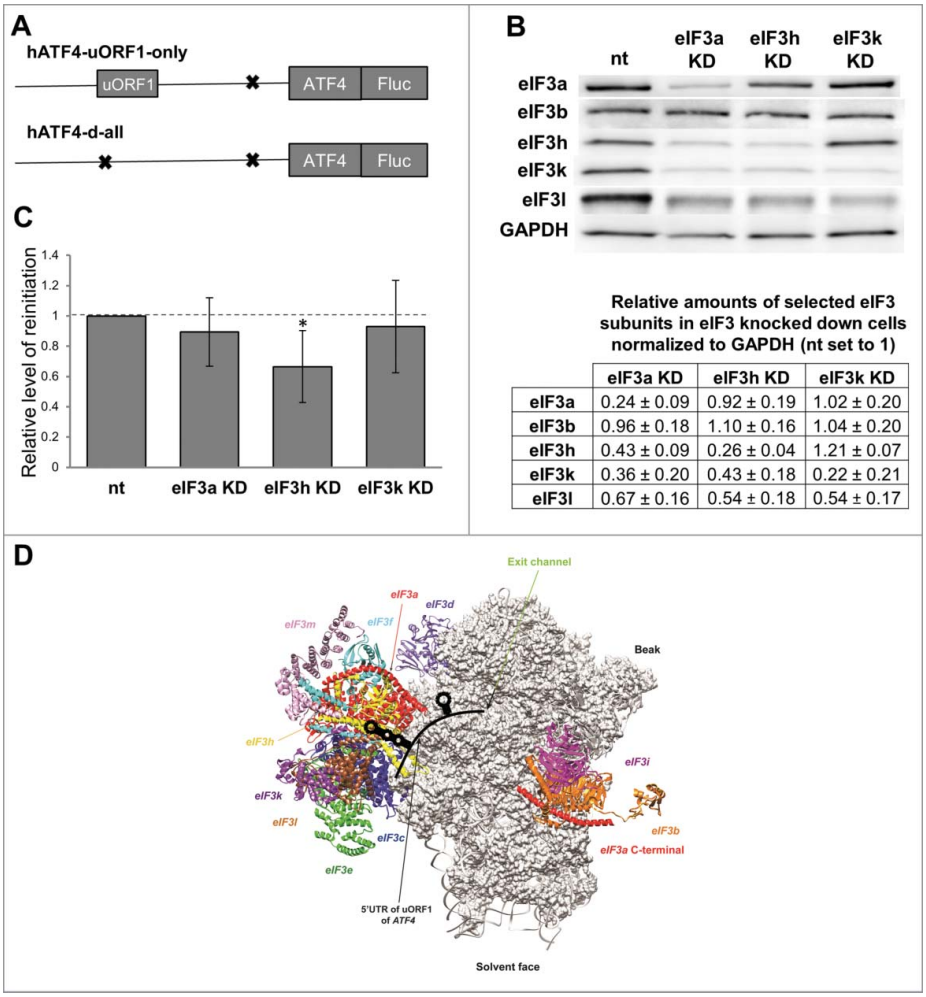

Relative amounts of selected eIF3 subunits in eIF3 knocked down cells normalized to GAPDH (nt set to 1)

	eIF3a KD	eIF3h KD	eIF3k KD
eIF3a	0.24 ± 0.09	0.92 ± 0.19	1.02 ± 0.20
eIF3b	0.96 ± 0.18	1.10 ± 0.16	1.04 ± 0.20
eIF3h	0.43 ± 0.09	0.26 ± 0.04	1.21 ± 0.07
eIF3k	0.36 ± 0.20	0.43 ± 0.18	0.22 ± 0.21
eIF3l	0.67 ± 0.16	0.54 ± 0.18	0.54 ± 0.17

Figure 2. The eIF3h subunit of human eIF3 enhances efficiency of resumption of scanning from *ATF4*s uORF1 for reinitiation downstream. A) Schematics of *hATF4-Fluc* constructs used in C). B) Efficiency of siRNA-mediated downregulation and co-downregulation of protein levels of selected eIF3 subunits normalized to house-keeping GAPDH and Non-targeted (nt) control cells estimated by Western blotting. C) Relative *Firefly* luciferase signals obtained from HeLa cells knocked down for indicated eIF3 subunits transfected with either the "uORF1-only" or "d-all" constructs (the latter was used for normalization purposes), expressed as relative percentages of *Fluc* signals obtained from Non-targeted control (nt) cells. The *Firefly* luciferase signals were individually normalized to mRNA levels of each reporter, which were beforehand normalized to the spike RNA added before the RNA extraction. Statistical analysis was performed using One sample *t* test; statistical significance is indicated by stars (one star means $P \leq 0.05$). D) Graphical illustration of the proposed arrangement of the post-termination complex on *ATF4*s uORF1 with its secondary structures interacting with the eIF3h subunit of eIF3 to promote resumption of scanning for REI on the *ATF4* mRNA. Depicted is the exit channel view of the 48S PIC (adopted from[47]) illustrating 12 color-coded eIF3 subunits with eIF3a and eIF3h indicated by an arrow. The 5′ UTR of the *ATF4*s uORF1 highlighting its secondary structures is shown in black.

are in general less repressive for REI than in yeast, usually reducing protein expression by 30 to 80% (i.e., they allow at least some resumption of scanning and reinitiation),[11] which suggests that there might be a smaller requirement for specific sequences.[9] Our results from both yeast and humans seem to agree with this theory, because whereas eliminating all *cis*-acting sequences flanking uORF1 or uORF2 of yeast *GCN4* fully abolished their REI potential,[16] substituting the similar sequences flanking *ATF4*s uORF1 with unstructured stretches of CAA repeats reduced the efficiency of REI "only" by ~65% (Fig. 1B; hATF4-CAAupanddown). Hence it does seem likely that most of mammalian uORFs are less inhibitory than in yeast, and only if they form an integral part of some sophisticated stress-related regulatory system often containing more than one uORF, nature equipped some of them with specific *cis*-acing features that render them highly permissive. What lies behind this difference between budding yeast and humans (mammals)?

It could very well be the nature of the two initiation factors that have been implicated in stimulating REI in one and/or the other organism; i.e., eIF3 and to a lesser extent also eIF4G,[20,21,29] and that differ most dramatically between yeast and vertebrates in several aspects. (1) Human eIF3 has practically twice as many subunits than its yeast counterpart; (2) human eIF4G is markedly longer and has more direct interacting partners; and 3), perhaps the most important difference is that mammalian eIF3 does directly interact with eIF4G; however, in yeasts this contact is supposedly only bridged by eIF5 and eIF1 (reviewed in [6,9]).

If we assume that eIF4G and eIF3 are indeed capable to persist throughout uORF translation on the mammalian 80S ribosome to stabilize the post-termination mRNA·40S complex, their direct contact could substantially empower this stabilization process. This would set the basal level of permissiveness for REI in mammals higher than it is set in the budding yeast, where these two factors do not directly interact, which may weaken the eIF4G interaction with elongating ribosomes. In the light of the recent findings, the fact that the recycling factor ABCE1 interacts with the intersubunit face of the 40S subunit

even after ribosomal recycling and most likely also promotes the initiation phase in close co-operation with eIF3[45,46] further suggests that eIF4G could, *via* its direct connection with eIF3, modulate ribosomal recycling in a way that would favor dissociation of only the 60S subunit and deacylated tRNA, which would stimulate REI. Since reinitiation-as a molecular phenomenon-is also rather interesting from the medical point of view (there is a rapidly growing number of articles reporting contributions of defective uORF functions to various human diseases[10]), more work is certainly needed to fully understand the mechanistic aspects of this intriguing difference, as well as the reinitiation mechanism as a whole.

Material and methods

Dual luciferase reporter assays

HEK293T cells were grown at 37°C and 5% CO_2 in 6-well plates in DMEM (Sigma, cat # D6429) supplemented with 10% FBS (Sigma, cat # F7524). The cells were lysed directly on plate with 1x Glo Lysis Buffer (Promega, cat # E266A) exactly 24 hours after the *Firefly* and *Renilla* reporter plasmids transfection with TurboFect (Thermo Scientific, cat # R0531). The lysate was then transferred into a white flat-bottom 96-well plate and part of the lysate was stored for RNA isolation. The Dual-Glo® Luciferase Assay System (Promega, cat # E2940) was used according to the vendor's instructions. The *Renilla* luciferase signal was used for normalization purposes. Total RNA was isolated using the RNA Blue reagent (Top Bio, cat # R013) according to the manufacturer's instructions. After the Turbo DNase digestion (Ambion, cat # AM2238), cDNA was synthesized using the High-capacity cDNA reverse transcription kit (Applied Biosystems, # 4368813). qPCR was performed using 5 × HOT FIREPol EvaGreen qPCR Mix Plus (Solis BioDyne # 08–25–00020). The mRNA levels of *Firefly* luciferase were normalized to *Renilla* luciferase mRNA levels. The obtained qPCR data were used for normalization of measured luciferase activities. qPCR primers are listed in Supplementary Table S1.

siRNA treatment, whole cell extract preparation and Western blotting

HeLa cells were grown at 37°C and 5% CO_2 in 6-well plates in DMEM (Sigma, cat # D6429) supplemented with 10% FBS (Sigma, cat # F7524). 24 hours after seeding, cells were transfected with the ON-TARGETplus siRNA cocktail system from Dharmacon at a final concentration of 5 nM (human eIF3a cat # L-019534–00, eIF3h cat # L-003883–00, eIF3k cat # L-020216–02 and Non-Targeting siRNA cat # D-001810–10). INTERFERin (Polyplus, cat # 409) was used as a transfection reagent and transfection was performed according to the vendor's instructions.

For Western blotting, cells were harvested 3 d after siRNA transfection in lysis buffer containing 1M Tris-HCl pH6.8, 20% glycerol, 20% SDS, 2% β-merkaptoethanol and 5% bromphenolblue. All samples were resolved using SDS-PAGE followed by Western blotting. All primary antibodies used in this study are listed in Supplementary Table S2. The Western signals were developed using the SuperSignal West Femto Maximum Sensitivity Substrate from Thermo Scientific (cat # 34096) and detected in a G-Box imager from Syngene using a series of varying exposure times. Signals were processed with Quantity One (BioRad). The resulting values were normalized as indicated in the corresponding figure legend.

For siRNA treatments followed by *Firefly* luciferase reporter assays, transfection of *Firefly* reporter plasmids was performed 48 hours after the siRNA treatment and cells were harvested 24 hours later as described above. The *Firefly* luciferase signal was normalized to the reporter's mRNA level, which was beforehand normalized to the spike RNA (particularly yeast *RPL41a* mRNA) added before the RNA extraction. In detail, HeLa cells in 6-well plates were lysed in 200 μl of 1x Glo Lysis Buffer (Promega, cat # E266A). 70 μl of this lysate was directly used for the luciferase reporter assay, and another 70 μl was mixed with 2 μl of yeast spike *RPL41a* mRNA to the final amount of approx. 100 ng per sample, and subsequently also with 750 μl of RNA Blue reagent (Top Bio, cat # R013). The total RNA was isolated according to the manufacturer's instructions. After the Turbo DNase digestion (Ambion, cat # AM2238), cDNA was synthesized using the High-capacity cDNA reverse transcription kit (Applied Biosystems, # 4368813). qPCR was performed using 5 × HOT FIREPol EvaGreen qPCR Mix Plus (Solis BioDyne # 08–25–00020). The signal from *Firefly* luciferase reporter plasmid was normalized to its mRNA levels, which were already normalized to the spike *RPL41a* mRNA to correct for any loss during the RNA isolation. The obtained values with individual constructs were finally normalized to the nt siRNA and the "d-all" control construct, the latter of which corrects for defects in general translation initiation.

Disclosure of potential conflicts of interest

No potential conflicts of interest were disclosed.

Acknowledgements

We are thankful to Ron Wek for the ATF4 reporter plasmids and advise, to Olga Krýdová for technical and administrative assistance, and to the members of the Valášek laboratory for helpful suggestions.

Funding

This research was supported by the Czech Science Foundation Grant GA15–10116S (to L.S.V.) and Charles University in Prague, project GA UK no. 10315 (to V.H.).

References

1. Shoemaker CJ, Green R. Kinetic analysis reveals the ordered coupling of translation termination and ribosome recycling in yeast. Proc Natl Acad Sci U S A. 2011;108:E1392-8. doi:10.1073/pnas.1113956108.
2. Pisarev AV, Hellen CUT, Pestova TV. Recycling of eukaryotic posttermination ribosomal complexes. Cell. 2007;131:286-99. doi:10.1016/j.cell.2007.08.041.
3. Pisarev AV, Skabkin MA, Pisareva VP, Skabkina OV, Rakotondrafara AM, Hentze MW, Hellen CU, Pestova TV. The role of ABCE1 in eukaryotic posttermination ribosomal recycling. Mol Cell. 2010;37:196-210. doi:10.1016/j.molcel.2009.12.034.

Downloaded by [Charles University in Prague] at 10:11 25 November 2017

Downloaded by [Charles University in Prague] at 10:11 25 November 2017

4. Skabkin MA, Skabkina OV, Dhote V, Komar AA, Hellen CU, Pestova TV. Activities of ligatin and MCT-1/DENR in eukaryotic translation initiation and ribosomal recycling. Genes Dev. 2010;24:1787-801. doi:10.1101/gad.1957510.
5. Guydosh NR, Green R. Dom34 rescues ribosomes in 3′ untranslated regions. Cell. 2014;156:950-62. doi:10.1016/j.cell.2014.02.006.
6. Valášek LS. 'Ribozoomin'-translation initiation from the perspective of the ribosome-bound Eukaryotic Initiation Factors (eIFs). Curr Protein Pept Sci. 2012;13:305-30. doi:10.2174/138920312801619385.
7. Beznosková P, Cuchalová L, Wagner S, Shoemaker CJ, Gunišová S, von der Haar T, Valášek LS. Translation initiation factors eIF3 and HCR1 control translation termination and stop codon read-through in yeast cells. PLoS Genet. 2013;9:e1003962. doi:10.1371/journal.pgen.1003962.
8. Beznoskova P, Wagner S, Jansen ME, von der Haar T, Valasek LS. Translation initiation factor eIF3 promotes programmed stop codon readthrough. Nucleic Acids Res. 2015;43:5099-111. doi:10.1093/nar/gkv421.
9. Jackson RJ, Hellen CU, Pestova TV. Termination and post-termination events in eukaryotic translation. Adv Protein Chem Struct Biol. 2012;86:45-93. doi:10.1016/B978-0-12-386497-0.00002-5.
10. Wethmar K. The regulatory potential of upstream open reading frames in eukaryotic gene expression. Wiley Interdiscip Rev RNA. 2014;5:765-78. doi:10.1002/wrna.1245.
11. Calvo SE, Pagliarini DJ, Mootha VK. Upstream open reading frames cause widespread reduction of protein expression and are polymorphic among humans. PNAS. 2009;106:7507-12. doi:10.1073/pnas.0810916106.
12. Barbosa C, Peixeiro I, Romao L. Gene expression regulation by upstream open reading frames and human disease. PLoS Genet. 2013;9:e1003529. doi:10.1371/journal.pgen.1003529.
13. Janich P, Arpat AB, Castelo-Szekely V, Lopes M, Gatfield D. Ribosome profiling reveals the rhythmic liver translatome and circadian clock regulation by upstream open reading frames. Genome Res. 2015;25:1848-59. doi:10.1101/gr.195404.115.
14. Hinnebusch AG. Translational regulation of GCN4 and the general amino acid control of yeast. Annu Rev Microbiol. 2005;59:407-50. doi:10.1146/annurev.micro.59.031805.133833.
15. Gunisova S, Valasek LS. Fail-safe mechanism of GCN4 translational control-uORF2 promotes reinitiation by analogous mechanism to uORF1 and thus secures its key role in GCN4 expression. Nucleic Acids Res. 2014;42:5880-93. doi:10.1093/nar/gku204.
16. Gunisova S, Beznoskova P, Mohammad MP, Vlckova V, Valasek LS. In-depth analysis of cis-determinants that either promote or inhibit reinitiation on GCN4 mRNA after translation of its four short uORFs. RNA. 2016;22:542-58. doi:10.1261/rna.055046.115.
17. Mueller PP, Hinnebusch AG. Multiple upstream AUG codons mediate translational control of *GCN4*. Cell. 1986;45:201-7. doi:10.1016/0092-8674(86)90384-3.
18. Kozak M. Constraints on reinitiation of translation in mammals. Nucleic Acids Res. 2001;29:5226-32. doi:10.1093/nar/29.24.5226.
19. Luukkonen BG, Tan W, Schwartz S. Efficiency of reinitiation of translation on human immunodeficiency virus type 1 mRNAs is determined by the length of the upstream open reading frame and by intercistronic distance. J Virol. 1995;69:4086-94
20. Szamecz B, Rutkai E, Cuchalová L, Munzarová V, Herrmannová A, Nielsen KH, Burela L, Hinnebusch AG, Valásek L. eIF3a cooperates with sequences 5′ of uORF1 to promote resumption of scanning by post-termination ribosomes for reinitiation on GCN4 mRNA. Genes Dev. 2008;22:2414-25. doi:10.1101/gad.480508.
21. Munzarová V, Pánek J, Gunišová S, Dányi I, Szamecz B, Valášek LS. Translation reinitiation relies on the interaction between eIF3a/TIF32 and progressively folded cis-acting mRNA elements preceding short uORFs. PLoS Genet. 2011;7:e1002137. doi:10.1371/journal.pgen.1002137.
22. Grant CM, Hinnebusch AG. Effect of sequence context at stop codons on efficiency of reinitiation in *GCN4* translational control. Mol Cell Biol. 1994;14:606-18. doi:10.1128/MCB.14.1.606.
23. Grant CM, Miller PF, Hinnebusch AG. Sequences 5′ of the first upstream open reading frame in *GCN4* mRNA are required for efficient translational reinitiation. Nuc Acids Res. 1995;23:3980-8. doi:10.1093/nar/23.19.3980.
24. Miller PF, Hinnebusch AG. Sequences that surround the stop codons of upstream open reading frames in *GCN4* mRNA determine their distinct functions in translational control. Genes and Development. 1989;3:1217-25. doi:10.1101/gad.3.8.1217.
25. Erzberger JP, Stengel F, Pellarin R, Zhang S, Schaefer T, Aylett CH, Cimermančič P, Boehringer D, Sali A, Aebersold R, et al. Molecular architecture of the 40SeIF1eIF3 translation initiation complex. Cell. 2014;158:1123-35. doi:10.1016/j.cell.2014.07.044.
26. Valášek L, Mathew AA, Shin BS, Nielsen KH, Szamecz B, Hinnebusch AG. The yeast eIF3 Subunits TIF32/a and NIP1/c and eIF5 make critical connections with the 40S Ribosome in vivo. Genes Dev. 2003;17:786-99. doi:10.1101/gad.1065403.
27. Kouba T, Dányi I, Gunišová S, Munzarová V, Vlčková V, Cuchalová L, Neueder A, Milkereit P, Valášek LS. Small ribosomal protein RPS0 stimulates translation initiation by mediating 40S-binding of eIF3 via its direct contact with the eIF3a/TIF32 Subunit. PLoS One. 2012;7:e40464. doi:10.1371/journal.pone.0040464.
28. Mohammad MP, Munzarova Pondelickova V, Zeman J, Gunisova S, Valasek LS. In vivo evidence that eIF3 stays bound to ribosomes elongating and terminating on short upstream ORFs to promote reinitiation. Nucleic Acids Res. 2017;45:2658-74. doi:10.1093/nar/gkx049.
29. Pöyry TA, Kaminski A, Jackson RJ. What determines whether mammalian ribosomes resume scanning after translation of a short upstream open reading frame? Genes Dev. 2004;18:62-75. doi:10.1101/gad.276504.
30. Roy B, Vaughn JN, Kim BH, Zhou F, Gilchrist MA, Von Arnim AG. The h subunit of eIF3 promotes reinitiation competence during translation of mRNAs harboring upstream open reading frames. RNA. 2010;16:748-61. doi:10.1261/rna.2056010.
31. Schepetilnikov M, Dimitrova M, Mancera-Martínez E, Geldreich A, Keller M, Ryabova LA. TOR and S6K1 promote translation reinitiation of uORF-containing mRNAs via phosphorylation of eIF3h. EMBO J. 2013;32:1087-102. doi:10.1038/emboj.2013.61.
32. Kozak M. Effects of intercistronic length on the efficiency of reinitiation by eucaryotic ribosomes. Mol Cell Biol. 1987;7:3438-45. doi:10.1128/MCB.7.10.3438.
33. Vattem KM, Wek RC. Reinitiation involving upstream ORFs regulates ATF4 mRNA translation in mammalian cells. Proc Natl Acad Sci U S A. 2004;101:11269-74. doi:10.1073/pnas.0400541101.
34. Lu PD, Harding HP, Ron D. Translation reinitiation at alternative open reading frames regulates gene expression in an integrated stress response. J Cell Biol. 2004;167:27-33. doi:10.1083/jcb.200408003.
35. Hofacker IL. RNA secondary structure analysis using the Vienna RNA package. Curr Protoc Bioinformatics. 2004;Chapter 12:Unit 12 2. doi:10.1002/0471250953.bi1202s04.
36. Wagner S, Herrmannova A, Malik R, Peclinovska L, Valasek LS. Functional and biochemical characterization of human eukaryotic translation initiation factor 3 in living cells. Mol Cell Biol. 2014;34:3041-52. doi:10.1128/MCB.00663-14.
37. Wagner S, Herrmannova A, Sikrova D, Valasek LS. Human eIF3b and eIF3a serve as the nucleation core for the assembly of eIF3 into two interconnected modules: The yeast-like core and the octamer. Nucleic Acids Res. 2016;44:10772-88. doi:10.1093/nar/gkw972.
38. Resch AM, Ogurtsov AY, Rogozin IB, Shabalina SA, Koonin EV. Evolution of alternative and constitutive regions of mammalian 5′UTRs. BMC Genomics. 2009;10:162. doi:10.1186/1471-2164-10-162.
39. Ingolia NT, Ghaemmaghami S, Newman JRS, Weissman JS. Genome-wide analysis in vivo of translation with nucleotide resolution using ribosome profiling. Science. 2009;324:218-23. doi:10.1126/science.1168978.
40. Lawless C, Pearson RD, Selley JN, Smirnova JB, Grant CM, Ashe MP, Pavitt GD, Hubbard SJ. Upstream sequence elements direct post-transcriptional regulation of gene expression under stress conditions in yeast. BMC Genomics. 2009;10:7. doi:10.1186/1471-2164-10-7.
41. Vilela C, Linz B, Rodrigues-Pousada C, McCarthy JE. The yeast transcription factor genes YAP1 and YAP2 are subject to differential

control at the levels of both translation and mRNA stability. Nucleic Acids Res. 1998;26:1150-9. doi:10.1093/nar/26.5.1150.
42. Yun DF, Laz TM, Clements JM, Sherman F. mRNA sequences influencing translation and the selection of AUG initiator codons in the yeast Saccharomyces cerevisiae. Mol Microbiol. 1996;19:1225-39. doi:10.1111/j.1365-2958.1996.tb02468.x.
43. Johnstone TG, Bazzini AA, Giraldez AJ. Upstream ORFs are prevalent translational repressors in vertebrates. EMBO J. 2016;35:706-23. doi:10.15252/embj.201592759.
44. Chew GL, Pauli A, Schier AF. Conservation of uORF repressiveness and sequence features in mouse, human and zebrafish. Nat Commun. 2016;7:11663. doi:10.1038/ncomms11663.
45. Heuer A, Gerovac M, Schmidt C, Trowitzsch S, Preis A, Kötter P, Berninghausen O, Becker T, Beckmann R, Tampé R. Structure of the 40S-ABCE1 post-splitting complex in ribosome recycling and translation initiation. Nat Struct Mol Biol. 2017;24:453-60. doi:10.1038/nsmb.3396.
46. Mancera-Martinez E, Brito Querido J, Valasek LS, Simonetti A, Hashem Y. ABCE1: A special factor that orchestrates translation at the crossroad between recycling and initiation. RNA Biol. 2017; in press; doi:10.1080/15476286.2016.1269993.
47. des Georges A, Dhote V, Kuhn L, Hellen CU, Pestova TV, Frank J, Hashem Y. Structure of mammalian eIF3 in the context of the 43S preinitiation complex. Nature. 2015;525:491-5. doi:10.1038/nature14891.

Downloaded by [Charles University in Prague] at 10:11 25 November 2017

TRANSLATIONAL CONTROL

An emergency brake for protein synthesis

The integrated stress response is able to rapidly shut down the synthesis of proteins in eukaryotic cells.

VLADISLAVA HRONOVÁ AND LEOŠ SHIVAYA VALÁŠEK

Related research article Jennings MD, Kershaw CJ, Adomavicius T, Pavitt GD. 2017. Fail-safe control of translation initiation by dissociation of eIF2α phosphorylated ternary complexes. *eLife* **6**: e24542. doi: 10.7554/eLife.24542

When driving a car it is usually best to brake gently when you want to stop. Occasionally, however, it is necessary to 'stand on the brakes' and perform an emergency stop. Surprisingly, perhaps, similar considerations can apply in protein synthesis because it is sometimes necessary for cells to stop the production of new proteins as quickly as possible. Now, in eLife, Graham Pavitt of the University of Manchester and colleagues – including Martin Jennings as first author, Christopher Kershaw and Tomas Adomavicius – report that they have identified an 'emergency brake' for stopping protein synthesis when cells are experiencing stress (***Jennings et al., 2017***).

The emergency brake – which is part of the integrated stress response in cells – shuts down the process by which messenger RNA molecules are translated into primary chains of amino acids, which then fold to form active proteins. Shutting down the process that transcribes DNA to form messenger RNA would also bring protein synthesis to a halt, but not as quickly as shutting down translation can stop it. Translational control thus allows cells to respond rapidly and flexibly to external signals and various forms of stress, and failures in this process have been linked to a number of diseases: for example, mutations in an initiation protein complex called eIF2B (which is short for eukaryotic translation initiation factor 2B) cause a fatal genetic disorder of the nervous system called leukodystrophy (***Pavitt and Proud, 2009***; ***Hinnebusch, 2014***; ***Chu et al., 2016***).

The integrated stress response is an elaborate signaling pathway that stops protein synthesis in eukaryotic cells when it is activated in response to various internal and external factors (reviewed in ***Pakos-Zebrucka et al., 2016***). The main internal factor is stress caused by the accumulation of unfolded proteins in the endoplasmic reticulum, and the external factors include viral infections and shortages of oxygen, amino acids or glucose. The integrated stress response is centered on an initiation protein complex called eIF2, and it is activated when a particular amino acid (serine 51 in its alpha subunit) is phosphorylated by a protein kinase: the identity of the kinase depends on the type of stress that the cell is responding to. This phosphorylation causes a robust reduction in general protein synthesis by blocking the initiation of translation for most messenger RNAs, but allowing the translation of selected messenger RNAs (for the production of proteins that can combat stress inside the cell).

Translation initiation begins with eIF2 binding to GTP and a molecule called initiator Met-tRNA to form a structure called the ternary complex. The role of the ternary complex is to ensure that the initiator Met-tRNA is delivered to the P-site on the ribosome and that translation begins at

© Copyright Hronová and Valášek. This article is distributed under the terms of the Creative Commons Attribution License, which permits unrestricted use and redistribution provided that the original author and source are credited.

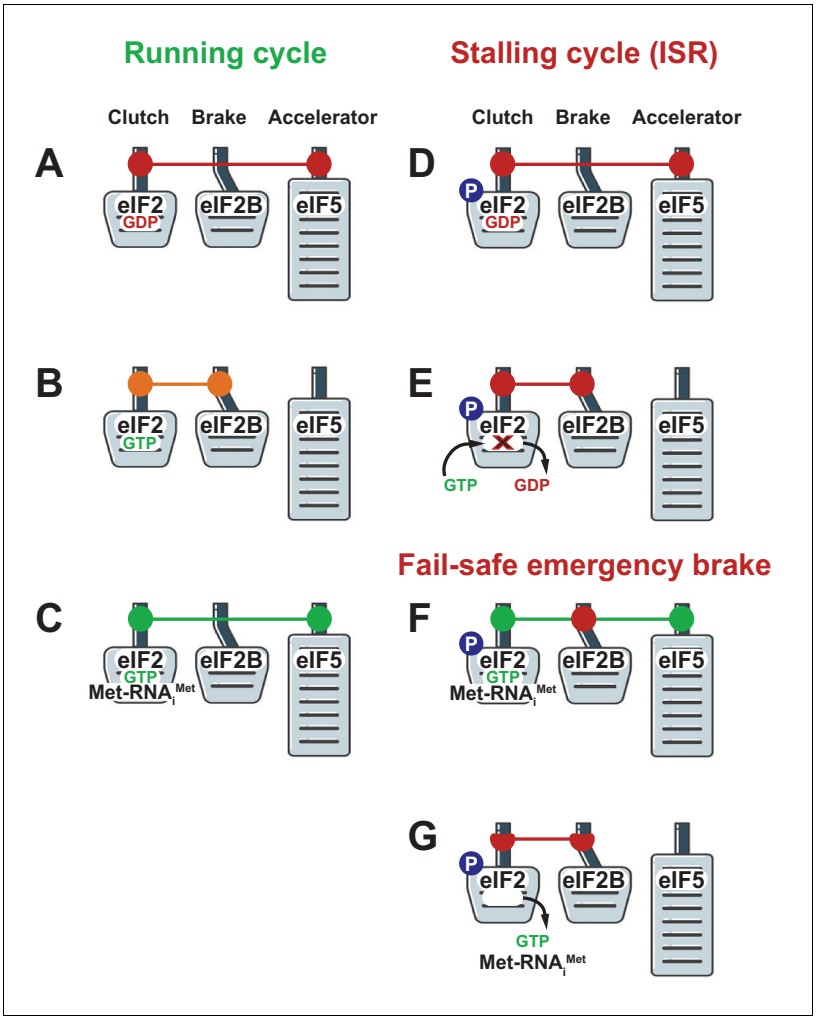

Figure 1. How translation can be stopped and started during protein synthesis. Three of the main players in the control of translation act like the clutch (eIF2), brake (eIF2B) and accelerator (eIF5) in a car. (**A**) Once the translation of an mRNA molecule has started, a complex containing eIF2-GDP (which is inactive) and eIF5 leaves the ribosome. (**B**) eIF2B then out-competes eIF5 and mediates the exchange of GDP and GTP to yield eIF2-GTP (which is active). (**C**) eIF2-GTP and initiator Met-tRNA then form a ternary complex, which is stabilized by eIF5, and a new cycle of translation can begin. (**D**) Sometimes a cell has to reduce protein synthesis in response to stress or other factors, and this response starts with the phosphorylation (P) of a specific amino acid (Ser51) in eIF2. (**E**) This phosphorylation has important consequences: eIF2B is unable to mediate the exchange of GDP and GTP, and translation cannot proceed. (**F, G**) Jennings et al. show that if the phosphorylation of Ser51 occurs on eIF2 present in an existing ternary complex, the phosphoryl group allows eIF2B to out-compete eIF5: this means that eIF5 cannot stabilize the ternary complex, so the complex falls apart and translation is stopped completely.

the correct start codon on each mRNA molecule (which involves scanning the mRNA to find the start codon, which is usually AUG). Besides eIF2, there are at least 11 other initiation factors that interact with messenger RNAs and/or subunits of the ribosome to form the so-called pre-initiation complex and ensure that translation is initiated properly. Two of these – eIF5 and eIF2B – constitute a regulatory circuit that cycles eIF2 between its active state (in which it is bound to GTP) and an inactive state (bound to GDP) that cannot initiate translation.

In some ways eIF5 resembles the accelerator of a car (***Figure 1***) in that it ensures that translation happens when the conditions are right for it: likewise, eIFB2 resembles a brake, slowing down the production of proteins in response to worsening conditions; and eIF2-GTP/GDP is like a clutch in that it allows the cell to change gears in response to varying conditions. However, in order to understand how these three factors perform these different roles and control protein synthesis in cells, we first need to understand the nature of their mutual interactions (for example, simultaneous versus mutually exclusive), as well as their varying affinities. It is known that eIF5 binds inactive eIF2-GDP and active eIF2-GTP with similar affinities (***Algire et al., 2005***), whereas initiator Met-tRNA binds eIF2-GTP with an affinity that is ~10 times greater than the affinity with which it binds eIF2-GDP (***Kapp and Lorsch, 2004***). Now, among other findings, Jennings et al. unexpectedly report that eIF2B binds eIF2-GDP and eIF2-GTP with similar affinities too, and that these binding affinities change in stress conditions.

Under normal conditions, when growth is permissible, the ternary complex binds the ribosome with help of other translation initiation factors, such as eIF5 and eIF3, to start scanning for the start codon. When this codon has been found eIF5 activates GTP hydrolysis on eIF2 and the resulting eIF2-GDP molecule (which is still bound to eIF5) leaves the pre-initiation complex (***Figure 1A***). eIF2B then out-competes eIF5 and mediates the exchange of GDP and GTP to bring eIF2 back to its active state (***Figure 1B***). Initiator Met-tRNA now binds to eIF2-GTP to form a new ternary complex that – together with eIF5 – can out-compete eIF2B, and this allows a new cycle of translation to begin (***Figure 1C***). In other words, all three factors – eIF2, eIF2B and eIF5 – co-operate and keep the car moving.

However, when the integrated stress response is activated, the eIF2-GDP-eIF5 complex leaving the pre-initiation complex after the

start codon has been recognized contains eIF2 in which serine 51 has been phosphorylated, and this results in the brakes being applied to the translation process by eIF2B. The dramatically increased strength of the binding between eIF2B and the phosphorylated eIF2-GDP means that the exchange of GDP and GTP does not occur, and that eIF5 cannot out-compete eIF2B in order to allow a new cycle of translation to begin (***Figure 1E***). We can think of this as the equivalent of the regular brakes on a car being used to slow it down. However, Jennings et al. show that cells have an additional 'fail-safe' emergency brake that completely stops the translation process.

The regular brake prevents the exchange of GDP and GTP on the phosphorylated eIF2-GDP-eIF5 complex as it leaves the pre-initiation complex, and thus blocks the formation of a new ternary complex: however, if the serine 51 site has been phosphorylated in the already-formed ternary complex, the emergency brake prevents it from beginning a new round of translation. It relies on eIF2B being able to out-compete eIF5 and thus destabilize the ternary complex. This way the translational vehicle is brought to a complete stop (***Figure 1F, 1G***).

Once we fully understand the role of eukaryotic initiation factors like eIF2, eIF2B and others in the regulation of gene expression, we will be in a better position to understand the molecular mechanisms underlying diseases caused by mutations in them.

Vladislava Hronová is in the Laboratory of Regulation of Gene Expression, Institute of Microbiology ASCR, Prague, Czech Republic
Leoš Shivaya Valášek is in the Laboratory of Regulation of Gene Expression, Institute of Microbiology ASCR, Prague, Czech Republic
valasekl@biomed.cas.cz
http://orcid.org/0000-0001-8123-8667

Competing interests: The authors declare that no competing interests exist.
Published 25 April 2017

References

Algire MA, Maag D, Lorsch JR. 2005. P_i release from eIF2, not GTP hydrolysis, is the step controlled by start-site selection during eukaryotic translation initiation. *Molecular Cell* **20**:251–262. doi: 10.1016/j.molcel.2005.09.008, PMID: 16246727

Chu J, Cargnello M, Topisirovic I, Pelletier J. 2016. Translation initiation factors: reprogramming protein synthesis in Cancer. *Trends in Cell Biology* **26**:918–933. doi: 10.1016/j.tcb.2016.06.005, PMID: 27426745

Hinnebusch AG. 2014. The scanning mechanism of eukaryotic translation initiation. *Annual Review of Biochemistry* **83**:779–812. doi: 10.1146/annurev-biochem-060713-035802, PMID: 24499181

Jennings MD, Kershaw CJ, Adomavicius T, Pavitt GD. 2017. Fail-safe control of translation initiation by dissociation of eIF2α phosphorylated ternary complexes. *eLife* **6**:e24542. doi: 10.7554/eLife.24542, PMID: 28315520

Kapp LD, Lorsch JR. 2004. GTP-dependent recognition of the methionine moiety on initiator tRNA by translation factor eIF2. *Journal of Molecular Biology* **335**:923–936. doi: 10.1016/j.jmb.2003.11.025, PMID: 14698289

Pakos-Zebrucka K, Koryga I, Mnich K, Ljujic M, Samali A, Gorman AM. 2016. The integrated stress response. *EMBO Reports* **17**:1374–1395. doi: 10.15252/embr.201642195, PMID: 27629041

Pavitt GD, Proud CG. 2009. Protein synthesis and its control in neuronal cells with a focus on vanishing white matter disease. *Biochemical Society Transactions* **37**:1298–1310. doi: 10.1042/BST0371298, PMID: 19909266

10948–10968 *Nucleic Acids Research, 2017, Vol. 45, No. 19* *Published online 14 September 2017*
doi: 10.1093/nar/gkx805

SURVEY AND SUMMARY

Embraced by eIF3: structural and functional insights into the roles of eIF3 across the translation cycle

Leoš Shivaya Valášek[1,*], Jakub Zeman[1], Susan Wagner[1], Petra Beznosková[1], Zuzana Pavlíková[1], Mahabub Pasha Mohammad[1], Vladislava Hronová[1], Anna Herrmannová[1], Yaser Hashem[2] and Stanislava Gunišová[1]

[1]Laboratory of Regulation of Gene Expression, Institute of Microbiology ASCR, Videnska 1083, Prague 142 20, the Czech Republic and [2]CNRS, Architecture et Réactivité de l'ARN UPR9002, Université de Strasbourg, 67084 Strasbourg, France

Received July 06, 2017; Revised August 21, 2017; Editorial Decision August 22, 2017; Accepted August 31, 2017

ABSTRACT

Protein synthesis is mediated *via* numerous molecules including the ribosome, mRNA, tRNAs, as well as translation initiation, elongation and release factors. Some of these factors play several roles throughout the entire process to ensure proper assembly of the preinitiation complex on the right mRNA, accurate selection of the initiation codon, errorless production of the encoded polypeptide and its proper termination. Perhaps, the most intriguing of these multitasking factors is the eukaryotic initiation factor eIF3. Recent evidence strongly suggests that this factor, which coordinates the progress of most of the initiation steps, does not come off the initiation complex upon subunit joining, but instead it remains bound to 80S ribosomes and gradually falls off during the first few elongation cycles to: (1) promote resumption of scanning on the same mRNA molecule for reinitiation downstream—in case of translation of upstream ORFs short enough to preserve eIF3 bound; or (2) come back during termination on long ORFs to fine tune its fidelity or, if signaled, promote programmed stop codon readthrough. Here, we unite recent structural views of the eIF3–40S complex and discus all known eIF3 roles to provide a broad picture of the eIF3's impact on translational control in eukaryotic cells.

OVERVIEW OF THE TRANSLATIONAL CYCLE

To begin a translational cycle, mRNA has to be brought to the ribosome in a way so that the start of the coding sequence that it carries is properly identified (reviewed in (1,2)). This is ensured by the initiator methionyl tRNA (Met-tRNA$_i^{Met}$) whose CAU anticodon is complementary to the most common initiation codon - AUG. Met-tRNA$_i^{Met}$ is delivered to the ribosome as a part of the so-called ternary complex (TC) together with the translation initiation factor 2 (eIF2) bound to a GTP molecule. Binding of the TC is aided by several other eIFs such as eIF1, 1A, 3 and 5 (Figure 1). Completion of this step results in a formation of the so-called 43S pre-initiation complex (PIC). Another co-operative role of eIFs 1, 1A, 3 and 5 is to prepare the small ribosomal subunit for mRNA docking by opening the 40S mRNA binding channel, initially believed to be mediated only by eIF1 and 1A. mRNA comes prebound by the group of the eIF4F factors, out of which eIF4E contacts the mRNA's 5′ 7-methyl guanosine cap, as well as the scaffold protein eIF4G (Figure 1). eIF4G further interacts with the helicase eIF4A and poly(A)-binding protein PABP1, and together with eIF3 represents the major driving force in mRNA recruitment and accommodation in the 40S mRNA binding channel. Binding of the 43S PIC to mRNA close to its cap structure yields the 48S PIC, which subsequently begins inspecting the sequence of nucleotides downstream of the cap in the process known as scanning. Scanning requires the action of helicases such as eIF4A (working together with its stimulatory factors eIF4B and eIF4H) and DHX29 (occurring only in higher eukaryotes) to unwind mRNA secondary structures for the ribosome to move smoothly along the 5′ UTR till the start codon (usually the first AUG) has been recognized. The AUG recogni-

*To whom correspondence should be addressed. Tel: +420 241 062 288; Fax: +420 241 062 665; Email: valasekl@biomed.cas.cz

© The Author(s) 2017. Published by Oxford University Press on behalf of Nucleic Acids Research.
This is an Open Access article distributed under the terms of the Creative Commons Attribution License (http://creativecommons.org/licenses/by/4.0/), which permits unrestricted reuse, distribution, and reproduction in any medium, provided the original work is properly cited.

Downloaded from https://academic.oup.com/nar/article-abstract/45/19/10948/4157872
by Department of Plant Physiology, Faculty of Science, Charles University user
on 25 November 2017

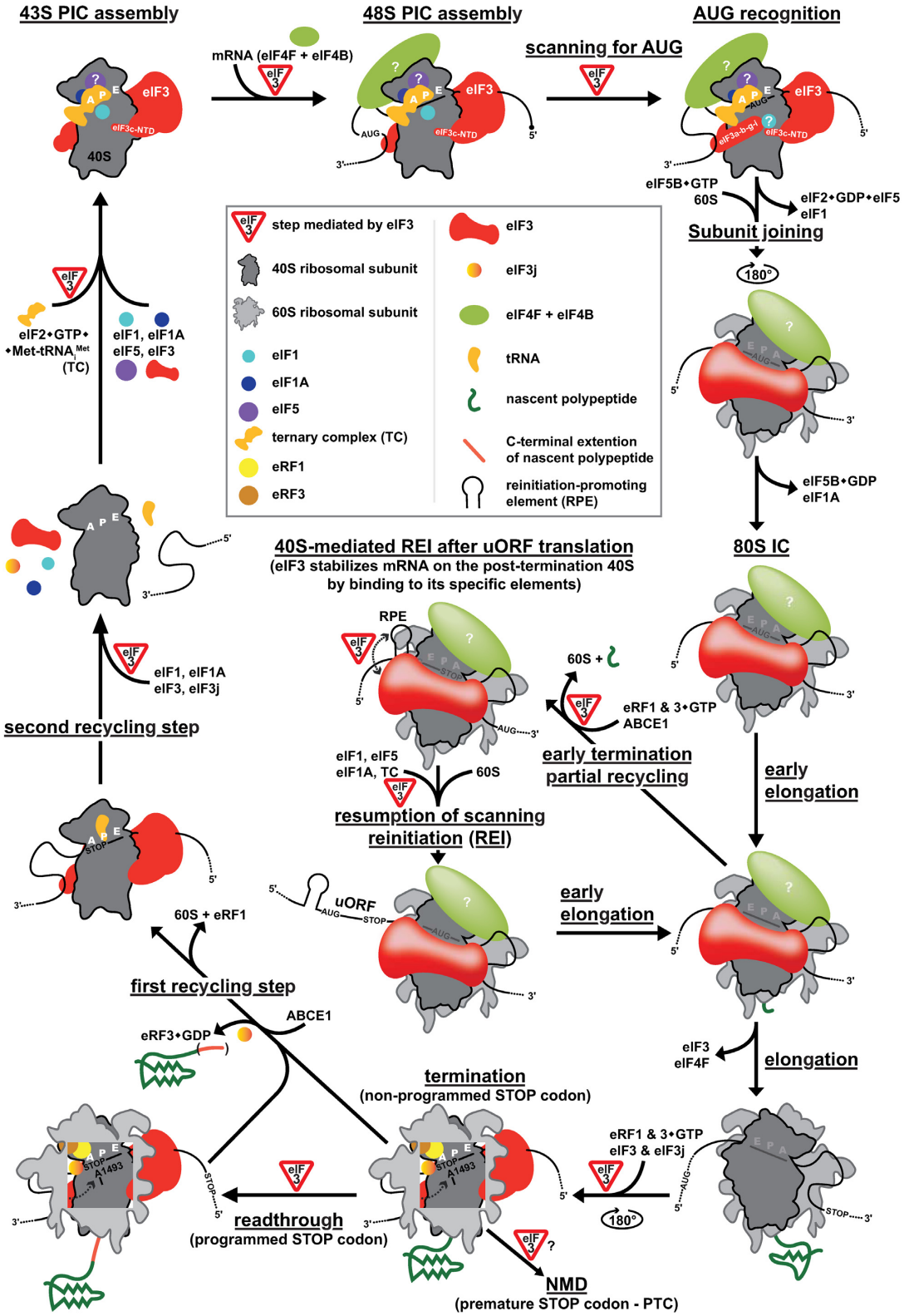

Figure 1. Schematics of the entire translational cycle with 'detours' for: (1) reinitiation, (2) programmed stop codon readthrough and (3) the Nonsense-mediated decay pathway, highlighting the role of eIF3 at the individual steps. For details, see the main text.

Downloaded from https://academic.oup.com/nar/article-abstract/45/19/10948/4157872
by Department of Plant Physiology, Faculty of Science, Charles University user
on 25 November 2017

tion triggers a series of intricate events and conformational changes in the PIC involving irreversible GTP hydrolysis on eIF2 co-operatively mediated by eIF5, eIF1, eIF1A and eIF3. This results in the closure of the 40S mRNA binding channel and ejection of most of the initiation factors from the 48S PIC (for example of the eIF2•GDP•eIF5 assembly) (1) (Figure 1). In contrast, accompanying these changes, the eIF1A binding to the 48S PIC becomes tighter. eIF5B bound to GTP then mediates subunit joining at the expense of the second and last GTP hydrolysis in the entire initiation phase. Ejection of eIF5B hand in hand with eIF1A marks the end of the initiation phase leaving the 80S initiation complex behind poised for elongation (3) (Figure 1). For the next round of initiation, eIF2B (the guanine nucleotide exchange factor - GEF) must first out-compete eIF5 from the eIF2•GDP•eIF5 assembly in order to mediate the exchange of GDP for GTP to bring eIF2 back to its active (GTP-bound) state (4,5).

The elongation phase consists of a string of repetitive events mediated by elongation factors eEF1A (a GTPase mediating the recruitment of aminoacyl-tRNAs to the A-site of the elongating ribosome), eEF1B (GEF for eEF1A) and eEF2 (a GTPase promoting translocation of the 80S ribosome by one triplet at a time), the purpose of which is to add one amino acid residue *per* each triplet following AUG into the growing polypeptide chain (Figure 1) (reviewed in (6)).

The termination phase commences with the stop codon slippage into the A-site during the last round of the eEF2•GTP-mediated translocation. In eukaryotes, all three existing stop codons are recognized by a single release factor eRF1 that comes in a complex with the GTPase eRF3 (reviewed in (7)). According to the most recent model, eRF3 senses the proper accommodation of eRF1 at the A-site occupied by the stop codon (8) (Figure 1). This triggers GTP hydrolysis on eRF3, which then leaves the pre-termination complex to make room for the recycling factor called ABCE1 (RLI1 in budding yeast). Binding of ABCE1, a member of the ATP-binding cassette (ABC) family of proteins (actually, it can bind and hydrolyze any NTP), promotes polypeptide release by pushing the GGQ motif of eRF1 into the peptidyl transferase center to kick off the hydrolysis of ester bond between the nascent polypeptide chain and the CCA end of the peptidyl-tRNA sitting at the P site. This NTP-independent step captures the production of a particular protein.

In order to complete the entire translational cycle and be able to start all over again, ABCE1 (RLI1 in yeast) hydrolyses its NTP and transforms the released energy into the mechanochemical force splitting the 80S termination complex into its individual subunits: 60S and 40S, the latter of which still contains de-acetylated P-site tRNA and mRNA (9–11) (Figure 1). Generally speaking, two scenarios are possible at this stage. (i) In case of long ORFs, the post-termination 40S-tRNA-mRNA complex is fully recycled by a joint action of canonical initiation factors eIF1, eIF1A and eIF3 or by eIF2D (known also as Ligatin or TMA64 in yeast), or by the heterodimer MCT1–DENR (known as TMA20 and TMA22 in yeast) corresponding to N-terminal and C-terminal regions of eIF2D, respectively (12,13). (ii) If the translated ORF is very short (up to 10 codons in yeast and 30 codons in higher eukaryotes) and surrounded by specific *cis*-acting features, the post-termination small ribosomal subunit may remain bound to the mRNA with help of eIF3 (and perhaps also of eIF4G), resume scanning and reinitiate protein synthesis from an AUG downstream of the stop codon (Figure 1) (reviewed in (2,7,14)).

In some specific cases, the stop codon does not signal the actual end of protein synthesis. This phenomenon is called stop codon readthrough or nonsense suppression and occurs when a near-cognate aminoacyl-tRNA (nc-tRNA) or a natural suppressor tRNA (fully cognate with a given stop codon) wins the otherwise uneven competition with eRF1 over the corresponding stop codon (Figure 1) (reviewed in (15,16)). It can be 'spontaneous' and thus relatively infrequent or it can be programmed to C-terminally extend the protein of interest as a response to specific environmental changes demanding an alteration of the corresponding protein's properties (17). Stop codon readthrough can also occur at a premature termination codon (PTC) within the coding region of a given gene, which is actually desirable because it can prevent the action of nonsense-mediated decay (NMD) pathway by ensuring the synthesis of a full-length protein (18). Numerous factors influence the efficiency of readthrough, such as for example the identity and the nucleotide context of the stop codon, the identity of the last two amino acids incorporated into the polypeptide chain, the identity of the P-site tRNA, the presence of stimulatory elements downstream from the stop codon (15), and last but not least, the identity and concentration of nc-tRNAs (19) and, rather unexpectedly, the presence of eIF3 in the pre-termination complex (20,21).

Here, we provide novel insights into all just described phases of translational cycle, as well as its modifications, from the perspective of the multitasking eukaryotic initiation factor eIF3.

THE ROLE OF eIF3 IN GENERAL TRANSLATION INITIATION

Translation initiation factor 3 (eIF3) has been considered the largest and the most complex of all eIFs ever since its first isolation (for review see (22)), yet its complete structure has not been determined yet. The *Saccharomyces cerevisiae* eIF3 (*S.c.*-eIF3) comprises five core essential subunits (a/TIF32, b/PRT1, c/NIP1, i/TIF34, and g/TIF35) (Figure 2) that have corresponding orthologs in the more complex mammalian eIF3 (m-eIF3), which contains seven additional subunits (eIF3d, e, f, h, k, l and m) reaching the total of 12 (reviewed in (2,23)) (see Table 1). Out of those 12, 8 subunits form the so-called octamer (a, c, e, f, h, k, l, m); eIF3b, g and i assemble into the so-called Yeast-Like-Core (YLC) together with the C-terminal region of the otherwise octameric eIF3a; and the remaining peripheral eIF3d subunit attaches to eIF3 *via* eIF3e (24,25) (Figure 3A). Originally, the yeast j/HCR1 (26) and its mammalian ortholog eIF3j (27) were believed to represent the 6th and 13th subunit of eIF3, respectively; however, recent evidence strongly indicates that they rather represent eIF3-associated factors (having mostly eIF3-independent roles) than the *bona fide* eIF3 subunits. For example, yeast j/HCR1 was proposed to play more important role in termination than in initiation

Downloaded from https://academic.oup.com/nar/article-abstract/45/19/10948/4157872
by Department of Plant Physiology, Faculty of Science, Charles University user
on 25 November 2017

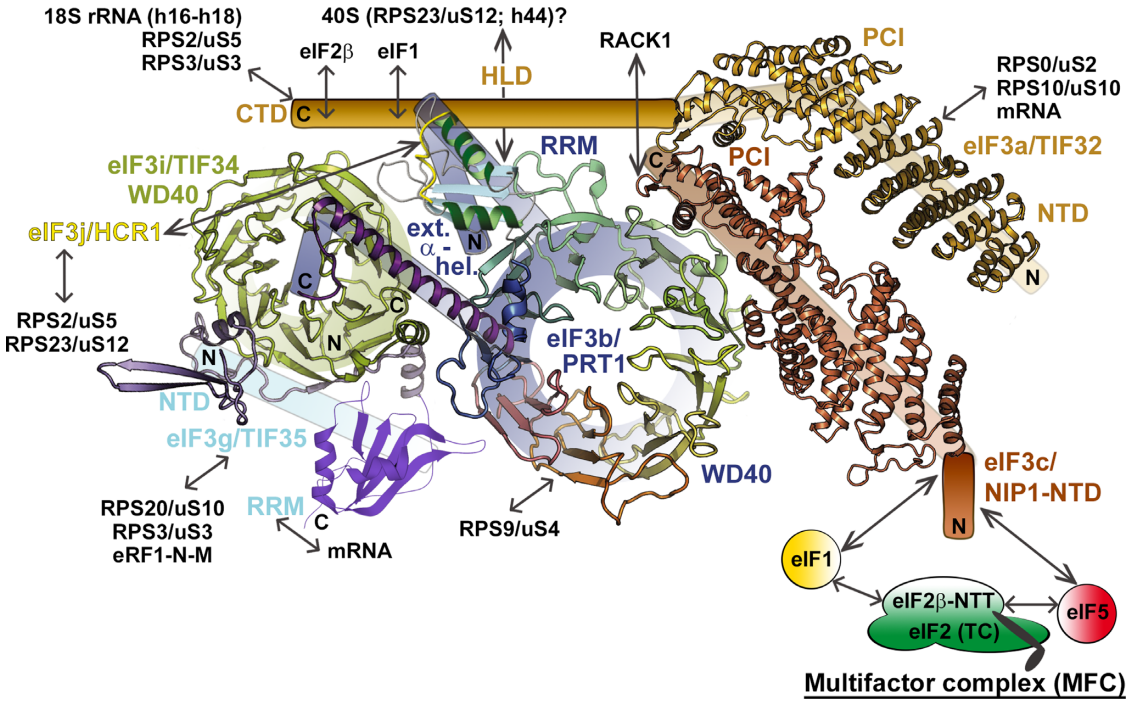

Figure 2. Schematics of the *S. cerevisiae* eIF3 complex. A 3D model of yeast eIF3 and its associated eIFs in the Multifactor complex (MFC) composed together to the best possible fit from all available structures of individual domains; namely the X-ray structure of the yeast i/TIF34 (full length)—g/TIF35-NTD (*S.c.* residues 1–135)—b/PRT1-extended-α-helix (*S.c.* residues 655–698) complex, the X-ray structure of the β-propeller (formed by nine WD40 repeats) of the middle domain of b/PRT1 (residues 132–626), the X-ray structure of the mutually interacting PCI domains of a/TIF32 (residues 1–496) and c/NIP1 (residues 251–812) (all taken from (64)); the NMR structure of the interaction between the RRM of human eIF3b (*H.s. residues* 170–274) and the N-terminal peptide of human eIF3j (*H.s. residues* 35–69) (37), and the NMR structure of the C-terminal RRM of human eIF3g (*H.s.* residues 231–320) (38). Arrows indicate all known interactions of eIF3 domains with other eIFs, ribosomal proteins and mRNA (see text for further details). NTD, N-terminal domain; CTD, C-terminal domain; HLD, HCR1-like domain; RRM, RNA recognition motif; PCI, PCI domain; WD40, WD40 domain; TC, ternary complex (composed of eIF2•GTP•Met-tRNA$_i^{Met}$).

(20), mammalian eIF3j and mRNA were found to bind anti-cooperatively to the 43S PIC (28), whereas the eIF3 complex is one of key factors promoting mRNA recruitment to the PICs, etc.

Over several decades of intensive research (mainly in budding yeast), eIF3 has been demonstrated to promote nearly every step of translation initiation. Briefly, the current knowledge is that eIF3 keeps the 40S and 60S subunits apart (29), several domains of its subunits directly stimulate the TC and mRNA recruitment to the PICs (30–36) and subsequently control the rate and processivity of scanning, as well as the fidelity of the start codon selection (30,31,35,37–44). eIF3 is apparently not actively involved in the subunit joining step even though it persists bound to the 80S initiation complex during early elongation (45–47). The breadth of the eIF3 roles in translation initiation most likely emanates from its complexity, as well as from the fact that it directly interacts with several other eIFs and to some degree co-ordinates their placement and functional conformations on the surface of the small ribosomal subunit (reviewed in (1,2)).

THE eIF3 STRUCTURE, ASSEMBLY AND PLACEMENT IN THE 48S PRE-INITIATION COMPLEX

Based on the most recent analysis of human and *N. crassa* 12-subunit eIF3 (25,41,48), as well as the earlier analysis of the 5-subunit S.c.-eIF3 (32,49–55), it seems likely that the eIF3 nucleation core is formed by the eIF3a and eIF3b subunits in most, if not all, organisms. They interact with each other via the N-terminal RNA recognition motif (RRM) of eIF3b and the C-terminal spectrin domain (the HCR1-like domain in yeast) of m-eIF3a (32,49,55,56) (Figures 2 and 3A). The extreme C-terminal end of eIF3b recruits eIF3g and eIF3i and their mutual interaction further fortifies this eIF3b–g–i module, at least in yeast (54). In mammals, the eIF3a spectrin domain most probably contributes to or takes over this fortification role by stabilizing the eIF3b–eIF3i interaction (56) (Figures 2 and 3A).

In less complex S.c.-eIF3, the C-terminal domain of eIF3b together with the N-terminal PCI domain of eIF3a interacts with eIF3c *via* its C-terminal and PCI domains, respectively, to complete the assembly (32,34,52) (Figure 2). In more sophisticated eIF3 complexes, the eIF3a subunit nucleates the formation of the octamer (Figure 3A); i.e. a structural scaffold that is shared by the functionally unrelated 19S proteasome lid, as well as the COP9 signalosome (57). The PCI/MPN octamer always contains six subunits with a PCI domain (for Proteasome-COP9 signalosome-eIF3) and two subunits with an MPN domain (for Mpr1-Pad1 N-terminal) (Figure 3A). Formation of the eIF3a–eIF3b nucleation core seems to be a strict prerequisite for the human octamer assembly *in vivo* (25), even though the octamer can be formed in a test tube from recombinant pro-

Downloaded from https://academic.oup.com/nar/article-abstract/45/19/10948/4157872
by Department of Plant Physiology, Faculty of Science, Charles University user
on 25 November 2017

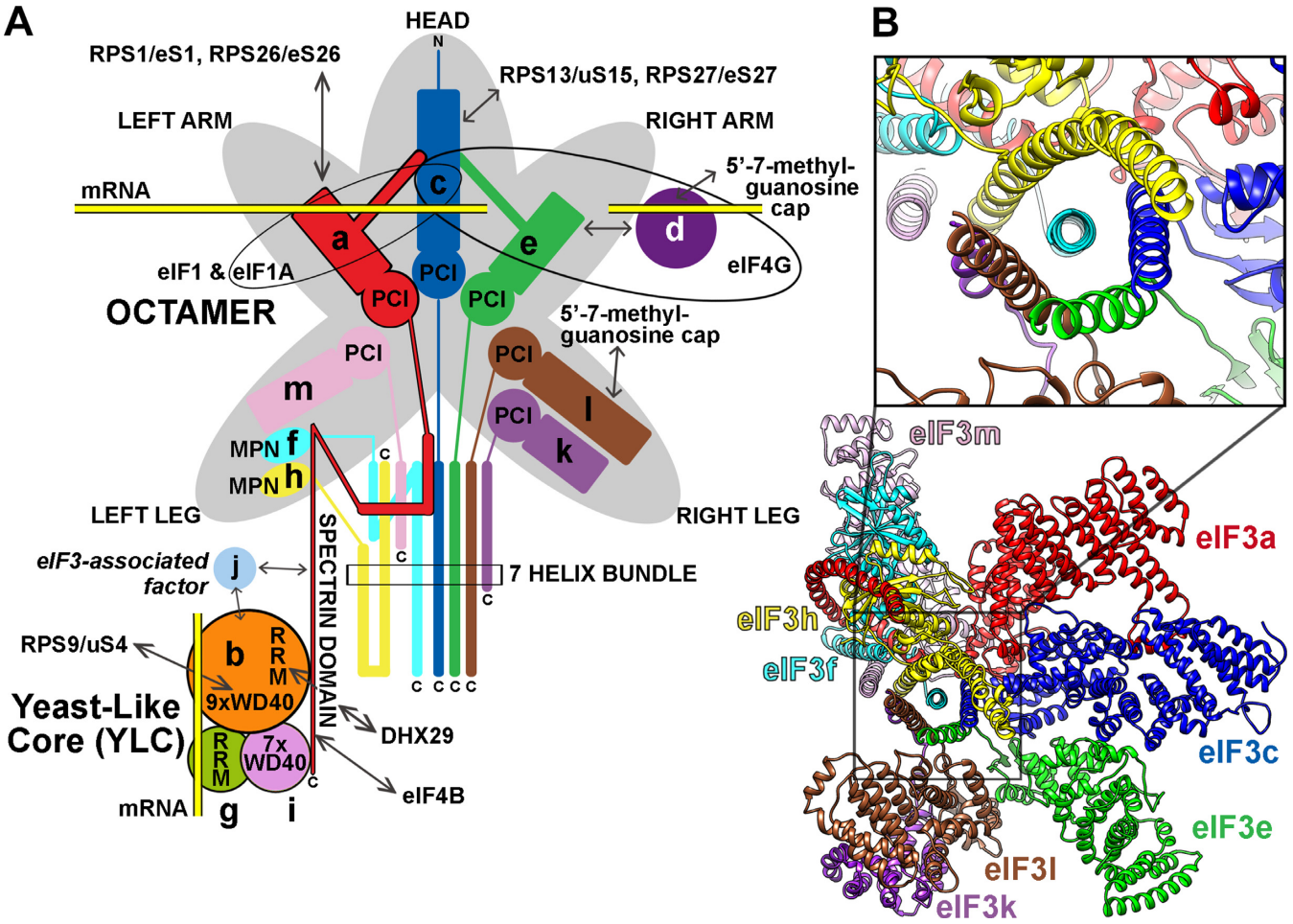

Figure 3. Schematics of the human eIF3 complex. (**A**) A schematic model of human eIF3 was adapted from (25). The eIF3 subunits forming the PCI/MPN octamer with the anthropomorphic shape are indicated by the grey background. The rectangle marks the seven α-helices involved in formation of the 7-helix bundle shown in panel C. The Yeast-Like Core (YLC) comprising the eIF3 subunits a, b, g and i (defined previously by (41)) is depicted and so is the eIF3-associated factor eIF3j with arrows indicating its contacts with other eIF3 subunits. The upper right-hand side arrow indicates the interaction between eIF3e and eIF3d that attaches eIF3d to the rest of eIF3 (48,59,159). Arrows indicate all known interactions of eIF3 domains with other eIFs, ribosomal proteins and mRNA (see text for further details). (**B**) Polyalanine-level model of the eIF3 octamer core with the close-up view of the 7-helix bundle formed by subunits h, c, e, f, l and k (adapted from (59)).

teins (58). In fact, it is possible that the formation of the eIF3a–b–g–i subcomplex (YLC) precedes the nucleation of the octamer because the YLC was shown to exist free in cytoplasm in human cells knocked down for the core octamer eIF3c, f and m subunits (25,41). According to the most recent data, the first step of the human octamer nucleation consists of the simultaneous addition of the eIF3c^{PCI}, f^{MPN} and m^{PCI} (and perhaps also of eIF3h^{MPN}) subunits to eIF3a^{PCI} from the 3a/3b nucleation core (25). This way the network of interactions among MPN and PCI domains nicknamed the β-sheet arc starts to build along with the additional multiple point of contacts called the α-helical bundle, to which all octameric subunits contribute by at least one α-helix (48,59) (Figure 3A and B). Subsequently, eIF3e^{PCI} together with its tightly binding partner represented by the non-octameric eIF3d subunit joins, followed by two tightly interacting octameric partners eIF3k^{PCI} and eIF3l^{PCI} to complete the assembly (25,48). It is noteworthy that the structural analysis of the recombinant human eIF3 out of the context of the ribosome resolved only the octameric subunits adopting a five-lobed structure with appendages reminiscent of a head, two arms, and legs (24,60); the structure of the rabbit octamer in the highest available resolution is shown in Figure 3B (59). Taking into account that neither eIF3d nor the YLC subunits could be determined suggests that all non-octameric subunits might be rather flexible.

The very first attempt to map the position of m-eIF3 on the small ribosomal subunit using the negatively stained EM images occurred in 1978 by the Freienstein's lab (61), followed by a similar study in the Frank's lab in 1992 (62). Both studies placed the eIF3 body close to the platform on the 40S solvent-exposed side. It took more than 20 years to visualize m-eIF3 in the 43S PIC in high-enough resolution to also predict the position of the YLC subunits (63) and later, in a more refined structure, to assign the observed densities to the individual subunits of m-eIF3 (59). Based on these structures, as well as on numerous biochemical reports that are in majority of cases consistent with the structural images, it is now clear that the major eIF3 body sits

Downloaded from https://academic.oup.com/nar/article-abstract/45/19/10948/4157872
by Department of Plant Physiology, Faculty of Science, Charles University user
on 25 November 2017

Table 1. Overview of eIF3 subunits and of the eIF3-associated factor eIF3j across species

Subunit	Domains	*S. cerevisiae*			*S. pombe*			*N. crassa*			*A. thaliana*			*H. sapiens*		
		Named	M.W. (kDa)	Essential[a]	Named	M.W. (kDa)	Essential[b]	Named	M.W. (kDa)	Essential[b]	Named	M.W. (kDa)	Essential	named	M.W. (kDa)	Essential[a]
eIF3a	PCI, Spectrin HLD (yeast)	**TIF32**	110.3	E	**p107**	107.1	E	**p110**	120.2	E	**p114**	114.3	?	**p170**	166.6	E
eIF3b	WD40, RRM	**PRT1**	88.1	E	**p84**	84.0	E	**p90**	85.6	E	**p82**	81.9	?	**p116**	92.5	E
eIF3c	PCI	**NIP1**	93.2	E	**p104**	104.4	E	**p93**	98.4	E	**p110**	103.0/91.7	?	**p110**	105.3	E
eIF3d	Cap-binding pocket?	-	-	-	**MOE1**	62.6	N	**eIF3d**	65.0	E	**p66**	66.7	?	**p66**	64.0	E
eIF3e	PCI	-	-	-	**INT6**	57.1	N	**INT6**	51.1	N	**p48**	51.8	E*	**p48**	52.2	E
eIF3f	MPN	-	-	-	**CSN6**	33.3	E	**eIF3f**	39.7	E	**p32**	31.9	E**	**p47**	37.6	E
eIF3g	RRM, Zn finger	**TIF35**	30.5	E	**TIF35**	31.5	E	**p33**	32.4	E	**eIF3g**	32,7/35,7	?	**p44**	35.6	E
eIF3h	MPN	-	-	-	**p40**	39.8	N	**eIF3h**	40.4	N	**p38**	38.4	E***	**p40**	39.9	N
eIF3i	WD40	**TIF34**	38.7	E	**SUM1**	36.8	E	**TIF34**	38.8	E	**p36**	36.4	?	**p36**	36.5	E
eIF3k	PCI	-	-	-	-	-	-	**p25**	26.8	N	**p25**	25.7	?	**p28**	25.1	N
eIF3l	PCI	-	-	-	-	-	-	**eIF3l**	54.5	N	**eIF3l**	60.2	?	**p67**	66.7	N
eIF3m	PCI	-	-	-	**CSN7B**	45.1	E	**eIF3m**	49.7	E.	**eIF3m**	46.8	?	**GA17**	42.5	E
associated factor eIF3j	-	**HCR1**	29.6	N	**p35**	30.5	N	**HCR1**	30.3	N	**eIF3j**	25.5	?	**p35**	29.1	N

[a]Essential: DEG, a Database of Essential Genes (161).
[b]Essential: (162).
*Gametogenesis.
**Pollen germination and embryogenesis.
***Significantly reduced fertility.

on the 40S solvent-exposed side, however, several of its subunits project into the ribosomal intersubunit side (Figure 4A and B). eIF3 thus embraces the small ribosomal subunit from both sides to control most, if not all, initiation reactions. In detail, the head and left arm represented by eIF3c and eIF3a were predicted to contact ribosomal proteins RPS13/uS15 and RPS27/eS27, and RPS1/eS1 and RPS26/eS26, respectively, occurring near the mRNA exit channel. Subunits eIF3e, h, k and l seem to stick out from the 40S-binding surface of the octamer into solution where they may mediate interactions with various partners to control the initiation rates in an mRNA-specific manner (see below).

Reconstruction and intensive integrative modeling of the yeast 40S–eIF1–eIF1A–eIF3 complex stabilized by crosslinking suggested that the eIF3a–eIF3c PCI heterodimer also sits near the mRNA exit channel, with the C-terminal portion of the eIF3a-PCI domain occupying the position of mammalian eIF3f and 3h subunits (64,65); the same arrangement was later observed even without cross-linking (66). In support, earlier biochemical experiments revealed that the N-terminal domain (NTD) of yeast eIF3a interacts with another 'mRNA exit channel' protein RPS0/uS2 (50,67) and contacts specific mRNA elements that promote translation reinitiation and are expected to reside in the vicinity of the mRNA exit channel (45–47). Similarly, m-eIF3a was crosslinked to 5′ UTR residues −14/−17 (relative to AUG) of model mRNA in the reconstituted 48S PICs and predicted to form a functionally important extension of the mRNA exit channel (68). Finally, using model mRNAs lacking contacts with the 40S entry or exit channels, we have recently uncovered a critical role for the a/TIF32-NTD in stabilizing mRNA interactions at the exit channel (35).

The outburst of recent cryo-EM reconstructions of both yeast and mammalian eIF3 in complex with the 40S subunit suggests that eIF3 can adopt several conformations depending on the actual initiation status. In particular, the eIF3b–g–i module is rather mobile, most probably thanks to the C-terminal domain of eIF3a that interacts with this module and thus may operate as a controllable mechanical arm (Figures 1, 4A and B). The first two mammalian structures predicted the densities observed near the mRNA entry channel to represent the β-propeller of eIF3b (thanks to the crystal structure showing that this propeller is atypically formed by 9 WD40 repeats (69)) with the disconnected, low-resolution density provisionally assigned as the eIF3b-RRM projecting laterally away from the 40S body (59,63,64) (Figure 4A). When viewed from the solvent-exposed side, the β-propeller of eIF3b is placed horizontally—touching RPS9/uS4 with the edge of one of its blades, whereas the seven-bladed WD40 β-propeller of eIF3i, which was assigned to another entry channel density thanks to the structure solved in (40), resides on the opposite side of the eIF3b β-propeller than the eIF3b-RRM in the vertical orientation (Figure 4C) (59). Both propellers are directly connected *via* the C-terminal extended α-helical domain of eIF3b, as shown before (40). The only part of the C-terminal mechanical arm of eIF3a that was resolved runs underneath the eIF3b β-propeller but it highly likely extends further towards the eIF3b-RRM domain (Figure 4A), because the major contact point between eIF3b and the eIF3a-CTD in both yeast and mammals is mediated *via* the eIF3b-RRM (32,54,56,70). Undoubtedly, it also connects with the octamer across the solvent side of the 40S ribosome towards its platform (see below); visualization of these particular contacts requires additional work (Figure 4A; red dashed lines). There was no apparent density for eIF3g in either of the structures.

In agreement, a nearly identical arrangement of the binary eIF3b–i subcomplex, represented by the RRM and both β-propellers attached to the eIF3a-CTD, was also deduced from the analysis of the yeast 40S–eIF1–eIF1A–eIF3 complex (64,65). In this yeast structure the eIF3g-NTD was assigned sandwiched between the eIF3i β-propeller and the 40S body (Figure 4A), in accord with the earlier work iden-

Downloaded from https://academic.oup.com/nar/article-abstract/45/19/10948/4157872
by Department of Plant Physiology, Faculty of Science, Charles University user
on 25 November 2017

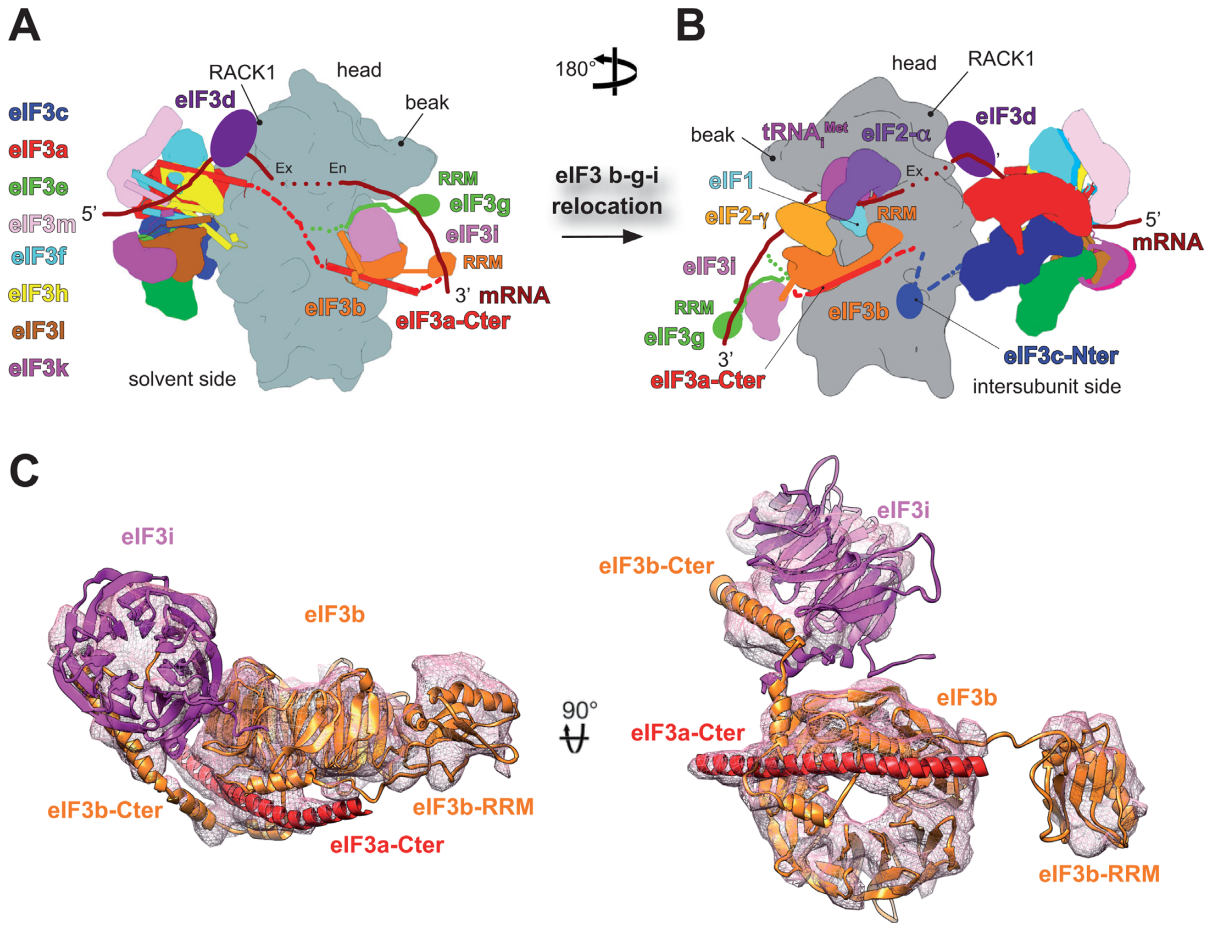

Figure 4. Schematic representation of the arrangement of eIF3 subunits in the two available conformations that are deduced from the available Cryo-EM analysis (adapted from (59)). (**A**) eIF3 binds to the solvent-exposed side with the octamer occupying the platform of the small ribosomal subunit connected with the eIF3b–g–i module (YLC)—sitting near the mRNA entry channel—*via* the extended C-terminal linker domain of eIF3a (a dashed red line indicates a predicted location of the eIF3a-CTD; placement of the eIF3g-RRM is also only our best guess) (59,63–65). Figure includes only those domains of eIF3 subunits for which the structures are known. The 40S subunit is depicted in grey surface; all other subunits are labelled and colored variably. The eIF3 helical bundles fortifying the intersubunit interactions are represented as cylinders. The predicted path of mRNA is shown in dark red; Ex and En—mRNA exit and entry channels, respectively. For details please see the main text. (**B**) In this conformation, the entire eIF3a-CTD–b–g–i module relocates from the solvent-exposed side to the intersubunit side, so that the eIF3b-RRM interacts with 18S rRNA and eIF1 and the eIF3b-propeller interacts with eIF2γ (66,70); a density presumably corresponding to the eIF3c-NTD residues 115–220 was in this structure identified not too far away from eIF1, where it could co-ordinate AUG recognition with other eIFs. Purely hypothetically, this could be the conformation that eIF3 adopts upon AUG recognition. Placement of the eIF3g–i unit held by the eIF3b-extended α-helix is only our best guess; for details please see the main text. (**C**) Atomic model of rabbit eIF3b (RRM, WD40 and the C-terminal extended α-helix domains - orange), yeast eIF3i-WD40 (purple) and a long α-helix (red) corresponding to a fragment of the C-terminal helical region of eIF3a. For details please see the main text.

tifying contacts between yeast g/TIF35 and RPS3/uS3 and RPS20/uS10, occurring at or near the mRNA entry channel (38). In addition, in this structure the density underneath the eIF3b β-propeller corresponding to the eIF3a-CTD extends N-terminally towards the eIF3a–3c PCI heterodimer clearly demonstrating that the eIF3a-CTD links both the PCI and eIF3b–g–i modules residing at or near the exit and entry channels, respectively, as suggested before (40). The overall placement of the yeast trimeric eIF3b–g–i module attached to the eIF3a-CTD is consistent with the previously identified contacts between the a/TIF32-CTD and RPS2/uS5 and RPS3/uS3 (39) and helices 16–18 of 18S rRNA (50), and between the eIF3b β-propeller and RPS9/uS4 (69). It also agrees with the protection of h16 nucleotides from chemical or enzymatic cleavage by m-eIF3 (68). In this conformation, the eIF3a-CTD–b–g–i module seems well positioned to interact with incoming mRNA by extending the mRNA entry channel and modulating the rate and processivity of scanning for AUG recognition *in vivo*, as experimentally evidenced (37–40,43,51) (Figure 4A). In accord, the recent biophysical work implicated both the entry and exit channel modules of yeast eIF3 in performing highly-specific roles during initiation, some of which are co-operative (like stabilizing the assembly of the PICs and mRNA recruitment), while some others are module-specific (35). For example, alterations to the a/TIF32-CTD and the eIF3b–g–i module significantly slowed mRNA recruitment and mutations within the eIF3b–g–i module destabilized eIF2•GTP•Met-tRNA$_i$ binding to the PIC, whereas alterations to the a/TIF32-NTD destabilized mRNA interactions with the PIC at the exit channel (35).

Downloaded from https://academic.oup.com/nar/article-abstract/45/19/10948/4157872
by Department of Plant Physiology, Faculty of Science, Charles University user
on 25 November 2017

The most recent yeast cryo-EM structures revealed the yeast 48S PICs during mRNA scanning (in the so-called py48S open conformation) and right at the start codon recognition (in the py48S closed conformation) (66) (Figure 4B). Apart from the eIF3a–eIF3c PCI dimer occurring at the 40S platform, a drum-like shape density at the 40S intersubunit face was observed near the RPS23/uS12, h44, and the eIF2γ subunit, and tentatively attributed to the eIF3i β-propeller with the extended α-helix of eIF3b and the eIF3g-NTD. Other isolated densities on the interface side were provisionally attributed to different parts of the yeast eIF3a-CTD and eIF3c-NTD (one of these, predicted to represent the extreme NTD of eIF3c-NTD, occurred next to eIF1 residing near the P-site, based on the known contact between these two molecules (31)). The authors suggested that this rather robust conformational rearrangement (mainly with respect to the eIF3g–i unit) may occur on mRNA binding. However, this assignment was later challenged because the 9-bladed β-propeller of eIF3b aligned much better to the drum-like density in the original cryo-EM map (70). Furthermore, the eIF3b-RRM motif closely matched the density in a direct contact with eIF1 (originally predicted to represent the c/NIP1-NTD (Figure 4B). The density linking the β-propeller and the RRM of eIF3b was intuitively predicted to be composed of the mostly unstructured eIF3b linker sequence loosely bundled with the extended α-helical region of the eIF3a-CTD (70) (Figure 4B); as mentioned above, the eIF3a-CTD and eIF3b-RRM directly interact (49) and the yeast eIF3a-CTD also interacts with eIF1 (32)). In fact, the projection of the eIF3a-CTD into the intersubunit space was - thanks to its contact with the eIF2β - already proposed earlier (32,50). Since these reassignments are definitely correct ((1) and José Llácer Guerri, personal communication), the positions of eIF3g and eIF3i in these particular yeast conformations remain unknown.

It is important to note that in Simonetti et al. we made an attempt to assign another intersubunit-side based density that we observed in our near-native conditions directly in cell extracts to the mammalian eIF3g–i unit (70); however, this density later turned out to be ABCE1 (71,72). Nonetheless, taken into account that the interaction between the eIF3b-extended α-helix and the eIF3g–i unit is highly conserved, it seems very likely that the entire eIF3a-CTD–b–g–i module relocates from the solvent-exposed side to the intersubunit side, so that the eIF3b-RRM interacts with 18S rRNA and eIF1 and the eIF3b-propeller interacts with eIF2γ (Figure 4B). Whether this remarkable rearrangement occurs on mRNA binding, or on the onset of scanning, or on the irreversible GTP hydrolysis upon AUG recognition remains to be determined. The proposed contacts with eIF2γ and eIF1 may slightly favor the latter idea; the eIF3b-RRM could stimulate the GTP hydrolysis on eIF2γ and help to kick eIF1 out of the P-site, which is one of the most critical steps underlying the proper AUG selection (reviewed in (1)).

The NTD of eIF3c was shown to mediate eIF3 interactions with eIF1 and 5 in yeast (Figure 2) (30,31,53,73) and with eIF1 in mammals (24,74), and also proposed to project into the intersubunit side to coordinate AUG recognition with the latter eIFs (50). Consistently, crosslinking mass spectrometry data predicted an interaction of the N-terminal segment of eIF3c with eIF1 bound to the 40S platform (64), and a density presumably corresponding to the eIF3c residues 115–220 was identified not too far away from eIF1 in both the py48S-closed/open complexes (66) (Figure 4B). Furthermore, several studies proposed intricate molecular interactions among the eIF3c-NTD and eIFs 1, 2 and 5 within the PIC that would enable rapid scanning-arrest at the start codon by removing eIF1 away from the ribosomal P-site (30,31,42). Since the eIF3c-NTD holds eIF1 in the so-called eIF3–1–2–5 multifactor complex (Figure 2) (73) and most likely promotes eIF1 delivery to the PICs (perhaps directly releasing it into the P-site), an intriguing idea is that upon AUG recognition, the NTD of eIF3c rebinds eIF1 and clears it away from the P-site to irreversibly stall the initiation machinery at the correct AUG (2,31,42) (Figure 1). Intuitively, this mechanism could only operate with the NTD of eIF3c stretching from the octamer base around the platform all the way to the 40S P-site (Figure 4B).

To complete the list of eIF3 interactions with other eIFs, mammalian eIF3a and eIF3c were, besides eIF1, also proposed to interact with eIF1A (24), and human eIF4G was (in contrast to yeast) shown to contain two distinct binding sites for eIF3, one of which contacts eIF3c and -d subunits, whereas the other binds eIF3e (75) (Figure 3A). These interactions were proposed to promote mRNA binding to the 40S ribosome in the eIF4G-dependent manner. eIF3a interacts with eIF4B (76) and its CTD, together with the eIF3b-RRM, associates with the initiation-specific non-processive mammalian helicase DHX29, and disruption of either contact impairs the DHX29 activity (77). It was proposed that DHX29 and eIF3 cooperate to promote scanning on structured mRNAs and to ensure stringency of AUG recognition (78), which is consistent with the eIF4B–eF3a contact and our previous yeast genetic data on g/TIF35 and a/TIF32 (38,39).

THE eIF3 ROLE IN SELECTIVE mRNA TRANSLATION INITIATION

Besides the indispensable role of eIF3 in general translation initiation, there is a growing number of reports suggesting that eIF3 also controls alternative modes of translation initiation on cellular transcripts. The Cate's lab used the PAR-CLIP technique to identify transcripts that specifically interact with eIF3 in human 293T cells (79). They identified ∼500 mRNAs falling into distinct groups like cell cycle, apoptosis and differentiation, the 5′ UTRs of which specifically crosslinked to eIF3a, b, d and g subunits. Specific structural elements were predicted to feature in the 5′ UTRs of these mRNAs and drive eIF3-specific, cap-dependent activation or inhibition of translation initiation (79). This indicates that (a) eIF3 is capable to directly promote mRNA recruitment to 43S PICs, in accord with our earlier report from yeast cells (33), and (b) that it might do so in a highly selective, mRNA-specific manner and thus contribute to a wide variety of translational control mechanisms. Later the same group showed that one of these eIF3 subunits, namely eIF3d, under specific conditions even directly contacts the 5′ cap (80). Using the mRNA encoding the cell proliferation regulator c-JUN as the model mRNA representing the

Downloaded from https://academic.oup.com/nar/article-abstract/45/19/10948/4157872
by Department of Plant Physiology, Faculty of Science, Charles University user
on 25 November 2017

entire 'crosslinked' group it was proposed that the eIF3d cap-binding pocket interacts with the 5′ cap of the c-JUN mRNA only upon its allosteric activation by other eIF3 subunits and/or by the c-JUN 5′ UTR-specific secondary structure. Interestingly, this particular mRNA also contains the eIF4F-inhibitory element, which could prevent it from being initiated *via* the canonical 5′ cap/eIF4F-dependent pathway *in vivo*. Besides eIF3d, the non-essential octameric subunit eIF3l (25) was also shown to interact with the 5′ cap *in vitro*, but only in context of the entire mammalian eIF3 (81). Even though the cap-binding activity of eIF3d was not detected in the latter study (81), together these findings suggest an intriguing possibility that eIF3 interacts with numerous mRNAs encoding regulatory proteins in various modes involving the 5′ cap and/or higher-order secondary structures and single-handedly mediates their binding to the 43S PICs to control their expression in response to various stresses and cellular signals. Recent findings of our laboratory suggest that human cells might besides the eIF3 holocomplex also contain several minor but still operational subcomplexes lacking for example eIF3d or eIF3l–k or eIF3e–d–l–k or eIF3h–l–k subunits (25). Hence it is conceivable that it could be the existence of these subcomplexes that stands behind the eIF3 modularity in gene-specific mRNA recruitment to the PICs. In fact, the imbalance in the expression levels of individual eIF3 subunits, often seen in cancers and other pathologies (for review see (82,83)), might dysregulate this modular mRNA expression profile, as well as the ability of the palette of eIF3 subcomplexes to contribute to stress adaptation, and as such lie behind many of these medical conditions.

In support, the *Schizosaccharomyces pombe* cells lacking therein non-essential eIF3e and eIF3d subunits failed to synthesize components of the mitochondrial electron transport chain, leading to a defect in respiration, endogenous oxidative stress, and premature aging (84). The cells managed to maintain the energy balance by a switch to anaerobic glycolysis with increased glucose uptake and strict dependence on a fermentable carbon source. Since human eIF3e, which is essential in higher eukaryotes, was also suggested to promote translation of metabolic mRNAs, the authors proposed that eIF3—*via* its eIF3d-eIF3e module—might orchestrate an mRNA-specific translational mechanism controlling energy metabolism that could be disrupted in cancer. Other recent examples of the selective mRNA regulatory role of eIF3 are: (1) a report showing that loss-of-function mutations in the non-essential genes encoding eIF3k and eIF3l subunits result in a 40% extension in lifespan and enhanced resistance to endoplasmic reticulum (ER) stress in *Caenorhabditis elegans* (85); (2) two studies together demonstrating that eIF3 interacts with YTHDF1, an N(6)-methyladenosine reader protein that recognizes the m(6)A-modified mRNAs, to promote their translation in a cap-independent manner as an alternative mechanism to IRES-mediated initiation under various stresses when the cap-dependent pathway is suppressed (86,87); (3) a work suggesting that eIF3e promotes binding of the eIF4E-specific kinase Mnk1 (MAPK signal-integrating kinase 1) to eIF4G to induce eIF4E phosphorylation that might regulate selective mRNA translation; and finally (4) eIF3h was proposed to specifically contribute to modulating a lens development in zebrafish by regulating translation of lens-associated crystallin isoform mRNAs most likely *via* their UTRs (88).

THE eIF3 ROLE IN IRES-MEDIATED INITIATION

Hepatitis C virus (HCV) and classical swine fever virus (CSFV) mRNAs contain related (HCV-like) internal ribosome entry sites (IRESs). Initiation on HCV-like IRESs relies on their specific interaction with the 40S subunit, which places the initiation codon into the P site, where it directly base-pairs with eIF2-bound Met-tRNA$_i^{Met}$ to form the 48S PIC. Importantly, only a subset of eIFs is needed for IRES-driven initiation; in fact different IRES classes have different requirements for eIFs (for review see (89)). It has been long known that eIF3 binds to the IIIabc four-way junction domain of the HCV IRES and is essential for its function in translation initiation (90–92). Earlier cryo-EM reconstructions suggested that the HCV IRES extends across eIF3 from the left arm to the right leg (60), which was later supported by demonstrating that the RNA-binding HLH motifs in eIF3a and eIF3c make direct contacts with the HCV IRES (93). Initially, it was believed that eIF3 actively promotes HCV IRES-mediated initiation (94), despite the fact that the ribosomal positions of eIF3 and the HCV IRES overlap. Our recent cryo-EM study of the CSFV-eIF3–40S complex resolved this paradox by showing that although the CSFV IRES interactions with the eIF3-bound 40S subunit were similar to those of the HCV IRES in the 40S-IRES binary complex, the eIF3 octamer was completely displaced from its typical ribosomal location and instead interacted with the apical region of the IRES domain III (95). Therefore, we proposed that the HCV-like IRESs actually prevent ribosomal association of eIF3 (at least that of the octamer because the YLC was not resolved) in their favor to be able to occupy the otherwise common 40S-binding site. As a consequence, they would also reduce formation of cellular PICs by sequestering eIF3 on viral PICs, thereby favoring translation of viral mRNAs. Hence, instead of being an IRES-translation-promoting factor, eIF3 may serve as an IRES-inhibitor. Actually, a negative role of eIF3 in a viral replicative cycle—but of a different kind—was also suggested by a study exploring the human immunodeficiency virus (HIV). It was shown that the eIF3d subunit inhibits the HIV replication and as such represents one of the targets-to-be-destroyed by the HIV protease, which specifically cleaves it during viral proliferation (96). On the other hand, binding of eIF3 together with PABP to the X-linked inhibitor of apoptosis (XIAP) IRES was recently shown to potentiate the ribosome recruitment to this IRES and thus to promote this IRES-driven translation (97). Given the diversity of the so far identified IRESs classes, it is conceivable that eIF3 may have stimulatory effects on some of them and inhibitory on some others—much like it was proposed for the structured cellular mRNAs (79). Precise biochemical analysis of each individual case are needed to corroborate especially those proposed molecular mechanisms that for their most part rely on structural and/or high-throughput studies only.

Downloaded from https://academic.oup.com/nar/article-abstract/45/19/10948/4157872
by Department of Plant Physiology, Faculty of Science, Charles University user
on 25 November 2017

THE eIF3 ROLE IN TRANSLATION TERMINATION, RIBOSOMAL RECYCLING AND STOP CODON READTHROUGH

The Pestova's lab revealed that after the ABCE1-mediated dissociation of post-termination complexes, the complete release of mRNA and deacylated P-site tRNA, which remain bound to post-termination 40S subunits, can be mediated by initiation factors eIF3, eIF1, eIF1A and the eIF3-associated factor eIF3j, at least *in vitro* (9,12). In detail, eIF1 with eIF1A relatively efficiently weakened the interaction of P-site deacylated tRNA with recycled 40S subunits, but complete dissociation of tRNA also required eIF3. In the absence of eIF3, eIF1/eIF1A-mediated release of P-site tRNA also led to mRNA dissociation; however, the presence of eIF3 resulted in less complete dissociation of mRNA from 40S subunits and efficient dissociation of mRNA required eIF3j. This is consistent with the stabilization role of eIF3 on mRNA binding (29,35), as well as with the reported negative cooperativity in 40S-binding between eIF3j and mRNA *in vitro* (28). Interestingly, at low concentrations of free Mg^{2+}, eIF3, eIF1, eIF1A and eIF3j were sufficient to promote complete recycling of post-termination complexes even in the absence of ABCE1, in which case splitting of post-termination ribosomes was principally mediated by eIF3 (12).

These findings prompted us to test the role of eIF3 in ribosomal recycling and perhaps even in translation termination in living yeast cells. By measuring the frequency of stop codon readthrough in a collection of eIF3 mutants using an established dual-luciferase reporter assay, we found many mutations in all five yeast eIF3 subunits showing a significant reduction in readthrough (20). Conversely, deletion of the non-essential eIF3-associated factor *hcr1* (encoding eIF3j) resulted in significantly increased readthrough. Furthermore, we revealed that: (i) a substantial amount of eIF3, eIF3j and eRF3 specifically co-sedimented with terminating ribosomes isolated from RNase-treated heavy polysomes in an eRF1-dependent manner; (ii) eIF3 and eIF3j also occurred in ribosome- and RNA-free complexes with both eRFs and the recycling factor ABCE1/RLI1; (iii) the g/TIF35-NTD directly interacted with the N-terminal plus middle domain (N-M) of eRF1 and (iv) eIF3 mutations reducing readthrough genetically interacted with mutant eRFs in a manner indicating that eRFs and eIF3 have antagonistic role at the same stage of the termination pathway. Hence, we proposed that wild-type eIF3 binds terminating ribosomes, perhaps in a complex with both eRFs, where it modulates the precision of stop codon recognition by eRF1 in order to fine tune the termination process (Figure 1).

In addition, we observed that the *hcr1* deletion resulted in accumulation of eRF3 in heavy polysomes in a manner suppressible by overexpressed ABCE1/RLI1, to which it directly binds to (98), and that high dosage of ABCE1/RLI1 fully suppressed the slow growth phenotype of *hcr1Δ,* as well as its termination but not initiation defects (20). Hence, we suggested that upon stop codon recognition, yeast eIF3j facilitates eRF3•GDP ejection from the post-termination complexes to allow binding of its interacting partner ABCE1/RLI1 near the A-site-based eRF1 to proceed with polypeptide release and ribosomal recycling. The fact that eIF3j was shown to reside next to eIF1A sitting near the 40S A-site (65), in agreement with earlier biochemical and genetic evidence suggesting that it spans across the mRNA entry channel (28,37), is consistent with this model. Importantly, these data implied that the termination function of eIF3j is more critical for optimal proliferation than its function in translation initiation, at least in yeast.

Interestingly, the cooperation of eIF3 and eIF3j with ABCE1 may easily reach beyond the termination phase. The recent structural studies revealed that ABCE1 interacts with the intersubunit face of the 40S subunit at the universally conserved GTPase binding site even after ribosomal recycling (71,72), and most likely participates in the initiation phase hand-in-hand with eIF3 and other eIFs, as proposed earlier (99). We proposed that ABCE1 could act as an anti-association factor preventing subunit joining until the AUG codon has been recognized by Met-$tRNA_i^{Met}$ and eIFs occurring at the ribosomal interface have been cleared away to allow formation of the 80S initiation complex (72).

The unexpected eIF3 role in termination sparked our curiosity to characterize its molecular basis; surprisingly, we revealed that it critically promotes programmed stop codon readthrough (Figure 1) (21). It *de novo* associates with pre-termination complexes, where it apparently interferes with the eRF1 decoding of the third/wobble position of any of the three stop codons set in the unfavorable termination context, thus allowing incorporation of near-cognate tRNAs with a mismatch at the same position. It is important to note that the eIF3 role in programmed readthrough was found to be conserved between yeast and humans (21). The precise molecular mechanism is still unknown; however, at least two possibilities come to mind. First possibility is based on the fact that a portion of the eIF3 body projects into the vicinity of the mRNA entry channel and several of its subunits interact with RNA (2,45,46,59,64,68); eIF3 could directly interact with the readthrough-promoting sequences surrounding the stop codon and perhaps even mediate their effects on shifting the equilibrium of stop codon recognition by eRF1 *versus* near-cognate tRNAs on the side of the latter.

The second possibility emanates from the proposal that the canonical stop codon recognition by eRF1 occurs in two steps (100). It is known that when the eRF1–eRF3•GTP complex enters the A-site with the stop codon in it, the pre-termination complex undergoes major conformational re-arrangements particularly at the A-site and around the mRNA entry channel (101–104). Part of these re-arrangements concerns the eRF1-NTD, which flips the 18S rRNA nucleotide A1493 (*Escherichia coli* nomenclature) so that it stacks on the second and third stop codon bases (103,104) (Figure 5A and B, right-handed panels). As a result, stop codon adopts the eukaryotic-specific U-turn-like conformation within a decoding pocket formed by the eRF1-NTD and the ribosome that is now also capable of accommodating the +4 base; i.e. the base immediately following the stop known to have a significant impact on the efficiency of readthrough (see for example (15,19)). To combine this U-turn-like stop codon tetranucleotide idea with the older, and in our opinion still valid, two-step model, we propose the following. In the first step, the first and sec-

Downloaded from https://academic.oup.com/nar/article-abstract/45/19/10948/4157872
by Department of Plant Physiology, Faculty of Science, Charles University user
on 25 November 2017

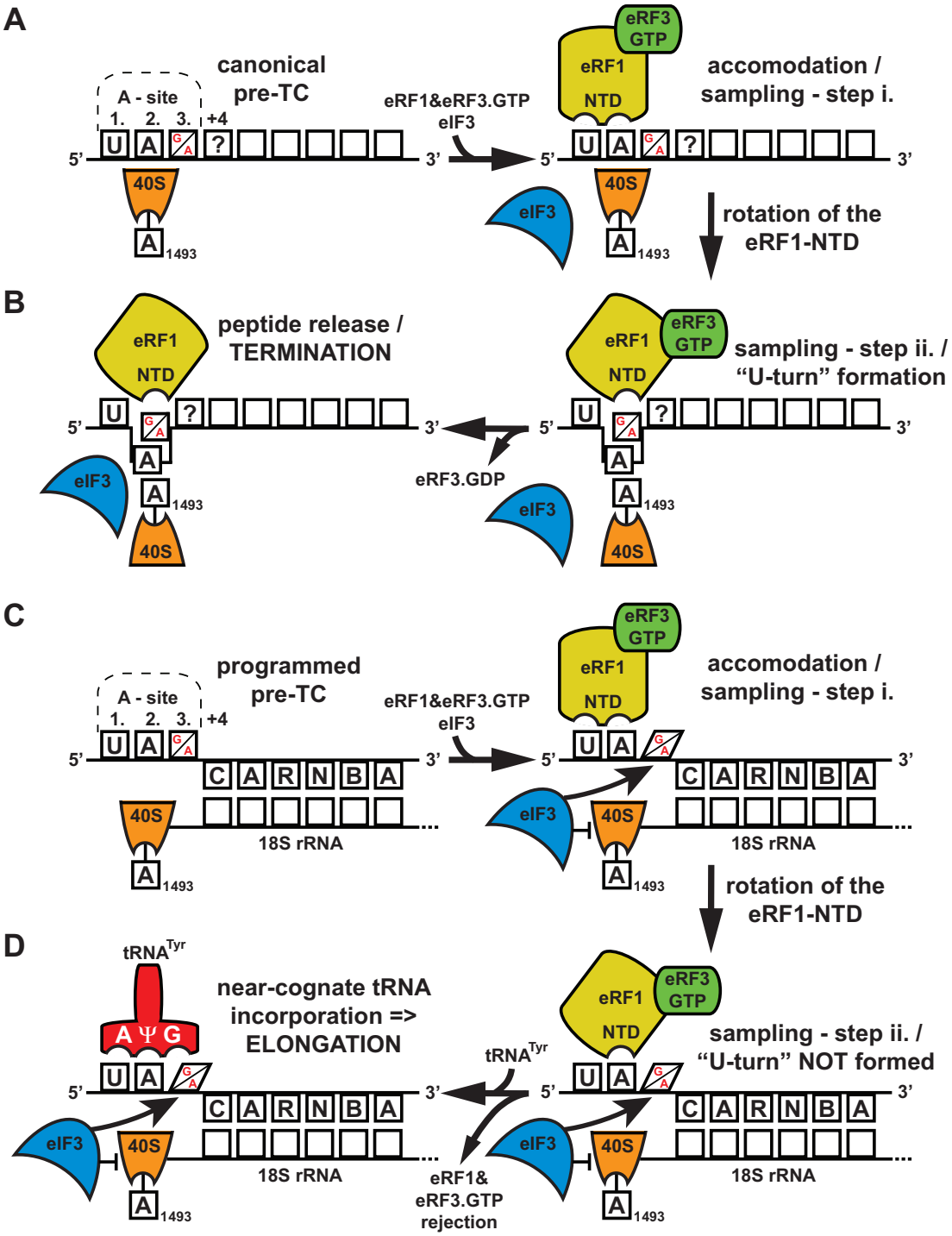

Figure 5. Translation initiation factor eIF3 promotes programmed stop codon readthrough - revised model adapted from (21). (**A** and **B**) Canonical termination; stop codon in the termination favorable context appears in the A-site (only UAG and UAA stop codons are indicated for illustration purposes; UGA works by the same mechanism; +4 base is indicated by a question mark), eRF1 in complex with eRF3.GTP binds to it and samples the codon in a two-step process (100). In the first step, the first and second nucleotides of the stop codon are recognized by specific residues of the eRF1-NTD. This is followed by the eRF1-NTD conformational re-arrangement during the second step, which probably includes flipping the A1493 base (according to the *E. coli* nomenclature) accompanied by formation of the U-turn-like conformation (103,104). This step permits decoding of the third nucleotide. As a result, eRF1 stably accommodates in the A-site triggering GTP hydrolysis on eRF3, followed by polypeptide release and ribosomal recycling. eIF3 has minimal, if any role here (see text for further details). (**C** and **D**) Programmed stop codon readthrough; stop codon occurs in the unfavorable termination context bearing specific consensus sequences like CAR-NBA in its 3′ UTR—in this particular case proposed to base-pair with 18S rRNA (160). The eIF3 presence in the pre-termination complex—perhaps in co-operation with these sequences—prevents the A1493 phosphate group to flip and thus specifically interferes with the proper decoding of the third position of programmed stop codons (19,21). This results in ejection of the eRF1–eRF3•GTP complex from the pre-termination complexes allowing incorporation of near-cognate tRNAs with the mismatch at the third position to read through the stop codon and continue with elongation. For details please see the main text.

Downloaded from https://academic.oup.com/nar/article-abstract/45/19/10948/4157872
by Department of Plant Physiology, Faculty of Science, Charles University user
on 25 November 2017

ond nucleotides of the stop codon are recognized by specific residues of the eRF1-NTD (Figure 5A). This is followed by the eRF1-NTD re-arrangement during the second step, which might actually include flipping the A1493 base accompanied by formation of the U-turn-like conformation, permitting decoding of the third nucleotide (Figure 5B). As a result, eRF1 stably accommodates in the A-site triggering GTP hydrolysis on eRF3. Where does eIF3 stand in this model?

Intriguingly, the A1493 nucleotide, which is required for efficient decoding by eRF1, is also targeted by the aminoglycoside paromomycin. This heavily-studied readthrough inducing drug, when bound to the termination complexes, displaces the A1493 phosphate group within the stop codon decoding pocket and deforms the near-cognate codon–anticodon helix in the A-site (105). As a result, the terminating ribosome does not actively sense the correct Watson–Crick base-pairing geometry and thus does not discriminate against near-cognate tRNAs; in other words relaxes the termination fidelity. Since the stimulatory effect of paromomycin on programmed stop codon readthrough is epistatic with that of eIF3 (19,21), it is tempting to speculate that eIF3 could also interfere with A1493. It could for example prevent its flipping, which most probably occurs during the transition from the first to the second step (Figure 5A and B, right-handed panels), and thus specifically interfere with the proper decoding of the third position of programmed stop codons (Figure 5C and D, right-handed panels), which was observed (single mismatches at the first or second stop codon positions showed no genetic interactions with eIF3) (19,21). This would lead to the ejection of the eRF1–eRF3•GTP complex from the pre-termination complexes allowing near-cognate tRNAs with a mismatch at the same position to incorporate into the A-site and continue elongating (Figure 5D, left-handed panel). How could eIF3 influence the position of A1493? Either directly, since it was proposed to reach the A-site *via* the a/TIF32-CTD (50,66,70) and interact with the N-M domain of eRF1 *via* its g/TIF35 subunit (20), or allosterically by binding to constituents of the decoding pocket such as RPS2/uS5 and RPS3/uS3 (38,39).

In fact, an earlier study carried out with the eRF1–eRF3•GMPPNP complex bound to terminating ribosomes may provide a solid support for the latter option. It was shown that another important part of the termination complex re-arrangements involves a movement of helix 16 (h16) of 18S rRNA and the NTD of RPS3/uS3 toward each other, which results in the establishment of a new head–body connection on the solvent side of the 40S subunit and a constriction of the mRNA entrance (106). Binding of the no-go mRNA decay complex DOM34–HBS1 to stalled yeast ribosomes also led to the appearance of a density bridging h16 and RPS3/uS3 (107). Strikingly, conformational changes involving 18S rRNA helices 16, 18 and 34, as well as RPS3/uS3 occur also during translation initiation and are controlled by a cooperative action of the eIF1, 1A, 2(TC) and 3 (66,108). First, binding of these eIFs dissolves the mRNA entry channel 'latch' formed by h18 in the body of the 40S and h34 and RPS3/uS3 in the head to open the channel for mRNA loading and subsequent ribosomal scanning. The reversal latch closure on AUG recognition, which is again triggered by the delicate interplay between eIF1, 1A, 2, 3 and 5 and involves the same ribosomal components (66,108), then clamps on the mRNA and arrests scanning (reviewed in (1)). This 'initiation' latch closure markedly resembles that provoked by eRF1–eRF3•GMPPNP during termination (106). Since mutations in the eIF3a-CTD (binds RPS3/uS3 and h16–18) and eIF3g (binds RPS3/uS3) confer phenotypes indicating destabilization of the closed PIC conformation (as the means of reducing start codon recognition), as well as phenotypes suggesting the opposite effect of destabilizing the open conformation of the PIC (as they appeared to reduce the processivity of scanning), it was proposed that the eIF3a-CTD and eIF3g regulate the transition between scanning-conducive and scanning arrested conformations (38,39). Therefore, it is very tempting to consider that in case of termination, the constriction at the mRNA entrance tunnel may include similar actors and serve the similar purpose; i.e. to clamp onto the mRNA to stabilize the termination complex as it prepares for peptide release. If true, multiple contacts that eIF3a and eIF3g establish with the constituents of the decoding pocket during this process could allosterically impact the position of the A1493 phosphate group in the decoding pocket, which would antagonize the conformational changes required for proper stop codon recognition by eRF1 and allow readthrough.

THE eIF3 PROSPECTIVE ROLE IN NONSENSE-MEDIATED DECAY (NMD) PATHWAY

Besides canonical stop codons, readthrough can also occur on premature stop codons (PTCs). There it is closely connected with the Nonsense-mediated decay (NMD) pathway, as majority of mRNAs containing PTCs are destined to degradation (109). Considering the eIF3 involvement in readthrough, it is no surprise that eIF3 has also been implicated in NMD (Figure 1) (110). According to one model, aberrant termination at a PTC occurring upstream of a post-splicing exon junction complex (EJC) in mammals results in UPF1-bridging the contact between eRFs and the EJC-associated UPF2/UPF3, which is followed by the SMG1-mediated phosphorylation of UPF1 triggering a series of downstream events. Based on *in vitro* experiments with human reconstituted system it was proposed that phospho-UPF1 set in the PTC termination complex directly interacts with eIF3 supposedly bound to the 48S PIC on the same mRNA molecule, and that this 'looping' interaction prevents formation of the elongation-competent 80S complex; i.e. initiation on this aberrant mRNA is repressed (110). Noteworthy, a recent proteomics study confirmed that eIF3 interacts with UPF1; however, independently of its phosphorylation status (111). Nonetheless, taken into account the eIF3 roles in termination events it remains to be unambiguously demonstrated that UPF1 really interacts with initiating and not terminating eIF3 and blocks initiation on NMD mRNA substrates by this proposed mechanism in living cells. Purely theoretically, the eIF3's critical role in readthrough and reinitiation (see below) could speak for the opposite effect of eIF3 on NMD; i.e. for its inhibition.

Downloaded from https://academic.oup.com/nar/article-abstract/45/19/10948/4157872
by Department of Plant Physiology, Faculty of Science, Charles University user
on 25 November 2017

A growing number of studies suggest that translational repression is one of the key steps that precedes mRNA delivery to the degradation machinery (112), which would support the first option; i.e. the UPF1-signalled, eIF3-mediated initiation arrest as an attractive mechanism by which eIF3 contributes to efficient degradation of PTC-containing mRNAs by NMD. In support, the eIF3g (113) and eIF3e (114) knockdowns were shown to strongly inhibit NMD, and immunoprecipitation experiments showed that eIF3e copurifies with UPF2 and the 'pioneer round' 5′ cap-binding protein CBP80. In addition, it was shown that several transcripts known to be upregulated by UPF1 or UPF2 depletion were also found to be stabilized when eIF3e was suppressed (114).

Major support for the second, NMD-inhibition option comes from the other well established model of NMD called the faux 3′ UTR-mediated NMD. Here the NMD is triggered by aberrant translation termination at stop codons located in an environment of the mRNP that is devoid of signals necessary for proper termination—like the presence of poly(A)-binding protein (PABP), which interacts with both eRFs and thus prevents their binding to UPF1 (115). Using tethering assays it was demonstrated that the three RRMs of human PABPC1, which mediate the PABC1 interaction with the eIF4G-NTD, were sufficient to antagonize NMD. Since tethering of the eIF4G-NTD, as well as of the eIF4G core in direct contact with eIF3 also suppressed NMD, the authors proposed that PABPC1, eIF4G and eIF3 directly cooperate with both eRFs in translation termination and NMD suppression (116). In fact, cooperation between eIF3, and PABPC1 and eIF4G (looping both mRNAs ends together) was suggested to lie behind the NMD-resistance conferred by mRNAs containing short uORFs (so-called the 'AUG-proximity effect'). First it was demonstrated that eIF3f and h subunits are required to prevent NMD of β-globin reporter transcripts with AUG proximal PTCs (117). Next the Romao's group proposed that simultaneous binding of PABPC1 to the poly(A) tail, as well as to the eIF4G/eIF3-bound early elongating ribosome, brings PABPC1 to close proximity with the termination complex allowing it to interact with eRF3, which in turn impairs the UPF1-eRF3 interaction and thus inhibits NMD (118). There is still much to be learnt about the eIF3 role (positive or negative) in NMD. It is entirely possible that some eIF3 subunits stimulate whereas some other inhibit NMD and the final outcome depends on the type and position of individual PTCs, which may employ different means of NMD-driven regulatory mechanisms (like EJC-mediated *versus* faux 3′ UTR-mediated NMD) under different conditions.

To conclude this and the previous chapters, we propose that in case of PTCs in the readthrough unfavorable context occurring in the false termination neighborhood and/or upstream of EJCs, eIF3 could block new rounds of initiation on defective mRNAs by a UPF1-mediated mechanism described by (110). However, if these PTCs are set in the readthrough favorable context, the eIF3 binding to pretermination complexes could override the NMD-triggering signals and promote efficient readthrough to allow synthesis of a full-length protein by a molecular mechanism that normally operates on genuine, programmed stops and is outlined above. In case of genuine but non-programmed stop codons and short uORFs, eIF3 can prevent NMD in cooperation with other 'canonical termination-signaling' factors to stabilize the mRNA.

THE eIF3 PRESENCE ON EARLY ELONGATING RIBOSOMES AND ITS ROLE IN REINITIATION

Translation reinitiation (REI) is a gene-specific regulatory mechanism that takes place on the same mRNA molecule after translation of an upstream ORF (usually very short) followed by incomplete ribosomal recycling; i.e. only the large 60S subunit and deacylated tRNA are recycled (Figure 1) (reviewed in (2,7,14)). The efficiency of canonical REI depends on: (i) *cis*–acting mRNA features surrounding a given short uORF; (ii) duration of the uORF elongation; (iii) some eIFs involved in the first initiation event and (iv) the intercistronic distance needed for the acquisition of the new TC (reviewed in (2)). It has been well established that uORFs are relatively widespread across all eukaryotic genomes (13%, 30%, 44% and 49% of yeast, *A. thaliana*, mouse, and human transcripts, respectively, contain uORFs (119–121)), and that most of them inhibit expression of the main ORF (some of them very severely) by completing the ribosomal recycling step after their translation. There are, however, exceptions in the so-called REI-permissive uORFs that inhibit the expression of the main ORF only very modestly, if at all. These are rarely alone, in fact they often precede REI-non-permissive uORFs or uORFs overlapping with the main ORF, and as such create mRNA-specific regulatory mechanisms modifying the expression of the main ORF in response to various environmental stimuli. Expression of various growth factors, transcription factors and other proto-oncogenes, proteins involved in differentiation, development, cell cycle, stress response, learning and memory can be found to be regulated *via* REI. Hence, it is no surprise that uORF polymorphism has also been implicated in a variety of human diseases (119,122,123).

The first hint that eIF3 may directly promote translation reinitiation came from the cauliflower mosaic virus (CaMV) polycistronic RNA (124). The cauliflower mosaic virus transactivator, TAV, was shown to physically interact with eIF3 (*via* its eIF3g subunit) and the 60S subunit to mediate efficient recruitment of eIF3 to polysomes, allowing translation of polycistronic mRNAs by reinitiation; however, after translation of long ORFs in this case. The eIF3g subunit stimulates REI also in the budding yeast *S cerevisiae* (38). Later the *Arabidopsis thaliana* eIF3h subunit was demonstrated to be required for REI efficiency of specific 5′ mRNA leader sequences containing series of upstream open reading frames like in case of the transcription factor ATB2/AtbZip11; eIF3h supposedly ensures that a fraction of uORF-translating ribosomes retain their competence to resume scanning for downstream REI (125,126). In support, the kinase cascade of the plant ortholog of mammalian target-of-rapamycin (mTOR) and S6 kinase (S6K) phosphorylates and thus activates eIF3h, which then contributes to efficient loading of uORF-containing mRNAs onto polysomes and their expression *via* the REI mechanism (127).

Downloaded from https://academic.oup.com/nar/article-abstract/45/19/10948/4157872
by Department of Plant Physiology, Faculty of Science, Charles University user
on 25 November 2017

Besides eIF3g, REI in yeast is critically promoted also by eIF3a (45). Genetic experiments carried out with the mRNA leader of the yeast transcriptional activator GCN4, which combines two REI-permissive uORFs with two non-permissive uORFs in an intricate fail-safe mechanism (128), revealed the following with respect to role of yeast eIF3 in REI. (Note that the *GCN4* regulatory mechanism responding to stress-induced changes in the TC levels is reviewed elsewhere (128–130).)

Both highly REI-permissive uORFs of the *GCN4* mRNA (uORF1 and uORF2) contain so-called REI-promoting elements (RPEs) upstream of their AUGs, some of which fold into specific structural features like hairpins and stem loops (46,128). In detail, uORF1 utilizes four RPEs (i–iv), whereas uORF2 separately utilizes only a single RPE v (similar in sequence with the uORF1-specific RPE i) and, in addition, 'shares' RPE ii with uORF1. We first showed that the RPEs i and iv of uORF1 and RPE v of uORF2 genetically interact with two separate segments encompassing amino acid residues 51–60 (nicknamed Box6) and 161–170 (Box17) of the a/TIF32-NTD (45,46). Mutating the latter RPEs or these eIF3a-Boxes severely reduced REI permissiveness of both uORFs and combining these mutations revealed genetic epistasis (46), suggesting that these molecules closely co-operate in promoting efficient REI. Taken into account a favorable location of the eIF3a-NTD on the 40S subunit next to the mRNA exit channel (50,65–67), we proposed that the eIF3a-Boxes 6/17 directly contact these RPEs that have, upon termination on uORF1 or uORF2, already emerged from the exit pore and became solvent-exposed (46). This interaction would be instrumental in preventing full ribosomal recycling by stabilizing the mRNA•40S post-termination complex to enable its subsequent resumption of scanning and reinitiation downstream (Figure 1). This would mean, however, that eIF3 has to either stay bound to 80S ribosomes elongating these short uORFs or leave the ribosome upon subunit joining but immediately come back as a part of the termination/recycling complex.

The former idea that some REI-specific eIFs remain transiently associated with elongating ribosomes and that increasing the uORF length or the ribosome transit time increases the likelihood that these factors are dropped off was not new (7,131). Besides our yeast genetics, *in vitro* experiments with mammalian reconstituted systems also suggested that eIF4F (particularly the eIF4G's central one-third fragment interacting with eIF3 and eIF4A), and presumably eIF3 as well, persistently interact with the post-initiation ribosomes for a few elongation cycles to stimulate resumption of scanning of the post-termination 40S subunit (132). It was shown that if the splitting of post-termination complexes proceeded in the presence of eIFs 3, 1, 1A and eIF2-TC *in vitro*, 40S subunits remained on mRNA and reinitiated at nearby upstream or downstream AUGs; imposing the 3′-directionality additionally required eIF4F (133). The eIF3–eIF4G co-operation in this process is easily conceivable because these two factors interact with each other (75,134) and both of them have a favorable location on the solvent-exposed side of the small subunit (2,59,65,66,135). However, direct *in vivo* evidence for their involvement in the establishment of the REI competence has been lacking and the molecular details of their REI-promoting role have been unclear.

To address this critical issue, firstly from the eIF3 point of view, and clearly distinguish between the aforementioned two possibilities (i.e. does eIF3 stay bound to elongating 80S ribosomes or does it come off before elongation commences and back on upon termination?), we recently developed a new *in vivo* RNA–protein Ni^{2+} pull down (Rap-Nip) assay. This yeast assay captures 80S ribosomes bound by initiation factors, in our case by eIF3, while translating and terminating on short uORFs (47). Using this *in vivo* assay we demonstrated that eIF3 does travel with early elongating ribosomes at all *GCN4* uORFs regardless their permissiveness for REI and gradually falls off as the length of any of these uORF grows. In support, recent ribosomal profiling experiments revealed the so-called '5′ ramp' of ribosomes at the beginning of the coding regions that was attributed to the engagement of some eIFs, particularly eIF3, with the 80S ribosome during early elongation transiently slowing down its rate (analogous to early transcription elongation) (136).

In case of *GCN4*, we propose the following model. During scanning for and translation of the REI-permissive uORFs, RPEs progressively fold into specific secondary structures that, upon termination, eIF3 interacts with *via* eIF3a-Box6/17 to stabilize the 40S subunit on the uORF1 (or uORF2) stop and prevent it from full recycling (Figure 6) (46,47). Thanks to that, the post-termination 40S subunit can, upon acquisition of other essential eIFs, resume scanning for REI downstream (Figure 1). Whether eIF4G also contributes to this process is currently under investigation. How yeast g/TIF35 participates in this mechanism is also unknown, except that its RRM domain, which occurs near the mRNA entry and not exit channel, does not stimulate REI in cooperation with any of known *GCN4 cis*-acting features (38).

To examine whether there is any mechanistic resemblance in the REI *modus operandi* between yeast and mammals, we have very recently analyzed the flanking sequences of the REI-permissive uORF1 from the mRNA leader of the human *GCN4* functional homolog, *ATF4*, encoding stress-inducible transcriptional activator, the regulation of which is governed in a similar fashion to that of *GCN4* (137). We revealed that its 5′ sequences contain two well conserved structural features resembling the *GCN4*'s RPEs. We also showed that the basic level of REI that the *ATF4*'s uORF1 allows is significantly increased by an independent contribution of both uORF1 flanking sequences, and that human eIF3h, like in plants, seems to stimulate efficient REI on *ATF4*. Whether it also interacts with the uORF1 5′ sequences like eIF3a does in yeast, however, remains to be determined (138).

eIF3 was also implicated in the mechanism of an exceptional case of termination/reinitiation after translation of a long ORF that is best described for the polycistronic mRNA of feline calicivirus (139,140). A specific 87-nt element (called TURBS for termination upstream ribosome binding site) preceding the overlapping termination/initiation site of two long ORFs folds into a special secondary structure that base-pairs with a specific segment of 18S rRNA and, at the same time, interacts with eIF3 *via* its several subunits in-

Downloaded from https://academic.oup.com/nar/article-abstract/45/19/10948/4157872
by Department of Plant Physiology, Faculty of Science, Charles University user
on 25 November 2017

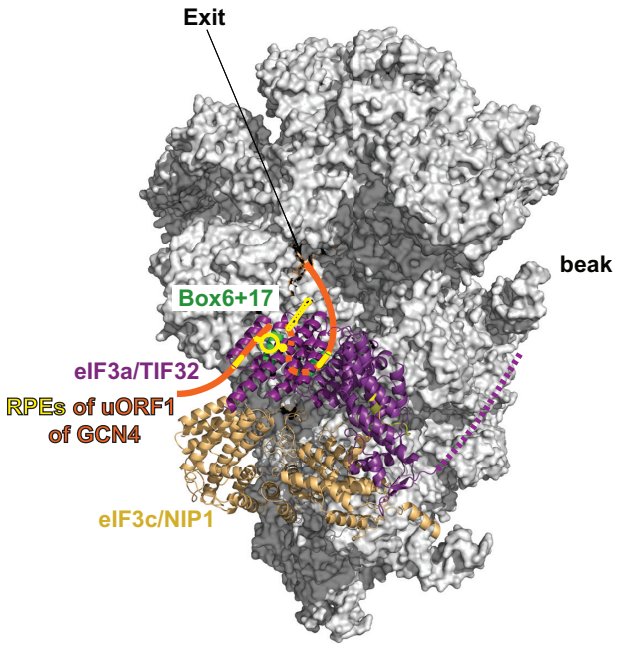

Figure 6. Graphical illustration (adapted from (47)) of the proposed arrangement of the post-termination complex on uORF1 with its RPEs interacting with Box 6 and Box 17 segments of the N-terminal domain of a/TIF32 to promote resumption of scanning for REI on *GCN4*. The exit channel view of the py48S-closed complex shows only two incomplete eIF3 subunits for simplicity: c/NIP1 in wheat and a/TIF32 in purple with its extreme NTD in light purple and its C-terminal HCR1-like domain (HLD) represented by a dotted line (its structure is unknown and thus its placement in the py48S complex was only predicted). The location of both a/TIF32 boxes is marked in green; the 5′-UTR of uORF1 is shown in orange with its RPEs depicted in yellow-orange.

cluding eIF3a and eIF3g. This intricate network of interactions should prevent dissociation of the mRNA/eIF3/40S complex in order to allow efficient REI on ORF3. However, whether or not the *in vivo* role of eIF3 in this process is critical must be further verified, because recent *in vitro* experiments showed that the post-termination ribosomal tethering of mRNA by TURBS diminishes dependence on the eIF3-mediated reinitiation by the post-termination 40S subunits, and instead allows reinitiation by the post-termination 80S ribosomes (141).

eIF3 IN HUMAN HEALTH AND DISEASE

Deregulation of eIF3 expression and/or function has been proposed to play either a causal role or at least contribute to the etiology of various diseases including cancer, neurodegenerative states etc.; some eIF3 subunits were even suggested to serve as oncogenes or tumor suppressors with potential prognostic values. The purpose of this chapter is not to cover all aspects of the prospective eIF3 involvement in various human diseases but to briefly discuss some of the discoveries reporting reduced or increased expression of various eIF3 subunits in the context of what we have recently learned about the human eIF3 integrity and potential consequences of imbalanced expression of its individual subunits (25). In other words, it has been long known that various types of cancer and other diseases are associated with altered expression levels of most, if not all, eIF3 subunits (for review see (82,83)). However, we recently demonstrated that these perturbations to the relatively balanced expression of eIF3 subunits lead to the formation of partial eIF3 subcomplexes that are associated with defects in the rate of translation and cell fitness. This may suggest that the observed pathological effects often attributed to alterations in the expression levels of a single eIF3 subunit are actually caused not only by the lack or excessive amount of this particular subunit *per se*, but by the loss or gain of function of partial eIF3 subcomplexes that could form in cancer and other sick cells as a result of these expression anomalies.

Perhaps the easiest interpretations of the functional consequences of altered expression levels in disease can be made with the eIF3d subunit, the siRNA-mediated knock down of which impact neither the expression levels of other eIF3 subunits nor the integrity of eIF3 *in vivo*, nonetheless confers severe defects in growth and translation rates (25). eIF3d was shown to be overexpressed in muscle invasive disease and ovarian cancer, whereas the eIF3d knock-down in metastatic T24M bladder cancer cells inhibited cell proliferation, migration, and colony formation *in vitro* and decreased tumor growth in xenograft models (142,143). eIF3d was also shown to be associated with hepatocellular carcinoma where it was up-regulated as a direct consequence of Hepatitis delta virus replication (144). Given what was said above, it is likely that these phenotypes are directly associated either with (i) malfunctioning of free eIF3d protein that occurs in excess to the rest of eIF3, or (ii) malfunctioning of eIF3 lacking its d subunit in these carcinoma cells.

The eIF3l subunit was found to interact with the Flavivirus NS5 and eIF3l overexpression was suggested to promote Flavivirus translation and thus to modulate the yellow fever virus replication cycle (145). Depletion of endogenous eIF3k de-sensitized simple epithelial cells to various types of apoptotic stimuli and promoted the retention of active caspase 3 in cytoplasmic inclusions by increasing Cas3 binding to keratins (146). Since knock downs of eIF3k and eIF3l mutually impact only their own expression and are dispensable for the integrity of the rest of the eIF3 complex (25), the above described phenotypes should be attributed to the changed expression levels of not only one of these subunits but to both of them. In accord, it was recently shown that the loss-of-function mutations in the *Caenorhabditis elegans* genes encoding eIF3k and eIF3l resulted in an identical phenotype; i.e. in a 40% extension in lifespan and enhanced resistance to endoplasmic reticulum (ER) stress (85).

Similarly, knock down of eIF3h leads to a concurrent downregulation of only the eIF3k and l subunits, hence observations that eIF3h is highly amplified for example in breast and prostate cancers (147) may imply that changes in the expression levels of eIF3k and l might be also expected, which could cause undesirable changes in expression profiles of numerous mRNAs contributing to malignancy.

eIF3e was perhaps the first eIF3 subunit the altered expression of which was connected with cancer (148). In particular, the introns of its gene were found to be a frequent integration site of mouse mammary tumor virus (MMTV)

Downloaded from https://academic.oup.com/nar/article-abstract/45/19/10948/4157872
by Department of Plant Physiology, Faculty of Science, Charles University user
on 25 November 2017

provoking changes in the eIF3e expression in an 'intron-specific' manner. For example, the MMTV integration at intron 6 resulted in a decreased expression of eIF3e in several human breast and lung carcinomas (149). We recently learnt that when eIF3e is significantly underexpressed, the expression of eIF3d, eIF3k and eIF3l is also dramatically reduced (25). As a result, the eIF3 subcomplex lacking only these four subunits forms, which might be responsible for the progression of the observed cancer phenotypes. On the other hand, the MMTV integration at intron 5 produced a truncated eIF3e protein with a malignant transformation potential that could, if still able to incorporate into eIF3, easily result from altered functional properties of the entire eIF3 complex (150).

The siRNA down regulation of either eIF3c or eIF3f or eIF3m subunits pretty much destroys the entire octamer preserving only the YLC (eIF3a–b–g–i) module (25), which is still capable to promote very basic eIF3 functions that are, however, insufficient to support life of human cells (41). Hence any reports describing pathological phenotypes stemming from altered expression of these three subunits should be at least partially regarded as a failure of the dramatically compromised eIF3 complex to ensure productive general translation initiation in sick cells; like underexpression of eIF3f in gastric, melanoma and pancreatic cancers supposedly deregulating apoptosis (151,152), eIF3f ubiquitination and proteosomal degradation during muscle atrophy (153), overexpression of eIF3m in human cancer cell lines and colon cancer patient tissues (154), as well as overexpression of eIF3c in testicular seminoma cells (155).

There are numerous reports implicating altered expression of eIF3a and eIF3b in numerous types of cancer (for review see (82,83)). However, knock down experiments with both of these subunits in HeLa and HEK293T cells clearly revealed that their expression is absolutely essential for formation and stability of the entire eIF3. As aforementioned, they serve as the nucleation core without which eIF3 does not assemble, and changes in their expression have dramatic impact on expression of all other eIF3 subunits (25). Hence, from this point of view we think that all these reports should be considered with caution and interpret the observed pathological anomalies as a consequence of the radically crippled eIF3 complex.

CONCLUDING REMARKS

Whereas the subunit composition of both forms of eIF3 (5-subunit Sc-eIF3 vs. 12-subunit m-eIF3) is now clear, individual initiation roles, as well as the assembly pathways have been elucidated, there is much to be learnt from the structural point of view. Several snapshots of eIF3 with or without other eIFs bound to PICs have been taken and provided an extremely valuable insight into particular initiation steps. However, we still do not know how both eIF3 forms look like free in solution, what structural rearrangements they have to undergo when they associate with other eIFs and mainly during their initial contact with the small ribosomal subunit.

We have learnt the mechanics of the mRNA entry channel latch opening and closure (1). However, we still do not understand when and how the eIF3a-CTD–eIF3b–i–g module swings to the ribosomal interface side, what it does there with respect to mRNA loading, scanning and AUG recognition (in particular considering its interactions with eIF2γ and eIF1 in the decoding center), and when it eventually comes back. Similarly, the mechanics of the eIF3c-NTD involvement in AUG recognition together with the P-site-based eIF1 and eIF5, the precise ribosomal placement of which remains a mystery, needs to be explored in the near future. Besides the need to reveal the eIF5 localization within the PICs, there is a similarly pressing need to identify a precise position of the eIF4F factors, as well as of PABP. The still improving methods of RNA interference and antisense approaches to knock down specific proteins, newly established CRISPR–Cas9 technology, revolutionized Cryo-electron microscopy, as well as the burst of specialized ribosomal profiling studies that are now available to capture scanning 48S PICs (156) should also help by a great deal in addressing most of these questions.

Apart from the initiation phase, it will be extremely valuable to determine how eIF3 associates with terminating ribosomes and uncover molecular details of its role in fine-tuning the termination fidelity and in promoting stop codon readthrough or reinitiation. What factors eIF3 really interacts with during these events and what are the molecular consequences of these contacts? For example, does eIF3 interact with eIF4F to promote reinitiation? What is the functional interplay between ABCE1 and eIF3 during ribosomal recycling followed by a new round of initiation? How does eIF3 manipulate the decoding pocket during termination to promote incorporation of near-cognate tRNAs to the A-site? What is the molecular mechanism of the eIF3 involvement in NMD? Does it vary with the placement and nature of the stop codon across the entire length of mRNA, under stress *versus* normal condition, etc.?

Considering the growing evidence of the eIF3 involvement in the transcript-specific translation regulation, it will also be important to identify all mRNAs that are subject to this eIF3-specific regulation, as well as other contributing factors (mRNA features and proteins). eIF3 was some time ago implicated in signal transduction pathways by recruiting protein kinases such as mTORC1 and S6K to the surface of the 40S subunit (157,158), which we did not cover here. It is entirely possible that signal transduction pathways may govern or at least markedly impact this peculiar role of eIF3.

And last but not least, taking into account numerous reports implicating eIF3 in cancer incidence, metastasis development, prognosis and therapeutic response, we should foster our effort to clarify the exact mechanism of the eIF3 involvement in oncogenesis and enlighten its real chances in cancer treatments, as these areas of research are indeed of the supreme interest for human health.

ACKNOWLEDGEMENTS

We would like to thank to Jose Luis Llacer for his valuable comments on our structure interpretations, and to all our colleagues from the fields of translational control and RNA biology for many supportive and inspirational discussions and thoughts. We also wish to apologize to those whose

Downloaded from https://academic.oup.com/nar/article-abstract/45/19/10948/4157872
by Department of Plant Physiology, Faculty of Science, Charles University user
on 25 November 2017

work was not cited due to the focus of this review or unintentional omissions.

FUNDING

Wellcome Trust [090812/B/09/Z]; Czech Science Foundation [GA17-06238S to L.S.V.]; 'Agence Nationale de la Recherche' (to Y.H.) as part of the 'Investissements d'Avenir' program [LabEx: ANR-10-LABX-0036_NETRNA and ANR-14-ACHN-0024 CryoEM80S]. Funding for open access charge: Wellcome Trust.
Conflict of interest statement. None declared.

REFERENCES

1. Hinnebusch,A.G. (2017) Structural insights into the mechanism of scanning and start codon recognition in eukaryotic translation initiation. *Trends Biochem. Sci.*, **42**, 589–611.
2. Valášek,L.S. (2012) 'Ribozoomin'—translation initiation from the perspective of the ribosome-bound eukaryotic initiation factors (eIFs). *Curr. Protein Pept. Sci.*, **13**, 305–330.
3. Fringer,J.M., Acker,M.G., Fekete,C.A., Lorsch,J.R. and Dever,T.E. (2007) Coupled release of eukaryotic translation initiation factors 5B and 1A from 80S ribosomes following subunit joining. *Mol. Cell Biol.*, **27**, 2384–2397.
4. Jennings,M.D., Kershaw,C.J., Adomavicius,T. and Pavitt,G.D. (2017) Fail-safe control of translation initiation by dissociation of eIF2alpha phosphorylated ternary complexes. *Elife*, **6**, e24542.
5. Hronova,V. and Valasek,L.S. (2017) An emergency brake for protein synthesis. *Elife*, **6**, e27085.
6. Dever,T.E. and Green,R. (2012) The elongation, termination, and recycling phases of translation in eukaryotes. *Cold Spring Harb. Perspect. Biol.*, **4**, a013706.
7. Jackson,R.J., Hellen,C.U. and Pestova,T.V. (2012) Termination and post-termination events in eukaryotic translation. *Adv. Protein Chem. Struct. Biol.*, **86**, 45–93.
8. Shoemaker,C.J. and Green,R. (2011) Kinetic analysis reveals the ordered coupling of translation termination and ribosome recycling in yeast. *Proc. Natl. Acad. Sci. U.S.A.*, **108**, E1392–E1398.
9. Pisarev,A.V., Skabkin,M.A., Pisareva,V.P., Skabkina,O.V., Rakotondrafara,A.M., Hentze,M.W., Hellen,C.U.T. and Pestova,T.V. (2010) The role of ABCE1 in eukaryotic posttermination ribosomal recycling. *Mol. Cell*, **37**, 196–210.
10. Becker,T., Franckenberg,S., Wickles,S., Shoemaker,C.J., Anger,A.M., Armache,J.P., Sieber,H., Ungewickell,C., Berninghausen,O., Daberkow,I. *et al.* (2012) Structural basis of highly conserved ribosome recycling in eukaryotes and archaea. *Nature*, **482**, 501–506.
11. Young,D.J., Guydosh,N.R., Zhang,F., Hinnebusch,A.G. and Green,R. (2015) Rli1/ABCE1 recycles terminating ribosomes and controls translation reinitiation in 3′UTRs in vivo. *Cell*, **162**, 872–884.
12. Pisarev,A.V., Hellen,C.U.T. and Pestova,T.V. (2007) Recycling of eukaryotic posttermination ribosomal complexes. *Cell*, **131**, 286–299.
13. Skabkin,M.A., Skabkina,O.V., Dhote,V., Komar,A.A., Hellen,C.U. and Pestova,T.V. (2010) Activities of Ligatin and MCT-1/DENR in eukaryotic translation initiation and ribosomal recycling. *Genes Dev.*, **24**, 1787–1801.
14. Wethmar,K. (2014) The regulatory potential of upstream open reading frames in eukaryotic gene expression. *Wiley Interdiscip. Rev. RNA*, **5**, 765–778.
15. Dabrowski,M., Bukowy-Bieryllo,Z. and Zietkiewicz,E. (2015) Translational readthrough potential of natural termination codons in eucaryotes—the impact of RNA sequence. *RNA Biol.*, **12**, 950–958.
16. Schueren,F. and Thoms,S. (2016) Functional translational readthrough: a systems biology perspective. *PLoS Genet.*, **12**, e1006196.
17. Dinman,J.D. (2012) Control of gene expression by translational recoding. *Adv. Protein Chem. Struct. Biol.*, **86**, 129–149.
18. Keeling,K.M., Xue,X., Gunn,G. and Bedwell,D.M. (2014) Therapeutics based on stop codon readthrough. *Annu. Rev. Genomics Hum. Genet.*, **15**, 371–394.
19. Beznoskova,P., Gunisova,S. and Valasek,L.S. (2016) Rules of UGA-N decoding by near-cognate tRNAs and analysis of readthrough on short uORFs in yeast. *RNA*, **22**, 456–466.
20. Beznosková,P., Cuchalová,L., Wagner,S., Shoemaker,C.J., Gunišová,S., Von der Haar,T. and Valášek,L.S. (2013) Translation initiation factors eIF3 and HCR1 control translation termination and stop codon read-through in yeast cells. *PLoS Genet.*, **9**, e1003962.
21. Beznoskova,P., Wagner,S., Jansen,M.E., von der Haar,T. and Valasek,L.S. (2015) Translation initiation factor eIF3 promotes programmed stop codon readthrough. *Nucleic Acids Res.*, **43**, 5099–5111.
22. Merrick,W.C. and Hershey,J.W.B. (1996) In: Hershey,JWB, Matthews,MB and Sonenberg,N (eds). *Translational Control*. Cold Spring Harbor Laboratory Press, NY, pp. 31–69.
23. Hinnebusch,A.G. (2006) eIF3: a versatile scaffold for translation initiation complexes. *Trends Biochem. Sci.*, **31**, 553–562.
24. Querol-Audi,J., Sun,C., Vogan,J.M., Smith,M.D., Gu,Y., Cate,J.H. and Nogales,E. (2013) Architecture of human translation initiation factor 3. *Structure*, **21**, 920–928.
25. Wagner,S., Herrmannova,A., Sikrova,D. and Valasek,L.S. (2016) Human eIF3b and eIF3a serve as the nucleation core for the assembly of eIF3 into two interconnected modules: the yeast-like core and the octamer. *Nucleic Acids Res.*, **44**, 10772–10788.
26. Valášek,L., Hašek,J., Trachsel,H., Imre,E.M. and Ruis,H. (1999) The *Saccharomyces cerevisiae HCRI* gene encoding a homologue of the p35 subunit of human translation eukaryotic initiation factor 3 (eIF3) is a high copy suppressor of a temperature-sensitive mutation in the Rpg1p subunit of yeast eIF3. *J. Biol. Chem.*, **274**, 27567–27572.
27. Block,K.L., Vornlocher,H.P. and Hershey,J.W.B. (1998) Characterization of cDNAs encoding the p44 and p35 subunits of human translation initiation factor eIF3. *J. Biol. Chem.*, **273**, 31901–31908.
28. Fraser,C.S., Berry,K.E., Hershey,J.W. and Doudna,J.A. (2007) 3j is located in the decoding center of the human 40S ribosomal subunit. *Mol. Cell*, **26**, 811–819.
29. Kolupaeva,V.G., Unbehaun,A., Lomakin,I.B., Hellen,C.U. and Pestova,T.V. (2005) Binding of eukaryotic initiation factor 3 to ribosomal 40S subunits and its role in ribosomal dissociation and anti-association. *RNA*, **11**, 470–486.
30. Valášek,L., Nielsen,K.H., Zhang,F., Fekete,C.A. and Hinnebusch,A.G. (2004) Interactions of eukaryotic translation initiation factor 3 (eIF3) subunit NIP1/c with eIF1 and eIF5 promote preinitiation complex assembly and regulate start codon selection. *Mol. Cell. Biol.*, **24**, 9437–9455.
31. Karaskova,M., Gunisova,S., Herrmannova,A., Wagner,S., Munzarova,V. and Valasek,L.S. (2012) Functional characterization of the role of the N-terminal domain of the c/Nip1 subunit of eukaryotic initiation factor 3 (eIF3) in AUG recognition. *J. Biol. Chem.*, **287**, 28420–28434.
32. Valášek,L., Nielsen,K.H. and Hinnebusch,A.G. (2002) Direct eIF2-eIF3 contact in the multifactor complex is important for translation initiation in vivo. *EMBO J.*, **21**, 5886–5898.
33. Jivotovskaya,A., Valášek,L., Hinnebusch,A.G. and Nielsen,K.H. (2006) Eukaryotic translation initiation factor 3 (eIF3) and eIF2 can promote mRNA binding to 40S subunits independently of eIF4G in yeast. *Mol. Cell. Biol.*, **26**, 1355–1372.
34. Khoshnevis,S., Gunišová,S., Vlčková,V., Kouba,T., Neumann,P., Beznosková,P., Ficner,R. and Valášek,L.S. (2014) Structural integrity of the PCI domain of eIF3a/TIF32 is required for mRNA recruitment to the 43S pre-initiation complexes. *Nucleic Acids Res.*, **42**, 4123–4139.
35. Aitken,C.E., Beznoskova,P., Vlckova,V., Chiu,W.L., Zhou,F., Valasek,L.S., Hinnebusch,A.G. and Lorsch,J.R. (2016) Eukaryotic translation initiation factor 3 plays distinct roles at the mRNA entry and exit channels of the ribosomal preinitiation complex. *Elife*, **5**, e20934.
36. Mitchell,S.F., Walker,S.E., Algire,M.A., Park,E.-H., Hinnebusch,A.G. and Lorsch,J.R. (2010) The 5′-7-methylguanosine cap on eukaryotic mRNAs serves both to stimulate canonical

Downloaded from https://academic.oup.com/nar/article-abstract/45/19/10948/4157872
by Department of Plant Physiology, Faculty of Science, Charles University user
on 25 November 2017

translation initiation and to block an alternative pathway. *Mol. Cell*, **39**, 950–962.
37. ElAntak,L., Wagner,S., Herrmannová,A., Karásková,M., Rutkai,E., Lukavsky,P.J. and Valášek,L. (2010) The indispensable N-terminal half of eIF3j co-operates with its structurally conserved binding partner eIF3b-RRM and eIF1A in stringent AUG selection. *J. Mol. Biol.*, **396**, 1097–1116.
38. Cuchalová,L., Kouba,T., Herrmannová,A., Danyi,I., Chiu,W.-l. and Valášek,L. (2010) The RNA recognition motif of eukaryotic translation initiation factor 3g (eIF3g) is required for resumption of scanning of posttermination ribosomes for reinitiation on GCN4 and together with eIF3i stimulates linear scanning. *Mol. Cell. Biol.*, **30**, 4671–4686.
39. Chiu,W.-L., Wagner,S., Herrmannová,A., Burela,L., Zhang,F., Saini,A.K., Valášek,L. and Hinnebusch,A.G. (2010) The C-terminal region of eukaryotic translation initiation factor 3a (eIF3a) promotes mRNA recruitment, scanning, and, together with eIF3j and the eIF3b RNA recognition motif, selection of AUG start codons. *Mol. Cell. Biol.*, **30**, 4415–4434.
40. Herrmannová,A., Daujotyte,D., Yang,J.C., Cuchalová,L., Gorrec,F., Wagner,S., Danyi,I., Lukavsky,P.J. and Valášek,L.S. (2012) Structural analysis of an eIF3 subcomplex reveals conserved interactions required for a stable and proper translation pre-Initiation complex assembly. *Nucleic Acids Res.*, **40**, 2294–2311.
41. Wagner,S., Herrmannova,A., Malik,R., Peclinovska,L. and Valasek,L.S. (2014) Functional and biochemical characterization of human eukaryotic translation initiation factor 3 in living cells. *Mol. Cell. Biol.*, **34**, 3041–3052.
42. Obayashi,E., Luna,R.E., Nagata,T., Martin-Marcos,P., Hiraishi,H., Singh,C.R., Erzberger,J.P., Zhang,F., Arthanari,H., Morris,J. *et al.* (2017) Molecular landscape of the ribosome pre-initiation complex during mRNA scanning: structural role for eIF3c and its control by eIF5. *Cell Rep.*, **18**, 2651–2663.
43. Nielsen,K.H., Szamecz,B., Valasek,L., J,A., Shin,B.S. and Hinnebusch,A.G. (2004) Functions of eIF3 downstream of 48S assembly impact AUG recognition and GCN4 translational control. *EMBO J.*, **23**, 1166–1177.
44. Pestova,T.V. and Kolupaeva,V.G. (2002) The roles of individual eukaryotic translation initiation factors in ribosomal scanning and initiation codon selection. *Genes Dev.*, **16**, 2906–2922.
45. Szamecz,B., Rutkai,E., Cuchalova,L., Munzarova,V., Herrmannova,A., Nielsen,K.H., Burela,L., Hinnebusch,A.G. and Valášek,L. (2008) eIF3a cooperates with sequences 5′ of uORF1 to promote resumption of scanning by post-termination ribosomes for reinitiation on GCN4 mRNA. *Genes Dev.*, **22**, 2414–2425.
46. Munzarová,V., Pánek,J., Gunišová,S., Dányi,I., Szamecz,B. and Valášek,L.S. (2011) Translation reinitiation relies on the interaction between eIF3a/TIF32 and progressively folded cis-acting mRNA elements preceding short uORFs. *PLoS Genet.*, **7**, e1002137.
47. Mohammad,M.P., Munzarova Pondelickova,V., Zeman,J., Gunisova,S. and Valasek,L.S. (2017) In vivo evidence that eIF3 stays bound to ribosomes elongating and terminating on short upstream ORFs to promote reinitiation. *Nucleic Acids Res.*, **45**, 2658–2674.
48. Smith,M.D., Arake-Tacca,L., Nitido,A., Montabana,E., Park,A. and Cate,J.H. (2016) Assembly of eIF3 mediated by mutually dependent subunit insertion. *Structure*.
49. Valášek,L., Phan,L., Schoenfeld,L.W., Valášková,V. and Hinnebusch,A.G. (2001) Related eIF3 subunits TIF32 and HCR1 interact with an RNA recoginition motif in PRT1 required for eIF3 integrity and ribosome binding. *EMBO J.*, **20**, 891–904.
50. Valášek,L., Mathew,A., Shin,B.S., Nielsen,K.H., Szamecz,B. and Hinnebusch,A.G. (2003) The yeast eIF3 subunits TIF32/a and NIP1/c and eIF5 make critical connections with the 40S ribosome in vivo. *Genes Dev.*, **17**, 786–799.
51. Nielsen,K.H., Valášek,L., Sykes,C., Jivotovskaya,A. and Hinnebusch,A.G. (2006) Interaction of the RNP1 motif in PRT1 with HCR1 promotes 40S binding of eukaryotic initiation factor 3 in yeast. *Mol. Cell. Biol.*, **26**, 2984–2998.
52. Phan,L., Schoenfeld,L.W., Valášek,L., Nielsen,K.H. and Hinnebusch,A.G. (2001) A subcomplex of three eIF3 subunits binds eIF1 and eIF5 and stimulates ribosome binding of mRNA and $tRNA_i^{Met}$. *EMBO J.*, **20**, 2954–2965.
53. Phan,L., Zhang,X., Asano,K., Anderson,J., Vornlocher,H.P., Greenberg,J.R., Qin,J. and Hinnebusch,A.G. (1998) Identification of a translation initiation factor 3 (eIF3) core complex, conserved in yeast and mammals, that interacts with eIF5. *Mol. Cell. Biol.*, **18**, 4935–4946.
54. Asano,K., Phan,L., Anderson,J. and Hinnebusch,A.G. (1998) Complex formation by all five homologues of mammalian translation initiation factor 3 subunits from yeast *Saccharomyces cerevisiae*. *J. Biol. Chem.*, **273**, 18573–18585.
55. Khoshnevis,S., Hauer,F., Milon,P., Stark,H. and Ficner,R. (2012) Novel insights into the architecture and protein interaction network of yeast eIF3. *RNA*, **18**, 2306–2319.
56. Dong,Z., Qi,J., Peng,H., Liu,J. and Zhang,J.T. (2013) Spectrin domain of eukaryotic initiation factor 3a is the docking site for formation of the a:b:i:g subcomplex. *J. Biol. Chem.*, **288**, 27951–27959.
57. Ellisdon,A.M. and Stewart,M. (2012) Structural biology of the PCI-protein fold. *Bioarchitecture*, **2**, 118–123.
58. Sun,C., Todorovic,A., Querol-Audi,J., Bai,Y., Villa,N., Snyder,M., Ashchyan,J., Lewis,C.S., Hartland,A., Gradia,S. *et al.* (2011) Functional reconstitution of human eukaryotic translation initiation factor 3 (eIF3). *Proc. Natl. Acad. Sci. U.S.A.*, **108**, 20473–20478.
59. des Georges,A., Dhote,V., Kuhn,L., Hellen,C.U., Pestova,T.V., Frank,J. and Hashem,Y. (2015) Structure of mammalian eIF3 in the context of the 43S preinitiation complex. *Nature*, **525**, 491–495.
60. Siridechadilok,B., Fraser,C.S., Hall,R.J., Doudna,J.A. and Nogales,E. (2005) Structural roles for human translation factor eIF3 in initiation of protein synthesis. *Science*, **310**, 1513–1515.
61. Emanuilov,I., Sabatini,D.D., Lake,J.A. and Freienstein,C. (1978) Localization of eukaryotic initiation factor 3 on native small ribosomal subunits. *Proc. Natl. Acad. Sci. U.S.A.*, **75**, 1389–1393.
62. Srivastava,S., Verschoor,A. and Frank,J. (1992) Eukaryotic initiation factor 3 does not prevent association through physical blockage of the ribosomal subunit-subunit interface. *J. Mol. Biol.*, **220**, 301–304.
63. Hashem,Y., des Georges,A., Dhote,V., Langlois,R., Liao,H.Y., Grassucci,R.A., Hellen,C.U., Pestova,T.V. and Frank,J. (2013) Structure of the mammalian ribosomal 43S preinitiation complex bound to the scanning factor DHX29. *Cell*, **153**, 1108–1119.
64. Erzberger,J.P., Stengel,F., Pellarin,R., Zhang,S., Schaefer,T., Aylett,C.H., Cimermancic,P., Boehringer,D., Sali,A., Aebersold,R. *et al.* (2014) Molecular architecture of the 40SeIF1eIF3 translation initiation complex. *Cell*, **158**, 1123–1135.
65. Aylett,C.H., Boehringer,D., Erzberger,J.P., Schaefer,T. and Ban,N. (2015) Structure of a yeast 40S-eIF1-eIF1A-eIF3-eIF3j initiation complex. *Nat. Struct. Mol. Biol.*, **22**, 269–271.
66. Llacer,J.L., Hussain,T., Marler,L., Aitken,C.E., Thakur,A., Lorsch,J.R., Hinnebusch,A.G. and Ramakrishnan,V. (2015) Conformational differences between open and closed states of the eukaryotic translation initiation complex. *Mol. Cell*, **59**, 399–412.
67. Kouba,T., Danyi,I., Gunišová,S., Munzarová,V., Vlčková,V., Cuchalová,L., Neueder,A., Milkereit,P. and Valášek,L.S. (2012) Small ribosomal protein RPS0 stimulates translation initiation by mediating 40S-binding of eIF3 via its direct contact with the eIF3a/TIF32 subunit. *PLoS One*, **7**, e40464.
68. Pisarev,A.V., Kolupaeva,V.G., Yusupov,M.M., Hellen,C.U.T. and Pestova,T.V. (2008) Ribosomal position and contacts of mRNA in eukaryotic translation initiation complexes. *EMBO J.*, **27**, 1609–1621.
69. Liu,Y., Neumann,P., Kuhle,B., Monecke,T., Schell,S., Chari,A. and Ficner,R. (2014) Translation initiation factor eIF3b contains a nine-bladed beta-propeller and interacts with the 40S ribosomal subunit. *Structure*, **22**, 923–930.
70. Simonetti,A., Brito Querido,J., Myasnikov,A.G., Mancera-Martinez,E., Renaud,A., Kuhn,L. and Hashem,Y. (2016) eIF3 Peripheral Subunits Rearrangement after mRNA Binding and Start-Codon Recognition. *Mol. Cell*, **63**, 206–217.
71. Heuer,A., Gerovac,M., Schmidt,C., Trowitzsch,S., Preis,A., Kotter,P., Berninghausen,O., Becker,T., Beckmann,R. and Tampe,R. (2017) Structure of the 40S-ABCE1 post-splitting complex in ribosome recycling and translation initiation. *Nat. Struct. Mol. Biol.*, **24**, 453–460.
72. Mancera-Martinez,E., Brito Querido,J., Valasek,L.S., Simonetti,A. and Hashem,Y. (2017) ABCE1: A special factor that orchestrates translation at the crossroad between recycling and initiation. *RNA Biol.*, doi:10.1080/15476286.15472016.11269993.

Downloaded from https://academic.oup.com/nar/article-abstract/45/19/10948/4157872
by Department of Plant Physiology, Faculty of Science, Charles University user
on 25 November 2017

73. Asano,K., Phan,L., Valasek,L., Schoenfeld,L.W., Shalev,A., Clayton,J., Nielsen,K., Donahue,T.F. and Hinnebusch,A.G. (2001) A multifactor complex of eIF1, eIF2, eIF3, eIF5, and tRNA(i)Met promotes initiation complex assembly and couples GTP hydrolysis to AUG recognition. *Cold Spring Harb. Symp. Quant. Biol.*, **66**, 403–415.
74. Fletcher,C.M., Pestova,T.V., Hellen,C.U.T. and Wagner,G. (1999) Structure and interactions of the translation initiation factor eIF1. *EMBO J.*, **18**, 2631–2639.
75. Villa,N., Do,A., Hershey,J.W. and Fraser,C.S. (2013) Human eukaryotic initiation factor 4G (eIF4G) binds to eIF3c, -d, and -e to promote mRNA recruitment to the ribosome. *J. Biol. Chem.*, **288**, 32932–32940.
76. Methot,N., Song,M.S. and Sonenberg,N. (1996) A region rich in aspartic acid, arginine, tyrosine, and glycine (DRYFG) mediates eukaryotic initiation factor 4B (eIF4B) self-association and interaction with eIF3. *Mol. Cell. Biol.*, **16**, 5328–5334.
77. Pisareva,V.P. and Pisarev,A.V. (2016) DHX29 and eIF3 cooperate in ribosomal scanning on structured mRNAs during translation initiation. *RNA*, **22**, 1859–1870.
78. Pisareva,V.P. and Pisarev,A.V. (2016) DHX29 reduces leaky scanning through an upstream AUG codon regardless of its nucleotide context. *Nucleic Acids Res.*, **44**, 4252–4265.
79. Lee,A.S., Kranzusch,P.J. and Cate,J.H. (2015) eIF3 targets cell-proliferation messenger RNAs for translational activation or repression. *Nature*, **522**, 111–114.
80. Lee,A.S., Kranzusch,P.J., Doudna,J.A. and Cate,J.H. (2016) eIF3d is an mRNA cap-binding protein that is required for specialized translation initiation. *Nature*, **536**, 96–99.
81. Kumar,P., Hellen,C.U. and Pestova,T.V. (2016) Toward the mechanism of eIF4F-mediated ribosomal attachment to mammalian capped mRNAs. *Genes Dev.*, **30**, 1573–1588.
82. Hershey,J.W. (2015) The role of eIF3 and its individual subunits in cancer. *Biochim. Biophy. Acta*, **1849**, 792–800.
83. Robichaud,N. and Sonenberg,N. (2017) Translational control and the cancer cell response to stress. *Curr. Opin. Cell Biol.*, **45**, 102–109.
84. Shah,M., Su,D., Scheliga,J.S., Pluskal,T., Boronat,S., Motamedchaboki,K., Campos,A.R., Qi,F., Hidalgo,E., Yanagida,M. *et al.* (2016) A transcript-specific eIF3 complex mediates global translational control of energy metabolism. *Cell Rep.*, **16**, 1891–1902.
85. Cattie,D.J., Richardson,C.E., Reddy,K.C., Ness-Cohn,E.M., Droste,R., Thompson,M.K., Gilbert,W.V. and Kim,D.H. (2016) Mutations in nonessential eIF3k and eIF3l genes confer lifespan extension and enhanced resistance to ER stress in Caenorhabditis elegans. *PLoS Genet.*, **12**, e1006326.
86. Meyer,K.D., Patil,D.P., Zhou,J., Zinoviev,A., Skabkin,M.A., Elemento,O., Pestova,T.V., Qian,S.B. and Jaffrey,S.R. (2015) 5 ' UTR m(6)A promotes Cap-independent translation. *Cell*, **163**, 999–1010.
87. Wang,X., Zhao,B.S., Roundtree,I.A., Lu,Z., Han,D., Ma,H., Weng,X., Chen,K., Shi,H. and He,C. (2015) N(6)-methyladenosine modulates messenger RNA translation efficiency. *Cell*, **161**, 1388–1399.
88. Choudhuri,A., Maitra,U. and Evans,T. (2013) Translation initiation factor eIF3h targets specific transcripts to polysomes during embryogenesis. *Proc. Natl. Acad. Sci. U.S.A.*, **110**, 9818–9823.
89. Lee,K.M., Chen,C.J. and Shih,S.R. (2017) Regulation mechanisms of viral IRES-driven translation. *Trends Microbiol.*, **25**, 546–561.
90. Kieft,J.S., Zhou,K., Grech,A., Jubin,R. and Doudna,J.A. (2002) Crystal structure of an RNA tertiary domain essential to HCV IRES-mediated translation initiation. *Nat. Struct. Biol.*, **9**, 370–374.
91. Sizova,D.V., Kolupaeva,V.G., Pestova,T.V., Shatsky,I.N. and Hellen,C.U. (1998) Specific interaction of eukaryotic translation initiation factor 3 with the 5′ nontranslated regions of hepatitis C virus and classical swine fever RNAs. *J. Virol.*, **72**, 4775–4782.
92. Buratti,E., Tisminetzky,S., Zotti,M. and Baralle,F.E. (1998) Functional analysis of the interaction between HCV 5′UTR and putative subunits of eukaryotic translation initiation factor eIF3. *Nucleic Acids Res.*, **26**, 3179–3187.
93. Sun,C., Querol-Audi,J., Mortimer,S.A., Arias-Palomo,E., Doudna,J.A., Nogales,E. and Cate,J.H. (2013) Two RNA-binding motifs in eIF3 direct HCV IRES-dependent translation. *Nucleic Acids Res.*, **41**, 7512–7521.
94. Otto,G.A. and Puglisi,J. (2004) The pathway of HCV IRES-mediated translation initiation. *Cell*, **119**, 369–380.
95. Hashem,Y., des Georges,A., Dhote,V., Langlois,R., Liao,H.Y., Grassucci,R.A., Pestova,T.V., Hellen,C.U. and Frank,J. (2013) Hepatitis-C-virus-like internal ribosome entry sites displace eIF3 to gain access to the 40S subunit. *Nature*, **503**, 539–543.
96. Jager,S., Cimermancic,P., Gulbahce,N., Johnson,J.R., McGovern,K.E., Clarke,S.C., Shales,M., Mercenne,G., Pache,L., Li,K. *et al.* (2012) Global landscape of HIV-human protein complexes. *Nature*, **481**, 365–370.
97. Thakor,N., Smith,M.D., Roberts,L., Faye,M.D., Patel,H., Wieden,H.J., Cate,J.H.D. and Holcik,M. (2017) Cellular mRNA recruits the ribosome via eIF3-PABP bridge to initiate internal translation. *RNA Biol.*, **14**, 553–567.
98. Yarunin,A., Panse,V.G., Petfalski,E., Dez,C., Tollervey,D. and Hurt,E. (2005) Functional link between ribosome formation and biogenesis of ironsulfur proteins. *EMBO J.*, **24**, 580–588.
99. Chen,Z.Q., Dong,J., Ishimura,A., Daar,I., Hinnebusch,A.G. and Dean,M. (2006) The essential vertebrate ABCE1 protein interacts with eukaryotic initiation factors. *J. Biol. Chem.*, **281**, 7452–7457.
100. Kryuchkova,P., Grishin,A., Eliseev,B., Karyagina,A., Frolova,L. and Alkalaeva,E. (2013) Two-step model of stop codon recognition by eukaryotic release factor eRF1. *Nucleic Acids Res.*, **41**, 4573–4586.
101. des Georges,A., Hashem,Y., Unbehaun,A., Grassucci,R.A., Taylor,D., Hellen,C.U., Pestova,T.V. and Frank,J. (2014) Structure of the mammalian ribosomal pre-termination complex associated with eRF1.eRF3.GDPNP. *Nucleic Acids Res.*, **42**, 3409–3418.
102. Preis,A., Heuer,A., Barrio-Garcia,C., Hauser,A., Eyler,D.E., Berninghausen,O., Green,R., Becker,T. and Beckmann,R. (2014) Cryoelectron microscopic structures of eukaryotic translation termination complexes containing eRF1-eRF3 or eRF1-ABCE1. *Cell Rep.*, **8**, 59–65.
103. Matheisl,S., Berninghausen,O., Becker,T. and Beckmann,R. (2015) Structure of a human translation termination complex. *Nucleic Acids Res.*, **43**, 8615–8626.
104. Brown,A., Shao,S., Murray,J., Hegde,R.S. and Ramakrishnan,V. (2015) Structural basis for stop codon recognition in eukaryotes. *Nature*, **524**, 493–496.
105. Bidou,L., Allamand,V., Rousset,J.P. and Namy,O. (2012) Sense from nonsense: therapies for premature stop codon diseases. *Trends Mol. Med.*, **18**, 679–688.
106. Taylor,D., Unbehaun,A., Li,W., Das,S., Lei,J., Liao,H.Y., Grassucci,R.A., Pestova,T.V. and Frank,J. (2012) Cryo-EM structure of the mammalian eukaryotic release factor eRF1-eRF3-associated termination complex. *Proc. Natl. Acad. Sci. U.S.A.*, **109**, 18413–18418.
107. Becker,T., Armache,J.P., Jarasch,A., Anger,A.M., Villa,E., Sieber,H., Motaal,B.A., Mielke,T., Berninghausen,O. and Beckmann,R. (2011) Structure of the no-go mRNA decay complex Dom34-Hbs1 bound to a stalled 80S ribosome. *Nat. Struct. Mol. Biol.*, **18**, 715–720.
108. Hussain,T., Llacer,J.L., Fernandez,I.S., Munoz,A., Martin-Marcos,P., Savva,C.G., Lorsch,J.R., Hinnebusch,A.G. and Ramakrishnan,V. (2014) Structural changes enable start codon recognition by the eukaryotic translation initiation complex. *Cell*, **159**, 597–607.
109. Keeling,K.M., Lanier,J., Du,M., Salas-Marco,J., Gao,L., Kaenjak-Angeletti,A. and Bedwell,D.M. (2004) Leaky termination at premature stop codons antagonizes nonsense-mediated mRNA decay in S. cerevisiae. *RNA*, **10**, 691–703.
110. Isken,O., Kim,Y.K., Hosoda,N., Mayeur,G.L., Hershey,J.W.B. and Maquat,L.E. (2008) Upf1 phosphorylation triggers translational repression during nonsense-mediated mRNA decay. *Cell*, **133**, 314–327.
111. Flury,V., Restuccia,U., Bachi,A. and Muhlemann,O. (2014) Characterization of phosphorylation- and RNA-dependent UPF1 interactors by quantitative proteomics. *J. Proteome Res.*, **13**, 3038–3053.
112. Decker,C.J. and Parker,R. (2012) P-bodies and stress granules: possible roles in the control of translation and mRNA degradation. *Cold Spring Harb. Perspect. Biol.*, **4**, a012286.
113. Choe,J., Oh,N., Park,S., Lee,Y.K., Song,O.K., Locker,N., Chi,S.G. and Kim,Y.K. (2012) Translation initiation on mRNAs bound by

Downloaded from https://academic.oup.com/nar/article-abstract/45/19/10948/4157872
by Department of Plant Physiology, Faculty of Science, Charles University user
on 25 November 2017

nuclear cap-binding protein complex CBP80/20 requires interaction between CBP80/20-dependent translation initiation factor and eukaryotic translation initiation factor 3g. *J. Biol. Chem.*, **287**, 18500–18509.
114. Morris,C., Wittmann,J., Jack,H.M. and Jalinot,P. (2007) Human INT6/eIF3e is required for nonsense-mediated mRNA decay. *EMBO Rep.*, **8**, 596–602.
115. Amrani,N., Ghosh,S., Mangus,D.A. and Jacobson,A. (2008) Translation factors promote the formation of two states of the closed-loop mRNP. *Nature*, **453**, 1276–1280.
116. Joncourt,R., Eberle,A.B., Rufener,S.C. and Muhlemann,O. (2014) Eukaryotic initiation factor 4G suppresses nonsense-mediated mRNA decay by two genetically separable mechanisms. *PLoS One*, **9**, e104391.
117. Peixeiro,I., Inacio,A., Barbosa,C., Silva,A.L., Liebhaber,S.A. and Romao,L. (2012) Interaction of PABPC1 with the translation initiation complex is critical to the NMD resistance of AUG-proximal nonsense mutations. *Nucleic Acids Res.*, **40**, 1160–1173.
118. Pereira,F.J., Teixeira,A., Kong,J., Barbosa,C., Silva,A.L., Marques-Ramos,A., Liebhaber,S.A. and Romao,L. (2015) Resistance of mRNAs with AUG-proximal nonsense mutations to nonsense-mediated decay reflects variables of mRNA structure and translational activity. *Nucleic Acids Res.*, **43**, 6528–6544.
119. Calvo,S.E., Pagliarini,D.J. and Mootha,V.K. (2009) Upstream open reading frames cause widespread reduction of protein expression and are polymorphic among humans. *PNAS*, **106**, 7507–7512.
120. Lawless,C., Pearson,R.D., Selley,J.N., Smirnova,J.B., Grant,C.M., Ashe,M.P., Pavitt,G.D. and Hubbard,S.J. (2009) Upstream sequence elements direct post-transcriptional regulation of gene expression under stress conditions in yeast. *BMC Genomics*, **10**, 7.
121. Kim,B.H., Cai,X., Vaughn,J.N. and von Arnim,A.G. (2007) On the functions of the h subunit of eukaryotic initiation factor 3 in late stages of translation initiation. *Genome Biol.*, **8**, R60.
122. Barbosa,C., Peixeiro,I. and Romao,L. (2013) Gene expression regulation by upstream open reading frames and human disease. *PLoS Genet.*, **9**, e1003529.
123. Janich,P., Arpat,A.B., Castelo-Szekely,V., Lopes,M. and Gatfield,D. (2015) Ribosome profiling reveals the rhythmic liver translatome and circadian clock regulation by upstream open reading frames. *Genome Res.*, **25**, 1848–1859.
124. Park,H.S., Himmelbach,A., Browning,K.S., Hohn,T. and Ryabova,L.A. (2001) A plant viral "reinitiation" factor interacts with the host translational machinery. *Cell*, **106**, 723–733.
125. Kim,T.H., Kim,B.H., Yahalom,A., Chamovitz,D.A. and von Arnim,A.G. (2004) Translational regulation via 5′ mRNA leader sequences revealed by mutational analysis of the Arabidopsis translation initiation factor subunit eIF3h. *Plant Cell*, **16**, 3341–3356.
126. Roy,B., Vaughn,J.N., Kim,B.-H., Zhou,F., Gilchrist,M.A. and Von Arnim,A.G. (2010) The h subunit of eIF3 promotes reinitiation competence during translation of mRNAs harboring upstream open reading frames. *RNA*, **16**, 748–761.
127. Schepetilnikov,M., Dimitrova,M., Mancera-Martinez,E., Geldreich,A., Keller,M. and Ryabova,L.A. (2013) TOR and S6K1 promote translation reinitiation of uORF-containing mRNAs via phosphorylation of eIF3h. *EMBO J.*, **32**, 1087–1102.
128. Gunisova,S. and Valasek,L.S. (2014) Fail-safe mechanism of GCN4 translational control-uORF2 promotes reinitiation by analogous mechanism to uORF1 and thus secures its key role in GCN4 expression. *Nucleic Acids Res.*, **42**, 5880–5893.
129. Hinnebusch,A.G. (2005) Translational regulation of GCN4 and the general amino acid control of yeast. *Annu. Rev. Microbiol.*, **59**, 407–450.
130. Gunisova,S., Beznoskova,P., Mohammad,M.P., Vlckova,V. and Valasek,L.S. (2016) In-depth analysis of cis-determinants that either promote or inhibit reinitiation on GCN4 mRNA after translation of its four short uORFs. *RNA*, **22**, 542–558.
131. Kozak,M. (2001) Constraints on reinitiation of translation in mammals. *Nucleic Acids Res.*, **29**, 5226–5232.
132. Pöyry,T.A., Kaminski,A. and Jackson,R.J. (2004) What determines whether mammalian ribosomes resume scanning after translation of a short upstream open reading frame? *Genes Dev.*, **18**, 62–75.
133. Skabkin,M.A., Skabkina,O.V., Hellen,C.U. and Pestova,T.V. (2013) Reinitiation and other unconventional posttermination events during eukaryotic translation. *Mol. Cell*, **51**, 249–264.
134. LeFebvre,A.K., Korneeva,N.L., Trutschl,M., Cvek,U., Duzan,R.D., Bradley,C.A., Hershey,J.W. and Rhoads,R. (2006) Translation initiation factor eIF4G-1 binds to eIF3 through the eIF3e subunit. *J. Biol. Chem.*, **281**, 22917–22932.
135. Yu,Y., Abaeva,I.S., Marintchev,A., Pestova,T.V. and Hellen,C.U. (2011) Common conformational changes induced in type 2 picornavirus IRESs by cognate trans-acting factors. *Nucleic Acids Res.*, **39**, 4851–4865.
136. Weinberg,D.E., Shah,P., Eichhorn,S.W., Hussmann,J.A., Plotkin,J.B. and Bartel,D.P. (2016) Improved ribosome-footprint and mRNA measurements provide insights into dynamics and regulation of yeast translation. *Cell Rep.*, **14**, 1787–1799.
137. Lu,P.D., Harding,H.P. and Ron,D. (2004) Translation reinitiation at alternative open reading frames regulates gene expression in an integrated stress response. *J. Cell Biol.*, **167**, 27–33.
138. Hronova,V., Mohammad,M.P., Wagner,S., Panek,J., Gunisova,S., Zeman,J., Poncova,K. and Valasek,L.S. (2017) Does eIF3 promote reinitiation after translation of short upstream ORFs also in mammalian cells? *RNA Biol.*, doi:10.1080/15476286.15472017.11353863.
139. Pöyry,T.A., Kaminski,A., Connell,E.J., Fraser,C.S. and Jackson,R.J. (2007) The mechanism of an exceptional case of reinitiation after translation of a long ORF reveals why such events do not generally occur in mammalian mRNA translation. *Genes Dev.*, **21**, 3149–3162.
140. Luttermann,C. and Meyers,G. (2009) The importance of inter- and intramolecular base pairing for translation reinitiation on a eukaryotic bicistronic mRNA. *Genes Dev.*, **23**, 331–344.
141. Zinoviev,A., Hellen,C.U. and Pestova,T.V. (2015) Multiple mechanisms of reinitiation on bicistronic calicivirus mRNAs. *Mol. Cell*, **57**, 1059–1073.
142. Lin,Y., Zhang,R. and Zhang,P. (2016) Eukaryotic translation initiation factor 3 subunit D overexpression is associated with the occurrence and development of ovarian cancer. *FEBS Open Biol.*, **6**, 1201–1210.
143. Zhang,F., Xiang,S., Cao,Y., Li,M., Ma,Q., Liang,H., Li,H., Ye,Y., Zhang,Y., Jiang,L. *et al.* (2017) EIF3Dpromotes gallbladder cancer development by stabilizing GRK2 kinase andactivating PI3K-AKT signaling pathway. *CellDeath Dis.*, **8**, e2868.
144. Mendes,M., Perez-Hernandez,D., Vazquez,J., Coelho,A.V. and Cunha,C. (2013) Proteomic changes in HEK-293 cells induced by hepatitis delta virus replication. *J. Proteomics*, **89**, 24–38.
145. Morais,A., Terzian,A.C., Duarte,D.V., Bronzoni,R.V., Madrid,M.C., Gavioli,A.F., Gil,L.H., Oliveira,A.G., Zanelli,C.F., Valentini,S.R. *et al.* (2013) The eukaryotic translation initiation factor 3 subunit L protein interacts with Flavivirus NS5 and may modulate yellow fever virus replication. *Virol. J.*, **10**, 205.
146. Lin,Y.M., Chen,Y.R., Lin,J.R., Wang,W.J., Inoko,A., Inagaki,M., Wu,Y.C. and Chen,R.H. (2008) eIF3k regulates apoptosis in epithelial cells by releasing caspase 3 from keratin-containing inclusions. *J. Cell Sci.*, **121**, 2382–2393.
147. Saramaki,O., Willi,N., Bratt,O., Gasser,T.C., Koivisto,P., Nupponen,N.N., Bubendorf,L. and Visakorpi,T. (2001) Amplification of EIF3S3 gene is associated with advanced stage in prostate cancer. *Am. J. Pathol.*, **159**, 2089–2094.
148. Marchetti,A., Buttitta,F., Miyazaki,S., Gallahan,D., Smith,G.H. and Callahan,R. (1995) *Int-6*, a highly conserved, widely expressed gene, is mutated by mouse mammary tumor virus in mammary preneoplasia. *J. Virol.*, **69**, 1932–1938.
149. Marchetti,A., Buttitta,F., Pellegrini,S., Bertacca,G. and Callahan,R. (2001) Reduced expression of INT-6/eIF3-p48 in human tumors. *Int. J. Oncol.*, **18**, 175–179.
150. Chiluiza,D., Bargo,S., Callahan,R. and Rhoads,R.E. (2011) Expression of truncated eukaryotic initiation factor 3e (eIF3e) resulting from integration of mouse mammary tumor virus (MMTV) causes a shift from cap-dependent to cap-independent translation. *J. Biol. Chem.*, **286**, 31288–31296.
151. Cheng,Y., Jia,C., Li,G. and Li,H. (2014) Expression of eukaryotic initiation factor 3f is associated with prognosis in gastric carcinomas. *Oncol. Res. Treat.*, **37**, 198–202.

Downloaded from https://academic.oup.com/nar/article-abstract/45/19/10948/4157872
by Department of Plant Physiology, Faculty of Science, Charles University user
on 25 November 2017

152. Doldan,A., Chandramouli,A., Shanas,R., Bhattacharyya,A., Leong,S.P., Nelson,M.A. and Shi,J. (2008) Loss of the eukaryotic initiation factor 3f in melanoma. *Mol. Carcinog.*, **47**, 806–813.
153. Lagirand-Cantaloube,J., Offner,N., Csibi,A., Leibovitch,M.P., Batonnet-Pichon,S., Tintignac,L.A., Segura,C.T. and Leibovitch,S.A. (2008) The initiation factor eIF3-f is a major target for atrogin1/MAFbx function in skeletal muscle atrophy. *EMBO J.*, **27**, 1266–1276.
154. Goh,S.H., Hong,S.H., Hong,S.H., Lee,B.C., Ju,M.H., Jeong,J.S., Cho,Y.R., Kim,I.H. and Lee,Y.S. (2011) eIF3m expression influences the regulation of tumorigenesis-related genes in human colon cancer. *Oncogene*, **30**, 398–409.
155. Rothe,M., Ko,Y., Albers,P. and Wernert,N. (2000) Eukaryotic initiation factor 3 p110 mRNA is overexpressed in testicular seminomas. *Am. J. Pathol.*, **157**, 1597–1604.
156. Archer,S.K., Shirokikh,N.E., Beilharz,T.H. and Preiss,T. (2016) Dynamics of ribosome scanning and recycling revealed by translation complex profiling. *Nature*, **535**, 570–574.
157. Holz,M.K., Ballif,B.A., Gygi,S.P. and Blenis,J. (2005) mTOR and S6K1 mediate assembly of the translation preinitiation complex through dynamic protein interchange and ordered phosphorylation events. *Cell*, **123**, 569–580.
158. Harris,T.E., Chi,A., Shabanowitz,J., Hunt,D.F., Rhoads,R.E. and Lawrence,J.C. Jr (2006) mTOR-dependent stimulation of the association of eIF4G and eIF3 by insulin. *EMBO J.*, **25**, 1659–1668.
159. Zhou,M., Sandercock,A.M., Fraser,C.S., Ridlova,G., Stephens,E., Schenauer,M.R., Yokoi-Fong,T., Barsky,D., Leary,J.A., Hershey,J.W. *et al.* (2008) Mass spectrometry reveals modularity and a complete subunit interaction map of the eukaryotic translation factor eIF3. *Proc. Natl. Acad. Sci. U.S.A.*, **105**, 18139–18144.
160. Namy,O., Hatin,I. and Rousset,J.P. (2001) Impact of the six nucleotides downstream of the stop codon on translation termination. *EMBO Rep.*, **2**, 787–793.
161. Luo,H., Lin,Y., Gao,F., Zhang,C.T. and Zhang,R. (2014) DEG 10, an update of the database of essential genes that includes both protein-coding genes and noncoding genomic elements. *Nucleic Acids Res.*, **42**, D574–D580.
162. Smith,M.D., Gu,Y., Querol-Audi,J., Vogan,J.M., Nitido,A. and Cate,J.H. (2013) Human-like eukaryotic translation initiation factor 3 from Neurospora crassa. *PLoS One*, **8**, e78715.

Downloaded from https://academic.oup.com/nar/article-abstract/45/19/10948/4157872
by Department of Plant Physiology, Faculty of Science, Charles University user
on 25 November 2017

OXFORD UNIVERSITY PRESS | FEMS Microbiology Reviews

http://mc.manuscriptcentral.com/fems

Please do not recycle! Translation reinitiation in microbes and higher eukaryotes.

Journal:	*FEMS Microbiology Reviews*
Manuscript ID	Draft
Manuscript Type:	Review Article
Date Submitted by the Author:	n/a
Complete List of Authors:	Gunisova, Stanislava; Institute of Microbiology CAS Hronova, Vladislava; Institute of Microbiology CAS Mohammad, Mahabub; Institute of Microbiology CAS Hinnebusch, Alan; National Institute of Child Health and Human Development Valasek, Leos Shivaya ; Institute of Microbiology CAS
Keywords:	translation reinitiation, termination-reinitiation, uORF, GCN4, eIF3, eIF2

SCHOLARONE™ Manuscripts

For Review

Please do not recycle!
Translation reinitiation in microbes and higher eukaryotes.

Stanislava Gunišová[1*], Vladislava Hronová[1], Mahabub Pasha Mohammad[1], Alan G. Hinnebusch[2*], and Leoš Shivaya Valášek[1*]

[1] Laboratory of Regulation of Gene Expression, Institute of Microbiology ASCR, Videnska 1083, Prague, 142 20, the Czech Republic
[2] Laboratory of Gene Regulation and Development, Eunice Kennedy Shriver National Institute of Child Health and Human Development, NIH, Bethesda, MD 20892, USA.

[*]To whom the correspondence should be addressed: valasekl@biomed.cas.cz
gunisova@biomed.cas.cz
ahinnebusch@nih.gov

One sentence summary

This review covers one of many means of gene-specific translational control called translational reinitiation that 1) occurs on mRNAs carrying more than one ORF, 2) can be mediated by either post-termination 40S or 80S ribosomes, and 3) is highly regulated in response to various stresses and many other intra- or extracellular signals.

Keywords: translation reinitiation, termination-reinitiation, uORF, GCN4, eIF2, eIF3

For Peer Review

ABSTRACT

Protein production must be strictly controlled at its beginning and end to synthesize a polypeptide that faithfully copies genetic information carried in mRNA by which it is encoded. In contrast to viruses and prokaryotes, the majority of eukaryotic mRNAs contain only one coding sequence resulting in production of a single protein. There are, however, several exceptional mRNAs that either carry short open reading frames upstream of the main coding sequence (uORFs) or even contain two or more long ORFs. A wide variety of mechanisms in microbes and higher eukaryotes has evolved to prevent recycling of all or some translational components upon termination of the first translated ORF (either short or long) in these mRNAs to enable subsequent translation of the next uORF or downstream coding sequences, which are often specifically regulated in response to various stimuli. Here we review short uORF-mediated versus long ORF-mediated mechanisms of translational reinitiation in all its forms to provide the current, complete picture of this intriguing type of translational control.

For Peer Review

ScholarOne Support 1-434/964-4100

INTRODUCTION

mRNA translation is a cyclic process regularly alternating four basic phases: initiation, elongation, termination, and ribosomal recycling. It is also one of the most energy consuming processes in the cells. Therefore, to keep the energy expenditure at the minimum, each cycle of protein synthesis reuses the components of the translation machinery that have been already used in the previous cycle, including mRNAs. The initiation phase is the most intricate process of all and its coordination relies on several initiation factors (eIFs). The G-protein complex eIF2 associates with GTP and Met-tRNA$_i^{Met}$ to form the ternary complex (eIF2-TC) that, with the help of eIF1, eIF1A, eIF5, and the multisubunit complex eIF3, is delivered to the small ribosomal subunit to form the 43S pre-initiation complex (PIC) (reviewed in (Valášek, 2012, Hinnebusch, 2017)) (Fig. 1). The eIF4E (mRNA cap-binding protein), eIF4G (a scaffold protein) and eIF4A (a DEAD-box helicase), together comprising the eIF4F complex, bind to the mRNA's 5' 7-methyl guanosine cap and thus mediate mRNA recruitment to the 43S PIC to form the 48S PIC. Subsequently, the eIF4F complex resolves secondary structures in the mRNA leader sequences to facilitate ribosomal scanning that occurs in the 5′ to 3′ direction until the AUG start codon has been recognized by base pairing with the anticodon of Met-tRNA$_i^{Met}$ (Hinnebusch, 2014). According to the "first AUG rule", for most mRNAs, the first AUG codon detected by the scanning complex is favored to be selected as the initiation codon of the ORF, and the surrounding nucleotide sequences together with eIFs 1, 1A, 2, 3, and 5 modulate the efficiency of its selection (Hinnebusch, 2017). Upon AUG selection and irreversible, eIF5-stimulated GTP hydrolysis on eIF2 (Algire *et al.*, 2005), the eIF2-GDP-eIF5 complex is released from the 48S PIC together with most other eIFs (reviewed in (Jennings & Pavitt, 2014, Dever *et al.*, 2016)), except for eIF3 (Szamecz *et al.*, 2008, Mohammad *et al.*, 2017, Valasek *et al.*, 2017) and probably also eIF4F (Pöyry *et al.*, 2004). eIF5B subsequently catalyzes the joining of the 60S subunit and upon GTP hydrolysis on eIF5B and its release from the ribosome (together with eIF1A) (Dever *et al.*, 2016), the 80S initiation complex thus formed is ready to enter the elongation phase. Protein synthesis then proceeds until a stop codon enters the ribosomal A-site and is recognized by the complex of eukaryotic release factors eRF1 and eRF3 (Fig. 1). eRF1 with help of the recycling factor ABCE1 (Rli1 in yeast) catalyzes the hydrolysis of the peptidyl-tRNA in the ribosomal P-site, releasing the completed polypeptide and producing the post-termination complex (post-TC) consisting of the 80S ribosome bound to mRNA with deacylated tRNA base-paired to the penultimate codon in the ribosomal P-site (Dever, 2012 #6042;Jackson, 2012 #5675}. ABCE1, perhaps together with eRF1, then initiates the recycling phase by splitting the subunits and releasing the 60S subunit from the remaining 40S post-TC (Pisarev *et al.*, 2010) (Fig. 1). It was shown *in vitro* that the ejection of the P-site tRNA and release of the 40S subunit from the mRNA can be achieved either by the combined action of canonical initiation factors eIF1, eIF1A, eIF3, and the eIF3-associated factor eIF3j (Hcr1 in yeast), or alternatively by a non-canonical initiation factor eIF2D (also known as Ligatin) or the DENR-MCT1 complex composed of two

For Peer Review

proteins that are homologous to the N- and C-terminal regions of eIF2D, respectively (Pisarev *et al.*, 2007, Skabkin *et al.*, 2010) (Fig. 1). The recycling phase thus ensures that at the end of each cycle, liberated mRNA and ribosomal subunits can immediately enter a new round of translation, which economizes the energetic resources of a cell and enables rapid regulatory responses when the demand for the synthesis of all or just a particular set of proteins changes.

Although ribosomal recycling is the natural sequence of events following translation termination, there are specific exceptions when the termination phase is followed by a second initiation event called reinitiation (REI) on the same mRNA molecule at a site downstream (or in some cases even upstream) of the stop codon. This can be achieved either by (i) incomplete post-TC recycling, particularly by allowing only dissociation of the 60S subunit by ABCE1, presumably followed by release of the deacylated tRNA from the P-site of the 40S post-TC to allow reinitiation *via* the small subunit in a manner similar to that of canonical initiation; or (ii) blocking the whole recycling process, in which case REI occurs with 80S post-TCs in a manner that may or may not require release of the deacylated tRNA (Fig. 1). One consequence of REI is the increase of the coding capacity of the genome and production of multiple proteins at calibrated levels from a single mRNA. Not surprisingly therefore, REI occurs widely in organisms with tightly packed genomes such as prokaryotes and viruses. In some instances, however, the production of the upstream peptide is not physiologically important (especially when it is very short) and translation of the first ORF merely provides the means of controlling the translation rate of the main ORF downstream. Unlike in prokaryotes and viruses, REI in eukaryotic cells is considered to be rare, as most cellular transcripts are monocistronic. Nevertheless, the fact that REI events frequently occur on mRNAs encoding key regulatory proteins in response to specific internal or external stimuli (e.g. during various stresses) underscores the physiological importance of this translational control mechanism in enabling cells to cope with, and adapt to, changing environmental conditions.

In this review, we describe all known types of translation REI, some of which have been identified only very recently. We summarize our current knowledge of molecular details of individual REI mechanisms with a particular focus on both *cis*-acting regulatory mRNA sequences and *trans*-acting regulatory proteins that have been discovered. Although it might seem at first glance that the different types of REI are largely unrelated mechanistically, many features and principles in common resurface after an in-depth analysis of the available information. In addition, we attempt to raise several questions that may spur future investigations and progress in this interesting field.

REINITIATION AFTER TRANSLATION OF SHORT uORFs

REI after short uORFs arguably represents the most widely recognized type. One reason is that, due to their minimal length, short uORFs are generally considered as merely regulatory elements governing expression of main ORFs without any

ScholarOne Support 1-434/964-4100

significant coding potential. In addition, the occurrence of short uORFs is relatively widespread across some viral and eukaryotic genomes: ~13%, 35% ~65%, ~44% and ~49% of yeast, plants, zebrafish, mouse and human transcripts, respectively, contain uORFs (Calvo *et al.*, 2009, Lawless *et al.*, 2009, von Arnim *et al.*, 2014, Chew *et al.*, 2016). Considering the nature of the scanning mechanism for start codon selection described above, uORFs represent a functional barrier for translation of a downstream cistron and indeed most uORFs effectively downregulate expression of the main ORFs (Calvo *et al.*, 2009, Barbosa *et al.*, 2013, von Arnim *et al.*, 2014, Wethmar, 2014, Hinnebusch *et al.*, 2016). Interestingly, uORFs are frequently found in certain classes of mRNAs with temporal or tissue-specific expression, or whose encoded proteins have dose-dependent functions, e.g. proto-oncogenes or other regulatory factors involved in differentiation, cell cycle, stress response, learning and memory formation (Calvo *et al.*, 2009, Barbosa *et al.*, 2013, von Arnim *et al.*, 2014, Wethmar, 2014, Janich *et al.*, 2015, Hinnebusch *et al.*, 2016), which are upregulated only upon specific internal or external signals. Hence it may not be surprising that deregulation of uORF translation and uORF polymorphisms have been implicated in a variety of human diseases (Calvo *et al.*, 2009, Barbosa *et al.*, 2013, Wethmar, 2014). Observations that near-cognate triplets (e.g. CUG, UUG, and GUG) can serve in addition to AUG as authentic initiation sites of short uORFs likely also contributes to the breadth of uORF-mediated translational control (Ingolia *et al.*, 2011, Fijalkowska *et al.*, 2017).

It is important to emphasize, however, that REI is not the only mechanism by which short uORFs control the expression of a downstream gene; others include increased uORF-triggered mRNA decay *via* the nonsense mediated decay pathway (NMD); constitutive or modulated leaky scanning, wherein the uORF start codon is bypassed by the scanning PIC; and regulated translational arrest or stalling within uORFs that modulate the efficiency of translation of the downstream ORF for example in response to an availability of a specific metabolite (for review see (Barbosa *et al.*, 2013, Wethmar, 2014, Hinnebusch *et al.*, 2016)). In fact, there are many examples, especially in transcripts of higher eukaryotes with multiple uORFs, where expression of the main gene is regulated in a more complex way by combining two or more of these mechanisms together (Barbosa *et al.*, 2013, Wethmar, 2014, Hinnebusch *et al.*, 2016).

By definition, a short uORF is an open reading frame occurring in the 5′ leader of a long ORF-containing mRNA. It is composed of a start codon and an in-frame termination codon separated by at least one additional sense codon. There are also examples of the shortest possible ‘start-stop uORFs’ that have been classified as canonical uORFs; however, since there is no elongation involved, they likely represent a separate class. In any case, the ability of an uORF to promote 40S-mediated REI (its REI-permissiveness) generally depends on four main factors: (i) *cis*–acting mRNA features surrounding the uORF, (ii) duration of uORF elongation, which is determined by its length and the propensity of its sequence to form stable secondary structures, (iii) a subset of initiation factors involved in primary initiation at the uORF start codon, and (iv) the intercistronic distance between the uORF and

ScholarOne Support 1-434/964-4100

main ORF, which determines the probability that the 40S subunit acquires a new eIF2-TC while traversing the leader from 5' to 3' before reaching the start codon of the downstream ORF, thus enabling recognition of the main ORF start codon by the anticodon of Met-tRNA$_i^{Met}$. Modulating the availability of the eIF2-TC also affects this probability. (Prior to the eIF2-TC acquisition the 40S subunit has no means to recognize the next AUG codon and, hence, this initial part of its journey will be referred to as "traversing" rather than "scanning") (Kozak, 1987, Pöyry *et al.*, 2004, Szamecz *et al.*, 2008, Cuchalová *et al.*, 2010, Roy *et al.*, 2010, Munzarová *et al.*, 2011, Mohammad *et al.*, 2017). According to the aforementioned criteria for efficient REI, uORFs that are too long or overlap the main ORF are expected to be REI-non-permissive. Studies indicate that REI-permissive uORFs are usually less than 10 codons in yeast, 16 codons in plants, and 30 codons in mammals (Kozak, 2001, Calvo *et al.*, 2009, von Arnim *et al.*, 2014).

Besides eIF2-TC, other eIFs, including eIF1 and 1A, are probably reacquired either at the onset of traversing or as the 40S traverses/scans further downstream from the uORF to promote proper recognition of the next start codon. It is well established that eIF1 restricts recognition of near-cognate start codons, and AUG start codons in poor Kozak context, and that changing the cellular availability of eIF1 alters the frequency of initiation events at such suboptimal start sites (Hinnebusch, 2017, Ivanov *et al.*, 2017). Recent genome-wide analysis demonstrated that eIF1 depletion in mammalian cells evoked upregulation of uORFs with suboptimal starts. Consequently, uORFs that acted as poor barriers of the main ORF under normal conditions became more prominent barriers at reduced eIF1 levels (Fijalkowska *et al.*, 2017). By extension, the efficiency of REI on main ORFs with suboptimal start sites might increase at reduced eIF1 levels.

It is generally considered that the eIF2-TC and other eIFs that bind at the subunit interface of the 40S subunit (eIF1, eIF1A) and are released on 60S joining must be reacquired from the cytosol post the uORF termination. However, there is a long-standing hypothesis that certain eIFs important for REI remain at least transiently associated with the elongating ribosome, and that increasing the uORF length or time required for its translation increases the likelihood that these eIFs dissociate before the completion of uORF translation (Kozak, 2001). When uORF translation takes a shorter period of time, these eIFs are still present at uORF termination and remain associated with the 40S post-TC following recycling of the 60S subunit, ready to enhance REI. So far, this ability has been directly demonstrated *in vivo* only for yeast eIF3 (Mohammad *et al.*, 2017), in accordance with the fact that it binds primarily to the surface of the 40S subunit that remains solvent-exposed in the translating 80S ribosome (Valášek *et al.*, 2003, Hashem *et al.*, 2013, Aylett *et al.*, 2015, des Georges *et al.*, 2015, Llacer *et al.*, 2015) (Fig. 1 and Supplementary Fig. 1, see below). However, genetic experiments suggest that participation of eIF3 in REI is conserved also in higher eukaryotes (Roy *et al.*, 2010, Hronova *et al.*, 2017). Studies in mammalian reconstituted systems indicate that eIF4F might represent another factor that persists transiently on elongating ribosomes and thereby facilitates REI following translation of short uORFs (Pöyry *et*

ScholarOne Support 1-434/964-4100

al., 2004, Skabkin *et al.*, 2013). eIF4F might function generally by opening the mRNA entry channel of the 40S ribosome that is traversing downstream, or it may be critical especially for REI events where the 40S subunit must traverse/scan sequences burdened with secondary structures that can be unwound by eIF4F (Sen *et al.*, 2015). Besides canonical eIFs, some short uORFs seem to utilize also other, REI-specific *trans*-acting factors (see below).

Regulation of reinitiation on short uORF(s)-containing mRNAs (like *GCN4* and *ATF4*) by eIF2α phosphorylation

Undoubtedly the best described example of regulation of REI of short uORF-containing mRNAs by eIF2α phosphorylation in response to nutritional stress is the *S. cerevisiae GCN4* gene (Fig. 2A). *GCN4* encodes a master basic leucine zipper (bZIP) transcription factor that activates, among many others, amino acid biosynthetic genes in response to amino acid limitation in the so-called general amino acid control (GAAC) pathway (reviewed in (Hinnebusch, 2005)). Simply speaking, this regulatory response pathway enables cells to swiftly limit consumption of amino acids by general protein synthesis while allowing their usage for inducing the synthesis of Gcn4 and ~600 other stress-response proteins under its control to increase amino acid availability or adjust to conditions of amino acid scarcity.

The *GCN4* mRNA leader contains four short AUG-initiated uORFs with a relatively close spacing between uORFs 1 and 2, even closer spacing between uORFs 3 and 4, and relatively larger separations between uORFs 2 and 3, and uORF4 and the *GCN4* ORF (Fig. 2A). Most of the experimental evidence establishing the mechanism of *GCN4* translational control is genetic and involves an extensive panel of mutations that systematically alter the individual uORFs or their surrounding sequences. The outcome on REI efficiency is measured by a reporter with the *GCN4* main ORF fused to *lacZ* and compares expression of WT *versus* mutant reporter constructs. It should be stressed that early studies justified the use of this reporter system as they confirmed that expression of various mutant *GCN4-lacZ* reporters paralleled the expression of particular Gcn4 target genes (or cellular phenotypes dependent on the GAAC response) in strains harboring the corresponding mutant *GCN4* alleles on single-copy plasmids (Mueller & Hinnebusch, 1986, Mueller *et al.*, 1988, Miller & Hinnebusch, 1989, Grant & Hinnebusch, 1994, Grant *et al.*, 1995).

The basic principles of the delayed REI mechanism on the *GCN4* mRNA can be best described using a simplified model featuring only uORFs 1 and 4 (Supplementary Fig. 2), as described in (Hinnebusch, 2005). The 5' proximal uORF1 is a positive, REI-promoting feature required for induction of *GCN4* in starved cells, while the 5' distal uORF4 is a negative, REI-suppressing feature required for *GCN4* repression in non-starved cells. Whereas uORF1 is highly permissive for REI, uORF4 is non-permissive, such that for *GCN4* translation, REI at uORF4 must be avoided. This is achieved by delaying the acquisition of eIF2-TC by 40S subunits traversing the *GCN4* leader following translation of uORF1, so that a fraction of them arrive at uORF4 without the eIF2-TC unable to recognize the AUG codon at this uORF. They

ScholarOne Support 1-434/964-4100

acquire the eIF2-TC only after bypassing uORF4 and so can reinitiate at *GCN4* instead. The key evidence for the importance of the delayed acquisition of the eIF2-TC came from progressively increasing the uORF1-uORF4 distance resulting in gradual decline in REI efficiency at the *GCN4* AUG (Abastado *et al.*, 1991). The delayed acquisition of the eIF2-TC is achieved in amino acid starved cells. Amino acids deficiency is sensed by the Gcn2 kinase that phosphorylates eIF2 on Ser51 of its alpha subunit and thus effectively prevents *de novo* formation of the eIF2-TC complexes. While this type of stress response shuts down general translation initiation, it at the same time stimulates *GCN4* expression (reviewed in (Hinnebusch, 2005, Jennings *et al.*, 2017).

Expanding the view back to the entire system, a comparison of individual REI efficiencies of all four uORFs, determined with *GCN4-lacZ* constructs harboring each solitary uORF, showed that their propensities to promote REI markedly differ. uORF1 and uORF2 are the most REI-permissive, allowing ~one third of the *GCN4-lacZ* expression observed in the absence of all four uORFs (Mueller & Hinnebusch, 1986). Normalizing the REI efficiency of uORF1 to 100%, uORF2 is ~90% efficient, whereas uORF3 and uORF4 are largely REI-non-permissive, enabling only ~18% and ~4% REI, respectively (Munzarová *et al.*, 2011, Gunisova & Valasek, 2014). As outlined below (Fig. 3), this arrangement of one pair of REI-permissive uORFs followed by another pair of REI-non-permissive uORFs creates a 'fail-safe' mechanism that ensures maximal *GCN4* induction under starvation conditions and, at the same time, tight inhibition of its expression under non-starvation conditions (Munzarová *et al.*, 2011, Gunisova & Valasek, 2014).

The ability of *GCN4* uORFs to allow or prevent REI is determined by several *cis*-elements. Sequences upstream of uORF1 are required for its high REI potential (Grant *et al.*, 1995) and multiple REI-promoting elements (RPEs) have been mapped upstream of both uORF1 and uORF2 that create a specific structural arrangement (the 5' enhancer) upstream of these two ORFs (Fig. 2A) (Munzarová *et al.*, 2011, Gunisova & Valasek, 2014). uORF1 utilizes four RPEs (i.–iv.), whereas uORF2 separately utilizes only a single RPE (v., with sequence similarity to RPE i.), and additionally shares RPE ii. with uORF1 (Fig. 2A). A combination of computational analysis and enzymatic probing showed that the shared RPE ii. forms a stable stem loop, whereas RPE iv. assembles into a double-circle hairpin (Munzarová *et al.*, 2011, Gunisova & Valasek, 2014) (Fig. 2A).

Besides the RPEs, two separate regions were identified within the extreme N-terminal domain (NTD) of the a/Tif32 subunit of eIF3 (called Box6 and Box17) that proved to be critical for high REI competence of these two uORFs in *trans* (Fig. 2B) (Szamecz *et al.*, 2008, Munzarová *et al.*, 2011). Genetic epistatic experiments revealed that RPEs i. and iv. of uORF1 and RPE v. of uORF2 co-operate with these two boxes to promote efficient REI (Munzarová *et al.*, 2011, Gunisova & Valasek, 2014). Importantly, the a/Tif32-NTD has a favorable location on the 40S subunit next to the mRNA exit channel (Valášek *et al.*, 2003, Kouba *et al.*, 2012, Aylett *et al.*, 2015), where it could directly contact these RPEs, which during termination on uORF1 or uORF2 will be emerging from the mRNA exit channel (Fig. 2B). This could

ScholarOne Support 1-434/964-4100

stabilize the 40S post-TC, particularly following dissociation of the deacylated tRNA cognate to the penultimate codon of the uORF (see below), to allow resumption of traversing/scanning downstream. The structural motif similar to RPE iv. was also identified upstream of the REI-permissive uORF in the mRNA leader of another yeast transcriptional activator Yap1. The fact that it likewise operates in an a/Tif32-NTD-dependent manner (Munzarová *et al.*, 2011) suggests that, at least in yeasts, the underlying molecular mechanism of REI on short uORFs might be conserved.

Based on these findings we proposed that while the eIF3-bound 40S ribosome scans through the region upstream of uORF1 (or uORF2) and subsequently translates one of these uORFs – retaining eIF3 during elongation, the RPEs progressively fold into the aforementioned secondary structures. Upon termination and dissociation of the 60S subunit, eIF3 interacts with the corresponding RPEs to specifically stabilize the 40S post-TC at the uORF1 (or uORF2) stop codon (Fig. 2B). Upon dissociation of the P-site bound deacylated tRNA and acquisition of other eIFs like eIF1 and eIF1A that might be needed for the subsequent step, the 40S subunit will resume traversing downstream. Once it reacquires the eIF2-TC, it switches into the scanning mode and begins “searching” for the next start codon. Employing a novel *in vivo* RNA–protein Ni^{2+}-pull down (RaP-NiP) assay, we provided direct *in vivo* evidence that eIF3 indeed remains transiently bound to elongating ribosomes post-initiation and interacts with the *cis*–acting elements of uORFs 1 and 2 (Mohammad *et al.*, 2017). More experiments are needed to reveal whether the co-operation between the a/Tif32-NTD and RPEs in rendering uORFs 1 and 2 REI-competent stems from a direct contact between them as opposed to an indirect functional interaction. Patches of positive charge on the surface of the a/Tif32-NTD and its ability to bind RNA (Khoshnevis *et al.*, 2014) may favor the model of direct contact. Molecular roles of RPE ii. and iii., which function independently of eIF3 (Munzarová *et al.*, 2011, Gunisova & Valasek, 2014), remain to be determined, as does the importance of eIF4F in REI in view of its predicted ability to remain associated with the ribosome during early elongation (Pöyry *et al.*, 2004, Skabkin *et al.*, 2013). Besides eIF3a, the g/Tif35 subunit that – based on its interactions with Rps3/uS3 and Rps20/uS10 (Cuchalová *et al.*, 2010) – appears to reside near the mRNA entry channel (Fig. 2B) (Aylett *et al.*, 2015) also stimulates REI after translation of both REI permissive uORFs ((Cuchalová *et al.*, 2010), S.G. and L.S.V., unpublished data); however, the molecular basis of its contribution is unknown.

In contrast to uORF2, the REI competence of uORF1 additionally depends on the AU-rich nature of sequences immediately following its stop codon, and replacing these sequences with the corresponding sequences from uORF4 impaired REI (Miller & Hinnebusch, 1989, Grant & Hinnebusch, 1994). The AU-rich motif identified within the first 12 nt of the uORF1 3’ sequences was recently shown as being critical for REI (Gunisova *et al.*, 2016) (Fig. 2A). Although nearly the same motifs occur in the 3’ sequences of uORFs 2 and 3, they do not promote REI of these two uORFs. In fact, the AU-rich motif operates only at uORF1, independently of the RPEs, in a manner strictly dependent on its position following the uORF1 stop codon; and is an essential prerequisite for the function of the 5′ enhancer at uORF1 (Munzarová *et al.*,

ScholarOne Support 1-434/964-4100

2011, Gunisova *et al.*, 2016). However, the molecular mechanism of the AU-rich element in uORF1 REI is unknown. Considering its position-specific role and the fact that it will be buried in the terminating ribosome at uORF1, it might function either to speed up the 60S and/or deacylated tRNA recycling steps or to prevent recycling of the post-termination 40S subunit, perhaps by a looping interaction with more remote sequences within the *GCN4* mRNA leader. Intriguingly, besides the REI-promoting sequences, REI-inhibiting sequences were found in more distal 3′ regions of uORF2 and uORF3 following their AU-rich motifs (Fig. 2A). These sequences function irrespectively of their distance from the *GCN4* start codon and to some extent decrease the REI potential of these two uORFs (Gunisova *et al.*, 2016), presumably to optimize the dynamic range of *GCN4* translational control. However, the molecular details of their action are also unknown.

The REI potential of *GCN4* uORFs is further modulated by their coding sequences, mainly by the character of the last sense codons (Miller & Hinnebusch, 1989, Grant & Hinnebusch, 1994, Gunisova *et al.*, 2016). At uORF1 and uORF2, UGC and UGU cysteine codons are found, respectively, while uORF3 and uORF4 both contain the CCG proline codon at that position (Fig. 2A). The presence of Cys and Pro codons as the last coding triplets of the short uORFs in *GCN4* mRNA is conserved in yeast species related to *S. cerevisiae*. Intriguingly, $tRNA^{Cys}$ was shown to be particularly prone to spontaneous dissociation from the ribosomal P-site in post-TCs analyzed *in vitro* (Skabkin *et al.*, 2013). Hence, the presence of Cys as the last sense codon at uORFs 1 and 2 might facilitate stabilization of the post-TC 40S subunits, as spontaneous dissociation of deacylated $tRNA^{Cys}$ could eliminate the need for the "2^{nd}-stage" recycling factors, eIF1 and eIF1A or eIF2D. Rapid, stochastic dissociation of deacylated $tRNA^{Cys}$ following 60S subunit recycling, combined with the known eIF3 role in mRNA stabilization on the ribosome (Kolupaeva *et al.*, 2005, Jivotovskaya *et al.*, 2006, Khoshnevis *et al.*, 2014, Aitken *et al.*, 2016), presumably *via* a/Tif32-NTD interactions with RPEs i. and iv. of uORF1 or RPE v. of uORF2 (Fig. 2B), could thus prevent full ribosomal recycling and allow the post-TC 40S subunit to resume traversing downstream. The presence of the CCG Pro codon, which suppresses the REI potential of uORF3 and uORF4, might be attributable to the spatially restricted conformation of the proline residue that could prevent efficient REI by slowing down the speed of uORF3 or 4 translation (Wohlgemuth *et al.*, 2008, Pavlov *et al.*, 2009), or by interfering with stop codon recognition in translation termination. Interestingly, the ~4-fold difference between the REI potential of uORF3 and uORF4 is largely determined by their different second codons and stop codon tetranucleotides (i.e. the stop codon plus the immediately following base), which at uORF4 further diminish its REI potential by allowing a higher frequency of stop codon readthrough (Beznoskova *et al.*, 2016, Gunisova *et al.*, 2016).

Taken all together, complex translational regulation of *GCN4* under nutrient replete *vs.* deplete conditions ultimately reflects the differential translation of all four uORFs that, according to their REI properties, control the fate of ribosomes terminating at their stop codons. The real decision makers are the REI-non-permissive uORFs 3 and 4, the expression of which prevents *GCN4* to be translated,

ScholarOne Support 1-434/964-4100

whereas their skipping allows it. The relatively high REI potential of uORF2 provides a 'fail-safe' mechanism for *GCN4* translational control. As summarized in Fig. 3, the REI-permissive uORF1 is efficiently translated under both nutrient-replete and depleted conditions. After its translation, the post-TC 40S subunit remains bound to the mRNA with help of eIF3 and resumes traversing downstream. uORF2 serves as a backup for uORF1 to capture ribosomes that leaky-scanned uORF1's AUG; thereby maximizing the REI potential of the whole system. This could be especially important during stress, where the frequency of leaky scanning appears to be elevated (Baird & Wek, 2012, Barbosa *et al.*, 2013). In non-starved cells, where the eIF2-TC levels are high, nearly all of the 5' to 3'-migrating ribosomes rebind the eIF2-TC before reaching uORF3 or uORF4. Since neither of them supports efficient REI, scanning ribosomes that reinitiate there will undergo full ribosomal recycling following termination and prevent REI at *GCN4* (Fig. 3). Under starvation conditions characterized by low levels of the eIF2-TC, a large proportion of the post-termination 40S ribosomes will bypass uORFs 3 and 4 and upon eventual acquisition of the eIF2-TC reinitiate at the *GCN4* start codon (Fig. 3). It is worth mentioning that besides the extensive genetic evidence supporting this model, key tenets of the mechanism were supported by analysis of ribosome-protected mRNA fragments by toe-printing and ribosome profiling techniques (Gaba *et al.*, 2001, Ingolia *et al.*, 2009).

Homologues of *GCN4* in filamentous fungi contain minimally two uORFs and it is generally assumed that they perform similar functions as uORF1 and uORF4 of *S. cerevisiae GCN4.* This assumption finds strong support in observations that each of the two REI-permissive uORFs in combination with either of the two REI-non-permissive uORFs suffice for the qualitative aspects of *GCN4* translational control in *S. cerevisiae* (Mueller & Hinnebusch, 1986, Gunisova & Valasek, 2014), as mentioned above. The best studied homologue in filamentous fungi is *cpc-1* of *Neurospora crassa*, whose translation is induced in starvation conditions through eIF2α phosphorylation by the Gcn2 homologue encoded by *cpc-3*. It is dependent on two uORFs, which orchestrate a cross-pathway control (CPC) response analogous to GAAC (Luo *et al.*, 1995, Sattlegger *et al.*, 1998). Recently, evidence was presented that post-termination 40S ribosomes efficiently reinitiate after translation of the 3-codons long uORF1 but not after translation of much longer uORF2 in the *cpc-1* mRNA leader (Ivanov *et al.*, 2017). However, whether there are any mechanistic parallels among the REI-promoting elements of *S. cerevisiae GCN4* uORF1 and its counterpart in *N. crassa cpc-1* remains to be seen.

GCN4 also has a functional homologue in mammalian genomes, *ATF4* (Activating transcription factor 4) that, like *cpc-1,* contains a 3-codon uORF1 and a longer uORF2, which in this case overlaps the beginning of the main ORF (Fig. 2C). In accordance with the *GCN4* model, phosphorylation of mammalian eIF2α induces *ATF4* translation (Lu *et al.*, 2004, Vattem & Wek, 2004), which can be achieved in principle by activation of any of four different mammalian eIF2α kinases: GCN2, PERK, PKR, and HRI1 (Pakos-Zebrucka *et al.*, 2016). Each of these kinases is activated by a different type of stress and their functions converge in the so-called

ScholarOne Support 1-434/964-4100

"integrated stress response" (ISR) (Pakos-Zebrucka *et al.*, 2016) (Note that budding yeasts contain only Gcn2).

Experiments with mouse reporter constructs revealed that, similar to *GCN4* uORFs 1 and 4, *ATF4* uORF1 is a positive, stimulatory feature allowing efficient REI after its translation, whereas translation of uORF2 inhibits *ATF4* expression and translation of uORF1 combined with low levels of the eIF2-TC are required to overcome its inhibitory effect (Lu *et al.*, 2004, Vattem & Wek, 2004). It was recently demonstrated that, by analogy with *GCN4* uORF1, *ATF4* uORF1 is surrounded by *cis*-acting, REI-promoting sequences, with the upstream sequences most probably forming specific secondary structures (Hronova *et al.*, 2017) (Fig. 2C). In addition, it was shown that efficient REI at human *ATF4* requires the eIF3h subunit, previously implicated in REI in plants (see below). Although it is not known whether eIF3h functionally co-operates with sequences upstream of *ATF4* uORF1, like eIF3a/Tif32 does in yeast, it seems likely that the basic molecular principles of REI are conserved between yeast *GCN4* and human *ATF4* (Fig. 2C).

Despite the evidence for translational control *via* uORF1-mediated REI underlying stress-induced ATF4 synthesis (Lu *et al.*, 2004, Vattem & Wek, 2004), many recent studies indicate that other outputs of phosphorylated eIF2α that are specific to higher eukaryotes, or even other regulatory pathways unrelated to the ISR, make important contributions to ATF4 induction. Various stresses were shown to stimulate *ATF4* transcription (see for example (Dey *et al.*, 2010)), increase the stability of *ATF4* mRNA by inhibition of NMD (Gardner, 2008), increase the level of ATF4 protein by preventing its degradation (see for example (Koditz *et al.*, 2007)), or boost *ATF4* translation by other mechanisms besides REI, such as by leaky scanning (Starck *et al.*, 2016). In fact, in direct contradiction with the original model, three independent studies noted increased translation of uORF2 under stress conditions (Andreev *et al.*, 2015, Sidrauski *et al.*, 2015, Starck *et al.*, 2016).

While there is little doubt that translational upregulation of *ATF4* during stress is achieved partly by uORF1-mediated REI; the contribution of this mechanism to the overall increase in ATF4 protein levels might be only ~2-fold *vs.* the ~6-fold originally reported ((Vattem & Wek, 2004, Andreev *et al.*, 2015), V.H. and L.S.V., unpublished data). It should be noted that even in yeasts, amino acid starvation increases the level of *GCN4* mRNA ~2-fold and the rate of Gcn4 degradation by the proteasome is also diminished under conditions of severe starvation, augmenting the translational induction of *GCN4* at different levels of gene expression (Hinnebusch, 2005). There are several other mammalian examples of the short uORF mediated REI mechanism regulating expression of *C/EBPα* and *C/EBPβ*, *CD36* and *ELK-1* that we will not discuss in detail (Calkhoven *et al.*, 2000, Griffin *et al.*, 2001, Rahim *et al.*, 2012). It suffices to say that translation control of these genes is also not mediated solely by REI but by a combination of REI with other translation control mechanisms like leaky scanning. Therefore it seems likely that there are no mammalian genes whose expression would be singlehandedly governed by REI, perhaps because the more complex organisms have evolved, the more complex translational control has become.

ScholarOne Support 1-434/964-4100

Regulation of reinitiation of short uORF(s)-containing mRNAs by eIF3h phosphorylation in *Arabidopsis thaliana*

The uORF-mediated control of translation has also been found to play a key role in complex growth and developmental processes in plants. In *Arabidopsis thaliana*, the mRNA leaders involved in such regulation typically contain multiple short or long uORFs that are frequently overlapping, which complicates the assessment of their contributions to REI efficiency. Well-studied examples of plant REI are receptor for kinase Clavata 1 (CLV1), leaf transcription factor ASYMETRIC LEAVES 1 (AS1), as well as several members of two families of transcription factors, namely Auxin Response Factors (ARFs) and bZIP factors. In all of these cases the intact eIF3h subunit of eIF3 is required to overcome the inhibitory effect of uORFs to allow efficient REI at the main ORF of the gene (Nishimura *et al.*, 2005, Kim *et al.*, 2007, Roy *et al.*, 2010, Zhou *et al.*, 2014). Strong specificity for eIF3h function in these REI events was demonstrated by showing that a C-terminal truncation of eIF3h that reduces the subunits association with the rest of eIF3 and the 43S PIC, selectively decreased translation of the aforementioned main ORFs while showing no impact on global translation initiation rates (Kim *et al.*, 2004, Kim *et al.*, 2007, Roy *et al.*, 2010). It was proposed that, by analogy with the function of yeast eIF3a/Tif32 discussed above, eIF3h (specifically its N-terminal part) might support efficient REI by preserving the competence of a fraction of uORF-translating ribosomes to resume traversing downstream (Roy *et al.*, 2010). Whether eIF3h stabilizes only eIF3 or mRNA, or both on the post-termination 40S subunits, and whether it acts on its own or in co-operation with some other eIF3 subunits or other factors, remains to be determined. In any case, polysomal microarray analysis clearly demonstrated that eIF3h is a general stimulator of efficient translation of short uORF(s)-containing mRNAs throughout the transcriptome (Kim *et al.*, 2007).

Interestingly, the efficiency of REI on ARF-encoding mRNAs and also on the auxin-unrelated *AtbZIP11* mRNA can be further increased upon activation of the auxin signaling pathway. Recent data revealed that transduction of the signal into activation of translation requires coordinated actions of phytohormone auxin, Rho-like small GTPase from plants 2 (ROP2), the central growth regulator serine/threonine protein kinase TOR (Target Of Rapamycin), and eIF3h (Schepetilnikov *et al.*, 2013) (Fig. 4). Ribosome fractionation experiments indicated that, in response to auxin, polysomes show increased accumulation of uORF-containing mRNAs (indicating enhanced translation), phosphorylated and thus activated TOR, and, interestingly, phosphorylated eIF3h. On the other hand, the downstream effector of TOR, the 40S ribosomal protein S6 kinase 1 (S6K1), resides in polysomes mainly in its inactive form and its polysome association is disrupted immediately upon its phosphorylation by TOR (Schepetilnikov *et al.*, 2013). Supporting this, a similar mechanism was previously shown to operate in mammals, where activated mTOR phosphorylates eIF3-bound S6K1 in PICs, which triggers S6K1 activation and its subsequent dissociation from PICs (Holz *et al.*, 2005). Hence the plant data suggested that

ScholarOne Support 1-434/964-4100

polysomes may after PICs serve as a second platform for S6K1 activation *via* phosphorylation by TOR. Because plant eIF3h physically interacts with S6K1, it was further suggested that eIF3h might be the downstream target of activated S6K1 (Schepetilnikov *et al.*, 2013). It is theoretically possible that eIF3h phosphorylation might be a trigger for S6K1 departure from polysomes. In a short summary, the current model proposes that the increased translation of main ORFs in short uORF(s)-containing mRNAs is triggered by activation of TOR by the GTP-bound ROP2 in response to auxin. Upregulated TOR is recruited to polysomes where it phosphorylates S6K1, which shortly before its release from polysomes phosphorylates eIF3h. This signaling cascade somehow ensures that ribosomes retain or adopt the REI-competent state to enable synthesis of the main ORF in response to auxin (Fig. 4).

In addition to eIF3h, the 60S ribosomal protein Rpl24/eL24 was also found to increase the REI competence of virtually the same classes of mRNAs (Fig. 4). Interestingly, mutations in either Rpl24/eL24 or eIF3h affects REI in similar fashion and confer similar developmental defects, indicating that the molecular functions of Rpl24/eL24 and eIF3h in plant REI are closely related (Nishimura *et al.*, 2005, Zhou *et al.*, 2010). However, the precise role of Rpl24/eL24, as well as the molecular details of the functional interaction between eIF3h and Rpl24/eL24 are unknown; nonetheless, considering their distant locations on the ribosome it is unlikely that they interact physically.

The key features just described for the auxin-stimulated REI mechanism, including hyperstimulation by a specific signal, involvement of TOR and ribosomal protein Rpl24/eL24, and the presumed requirement for retaining eIF3 during translation elongation, bear remarkable similarities with another REI mechanism found in *Cauliflower mosaic virus* (CaMV) that, by contrast, promotes REI after translation of long ORFs (Thiebeauld *et al.*, 2009, Schepetilnikov *et al.*, 2011) (for details see below). What is the purpose of having all these features in place at the same time? Perhaps, the answer lies in the fact that the leaders of investigated mRNAs contain multiple uORFs and usually at least one of them is too long (often even longer than 90 codons) to enable the efficient short uORF-mediated REI defined above. It is therefore conceivable that two types of REI mechanism may operate together on the same mRNA bearing multiple uORFs of different lengths (Fig. 4). Whereas REI after short uORFs would rely on the four requirements established above, REI after longer uORFs might require the signaling cascade that allows eIF3, *via* its h subunit, to persist longer on elongating ribosomes. Specific conformational changes of the ribosome mediated either directly or indirectly by ribosomal proteins, such as Rpl24/eL24, perhaps in response to signaling, may further buttress the requirement for eIF3 retention. These thoughts find some support in reports showing that inhibition of TOR signaling did not affect translation of a reporter containing only a very short uORF, and that REI-dependence on eIF3h was lost when the longest uORF (>40 codons) in the multiple uORF mRNA leader of *AtbZIP11* was removed (the remaining uORFs had a maximal length of only 20 codons) (Kim *et al.*, 2007, Schepetilnikov *et al.*, 2013).

ScholarOne Support 1-434/964-4100

DENR-MCT1 as REI-specific factors

The two subunits of the heterodimeric complex DENR–MCT1 (MCTS1 in human) were identified as REI-specific *trans*-acting factors for certain short uORFs in *Drosophila* and humans (Schleich *et al.*, 2014, Schleich *et al.*, 2017). In *Drosophila*, DENR-MCT1 was found to regulate a specific group of mRNAs possessing strong Kozak context at the AUG codons of their short uORFs; no additional *cis*-acting sequences seemed to be necessary (Fig. 5). The DENR-MCT1 heterodimer promotes REI even in non-stressed, normally proliferating cells; i.e. when general translation is not compromised, and independently of the distance between an uORF and the main ORF (Schleich *et al.*, 2014). This implies that, unlike the *GCN4*-like mechanisms, REI seems to occur independently of the eIF2-TC abundance. Importantly, in contrast to eIF3 or eIF4F, the DENR-MCT1 heterodimer is not required for initiation on uORF-less mRNAs (Schleich *et al.*, 2014), apparently uncoupling REI from standard initiation. However, the ability of DENR-MCT1 to promote REI declines as uORFs become longer, suggesting that some eIFs from the primary initiation event are still needed to ensure maximal REI capacity. The uORF length requirements were even more strict in human cells, where somewhat unexpectedly DENR-MCT1 supported REI only on reporter mRNAs bearing minimal 'start-stop uORFs' with AUGs in strong Kozak context (Schleich *et al.*, 2017). Interestingly, mRNA leaders of this type were found to be enriched in neuron-specific genes (Schleich et al., 2017). These remarkable findings suggesting that REI-specific factors are not involved in canonical initiation raises many questions. Are there different types of short uORFs with markedly varying needs for auxiliary factors? It is possible that DENR-MCT1-mediated REI can occur only in specific tissues or during restricted periods throughout development as a function of modulated expression of DENR or MCT1 proteins.

It should be recollected that DENR-MCT1 were shown *in vitro* to promote dissociation of deacylated tRNA and mRNA from the post-TC 40S subunits in the second step of ribosome recycling (Fig. 1) (Skabkin *et al.*, 2010). In contrast to removal of the deacylated tRNA from the P-site, the mRNA dissociation function of DENR-MCT1 would be expected to inhibit rather than promote REI *in vivo*. DENR-MCT1 were also shown *in vitro* to recruit Met-tRNA$_i^{Met}$ to the 40S subunit in a non-canonical, eIF2-independent manner on certain viral mRNAs that position the start codon directly in the P-site without any scanning (Skabkin *et al.*, 2010). This ability could have a stimulatory function instead. If DENR-MCT1 exerts these functions also in living cells, it implies that the first function would have to be inhibited in order to utilize the second function to stimulate REI. The question is then what determines whether DENR-MCT1 completes the recycling phase or promotes REI?

Since the ability of DENR-MCT1 to promote REI decreases with increasing uORF length, it seems clear that the uORF length (and everything what is related to it) dictates the fate of the DENR-MCT1-bound terminating ribosomes. This might favor the idea that DENR-MCT1 co-operates with some factors that were involved in

ScholarOne Support 1-434/964-4100

the primary initiation event and subsequently carried along with the elongating ribosomes for a limited number of elongation rounds – like eIF3 in yeast (Fig. 5).

Some insights into the DENR-MCT1 functions has recently been provided by two independent groups that resolved structures of human 40S complexes with DENR-MCT1 or the related single polypeptide eIF2D (Lomakin *et al.*, 2017, Weisser *et al.*, 2017); one of which also contained mRNA with Met-tRNA$_i^{Met}$ based-paired with AUG in the P-site (Weisser *et al.*, 2017). The structures identified specific contacts of DENR-MCT1 or eIF2D with the 40S subunit in the vicinity of the P-site, as well as contacts with both aminoacyl acceptor and anticodon arms of initiator tRNA that at least partially overlap with the known 40S-binding sites of eIF1, eIF2, and most probably also eIF1A. Interestingly, the positions of DENR-MCT1 or eIF2D were also predicted to overlap with 40S contacts of specific domains of the eIF3a and eIF3b subunits known to transiently relocate to the 40S interface surface (Llacer *et al.*, 2015 Weisser, 2017 #6176, Lomakin *et al.*, 2017, Valasek *et al.*, 2017) while the majority of eIF3 stably resides on the solvent-exposed side of the 40S (Supplementary Fig. 1). The contacts that eIF3 retains on the solvent side of the 40S subunit in the elongation complex (Mohammad *et al.*, 2017) could co-exist with DENR-MCT1 bound to the interface surface. Hence it is tempting to speculate that the persistence of eIF3 on elongating ribosomes inhibits the mRNA recycling function of DENR-MCT1 during termination on certain short uORFs in favor of REI (Fig. 5). Since this works specifically only on some uORFs with strong Kozak context, even if our speculation holds true, it would not be the end of the story. The *in vitro* documented ability of DENR-MCT1 to replace the deacylated tRNA in the P-site with Met-tRNA$_i^{Met}$, which gains support in the partial overlap of DENR-MCT1 with the 40S-binding site of eIF2, could then eliminate the need of the post-termination 40S ribosome to rebind the eIF2-TC (Fig. 5), and thus eliminate the requirement for a minimum intercistronic distance between the uORF and main ORF during REI. In short, eIF3 could block dissociation of mRNA from the 40S by DENR-MCT1, while allowing DENR-MCT1 to replace the P-site deacylated tRNA with Met-tRNA$_i^{Met}$ (Fig. 5). This could explain why this mechanism works most efficiently for the 'start-stop uORFs', as AUGs of these minimal uORFs occur upon termination directly in the in P-site. Why there is a specific requirement for the strong Kozak context is not known. It is also not known whether DENR-MCT1 travels with post-termination 40S ribosomes downstream to finally reinitiate at the main ORF, like eIF3 does, however if it does, its partial overlap with 40S-binding sites of eIF1 and maybe eIF1A could also eliminate their need for proper AUG selection of the main ORF. Taking into account that MCT1, DENR and eIF2D share homologs also in budding yeast (represented by thus far only poorly characterized proteins Tma20, Tma22 and Tma64, respectively), it will be intriguing to explore whether these yeast counterparts also play some role in REI in this unicellular organism.

REINITIATION AFTER TRANSLATION OF LONG ORFs

ScholarOne Support 1-434/964-4100

In contrast to REI after short uORFs, reinitiation after translation of long ORFs; i.e. those encoding cellular proteins, is considered to be a very rare event because most ribosomes translating canonical ORFs undergo full ribosomal recycling upon completion of protein synthesis. In addition, it is presumably impossible to retain any initiation factors involved in the primary initiation event, including eIF3, during the extended period of elongation required to translate upstream long ORFs. Nonetheless, there are quite a few exceptions to this rule, especially among viral mRNAs, where REI after long ORFs provides the means for: 1) maximizing the genome coding capacity, 2) regulating the levels of expressed proteins, and 3) redirecting the host translational machinery to the virus. A number of distinct strategies appear to be used involving REI mediated by either 40S or 80S species with peculiar ways of REI start site selection and varying requirements for interactions that viral proteins or mRNA establish with ribosomal subunits or eIFs. Interestingly, some recent data indicate that REI after translation of long ORFs may even represent an integral aspect of translational control in eukaryotic cells.

Coupled termination-reinitiation

Although termination-reinitiation is represented in the literature mainly by the TURBS-mediated mechanism in caliciviral protein synthesis, described at length below, it comprises a fairly heterogeneous group of molecular processes utilizing specific mRNA sequence motifs or structures upstream or downstream of the termination-REI start site to ensure efficient translational coupling between termination on the upstream ORF and subsequent REI on the downstream ORF. This is achieved by the retention of the post-termination 40S subunit on mRNA following the first recycling step (dissociation of the 60S subunit). Based on *in vitro* experiments it is theoretically possible that in some cases ribosomal recycling does not occur and termination-REI is mediated by the post-termination 80S ribosomes; however, *in vivo* evidence is missing. The common feature linking all of these processes is the existence of a region between the two ORFs, where the stop codon of an upstream ORF is functionally connected with the start codon of the downstream ORF. Frequently, the stop and start codons are in close proximity, which is often expressed by the formula AUGn$_x$UGA (with X being 2, 5, 8 or 14 nt); alternatively, they may overlap each other, as follows: UAAUG or AUGA. A longer separation, greater than 14 nt, has been observed in some cellular mRNAs; however, in these cases the REI start codon always precedes the upstream ORF termination codon. The proximity of stop-start codons in these systems places the post-termination ribosomes in the vicinity of the next start codon and should obviate the need for traversing/scanning during REI. This presumably reflects the absence of all initiation factors associated with the post-TCs, including eIF3, owing to the extended period of elongation involved in translating the long, upstream cistron.

Termination-reinitiation in caliciviruses

ScholarOne Support 1-434/964-4100

The most extensively studied viral reinitiation events occur in the single-stranded positive sense RNA viruses of different genera of the family *Caliciviridae*, including rabbit hemorrhagic disease virus (RHDV) (Meyers, 2003, Meyers, 2007), feline calicivirus (FCV) (Luttermann & Meyers, 2007, Pöyry *et al.*, 2007), and bovine, human, and murine noroviruses (NVs) (McCormick *et al.*, 2008, Napthine *et al.*, 2009, Luttermann & Meyers, 2014). Caliciviruses produce 3′ co-terminal subgenomic mRNAs that are always dicistronic (for simplicity these two cistrons will be designated here as ORF1 and ORF2, although according to their original position in full-length genomic mRNA they are usually described as ORF2 and ORF3, respectively). ORF1 encodes a major capsid protein and the downstream ORF2 encodes a small basic protein, which is essential for infectivity and was proposed to be involved in different regulatory functions. The ORF2/ORF1 expression ratio varies from ~3% (in human NV) (Luttermann & Meyers, 2014) to about 20% (in RHDV) (Meyers, 2003, Meyers, 2007). Depending on the viral species, the two ORFs overlap by 1–14 nt. Thus, even though the ORF1 stop codon is always close to the ORF2 AUG codon, there exists a certain degree of flexibility in their spacing; and as might be expected, the REI frequency drops with increasing distance between the stop and start sites. These observations are in sharp contrast with REI after short uORFs (such as in the case of *GCN4*), where the efficiency of REI increases with increasing distance between the two ORFs, thus demonstrating that distinct mechanisms apply.

Detailed *in vitro* and *in vivo* mutational analyses have shown that the termination-REI process in caliciviruses depends on specific mRNA sequence motifs typically situated within the 40–90 nucleotides upstream of the ORF1 termination codon, designated as the termination upstream ribosome binding site (TURBS) (Fig. 6). Since ORF2 could be replaced by various reporter genes with no effect on the REI efficiency (Meyers, 2003, Pöyry *et al.*, 2007), no dependence on particular downstream sequences has been considered likely. However, a recent study suggested that, at least in the case of FCV, the efficiency of ORF2 expression is also modulated by the primary and secondary structures of the region downstream of the stop-restart signal (Habeta et al., 2014). Additional analyses are thus required to resolve this potential discrepancy. Also, no requirement for a virus-encoded transactivator protein has been reported so far.

The TURBS region contains three essential motifs, designated as 1, 2, and 2* (Fig. 6B). Motif 1 contains a conserved UGGGA core sequence located at a similar position relative to the stop-restart site within all caliciviral mRNAs. Importantly, the UGGGA sequence is complementary to the single-stranded loop at the tip of helix 26 of 18S rRNA, residing near the exit pore of the mRNA-binding channel (Luttermann & Meyers, 2007, Meyers, 2007) (Fig. 6B). With help of yeast genetics it was shown that this hybridization interaction is critical for tethering the post-termination 40S subunits to the viral mRNA (Fig. 6A); mutations within motif 1 reduced REI efficiency of a reporter mRNA in a manner rescued by complementary changes in 18S rRNA (Luttermann & Meyers, 2009). In contrast to motif 1, motifs 2 and 2* are species-specific and complementary to one another. Base pairing between these motifs allows formation of a stem loop structure in which the conserved UGGGA nucleotides

ScholarOne Support 1-434/964-4100

of motif 1 are exposed in an internal loop. Occurrence of this structure in ORF1 at a defined distance upstream of the termination-REI site was proposed to enable placement of motif 1-bound 40S subunits directly at, or at least in proximity to, the REI start codon (Luttermann & Meyers, 2007, Meyers, 2007). Moreover, it was suggested that this tethering interaction stabilizing post-TC 40S subunits on viral mRNA might provide sufficient time for recruitment of initiation factors (mainly the eIF2-TC) that are critical for recognition of the REI start codon. The key importance of TURBS sequences was recently also confirmed in a mammalian *in vitro* reconstituted system using model RHDV mRNAs with mutated motif 1 and motif 2* (Zinoviev *et al.*, 2015).

Interestingly, in some caliciviruses, as well as in *Influenza B* (see below), two alternative structural isoforms of TURBS were proposed based on secondary-structure predictions and enzymatic and chemical probing (Powell *et al.*, 2008, Napthine *et al.*, 2009). In one of these structures motif 1 is sequestered by base-pairing with another region of the viral mRNA, which makes it inaccessible for the tethering interaction, while the other structure shows the original arrangement with motif 1 accessible in the apical loop (Powell, 2010). It was therefore suggested that translation through ORF1 might be required for structural remodeling of the TURBS to expose motif 1 for base-pairing with 18S rRNA (Powell, 2010). This suggestion invokes an interesting analogy with the folding of the 5´ enhancer structure preceding the *GCN4*'s uORFs 1 and 2 after its sequence has emerged from the mRNA exit channel, which we discussed above (Munzarová *et al.*, 2011, Gunisova & Valasek, 2014). The proposed need for the translation-dependent remodeling of TURBS could help explain why the REI event occurs only after termination at a nearby stop codon. It is possible that constitutive formation of the TURBS conformation that exposes motif 1 would allow it to act as an internal ribosome entry site (IRES), promoting internal initiation by direct recruitment of the small ribosomal subunit to the ORF2 start site, without prior uORF1 translation. Uncoupling ORF2 translation from ORF1 in this way would alter the relative amounts of the two gene products and could be detrimental to virus propagation.

Various studies have demonstrated that caliciviral termination-REI is extraordinarily insensitive to substitutions in the REI start codon, being largely insensitive to single substitutions and not fully impaired even when two or all three positions are mutated (Meyers, 2003, Luttermann & Meyers, 2007, Meyers, 2007, Pöyry *et al.*, 2007, Napthine *et al.*, 2009, Luttermann & Meyers, 2014). Regardless of the REI start codon alterations, the initiating amino-acid residue in most of the ORF2 FCV proteins is still methionine, indicating decoding of near-cognate or even non-cognate start codons by Met-tRNA$_i^{Met}$ (Luttermann & Meyers, 2007). Since investigations of human NV revealed that the Kozak context also has no influence on the REI rates measured with an AUG start site (Luttermann & Meyers, 2014), it is clear that the mechanism of its selection is not canonical.

Interestingly, if a second AUG is introduced downstream of the WT ORF2 AUG codon, most REI occurs at the the original REI start site (Luttermann & Meyers, 2014). However, when the AUG triplet is introduced close to a mutated version of the

ScholarOne Support 1-434/964-4100

original REI start site, the new AUG is now preferred over the mutated start site (Luttermann & Meyers, 2014). This indicates that base pairing with the anticodon of Met-tRNA$_i^{Met}$ still contributes to selection of the REI start site even though a perfect codon:anticodon duplex is not critical for REI to occur. The relaxed requirement for a canonical AUG start codon on the one hand and the critical importance of maintaining a specific distance between the terminating ribosome and TURBS on the other clearly support the idea that the tethered post-termination 40S subunit is delivered directly to the ORF2 REI start site. The limited flexibility with respect to the juxtaposition of termination and REI start sites is believed to reflect a restricted mobility of the tethered 40S subunit following termination. The range of this spatially limited lateral migration during REI start codon selection is probably determined by the reach that the ribosomal P-site of the TURBS-bound 40S subunit has on each side of the ORF1 stop codon.

All data presented so far suggest that the caliciviral REI mechanism is mediated strictly by the post-termination 40S complexes. However, a recent study challenged this issue by investigating the plasticity in requirements for REI start codon selection by post-termination 40S subunits *versus* post-termination 80S ribosomes using mutant RHDV and NV mRNAs in an *in vitro* reconstituted system (Zinoviev *et al.*, 2015). At the AUG REI start site or when it was replaced by near-cognate codons, the post-termination 40S subunits reinitiated *via* base-pairing with Met-tRNA$_i^{Met}$ (as observed before) and required the combined assistance of eIFs 1, 1A and eIF2, or eIF2D (Ligatin) only. By contrast, REI at non-cognate codons could be achieved solely with eIF2D (Ligatin) and cognate aminoacyl-tRNA (Zinoviev *et al.*, 2015). As observed before, the position of the original REI start site was strongly preferred over a second AUG inserted into ORF2, and more efficient REI took place from the inserted AUG only when the original AUG was mutated (Zinoviev *et al.*, 2015). Strikingly, these authors showed that REI on caliciviral mRNAs *in vitro* could be also executed by post-termination 80S ribosomes that efficiently reacquired Met-tRNA$_i^{Met}$ and moved a few nt upstream (for RHDV) or downstream (for NV) to reinitiate at AUG of their ORF2 or, in the case of RHDV, at the near-cognate codon in place of AUG. Interestingly, post-termination 80S ribosomes could also migrate to, and initiate at, nearby non-cognate codons, in which case REI required binding of the respective cognate elongator tRNAs directly to the P-site (Zinoviev *et al.*, 2015). Whether such termination-REI events involving post-termination 80S ribosomes occur *in vivo* is presently not known.

Recent work of (Luttermann & Meyers, 2014) showed that when the original REI start codon is mutated, REI in human NV can also occur at more distant downstream sites (up to 78 codons), though with a much lower efficiency. Interestingly, this downstream REI was dependent on the Kozak sequence context. Movement of the 40S subunit along the mRNA in the 5' to 3' direction together with the requirement for a strong Kozak context are reminiscent of the scanning process in standard cap-dependent translation initiation. Thus, it was suggested that in addition to the specific TURBS-dependent positioning of the post-termination 40S complex onto the REI start site, start site selection during termination-REI in

ScholarOne Support 1-434/964-4100

caliciviruses can be achieved by an alternative, 'back-up' mechanism. When the TURBS-captured 40S subunits cannot establish stable codon-anticodon interaction at the original REI start site, a certain percentage of these 40S subunits may adopt a "short uORF-like" mode of REI by acquiring initiation factors and scanning downstream to the next AUG codon with strong Kozak context (Luttermann & Meyers, 2014).

Tethering the post-termination 40S subunit to the viral mRNA is not the only function that has been attributed to TURBS. UV-cross-linking assays with the FCV TURBS demonstrated that it binds eIF3 (Fig. 6) (in particular, the eIF3a, eIF3b, eIF3d, eIF3l, and eIF3g subunits were cross-linked to the FCV element), and TURBS mutants with reduced REI activity were shown to be defective in either eIF3 or 40S subunit binding, or both (Pöyry *et al.*, 2007). The proposed eIF3 involvement in termination-REI might resemble REI after short uORFs in yeast cells discussed above, where eIF3 critically stabilizes the post-termination 40S-mRNA complex (Munzarová *et al.*, 2011, Mohammad *et al.*, 2017). Even though efficient REI after short uORFs in mammalian systems also appears to require the eIF4F complex (Pöyry *et al.*, 2004), in addition to eIF3 (Hronova *et al.*, 2017), the TURBS-mediated reinitiation event seems to have no requirement for any of the eIF4F components (Pöyry *et al.*, 2007). This makes sense because the TURBS-captured 40S subunits are most likely loaded directly onto the REI start codon of the downstream cistron, obviating the need for eIF4F function in promoting *de novo* mRNA recruitment and scanning through structured mRNA leaders.

Owing to the proposed role of eIF3 in ribosomal recycling (Pisarev *et al.*, 2007), it was originally suggested that its interaction with TURBS increases the rate of 60S subunit recycling and as such provides the tethered post-termination 40S subunit with more time to acquire initiation factors (like eIF2-TC) necessary for REI (Pöyry *et al.*, 2007). However, the eIF3-mediated 80S splitting occurs only in a narrow range of low Mg^{2+} concentrations (Pisarev *et al.*, 2007), and subsequent *in vitro* and *in vivo* experiments showed that subunit splitting is primarily performed by the canonical recycling factor ABCE1 (Pisarev *et al.*, 2010, Shoemaker & Green, 2011, Young *et al.*, 2015), ostensibly at odds with the original suggestion. What could be the eIF3 contribution then, if any? It was shown that, after the ABCE1-mediated splitting, eIF3 prevents mRNA dissociation from the 40S post-TC complex (Kolupaeva *et al.*, 2005, Pisarev *et al.*, 2010), in accord with the importance of eIF3 in mRNA recruitment and stabilization on the 40S subunit (Kolupaeva *et al.*, 2005, Jivotovskaya *et al.*, 2006, Khoshnevis *et al.*, 2014, Aitken *et al.*, 2016). This mRNA-40S stabilization function, perhaps together with the role of eIF3 in 60S subunit recycling and in preventing ribosomal subunit re-association (Kolupaeva *et al.*, 2005), might explain how eIF3 promotes termination-REI after long ORFs (see our model below).

New insights into the role of eIF3 and other eIFs in this mechanism were recently provided by the *in vitro* reconstitution experiments mentioned above using two model caliciviral mRNAs containing RHDV or human NV TURBS elements (Zinoviev *et al.*, 2015). Unexpectedly, the experiments that monitored the fate of 40S

ScholarOne Support 1-434/964-4100

subunits following the subunit splitting in the presence or absence of ABCE1 suggested that eIF3 was not essential for efficient REI, and that only eIF1, 1A and eIF2-TC, or just eIF2D (Ligatin) alone, sufficed. In fact, the role of eIF2D (Ligatin) or DENR-MCT1 in REI on RHDV mRNA is consistent with their abilities to stimulate eIF2-independent recruitment of Met-tRNA$_i^{Met}$ to mRNA-40S complexes in which the start codon is placed directly in the P-site (Skabkin *et al.*, 2010), which is ensured by the TURBS-18S rRNA interaction. The fact that this model system revealed no eIF3 dependence could be explained by non-physiological conditions of the *in vitro* system or by proposing that the eIF3 contribution to termination-REI varies for different caliciviruses, perhaps in inverse relation to the strength of their TURBS-40S interactions. Interestingly, some stimulatory role for eIF3 even in this system was observed when concentrations of other factors became limiting, e.g. when eIF1 or eIF1A were present individually, when eIF2-TC was added following a delay, or when the TURBS elements were mutated; in the latter eIF3 became nearly essential for REI (Zinoviev *et al.*, 2015). These findings may suggest the following. Besides ribosomal recycling, eIF3 was recently shown to control translation termination and thus it is expected to associate with early terminating ribosomes; perhaps in a complex with eRFs that was shown to exist *in vivo* (Beznosková *et al.*, 2013). This might mean that termination complexes in living cells come into contact with eIF3 much earlier than other eIFs, shown to be relatively more important for REI in the *in vitro* system. This could impose a marked *in vivo* requirement for the mRNA stabilization role of eIF3 during the onset of the termination-REI mechanism (fortifying the TURBS-40S contact), as discussed above.

To summarize, the TURBS-40S interaction represents the critical requirement for the termination-reinitiation mechanism to occur (Fig. 6A). eIF3 may further stabilize the mRNA-40S complex and, in the case that eIF2D (Ligatin) ensures the subsequent replacement of deacylated tRNA with Met-tRNA$_i^{Met}$, it may also prevent the Ligatin's ability to dissociate 40S post-TCs, as suggested above. Alternatively, dissociation of the deacylated tRNA would be mediated by eIFs 1 and 1A, and eIF2 would subsequently deliver Met-tRNA$_i^{Met}$ to the P-site to form the TURBS reinitiation complex poised for elongation. It will be of great importance to investigate the functions of eIF1, eIF1A, eIF2-TC, eIF3 and eIF2D (Ligatin) in TURBS-mediated REI *in vivo* to find out what is their true physiological contribution to this mechanism. Another interesting question is how the caliciviral TURBS-mediated termination-REI mechanism would respond to decreased levels of the eIF2-TC provoked by stress-activated eIF2α phosphorylation by kinases such as PKR and PERK, whose activation is triggered by viral infections to produce a systematic shutdown of protein synthesis. To the best of our knowledge, there is currently no information about the control of the eIF2α phosphorylation during calicivirus infection.

Termination-reinitiation in Influenza B

The termination-REI mechanism has been quite extensively studied also in the single-stranded negative sense RNA Orthomyxovirus *Influenza B*, where numerous

ScholarOne Support 1-434/964-4100

similarities to the caliciviral mechanism have been observed (Horvath *et al.*, 1990, Powell *et al.*, 2008, Hatta *et al.*, 2009). Its segment 7 encodes two proteins whose coding sequences overlap in a typical UAAUG stop-restart arrangement and ~10% of ribosomes terminating at the ORF1 stop codon were shown to reinitiate at the ORF2 AUG (Powell *et al.*, 2008). Efficient REI on ORF2 is dependent on proximity of the stop-restart sequence and the ~45 nt long TURBS region upstream of the overlap, which contains the motif 1 UGGGA core sequence, as well as complementary motifs 2 and 2* (Horvath *et al.*, 1990, Powell *et al.*, 2008, Hatta *et al.*, 2009). Oligonucleotide targeting experiments and expression studies in yeast cells support the hypothesis that motif 1, like in caliciviruses, interacts directly with helix 26 of 18S rRNA (Powell *et al.*, 2011). Whether or not there is also a need for the TURBS-specific mRNA secondary structure remains to be resolved since the most recent experimental data provided only limited support for the initial secondary structure predictions and translational remodeling hypothesis (Powell *et al.*, 2008, Powell, 2010, Powell *et al.*, 2011). In further analogy, a variety of non-canonical initiation codons can be utilized and there is also a minimal requirement for optimal start codon context (Powell *et al.*, 2008). Accordingly, it was suggested that the decreased stringency in REI start codon selection may reflect the reduced requirement for the full complement of initiation factors in the termination-REI process, such as eIF1 and eIF1A—key players in canonical start site recognition (Hinnebusch, 2017). As stated above, the pace of the termination-REI mechanism *in vivo* may simply be too quick for these factors to bind the post-termination mRNA–40S complex on time. Alternatively or in addition, the reduced stringency might result from the fact that the 40S subunit is tethered rather than scanning, which increases the dwell time over the start codon. This option is in analogy with earlier findings of Kozak that a stable stem loop inserted downstream of the start site at a position that would arrest the scanning PIC with the start codon in the P-site increases initiation at AUGs in poor context (Kozak, 1991).

Also as in case of caliciviruses, it was shown that when termination occurs at the normal distance relative to the TURBS, a certain proportion of ribosomes is able to locate AUG codons placed at a relatively remote location (63 nt) downstream of the mutated original REI start codon (Powell *et al.*, 2011). Since REI on distant AUGs was not inhibited in the eIF4G-depleted rabbit reticulocyte lysates, it was suggested that the tethered 40S subunit can move some distance in a linear, eIF4F-independent manner akin to scanning, or that a direct transfer of the 40S subunit from the TURBS to the distant AUGs might be facilitated by looping out of the mRNA segment between the tethered 40S subunit and downstream AUG (Powell *et al.*, 2011).

Influenza B REI can be also stimulated by exogenously added eIF3, even when TURBS was rendered defective (by mutated motif 1), further supporting the view that eIF3 can substitute for the TURBS-18S rRNA interaction to prevent dissociation of post-termination 40S subunit from viral mRNA and ensure its transfer to the REI start site (Powell *et al.*, 2011). Thus, all of these data suggest that the *Influenza B* termination-REI mechanism is mechanistically very similar to that of

ScholarOne Support 1-434/964-4100

caliciviruses and depends on direct placement of the post-termination 40S subunit onto or nearby the REI start codon.

Termination-reinitiation in other viruses and retrotransposons

There is evidence that other unrelated viral RNAs employ coupled termination–REI with similar molecular mechanisms. In pneumo- and metapneumoviruses, termination–REI was demonstrated to regulate the synthesis of a downstream cistron from a single transcript (Ahmadian *et al.*, 2000, Gould & Easton, 2005, Gould & Easton, 2007). As in caliciviruses, the REI start site must be in close proximity to the termination codon of the upstream ORF, although in some cases larger separations of up to 29 nt can be tolerated (Ahmadian *et al.*, 2000). Efficient REI is also dependent on sequences upstream of the termination codon, but the identified region is quite large (up to ~200 nt) and apparently contains extensive secondary structures (Gould & Easton, 2005). Unlike in caliciviruses, however, this region lacks an obvious motif 1 and thus its exact function is unknown. Similarly, in victoriviruses the stop and REI start sites of REI-regulated cistrons often overlap, and the upstream sequence—in particular the 32 nt long region immediately upstream of the stop-start site—was shown to be important for efficient REI (Li *et al.*, 2011). This region is predicted to adopt a specific pseudoknot structure but also lacks the motif 1 sequence. In hypoviruses, where the downstream cistron appears to be translated by the termination-REI mechanism *via* an overlapping stop-start site at a frequency of less than 5%, no motif 1 has been identified; however, an upstream sequence involved in the putative REI shows some complementarity to 18S rRNA (Guo *et al.*, 2009). Interestingly, the protein encoded by the upstream hypoviral cistron seems to participate in REI of the downstream ORF by a yet to be identified mechanism (Guo *et al.*, 2009).

A specific translational coupling of a similar nature to those described above has been observed also in the non-LTR silkworm retrotransposon SART1, with one apparent exception; the complex secondary structure needed for proper functioning of this mechanism was located downstream – not upstream – of the overlapping stop-restart site (Kojima *et al.*, 2005). An unconventional termination-REI mechanism has been also proposed for another non-LTR retrotransposon, mammalian LINE-1, where sequences within ORF2 may play a role in positioning the ribosome onto or nearby the ORF2 AUG codon (Alisch *et al.*, 2006). Here, however, ORF1 and ORF2 are separated by a 63 nt long inter-ORF spacer and in order to reach the downstream cistron, some sort of scanning through this spacer might have to occur, unless the ORF1 stop and ORF2 start are brought together by a looping mechanism mentioned above.

Termination-reinitiation in cellular mRNAs

The fact that the termination-REI mechanism is widespread in viruses and does not seem to require specific viral-encoded proteins raises the question whether some of

ScholarOne Support 1-434/964-4100

the rarely occurring cellular bi- or polycistronic mRNAs (with at least two long ORFs) utilize a similar mechanism. Recently, (Gould *et al.*, 2014) identified more than 2000 genes in the human genome whose transcripts contained a major ORF overlapping with a second ORF comprising at least 50 codons. From 24 experimentally investigated transcripts, 22 expressed an ORF2-encoded protein, which may indicate that the protein-coding potential of 3' UTRs of cellular mRNAs is greater than generally believed. Importantly, five transcripts were shown to use a coupled termination-REI mechanism for access to the ORF2 AUG codon; however, none of these mRNAs contained an upstream sequence that resembles the TURBS or any other viral REI-promoting sequences. In fact, detailed analysis of one of these transcripts, encoding the CASQ2 protein, revealed that the termination-REI mechanism did not depend on any mRNA sequences at all, and required instead an aspartate-rich repeat region at the C-terminus of CASQ2. Quantification of the coupling efficiency demonstrated that the levels of downstream protein were ~82-fold lower compared to the upstream product. It was suggested that the aspartate-rich region might act to slow down the elongating ribosomes or cause them to pause at the end of ORF1, but how this would promote REI at ORF2 remains to be determined.

Another example of a cellular mRNA likely to be regulated by translational coupling is the mouse embryonic mRNA splicing variant of glutamic acid decarboxylase (GAD) (Kojima *et al.*, 2005). The bicistronic RNA of GAD contains UGAUG overlapping stop-start codons and its downstream ORF was shown to be translated *in vivo* (Szabo *et al.*, 1994). Strikingly, a putative TURBS motif 1 has been identified within the sequence preceding the stop-restart signal, as were the complementary motifs 2 and 2* (Powell, 2010). The sequence related to the TURBS core sequence UGGGA has also been found in the 5´ leader sequence of the long isoform of the human *SLAMF1* gene (encoding the CD150 membrane protein), where the stop codon of the last 29-codon uORF (of altogether four uORFs) overlaps the start codon of the main reading frame by 1 nt (UGAUG) (Putlyaeva *et al.*, 2014)). Although this uORF, according to its relatively short length, might still qualify as a REI-permissive uORF, the fact that it overlaps the main ORF by even 1 nt likely precludes it from functioning as a typical REI-permissive uORF, in which an appreciable distance/time is required for the traversing/scanning 40S subunit to rebind eIF2-TC *en route* to the downstream ORF. It remains to be determined whether the TURBS-mediated termination-REI mechanism operates on the *SLAMF1* gene. If so, the short length of the uORF might allow eIF3 to persist on elongating ribosomes over its entire length (see above) and co-operate with TURBS immediately on the onset of termination to promote efficient termination-REI. This example illuminates a theoretical possibility how some features of the fundamentally different REI mechanisms may act together to potentiate the final outcome.

Clearly, dissecting the intricate ways in which viral genomes exploit the host molecular machineries to produce all of their proteins in the proper stoichiometries has revealed an important mechanism of REI. It will be valuable to determine whether this coupled termination–reinitiation mechanism is widespread in cellular

For Peer Review

ScholarOne Support 1-434/964-4100

mRNAs, where it could provide an appreciated means of expanding the coding capacity of mammalian genomes.

Transactivation of translation on long ORFs by a viral factor

In plants, an exceptional strategy to ensure translation of all cistrons in polycistronic mRNAs has been uncovered in *Cauliflower mosaic virus* (CaMV) and some related pararetroviruses of the icosahedral *Caulimoviridae* family, wherein the REI mechanism is strictly dependent on a virus-encoded transactivator protein called TAV (transactivator/viroplasmin) (Fig. 7) (Bonneville *et al.*, 1989, Park *et al.*, 2001). Upon infection, the CaMV genome is transcribed into pregenomic RNA (pgRNA) containing seven long ORFs, which can be further internally spliced into individual derivatives containing at least four long ORFs. All ORFs (except for the TAV ORF) are tightly spaced and usually exhibit short regions of overlap, compatible with linked translation. Interestingly, increasing overlap between the two long CaMV ORFs (by more than ~130 nt) was found to inhibit transactivation by TAV (Futterer & Hohn, 1991), which may imply that the backward movement of reinitiating ribosomes is somehow limited. In addition to activating translation of consecutive long viral ORFs, TAV is able to promote REI on completely artificial bicistronic reporters, indicating that specific *cis*-sequence signals are not required for transactivation of the second ORF translation (Bonneville *et al.*, 1989, Futterer & Hohn, 1991, Futterer & Hohn, 1992). TAV-mediated REI is also not affected by the distance between the two consecutive long ORFs—occurring efficiently with distances between the uORF and downstream ORF ranging from only a few nt up to 700 nt (Futterer & Hohn, 1991). This contrasts with the REI mechanism mediated by short uORFs, where a minimum intercistronic distance is required to provide sufficient time for efficient eIF2-TC recruitment as the 40S ribosome traverses from the uORF to the downstream ORF.

Studies from Ryabova's laboratory on the molecular mechanism of CaMV REI indicate that a key feature is the retention of reinitiation-supporting factors, namely eIF3 (Park *et al.*, 2001), RISP (Thiébeauld et al, 2009), and TOR (Schepetilnikov *et al.*, 2011) on ribosomes translating the first long ORF (Fig. 7). TAV was shown to interact with these factors and other components of the host translational machinery (namely 60S ribosomal proteins Rpl13/eL13, Rpl18/eL18 and Rpl24/eL24) directly *via* its two central domains that are essential for REI.

The initial *in vitro* studies demonstrated that TAV can form two stable complexes; in the first TAV bridges interaction between eIF3 (*via* its g subunit) and the 60S subunit (*via* Rpl18/eL18 or potentially also Rpl13/eL13); and in the second complex eIF3 connects TAV with the 40S subunit (Park *et al.*, 2001). Later it was shown that the TAV-eIF3-40S complex can join with the 60S subunit to form an 80S-eIF3-TAV complex *in vitro*, which was also observed after fractionation of cell extracts by sucrose gradient centrifugation (Park *et al.*, 2001). Consistently, analysis of extracts from CaMV-infected plants revealed significant accumulation of TAV and eIF3 in the polysomal fractions (Park *et al.*, 2001). These observations suggested that the TAV-eIF3 complex is associated with elongating ribosomes *in vivo* and that

ScholarOne Support 1-434/964-4100

TAV might prevent spontaneous eIF3 dissociation from ribosomes translating long ORFs, through its mutual interaction with eIF3 and 60S proteins Rpl18/eL18 or Rpl13/eL13, to maintain their REI competence post termination (Fig. 7). Because Rpl24/eL24 is located at the intersubunit surface and serves as one of the intersubunit bridges, its role in eIF3 retention on elongating ribosomes is highly unlikely. Instead it was proposed that its interaction with TAV might actually lead to inhibition of protein synthesis during the late phase of viral infection, promoting a switch to viral assembly (Park *et al.*, 2001).

Later it was shown that eIF4B (a factor stimulating the RNA helicase activity of eIF4A that is, however, not essential in plants (Altmann *et al.*, 1995)) shares the same binding site on eIF3g with TAV and potently outcompetes TAV for binding to the eIF3-40S complexes both *in vitro* and *in vivo* (Park *et al.*, 2004). Consistently, transient overexpression of eIF4B in plant protoplasts specifically inhibited TAV-mediated REI at a second ORF (Park *et al.*, 2004). eIF4B did not displace eIF3 from the eIF3-TAV-60S complexes, however, 60S subunit joining disrupted only the eIF4B-eIF3-40S and not the TAV-eIF3-40S complexes *in vitro* (Park *et al.*, 2004). These data indicated that eIF4B precludes the TAV-eIF3-40S complex formation during the first initiation event and that TAV enters the host translation machinery after eIF4B removal from the 48S PIC (i.e. at or shortly before subunit joining) to stabilize eIF3 on the translating ribosome (Fig. 7). If true, it would explain why TAV affects exclusively the second and all following rounds of initiation on polycistronic mRNA.

Subsequently, a novel plant-specific REI supporting protein (RISP) was identified and proposed to act as an indispensable host factor enhancing TAV function in REI (Thiebeauld *et al.*, 2009). Knock-out of *rispa* (encoding RISP) caused a delay in viral replication and reduced TAV-mediated transactivation of REI (Thiebeauld *et al.*, 2009); the innate RISP function in non-infected plant cells is not known. RISP has a predicted coiled-coil structure characterized by four helices, H1–H4. The interaction between TAV and RISP was mapped within putative helix H3, while segments represented by helices H2 and H4 were found to interact with eIF3a and eIF3c subunits, and with the C-terminus of Rpl24/eL24, respectively (Thiebeauld *et al.*, 2009). Binding of RISP to the 40S subunit occurred only with preformed RISP–eIF3 complexes suggesting that RISP enters the cell translational machinery together with eIF3 at the stage of 43S PIC formation (Fig. 7) (Thiebeauld *et al.*, 2009). Importantly, RISP accumulation in polysomes required TAV indicating that 1) RISP is recruited to or stabilized in polysomes in CaMV-infected cells, and 2) that, analogous to eIF3, TAV prevents RISP dissociation from the translating ribosomes during prolonged elongation (Thiebeauld *et al.*, 2009). Quaternary complexes composed of eIF3-TAV-RISP-eL24 could form *in vitro* (Thiebeauld *et al.*, 2009) which may suggest that, upon termination, RISP and TAV could bridge the interaction between eIF3-bound 40S and Rpl24/eL24 of 60S to enhance recruitment of 60S subunits while the post-termination 40S subunit is engaged in AUG-searching process before each initiation event on polycistronic mRNA (Fig. 7).

ScholarOne Support 1-434/964-4100

Besides eIF3 and RISP, TAV function requires its physical interaction with the plant protein kinase TOR and its downstream effector S6K1; the TAV-TOR association is critical for viral fitness and, consistently, TOR-deficient plants are resistant to viral infection (Schepetilnikov *et al.*, 2011). As demonstrated both *in vitro* and *in vivo*, TAV overexpression (or viral infection) triggers TOR hyperactivation and high levels of S6K1 phosphorylation (Schepetilnikov *et al.*, 2011). Sucrose gradient fractionations revealed that activated TOR binds to polysomes simultaneously with TAV, eIF3 and RISP; although TOR binding does not seem to be a prerequisite for polysome association of these other three factors (Schepetilnikov *et al.*, 2011). Importantly, however, polysomal association of TOR correlated with increased phosphorylation of polysome-associated RISP, a putative novel substrate of S6K1; and RISP was found to stimulate TAV-mediated REI only in its phosphorylated state (Schepetilnikov *et al.*, 2011). Collectively, these findings may suggest that the essential function of TOR in TAV-mediated REI is to keep polysomal RISP in its phosphorylated state (Fig. 7). Interestingly, a non-phosphorylatable mutant of RISP showed increased affinity for eIF3 but decreased affinity for TAV and Rpl24/eL24 (Schepetilnikov *et al.*, 2011) suggesting that selective alterations in RISP binding affinities upon its phosphorylation might be an important part of the regulatory mechanism. Notably, as discussed above, TOR-S6K1 connections with eIF3 were implicated in REI on the ARF-encoding mRNAs in *Arabidopis* (Schepetilnikov *et al.*, 2013), as well as in the PIC assembly during canonical translation initiation in mammals (Holz *et al.*, 2005).

All of these findings were combined in the following elaborate model for TAV function in REI (Fig. 7). Upon infection, the overexpressed TAV binds to and activates TOR. Attendant S6K1 activation by TOR leads to RISP phosphorylation in the context of eIF3-bound PICs. During the 60S subunit joining step, eIF4B is ejected from the 40S subunit, enabling TAV to bind and thus stabilize the eIF3 and phosphorylated RISP binding to the 80S ribosome. Hypothetically, TAV may enter the assembly pre-bound to the 60S subunit (through Rpl13/eL13 and/or Rpl18/eL18) during subunit joining at the start codon of ORF1 or (since eIF3 can persist transiently on elongating ribosomes (Mohammad *et al.*, 2017)) during the first few rounds of elongation. The major role of TAV at this stage is to prevent dissociation of eIF3 and RISP during elongation on ORF1. Since binding of eIF3 to the solvent-exposed side of the 40S subunit has been firmly established (reviewed in (Valasek *et al.*, 2017)) (Supplementary Fig. 1), it seems reasonable to propose that the TAV-eIF3-RISP complex resides at least initially at this canonical eIF3 binding site on the 40S subunit. However, the model posits that TAV-bound eIF3 and RISP disengage from the 40S at the onset of elongation and relocates to the solvent surface of the 60S subunit *via* TAV binding to Rpl18/eL18 (and/or Rpl13/eL13), presumably to allow retention of the eIF3-TAV-RISP assembly throughout the prolonged period of elongation required to translate ORF1. It would be intriguing to see how TAV is arranged on the surface of the 80S ribosome, contacting Rpl18/eL18 or Rpl13/eL13 and interacting with eIF3 and RISP, without hampering the elongation process. The phosphorylated (or rephosphorylated) state of RISP is maintained by activated TOR-

For Peer Review

ScholarOne Support 1-434/964-4100

S6K1. Upon termination, the eIF3–TAV-RISP complex would need to be transferred back to the 40S subunit where its components can facilitate reassembly of a complex capable of recruiting eIF2-TC for REI. As mentioned above, the RISP–TAV complex is believed to bridge the 40S–60S interaction through contacts with eIF3 and Rpl24/eL24 and thus prevent ribosomal recycling at the ORF1 stop codon and enable reuse of the same 60S subunit during subsequent REI events. It was also speculated that the 40S–60S association would need to be sufficiently relaxed to allow efficient eIF2-TC binding during traversing of the putative 80S complex along viral mRNA. Considering the multiple interactions of TAV and other involved factors, as well as the rather dramatic relocation of eIF3-TAV-RISP from the 40S to 60S subunit and back postulated in this model, which were identified and proposed primarily based on biochemical experiments, it will be important to analyze the individual proposed steps in reconstituted, as well as *in vivo* systems. Structural analysis of different TAV complexes free or ribosome-bound would also shed more light on this intriguing REI mechanism and its unique reliance on non-canonical REI factors.

Reinitiation in the 3´ UTR

REI in 3' untranslated regions (UTRs) has generally not been considered as feasible until recently, when the application of ribosome profiling techniques revealed ribosome protected fragments (RPFs) in many non-coding regions including 3´ UTRs of conventional mRNAs (Guydosh & Green, 2014, Ji *et al.*, 2015, Miettinen & Bjorklund, 2015, Young *et al.*, 2015, Mills *et al.*, 2016). Depending on experimental conditions, the proportion of reads arising from 3´ UTRs varied between very low (<1%) to up to 20-25% of all generated RPFs. Interestingly, an increased density of 3´ UTR RPFs was found in some specific cellular lineages or for example in yeast cells lacking Dom34, a factor that rescues ribosomes stalled during elongation on cellular mRNAs (Guydosh & Green, 2014, Miettinen & Bjorklund, 2015, Mills *et al.*, 2016). The vast majority of these RPFs were, however, suggested to arise from non-translating 80S ribosomes. One study estimated that ~4% of all translated coding sequences in normal human cells derive from the 3' UTRs of transcripts encoding primary annotated ORFs (Ji *et al.*, 2015).

In the recent work of (Young *et al.*, 2015) a special case of non-canonical REI involving 80S ribosomes was found to occur broadly in 3´ UTRs in mutant yeast cells where the first stage of ribosome recycling (removal of 60S subunit) following termination was impaired (Fig. 8). Conditional depletion of the essential recycling factor, Rli1 (ABCE1) led to increased accumulation of 80S ribosomes at stop codons and in the adjacent 3′ UTRs of virtually all yeast genes. Three critical observations provided evidence that the 3′ UTR ribosomes are frequently engaged in translation and that this form of translation represents new REI events as opposed to readthrough of the main ORF stop codon. First, numerous ribosome occupancy peaks were identified to coincide with stop codons in the 3′ UTRs in all three reading frames relative to the main ORF, as expected from defective 60S subunit recycling

ScholarOne Support 1-434/964-4100

For Peer Review

on the main ORF and subsequent random reinitiation. Second, induction of histidine starvation specifically increased ribosome occupancy at histidine codons located in the same 3' UTR reading frame upstream of the prominent 3′ UTR stop codon peaks present in non-starved cells, consistent with stalled elongation at 3' UTR histidine codons. Finally, synthesis of small peptide products predicted from the 3′ UTR ribosome occupancies at different genes, and representing all three reading frames, was identified by Western blotting and mass spectrometry analyses.

Surprisingly, REI frequently occurred relatively close to the main ORF stop codon (within ~10 nt upstream or downstream), but neither AUG codons nor triplets complementary to the ultimate P-site tRNA were preferred as start sites (Young *et al.*, 2015). This strongly suggests that: 1) the 3′ UTR REI does not involve scanning and start site selection *via* complementarity to either Met-tRNA$_i^{Met}$ in eIF2-TC or the deacylated tRNA in the P-site of post-termination 80S ribosomes; and 2) that this mechanism radically differs from that described in an *in vitro* reconstituted system, where it appeared that REI by unrecycled post-termination 80S ribosomes was directed by complementarity to deacylated tRNA in the P-site (Skabkin *et al.*, 2013). Could this difference arise from the fact that the *in vivo* study followed the fate of post-termination ribosomes after translation of long ORFs, whereas the *in vitro* study monitored the situation after translation of short uORFs? What is the mechanism of REI in 3′ UTRs by unrecycled 80S ribosomes *in vivo*?

Young et al. (Young *et al.*, 2015) have proposed that, following termination at the main ORF stop codon and polypeptide release, the splitting of the 60S subunit from the 80S post-TCs fails due to insufficient Rli1 (Fig. 8). The 80S post-TC thus releases only eRF1 from the A-site, allowing the deacylated P-site tRNA to adopt the pre-translocation P/E hybrid state required for freeing the 80S post-TC to migrate in either direction towards new sense codons. Choice of the REI start site is probably stochastic, determined by base-pairing between a particular sense codon that appears in the A-site and the cognate eEF1A-GTP-aa-tRNA-ternary complex (as stated above, no scanning is involved). Upon base-pairing, a pseudo-translocation event - similar to that occurring during the A-site-initiated translation initiation directed by the dicistrovirus IGR IRES (Thompson, 2012) – would occur to translocate the codon:aa-tRNA-ternary complex assembly into the P-site, exposing the next triplet in the A-site and allowing conventional elongation to commence (Fig. 8) (Young *et al.*, 2015). Whether this idea is correct and, if so, what other factors might be involved, remains to be shown.

It is interesting to note that whereas depletion of Rli1 produced translating 80S ribosomes in 3' UTRs (Young *et al.*, 2015), it appeared that deletion of *DOM34* led primarily to accumulation of 80S ribosomes at the 3' UTR junction with the mRNA poly(A) tail (Guydosh & Green, 2014). The fact that this phenomenon in *dom34Δ* cells was suppressed by Rli1 overexpression indicates that the accumulating 80S ribosomes originate from failed 60S recycling at main ORF stop codons, despite WT levels of Rli1. To explain why a deficiency in Rli1 recycling leads primarily to 80S accumulation at the poly(A) tail in *dom34Δ* cells but not in the *DOM34* cells depleted of Rli1, it was suggested that Dom34 serves to rescue the class of 80S ribosomes

ScholarOne Support 1-434/964-4100

that arrive at the poly(A) junction after failing to reinitiate at all or while still engaged in translation. By contrast, the reinitiating ribosomes observed on Rli1 depletion represent the class that escaped Dom34 rescue.

This brings us to three fundamental questions. Does this type of 80S REI occur in normal cells? What is its frequency? And what purpose is served (if any) by the 3' UTR-encoded peptides produced in this way? Some of these peptides could easily be toxic and their production should be suppressed. Since REI products encoded in the *CWP2* 3′ UTR were detected at low levels in WT yeast cells, and their synthesis was diminished by overexpressing Rli1 (Young *et al.*, 2015), it was suggested that this mechanism does operate at some level in living cells. Since elevated levels of 3′ UTR-localized ribosomes were also detected during stress (Young *et al.*, 2015), it was suggested that the wild-type level of Rli1 activity is just below the threshold of sufficiency for complete recycling, and that under stress this threshold may increase (or Rli1 levels might decrease) to enhance the frequency of 80S REI in 3' UTRs.

Reinitiation of translation in prokaryotes

In contrast to eukaryotes, reinitiation in prokaryotes is considered to be a frequent event, which is not surprising owing to the fact that most of prokaryotic transcripts are naturally bi- or polycistronic. In addition, more than 75% of the intercistronic distances in *E. coli* transcripts are shorter than 30 nt, which is considered too short to allow *de novo* initiation on the downstream cistron in view of the length of mRNA covered by one ribosome (34 – 38 nt) (Yamamoto *et al.*, 2016). However, our knowledge of the mechanism of prokaryotic REI has been quite limited. The recent *in vitro* studies of (Yamamoto *et al.*, 2016) revealed somewhat unexpectedly that traversing to and translation of the downstream cistron is achieved by 70S ribosomes. In fact, 70S ribosomes were also able to initiate translation on monocistronic mRNA provided that its 5′ UTR did not contain strong secondary structures. Using various reporters in an *in vitro* reconstituted system, these authors demonstrated that after termination, 70S ribosomes scan the sequence surrounding the termination codon for the presence of the Shine-Dalgarno (SD) motif which, through base pairing with the 3' end of 16S rRNA, positions the start codon of the downstream cistron in the ribosome P-site to produce a 70S initiation complex ready to commence translation (Fig. 9). The scanning process was triggered by fMet-$tRNA_f^{Met}$, did not require energy and was found to be regulated by IFs 1 and 3. Whereas the function of IF3 was essential to keep 70S ribosomes in the scanning-competent mode, IF1 stimulated 70S-mediated REI most probably by preventing deleterious entry of the elongation ternary complexes (EF-Tu-GTP-aa-tRNA), which could interrupt the scanning process before the SD was located. The scanning-like movement of post-termination ribosomes was also detected in earlier *in vivo* studies, where its radius of action exceeded more than 40 nt in both directions and REI occurred at the first start codon encountered that was preceded by a SD-like sequence (Adhin & van Duin, 1990). The just described mechanism of 70S REI

ScholarOne Support 1-434/964-4100

bears some features that are similar to eukaryotic REI by post-termination 80S ribosomes as described above (Skabkin *et al.*, 2013, Young *et al.*, 2015, Zinoviev *et al.*, 2015). In addition, the eukaryotic functional counterparts of IF3 and IF1, namely eIF1 and eIF1A, have also been implicated in scanning by 43S PICs during conventional initiation (Hinnebusch, 2017). However, it is questionable whether eIF1 and eIF1A binding to the interface surface of the 40S subunit could be maintained in an 80S ribosome. Perhaps an even more crucial difference between the two systems is the absence of the SD:rRNA interaction in eukaryotes and a different mode of termination and ribosomal recycling mediated by unrelated factors (Myasnikov *et al.*, 2009, Buskirk & Green, 2017, Hinnebusch, 2017).

REINITIATION OCCURING WITHIN CODING REGIONS

The following section deals with two mechanistically distinct processes that can be considered as specific types of REI even though they drive new translation from within the same coding sequence. The first, called retroreinitiation (retroREI) resembles 80S-mediated REI after long ORFs as it requires recognition of a stop codon. In this case, however, the stop codon is introduced by a nonsense mutation that prematurely terminates the decoding of the ORF. The second mechanism, designated as Stop-Carry On or StopGo, completely interrupts elongation and produces two discrete, sequentially synthetized peptides from the same ORF.

Retroreinitiation

RetroREI is believed to represent a specific REI mechanism occurring within a conventional ORF that happens to be interrupted by a premature termination codon (PTC). Such PTCs are normally recognized as aberrant and the corresponding mRNAs are targeted for degradation by the NMD pathway (for review see (He & Jacobson, 2015)). Using toe-printing analysis to map the positions of stable ribosomal complexes in yeast cell-free systems it was noted that, in contrast to regular stop codons, ribosomes failed to be efficiently released when they encountered a PTC on the *CAN1* reporter mRNA (Amrani *et al.*, 2004). Subsequent addition of the elongation inhibitor cycloheximide allowed detection of additional signals that were attributed to 80S ribosomes with their P-sites centered on AUG codons in proximity to the PTC (Amrani *et al.*, 2004). This led to the suggestion that ribosomes that failed to be released from the PTC could migrate preferentially in the 5' direction (accounting for the designation retroREI), and reinitiate from nearby AUGs (Fig. 10). This event was shown to depend on PTC recognition by eRF1 and execution of peptide hydrolysis because the presence of defective eRF1 led to ribosomal stalling at the PTCs (Amrani *et al.*, 2004). This is consonant with the data from *in vitro* reconstituted termination on short uORF containing mRNAs where migration of 80S ribosomes in the 5' direction strictly depended on previous peptide release (Skabkin *et al.*, 2013). Even though migration to codons cognate to the deacylated P-site tRNA prevailed in this *in vitro* system, a small proportion of 80S

ScholarOne Support 1-434/964-4100

ribosomes apparently lacking the deacylated tRNA could rebind Met-tRNA$_i^{Met}$ and migrate to upstream AUGs (Skabkin *et al.*, 2013)—which might also be the case in retroREI. Interestingly, inactivation of factors involved in NMD (Upf1 and Upf2) diminished the retroREI toe-prints at upstream AUGs suggesting that, besides eRF1 recognition of the PTC as a stop codon, NMD factors—required to couple PTC recognition to mRNA decay—also contribute to efficient retroREI (Fig. 10). The physiological importance of retroREI is debatable; i.e. whether any benefit could be derived from synthesis of truncated proteins, often out of frame, from aberrant mRNAs that are being targeted for degradation to prevent the synthesis of potentially harmful truncated proteins. Nevertheless, the findings that ribosome recycling is inhibited at PTCs and that NMD factors are required for a scanning-like retro-migration of post-termination complexes deserve additional investigation.

Stop-Carry On or StopGo translation

Stop-Carry On or StopGo translation represents a rather peculiar REI mechanism where translation elongation arrest leads to termination at a specific sense codon ("Stop"), release of the nascent polypeptide, and subsequent reinitiation ("Go") at the next in-frame codon, resulting in the synthesis of a separate downstream protein product (Atkins *et al.*, 2007, Brown & Ryan, 2010). In other words, within the coding sequence the synthesis of one specific peptide bond is skipped. The mechanism was first described in the FMDV (Foot and Mouth Disease Virus) apthovirus and in the EMCV (EncephaloMyoCarditis Virus) cardiovirus of the *Picornaviridae* family as a strategy used in the biogenesis of viral proteins (Donnelly *et al.*, 2001, Brown & Ryan, 2010). Since then it was found in many other positive-strand RNA viruses known for the production of multiple proteins from a single long ORF, including other mammalian *Picornaviridae* subgroups (erboviruses, teschoviruses and parechoviruses) and insect Iflaviviruses and *Tetraviridae* and *Dicistroviridae* families (Luke *et al.*, 2008). Apparently, such unconventional REI events provide an alternative to proteolytic processing of a polyprotein in single-stranded RNA viruses. StopGo translation has been also identified in mammalian (rotaviruses), insect (cypoviruses) and crustacean (*Totiviridae*) double-stranded RNA viruses, and in sequences derived from non-LTR retrotransposons of trypanosomes and the purple sea urchin (Donnelly *et al.*, 2001, Heras *et al.*, 2006, Luke *et al.*, 2008). Interestingly, in the latter species, this mechanism may also control cellular protein synthesis and was suggested to participate in the innate immune system (Brown & Ryan, 2010).

In cardio- and apthoviruses, the StopGo occurs between segments 2A and 2B of the polyprotein that form the boundary between viral upstream capsid proteins and downstream RNA replication factors (Fig. 11). Alignment of their 2A sequences (which are only 18 aa long in apthoviruses compared to ~150 aa in cardioviruses) led to identification of a conserved motif DxExNPG/P (where x is any amino acid) situated at the C-terminal end of 2A with the last conserved proline residue representing the N-terminal residue of the 2B segment (Fig. 11) (Donnelly *et al.*, 1997). Similar motifs were later found in other viral genera or cellular genes utilizing

ScholarOne Support 1-434/964-4100

StopGo (Luke *et al.*, 2008, Brown & Ryan, 2010). The 2A penultimate proline (proline-17; according to apthoviruses) and ultimate glycine (glycin-18) residues are completely conserved and essential among all active 2A and 2A-like sequences, while the 2B proline (proline-19) can be substituted by glycine at the expense of lower efficiency (Donnelly *et al.*, 2001). Remarkably, 2A peptides work in all eukaryotic systems but not in prokaryotes (Ryan & Drew, 1994, Donnelly *et al.*, 1997). Interestingly, phylogenetic analyses of 2A and 2A-like sequences indicated multiple, independent acquisitions of these sequences at different stages during virus evolution (Luke *et al.*, 2008).

In contrast to proteins analyzed from the FMDV infected cells where no full-length protein products including both 2A and 2B segments were observed, expression of artificial proteins from a bicistronic reporter construct with the 2A segment inserted in-frame between the two cistrons revealed an imbalance in the accumulated translation products (Donnelly *et al.*, 1997, Donnelly *et al.*, 2001, Donnelly *et al.*, 2001). These and other experiments indicated that besides the 2A segment, its surrounding sequences also contribute to the efficiency of StopGo. In accord, natural extension of the FMDV 2A segment to ~30 aa regained 100% of the StopGo efficiency, no fusion products were observed and reporter proteins were produced in equimolar ratios (Donnelly *et al.*, 1997, Donnelly *et al.*, 2001).

The molecular mechanism of StopGo REI is distinctively associated with the specific nature of the essential glycine-18 and proline-19 residues. Toe-printing analysis and puromycin treatment indicated that the StopGo event might begin with the ribosomal pausing at the end of the 2A-coding sequence, with the glycine-18 codon in the P-site and the proline-19 codon in the A-site (Fig. 11) (Donnelly *et al.*, 2001, Doronina *et al.*, 2008). Ribosomal pausing and subsequent inhibition of the peptide bond formation is presumably caused by specific biochemical properties of these two residues, such as poor chemical attractiveness between their reaction centers and spatially restrained conformation of proline-19. It was also suggested that the conserved proline-17 may aid to reorient the glycyl-peptidyl-tRNA to disfavor peptide bond formation by adopting a tight-turn (Donnelly *et al.*, 2001). Further constrains to peptide bond formation may be induced by sequences upstream of the 2A motif that could, depending on their length, establish interactions inside of the ribosomal exit tunnel and thus provoke ribosomal stalling (Donnelly *et al.*, 2001).

More insights into the StopGo REI were gained by an indirect evidence suggesting that eRF1 and eRF3 contribute to this unusual termination on a sense codon (Fig. 11). In particular, depletion of eRF1 both *in vivo* and *in vitro* was accompanied by ~30-40% reduction in the efficiency of the StopGo REI resulting in an increased amount of the full length polyprotein (Doronina *et al.*, 2008). This implies that eRF1 can under specific circumstances recognize the sense codon as a stop codon and that its hydrolytic activity contributes to the breakage of the ester bond of the P-site glycyl-peptidyl-tRNA. In contrast, impairing the eRF3 GTPase activity prevented majority of ribosomes to translate beyond 2A, substantially reducing the amounts of the downstream translation product (Doronina *et al.*, 2008). This indicates that while the compromised eRF3 activity increases the efficiency of

ScholarOne Support 1-434/964-4100

the sense-codon termination, it markedly impairs the “Go” phase. Therefore it was suggested that in order to neutralize the decoding function of eRF1 for the “Stop” phase, hydrolysis of the nascent chain may be uncoupled from GTP hydrolysis on eRF3 (GTP hydrolysis on eRF3 normally senses a perfect match between the stop codon and eRF1). In other words, hydrolysis of the nascent chain does not follow GTP hydrolysis as during canonical termination but may occur independently of it. The delay in GTP hydrolysis on eRF3 may extend the occupancy of both eRFs on the ribosome, thereby increasing the time window for both ester bond hydrolysis and release of the 2A peptide from the ribosome (Doronina *et al.*, 2008, Brown & Ryan, 2010).

In the current model of the StopGo REI (Fig. 11), ribosomes translate the 2A sequence until glycine-18 has been incorporated into the nascent chain and its tRNA translocated into the P-site. This makes the ribosome to pause and enables the entry of eRFs into the A-site over the prolyl-tRNA. Subsequent hydrolysis of the ester bond, uncoupled from GTP hydrolysis on eRF3, allows the release of the 2A peptide and both eRFs from the “Stop” ribosome followed by an entry of the prolyl-tRNA to the A-site. Since there is only the deacylated tRNA left in the P/E-site, the pseudo-translocation promoted by eEF2 described above (Thompson, 2012) is probably needed to transfer prolyl-tRNA to the P-site without a peptide bond formation to begin the “Go” phase. In support, early studies with the EMCV cardiovirus revealed that low levels of eEF2 prevented translation of products corresponding to proteins downstream of 2A, which could be overcome by the addition of purified eEF2 (Svitkin & Agol, 1983). To define the full spectrum of factors promoting/inhibiting the StopGo REI and understand its molecular mechanics – for example how this mechanism prevents ribosomal recycling that normally follows termination by eRFs – more work including structural analysis of the StopGo complexes is needed. It is noteworthy that the autonomous function and high efficiency of the StopGo REI mechanism in various eukaryotic translation systems has been extensively exploited for many practical purposes; in biotechnology to achieve stoichiometric co-expression of different proteins, in a recent remake of the dual luciferase reporter system detecting stop codon readthrough to avoid artefacts that can arise from translation of fused dual reporters (Loughran *et al.*, 2017), or for generation of multiple genes expressing vectors for gene therapy and biomedical research (Luke *et al.*, 2010).

CONCLUDING REMARKS AND FUTURE PROSPECTS

Cumulative evidence documented in detail in this review clearly shows that translation reinitiation has many forms and takes place at practically any position within mRNAs. From the mechanistic point of view, the major difference is between REI promoted by 40S *versus* 80S post-termination complexes. To capture our efforts to describe all existing REI mechanisms, we present simplified models for each of them emphasizing only the features that are at least partially shared by most members of each group.

ScholarOne Support 1-434/964-4100

For 40S-mediated REI, it is essential that following translation termination only the first step of ribosome recycling occurs, i.e. the 60S dissociation catalyzed by ABCE1, to produce a post-termination 40S subunit bound to the mRNA at the stop codon of the upstream ORF. This means that the second recycling step must be prevented to preserve the 40S-mRNA post-TC. At the same time, the ultimate deacylated tRNA should be released from the P-site to allow its replacement by Met-$tRNA_i^{Met}$, either in the form of eIF2-TC or on its own presumably by DENR-MCT1 (or Ligatin), which is needed for recognition of the downstream AUG codon selected for REI (see below). There is now experimental evidence that eIF3 is the key factor capable of stabilizing interaction of the post-termination 40S subunit with mRNA, and might compensate for loss of the stabilizing codon:anticodon interaction involving the ultimate deacylated tRNA. In order to exert this function, eIF3 must be retained by the elongating ribosome during translation of ORF1, which is possible because its primary interactions with the 40S are confined to the solvent-exposed surface that remains accessible in the 80S ribosome (Fig. 2B and Supplementary Fig. 1). However, owing to stochastic dissociation of eIF3 from elongating 80S complexes, it can be retained at appreciable levels only during translation of short uORFs, which helps to explain the fact that the basic level of REI occurs without specialized mRNA-ribosome interactions only for short uORFs. Although eIF3 acts during primary initiation to stabilize PIC interactions with the mRNA, especially at the exit channel, its ability to markedly enhance REI following short-uORF translation requires specialized mRNA sequences which it functionally (and perhaps physically) interacts with in the 40S post-TC, exemplified by some of the REI-promoting sequences upstream of *GCN4* uORFs 1 and 2 (Fig. 2A).

In the case of REI following long ORFs, specialized mechanisms are required either to prevent the release of eIF3 from elongating ribosomes during the prolonged period required to translate the first long ORF, or to complement or substitute the stabilizing role of eIF3 with specialized mRNA sequences that physically tether the 40S subunit to the mRNA. TAV-stimulated REI exemplifies the first case, wherein proteins without general functions in translation (TAV and RISP) collaborate to retain eIF3 on one or both subunits of the elongating 80S ribosome during translation of the first ORF, and so does the phosphorylation of eIF3h observed in *Arabidopsis thaliana*. The TURBS-18S rRNA interaction exemplifies the second strategy. In contrast to the first strategy, however, the tethering of the 40S subunit to the TURBS element located at the 3' end of the first ORF imposes limitations on where REI can occur, restricting it to a start codon for ORF2 located fairly close to the ORF1 stop codon. In special cases, when for example physical constrains for the 40S movement are imposed by the TURBS-18S rRNA interaction, REI can occur close to the stop codon from AUGs, as well as non-canonical restart sites, lying either downstream or upstream of it.

Because 40S REI generally utilizes an AUG start codon in the downstream ORF, Met-$tRNA_i^{Met}$ must be reacquired by the post-TC 40S subunit to allow recognition of the downstream AUG start codon by standard base pairing with the anticodon of Met-$tRNA_i^{Met}$. In the case of REI following short uORFs, this generally

ScholarOne Support 1-434/964-4100

involves rebinding of the eIF2-GTP-Met-tRNA$_i^{Met}$ (eIF2-TC) as the 40S subunit traverses the intercistronic spacer between the uORF and main ORF. Upon rebinding of the eIF2-TC, traversing changes into real scanning for AUG recognition. In the case of the highly structured intercistronic spacer, traversing/scanning of the 40S might require the activity of helicases to dissolve the mRNA's secondary structures which can be achieved by the eIF4F complex. In TURBS-mediated REI, the established TURBS-40S interaction upon termination not only ensures that reinitiation occurs close to the stop codon but also allows sufficient time for the eIF2-TC reacquisition. In some instances, DENR-MCT1 (or Ligatin) might promote the reacquisition of Met-tRNA$_i^{Met}$ instead of eIF2, either coupled with or uncoupled from ejection of the ultimate deacylated tRNA from the P-site, which remains to be experimentally tested. Other important questions that need to be addressed are when eIFs 1, 1A and 5 join the 40S ribosome *en route* to the next ORF and whether DENR-MCT1 (or Ligatin) is capable to persist on reinitiating ribosomes and substitute for the activities of the latter eIFs during AUG recognition on the downstream ORF.

In contrast to 40S-mediated REI, where several *cis*- and *trans*-acting factors actively cooperate to prevent dissociation of mRNA form the 40S post-TCs, 80S-mediated REI can be viewed as a passive process stemming from either the elongation failure (in particular, an inability to form a peptide bond) or the termination/recycling failure (an inability to recycle the 80S post-TC upon termination on regular or premature stop codons). These 'failures' may under specific circumstances become advantageous and as such they are often exploited by numerous viruses. For 80S-mediated REI, the mRNA is stable anchored in the mRNA binding channel, locked by the deacylated P-site tRNA, hence there is no requirement for an active mRNA retention. Upon polypeptide release and departure of both eRFs, the post-termination 80S ribosome may begin to traverse in both directions (even though the upstream movement might be limited by the elongating 80S ribosome approaching the same stop codon from the mRNA's 5' end) and eventually reinitiate at start sites, the nature of which is probably determined by the identity of the A- and/or P-site tRNAs, as well as the conformational states of the post-termination 80S ribosomes. Considering the fact that a substantial number of these unorthodox REI events is most probably prevented to occur by cellular surveillance factors such as Dom34/PELO, the fundamental question that remains to be answered is to what extent are the 80S-mediated REI events physiologically relevant as opposed to being a byproduct of translational malfunctioning.

Despite the tremendous progress that has recently been made in identification of factors promoting REI both in *cis* and *trans* in various organisms, the molecular details of their particular functions are only partly understood. Besides the classical 'wet-lab' approaches such as genetics, *in vitro* reconstituted systems, etc., structural studies revealing 'snap-shots' of complexes involved in individual REI mechanisms should substantially increase our understanding of how they rewire the translational cycle. Although there are many features that are shared among different REI mechanisms, the observed peculiarities may allow us to develop specific strategies for controlled altering their efficiencies, which could – in the long run – help to cope

ScholarOne Support 1-434/964-4100

with deregulation of the REI-mediated translational control and uORF polymorphism implicated in a variety of human diseases (Calvo *et al.*, 2009, Barbosa *et al.*, 2013, Janich *et al.*, 2015).

Funding

This particular work was supported by the Czech Science Foundation Grant GA15-10116S (to LSV), and by Intramural Research Program of the National Institutes of Health (to AGH).

Acknowledgements

We would like to thank all past and present members of the both laboratories for their excellent experimental, as well as intellectual contributions to this work, and to all our colleagues from the fields of translational control and RNA biology for many supportive and inspirational discussions and thoughts. We also wish to apologize to those whose work was not cited due to the focus of this review or unintentional omissions.

References

Abastado JP, Miller PF, Jackson BM & Hinnebusch AG (1991) Suppression of ribosomal reinitiation at upstream open reading frames in amino acid-starved cells forms the basis for *GCN4* translational control. *Mol Cell Biol* **11**: 486-496.

Adhin MR & van Duin J (1990) Scanning model for translational reinitiation in eubacteria. *J Mol Biol* **213**: 811-818.

Ahmadian G, Randhawa JS & Easton AJ (2000) Expression of the ORF-2 protein of the human respiratory syncytial virus M2 gene is initiated by a ribosomal termination-dependent reinitiation mechanism. *EMBO J* **19**: 2681-2689.

Aitken CE, Beznoskova P, Vlckova V, Chiu WL, Zhou F, Valasek LS, Hinnebusch AG & Lorsch JR (2016) Eukaryotic translation initiation factor 3 plays distinct roles at the mRNA entry and exit channels of the ribosomal preinitiation complex. *Elife* **5**.

Algire MA, Maag D & Lorsch JR (2005) Pi release from eIF2, not GTP hydrolysis, is the step controlled by start-site selection during eukaryotic translation initiation. *Mol Cell* **20**: 251-262.

Alisch RS, Garcia-Perez JL, Muotri AR, Gage FH & Moran JV (2006) Unconventional translation of mammalian LINE-1 retrotransposons. *Genes Dev* **20**: 210-224.

Altmann M, Wittmer B, Methot N, Sonenberg N & Trachsel H (1995) The *Saccharomyces cerevisiae* translation initiation factor Tif3 and its mammalian homologue, eIF-4B, have RNA annealing activity. *EMBO Journal* **14**: 3820-3827.

Amrani N, Ganesan R, Kervestin S, Mangus DA, Ghosh S & Jacobson A (2004) A faux 3'-UTR promotes aberrant termination and triggers nonsense-mediated mRNA decay. *Nature* **432**: 112-118.

Andreev DE, O'Connor PB, Fahey C, Kenny EM, Terenin IM, Dmitriev SE, Cormican P, Morris DW, Shatsky IN & Baranov PV (2015) Translation of 5' leaders is pervasive in genes resistant to eIF2 repression. *Elife* **4**: e03971.

Atkins JF, Wills NM, Loughran G, Wu CY, Parsawar K, Ryan MD, Wang CH & Nelson CC (2007) A case for "StopGo": reprogramming translation to augment codon meaning of GGN by promoting unconventional termination (Stop) after addition of glycine and then allowing continued translation (Go). *RNA* **13**: 803-810.

ScholarOne Support 1-434/964-4100

Aylett CH, Boehringer D, Erzberger JP, Schaefer T & Ban N (2015) Structure of a yeast 40S-eIF1-eIF1A-eIF3-eIF3j initiation complex. *Nat Struct Mol Biol* **22**: 269-271.

Baird TD & Wek RC (2012) Eukaryotic Initiation Factor 2 Phosphorylation and Translational Control in Metabolism. *Advances in Nutrition: An International Review Journal* **3**: 307-321.

Barbosa C, Peixeiro I & Romao L (2013) Gene expression regulation by upstream open reading frames and human disease. *PLoS Genet* **9**: e1003529.

Beznoskova P, Gunisova S & Valasek LS (2016) Rules of UGA-N decoding by near-cognate tRNAs and analysis of readthrough on short uORFs in yeast. *RNA* **22**: 456-466.

Beznosková P, Cuchalová L, Wagner S, Shoemaker CJ, Gunišová S, Von der Haar T & Valášek LS (2013) Translation initiation factors eIF3 and HCR1 control translation termination and stop codon read-through in yeast cells. *PLoS Genet* **9**: e1003962.

Bonneville JM, Sanfacon H, Futterer J & Hohn T (1989) Posttranscriptional trans-activation in cauliflower mosaic virus. *Cell* **59**: 1135-1143.

Brown JD & Ryan MD (2010) Ribosome “Skipping”: “Stop-Carry On” or “StopGo” Translation. *Recoding: Expansion of Decoding Rules Enriches Gene Expression,*(Atkins JF & Gesteland RF, eds.), p.^pp. 101-121. Springer New York, New York, NY.

Buskirk AR & Green R (2017) Ribosome pausing, arrest and rescue in bacteria and eukaryotes. *Philos Trans R Soc Lond B Biol Sci* **372**.

Calkhoven CR, Muller C & Leutz A (2000) Translational control of C/EBPa and C/EBPb isoform expression. *Genes Dev* **14**: 1920-1932.

Calvo SE, Pagliarini DJ & Mootha VK (2009) Upstream open reading frames cause widespread reduction of protein expression and are polymorphic among humans. *PNAS* **106**: 7507-7512.

Cuchalová L, Kouba T, Herrmannová A, Danyi I, Chiu W-l & Valášek L (2010) The RNA Recognition Motif of Eukaryotic Translation Initiation Factor 3g (eIF3g) Is Required for Resumption of Scanning of Posttermination Ribosomes for Reinitiation on GCN4 and Together with eIF3i Stimulates Linear Scanning. *Mol Cell Biol* **30**: 4671-4686.

des Georges A, Dhote V, Kuhn L, Hellen CU, Pestova TV, Frank J & Hashem Y (2015) Structure of mammalian eIF3 in the context of the 43S preinitiation complex. *Nature* **525**: 491-495.

Dever TE, Kinzy TG & Pavitt GD (2016) Mechanism and Regulation of Protein Synthesis in Saccharomyces cerevisiae. *Genetics* **203**: 65-107.

Dey S, Baird TD, Zhou D, Palam LR, Spandau DF & Wek RC (2010) Both transcriptional regulation and translational control of ATF4 are central to the integrated stress response. *J Biol Chem* **285**: 33165-33174.

Donnelly ML, Gani D, Flint M, Monaghan S & Ryan MD (1997) The cleavage activities of aphthovirus and cardiovirus 2A proteins. *J Gen Virol* **78 (Pt 1)**: 13-21.

Donnelly ML, Hughes LE, Luke G, Mendoza H, ten Dam E, Gani D & Ryan MD (2001) The 'cleavage' activities of foot-and-mouth disease virus 2A site-directed mutants and naturally occurring '2A-like' sequences. *J Gen Virol* **82**: 1027-1041.

Donnelly ML, Luke G, Mehrotra A, Li X, Hughes LE, Gani D & Ryan MD (2001) Analysis of the aphthovirus 2A/2B polyprotein 'cleavage' mechanism indicates not a proteolytic reaction, but a novel translational effect: a putative ribosomal 'skip'. *J Gen Virol* **82**: 1013-1025.

ScholarOne Support 1-434/964-4100

Doronina VA, Wu C, de Felipe P, Sachs MS, Ryan MD & Brown JD (2008) Site-specific release of nascent chains from ribosomes at a sense codon. *Mol Cell Biol* **28**: 4227-4239.

Fijalkowska D, Verbruggen S, Ndah E, Jonckheere V, Menschaert G & Van Damme P (2017) eIF1 modulates the recognition of suboptimal translation initiation sites and steers gene expression via uORFs. *Nucleic Acids Res* **45**: 7997-8013.

Futterer J & Hohn T (1991) Translation of a polycistronic mRNA in the presence of the cauliflower mosaic virus transactivator protein. *EMBO J* **10**: 3887-3896.

Futterer J & Hohn T (1992) Role of an upstream open reading frame in the translation of polycistronic mRNAs in plant cells. *Nucleic Acids Res* **20**: 3851-3857.

Gaba A, Wang Z, Krishnamoorthy T, Hinnebusch AG & Sachs MS (2001) Physical evidence for distinct mechanisms of translational control by upstream open reading frames. *EMBO J* **20**: 6453-6463.

Gardner LB (2008) Hypoxic inhibition of nonsense-mediated RNA decay regulates gene expression and the integrated stress response. *Mol Cell Biol* **28**: 3729-3741.

Gould PS & Easton AJ (2005) Coupled translation of the respiratory syncytial virus M2 open reading frames requires upstream sequences. *J Biol Chem* **280**: 21972-21980.

Gould PS & Easton AJ (2007) Coupled translation of the second open reading frame of M2 mRNA is sequence dependent and differs significantly within the subfamily Pneumovirinae. *J Virol* **81**: 8488-8496.

Gould PS, Dyer NP, Croft W, Ott S & Easton AJ (2014) Cellular mRNAs access second ORFs using a novel amino acid sequence-dependent coupled translation termination-reinitiation mechanism. *RNA* **20**: 373-381.

Grant CM & Hinnebusch AG (1994) Effect of sequence context at stop codons on efficiency of reinitiation in *GCN4* translational control. *Mol Cell Biol* **14**: 606-618.

Grant CM, Miller PF & Hinnebusch AG (1995) Sequences 5' of the first upstream open reading frame in *GCN4* mRNA are required for efficient translational reinitiation. *Nuc Acids Res* **23**: 3980-3988.

Griffin E, Re A, Hamel N, Fu C, Bush H, McCaffrey T & Asch AS (2001) A link between diabetes and atherosclerosis: Glucose regulates expression of CD36 at the level of translation. *Nat Med* **7**: 840-846.

Gunisova S & Valasek LS (2014) Fail-safe mechanism of GCN4 translational control-uORF2 promotes reinitiation by analogous mechanism to uORF1 and thus secures its key role in GCN4 expression. *Nucleic Acids Res* **42**: 5880-5893.

Gunisova S, Beznoskova P, Mohammad MP, Vlckova V & Valasek LS (2016) In-depth analysis of cis-determinants that either promote or inhibit reinitiation on GCN4 mRNA after translation of its four short uORFs. *RNA* **22**: 542-558.

Guo LH, Sun L, Chiba S, Araki H & Suzuki N (2009) Coupled termination/reinitiation for translation of the downstream open reading frame B of the prototypic hypovirus CHV1-EP713. *Nucleic Acids Res* **37**: 3645-3659.

Guydosh NR & Green R (2014) Dom34 rescues ribosomes in 3' untranslated regions. *Cell* **156**: 950-962.

Hashem Y, des Georges A, Dhote V, Langlois R, Liao HY, Grassucci RA, Hellen CU, Pestova TV & Frank J (2013) Structure of the Mammalian Ribosomal 43S Preinitiation Complex Bound to the Scanning Factor DHX29. *Cell* **153**: 1108-1119.

Hatta M, Kohlmeier CK, Hatta Y, Ozawa M & Kawaoka Y (2009) Region required for protein expression from the stop-start pentanucleotide in the M gene of influenza B virus. *J Virol* **83**: 5939-5942.

ScholarOne Support 1-434/964-4100

He F & Jacobson A (2015) Nonsense-Mediated mRNA Decay: Degradation of Defective Transcripts Is Only Part of the Story. *Annu Rev Genet* **49**: 339-366.

Heras SR, Thomas MC, Garcia-Canadas M, de Felipe P, Garcia-Perez JL, Ryan MD & Lopez MC (2006) L1Tc non-LTR retrotransposons from Trypanosoma cruzi contain a functional viral-like self-cleaving 2A sequence in frame with the active proteins they encode. *Cell Mol Life Sci* **63**: 1449-1460.

Hinnebusch AG (2005) Translational regulation of GCN4 and the general amino acid control of yeast. *Annu Rev Microbiol* **59**: 407-450.

Hinnebusch AG (2014) The scanning mechanism of eukaryotic translation initiation. *Annu Rev Biochem* **83**: 779-812.

Hinnebusch AG (2017) Structural Insights into the Mechanism of Scanning and Start Codon Recognition in Eukaryotic Translation Initiation. *Trends Biochem Sci*.

Hinnebusch AG, Ivanov IP & Sonenberg N (2016) Translational control by 5'-untranslated regions of eukaryotic mRNAs. *Science* **352**: 1413-1416.

Holz MK, Ballif BA, Gygi SP & Blenis J (2005) mTOR and S6K1 Mediate Assembly of the Translation Preinitiation Complex through Dynamic Protein Interchange and Ordered Phosphorylation Events. *Cell* **123**: 569-580.

Horvath CM, Williams MA & Lamb RA (1990) Eukaryotic coupled translation of tandem cistrons: identification of the influenza B virus BM2 polypeptide. *EMBO J* **9**: 2639-2647.

Hronova V, Mohammad MP, Wagner S, Panek J, Gunisova S, Zeman J, Poncova K & Valasek LS (2017) Does eIF3 promote reinitiation after translation of short upstream ORFs also in mammalian cells? *RNA biol* doi: 10.1080/15476286.15472017.11353863.

Chew GL, Pauli A & Schier AF (2016) Conservation of uORF repressiveness and sequence features in mouse, human and zebrafish. *Nat Commun* **7**: 11663.

Ingolia NT, Lareau LF & Weissman JS (2011) Ribosome profiling of mouse embryonic stem cells reveals the complexity and dynamics of mammalian proteomes. *Cell* **147**: 789-802.

Ingolia NT, Ghaemmaghami S, Newman JRS & Weissman JS (2009) Genome-Wide Analysis in Vivo of Translation with Nucleotide Resolution Using Ribosome Profiling. *Science* **324**: 218-223.

Ivanov IP, Wei J, Caster SZ*, et al.* (2017) Translation Initiation from Conserved Non-AUG Codons Provides Additional Layers of Regulation and Coding Capacity. *MBio* **8**.

Janich P, Arpat AB, Castelo-Szekely V, Lopes M & Gatfield D (2015) Ribosome profiling reveals the rhythmic liver translatome and circadian clock regulation by upstream open reading frames. *Genome Res* **25**: 1848-1859.

Jennings MD & Pavitt GD (2014) A new function and complexity for protein translation initiation factor eIF2B. *Cell Cycle* **13**: 2660-2665.

Jennings MD, Kershaw CJ, Adomavicius T & Pavitt GD (2017) Fail-safe control of translation initiation by dissociation of eIF2alpha phosphorylated ternary complexes. *Elife* **6**.

Ji Z, Song R, Regev A & Struhl K (2015) Many lncRNAs, 5'UTRs, and pseudogenes are translated and some are likely to express functional proteins. *Elife* **4**: e08890.

Jivotovskaya A, Valášek L, Hinnebusch AG & Nielsen KH (2006) Eukaryotic translation initiation factor 3 (eIF3) and eIF2 can promote mRNA binding to 40S subunits independently of eIF4G in yeast. *Mol Cell Biol* **26**: 1355-1372.

Khoshnevis S, Gunišová S, Vlčková V, Kouba T, Neumann P, Beznosková P, Ficner R & Valášek LS (2014) Structural integrity of the PCI domain of eIF3a/TIF32 is

ScholarOne Support 1-434/964-4100

required for mRNA recruitment to the 43S pre-initiation complexes. *Nucleic Acids Research* **42**: 4123-4139.
Kim BH, Cai X, Vaughn JN & von Arnim AG (2007) On the functions of the h subunit of eukaryotic initiation factor 3 in late stages of translation initiation. *Genome Biol* **8**: R60.
Kim TH, Kim BH, Yahalom A, Chamovitz DA & von Arnim AG (2004) Translational regulation via 5' mRNA leader sequences revealed by mutational analysis of the Arabidopsis translation initiation factor subunit eIF3h. *Plant Cell* **16**: 3341-3356.
Koditz J, Nesper J, Wottawa M, Stiehl DP, Camenisch G, Franke C, Myllyharju J, Wenger RH & Katschinski DM (2007) Oxygen-dependent ATF-4 stability is mediated by the PHD3 oxygen sensor. *Blood* **110**: 3610-3617.
Kojima KK, Matsumoto T & Fujiwara H (2005) Eukaryotic translational coupling in UAAUG stop-start codons for the bicistronic RNA translation of the non-long terminal repeat retrotransposon SART1. *Mol Cell Biol* **25**: 7675-7686.
Kolupaeva VG, Unbehaun A, Lomakin IB, Hellen CU & Pestova TV (2005) Binding of eukaryotic initiation factor 3 to ribosomal 40S subunits and its role in ribosomal dissociation and anti-association. *RNA* **11**: 470-486.
Kouba T, Danyi I, Gunišová S, Munzarová V, Vlčková V, Cuchalová L, Neueder A, Milkereit P & Valášek LS (2012) Small Ribosomal Protein RPS0 Stimulates Translation Initiation by Mediating 40S-binding of eIF3 via its Direct Contact with the eIF3a/TIF32 Subunit. *PLoS One* **7**: e40464.
Kozak M (1987) Effects of intercistronic length on the efficiency of reinitiation by eucaryotic ribosomes. *Mol Cell Biol* **7**: 3438-3445.
Kozak M (1991) Structural features in eukaryotic mRNAs that modulate the initiation of translation. *J Biol Chem* **266**: 19867-19870.
Kozak M (2001) Constraints on reinitiation of translation in mammals. *Nucleic Acids Res* **29**: 5226-5232.
Lawless C, Pearson RD, Selley JN, Smirnova JB, Grant CM, Ashe MP, Pavitt GD & Hubbard SJ (2009) Upstream sequence elements direct post-transcriptional regulation of gene expression under stress conditions in yeast. *BMC Genomics* **10**: 7.
Li H, Havens WM, Nibert ML & Ghabrial SA (2011) RNA sequence determinants of a coupled termination-reinitiation strategy for downstream open reading frame translation in Helminthosporium victoriae virus 190S and other victoriviruses (Family Totiviridae). *J Virol* **85**: 7343-7352.
Llacer JL, Hussain T, Marler L, Aitken CE, Thakur A, Lorsch JR, Hinnebusch AG & Ramakrishnan V (2015) Conformational Differences between Open and Closed States of the Eukaryotic Translation Initiation Complex. *Mol Cell* **59**: 399-412.
Lomakin IB, Stolboushkina EA, Vaidya AT, Zhao C, Garber MB, Dmitriev SE & Steitz TA (2017) Crystal Structure of the Human Ribosome in Complex with DENR-MCT-1. *Cell Rep* **20**: 521-528.
Loughran G, Howard MT, Firth AE & Atkins JF (2017) Avoidance of reporter assay distortions from fused dual reporters. *RNA* **23**: 1285-1289.
Lu PD, Harding HP & Ron D (2004) Translation reinitiation at alternative open reading frames regulates gene expression in an integrated stress response. *J Cell Biol* **167**: 27-33.
Luke G, Escuin H, De Felipe P & Ryan M (2010) 2A to the fore - research, technology and applications. *Biotechnol Genet Eng Rev* **26**: 223-260.
Luke GA, de Felipe P, Lukashev A, Kallioinen SE, Bruno EA & Ryan MD (2008) Occurrence, function and evolutionary origins of '2A-like' sequences in virus genomes. *J Gen Virol* **89**: 1036-1042.

ScholarOne Support 1-434/964-4100

Luo Z, Freitag M & Sachs MS (1995) Translational regulation in response to changes in amino acid availability in *Neurospora crassa*. *Mol Cell Biol* **15**: 5235-5245.

Luttermann C & Meyers G (2007) A bipartite sequence motif induces translation reinitiation in feline calicivirus RNA. *J Biol Chem* **282**: 7056-7065.

Luttermann C & Meyers G (2009) The importance of inter- and intramolecular base pairing for translation reinitiation on a eukaryotic bicistronic mRNA. *Genes Dev* **23**: 331-344.

Luttermann C & Meyers G (2014) Two alternative ways of start site selection in human norovirus reinitiation of translation. *J Biol Chem* **289**: 11739-11754.

McCormick CJ, Salim O, Lambden PR & Clarke IN (2008) Translation termination reinitiation between open reading frame 1 (ORF1) and ORF2 enables capsid expression in a bovine norovirus without the need for production of viral subgenomic RNA. *J Virol* **82**: 8917-8921.

Meyers G (2003) Translation of the minor capsid protein of a calicivirus is initiated by a novel termination-dependent reinitiation mechanism. *J Biol Chem* **278**: 34051-34060.

Meyers G (2007) Characterization of the sequence element directing translation reinitiation in RNA of the calicivirus rabbit hemorrhagic disease virus. *J Virol* **81**: 9623-9632.

Miettinen TP & Bjorklund M (2015) Modified ribosome profiling reveals high abundance of ribosome protected mRNA fragments derived from 3' untranslated regions. *Nucleic Acids Res* **43**: 1019-1034.

Miller PF & Hinnebusch AG (1989) Sequences that surround the stop codons of upstream open reading frames in *GCN4* mRNA determine their distinct functions in translational control. *Genes and Development* **3**: 1217-1225.

Mills EW, Wangen J, Green R & Ingolia NT (2016) Dynamic Regulation of a Ribosome Rescue Pathway in Erythroid Cells and Platelets. *Cell Rep* **17**: 1-10.

Mohammad MP, Munzarova Pondelickova V, Zeman J, Gunisova S & Valasek LS (2017) In vivo evidence that eIF3 stays bound to ribosomes elongating and terminating on short upstream ORFs to promote reinitiation. *Nucleic Acids Res* **45**: 2658-2674.

Mueller PP & Hinnebusch AG (1986) Multiple upstream AUG codons mediate translational control of *GCN4*. *Cell* **45**: 201-207.

Mueller PP, Jackson BM, Miller PF & Hinnebusch AG (1988) The first and fourth upstream open reading frames in }I}GCN4}i} mRNA have similar initiation efficiencies but respond differently in translational control to changes in length and sequence. *Mol Cell Biol* **8**: 5439-5447.

Munzarová V, Pánek J, Gunišová S, Dányi I, Szamecz B & Valášek LS (2011) Translation Reinitiation Relies on the Interaction between eIF3a/TIF32 and Progressively Folded cis-Acting mRNA Elements Preceding Short uORFs. *PLoS Genet* **7**: e1002137.

Myasnikov AG, Simonetti A, Marzi S & Klaholz BP (2009) Structure-function insights into prokaryotic and eukaryotic translation initiation. *Curr Opin Struct Biol* **19**: 300-309.

Napthine S, Lever RA, Powell ML, Jackson RJ, Brown TD & Brierley I (2009) Expression of the VP2 protein of murine norovirus by a translation termination-reinitiation strategy. *PLoS One* **4**: e8390.

Nishimura T, Wada T, Yamamoto KT & Okada K (2005) The Arabidopsis STV1 Protein, Responsible for Translation Reinitiation, Is Required for Auxin-Mediated Gynoecium Patterning. *THE PLANT CELL* **17**: 2940-2953.

For Peer Review

Pakos-Zebrucka K, Koryga I, Mnich K, Ljujic M, Samali A & Gorman AM (2016) The integrated stress response. *EMBO Rep* **17**: 1374-1395.

Park HS, Browning KS, Hohn T & Ryabova LA (2004) Eucaryotic initiation factor 4B controls eIF3-mediated ribosomal entry of viral reinitiation factor. *EMBO J* **23**: 1381-1391.

Park HS, Himmelbach A, Browning KS, Hohn T & Ryabova LA (2001) A plant viral "reinitiation" factor interacts with the host translational machinery. *Cell* **106**: 723-733.

Pavlov MY, Watts RE, Tan Z, Cornish VW, Ehrenberg M & Forster AC (2009) Slow peptide bond formation by proline and other N-alkylamino acids in translation. *Proc Natl Acad Sci U S A* **106**: 50-54.

Pisarev AV, Hellen CUT & Pestova TV (2007) Recycling of Eukaryotic Posttermination Ribosomal Complexes. *Cell* **131**: 286–299.

Pisarev AV, Skabkin MA, Pisareva VP, Skabkina OV, Rakotondrafara AM, Hentze MW, Hellen CUT & Pestova TV (2010) The Role of ABCE1 in Eukaryotic Posttermination Ribosomal Recycling. *Mol Cell* **37**: 196-210.

Powell ML (2010) Translational termination-reinitiation in RNA viruses. *Biochem Soc Trans* **38**: 1558-1564.

Powell ML, Napthine S, Jackson RJ, Brierley I & Brown TD (2008) Characterization of the termination-reinitiation strategy employed in the expression of influenza B virus BM2 protein. *RNA* **14**: 2394-2406.

Powell ML, Leigh KE, Poyry TA, Jackson RJ, Brown TD & Brierley I (2011) Further characterisation of the translational termination-reinitiation signal of the influenza B virus segment 7 RNA. *PLoS One* **6**: e16822.

Pöyry TA, Kaminski A & Jackson RJ (2004) What determines whether mammalian ribosomes resume scanning after translation of a short upstream open reading frame? *Genes Dev* **18**: 62-75.

Pöyry TA, Kaminski A, Connell EJ, Fraser CS & Jackson RJ (2007) The mechanism of an exceptional case of reinitiation after translation of a long ORF reveals why such events do not generally occur in mammalian mRNA translation. *Genes Dev* **21**: 3149-3162.

Putlyaeva LV, Schwartz AM, Korneev KV, Covic M, Uroshlev LA, Makeev VY, Dmitriev SE & Kuprash DV (2014) Upstream open reading frames regulate translation of the long isoform of SLAMF1 mRNA that encodes costimulatory receptor CD150. *Biochemistry (Mosc)* **79**: 1405-1411.

Rahim G, Araud T, Jaquier-Gubler P & Curran J (2012) Alternative splicing within the elk-1 5' untranslated region serves to modulate initiation events downstream of the highly conserved upstream open reading frame 2. *Mol Cell Biol* **32**: 1745-1756.

Roy B, Vaughn JN, Kim B-H, Zhou F, Gilchrist MA & Von Arnim AG (2010) The h subunit of eIF3 promotes reinitiation competence during translation of mRNAs harboring upstream open reading frames. *RNA* **16**: 748-761.

Ryan MD & Drew J (1994) Foot-and-mouth disease virus 2A oligopeptide mediated cleavage of an artificial polyprotein. *EMBO J* **13**: 928-933.

Sattlegger E, Hinnebusch AG & Barthelmess IB (1998) *cpc-3*, the *Neurospora crassa* homologue of yeast *GCN2,* encodes a polypeptide with juxtaposed eIF2a kinase and histidyl-tRNA synthetase-related domains required for general amino acid control. *Journal of Biological Chemistry* **273**: 20404-20416.

Sen ND, Zhou F, Ingolia NT & Hinnebusch AG (2015) Genome-wide analysis of translational efficiency reveals distinct but overlapping functions of yeast DEAD-box RNA helicases Ded1 and eIF4A. *Genome Res* **25**: 1196-1205.

For Peer Review

ScholarOne Support 1-434/964-4100

Shoemaker CJ & Green R (2011) Kinetic analysis reveals the ordered coupling of translation termination and ribosome recycling in yeast. *Proc Natl Acad Sci U S A* **108**: E1392-1398.

Schepetilnikov M, Dimitrova M, Mancera-Martinez E, Geldreich A, Keller M & Ryabova LA (2013) TOR and S6K1 promote translation reinitiation of uORF-containing mRNAs via phosphorylation of eIF3h. *EMBO J* **32**: 1087-1102.

Schepetilnikov M, Kobayashi K, Geldreich A, Caranta C, Robaglia C, Keller M & Ryabova LA (2011) Viral factor TAV recruits TOR/S6K1 signalling to activate reinitiation after long ORF translation. *EMBO J* **30**: 1343-1356.

Schleich S, Acevedo JM, Clemm von Hohenberg K & Teleman AA (2017) Identification of transcripts with short stuORFs as targets for DENR*MCTS1-dependent translation in human cells. *Sci Rep* **7**: 3722.

Schleich S, Strassburger K, Janiesch PC*, et al.* (2014) DENR-MCT-1 promotes translation re-initiation downstream of uORFs to control tissue growth. *Nature* **512**: 208-212.

Sidrauski C, McGeachy AM, Ingolia NT & Walter P (2015) The small molecule ISRIB reverses the effects of eIF2alpha phosphorylation on translation and stress granule assembly. *Elife* **4**.

Skabkin MA, Skabkina OV, Hellen CU & Pestova TV (2013) Reinitiation and other unconventional posttermination events during eukaryotic translation. *Mol Cell* **51**: 249-264.

Skabkin MA, Skabkina OV, Dhote V, Komar AA, Hellen CU & Pestova TV (2010) Activities of Ligatin and MCT-1/DENR in eukaryotic translation initiation and ribosomal recycling. *Genes Dev* **24**: 1787-1801.

Starck SR, Tsai JC, Chen K, Shodiya M, Wang L, Yahiro K, Martins-Green M, Shastri N & Walter P (2016) Translation from the 5' untranslated region shapes the integrated stress response. *Science* **351**: aad3867.

Svitkin YV & Agol VI (1983) Translational barrier in central region of encephalomyocarditis virus genome. Modulation by elongation factor 2 (eEF-2). *Eur J Biochem* **133**: 145-154.

Szabo G, Katarova Z & Greenspan R (1994) Distinct protein forms are produced from alternatively spliced bicistronic glutamic acid decarboxylase mRNAs during development. *Mol Cell Biol* **14**: 7535-7545.

Szamecz B, Rutkai E, Cuchalova L, Munzarova V, Herrmannova A, Nielsen KH, Burela L, Hinnebusch AG & Valášek L (2008) eIF3a cooperates with sequences 5' of uORF1 to promote resumption of scanning by post-termination ribosomes for reinitiation on GCN4 mRNA. *Genes Dev* **22**: 2414-2425.

Thiebeauld O, Schepetilnikov M, Park HS, Geldreich A, Kobayashi K, Keller M, Hohn T & Ryabova LA (2009) A new plant protein interacts with eIF3 and 60S to enhance virus-activated translation re-initiation. *EMBO J* **28**: 3171-3184.

Thompson SR (2012) Tricks an IRES uses to enslave ribosomes. *Trends Microbiol* **20**: 558-566.

Valasek LS, Zeman J, Wagner S, Beznoskova P, Pavlikova Z, Mohammad MP, Hronova V, Herrmannova A, Hashem Y & Gunisova S (2017) Embraced by eIF3: structural and functional insights into the roles of eIF3 across the translation cycle. *Nucleic Acids Res* doi: 10.1093/nar/gkx1805.

Valášek L, Mathew A, Shin BS, Nielsen KH, Szamecz B & Hinnebusch AG (2003) The Yeast eIF3 Subunits TIF32/a and NIP1/c and eIF5 Make Critical Connections with the 40S Ribosome in vivo. *Genes Dev* **17**: 786-799.

For Peer Review

ScholarOne Support 1-434/964-4100

Valášek LS (2012) 'Ribozoomin' – Translation Initiation from the Perspective of the Ribosome-bound Eukaryotic Initiation Factors (eIFs). *Curr Protein Pept Sci* **13**: 305-330.

Vattem KM & Wek RC (2004) Reinitiation involving upstream ORFs regulates ATF4 mRNA translation in mammalian cells. *Proc Natl Acad Sci U S A* **101**: 11269-11274.

von Arnim AG, Jia Q & Vaughn JN (2014) Regulation of plant translation by upstream open reading frames. *Plant Sci* **214**: 1-12.

Weisser M, Schafer T, Leibundgut M, Bohringer D, Aylett CHS & Ban N (2017) Structural and Functional Insights into Human Re-initiation Complexes. *Mol Cell* **67**: 447-456 e447.

Wethmar K (2014) The regulatory potential of upstream open reading frames in eukaryotic gene expression. *Wiley Interdiscip Rev RNA* **5**: 765-778.

Wohlgemuth WA, Safonova O, Engelhardt M, Freitag M, Wolfle K & Kirchhof K (2008) Improvement of the quality of life concerning the health of patients with peripheral arterial disease (PAD) after successful bypass surgery. *Vasa* **37**: 338-344.

Yamamoto H, Wittek D, Gupta R, Qin B, Ueda T, Krause R, Yamamoto K, Albrecht R, Pech M & Nierhaus KH (2016) 70S-scanning initiation is a novel and frequent initiation mode of ribosomal translation in bacteria. *Proc Natl Acad Sci U S A* **113**: E1180-1189.

Young DJ, Guydosh NR, Zhang F, Hinnebusch AG & Green R (2015) Rli1/ABCE1 Recycles Terminating Ribosomes and Controls Translation Reinitiation in 3'UTRs In Vivo. *Cell* **162**: 872-884.

Zhou F, Roy B & von Arnim AG (2010) Translation reinitiation and development are compromised in similar ways by mutations in translation initiation factor eIF3h and the ribosomal protein RPL24. *BMC Plant Biol* **10**: 193.

Zhou F, Roy B, Dunlap JR, Enganti R & von Arnim AG (2014) Translational control of Arabidopsis meristem stability and organogenesis by the eukaryotic translation factor eIF3h. *PLoS One* **9**: e95396.

Zinoviev A, Hellen CU & Pestova TV (2015) Multiple mechanisms of reinitiation on bicistronic calicivirus mRNAs. *Mol Cell* **57**: 1059-1073.

For Peer Review

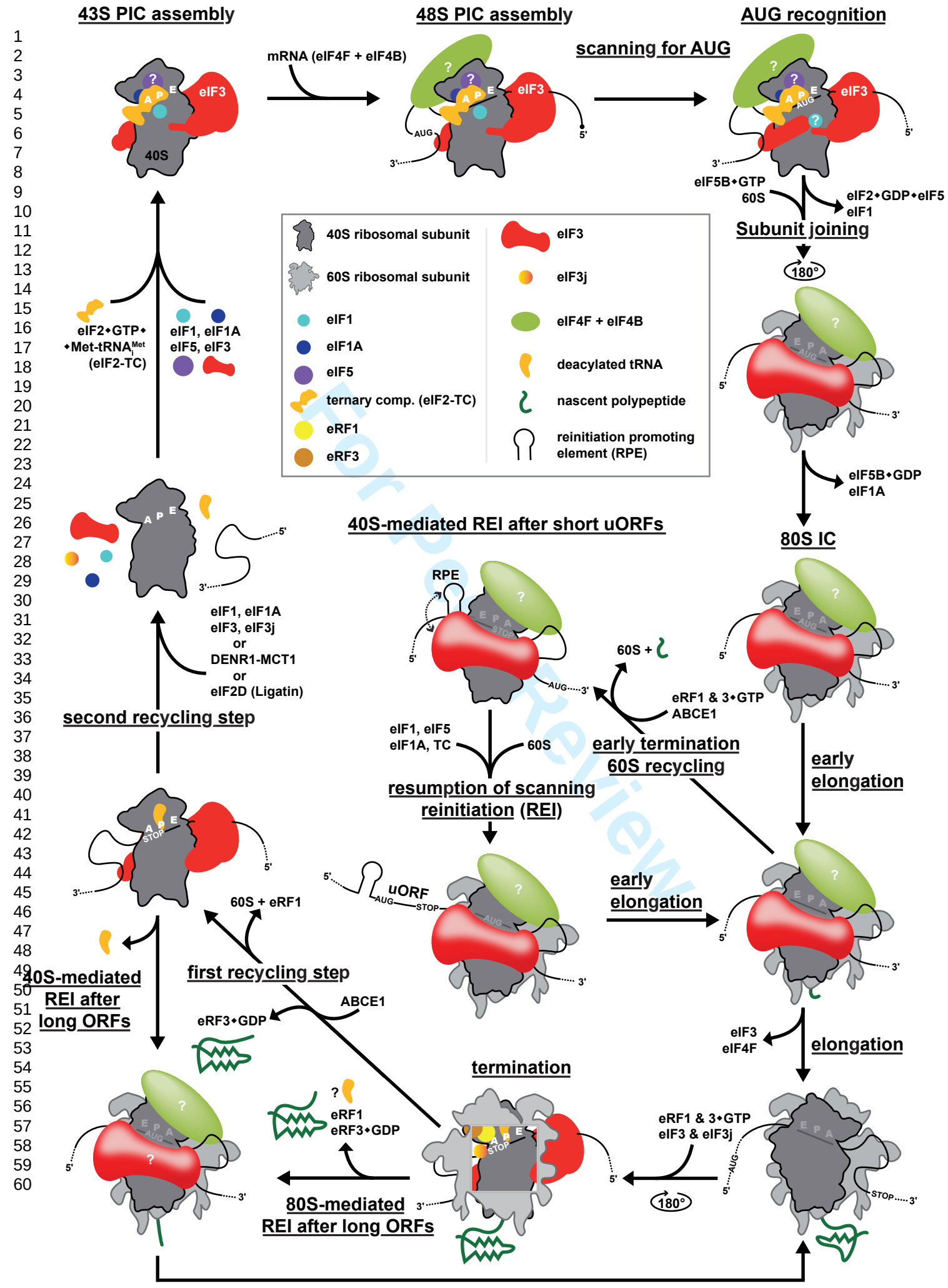

For Peer Review

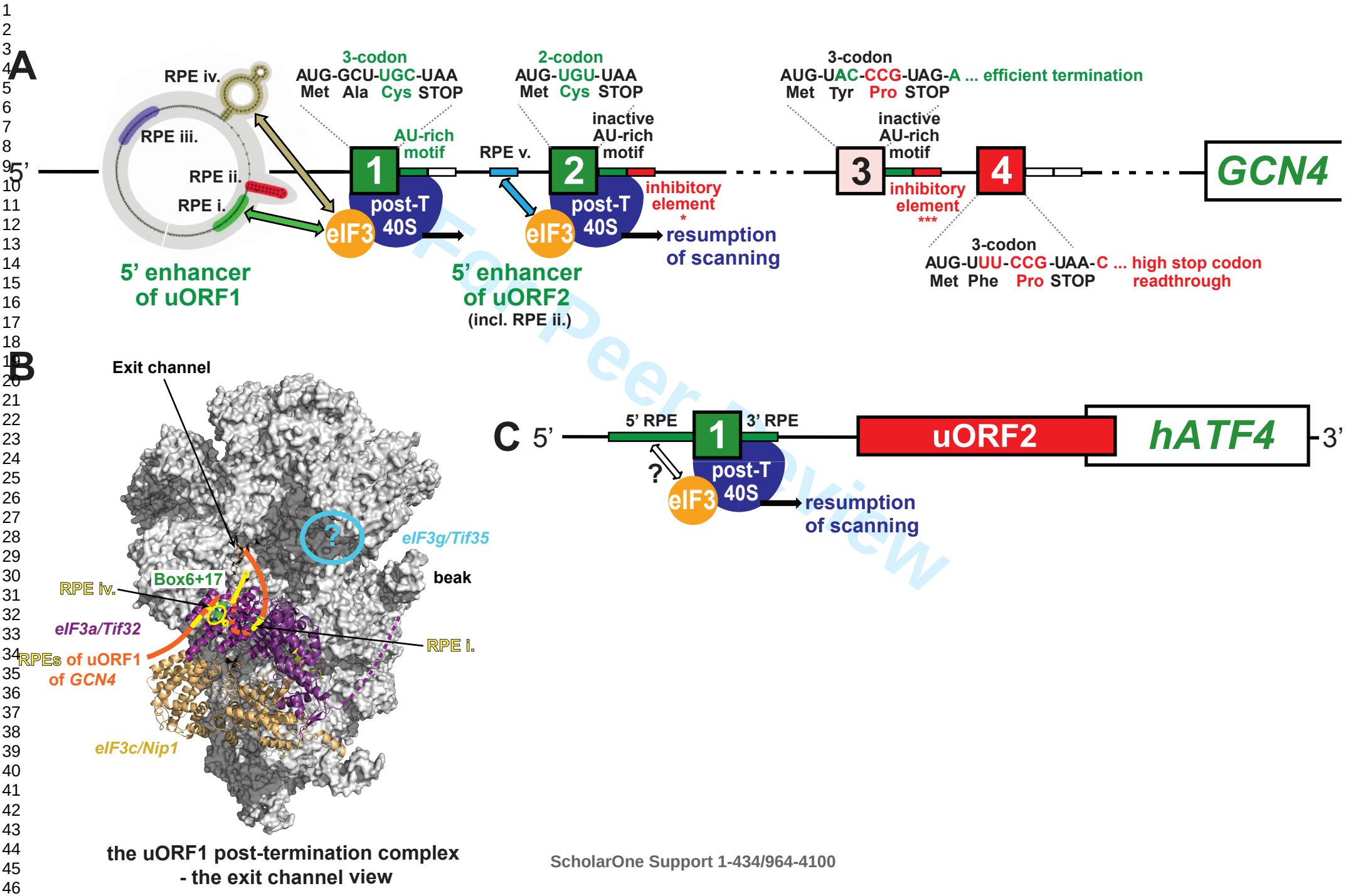

For Peer Review

FAIL-SAFE mechanism of *GCN4* translation control via REINITIATION

NON-STARVATION: *GCN4* translation is REPRESSED
(high levels of TC)

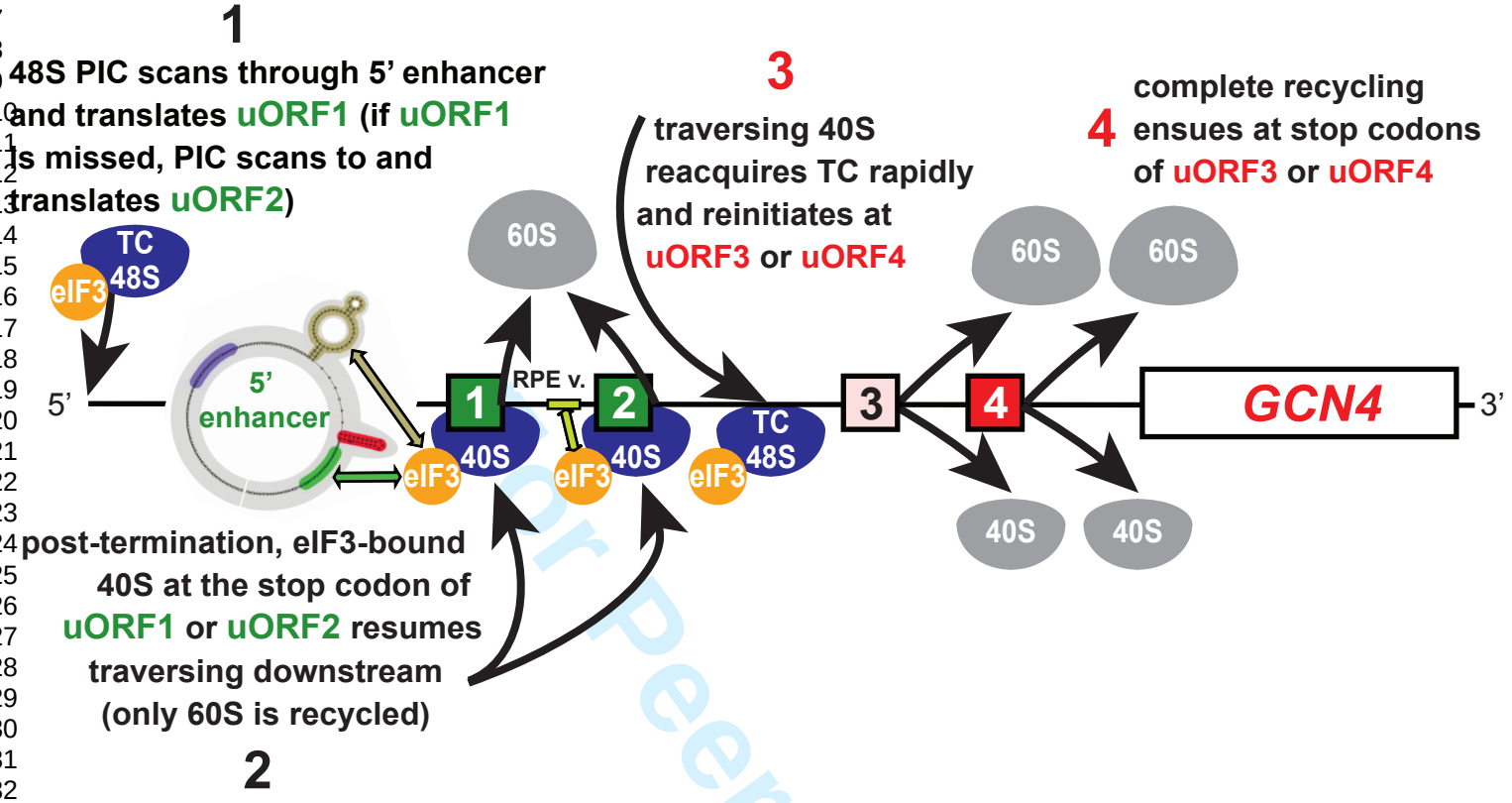

STARVATION: *GCN4* translation is DEREPRESSED
(uncharged tRNAs => GCN2 => eIF2α-P => **low levels of TC**)

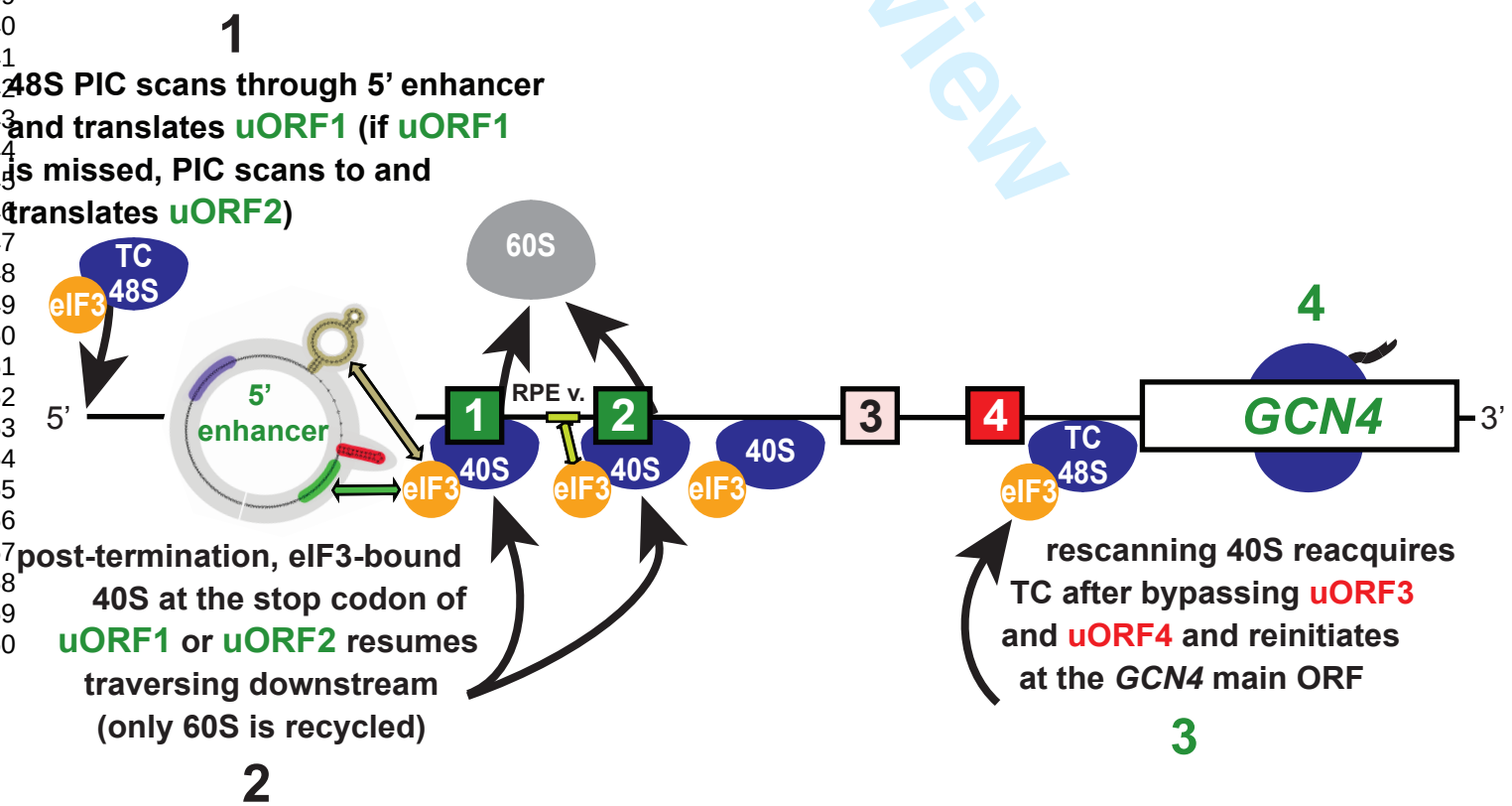

For Peer Review

Gunisova Fig. 4

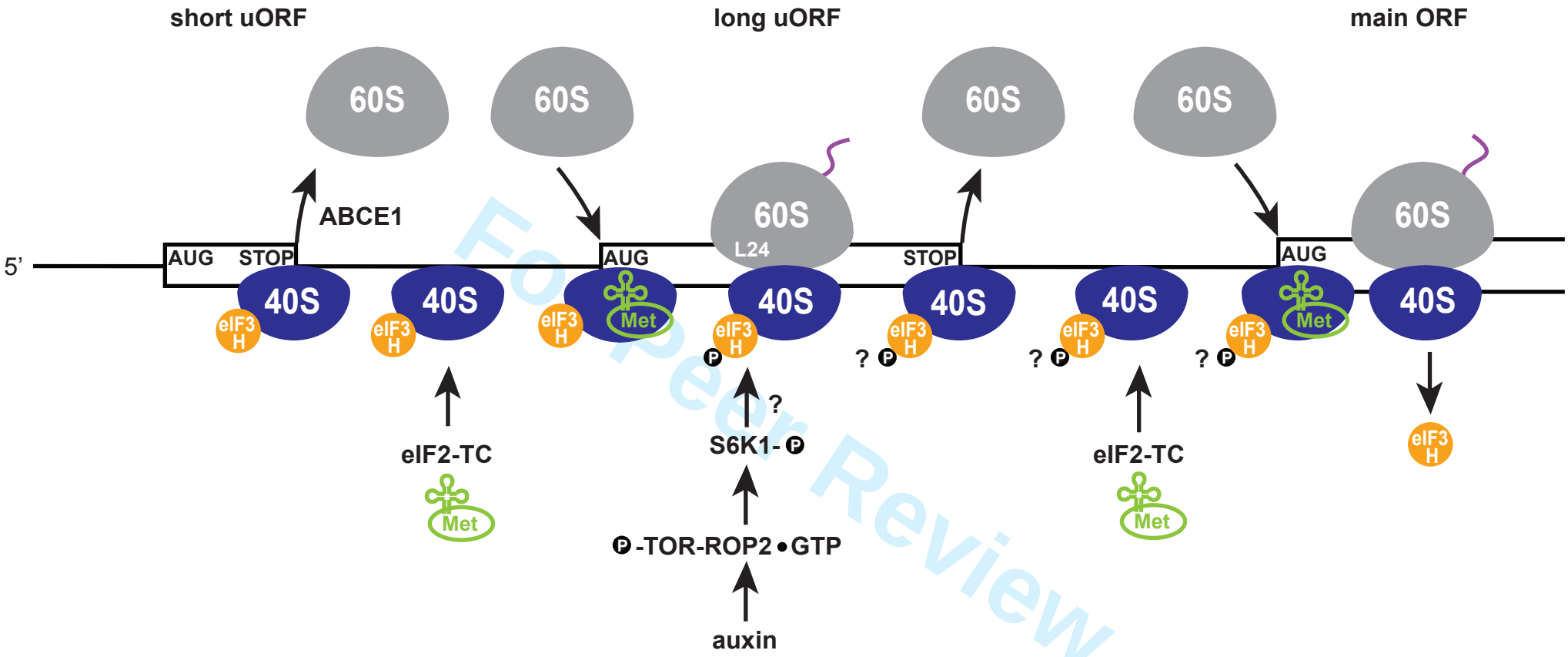

For Peer Review

Gunisova Fig. 5

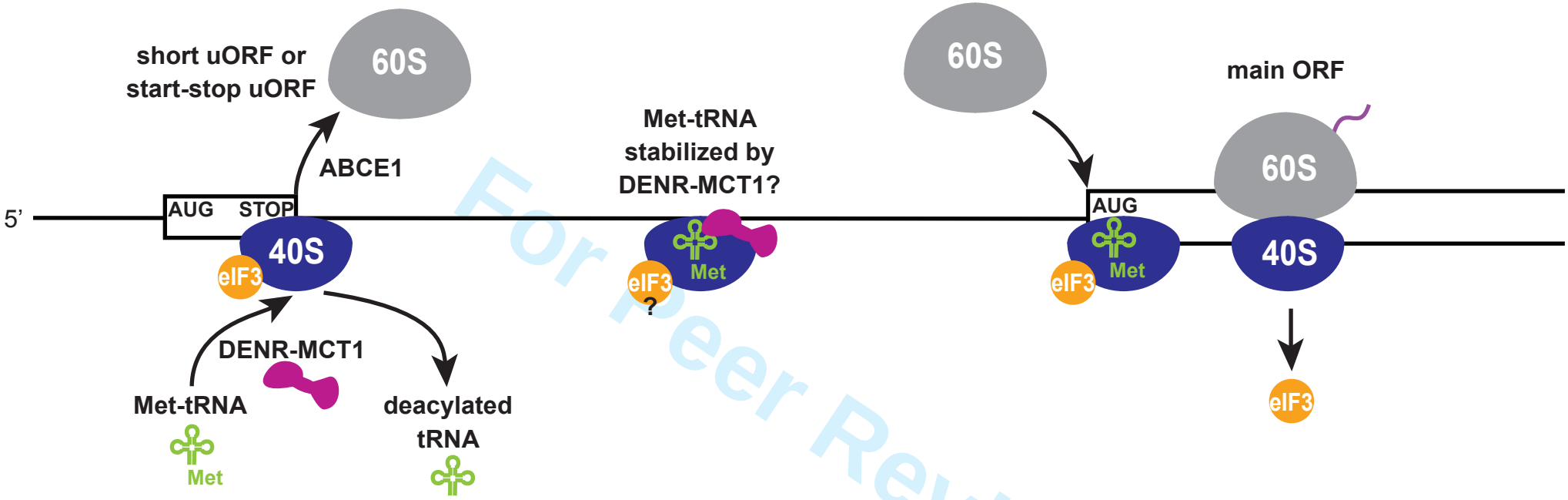

For Peer Review

Gunisova Fig. 6

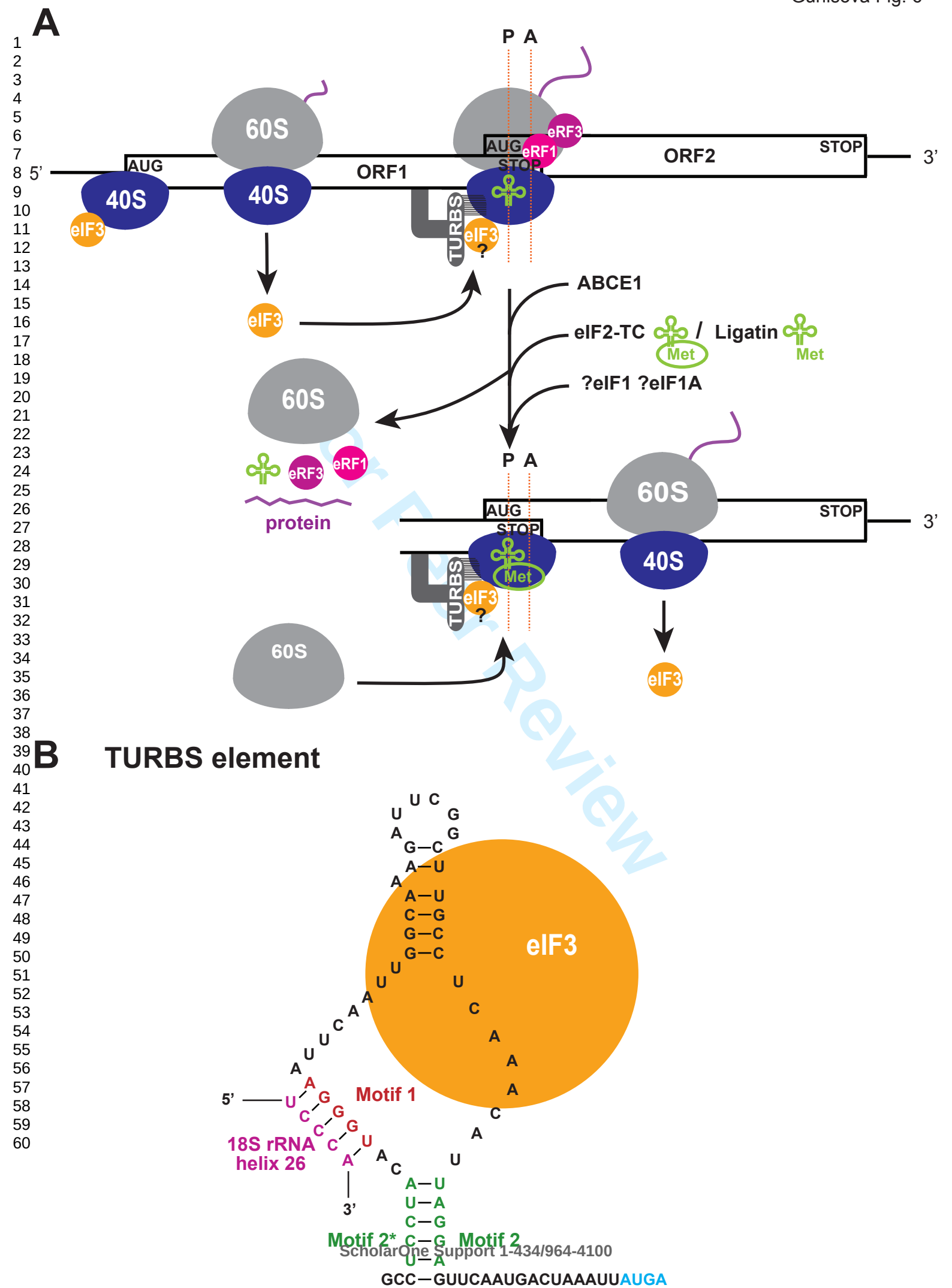

For Peer Review

ScholarOne Support 1-434/964-4100

Gunisova Fig. 7

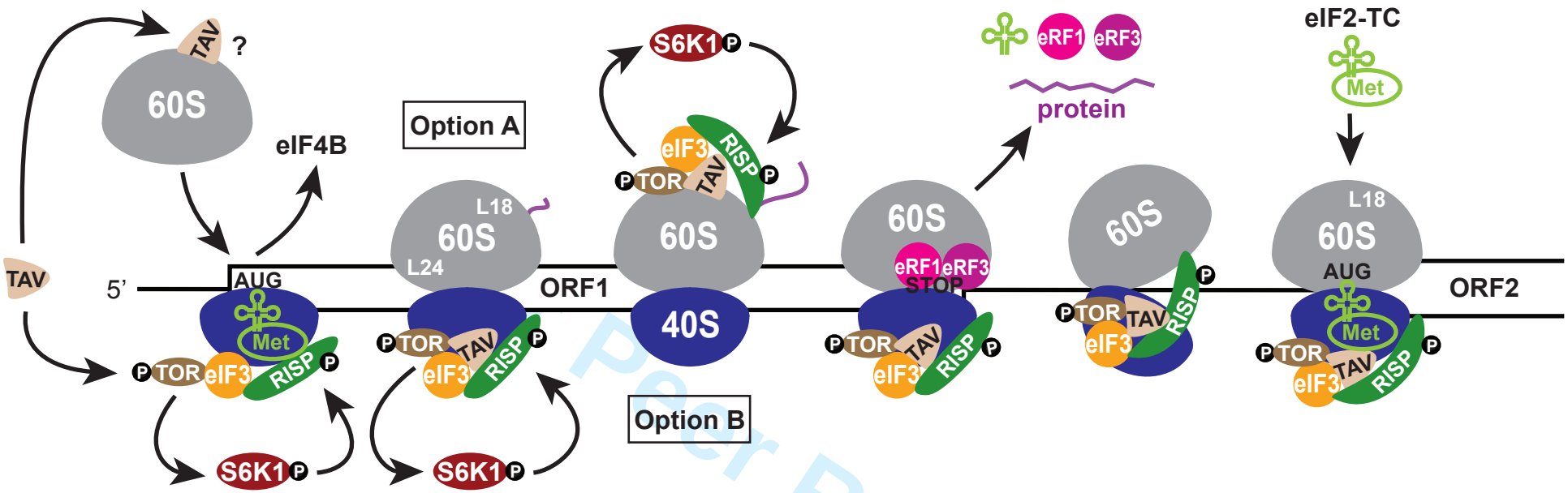

Peer Review

Gunisova Fig. 8

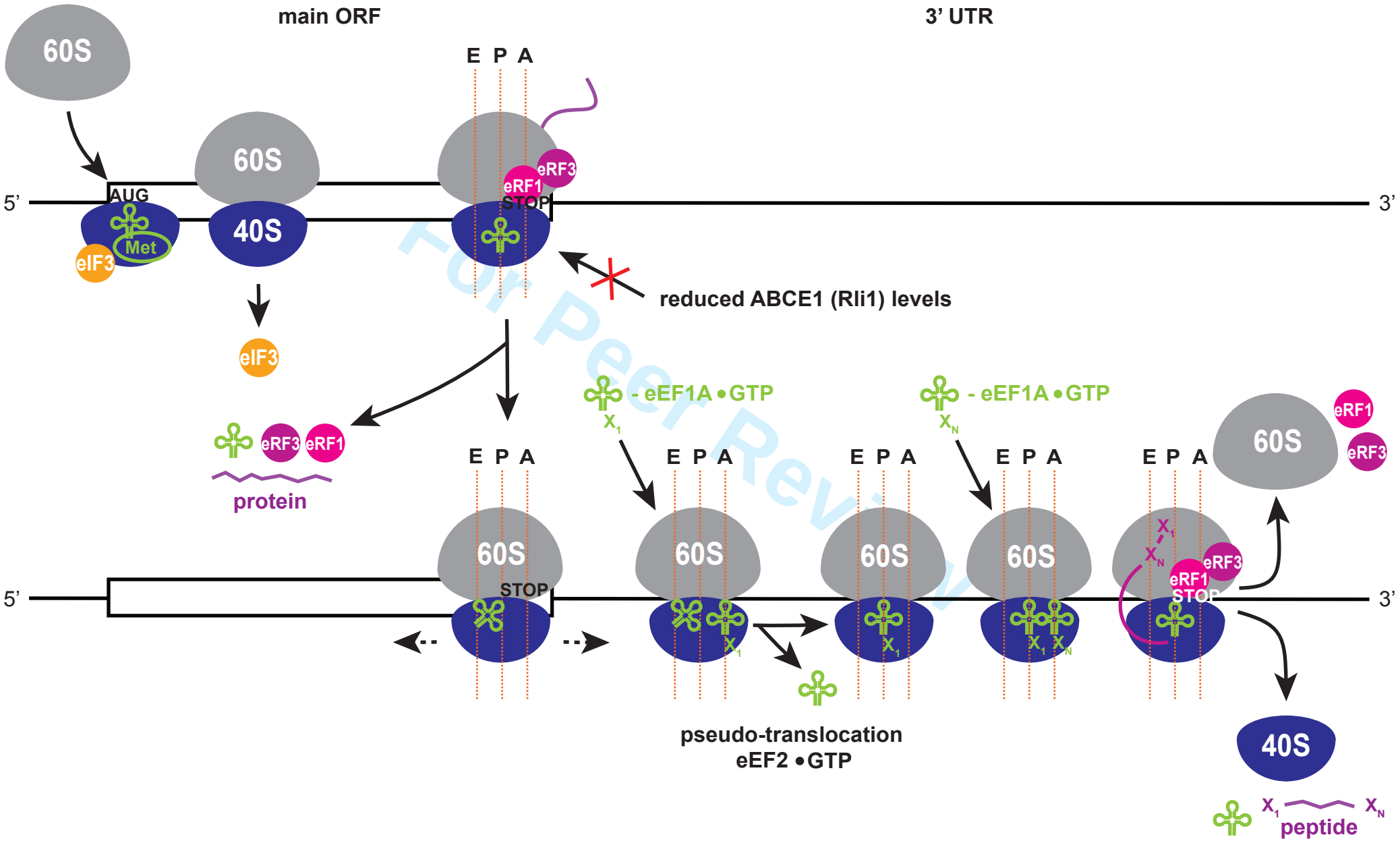

For Peer Review

Gunisova Fig. 9

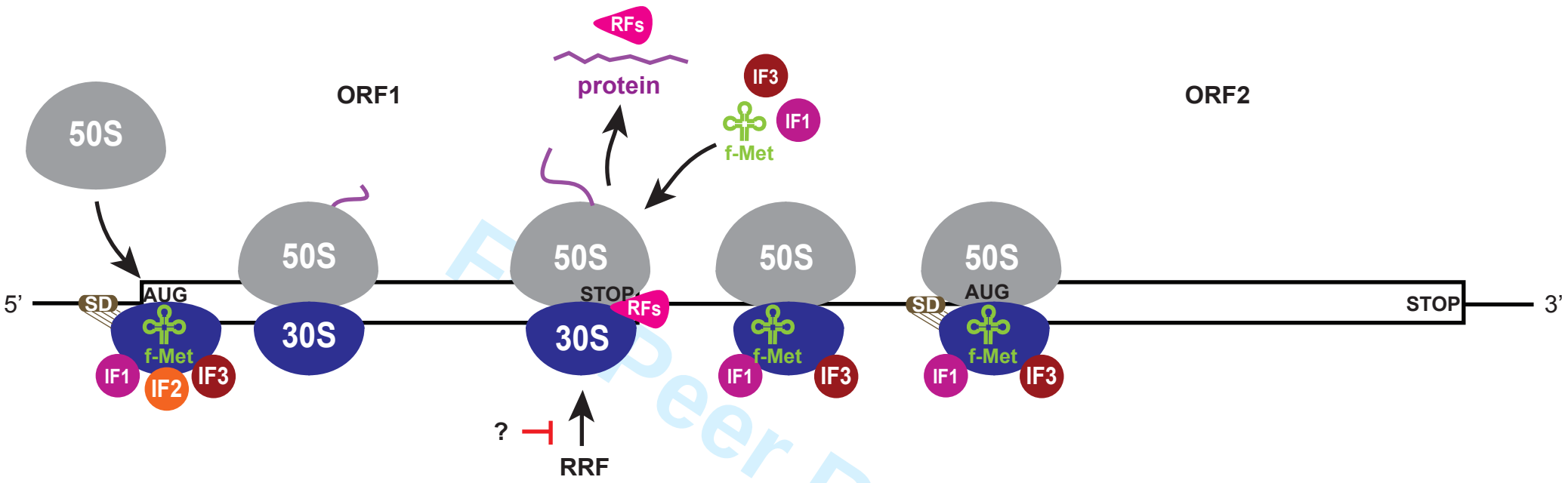

For Peer Review

Gunisova Fig. 10

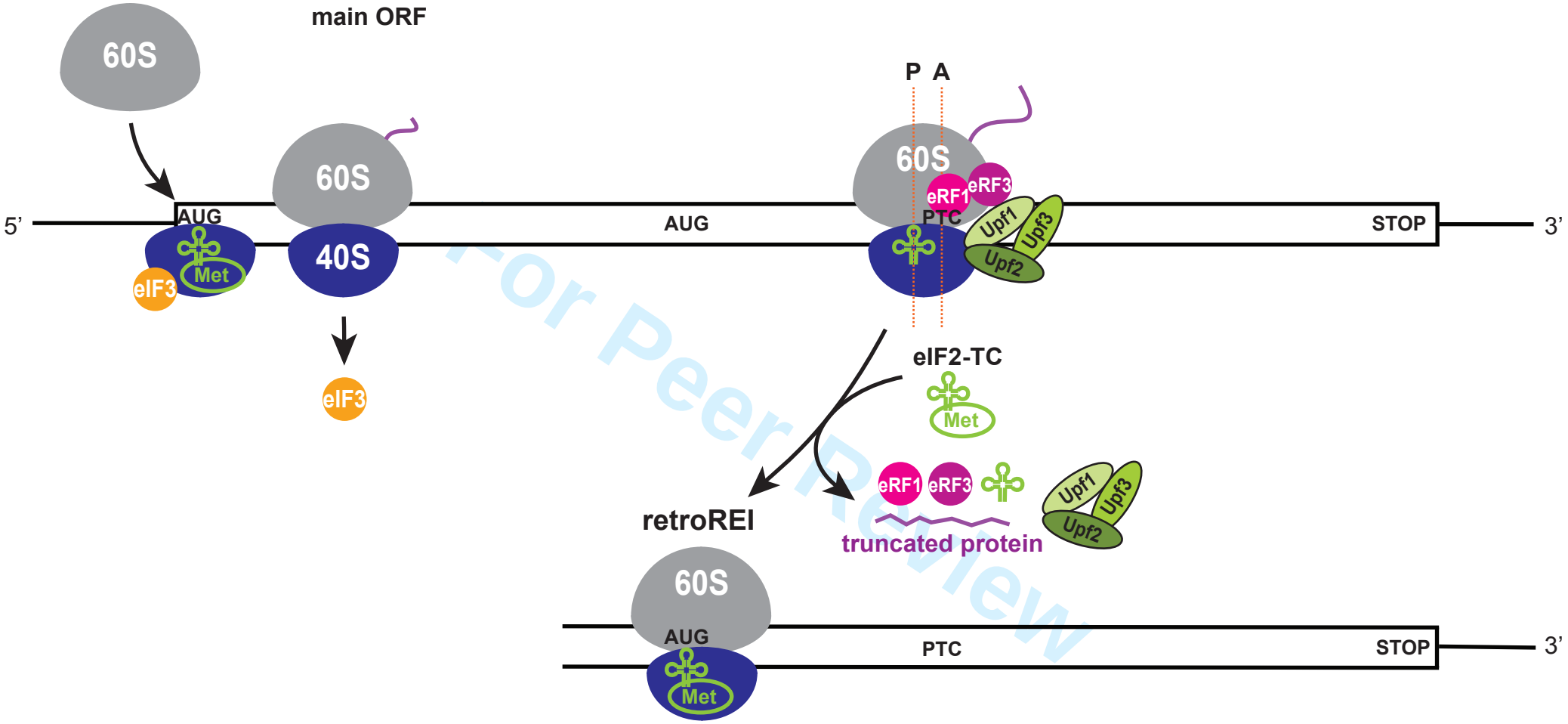

For Peer Review

Gunisova Fig. 11

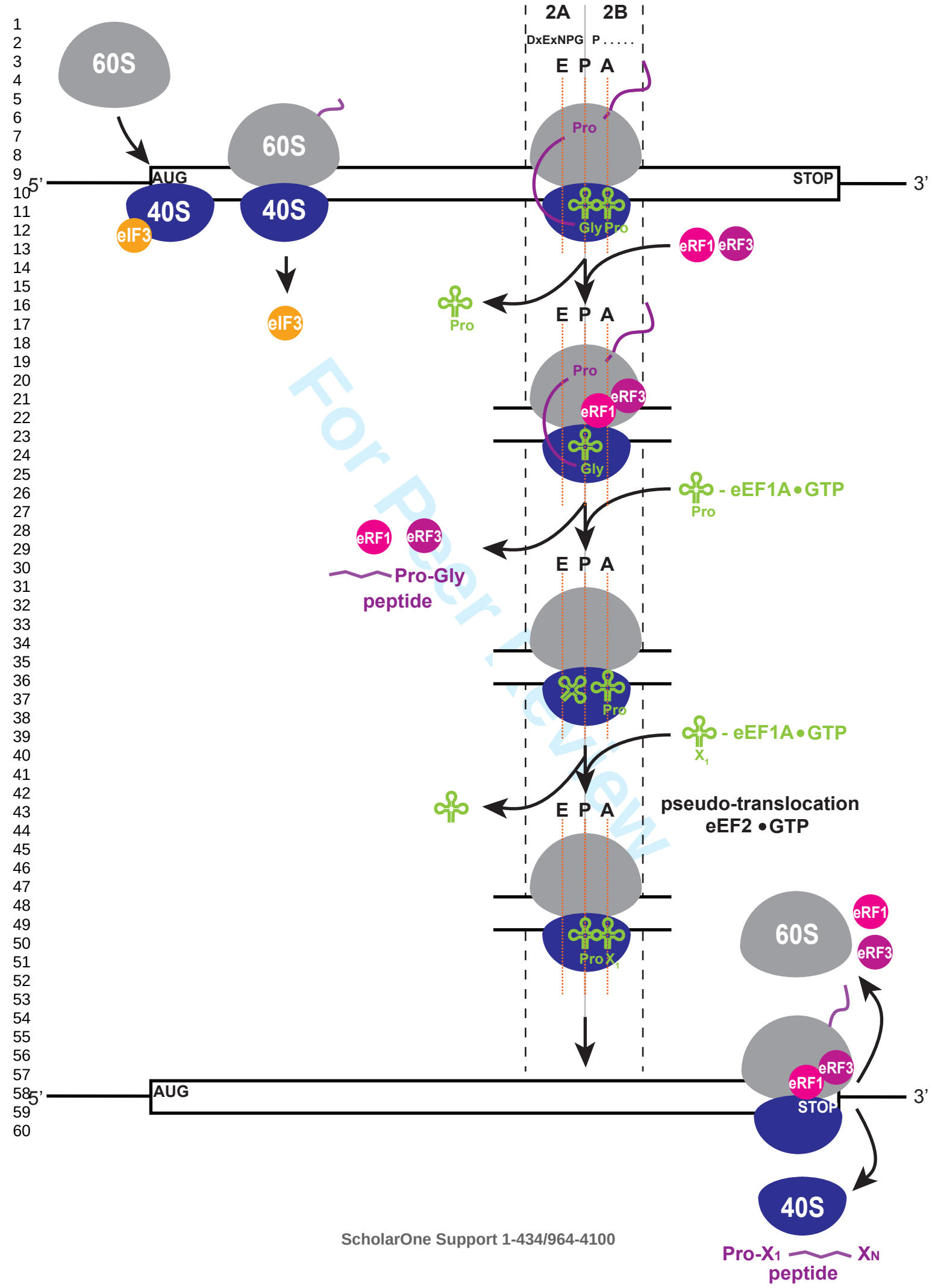

For Peer Review

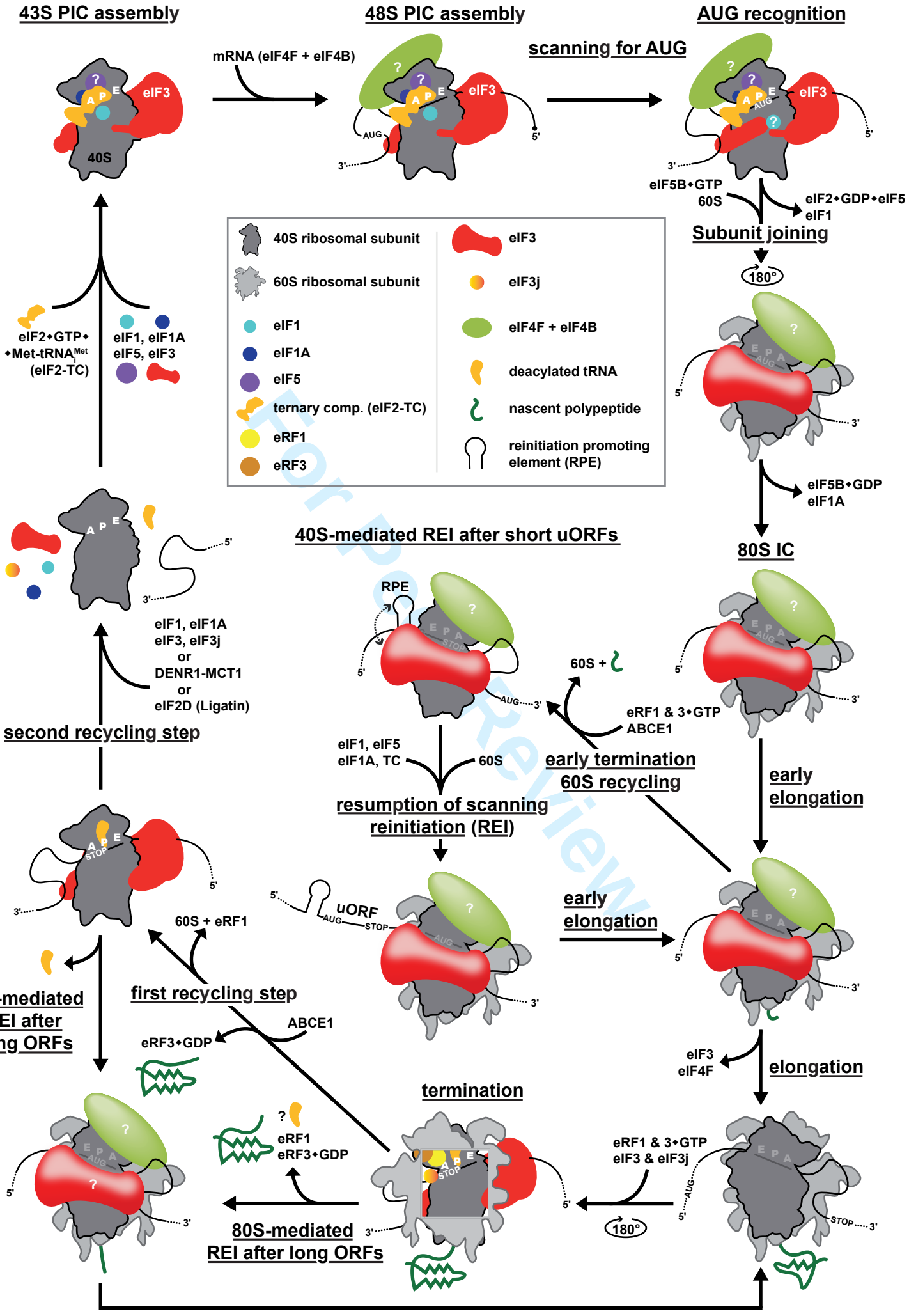

For Peer Review

Figure legends

Figure 1. Model of the entire translational cycle with two basic ways of translation reinitiation: 1) the 40S-mediated REI after short *versus* long uORFs, 2) the 80S-mediated REI after long ORFs. For details please see the main text (adapted from (Valasek *et al.*, 2017)).

Figure 2. (A) Model of the 5' leader of *GCN4* mRNA with its four short uORFs summarizing all REI-promoting and inhibiting RNA and protein features (adapted from (Gunisova *et al.*, 2016)). For details please see the main text. (B) Graphical illustration of the proposed arrangement of the post-termination complex on uORF1 with its RPEs interacting with Box 6 and Box 17 segments of the N-terminal domain of a/Tif32 to promote resumption of scanning for REI on *GCN4* (adopted from (Mohammad *et al.*, 2017)). The exit channel view of the 48S-closed complex shows only two incomplete eIF3 subunits for simplicity: eIF3c/Nip1 in light gold and eIF3a/Tif32 in purple, with its CTD represented by a dotted line (the structure of this domain is unknown and thus its placement in the 48S complex was only predicted). The location of Boxes 6 + 17 is indicated in green. The 5' leader of uORF1 is shown in orange with its RPEs depicted in yellow. The predicted position of eIF3g/Tif35 is indicated by blue circle. (C) Model of the *ATF4* mRNA; REI promoting elements (RPEs) surrounding uORF1 are depicted in green and the prospective interaction between eIF3 and the 5´ RPE is indicated. For details please see the main text.

Figure 3. Model for *GCN4* translational control under non-starvation *versus* starvation conditions mediated *via* reinitiation in response to changing levels of the eIF2-TC. For details please see the main text (adapted from (Gunisova & Valasek, 2014)).

Figure 4. Model for translational control of short and long uORFs-containing mRNAs mediated *via* reinitiation promoted by eIF3h phosphorylation in *Arabidopsis thaliana.* For details please see the main text.

Figure 5. Model for translational control of short uORFs or start-stop uORFs-containing mRNAs mediated *via* reinitiation promoted by DENR-MCT1 as the REI-specific factors. For details please see the main text.

Figure 6. (A) Model for the termination-reinitiation mechanism in caliciviruses with overlapping ORFs mediated *via* TURBS base-pairing with 18S rRNA, which can be perhaps further potentiated by eIF3 binding to both TURBS and the 40S. For details please see the main text. (B) Predicted secondary structure of the FCV TURBS illustrating base-pairing between motif 1 and helix 26 of 18S rRNA, motifs 2 and 2*, as well as the schematic interaction of TURBS with eIF3 (based on (Jackson *et al.*, 2012)).

For Peer Review

ScholarOne Support 1-434/964-4100

Figure 7. Model for translational control of the Cauliflower mosaic virus (CaMV) mRNA mediated *via* reinitiation promoted by the virus-encoded transactivator protein called TAV and the plant-specific REI supporting protein (RISP). For details please see the main text.

Figure 8. Model for translation reinitiation in the 3´ UTR. For details please see the main text.

Figure 9. Model for translation reinitiation in prokaryotes; SD – Shine-Dalgarno sequence; RRF – ribosome recycling factor. For details please see the main text.

Figure 10. Model for retroreinitiation within the coding region; PTC – premature termination codon. For details please see the main text.

Figure 11. Model for the StopGo translation reinitiation. For details please see the main text.

For Peer Review

ScholarOne Support 1-434/964-4100

Please do not recycle!

Translation reinitiation in microbes and higher eukaryotes.

Stanislava Gunišová[1*], Vladislava Hronová[1], Mahabub Pasha Mohammad[1], Alan G. Hinnebusch[2*], and Leoš Shivaya Valášek[1*]

[1] Laboratory of Regulation of Gene Expression, Institute of Microbiology ASCR, Videnska 1083, Prague, 142 20, the Czech Republic

[2] Laboratory of Gene Regulation and Development, Eunice Kennedy Shriver National Institute of Child Health and Human Development, NIH, Bethesda, MD 20892, USA.

For Peer Review

SUPPLEMENTARY DATA

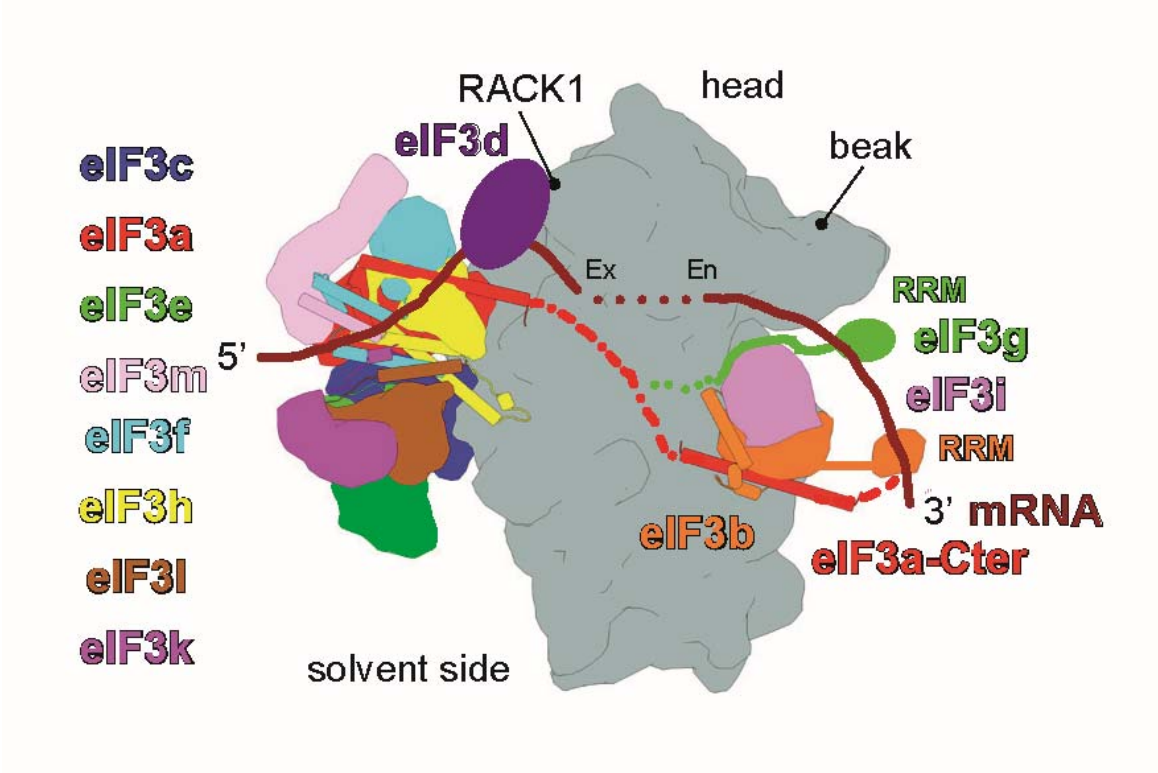

Supplementary Figure 1. Schematic representation of the arrangement of mammalian eIF3 subunits on the solvent-exposed side of 40S subunit (adapted from (Valasek *et al.*, 2017)). eIF3 binds to the solvent-exposed side with the octamer occupying the platform of the small ribosomal subunit connected with the eIF3b–g–i module (YLC) – sitting near the mRNA entry channel – *via* the extended C-terminal linker domain of eIF3a (a dashed red line indicates a predicted location of the eIF3a-CTD (eIF3a-Cter); placement of the eIF3g-RRM is also only our best guess). Figure includes only those domains of eIF3 subunits for which the structures are known. The 40S subunit is depicted in grey surface; all other subunits are labelled and colored variably. The eIF3 helical bundles fortifying the intersubunit interactions are represented as cylinders. The predicted path of mRNA is shown in dark red; Ex and En – mRNA exit and entry channels, respectively. For details please see the main text.

For Review

ScholarOne Support 1-434/964-4100

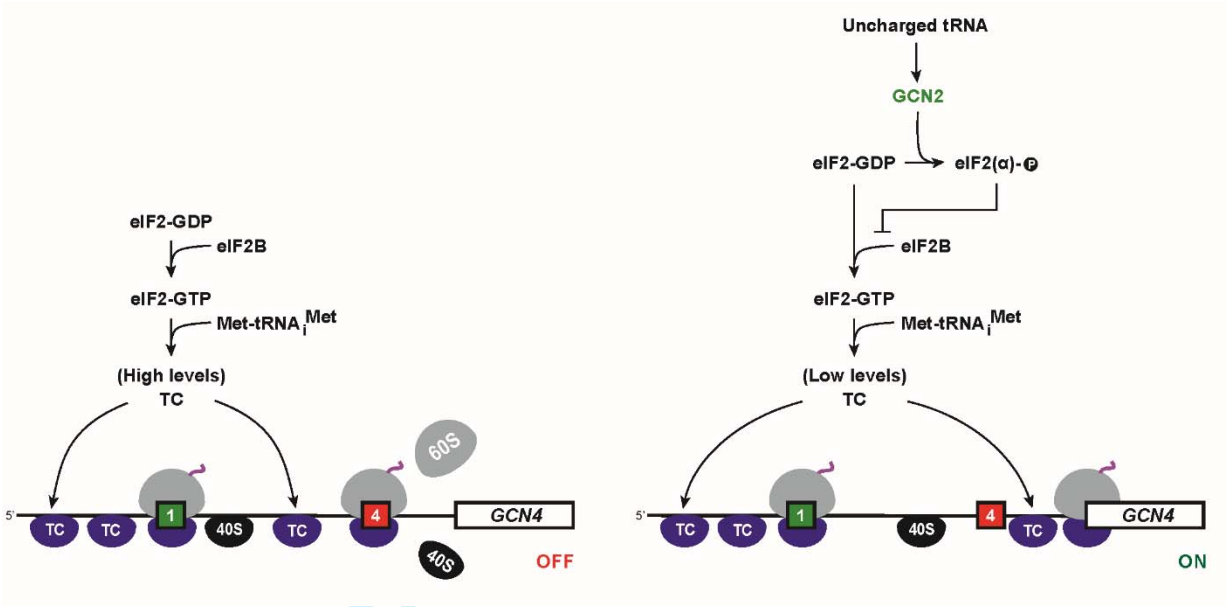

Supplementary Figure 2. Simplified model for the delayed REI mechanism on the *GCN4* mRNA under non-starvation *versus* starvation conditions depicting only uORFs 1 and 4; for details please see the main text (based on (Hinnebusch, 2005)).

For Peer Review

ScholarOne Support 1-434/964-4100